frontiers | Research Topics

Repurposed drugs targeting cancer signaling pathways: clinical insights to improve oncologic therapies, volume II

Edited by
Gerardo Leyva-Gómez, Teresita Padilla-Benavides and Alma D. Campos-Parra

Published in
Frontiers in Oncology

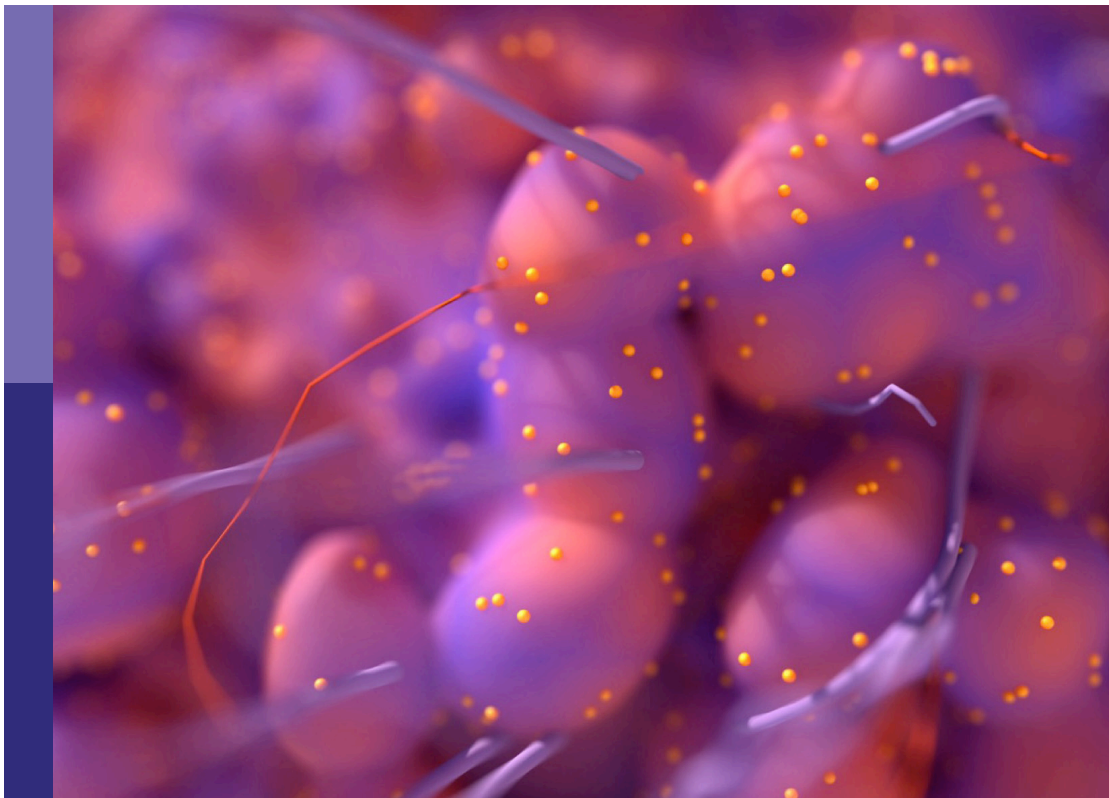

ISSN 1664-8714
ISBN 978-2-8325-6435-6
DOI 10.3389/978-2-8325-6435-6

About Frontiers

Frontiers is more than just an open access publisher of scholarly articles: it is a pioneering approach to the world of academia, radically improving the way scholarly research is managed. The grand vision of Frontiers is a world where all people have an equal opportunity to seek, share and generate knowledge. Frontiers provides immediate and permanent online open access to all its publications, but this alone is not enough to realize our grand goals.

Frontiers journal series

The Frontiers journal series is a multi-tier and interdisciplinary set of open-access, online journals, promising a paradigm shift from the current review, selection and dissemination processes in academic publishing. All Frontiers journals are driven by researchers for researchers; therefore, they constitute a service to the scholarly community. At the same time, the *Frontiers journal series* operates on a revolutionary invention, the tiered publishing system, initially addressing specific communities of scholars, and gradually climbing up to broader public understanding, thus serving the interests of the lay society, too.

Dedication to quality

Each Frontiers article is a landmark of the highest quality, thanks to genuinely collaborative interactions between authors and review editors, who include some of the world's best academicians. Research must be certified by peers before entering a stream of knowledge that may eventually reach the public - and shape society; therefore, Frontiers only applies the most rigorous and unbiased reviews. Frontiers revolutionizes research publishing by freely delivering the most outstanding research, evaluated with no bias from both the academic and social point of view. By applying the most advanced information technologies, Frontiers is catapulting scholarly publishing into a new generation.

What are Frontiers Research Topics?

Frontiers Research Topics are very popular trademarks of the *Frontiers journals series*: they are collections of at least ten articles, all centered on a particular subject. With their unique mix of varied contributions from Original Research to Review Articles, Frontiers Research Topics unify the most influential researchers, the latest key findings and historical advances in a hot research area.

Find out more on how to host your own Frontiers Research Topic or contribute to one as an author by contacting the Frontiers editorial office: frontiersin.org/about/contact

Repurposed drugs targeting cancer signaling pathways: clinical insights to improve oncologic therapies, volume II

Topic editors

Gerardo Leyva-Gómez — National Autonomous University of Mexico, Mexico
Teresita Padilla-Benavides — Wesleyan University, United States
Alma D. Campos-Parra — Universidad Veracruzana, Mexico

Citation

Leyva-Gómez, G., Padilla-Benavides, T., Campos-Parra, A. D., eds. (2025). *Repurposed drugs targeting cancer signaling pathways: clinical insights to improve oncologic therapies, volume II*. Lausanne: Frontiers Media SA.
doi: 10.3389/978-2-8325-6435-6

Table of contents

frontiers | Frontiers in Oncology

TYPE Editorial
PUBLISHED 28 May 2025
DOI 10.3389/fonc.2025.1628842

OPEN ACCESS

EDITED AND REVIEWED BY
Luisa Lanfrancone,
European Institute of Oncology (IEO), Italy

*CORRESPONDENCE
Alma D. Campos-Parra
almcampos@uv.mx
Teresita Padilla-Benavides
tpadillabena@wesleyan.edu

†These authors have contributed equally to this work

RECEIVED 14 May 2025
ACCEPTED 16 May 2025
PUBLISHED 28 May 2025

CITATION
Campos-Parra AD, Leyva-Gomez G and Padilla-Benavides T (2025) Editorial: Repurposed drugs targeting cancer signaling pathways: clinical insights to improve oncologic therapies, volume II.
Front. Oncol. 15:1628842.
doi: 10.3389/fonc.2025.1628842

Editorial: Repurposed drugs targeting cancer signaling pathways: clinical insights to improve oncologic therapies, volume II

Alma D. Campos-Parra [1*†], Gerardo Leyva-Gomez [2] and Teresita Padilla-Benavides [3*†]

[1]Instituto de Salud Pública, Universidad Veracruzana, Xalapa, Mexico, [2]Departamento de Farmacia, Facultad de Química, Universidad Nacional Autónoma de México, Ciudad de Mexico, Mexico, [3]Molecular Biology and Biochemistry Department, Wesleyan University, Middletown, CT, United States

KEYWORDS

drug repositioning, cancer, signaling pathways, treatments, personalize therapy

Editorial on the Research Topic
Repurposed drugs targeting cancer signaling pathways: clinical insights to improve oncologic therapies, volume II

Introduction

Drug repurposing in oncology is a strategy that attempts to identify new therapeutic uses of drugs already approved for other diseases to treat cancer. This strategy has gained interest because of its potential to reduce costs and accelerate the development of oncology treatments. This Research Topic aims to provide information on repositioned drugs in different types of cancer, to personalize and improve cancer therapies. Ten manuscripts in this Research Topic examine various but interconnected aspects of drug repurposing, highlighting the rapid advancement of the field and increasing complexity.

Repositioning existing drugs for the treatment of common cancers

Common tumors refer to cancers with high incidence and prevalence across global populations, making them some of the most frequently diagnosed malignancies. These typically include solid tumors such as breast, lung, colorectal, prostate, ovarian, pancreatic, liver, and bladder cancers. Characterized by well-established clinical and biological profiles, these tumors are often supported by robust preclinical models and extensive clinical trial data. Due to their prevalence and clinical impact, they are strong candidates for drug repurposing to enhance outcomes, particularly in resistant cases or when treatment options are limited.

In this sense, triple negative breast cancer (TNBC) is usually an aggressive and difficult-to-treat cancer. On this topic, Carrion-Estrada et al. demonstrated a compelling strategy for targeting TNBC by stabilizing the oncogenic K-Ras4B G13D/PDE6δ complex using novel compounds (C14 and P8). These agents suppressed tumor growth in both *in vitro* and *in vivo* models, including resistant TNBC subtypes, highlighting their potential as adjuvant treatments when standard therapies fail. In a related effort to expand treatment options through drug repositioning, Hajihosseini et al. conducted a meta-analysis showing that olaparib, typically used in BRCA1/2-mutant breast and ovarian cancer, improved progression-free survival when used as monotherapy in lung cancer compared to combination regimens with durvalumab or gefitinib. In parallel, Pernot et al. explored an immunomodulatory approach through the repurposing of sulconazole, an antifungal compound that inhibits PD-1 expression in immune and cancer cells by blocking NF-κB and calcium signaling. The ability of sulconazole to restore immune activity while repressing malignant traits further highlights the value of nontraditional compounds in oncology, especially for immunologically evasive tumors (https://doi.org/10.3389/fimmu.2023.1278630).

Complementing these findings, Villegas-Vázquez et al. provided a comprehensive review on drug repositioning for ovarian cancer, emphasizing the critical role of cell line and animal models in preclinical drug screening. Although clinical application remains in early stages, these models are key to developing future therapies aimed at improving outcomes in patients with gynecologic cancers.

At the genomic level, Martinez-Montiel et al. discussed a paradigm shift by focusing on alternative splicing events in prostate cancer. As splicing errors increasingly emerge as hallmarks of malignancy, this review advocates for the development of diagnostics and therapies that target cancer-specific splicing isoforms, an especially timely strategy given the rising global burden of disease in low-resource settings. Additionally, Sánchez-Marín et al. discussed thyroid cancer at the genomic levels and identified 13 genes with missense mutations and 10 for gene fusions as potential therapeutic targets for drug repositioning. This which represents promising area for therapeutics, as treatment for this cancer is limited.

Therapeutic opportunities through drug repositioning in uncommon cancers

Uncommon tumors are rare cancers with limited epidemiological data, including sarcomas, neuroendocrine tumors, certain pediatric cancers, and site-specific malignancies. Their low incidence often leads to underrepresentation in clinical trials and reliance on limited or extrapolated treatment evidence. Their rarity poses challenges for diagnosis, research, and treatment development, but also makes them ideal candidates for drug repurposing, offering quicker, cost-effective options where standard therapies are limited or ineffective.

Osteosarcoma is a rare and aggressive bone cancer, with complex diagnosis and treatment due to tumor heterogeneity. Despite its prevalence across age groups, comparative genomic data has been limited. A study by Zou et al. analyzed 194 patients and found age-related molecular differences. While common mutations like TP53 appeared across all ages, younger patients had more gene amplifications and homologous recombination deficiency, whereas adults had higher tumor mutational burden. Children showed more angiogenesis-related mutations, while older groups had alterations in PI3K/mTOR and cell cycle pathways. Notably, 58% of patients had actionable mutations, with treatment targets varying by age.

Giant cell tumor of bone (GCT) is a rare neoplasm with limited treatment options. In this context, McAllister et al. were the first to report the expression of Prostate-Specific Membrane Antigen (PSMA) in GCT. PSMA is the molecular target for the radioligand therapies Locametz and Pluvicto, currently approved for prostate cancer. Based on their findings, the authors suggest the potential repositioning of Locametz and Pluvicto as therapeutic options for GCT.

A broader overview of glioblastoma therapy shed light on the systemic challenges in treating this notoriously intractable disease. The review by Han Bae et al. emphasize the importance of biomarker discovery and innovative drug delivery technologies (e.g., nanoparticles, focused ultrasound) alongside drug repurposing, a strategy echoed in the sulconazole and C14/P8 studies, for overcoming barriers like the blood-brain barrier and tumor heterogeneity.

Finally, home chemotherapy initiatives have emerged as a viable and safe alternative to traditional hospital treatment for oncology patients, a safe alternative that could reduce costs and hospital burden. In this regard, Villegas et al. presented several recommendations based on the published literature and an expert panel in order to have a basis for the development of future initiatives, as they represent a new model of patient-centered oncology care.

Summary and concluding remarks

This growing body of research emphasizes the promise of drug repurposing as a faster, cost-effective way to develop new cancer therapies by using existing drugs with known safety profiles. It highlights a shift toward targeted, mechanism-based treatments, aiming to improve outcomes, especially for difficult or understudied cancers. By combining molecular insights with innovative therapeutic approaches, these studies move the field closer to personalized and effective cancer care.

Author contributions

AC: Supervision, Writing – review & editing, Investigation, Writing – original draft, Validation, Project administration, Visualization, Conceptualization. GL: Visualization, Validation, Writing – review & editing. TP-B: Writing – original draft, Project administration, Visualization, Validation, Supervision, Investigation, Writing – review & editing.

Acknowledgments

We are grateful to all the colleagues who contributed to the present special topic.

Conflict of interest

The authors declare that the research was conducted in the absence of any commercial or financial relationships that could be construed as a potential conflict of interest.

The author(s) declared that they were an editorial board member of Frontiers, at the time of submission. This had no impact on the peer review process and the final decision.

Generative AI statement

The author(s) declare that no Generative AI was used in the creation of this manuscript.

Publisher's note

frontiers | Frontiers in Immunology

TYPE Original Research
PUBLISHED 05 January 2024
DOI 10.3389/fimmu.2023.1278630

OPEN ACCESS

EDITED BY
Teresita Padilla-Benavides,
Wesleyan University, United States

REVIEWED BY
Qibin Liao,
Shenzhen Third People's Hospital, China
Dalia Haydar,
Children's National Hospital, United States

*CORRESPONDENCE
Abdel-Majid Khatib
majid.khatib@inserm.fr
Geraldine Siegfried
geraldine.siegfried@inserm.fr

†PRESENT ADDRESS
Mercedes Tomé,
Group of Metabolism and Cell Signaling, Andalusian Molecular Biology and Regenerative Medicine Centre-CABIMER-CSIC, Seville, Spain

‡These authors share first authorship

RECEIVED 16 August 2023
ACCEPTED 30 November 2023
PUBLISHED 05 January 2024

CITATION
Pernot S, Tomé M, Galeano-Otero I, Evrard S, Badiola I, Delom F, Fessart D, Smani T, Siegfried G, Villoutreix BO and Khatib A-M (2024) Sulconazole inhibits PD-1 expression in immune cells and cancer cells malignant phenotype through NF-κB and calcium activity repression.
Front. Immunol. 14:1278630.
doi: 10.3389/fimmu.2023.1278630

Sulconazole inhibits PD-1 expression in immune cells and cancer cells malignant phenotype through NF-κB and calcium activity repression

Simon Pernot[1,2‡], Mercedes Tomé[1†‡], Isabel Galeano-Otero[1], Serge Evrard[1,2], Iker Badiola[3], Frederic Delom[1,2], Delphine Fessart[1,2], Tarik Smani[4], Geraldine Siegfried[1,2*], Bruno O. Villoutreix[5] and Abdel-Majid Khatib[1,2*]

[1]Reprograming tumor activitY and associaTed MicroenvironmEnt (Rytme), Bordeaux Institute of Oncology (BRIC)-UMR1312 Inserm, Université of Bordeaux, Pessac, France, [2]Institut Bergonié, Bordeaux, France, [3]Department of Cell Biology and Histology, Faculty of Medicine and Nursing, University of the Basque Country (UPV/EHU), Leioa, Spain, [4]Group of Cardiovascular Pathophysiology, Institute of Biomedicine of Seville, University Hospital of Virgen del Rocío/University of Seville/CSIC, Seville, Spain, [5]Integrative Computational Pharmacology and Data Mining, INSERM UMR 1141, Rob-ert-Debré Hospital, Paris, France

The overexpression of the immunoinhibitory receptor programmed death-1 (PD1) on T-cells is involved in immune evasion in cancer. The use of anti-PD-1/PDL-1 strategy has deeply changed the therapies of cancers and patient survival. However, their efficacy diverges greatly along with tumor type and patient populations. Thereby, novel treatments are needed to interfere with the anti-tumoral immune responses and propose an adjunct therapy. In the current study, we found that the antifungal drug Sulconazole (SCZ) inhibits PD-1 expression on activated PBMCs and T cells at the RNA and protein levels. SCZ repressed NF-κB and calcium signaling, both, involved in the induction of PD-1. Further analysis revealed cancer cells treatment with SCZ inhibited their proliferation, and migration and ability to mediate tumor growth in zebrafish embryos. SCZ found also to inhibit calcium mobilization in cancer cells. These results suggest the SCZ therapeutic potential used alone or as adjunct strategy to prevent T-cell exhaustion and promotes cancer cell malignant phenotype repression in order to improve tumor eradication.

KEYWORDS

PD-1, Jurkat T cells, PBMCs, NF-κB, calcium, cancer, zebrafish

1 Introduction

The inhibitory receptor programmed cell death protein-1 (PD-1, PDCD1) is a member of the immunoglobulin (lg) superfamily (1). The expression of this type I transmembrane protein is induced in various immune cells including T cells, B cells, macrophages, and several dendritic cell subsets (2–4). Two main ligands of PD-1, namely programmed cell death ligand 1 and 2 (PD-L1/PD-L2) (5) are expressed in various tumor cell types and immune cells (5, 6). By binding to PD-1, PD-L1 inhibits T cell activation, leading to immune escape. Thereby, interfering with PD-1 and PD-L1 interaction or signaling pathways was proposed as a therapeutic approach to prevent cancer cells from avoiding the anti-tumoral immune response. This by reactivating the T-cell-mediated tumor cell cytotoxicity and elimination (1–5). Indeed, previous studies indicated that the inhibition of PD-1 promotes an effective immune response against cancer cells (1–5) and targeting PD-L1 or PD-1 using monoclonal antibody blocking PD-1 or PD-L1 has been associated with significant clinical response in a wide range of malignancies (7, 8). However, although blockade of PD-1/PD-L1 with these monoclonal antibodies shows therapeutic effect for cancer patients, their use displayed some restrictions. These include the reduced response frequency and several adverse effects observed in some cancer patients (7, 8). Therefore, to overcome these difficulties the development of other efficient strategies is now necessary.

Antifungal imidazole derivatives are commonly used for the treatment of topical and systemic infections including candidal infections and mycoses (9). Imidazole derivatives, including ketoconazole (KET), miconazole (MIC), tioconazole (TIO), clotrimazole (CLO), and sulconazole (SCZ), were initially identified as ligands of the heme iron atom of cytochrome P450 (CYP) (10–12). Furthermore, the effect of these drugs have been studied in the context of human pathologies treatment including cancer (13). Of these, SCZ is an antifungal agent with a broad spectrum of activity and is proposed for the treatment of skin infections such as dermatophyte infections (14–16). Compared to several imidazoles, SCZ shows enhanced antifungal activity (14–16) and was reported to inhibit the malignant phenotype of breast cancer cells (13). In this study we demonstrate the ability of SCZ to inhibit the expression of PD-1 on activated T cells and PBMCs through NF-κB activity and calcium mobilization repression. Sulconazole was also able to inhibit colon cancer and breast cancer cells as well as melanoma proliferation, and migration, suggesting the dual therapeutic effect of this drug.

2 Materials and methods

2.1 PBMCs, T cells and cancer cells culture and PBMCs activation

Human peripheral blood mononuclear cells (hPBMCs) were obtained following written informed consent approved by Bergonié Institute (Bordeaux, France). PBMCs were isolated from healthy donors by density gradient centrifugation with Pancoll (PANBiotech; human, density 1,077g/ml) and were cultured in RPMI 1640 (PAN-Biotech) supplemented with 10% FBS (Gibco), 2mM L-glutamine (Gibco) and penicillin/streptomycin solution (Dominique Dutscher). Human T cells were purified from blood using the MACSxpress® Whole Blood Pan T Cell Isolation Kit (Miltenyi Biotec). The murine colon cancer cells CT-26, the human colon cancer cells HT29, melanoma cells M10 and Jurkat T and J.RT3-T3.5 (JRT3) cell lines were cultured in RPMI 1640 complete media. The breast cancer cells MDA-MB 231 were cultured in DMEM complete media. All the cells were grown at 37°C in a 95% air, 5% CO2 humidified incubator. Activation of Jurkat T cells, purified T cells and PBMCs was induced by phorbol myristate acetate (PMA,100ng/ml) and Ionomycin (Io,1ug/ml), as previously described (17).

2.2 Real-time qPCR

Total RNA was isolated using the Nucleospin RNA kit (Macherey-Nagel) prior reverse transcription in a reaction mixture containing 50mM Tris-HCl (pH 8.3), 30mMKCl, 8mM MgCl2, 1mM dNTPs, and 0.2U Superscript reverse transcriptase (Invitrogen), as previously described (17, 18) in a VeritiThermal Cycler (Applied Biosystem). Quantitative real-time PCR was performed using specific TaqMan primers and Master Mix (Eurogentec), in a StepOne Plus Real-Time PCR system following manufacturer's instructions (Applied Biosystem). GAPDH was used for normalization. The PDCD1 primers used are F 5'-CTACAACTGGGCTGGCGG-3' and R 5'-TGTGTTGGAGAAGCTGCAGG-3, respectively. The primers for CTLA4 were derived from BioRad Unique Assay (ID qHsaCED0003794).

2.3 Ca^{2+} mobilization measurement quenching assay

Indicated cells were treated for 48 h with 10 µM of Sulconazole or vehicle (DMSO) in their culture media, and then Ca^{2+} influx was evaluated using 2 µM Fura-2 AM (ThermoFisher Scientific, US) and microfluorometry system, for adherent cells, or CLARIOstar® Plus microplate reader (BMG Labtech; Germany), for T cells. The microfluorometry system includes inverted microscope Leica (Wetzlar, Germany) with a 20×/0.75 NA objective, a monochromator (Polychrome V, Till Photonics, Munich, Germany), a CCD camera and HP software (Hamamatsu Photonics, Japan). In both cases, the changes of intracellular Ca^{2+} concentration ($[Ca^{2+}]_i$) were shown as the ratio of Fura-2 AM fluorescence after excitation at 340 and 380 nm (ratio = F_{340}/F_{380}). Experiments were done following the period sequence: 4 min in (1) free Ca^{2+} solution (140 mM NaCl, 2.7 mM KCl, 4 mM $MgCl_2$, 0.5 mM EGTA, 10 mM HEPES, pH = 7.4) with 2 µM of thapsigargin, in order to stimulate Store Operated Ca^{2+} Entry (SOCE), and 6 min in (2) 2-2.5 mM Ca^{2+} solution (2-2.5 mM $CaCl_2$; 140 NaCl, 2.7 KCl, 1 $MgCl_2$, 0.5 EGTA, 10 HEPES, pH = 7.4). Then, Ca^{2+} influx (Δratio)

was computed as the difference between the peak ratio after 2 min of extracellular Ca^{2+} re-addition and its level just before.

2.4 JRT3 functional assay

This functional assay, is based on Jurkat T-cell line stably expressing the human LES -γδ TCR (JRT3-LES) incubated with the colon cancer cell line HT29 overexpressing the endothelial protein C receptor (HT29-EPCR), as previously described (17). The activation of JRT3-LES cells was evaluated by the expression of CD69.

2.5 Proliferation assay

The proliferation of indicated cells was performed using the IncuCyte live-cell microscopy incubator (Essen Bioscience). Cells (2×10^5) were treated with indicated concentrations of SCZ in the presence of 3% and 10% serum and placed in the IncuCyte incubator, and phase-contrast images were taken at regular intervals over 96 hours. Results were calculated by the IncuCyte software and presented as confluence relative to time 0. Images were taken with a ×4 objective. Four images were taken from each well, and each condition had more than 6 wells.

2.6 Wound healing assay

Cells were seeded in 96-well plates and allowed to grow until they reached 90% confluence (2×10^6 cells per well of each cell line). The cell wound was performed using Incucyte® Wound Maker 96-Tool, and cells were treated with various concentration of SCZ during various time periods. Plates were placed in the IncuCyte incubator which took 4 phase-contrast images and calculated cell-free area of each well at regular intervals over 48 hours. Results were shown as relative wound density.

2.7 Immunocytochemistry

Detection of PD-1 in Jurkat T cells were monitored using an anti-PD-1 antibody at 1:100 in TBS with 5% BSA, as previously described (17). Confocal immunofluorescence images were taken using the inverted microscope Nikon C2si Eclipse Ti-S with NIS-ElementsAR software (NikonInstruments Europe B.V.).

2.8 Flow cytometry analysis

Cells were stained with fluorophore-conjugated antibodies: PE-anti-PD-1 mAb (MIH4, #560908 eBiosciences) and Flowcytometry data were acquired with BD Accuri C6 (BD Biosciences). Flow cytometry analyses were performed using BD Accuri C6 software and FlowJo 9.3.2 (TreeStar), as previously described (17).

2.9 Western blotting

Cells were lysed in PBS containing 2% NP-40 and lysates were subjected to SDS-PAGE (BioRad Miniprotein) and proteins were blotted onto polyvinylidene difluoride membrane (PVDF, Amersham Pharmacia Biotech). The primary antibodies anti-NF-κB p65 (#sc-8008, dilution 1/500) from Santa Cruz Biotech, phospho-NF-κBp65 (#3033, dilution 1/500) from Cell signaling, TRPC1: rabbit anti-TRPC1 (1:500, T8276; Sigma-Aldrich, United States), STIM1: rabbit anti-STIM1 (1:500, 4916S; Cell Signaling, United States) and Orai1: rabbit anti-Orai1(1:250, O8264; Sigma-Aldrich, United States) were revealed by HPR-conjugated secondary antibodies (Amersham Pharmacia Biotech) and enhanced chemiluminescence (Pierce ECL Plus, Thermo Scientific) according to the manufacturer's instructions. Images were acquired with a Genegnome system and GeneSyssoftware (Syngene) (17–19).

2.10 Tumorigenicity assay

All experiments performed in this study were approved by the university of Bordeaux Animal Ethics. Adult AB zebrafish strain (ZIRC, USA) were maintained following the French Directive under permission number A33-063-935. All the procedures were conducted in compliance with the European Communities Council Directive (2010/63/EU). Following the production of embryos by adult zebrafish, embryos were allowed to grow in E3 medium (5 mM NaCl, 0.17 mM KCl, 0.33 mM CaCl2, 0.33 mM MgSO4) at 28°C, as described previously (20, 21). After dechorionation, 2-day post fertilization (dpf) zebrafish embryos were anaesthetized with 0.003% tricaine (Sigma, USA) and placed in 3% methylcellulose on a dish coated with 1% agarose. MDA-MDB-231 cells were detached using Versaine solution and $2.5{\cdot}10^6$ cells were resuspended in 50 µl of PBS containing 1% phenol red. Immediately, cell suspension was loaded into Femtotip II capilar needles (Eppendorf, Germany) and injections were performed using a pump (Femtojet 4i; Eppendorf, Germany) and a micromanipulator (Phymep). Around 500 cells per embryos were inserted above the duct of Cuvier in perivitelline space of the embryo, as previously described (22). After checking the implantation with mammalian cells, zebrafish embryos were maintained in 24-well plates at 36.3°C. Then, SCZ (1 µM) or vehicle (DMSO) we added of to each well. Tumor imaging was done after 48-h post injection (hpi) using Nikon EclipseTS100 microscope. The tumor size was evaluated using the area of the developed tumors.

2.11 Statistical analysis

Unless otherwise indicated, data are presented as mean ± SEM. A 2-tailed t test was used to analyze the data in GraphPad Prism (GraphPad Software). The statistical significance level is illustrated with P (p-values). Statistical P was set than 0.05.

10.3389/fimmu.2023.1278630

3 Results

3.1 Sulconazole inhibits PD-1 expression in T cells and PBMCs

A potent T cell response requires PKC signaling (23). To induce PBMCs, human purified T cells activation we first used combination of PMA and Io (PMA/Io) that mimics T-cell receptor (TCR) activation. Indeed, PMA binds to and activates PKC whereas ionomycin (Io) is a calcium ionophore that enhances membrane permeability to calcium. Incubation of indicated cells with PMA/Io for 24h induced PD-1 mRNA expression in all indicated cells (Figures 1A, B). In the presence of SCZ (5µM), PD-1 mRNA expression was considerably decreased after 24h of treatment, as assessed by real time-PCR. Similarly, using the Jurkat T cells, their treatment with SCZ, also affect PD-1 expression (Figure 1C). These observations indicate that PD-1 expression on T cells and PBMCs can be repressed.

To evaluate the expression of PD-1 in PBMCs and T cells at the protein level, we first treated the PMA/Io activated-Jurkat T

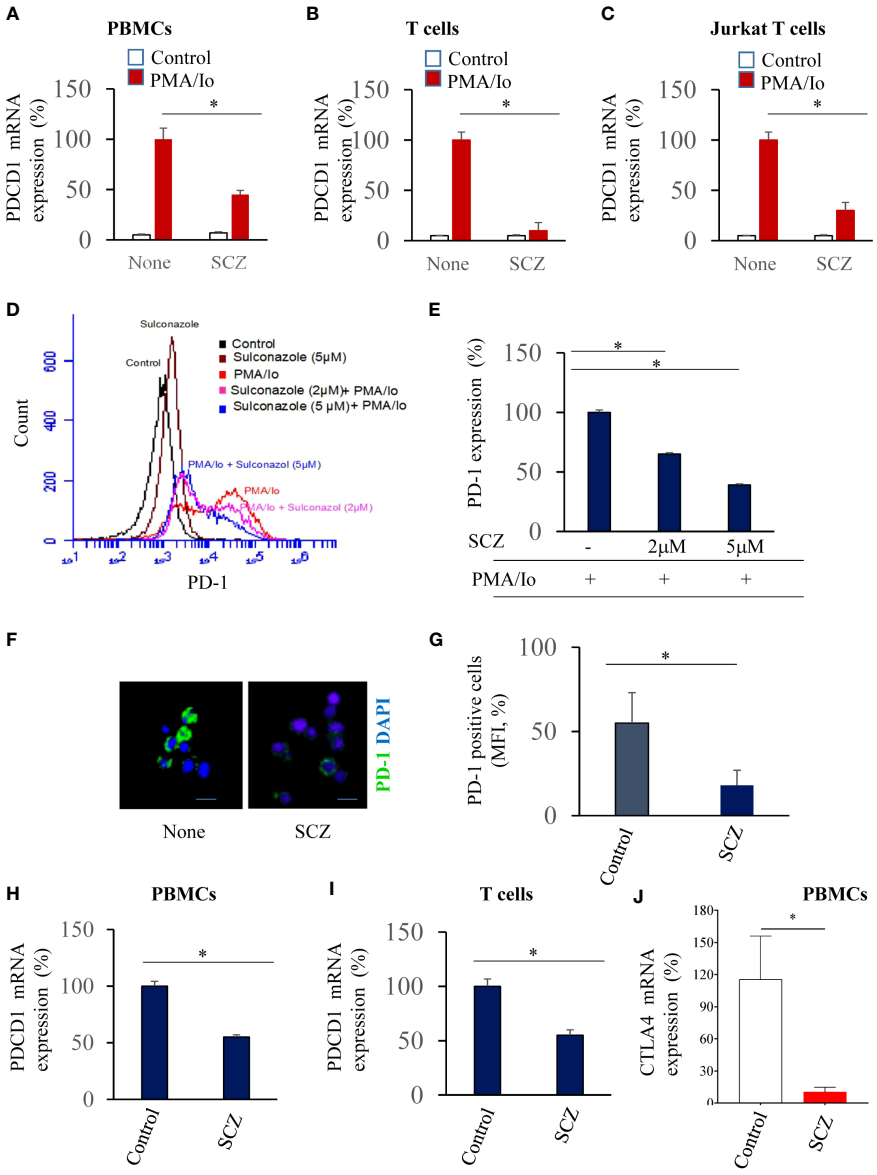

FIGURE 1
Inhibition of PDCD1 expression in PBMCs **(A)**, purified T cells **(B)** and Jurkat T cells **(C)** by Sulconazole (SCZ). PD-1 mRNA level upon PMA/Io stimulation in the absence and presence of SCZ (5µM) at 24h, assessed by real time-PCR. Data are represented as fold change to PMA/Io-stimulated cells that was assigned 100% as mean ± SEM from three independent experiments. *, $P < 0.05$. **(D, E)** Jurkat T cells were treated with indicated SCZ concentrations prior their incubation with PMA/Io. PD-1 expression was analyzed by Flow cytometry. **(F, G)** Representative confocal microscopy images of PD-1 immunostaining (green) of PMA/Io-activated Jurkat T cells in the absence and presence of SCZ. **(H, I)** PD-1 expression in PBMCs **(H)** and purified T **(I)** cells treated with SCZ prior their incubation with PMA/Io, as assesses by Flow cytometry. **(J)** CTLA-4 mRNA level upon PMA/Io stimulation in the absence and presence of SCZ (5µM) at 24h, assessed by real time-PCR. Scale bar, 10 µm. Data are represented as mean ± SEM from three independent experiments. MFI, mean fluorescence intensity (arbitrary unit). * $P < 0.05$.

cells with indicated SCZ concentrations. Flow cytometry analysis revealed that PD-1 expression is also induced at the protein level in the presence of PMA/Io that was repressed by sulconazole in a dose-dependent manner (Figures 1D, E). PD-1 expression was reduced by up to 60% with 5µM of SCZ. The use of immunofluorescence staining under these conditions confirmed that PD-1 expression was greatly decreased in the presence of sulconazole (Figures 1F, G). The use of PMA/Io-treated-PBMCs and purified T cells also revealed their reduced PD-1 expression in the presence of SCZ (Figures 1H, I). These observations indicate that SCZ can impede PD-1 expression at the RNA and protein levels in PBMCs and T cells. To evaluate whether SCZ is also able to affect the expression of other immune checkpoint inhibitors involved in T cell exhaustion, such as CTLA-4. As illustrated in Figure 1J, treatment of activated PBMCs with SCZ (5µM), significantly affected CTLA-4 expression.

3.2 Repression of NF-κB expression and calcium mobilization by sulconazole

NF-kB activation and calcium mobilization has previously been reported to be involved in PD-1 expression (17, 24). Thereby, we next investigated the effect of SCZ on these two PD-1 signaling pathways. As illustrated in Figures 2A, B incubation of Jurkat T cells at the indicated time points with PMA/Io induced NF-κB phosphorylation. Maximal stimulation was observed after 10-20 min and was downregulated after 40 min of cells stimulation. The presence of SCZ significantly reduced NF-κB activation. The inhibitory effect of SCZ was significant after 20 min and maximal after 40 min of cells incubation. These results show that SCZ represses the activation of NF-κB required for PD-1 expression. Similarly, store-operated Ca^{2+} entry (SOCE) is a mechanism for Ca^{2+} influx across the plasma membrane activated in response to depletion of intracellular Ca^{2+}

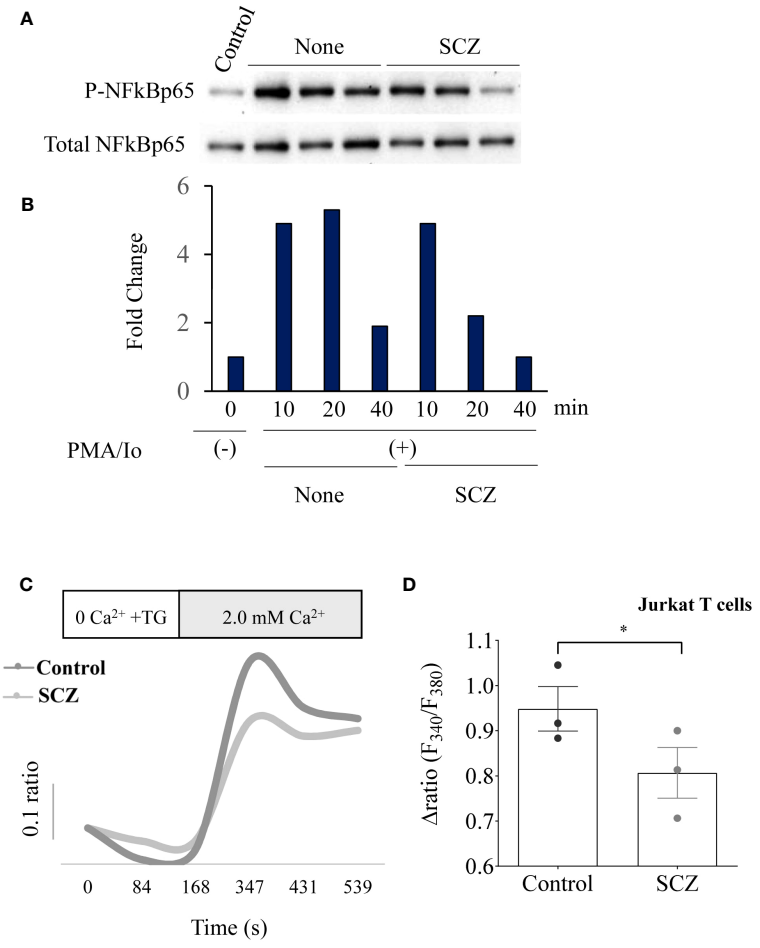

FIGURE 2
Inhibition of NF-κB phosphorylation and calcium mobilisation by Sulconazole (SCZ) in Jurkat T cells. **(A)** Jurkat T cells were treated with SCZ prior their incubation with PMA/Io and the phosphorylation of NF-κB was analyzed by western blotting at the indicated time points. **(B)** Results of NF-κB phosphorylation quantification are shown in the bar graph and calculated, as the ratio of p-NF-κB/Total NF-κB and are representative of three independent experiments. **(C)** Representative recordings of thapsigargin-induced changes in the intracellular calcium concentration expressed as fluorescence ratio (F340/F380). Jurkat cells were incubated for 4 min in a free Ca^{2+} solution in the presence of 2µM of thapsigargin and Ca^{2+} (2.0 mM) was re-added. **(D)** Bar graph shows the percentage of delta ratio increase after and before adding Ca^{2+} in cells treated with or without SCZ (10µM). Data are represented as mean ± SEM from three independent experiments. * $P < 0.05$.

10.3389/fimmu.2023.1278630

stores, mostly in the ER. To evaluate the effect of SCZ on Ca^{2+} mobilization, Jurkat T cells were incubated with sulconazole (10 µM), and Ca^{2+} levels were measured. Cells were loaded with fura-2, and then stimulated with 2 µM thapsigargin to deplete the ER and activate SOCE. As illustrated in Figures 2C, D, SCZ inhibited Ca^{2+} entry into cells. These observations, together with the finding that SCZ was able to regulate NF-κB activation, indicate SCZ ability in the repression of different pathways involved in the PD-1 expression on T cells.

3.3 Functional and survival of Jurkat T cells in the presence of sulconazole

To evaluate the effect SCZ on Jurkat T cells function, we next analyzed the expression of CD69, a T-cell activation marker, by flow cytometry to analyze antigen-TCR binding and therefore, downstream T-cell activation. Thereby we used the TCR-deficient Jurkat T cells (JRT3), expressing a specific TCR (LES) that recognizes the EPCR protein that were cocultured with EPCR-expressing HT29 cancer cells. As illustrated in Figures 3A, B the expression of CD69 was upregulated when JRT3-LES cells were cocultured with EPCR-expressing HT29 cells. Similarly, Following JRT3-LES treatment with SCZ (5µM) for 24 hours in the presence of EPCR-expressing HT29 cancer cells also strongly upregulated CD69 expression (Figures 3A, B). We next evaluated the effect of SCZ on cell survival. Thereby, T cells were incubated with SCZ in the absence and presence of serum and flow-cytometric analysis of cell death was performed using annexin V and 7AAD as markers. Flow cytometric analysis revealed that Jurkat T cells incubation with up to 5 µM SCZ had no effect on cell survival. In the absence of

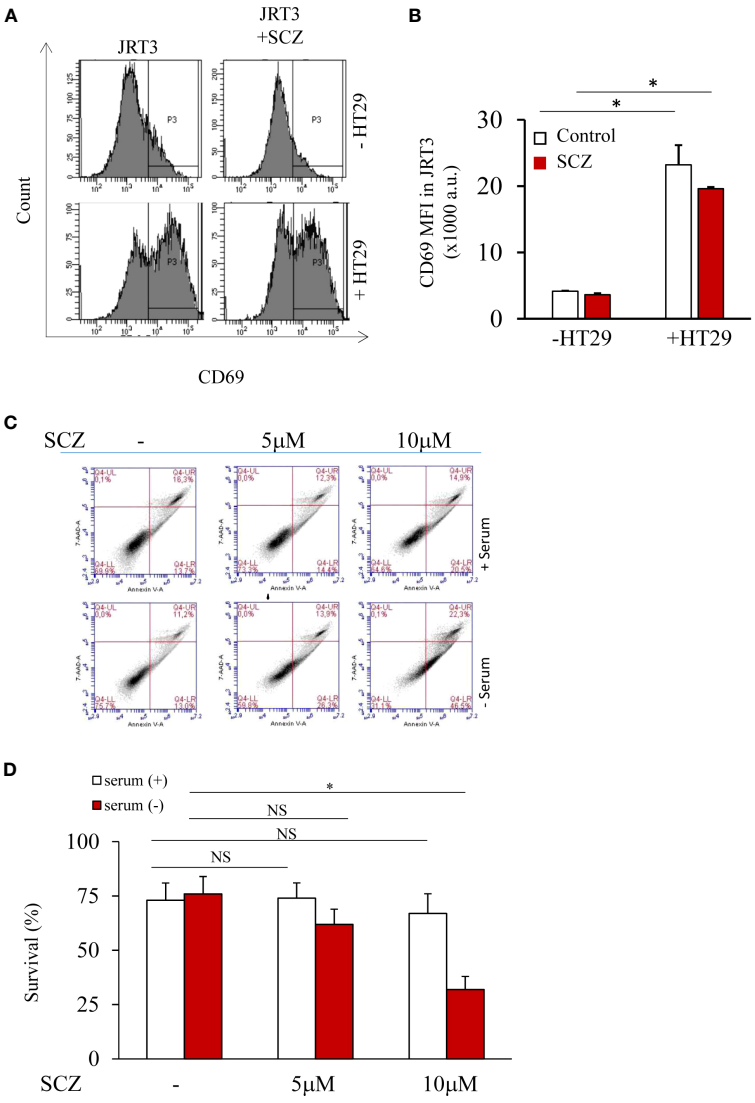

FIGURE 3
T cell activity and survival are not affected by sulconazole. **(A, B)** Flow cytometry analysis of TCR-activation marker CD69 in JRT3 cells upon binding to HT29 cancer cells in the presence and absence of SCZ **(C, D)** Fluorescence-activated cell sorter scatter plots of Jurkat T cells incubated for 24h without or with serum (5%) at indicated SCZ concentrations. After incubation, cells were double stained with annexin V and 7AAD. The use of fluorescence-activated cell sorter detected viable (negative for both dyes; lower left), early apoptotic (Annexin+/7AAD–, lower right), necrotic cells (Annexin–/7AAD+, upper left) and late apoptotic (Annexin+/7AAD+, upper right) cells. Data represented as mean ± SEM from three independent experiments. *, $P < 0.05$. NS, not significant.

serum, only the concentration of 10μM induced cell death (Figures 3C, D).

3.4 Sulconazole inhibits calcium mobilization in cancer cells

Calcium is considered as a regulator of the malignant phenotype of cancer cells, therefore, we further investigated the effects of SCZ on Ca^{2+} influx. First, the breast cancer cells MDA-MB-231 were pretreated with SCZ and then calcium signals were detected. As shown in Figures 4A, B, Ca^{2+} influx induced by thapsigargin was blocked by SCZ (10 μM). These results implied that SCZ blocked calcium mobilization, a signal pathway required for various processes required for the acquisition of the malignant phenotype of cancer cells, including cell proliferation, and migration. Further analysis revealed that the effect of SCZ on calcium mobilization is not mediated by changes in the levels of the calcium channels STIM1, ORAI1 and TRPC1, as assessed by western blotting analysis (Supplementary Figure 1).

3.5 Sulconazole inhibits cancer cell proliferation and migration

To determine the effect of SCZ on the malignant phenotype, the proliferation of several cancer cells, including the melanoma M10, the breast MD-MB231 and the colon CT-26 cancer cell lines were treated with indicated concentrations of SCZ in the presence of low (3%) and high (10%) concentration of serum and their proliferation was measured using the IncuCyte Live Cell Analysis System (Figures 5A–I). As illustrated, treatment of these cells with SCZ significantly decreased their confluence rate. The effect of SCZ was more efficient in the presence of low concentration of serum. We next evaluated the effect of SCZ on the migration of these cancer cells in a wound-healing assay. As illustrated in Figures 6A–D, treatment with SCZ for indicated time periods, reduced cancer cell motility in a concentration and time-dependent manner.

3.6 Sulconazole inhibits tumor growth in zebrafish

To directly assess the effect of SCZ on tumor growth, we used zebrafish embryos injected with MDA-MB-231 cancer cells, as *in vivo* model. Indeed, the adaptive immune system of zebrafish matures at 28 dpf (25–27). Previously, the development of T cells in zebrafish was reported to occur post 5 days post-fertilization (dpf). This temporal sequence corresponds to the infiltration of the thymus by lymphoid progenitor cells around c with subsequent egress from the thymus occurring between 6 dpf and 7 dpf, facilitating entry into the peripheral circulation (28). Thereby, multiple cancer models have been generated in zebrafish and proven similar to their human counterparts molecularly and pathologically (22, 29, 30). To assess the effect of SCZ on tumor growth we used 2 dpf zebrafish embryos to inject 500 cells/fish (25-30 fish) and allowed to grow for 48h in the absence and presence of SCZ (1μM). As shown in Figures 7A, B, the presence of SCZ in the embryo's media reduced up to ~ 4-fold time MDA-MB-231 cancer cells ability to induce tumor growth in zebrafish embryos, confirming the antitumorigenic effect of SCZ *in vivo*.

4 Discussion

The interaction between PD-1 on T cells and its ligand PDL-1 expressed on tumor cells directly affects the cytotoxic function of T cells required for cancer cells eradication (1, 6). However, the tumor

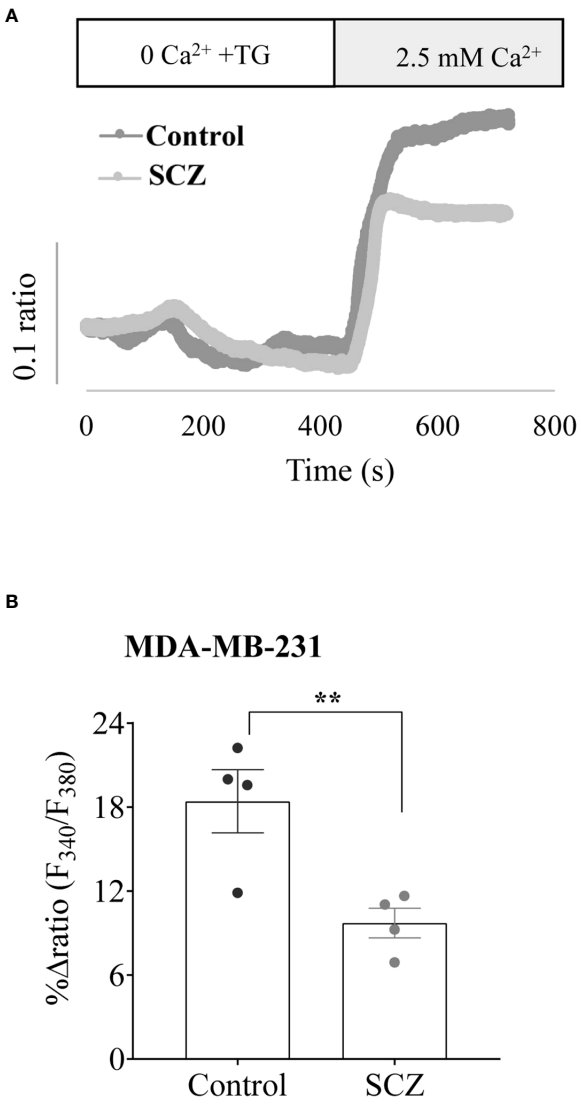

FIGURE 4
Inhibition of calcium mobilisation by Sulconazole in cancer cells. **(A)** Representative recordings of thapsigargin-induced changes in the intracellular calcium concentration expressed as fluorescence ratio (F340/F380). MDA-MB-231 cells were incubated for 4 min in a free Ca^{2+} solution in the presence of 2μM of thapsigargin and Ca^{2+} (2.5 mM) was re-added. **(B)** Bar graph shows the percentage of delta ratio increase after and before adding Ca^{2+} in cells treated with or without SCZ (10μM). Data are represented as mean ± SEM from four independent experiments.

10.3389/fimmu.2023.1278630

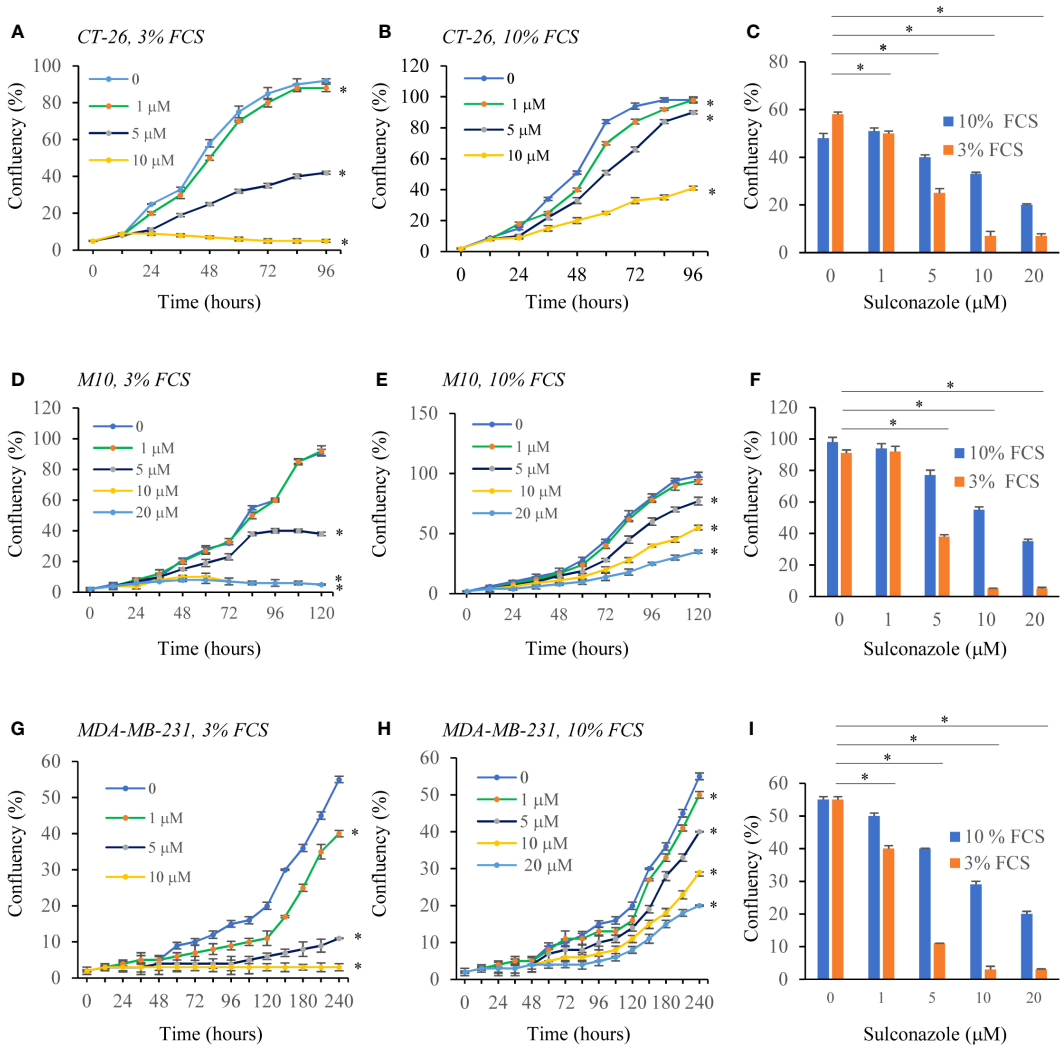

FIGURE 5
Inhibition of cancer cells proliferation by Sulconazole. colon cancer cells (CT-26) **(A–C)**, Melanoma cells M10 **(D–F)** and breast cancer cells MDA-MB-231 **(G–I)** and were plated at low confluence for time-lapse phase-contrast videomicroscopy (IncuCyte microscope) in the absence and presence of different concentrations of SCZ and serum, and cell proliferation was monitored by automated confluence analysis at set intervals after plating. Data are represented as mean ± SEM from three independent experiments (n = 6 wells per group). * $P < 0.05$.

microenvironment (TME) including the components of the extracellular matrix of various TME cells affect the expression of PD-1 on T cells leading to immune evasion. The monoclonal antibodies used to target PD-1 and PD-L1 were found to be potent immune checkpoint inhibitors and were used for various cancers treatment such as melanoma, lung cancer and gastric cancer. Indeed, since 2014, FDA has approved various anti-PD-1 and anti-PD-L1 monoclonal antibody drugs. These drugs have made serious improvement in the clinical treatment of various tumors and prolonged the survival of cancer patients. For several cancer patients, these drugs mediated complete remission. However, other patients with solid tumors, including colorectal cancers [except the microsatellite-instable (MSI) subset] are refractory to these treatments (6, 8).

The failure to respond to anti-PD-1 drug is mainly due to the presence of irreversibly exhausted T cells. In addition, various adverse responses are mediated by these inhibitors that are mainly immune-related adverse reactions found to affect several tissues and organs of the treated patients (31, 32). Other studies also showed that it is difficult for antibody drugs to successfully infiltrate tumor tissues and reach all areas of the tumor microenvironment in order to be accumulated at an adequate and efficient concentration (17). Other studies revealed that the efficacy of these drugs can be reduced with time and was linked to their immunogenicity that induces the production of anti-antibodies during the treatment (32). Therefore, it is necessary to develop novel inhibitors such as small molecules with confirmed efficacy and safety to target the PD-1/PD-L1 interaction. Indeed, compared to monoclonal antibodies that are difficult to produce, small molecule present various advantages to make them promising for clinical treatments (33). Small molecule inhibitors are more appropriate for oral management, and can be used to avoid immune-related adverse effects due to the facility of their changeable half-life. In this study, we demonstrate that SCZ is able to repressses the expression of PD-1

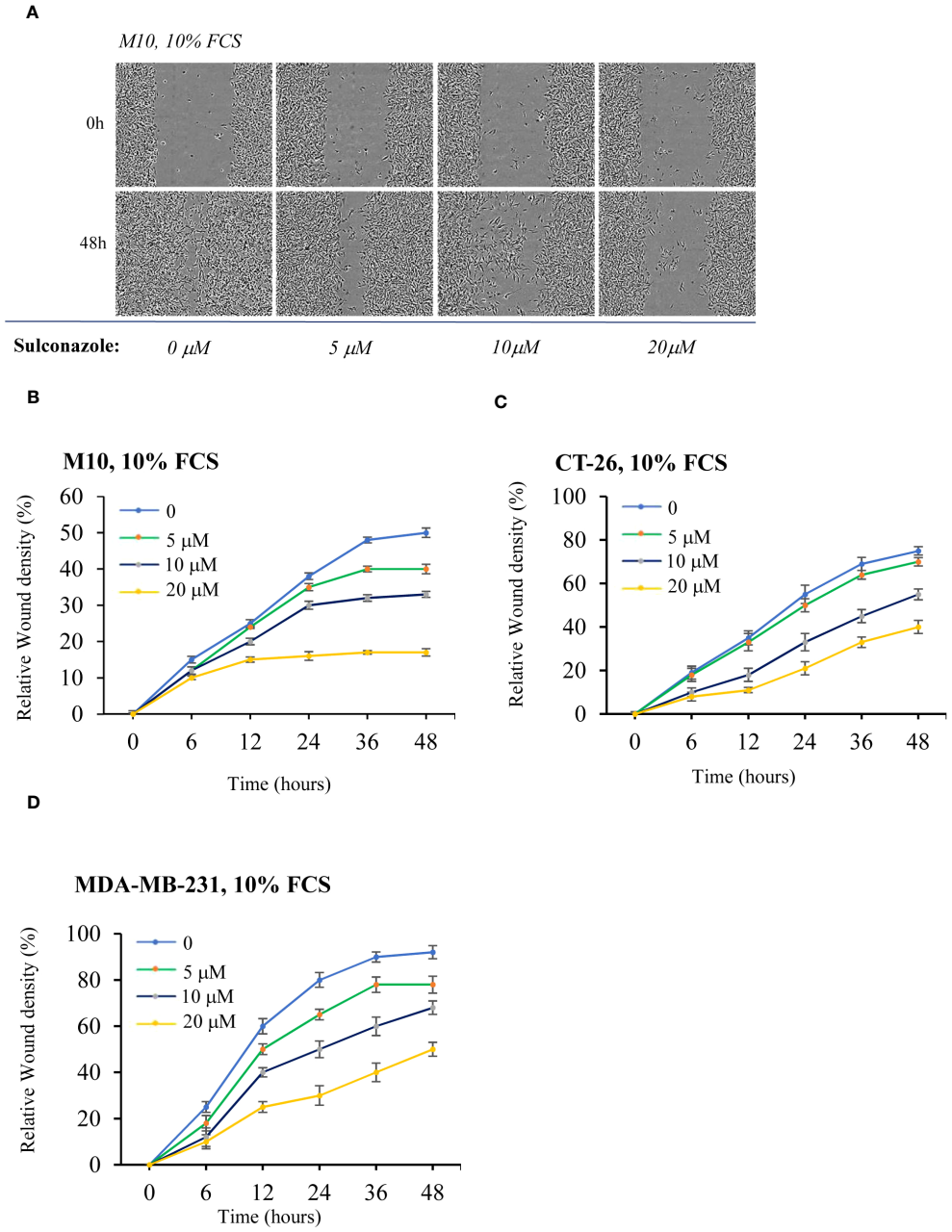

FIGURE 6
Inhibition of cancer cells migration by Sulconazole. **(A–D)** cancer cell migration was analyzed by scratch wound assay. M10 **(A, B)** CT-26) **(C)**, and MDA-MB-231 **(D)** cells were treated with various SCZ concentrations and were subjected to scratch wounds and imaged using IncuCyte microscope during 48h (*n* = 6 wells per group, 3 independent experiments). **(B–D)** Quantification of wound closure during indicated time periods. Data are represented as mean ± SEM.

on T cells and PBMCs and reduces cancer proliferation, migration and tumor growth *in vivo* using zebrafish embryos model.

Previously, NF-κB and calcium signaling pathways were reported to be required for PD-1 expression on T cells (17). We found that SCZ inhibited these pathways and thereby linking PD-1 repression by SCZ in T cells to NF-κB activity and calcium mobilization inhibition. Further analysis revealed that SCZ is also able to repress CTLA-4 expression in PBMCs. Our results identified SCZ, as small not toxic molecule medicine that may constitute a starting point for the identification of new class of immune checkpoint inhibitor regulators that will have the chance to be used at the clinical setting since their none toxicity was previously established. Indeed, current preclinical studies revealed that small molecule compounds have a better capability than antibodies to repress tumor growth progression (25), suggesting their use to overcome the existing problems of antibody drugs and allow them to replace monoclonal antibodies or serve as complementary therapies.

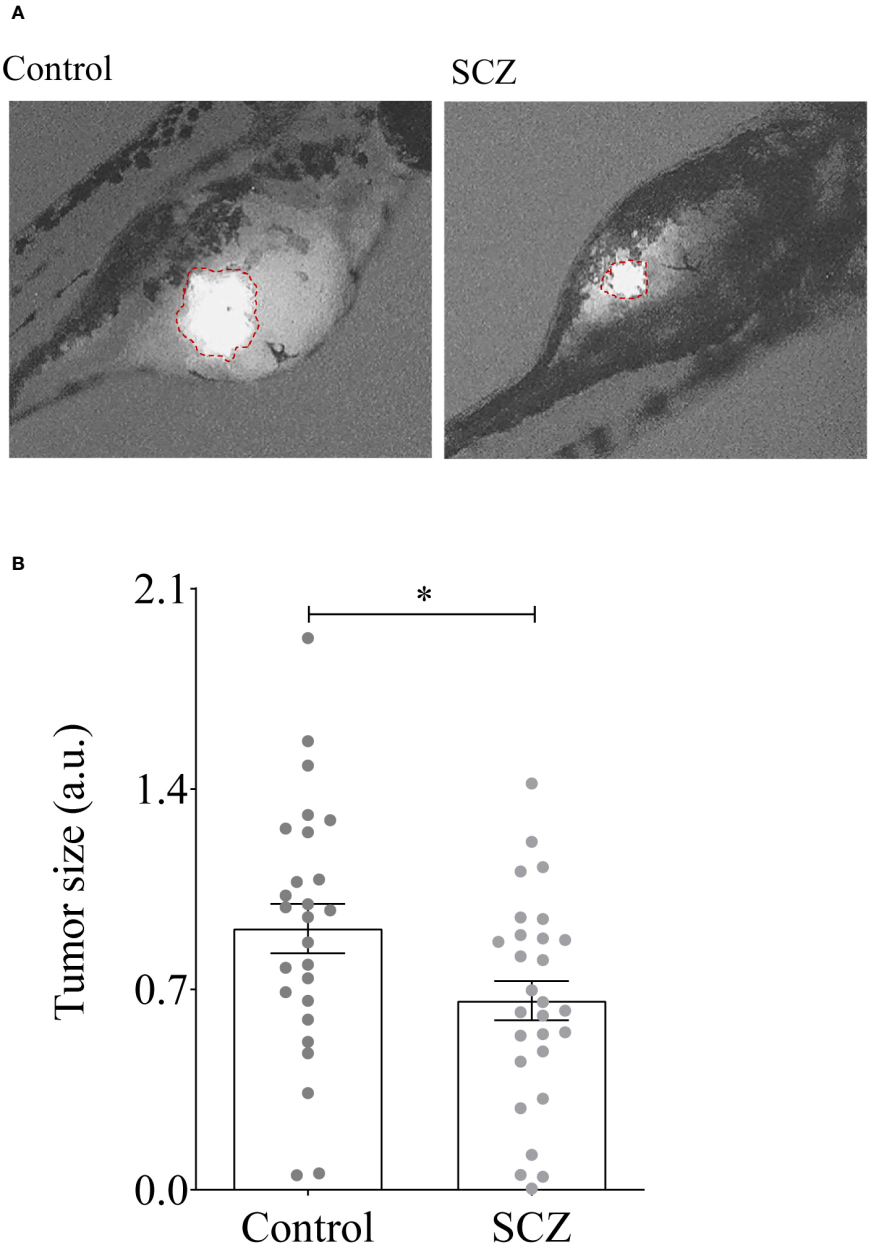

FIGURE 7
Inhibition of tumor growth by Sulconazole. **(A, B)** MDA-MB-231 cells (500) were injected above the duct of Cuvier in perivitelline space of the embryos and SCZ (1 µM) or vehicle (DMSO) were added to embryo E3 medium. Tumor imaging was performed after 48-h post injection. Results are representative of 4 experiments. Values are mean ± SEM (n = 25-30 per group). *$P < 0.05$.

5 Conclusions

Innovative pharmacological methods are needed to improve treatments of advanced cancers, regardless of the considerable benefit of immunotherapy. Indeed, new drugs are needed for to complement the used monoclonal antibodies to target PD-1 and/or PD-L1 immune checkpoint proteins. Here, we have identified SCZ a known antifungal drug which could reinforce immunotherapy based on their capacity to modulate PD-1 expression. We revealed that SCZ repress PD-1 expression on activated T cells through NFκB and calcium mobilization inactivation. It will be of additional interest to explore whether SCZ induces T cells infiltration in tumors and mediates synergic effect with the current immunotherapy.

Data availability statement

The raw data supporting the conclusions of this article will be made available by the authors, without undue reservation.

Ethics statement

The studies involving humans were approved by Bergonié Institute (Bordeaux, France). The studies were conducted in accordance with the local legislation and institutional requirements. The human samples used in this study were acquired from a by-product of routine care or industry. Written informed consent for participation was not required from the participants or the participants' legal guardians/next of kin in accordance with the national legislation and institutional requirements.

Author contributions

SP: Conceptualization, Methodology, Writing – original draft. MT: Conceptualization, Investigation, Methodology, Writing – review & editing. IG: Conceptualization, Methodology, Writing – original draft. SE: Conceptualization, Methodology, Writing – original draft. IB: Formal analysis, Writing – review & editing. FD: Investigation, Methodology, Writing – review & editing. DF: Writing – review & editing. TS: Investigation, Methodology, Writing – original draft, Writing – review & editing. GS: Investigation, Methodology, Writing – original draft, Writing – review & editing. BV: Conceptualization, Writing – original draft, Writing – review & editing. A-MK: Conceptualization, Funding acquisition, Methodology, Supervision, Writing – original draft, Writing – review & editing.

Funding

The author(s) declare financial support was received for the research, authorship, and/or publication of this article. This research was funded by La Region Nouvelle Aquitaine, Planet Vegetal, Ligue Contre le cancer and INSERM.

Acknowledgments

We thank Dr Angela Pappalardo for technical advices and assistance.

Conflict of interest

The authors declare that the research was conducted in the absence of any commercial or financial relationships that could be construed as a potential conflict of interest.

Publisher's note

Supplementary material

The Supplementary Material for this article can be found online at: https://www.frontiersin.org/articles/10.3389/fimmu.2023.1278630/full#supplementary-material

References

1. du Rusquec P, de Calbiac O, Robert M, Campone M, Frenel JS. Clinical utility of pembrolizumab in the management of advanced solid tumors: an evidence-based review on the emerging new data. *Cancer Manag Res* (2019) 11:4297–312. doi: 10.2147/CMAR.S151023

2. Inokuchi J, Eto M. Profile of pembrolizumab in the treatment of patients with unresectable or metastatic urothelial carcinoma. *Cancer Manag Res* (2019) 11:4519–28. doi: 10.2147/CMAR.S167708

3. Nakamura Y. Biomarkers for immune checkpoint inhibitor-mediated tumor response and adverse events. *Front Med (Lausanne)* (2019) 6:119. doi: 10.3389/fmed.2019.00119

4. Ishida Y, Agata Y, Shibahara K, Honjo T. Induced expression of PD-1, a novel member of the immunoglobulin gene superfamily, upon programmed cell death. *EMBO J* (1992) 11:3887–95. doi: 10.1002/j.1460-2075.1992.tb05481.x

5. Latchman Y, Wood CR, Chernova T, Chaudhary D, Borde M, Chernova I, et al. PD-L2 is a second ligand for PD-1 and inhibits T cell activation. *Nat Immunol* (2001) 2:261–8. doi: 10.1038/85330

6. Okazaki T, Honjo T. PD-1 and PD-1 ligands: from discovery to clinical application. *Int Immunol* (2007) 19:813–24. doi: 10.1093/intimm/dxm057

7. Iwai Y, Hamanishi J, Chamoto K, Honjo T. Cancer immunotherapies targeting the PD-1 signaling pathway. *J BioMed Sci* (2017) 24:26. doi: 10.1186/s12929-017-0329-9

8. Postow MA. Managing immune checkpoint-blocking antibody side effects. *Am Soc Clin Oncol Educ Book* (2015) 35:76–83. doi: 10.14694/EdBook_AM.2015.35.76

9. Rani N, Sharma A, Gupta GK, Singh R. Imidazoles as potential antifungal agents: a review. *Mini Rev Med Chem* (2013) 13:1626–55. doi: 10.2174/13895575113139990069

10. Sheets JJ, Mason JI, Wise CA, Estabrook RW. Inhibition of rat liver microsomal cytochrome P-450 steroid hydroxylase reactions by imidazole antimycotic agents. *Biochem Pharmacol* (1986) 35:487–91. doi: 10.1016/0006-2952(86)90224-8

11. Katz HI. Drug interactions of the newer oral antifungal agents. *Br J Dermatol* (1999) 141 Suppl 56:26–32. doi: 10.1046/j.1365-2133.1999.00011.x

12. Maurice M, Pichard L, Daujat M, Fabre I, Joyeux H, Domergue J, et al. Effects of imidazole derivatives on cytochromes P450 from human hepatocytes in primary culture. *FASEB J* (1992) 6:752–8. doi: 10.1096/fasebj.6.2.1371482

13. Bae SH, Park JH, Choi HG, Kim H, Kim SH. Imidazole antifungal drugs inhibit the cell proliferation and invasion of human breast cancer cells. *Biomol Ther (Seoul)* (2018) 26:494–502. doi: 10.4062/biomolther.2018.042

14. Benfield P, Clissold SP. Sulconazole. A review of its antimicrobial activity and therapeutic use in superficial dermatomycoses. *Drugs* (1988) 35:143–53. doi: 10.2165/00003495-198835020-00004

15. Gugnani HC, Gugnani A, Malachy O. Sulconazole in the therapy of dermatomycoses in Nigeria. *Mycoses* (1997) 40:139–41. doi: 10.1111/j.1439-0507.1997.tb00203.x

16. Hercelin B, Delaunay-Vantrou M, Alamichel F, Mazza M, Marty JP. Pharmacokinetics of cutaneous Sulconazole nitrate in the hairless rat: absorption, excretion, tissue concentrations. *Eur J Drug Metab Pharmacokinet* (1993) 18:149–54. doi: 10.1007/BF03188789

17. Tomé M, Pappalardo A, Soulet F, López JJ, Olaizola J, Leger Y, et al. Inactivation of proprotein convertases in T cells inhibits PD-1 expression and creates a favorable immune microenvironment in colorectal cancer. *Cancer Res* (2019) 79:5008–21. doi: 10.1158/0008-5472.CAN-19-0086

18. He Z, Khatib A-M, Creemers JWM. Loss of the proprotein convertase Furin in T cells represses mammary tumorigenesis in oncogene-driven triple negative breast cancer. *Cancer Lett* (2020) 484:40–9. doi: 10.1016/j.canlet.2020.05.001

19. Scamuffa N, Siegfried G, Bontemps Y, Ma L, Basak A, Cherel G, et al. Selective inhibition of proprotein convertases represses the metastatic potential of human colorectal tumor cells. *J Clin Invest* (2008) 118:352–63. doi: 10.1172/JCI32040

20. Ma J, Evrard S, Badiola I, Siegfried G, Khatib A-M. Regulation of the proprotein convertases expression and activity during regenerative angiogenesis: Role of hypoxia-inducible factor (HIF). *Eur J Cell Biol* (2017) 96:457–68. doi: 10.1016/j.ejcb.2017.06.001

21. Hagedorn M, Siegfried G, Hooks KB, Khatib A-M. Integration of zebrafish fin regeneration genes with expression data of human tumors in silico uncovers potential novel melanoma markers. *Oncotarget* (2016) 7:71567–79. doi: 10.18632/oncotarget.12257

22. Gounou C, Bouvet F, Liet B, Prouzet-Mauléon V, d'Agata L, Harté E, et al. Annexin-A5 and annexin-A6 silencing prevents metastasis of breast cancer cells in zebrafish. *Biol Cell* (2023) 115:e202200110. doi: 10.1111/boc.202200110

23. Salerno F, Paolini NA, Stark R, von Lindern M, Wolkers MC. Distinct PKC-mediated posttranscriptional events set cytokine production kinetics in CD8+ T cells. *Proc Natl Acad Sci U.S.A.* (2017) 114:9677–82. doi: 10.1073/pnas.1704227114

24. Bally APR, Lu P, Tang Y, Austin JW, Scharer CD, Ahmed R, et al. NF-κB regulates PD-1 expression in macrophages. *J Immunol* (2015) 194:4545–54. doi: 10.4049/jimmunol.1402550

25. Lam SH, Chua HL, Gong Z, Lam TJ, Sin YM. Development and maturation of the immune system in zebrafish, Danio rerio: a gene expression profiling, *in situ* hybridization and immunological study. *Dev Comp Immunol* (2004) 28:9–28. doi: 10.1016/s0145-305x(03)00103-4

26. Langenau DM, Ferrando AA, Traver D, Kutok JL, Hezel J-PD, Kanki JP, et al. *In vivo* tracking of T cell development, ablation, and engraftment in transgenic zebrafish. *Proc Natl Acad Sci U.S.A.* (2004) 101:7369–74. doi: 10.1073/pnas.0402248101

27. Nicoli S, Ribatti D, Cotelli F, Presta M. Mammalian tumor xenografts induce neovascularization in zebrafish embryos. *Cancer Res* (2007) 67:2927–31. doi: 10.1158/0008-5472.CAN-06-4268

28. Bajoghli B, Dick AM, Claasen A, Doll L, Aghaallaei N. Zebrafish and medaka: two teleost models of T-cell and thymic development. *Int J Mol Sci* (2019) 20:4179. doi: 10.3390/ijms20174179

29. Blackburn JS, Langenau DM. Zebrafish as a model to assess cancer heterogeneity, progression and relapse. *Dis Model Mech* (2014) 7:755–62. doi: 10.1242/dmm.015842

30. Kobar K, Collett K, Prykhozhij SV, Berman JN. Zebrafish cancer predisposition models. *Front Cell Dev Biol* (2021) 9. doi: 10.3389/fcell.2021.660069

31. Su C, Wang H, Liu Y, Guo Q, Zhang L, Li J, et al. Adverse effects of anti-PD-1/PD-L1 therapy in non-small cell lung cancer. *Front Oncol* (2020) 10:554313. doi: 10.3389/fonc.2020.554313

32. Naidoo J, Page DB, Li BT, Connell LC, Schindler K, Lacouture ME, et al. Toxicities of the anti-PD-1 and anti-PD-L1 immune checkpoint antibodies. *Ann Oncol* (2015) 26:2375–91. doi: 10.1093/annonc/mdv383

33. Chen S, Lee L-F, Fisher TS, Jessen B, Elliott M, Evering W, et al. Combination of 4-1BB agonist and PD-1 antagonist promotes antitumor effector/memory CD8 T cells in a poorly immunogenic tumor model. *Cancer Immunol Res* (2015) 3:149–60. doi: 10.1158/2326-6066.CIR-14-0118

frontiers | Frontiers in Oncology

TYPE Original Research
PUBLISHED 16 February 2024
DOI 10.3389/fonc.2024.1335344

OPEN ACCESS

EDITED BY
Alma D. Campos-Parra,
Universidad Veracruzana, Mexico

REVIEWED BY
Giovanni Rosti,
San Matteo Hospital Foundation (IRCCS), Italy
Oscar Medina-Contreras,
Mexico Children's Hospital, Mexico

*CORRESPONDENCE
Miguel Angel Seguí
masegui@gmail.com

RECEIVED 11 December 2023
ACCEPTED 12 January 2024
PUBLISHED 16 February 2024

CITATION
Villegas E, Arruñada M, Casado MÁ, González S, Moreno-Martínez ME, Peñuelas MÁ, Torres AM, Sierra Y and Seguí MA (2024) National expert consensus on home-administered oncologic therapies in Spain. *Front. Oncol.* 14:1335344. doi: 10.3389/fonc.2024.1335344

National expert consensus on home-administered oncologic therapies in Spain

Eulalia Villegas[1], María Arruñada[2], Miguel Ángel Casado[2], Sonia González[3,4,5], María Estela Moreno-Martínez[6], María Ángeles Peñuelas[7], Ana Maria Torres[1], Yanik Sierra[8] and Miguel Angel Seguí[9,10]*

[1]Dos de Maig Hospital, Barcelona, Spain, [2]Pharmacoeconomics & Outcomes Research Iberia (PORIB), Madrid, Spain, [3]Innovation in Clinical Pharmacy Research Group (i-FARMA-Vigo), Vigo, Spain, [4]Galicia Sur Health Research Institute (IIS Galicia Sur), Vigo, Spain, [5]University Hospital Complex of Vigo (SERGAS-UVIGO), Vigo, Spain, [6]Pharmacy Service, de la Sant a Creu i Sant Pau Hospital, Barcelona, Spain, [7]Vall d'Hebron University Hospital, Barcelona, Spain, [8]Eisai Farmaceutica SA, Madrid, Spain, [9]Parc Taulí Foundation, Barcelona, Spain, [10]Autonomous University of Barcelona, Barcelona, Spain

The diagnosis and treatment of cancer impose a significant emotional and psychological burden on patients, families, and caregivers. Patients undergo several interventions in a hospital setting, and the increasing number of patients requiring extended care and follow-up is driving the demand for additional clinical resources to address their needs. Hospital at Home (HaH) teams have introduced home-administered oncologic therapies that represent a new model of patient-centered cancer care. This approach can be integrated with traditional models and offers benefits to both patients and healthcare professionals (HCPs). Home-administered treatment programs have been successfully piloted globally, demonstrated as a preferred option for most patients and a safe alternative that could reduce costs and hospital burden. The document aims to establish the minimum recommendations for the home administration of oncologic therapies (ODAH) based on a national expert agreement. The expert panel comprised seven leading members from diverse Spanish societies and three working areas: clinical and healthcare issues, logistical and administrative issues, and economic, social, and legal issues. The recommendations outlined in this article were obtained after a comprehensive literature review and thorough discussions. This document may serve as a basis for the future development of home-administered oncologic therapy programs in Spain.

KEYWORDS

oncology, home administration, expert recommendations, quality of life, oncology therapies

1 Introduction

Cancer remains a major global health problem despite scientific efforts in the development of new therapies (1, 2). According to GLOBOCAN data, 19.3 million new cases and 10 million cancer deaths were reported in 2020 worldwide, and a 47% increase in new cases will occur in 2040 if the current rates remain constant (3). In Spain, 277,394 new cases were diagnosed in 2020, currently being the second cause of death and accounting for 22.2% of total deceases (109,706 cancer deaths). According to Spanish Network of Cancer Registries (REDECAN) data, 280,100 newly diagnosed patients are expected by the end of 2022 (4).

Patients with cancer undergo multiple interventions, typically performed within a hospital setting that provides the requisite logistical resources. The reliance on the hospital environment has been amplified by the necessity for a multidisciplinary team of healthcare professionals (HCPs) and the development and deployment of new technologies for diagnosis and treatment. Nevertheless, the COVID-19 pandemic has had adverse effects in various routine clinical procedures due to hospital saturation, insufficient resources, and recommended restrictions aimed at reducing the risk of infection (5–7). Consequently, the regular activity of the oncology units was affected (6, 7). A meta-analysis reported a reduction in general clinical activity in 58% of the centers worldwide during the first wave (6). Frequently, treatment delay or cancellation, change in treatment plans, and delay in outpatient visits (in 58%, 65%, and 75% of centers, respectively) were registered, and many centers (72%) implemented virtual visits (6).

Hospital at Home Service (HaH) is hospital-level substitutive care delivered at home for acute patients who required hospital admission. HaH has been associated with several advantages, including patient safety, reduction of nosocomial complications, similar or even better health outcomes compared to conventional hospitalization, high satisfaction levels from both patients and caregivers, and cost savings (8, 9).

HaH teams are trained to perform complex interventions at home, which would reduce the hospital burden preventing the negative consequences of this overload on cancer patients (10–13). Moreover, treating cancer patients at home can help to control high-risk situations such as the exposure to epidemics of multidrug-resistant pathogens or community viral infections with high morbidity and mortality (14).

Despite the growing interest, the available literature exploring the possibilities and benefits of oncologic drug administration at home (ODAH) and supportive care treatments in oncology patients is still limited and controversial, especially in Spain. The aim of the present document is to establish the minimum recommendations for an ODAH based on a national expert consensus. It should be noted that in the present document this setting refers to all healthcare-related procedures coordinated by a multidisciplinary group of HCPs that attend to the diagnostic and therapeutic needs of selected oncology patients at their homes. This home-based care is a complementary element of the protocol designed for those patients and, thus, it must be integrated as part of it. Due to their singularities, pediatric oncologic patients and those with haemato-oncologic diseases are not considered in the elaboration of this recommendations.

2 Materials and methods

2.1 Expert selection and panel composition

The panel of experts was multidisciplinary and included seven professionals from Madrid, Barcelona and Vigo involved in cancer treatment and who belong to diverse scientific societies: SEFH (Spanish Society of Hospital Pharmacy), SEHAD (Spanish Society of Home Hospitalization), SEEO (Spanish Oncology Nursing Society), and SEOM (Spanish Society of Medical Oncology). The panel included experts in the field of oncology, nursing, HaH, hospital pharmacy, and health economics. Three working areas were defined: 1) clinical and healthcare issues, 2) logistical and administrative issues, and 3) economic, social, and legal issues. Experts were assigned to a working group according to their knowledge and expertise (Supplementary Table 1).

2.2 Literature screening and questions formulation

A series of relevant questions for each section were prepared (see Supplementary Table 2). The experts reviewed the literature and provided individual responses, but a systematic review was not conducted. The working group then deliberated on the responses and arrived at a consensus on the recommendations. The decisions were primarily guided by expert opinions and were reinforced by the existing literature. In instances where evidence was lacking, only expert opinions were taken into account.

2.3 Consensus meeting and agreement

The consensus meeting took place on November 16th, 2022. The recommendations of each working group were presented to all experts and discussed in the meeting to reach a final agreement. The present recommendations are presented in question-answer format and have been endorsed by all participants. The role and functions of the main stakeholders involved in home administration of oncologic therapies were defined and summarized in Supplementary Table 3.

3 Results

3.1 Section 1: clinical and healthcare issues

When considering the feasibility of a home-based oncology treatment program, it is important to take into account various factors related to the oncology drug, therapy, patient characteristics, and healthcare environment.

3.1.1 Item A. Related to drug/therapy

Question 1. Which drugs are potentially suitable for home administration?

When planning a home-based oncology treatment program, it is important to consider the pharmaceutical and clinical

characteristics of the administered treatment, including its posology, stability, route and duration of administration, and safety profile. Most articles describing ODAH focus on parenterally administered treatments, with oral medications not typically considered as home-administered chemotherapy (12, 15). Oncologic therapies that have a non-complex administration protocol and a known and manageable safety profile are good candidates for home-base administration (15). The duration of chemotherapy treatment typically varies from two to eight months, and shorter administration times are generally preferable to longer ones (16). Prolonged home-administered therapy, especially if it requires the presence of a nurse throughout the entire procedure, can result in a waste of resources for hospitals and increase costs (15, 17, 18). According to published initiatives, the infusion duration of home-administered drugs usually took less than four hours (15). Moreover, guaranteeing drug stability for its administration at home is essential to ensure the best treatment for the patient (19).

An indicative list of oncologic drugs that can potentially be administered at home is presented in Table 1, although there is significant variability in the types of antineoplastic drugs used in home-based therapy programs (12, 15, 20–22).

TABLE 1 Potential oncologic treatments for home administration.

Drug	Posology	Ad. route	Premedication
5-Fluorouracil	15 mg/kg or 600 mg/m^2 once a week (initial treatment) *	IV	None
Eribulin	1.23 mg/m^2 (days 1 and 8 every 21-day cycle)	IV	None
Methotrexate	single doses ranged 20-40 mg (10-20 ml)/m^2 BSA*	IM/SC	None
Nivolumab	240 mg/2 weeks (~30 min) * 480 mg/4 weeks (~60 min) *	IV (not push or bolus)	None
Pembrolizumab	200 mg/3 weeks 400 mg/6 weeks	IV	Antiemetics
Pemetrexed	500 mg/m^2 BSA*	IV	Corticosteroids
Pertuzumab	Initial dose of 840 mg (~60 min) Maintenance dose 420 mg/3 weeks (~30-60 min)	IV	None
Trabectidin	1,5 mg/m2 BSA (over 24 h, 3-week interval between cycles) *	IV	None
Trastuzumab	Dose and regimen depend on indication (weekly or 3-weekly schedules)	IV (not bolus)/ SC	None

BSA, body surface area; EPOCH, etoposide, vincristine, doxorubicin, cyclophosphamide, and prednisone; IM, intramuscular; IV, intravenous; SC, subcutaneous.
*Dose and regimen may depend on indication, patient's condition, or previous/concomitant treatment.

3.1.2 Item B. Related to patients

Question 2. What profile of patients would benefit from oncology treatment administered at home?

Eligibility criteria for ODAH is crucial to maintain the safety and should be based on patient and caregiver readiness, diagnosis, characteristics and co-morbidities, treatment regimen, and hospital proximity and home environment (Table 2) (15, 16). Inclusion criteria should be related to the clinical and physical state, cancer type and grade, and type of treatment. External factors, such as the distance to the hospital, presence of a caregiver/relative and housing conditions should also be assessed by a multidisciplinary team of HCPs (16).

3.1.3 Item C. Related to healthcare settings

Question 3. How would ODAH compromise the efficacy, safety, and quality of life of systemic treatments?

Research has shown that home-administered oncology treatment can be just as effective and safe as hospital-administered treatment and may lead to improvements in quality of life and patient satisfaction (12, 15, 16). Recently, a systematic review found that ODAH presented no statistically significant differences in quality of life compared to hospital administered setting (12, 23). Safety data showed that toxicities were expected regardless of the location of administration. In Spain, a randomized controlled trial comparing home-based chemotherapy to hospital treatment revealed higher satisfaction with home-based administration in terms of the perception of nursing availability and communication (24). Another systematic review, exploring the advantages of home chemotherapy pointed that the results obtained in several trials sustained that treatment administration at home was safe and feasible, and preferred by patients and caregivers (25).

However, some clinicians may still have concerns about patient safety (26), but the appropriate preparation and education can help ensure the safety of the procedure (16). Patients and caregivers should receive educational and supporting material that explains the program implications in simple and easy-to-understand vocabulary. Periodic satisfaction surveys can also help to monitor the patient experience and identify areas for improvement. Also, further research is needed to compare the efficacy, safety, and quality of home-administered therapy to hospital treatment.

Question 4. **What kind of education, accreditation or training should receive the HCPs involved?**

Oncology, HaH and Pharmacy Services must be coordinated for drug prescription, validation, evaluation of the clinical state before drug administration, detection of adverse events, and patient follow-up. Therefore, an interdisciplinary group of HCPs with defined responsibilities is required along with specialized education and training (15, 27).

Furthermore, antineoplastic drug administration is a complex procedure that must be performed by a qualified professional to avoid undesirable incidents (28–31). Specialized nurses are responsible for the chemotherapy and biotherapy administration, and they have specific education and training that ensure the safe care of the patient (28, 32).

TABLE 2 Recommended inclusion and exclusion criteria to select the most adequate patients for home-administered chemotherapy.

Inclusion criteria	Exclusion criteria
Diagnosis of oncological disease requiring systemic treatment.	Lack of availability or capacity of the HaH to undertake the procedure.
Patient of legal age and with capacity to make autonomous decisions.	Severe delayed toxicity associated with treatment or prior requirement for medical attention.
Explicit acceptance of the on-home administration care resource by the patient or his/her legal guardian.	Clinical instability that limits the procedure.
Geographical area within the responsibility of HaH.	Pharmacological treatments with risk of drug-drug interaction after assessing that is a threat to the patient.
Previous administration of medication in the hospital centre without serious adverse reactions.	Inclusion in a clinical trial.
1-3 treatment cycles without incident.*	Patients with risky behavioural alterations.
General clinical stability with no evidence of acute intercurrent conditions.	Unhealthy or unsanitary conditions at home.
Mobility problems or severe functional disability that makes movement difficult.	
Difficulty of the patient to reconcile work or family life in attending the Day Hospital.	
Comorbidities that make access to the Day Hospital difficult or inadvisable.	
Accompaniment of the patient during the intervention.	
Existence of a trained primary caregiver and its compliance in case of disabilities.	
Availability for telephone communication or teleassistance.	

*The minimum number of cycles it will depend on the selected drug and individual patient evaluation.

Implementing this strategy will typically necessitate the establishment of specialized teams dedicated to administering antineoplastic treatments in patients' homes. While it is feasible to utilize home hospitalization resources or hospital nursing to a certain extent, this approach generally entails a greater demand for human and material resources.

Question 5. What kind of controls should be performed?

Experts suggest and agree that certain minimum requirements must be met by the hospital when considering a ODAH program: 1) to have a Medical Oncology Service; 2) to have a territorial/regional HaH Service; 3) to have a Pharmacy Service that ensures the highest quality of care for patients; 4) to be provided with minimum healthcare resources in the units and available involved Services; and 5) to perform a demographic and geographic evaluation of the healthcare area.

An initial pilot program should be set up to evaluate the results and determine the compliance of requirements. Standardized approaches and procedures, along with interdisciplinary professional review, can help avoid medication mistakes (28–30). An indicative checklist is provided in Table 3 and a standardized nurse visit is shown in Supplementary Figure 1.

Question 6. What would be the minimum instruments, apparatus or equipment required?

Table 4 includes a list of materials to be considered for an ODAH program. The minimum required material will depend on the therapy and clinical state of the patient (18).

Question 7. Which aspects should be considered for drug preparation?

To ensure the best treatment for the patient, it is crucial to maintain drug stability during home delivery. This requires a review of all factors involved in drug preparation and transport, and the implementation of protocols and controls to assess drug stability for optimal implementation of a home-based therapy program (19).

3.1.4 Recommendations of the experts panel for the section 1

Table 5 contains the agreed recommendations made by the panel of experts regarding clinical and healthcare issues section.

3.2 Section 2: logistical and administrative issues

Question 8. To consider the ODAH, what are the requirements that must be fulfilled by the oncology department/hospital?

Simplifying the patient's journey and ensuring the availability of necessary resources and adherence to schedules and processes is crucial. This can be achieved by developing agreed protocols and plans that outline all the steps, stakeholders, and professionals

TABLE 3 Checklist of the optimal steps to perform the ODAH.

Time point	To check/perform:
Before administration	- Clinical state (diagnosis and treatment scheme) - Prescribed medication (antineoplastics, concomitant, premedication). * - Patient medical record (allergies, comorbidities, venous accesses, etc). - Need of previous medical controls. - Administration system required. - Patient's identity. - Administration scheme.
During administration	- Assure patient's identity and administration scheme. - Periodically check the adverse events and administration route state. - Clinical and hemodynamic stability. - Ask about previous tolerance to treatment. - Give recommendations about toxicity.
After administration	- Venous/cutaneous state (e.g., ensure for no extravasation). - Healing/catheter registration. - Ensure the patient understand the recommendations for toxicities detection. - Register necessary information in the medical record. - Adequate medical waste disposal.

*Verification by at least two health-care professionals.

TABLE 4 Basic and additional materials needed for ODAH procedure.

Category	Materials
Basic	- Reference manual for the ODAH. - Extravasation kit. - Spill kit. - Emergency kit. - Venepuncture material. - Medical prescription. - Computer or similar for informatic access. - Material for waste management. - Sphygmomanometer, pulse oximeter, and stethoscope. - Temperature-controlled box for dug transport. - Basic life support.
For venous cannulation	- Endovenous catheter. - 10cc saline solution injections (pre-filled or not). - Sterile gauzes and dressings, antiseptic, absorbent towel. - Container for sharp objects. - Port-a-catch needle. - Catheter Abbocath No. 22. - Adhesive skin sutures. - Sodium heparin for catheter flushing. - Healing material for peripheral venous catheter.
Visiting HCPs equipment	- Protection material (gloves, mask, disposable gown, glasses). - Container group IV.
Vehicle equipment	- Hermetic refrigerator for transport of cytostatic drugs. - Container for cytostatic drugs. - Emergency kit. - Infusion pumps. - Container group IV and for sharp objects.
Diagnosis material (HBH Service)	- Electrocardiogram. - Pulse oximeter. - Automated external defibrillator (AED). - Necessary equipment for sample collection and analysis.
Additional therapeutic material (HBH Service)	- Oxygen therapy. - Aerosol therapy. - Elastomeric and perfusion pumps. - Transfusions of blood components. - Material for ostomy and tracheostomy management. - Mechanical ventilation instruments (BiPAP, CPAP). - Digit puncture for measurement of INR. - Material for enteral or invasive nutrition. - Surgical drainages. - Bladder catheterization. - Replacements of probes and cannulas. - Negative pressure therapy treatments. - Advanced life support.

AED, Automated external defibrillator; BiPAP, Bi-level Positive Airway Pressure; CPAP, Continuous Positive Airway Pressure; HBH, home-based hospitalization; HCPs, healthcare professionals; INR, international normalized ratio.

involved. Therefore, it is essential to collaborate and coordinate among nursing, pharmacy, oncology and HaH Services, and all the other involved parties for the program's success (16, 33, 34). Figure 1 depicts a recommended circuit model for ODAH.

Question 9. When should be considered ODAH and for what duration?

The inclusion of a cancer patient into ODAH will be based on compliance with the defined inclusion criteria. Once the oncologist has approved the treatment and the patient is considered a potential candidate, the Oncology Service is able to coordinate with the HaH Service to determine the patient's eligibility.

Question 10. How should the telephone for medical support be implemented?

A dedicated telephone line for cancer patients has been shown to be effective in reducing unnecessary emergency evaluations and hospital admissions, leading to lower healthcare costs and improved patient quality of life. Oncologists and specialized nurses can detect potential adverse events early, reducing the need for hospital visits, while telephone support can enhance patient-centred care (33, 35).

Question 11. How could be defined the hospital logistic route?

Typically, oncology patients follow a pathway for treatment that includes: 1) access/referral to Oncology Service; 2) assessment and decision to treat; 3) patient consent for treatment. In home-based chemotherapy programs, eligibility for home-administered therapy is determined after the treatment decision has been made (16).

3.2.1 Recommendations of the experts panel for the section 2.

Table 6 contains the agreed recommendations regarding section 2.

3.3 Section 3: economic, social and legal issues

Question 12. How can the efficiency of ODAH be determined?

Health interventions must provide information on their socio-economic value, including the economic impact and whether the additional benefit justifies the cost. Healthcare policy and decision-making processes are recognizing the need to limit resources to finance available interventions while incorporating the concept of opportunity cost from a societal perspective. Therefore, healthcare programs should consider incorporating health outcomes and their incremental costs to provide necessary evidence for evaluating new interventions. A similar methodology should be employed to evaluate the efficiency of ODAH.

Firstly, to evaluate the efficiency of ODAH, the perspective of the analysis has to be established. As ODAH has potential benefits for both patients and the Spanish NHS, the analysis should be conducted from a societal perspective, which considers direct healthcare costs such as the cost of medication, premedication, hydration, and used materials, as well as possible adverse reactions. Direct non-healthcare costs, such as patient or family transportation expenses, the cost of time spent on these trips, and the cost of time spent waiting, should also be considered. Finally, indirect costs such as losses in productivity should be factored in as well.

TABLE 5 Expert recommendations for clinical and healthcare issues.

Section 1. Clinical and healthcare issues	
1A. Related to drug/therapy	
Question	**Recommendations**
1. Which drugs are potentially suitable for home administration?	Recommendation 1.1: ODAH should be limited to parenterally administered drugs (intravenous, intramuscular, or subcutaneous) using electric infusers or elastomeric devices in increasing or decreasing doses. Caregivers should be trained to detect incidents during prolonged infusions, and healthcare personnel should be available if needed. Recommendation 1.2: Drug administration schedule (e.g., daily, weekly, twice per week) and complete duration of treatment (number of cycles) should be considered, but not discriminatory. Recommendation 1.3: Drug administration should take less than 2 hours, including all the steps in the treatment scheme except analytical controls (e.g., previous clinical controls, premedication, drug administration, cleaning and hydration, and aftercare). Longer procedures may be individually considered. Recommendation 1.4: The drug safety profile should be predictable and manageable, and the dispensed drug must not frequently cause pain or infusion-related adverse reactions. Recommendation 1.5: Clinical and analytical controls should be easily performed before administration at the patient's home, and the results should be available for treatment validation (Pharmacy Service). Recommendation 1.6: Drug quality has to be maintained during production, transport, and at-home administration.
1B. Related to patients	
Question	**Recommendations**
2. What profile of patients would benefit from oncology treatment administered at home?	Recommendation 2.1: It is recommended to initiate the first infusion in the hospital to monitor the adverse reactions such as allergies or anaphylaxis. Recommendation 2.2: Standardized patient selection criteria should be established to ensure safe home-administered oncologic therapies. However, individual characteristics of each patient should also be considered. Recommendation 2.3: A multidisciplinary committee should be responsible for regularly reviewing and revising inclusion and exclusion criteria. An internal procedure should also be established for the rapid assessment and periodic revisions.
1C. Related to healthcare settings	
Question	**Recommendations**
3. How ODAH would compromise the efficacy, safety, and quality of life of systemic treatments?	Recommendation 3.1: Complying with inclusion criteria is crucial for the safe and effective administration of oncology treatment at home. Recommendation 3.2: Standardized protocols and digital platforms utilized in day hospital units can mitigate risks and promote safety for patients and HCPs during validation, preparation, dispensing, and administration. Recommendation 3.3: Drugs that may jeopardize patient safety, quality of life, or treatment efficacy must not be permitted.
4. What kind of education, accreditation or training should receive the HCPs involved?	Recommendation 4.1: HCPs involved in ODAH programs require knowledge and experience in drug administration and patient care, along with the ability to coordinate and communicate with various levels of care, both within hospital and territory. Recommendation 4.2: Nurses responsible for ODAH require training in early detection and management of adverse events, extravasations, spills, antineoplastic treatment administration, and home hospitalization. Also, they should have a minimum experience and capacitation according to the particular needs. Recommendation 4.3: The staff involved should receive adequate training to identify socio-family problems and environments that may not be suitable for administering treatment.
5. What kind of controls should be performed?	Recommendation 5.1: A consensus manual is essential and should include pre-, during, and post-treatment instructions, signs/symptoms to watch for, transport, handling, disposal of medication and materials, and procedures for responding to adverse reactions, extravasations, spills, or incidents with the central/peripheral venous catheter. Recommendation 5.2: The HaH Service is the responsible of performing the controls during the ODAH procedure (before, during and after administration). These controls should be adequate to patients, their environment, and the administered drug. Recommendation 5.3: The ODAH schedule should be verified by at least two HCPs, especially the infusion rate of the pumps.
6. What would be the minimum instruments, apparatus or equipment required?	Recommendation 6.1: It is essential to provide a reference manual detailing procedure. Recommendation 6.2: Ensure proper disposal of essential and additional materials, as well as biological waste by providing containers.
7. Which aspects should be considered for drug preparation?	Recommendation 7.1: The chemotherapy should be prepared in the Pharmacy Service following hospital center safety procedures, labelled for home administration. Recommendation 7.2: The risk of exposure to HCPs administering the treatment, patients or caregivers should be minimal. Therefore, treatments must be prepared and conditioned in sterile class II biosafety cabinet; intravenous drugs must be prepared in closed transfer systems and, if possible, will be dispensed with the closed system infusion set purged with the compatible serum; for subcutaneous or intramuscular drugs the syringes will be loaded with safety anti-reflux caps. Recommendation 7.3: Once at patient home, the material should be prepared on an absorbent towel to prevent any type of spill.

To optimize ODAH efficiency, experts suggest conducting societal perspective evaluations, which can benefit patients and public healthcare administration by reducing hospital load. For oncological therapies, recommendations include implementing efficiency analysis and considering greater patient comfort and satisfaction, avoiding travel, and reduced Services saturation. If only the Spanish NHS perspective is considered, the cost of home administration may appear higher than hospital administration.

To fulfil the quality-of-life assessment, it is essential to measure outcomes related with patient perception (Patient-Reported Outcomes Measures-PROM/Patient-Reported Experience Measures-PREM) through validated questionnaires (e.g., from CatSalut in the case of Catalonia, or from the Patient Care Unit of the reference hospital). Ultimately, the results obtained in HaH can be compared to those obtained in cost-benefit analysis of the Day Care Hospital.

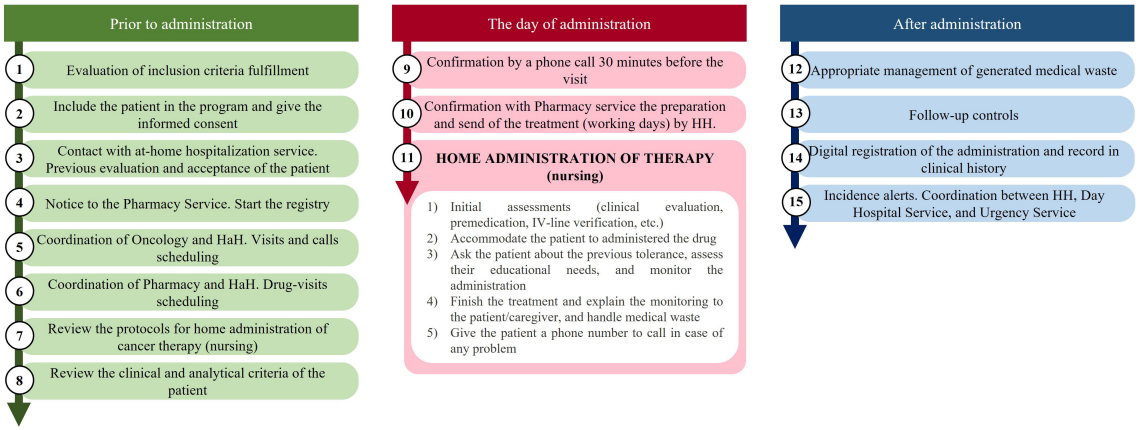

FIGURE 1
Diagram of the recommended logistic rout for home administration oncologic therapies.

The implementation of an ODAH offers numerous benefits for patients, caregivers, and society as: (i) it eliminates the need for patients and caregivers to travel to the hospital for oncological therapies, thus saving time and effort; (ii) it prevents work productivity losses for the patient's family or caregivers who would have otherwise accompanied them to the hospital; (iii) it reduces the care burden at the oncological day hospital, freeing up critical hospital resources; (iv) it potentially improves adherence and persistence to treatment since nursing staff regularly visit the patient's home. Without home administration, there is a potential risk of non-attendance, which could result in medication non-receipt; (v) patients may experience greater satisfaction with

TABLE 6 Expert recommendations for logistical and administrative issues.

Section 2. Logistical and administrative issues	
Question	**Recommendations**
8. To consider the ODAH, what are the requirements that must be fulfilled by the oncology department/hospital?	Recommendation 8.1: ODAH programs require the presence of an interdisciplinary HaH Service in the healthcare centre formed by experienced HCPs that comply with the healthcare model of each region. At least one of these professionals must have onco-hematologic training. Recommendation 8.2: The Pharmacy Service should have an oncology pharmacist with expertise in home healthcare protocols, a standardized method to manage medical waste, and an electronic health record system or pharmacotherapeutic history. A teleassistance system or application is also recommended. Recommendation 8.3: The healthcare center should have a significant volume of treatment, extensive experience in outpatient administration of antineoplastic drugs, and a well-established home hospitalization program. Recommendation 8.4: The center should meet the minimum requirements for ensuring quality Service, including maintaining schedules and providing a simple and comfortable patient journey. Recommendation 8.5: In the event of unforeseen circumstances requiring a return of the drug, it should be sent back to the Pharmacy Service.
9. When should be considered the ODAH and for what duration?	Recommendation 9.1: Patients can be considered for home-administered chemotherapy from treatment initiation until discontinuation, with agreement from the patient and their caregiver. Recommendation 9.2: Acceptance of home-administered chemotherapy does not preclude hospital visits when necessary. Recommendation 9.3: Discontinuation of home-administered chemotherapy may be decided by the patient/legal representative, the oncology Service (due to adverse events, disease progression, etc.), or the HaH Service (due to non-compliance with inclusion criteria or logistical difficulties).
10. How should the telephone for medical support be implemented?	Recommendation 10.1: Medical support telephone should be attended by the oncologist, but internal specialist in HaH Service will visit and treat the patient at home. Recommendation 10.2: The communication between Oncology, Pharmacy, and HaH Services must be direct and fluid throughout the home administration treatment. The involved nurses should have the ability to contact the oncologist directly.
11. How could be defined the hospital logistic route?	Recommendation 11.1: The HaH, Pharmacy, and Oncology Services should collaborate closely to provide personalized follow-up for ODAH patients. The HaH Service can also coordinate additional procedures, such as treating infectious complications or providing transfusion support. Recommendation 11.2: The HaH Service should maintain a schedule for patients enrolled in the program and coordinate with the Pharmacy and Oncology Services to ensure proper patient monitoring. Recommendation 11.3: Medical waste management protocols should be adapted for home settings to ensure the safety of patients, caregivers, and HCPs. This involves a thermally insulated, airtight, resistant, and well-labelled cytostatic container, collected upon discharge. The Maintenance Service of the hospital could provide the appropriate container. Recommendation 11.4: Safety incidents must be reported immediately to healthcare authorities due to the biological hazard of the drugs administered.

treatment and improved humanization of care, as the home environment reduces the feeling of medicalization and increases comfort during administration, potentially leading to an improvement in health-related quality of life.

In turn, adequate organizational support, including sufficient budgetary and human resources, is necessary to meet the needs of patients in implementing an ODAH. This includes incorporating qualified technical staff and obtaining appropriate materials to carry out the project effectively. It is also recommended to carry out a pilot program in order to conduct an economic evaluation (Figure 2).

Beyond this, other proposals could aid in implementing the ODAH setting, including the possibility of the laboratory covering the differential costs for home administration by sponsoring each patient attended or providing indirect resources, or by removing the VAT associated with drugs for home administration (as done in the United Kingdom) to utilize the potential savings to cover the additional expenses related (18).

In a systematic review by Cool et al. that evaluated the cost efficiency of Oncological Day Hospital at Home (ODAH), nine studies were reviewed (12). Of these, five studies estimate the difference in costs for one home-administered treatment versus hospital-administered from the perspective of the National Health Insurance. These studies reported reductions in costs (ranging from 9% to 53%) that favored home administration (12, 36, 37). Another study evaluated the cost per cycle and resulted in a 3.8% reduction of the costs from a societal perspective (12, 26). Additional systematic review, which included 13 heterogeneous articles, reported that home chemotherapy could result in savings ranging from $1,928 and $2,974 per treatment (38). Recent economic studies also suggest that ODAHs could lead to lower costs (39, 40). Nonetheless, current data do not fully confirm the potential cost reduction derived from home administration, but it is likely that better results of PROMs and PREMs would be obtained (12).

Question 13: How can the economic impact of ODAH be determined?

To conform with the guidelines presented in the CatSalut Guide for Economic Evaluations and Budgetary Impact Analyses, it is important to conduct separate assessments of an intervention's efficiency and its economic impact in order to ensure proper evaluation (41).

As previously mentioned, the societal perspective is the most appropriate since it takes into account the benefits for the patient and their relatives and caregivers. Once the perspective has been defined, costs can be identified, quantified, and evaluated (42).

From a methodological perspective, it is necessary to conduct an economic impact assessment to estimate the difference in costs between ODAH and standard hospital administration (43, 44). To achieve this, two different scenarios should be developed for cancer patients who are suitable for home administration. In the current scenario, named as scenario 1, (S1; hospital administration) all patients received chemotherapy at the hospital, whereas in the potential scenario, named as scenario 2, (S2; home administration) all patients received the treatment at home. The economic impact of ODAH would be the difference between these two scenarios (Figure 3). Then, three possible results can be obtained after the estimation: 1) S1 costs higher than S2 costs; 2) S1 costs lower than S2; and 3) the same costs for S1 and S2.

While it would be reasonable to assume that the costs of scenario S1 would be comparable to those of scenario S2, if it is found that the costs of S1 are actually higher than those of S2, this could provide additional support for the adoption of ODAH programs from a healthcare administration perspective.

Question 14. Are there legal and ethical issues to be solved to implement the program?

Currently, there is no specific national legislation that regulates the ODAHs. Consequently, HCPs who provide home-administered treatments are legally covered as if they were delivering them at a hospital. Nevertheless, the administration of antineoplastic therapies must be carried out by qualified and experienced professionals to minimize potential risks for the patient and the handler. In case of accidental contamination such as breakage, spillage, or any other incident, the HCPs should be aware of the appropriate measures to manage it. Therefore, the administration of

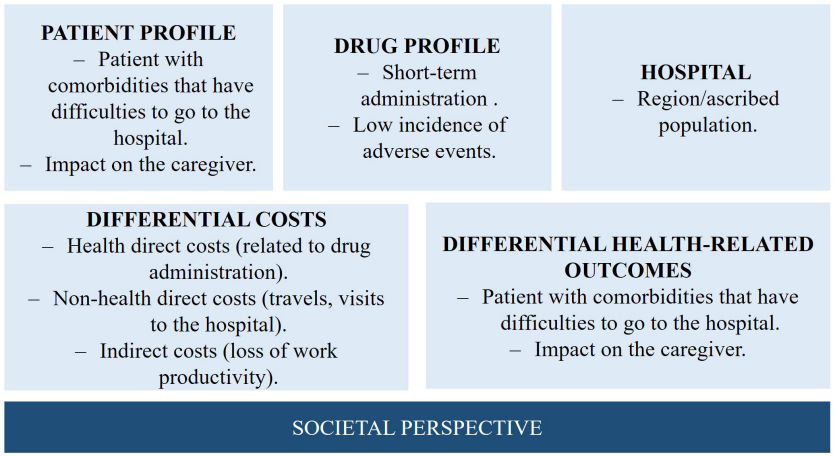

FIGURE 2
Factors to be considered for the implementation of a pilot study with the aim of assessing the efficiency of the ODAH.

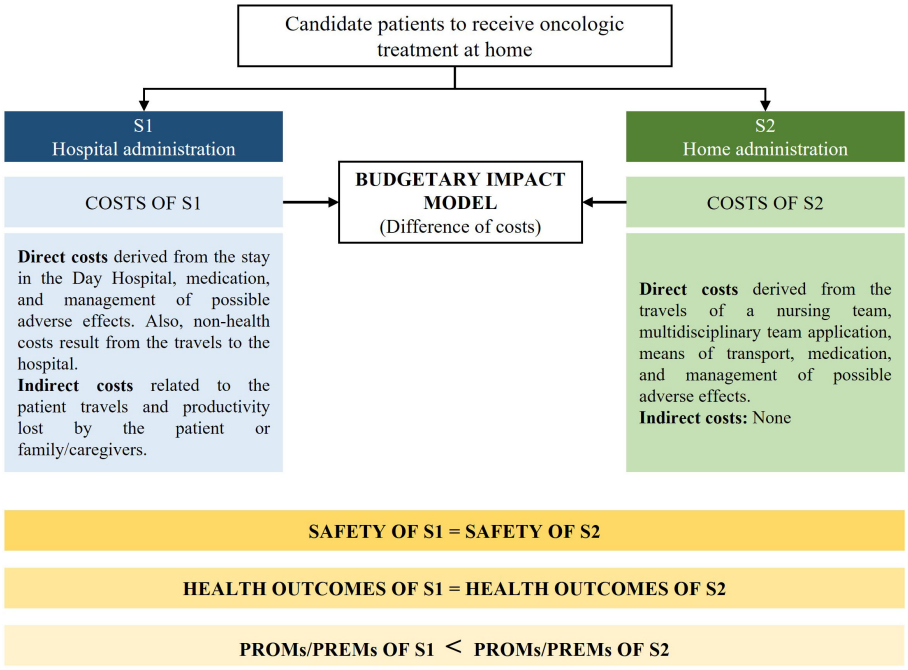

PREMs: patient-reported experience measures; PROMs: patient-reported outcomes measures; SC: scenario

FIGURE 3
Scheme of the relevant aspects to consider during the economic evaluation of home-administered oncologic therapies.

cytostatic agents should be restricted to HCPs who are trained and experienced in the safe handling of chemotherapeutic drugs (45).

3.3.1 Recommendations of the experts panel for the section 3.

Table 7 summarizes the agreed recommendations for the panel of experts regarding section 3.

TABLE 7 Expert recommendations for economic, social and legal issues.

Section 3. Economic, social and legal issues	
Question	**Recommendations**
12. How can the efficiency of ODAH be determined?	Recommendation 12.1: To evaluate the efficiency of ODAH, it is recommended to conduct an economic analysis from a societal perspective, given the potential benefits it offers to patients and the Spanish NHS. Recommendation 12.2: It is advised to implement a pilot program to perform an economic evaluation of ODAH.
13. How can the economic impact of ODAH be determined?	Recommendation 13.1: For economic impact determination, the resulting costs of the ODAH and in the hospital should be compared. Recommendation 13.2: Despite the potential difficulty in measuring PROMs and PREMs, it should be considered in the evaluation. Recommendation 13.3: To adequately capture potential patient benefits associated with home administration, efficiency evaluations should be conducted from a societal perspective. Recommendation 13.4: It is essential to employ validated questionnaires that can effectively gather and assess

(Continued)

TABLE 7 Continued

Section 3. Economic, social and legal issues	
Question	**Recommendations**
	PROMs and PREMs to generate evidence regarding the health-related outcomes perceived by patients.
14. Are there legal and ethical issues to be solved to implement the program?	Recommendation 14.1: ODAH programs should adhere to the legal regulations of the respective country or region to ensure legal coverage for HCPs and procedures. Recommendation 14.2: Standard protocols for collecting and responding to claims should be followed by each center, and patients should be informed through a formal consent before starting treatment. Recommendation 14.3: Efforts should be made to expand the availability of ODAH programs to more patients while ensuring the safety and efficacy of the treatment is not compromised.

4 Conclusions

Home-based chemotherapy initiatives have emerged as a viable and safe alternative to traditional hospital treatment for oncology patients. These programs offer several advantages over traditional hospital-based treatment, including increased patient comfort and convenience, improved control of high-risk situations, and reduced costs and hospital overload. While most programs currently operate in urban environments where a high concentration of patients can be found, we believe that this strategy can also be successfully employed in areas with dispersed populations, as long as the travel

time does not exceed 30-45 minutes. Furthermore, by providing patient-centered care and reducing the psychological and emotional burden of treatment, ODAH programs have the potential to significantly improve the quality of life of patients with cancer.

To support the development and implementation of these programs, a multidisciplinary group of experts have developed a list of recommendations based on the published literature and the collective expertise of the group aiming to serve as a foundation for the development of future initiatives.

Overall, ODAHs have the potential to revolutionize the way in which oncology patients receive treatment. By providing safe, effective, and patient-centered care, these programs can help to improve the overall experience of cancer treatment for patients and reduce the burden on healthcare systems. Also, an adequate financial investment and the training of specialized teams would be critical. It is therefore important that healthcare providers, policy makers, and other stakeholders work together to support the development and implementation of these programs to improve the quality of life for patients with cancer.

Data availability statement

The original contributions presented in the study are included in the article/Supplementary Material. Further inquiries can be directed to the corresponding author.

Author contributions

EV: Conceptualization, Methodology, Validation, Writing – review & editing. MA: Conceptualization, Methodology, Validation, Writing – review & editing. MC: Conceptualization, Methodology, Validation, Writing – review & editing. SG: Conceptualization, Methodology, Validation, Writing – review & editing. MEM-M: Conceptualization, Methodology, Validation, Writing – review & editing. MP: Conceptualization, Methodology, Validation, Writing – review & editing. AT: Conceptualization, Methodology, Validation, Writing – review & editing. YS: Conceptualization, Methodology, Validation, Writing – review & editing. MS: Conceptualization, Methodology, Validation, Writing – review & editing.

Funding

The author(s) declare financial support was received for the research, authorship, and/or publication of this article.

Acknowledgments

Authors would like to thank Meisys for the assistance, whose service has been founded by Eisai Pharmaceuticals S.A.

Conflict of interest

Authors MA and MC were employed by the company Pharmacoeconomics & Outcomes Research Iberia (PORIB). Author YS was employed by the company Eisai Farmaceutica S.A. All authors have received honoraria from Eisai Pharmaceuticals S.A.

The authors declare that this study received funding from Eisai Farmaceutica, S.A. The funder had the following involvement in the study: responsible for contacting the project coordinator, setting the project goals, and developing the initial work plan. It was also in charge of gathering information from different sources about professional experts that could be invited to join in and, along with the project coordinator, invite them. Eisai provided the logistic support for the meetings (all via teleconference), selected the medical writing agency and the funding for the professional participants fees and external medical writer honorarium. Two members of the local Oncology Medical Affairs Department attended to the expert discussion meetings as observers, but they have not righted to review or modify the manuscript and the final consensus document.

Publisher's note

Supplementary material

The Supplementary Material for this article can be found online at: https://www.frontiersin.org/articles/10.3389/fonc.2024.1335344/full#supplementary-material

References

1. Sawada NO, Nicolussi AC, de Paula JM, Garcia-Caro MP, Marti-Garcia C, Cruz-Quintana F. Quality of life of Brazilian and Spanish cancer patients undergoing chemotherapy: an integrative literature review. *Rev Lat Am Enfermagem* (2016) 24: e2688. doi: 10.1590/1518-8345.0564.2688

2. Meneguin S, Matos TDS, Ferreira M. Perception of cancer patients in palliative care about quality of life. *Rev Bras Enferm* (2018) 71(4):1998–2004. doi: 10.1590/0034-7167-2017-0360

3. Sung H, Ferlay J, Siegel RL, Laversanne M, Soerjomataram I, Jemal A, et al. Global cancer statistics 2020: GLOBOCAN estimates of incidence and mortality worldwide for 36 cancers in 185 countries. *CA Cancer J Clin* (2021) 71(3):209–49. doi: 10.3322/caac.21660

4. *Red Española de Registros de Cáncer (REDECAN.Estimaciones de la incidencia del cáncer en España* (2022). Available at: https://redecan.org/storage/documents/873877e1-af1b-43fe-8d97-0ee1434fe261.pdf (Accessed October 2022).

5. Alkatout I, Biebl M, Momenimovahed Z, Giovannucci E, Hadavandsiri F, Salehiniya H, et al. Has COVID-19 affected cancer screening programs? A systematic review. *Front Oncol* (2021) 11:675038 From NLM. doi: 10.3389/fonc.2021.675038

6. Di Cosimo S, Susca N, Apolone G, Silvestris N, Racanelli V. The worldwide impact of COVID-19 on cancer care: A meta-analysis of surveys published after the first wave of the pandemic. *Front Oncol* (2022) 12:961380 From NLM. doi: 10.3389/fonc.2022.961380

7. Riera R, Bagattini Â M, Pacheco RL, Pachito DV, Roitberg F, Ilbawi A. Delays and disruptions in cancer health care due to COVID-19 pandemic: systematic review. *JCO Glob Oncol* (2021) 7:311–23. doi: 10.1200/go.20.00639

8. Leff B, Burton L, Mader SL, Naughton B, Burl J, Inouye SK, et al. Hospital at home: feasibility and outcomes of a program to provide hospital-level care at home for acutely ill older patients. *Ann Intern Med* (2005) 143(11):798–808. doi: 10.7326/0003-4819-143-11-200512060-00008

9. Conley J, O'Brien CW, Leff BA, Bolen S, Zulman D. Alternative strategies to inpatient hospitalization for acute medical conditions: A systematic review. *JAMA Intern Med* (2016) 176(11):1693–702. doi: 10.1001/jamainternmed.2016.5974

10. Sanguinetti JM, Martinez D, Dimase F, Streich G, Castro P, Vega V, et al. Patient safety and satisfaction in home chemotherapy. *Home Healthc Now* (2021) 39(3):139–44. doi: 10.1097/NHH.0000000000000958

11. Murthy V, Wilson J, Suhr J, James L, Tombs H, Shereef E, et al. Moving cancer care closer to home: a single-centre experience of home chemotherapy administration for patients with myelodysplastic syndrome. *ESMO Open* (2019) 4(2):e000434. doi: 10.1136/esmoopen-2018-000434

12. Cool L, Vandijck D, Debruyne P, Desmedt M, Lefebvre T, Lycke M, et al. Organization, quality and cost of oncological home-hospitalization: A systematic review. *Crit Rev Oncol Hematol* (2018) 126:145–53. doi: 10.1016/j.critrevonc.2018.03.011

13. De Zen L, Del Rizzo I, Ronfani L, Barbieri F, Rabusin M, Dall'Amico R, et al. Safety and family satisfaction of a home-delivered chemotherapy program for children with cancer. *Ital J Pediatr* (2021) 47(1):43. doi: 10.1186/s13052-021-00993-x

14. Sandman KE, Bell TJ. Patient-Focused Benefits of at-Home Versus in-Clinic Administration of Cancer Therapy: New Considerations for the COVID-19 Era. *Blood* (2020) 136:35–6. doi: 10.1182/blood-2020-137560

15. Evans JM, Qiu M, MacKinnon M, Green E, Peterson K, Kaizer LA. multi-method review of home-based chemotherapy. *Eur J Cancer Care (Engl)* (2016) 25 (5):883–902. doi: 10.1111/ecc.12408

16. Corbett M, Heirs M, Rose M, Smith A, Stirk L, Richardson G, et al. *The delivery of chemotherapy at home: an evidence synthesis*. Southampton (UK: NIHR Journals Library (2015). doi: 10.3310/hsdr03140

17. *American society of clinical oncology (ASCO) position statement home infusion of anticancer therapy.* (2020). Available at: https://old-prod.asco.org/sites/new-www.asco.org/files/content-files/advocacy-and-policy/documents/2020_Home-Infusion-Position-Statement.pdf (Accessed January 2023).

18. Burns V, Misra V, Paton N. Systemic anti-cancer therapy delivery in the home: a service model. *Br J Nurs* (2020) 29(10):S22–9. doi: 10.12968/bjon.2020.29.10.S22

19. Swinden J, Barton S, Peron JMR, Nabhani-Gebara S. *Improving drug stability to promote home cancer therapy.* (2014). Available at: https://hospitalpharmacyeurope.com/news/editors-pick/improving-drug-stability-to-promote-home-cancer-therapy/ (Accessed January 2023).

20. Vokes EE, Schilsky RL, Choi KE, Magid DM, Guarnieri CM, Whaling SM, et al. A randomized study of inpatient versus outpatient continuous infusion chemotherapy for patients with locally advanced head and neck cancer. *Cancer* (1989) 63(1):30–6. doi: 10.1002/1097-0142(19890101)63:1<30::aid-cncr2820630105>3.0.co;2-m

21. Cox K, Visintin L, Kovac S, Childs A, Kelleher H, Murray B, et al. Establishing a programme for continuous ambulatory infusion chemotherapy. *Aust N Z J Med* (1997) 27(6):680–4. doi: 10.1111/j.1445-5994.1997.tb00998.x

22. Rischin D, White MA, Matthews JP, Toner GC, Watty K, Sulkowski AJ, et al. A randomised crossover trial of chemotherapy in the home: patient preferences and cost analysis. *Med J Aust* (2000) 173(3):125–7. doi: 10.5694/j.1326-5377.2000.tb125563.x

23. Cool L, Missiaen J, Vandijck D, Lefebvre T, Lycke M, De Jonghe PJ, et al. An observational pilot study to evaluate the feasibility and quality of oncological home-hospitalization. *Eur J Oncol Nurs* (2019) 40:44–52. doi: 10.1016/j.ejon.2019.03.003

24. Borras JM, Sanchez-Hernandez A, Navarro M, Martinez M, Mendez E, Ponton JL, et al. Compliance, satisfaction, and quality of life of patients with colorectal cancer receiving home chemotherapy or outpatient treatment: a randomised controlled trial. *BMJ* (2001) 322(7290):826. doi: 10.1136/bmj.322.7290.826

25. Álvarez-Velásquez S, Sanz-Valero J. Home chemotherapy advantages in adult neoplasia sufferers: a systematic review. *Hosp Domicilio* (2020) 4(1):24–41. doi: 10.22585/hospdomic.v4i1.98

26. Corrie PG, Moody AM, Armstrong G, Nolasco S, Lao-Sirieix SH, Bavister L, et al. Is community treatment best? a randomised trial comparing delivery of cancer treatment in the hospital, home and GP surgery. *Br J Cancer* (2013) 109(6):1549–55. doi: 10.1038/bjc.2013.414

27. (ESMO), E. S. f. M. O. *ESMO Standard Operating Procedures (SOPs) for Consensus Conference (CC) recommendations* . Available at: https://www.esmo.org/content/download/77792/1426729/1/ESMO-ConsensusConference-SOPs.pdf (Accessed October 2022).

28. Neuss MN, Gilmore TR, Belderson KM, Billett AL, Conti-Kalchik T, Harvet BE, et al. 2016 Updated American society of clinical oncology/Oncology nursing society chemotherapy administration safety standards, including standards for pediatric oncology. *Oncol Nurs Forum* (2017) 44(1):31–43. doi: 10.1188/17.ONF.31-43

29. Jacobson JO, Polovich M, Gilmore TR, Schulmeister L, Esper P, Lefebvre KB, et al. Revisions to the 2009 american society of clinical oncology/oncology nursing society chemotherapy administration safety standards: expanding the scope to include inpatient settings. *J Oncol Pract* (2012) 8(1):2–6. doi: 10.1200/JOP.2011.000339

30. Ewen BM, Combs R, Popelas C, Faraone GM. Chemotherapy in home care: one team's performance improvement journey toward reducing medication errors. *Home Healthc Nurse* (2012) 30(1):28–37. doi: 10.1097/NHH.0b013e318233a75e

31. Nabhani-Gebara S, Salma D. Delivering chemotherapy at home: how much do we know? *Br J Community Nurs* (2019) 24(10):482–4. doi: 10.12968/bjcn.2019.24.10.482

32. Olsen M, LeFebvre K, Brassil K. Chemotherapy and immunotherapy guidelines and recommendations for practice. *Oncol Nurs Soc* (2019).

33. Tralongo P, Ferrau F, Borsellino N, Verderame F, Caruso M, Giuffrida D, et al. Cancer patient-centered home care: a new model for health care in oncology. *Ther Clin Risk Manag* (2011) 7:387–92. doi: 10.2147/TCRM.S22119

34. Casteli CPM, Mbemba GIC, Dumont S, Dallaire C, Juneau L, Martin E, et al. Indicators of home-based hospitalization model and strategies for its implementation: a systematic review of reviews. *Syst Rev* (2020) 9(1):172. doi: 10.1186/s13643-020-01423-5

35. Sweeney L, Halpert A, Waranoff J. Patient-centered management of complex patients can reduce costs without shortening life. *Am J Manag Care* (2007) 13(2):84–92.

36. Lassalle A, Thomare P, Fronteau C, Mahe B, Jube C, Blin N, et al. Home administration of bortezomib in multiple myeloma is cost-effective and is preferred by patients compared with hospital administration: results of a prospective single-center study. *Ann Oncol* (2016) 27(2):314–8. doi: 10.1093/annonc/mdv563

37. Touati M, Lamarsalle L, Moreau S, Vergnenegre F, Lefort S, Brillat C, et al. Cost savings of home bortezomib injection in patients with multiple myeloma treated by a combination care in Outpatient Hospital and Hospital care at Home. *Support Care Cancer* (2016) 24(12):5007–14. doi: 10.1007/s00520-016-3363-3

38. Polinski JM, Kowal MK, Gagnon M, Brennan TA, Shrank WH. Home infusion: Safe, clinically effective, patient preferred, and cost saving. *Healthc (Amst)* (2017) 5(1-2):68–80. doi: 10.1016/j.hjdsi.2016.04.004

39. Sharma D, Wojtynek J, Fox KM, Cooper C, Dokubo I. Cost of home vs clinic administration of paclitaxel in metastatic breast cancer. *Am J Manag Care* (2021) 27(2 Spec. No.):SP46–50. doi: 10.37765/ajmc.2021.88563

40. Kulthanachairojana N, Chansriwong P, Thokanit NS, Sirilerttrakul S, Wannakansophon N, Taychakhoonavudh S. Home-based chemotherapy for stage III colon cancer patients in Thailand: Cost-utility and budget impact analyses. *Cancer Med* (2021) 10(3):1027–33. doi: 10.1002/cam4.3690

41. Servei Català de la Salut [CatSalut]. *Guía y recomendaciones para la realización y presentación de evaluaciones económicas y análisis de impacto presupuestario de medicamentos en el ámbito del CatSalut.* Available at: https://catsalut.gencat.cat/web/.content/minisite/catsalut/proveidors_professionals/medicaments_farmacia/farmaeconomica/caeip/gaeip_publica_castellano_octubre2014_catsalut.pdf (Accessed March 2023).

42. Prieto L, Sacristán JA, Pinto JL, Badia X, Antoñanzas F, del Llano J. Análisis de costes y resultados en la evaluación económica de las intervenciones sanitarias. *Evaluación económica para clínicos* (2004) 122(11):423–9. doi: 10.1016/S0025-7753(04)74260-8

43. Brosa M, Gisbert R, Rodríguez JM, Soto J. Principios, métodos y aplicaciones del análisis del impacto presupuestario en el sector sanitario. *Pharmacoecon. Span. Res Artic* (2005) 2:65–78. doi: 10.1007/BF03320900

44. Sullivan SD, Mauskopf JA, Augustovski F, Jaime Caro J, Lee KM, Minchin M, et al. Budget impact analysis-principles of good practice: report of the ISPOR 2012 Budget Impact Analysis Good Practice II Task Force. *Value Health* (2014) 17(1):5–14. doi: 10.1016/j.jval.2013.08.2291

45. Comisión de Salud Pública (Consejo Interterritorial del Sistema Nacional de Salud). *Protocolo de Vigilancia Sanitaria Específica para los trabajadores expuestos a Agentes Citostáticos* (2003). Available at: https://www.sanidad.gob.es/ciudadanos/saludAmbLaboral/docs/Agentescitostaticos.pdf (Accessed 2023).

frontiers | Frontiers in Oncology

TYPE Original Research
PUBLISHED 20 March 2024
DOI 10.3389/fonc.2024.1341766

OPEN ACCESS

EDITED BY
Teresita Padilla-Benavides,
Wesleyan University, United States

REVIEWED BY
Monserrat Avila Zozaya,
Boston University, United States
Danijela M Cvetković,
University of Kragujevac, Serbia

*CORRESPONDENCE
Miguel Vargas
mavargas@cinvestav.mx

RECEIVED 20 November 2023
ACCEPTED 31 January 2024
PUBLISHED 20 March 2024

CITATION
Carrión-Estrada DA, Aguilar-Rojas A, Huerta-Yepez S, Montecillo-Aguado M, Bello M, Rojo-Domínguez A, Arechaga-Ocampo E, Briseño-Díaz P, Meraz-Ríos MA, Thompson-Bonilla MdR, Hernández-Rivas R and Vargas M (2024) Antineoplastic effect of compounds C14 and P8 on TNBC and radioresistant TNBC cells by stabilizing the K-Ras4B^{G13D}/PDE6δ complex. *Front. Oncol.* 14:1341766. doi: 10.3389/fonc.2024.1341766

Antineoplastic effect of compounds C14 and P8 on TNBC and radioresistant TNBC cells by stabilizing the K-Ras4B^{G13D}/PDE6δ complex

Dayan A. Carrión-Estrada[1], Arturo Aguilar-Rojas[2], Sara Huerta-Yepez[3], Mayra Montecillo-Aguado[3], Martiniano Bello[4], Arturo Rojo-Domínguez[5], Elena Arechaga-Ocampo[5], Paola Briseño-Díaz[6], Marco Antonio Meraz-Ríos[1], María del Rocío Thompson-Bonilla[7], Rosaura Hernández-Rivas[1] and Miguel Vargas[1]*

[1]Department of Molecular Biomedicine, Center for Research and Advanced Studies of the National Polytechnic Institute (CINVESTAV-I.P.N.), Mexico City, Mexico, [2]Medical Research Unit in Reproductive Medicine, Mexican Social Security Institute (IMSS), High Specialty Medical Unit in Gynecology and Obstetrics No. 4 Dr. Luis Castelazo Ayala, Mexico City, Mexico, [3]Research Unit in Oncological Diseases, Children's Hospital of Mexico Federico Gómez, Mexico City, Mexico, [4]Laboratory for the Design and Development of New Drugs and Biotechnological Innovation, Higher School of Medicine, National Polytechnic Institute, Mexico City, Mexico, [5]Department of Natural Sciences, Metropolitan Autonomous University Cuajimalpa Unit, Mexico City, Mexico, [6]Department of Biochemistry of the Faculty of Medicine of the National Autonomous University of Mexico (UNAM), Mexico City, Mexico, [7]Biomedical and Transnational Research, Genomic Medicine Laboratory, Hospital 1° de Octubre, Institute of Security and Social Services of State Workers (ISSSTE), Mexico City, Mexico

Introduction: Breast cancer (BC) is the leading cause of cancer-related deaths among women, with triple-negative breast cancer (TNBC) representing one of the most aggressive and treatment-resistant subtypes. In this study, we aimed to evaluate the antitumor potential of C14 and P8 molecules in both TNBC and radioresistant TNBC cells. These compounds were chosen for their ability to stabilize the complex formed by the overactivated form of K-Ras4B^{G13D} and its membrane transporter (PDE6δ).

Methods: The antitumor potential of C14 and P8 was assessed using TNBC cell lines, MDA-MB-231, and the radioresistant derivative MDA-MB-231RR, both carrying the K-Ras4B>^{G13D} mutation. We investigated the compounds' effects on K-Ras signaling pathways, cell viability, and tumor growth in vivo.

Results: Western blotting analysis determined the negative impact of C14 and P8 on the activation of mutant K-Ras signaling pathways in MDA-MB-231 and MDA-MB-231RR cells. Proliferation assays demonstrated their efficacy as cytotoxic agents against K-Ras^{G13D} mutant cancer cells and in inducing apoptosis. Clonogenic assays proven their ability to inhibit TNBC and radioresistant TNBC cell clonogenicity. In In vivo studies, C14 and P8 inhibited tumor growth and reduced proliferation, angiogenesis, and cell cycle progression markers.

Discussion: These findings suggest that C14 and P8 could serve as promising adjuvant treatments for TNBC, particularly for non-responders to standard therapies. By targeting overactivated K-Ras and its membrane transporter, these compounds offer potential therapeutic benefits against TNBC, including its radioresistant form. Further research and clinical trials are warranted to validate their efficacy and safety as novel TNBC treatments.

KEYWORDS

K-Ras4B, PDE6δ, breast cancer, triple negative breast cancer (TNBC), radioresistant, antitumor compounds, C14, P8

1 Introduction

Breast cancer (BC) is the most frequently diagnosed cancer and the leading cause of cancer deaths among women worldwide. In 2020 alone, BC accounted for 2.3 million new cases in women, representing 24.5% of the total cancer cases, with a 15.5% mortality rate among cancer cases (1, 2). This disease manifests as a highly heterogeneous and complex entity, encompassing various clinical and molecular subtypes, each posing distinct challenges. According to the expression of specific markers, such as estrogen receptor (ER), progesterone receptor (PR), epidermal growth factor receptor 2 (HER2), and the proliferation marker Ki-67, BC has been principally classified into five subtypes: luminal A, luminal B, luminal B-like, HER2-enriched, and triple-negative breast cancer (TNBC) (3). TNBC represents approximately 15%–20% of all breast cancer cases and is considered one of the most aggressive BC subtypes. It is characterized by the absence of ER, PR, and HER2 expression, coupled with elevated Ki-67 levels, leading to rapid growth, high recurrence rates, metastatic potential, worse prognosis, and limited treatment options than other BC subtypes (4, 5) (4, 6). Currently, the standard of care to treat high-risk and locally advanced TNBC is chemotherapy, radiotherapy, and, recently, immune checkpoint blockade (ICB) agents (7). Although all those therapeutic schemes have shown their effectiveness against TNBC, this is limited especially by the development of resistance, tumoral recurrences, metastasis, and the emergence of serious adverse side effects (8). For example, there is a 40% mortality rate within the first 5 years after diagnosis, and a substantial number of patients develop distant metastasis (46%) and recurrent disease after surgery (>25%) (6, 9). Additionally, the development of resistance to treatments in these patients has been observed. For example, a significant portion of TNBC patients are not able to respond to chemotherapy and radiation schemes (60%–70%). This tumoral aggressiveness has been associated with various factors. In this context, one of the most important events according to genomic landscape studies is the overactivation of KRAS and its associated signaling pathways, which are the driving force behind the malignant behavior observed in these tumors, including the acquisition of early tumor relapse, local invasion, and metastatic spread (10). Likewise, according to previous reports, patients who express overactive mutant forms of KRAS also have been associated with the development of chemoresistance (11, 12). In this case, although the development of chemoresistant phenotypes in TNBC is implicated in the activation of multiple signaling pathways, context-dependent compensatory pathway crosstalk, synergy, antagonism, and reconfiguration of signaling network (8), overactivation of the EGFR/K-RAS/MAPK pathway is highly prevalent in chemoresistant, recurrent, locally advanced, and metastatic TNBC (13).

Additionally, TNBC patients with KRAS mutations often display resistance to radiation therapy, a key component of breast cancer treatment. The resistance observed in TNBC patients may stem from the highly heterogeneous nature of these tumors such as high diversity in tumoral cell populations, the presence of cancer stem cells, and epithelial–mesenchymal transition characteristics. These factors can lead to a reduced response to radiotherapy (14, 15). Overcoming radioresistance in TNBC remains a critical area of research, with ongoing efforts focused on identifying novel therapeutic strategies to enhance the effectiveness of treatments and radiation therapy in this aggressive and challenging breast cancer subtype (15).

Considering this, KRAS has emerged as a promising therapeutic target. K-Ras4B is the more abundant isoform of the K-Ras protein (16). Mutant K-Ras4B is associated with various cancers, such as pancreatic cancer (60%), colon cancer (32%), lung cancer (17%), and approximately 5%–15% of breast cancers, including TNBC, and plays a role in tumorigenesis by driving key signaling pathways like RAF/MEK/MAPK (17). In the specific case of breast cancer, up to 23% of premenopausal women with TNBC have been shown to have higher rates of mutations in KRAS gene. Mutant KRAS in TNBC correlates with therapy resistance, reduced expression of estrogen receptor alpha (Erα), development of resistance to antiestrogen treatments, and negative prognostic outcomes, making it one of the pivotal factors in the progression of aggressive BC cases (18–20). With its role in driving TNBC, it offers an attractive target for therapeutic intervention, especially since patients with active mutant KRAS have an increased susceptibility to ovarian cancer as well (21). This not only

highlights the significance of KRAS in promoting therapy resistance but also underscores its role in driving the development of the most aggressive forms of breast cancer.

Therefore, targeting the overactivated form of K-Ras4B emerges as a promising alternative for treating TNBC tumors, aiming to reduce Ras signaling-dependent pathways and signaling pathways associated with radioresistance (22). In oncogenic forms of K-Ras4B, 19 activating codon substitutions occur at codons 12, 13, or 61, displaying a specific pattern depending on the type of tumor. Notably, mutations in G12D, G12V, G12C, G13D, and Q61R collectively account for approximately 70% of all Ras-mutant patients (23). The substitution of glycine with aspartic acid at position 12 (G12D) is the most frequent, occurring in the range of 30% to 50% of solid tumors, with the highest incidence observed in pancreatic cancer and the lowest in lung adenocarcinoma but also is found in an isolated sample of TNBC (24). Another common mutation is G12V, which is the most prevalent in ovarian cancer and least common in cholangiocarcinoma. The G12C mutation is highly prevalent in lung adenocarcinoma (nearly 40%), but it occurs much less frequently in other tumors (approximately 10%) (25). G13D is primarily reported in colorectal cancer (12%) (26), but it is also found in the TNBC cell line MDA-MB-231 (27). Regarding Q61R, this codon represents only 2% of K-Ras4B mutations across all cancers and 5% in pancreatic ductal adenocarcinoma (PDAC) (28).

Although mutant forms of K-Ras4B play an essential role in the development, maintenance, and progression of breast cancer, there is limited information about the type and frequency of activating mutations in this neoplasia. For instance, the presence of the G12D mutation has been reported in an isolated sample of triple-negative breast cancer tumors (24). Similarly, the cell line MDA-MB-231 expresses the G13D form and is the only cellular model available to study the oncogenic function of K-Ras4B in BC.

Regarding the prevalence of K-Ras4B mutations in breast cancer, it has been reported to be between 7% and 12% (29). Specifically, the mutation frequency of K-Ras4B is 2% in luminal A tumors, 20% in luminal B tumors, 17.4% in HER2+ tumors, and 7.7% in TNBC (29). In this case, it is important to mention that there are few studies reporting the frequencies of mutant forms of this GTPase in breast cancer patients, and there are not enough studies demonstrating the specific types of mutations in patients with BC. As a result, the type, frequency, and effects of mutant forms of K-Ras4B on the population could be underestimated. For example, according to estimations made in 2018 by the United States, there were 268,670 new cases of breast cancer in that year. Even when considering a low frequency of K-Ras4B mutations in the population, it is estimated that there would be 3,578 cases associated with the presence of overactivated forms of K-Ras4B (30). Given the limited therapeutic options, the unfavorable prognosis, and the high amount of TNBC patients, the utilization of new drugs to decrease the mortality rate associated with this disease is essential.

However, targeting oncogenic forms of K-Ras4B has been a significant challenge due to its cellular localization requirements and the number of mutations. For this reason, our research group has been working in this area to propose a novel strategy to reduce the oncogenic potential of this protein. This new approach involves the use of a family of small molecules, including the compounds known as C14 and P8, which act as molecular staples (31–33). C14 is denoted as 2-[(3-chlorophenyl)-methyl-methyl-amino]-*N*-croman-4-yl-acetamide with a molecular weight of 344.83 g/mol. Five rotatable bonds, a hydrogen bridge donor atom, and three hydrogen bridge acceptor atoms are possessed by the molecule. The functional groups included benzopyrene or chromeno, which is a rigid structure formed by a benzene ring and a six-atom heterocycle with hydrogen at position 1 and a *N*-methylacetamide group (Supplementary Figure 1A). P8 is designated as 2-[4-(3-chlorophenyl)piperazin-1-yl]-*N*-[(4*R*)-chroman-4-yl]acetamide with a molecular weight of 385.9 g/mol and is an analog of the base compound C14 (Supplementary Figure 1B) (33). Both compounds are capable of binding to the complex formed by K-Ras4B and the phosphodiesterase subunit delta (PDE6δ) to reduce the activity of this GTPase and its associated signaling pathways. Through this strategy, it has been possible to disrupt tumor growth in xenograft mouse models, pancreatic cancer cell lines, and colon cancer cell lines as previously shown (31–33).

Considering the high mortality rate among patients with triple-negative tumors, coupled with their limited therapeutic options and the significant proportion of them developing resistance to conventional treatments such as radiotherapy, this study aims to assess the antitumor effects of the compounds known as C14 and P8 in models representing advanced stages of BC. For this purpose, the TNBC cell line MDA-MB-231 and the radioresistant TNBC MDA-MB-231RR (34) were employed. To the best of our group's knowledge, these cell lines are the only *in vitro* models of BC that naturally express the K-Ras4B^{G13D} mutant form. For this reason, they have been selected as models to represent the most aggressive form of BC.

2 Materials and methods

2.1 *In silico* docking simulations and molecular dynamics simulations

Compounds C14 and P8 were selected through docking from the ENAMINE database 3D Diversity set (www.enamine.net). The crystallographic structure of the wild-type (K-Ras4B^{WT}/PDE6δ) system was derived from PDB file 5TAR. Mutation for obtaining the K-Ras4B^{G13D}/PDE6δ complex was introduced with the mutagenesis tool in Molecular Operating Environment (MOE; www.chemcomp.com) followed by local energy minimization of the new side chain and then minimization of surrounding atoms. Docking studies were performed using both MOE and GOLD (35). Protein–protein interaction energies between K-Ras4BWT/PDE6δ and K-Ras4B^{G13D}/PDE6δ systems with the C14 and P8 compounds were calculated using the HawkDock Server (http://cadd.zju.edu.cn/hawkdock/), taking into account force field interactions and solvation energies (36, 37).

Extensive docking calculations were conducted on the macromolecular system, initially through a blind search of the surface, followed by a focus on the resulting main cavity. In the

case of MOE, a set of conformers was prepared using the MMFF94x force field, followed by five rounds of extensive testing; 15,000 poses for each conformer on the receptor target (crystallographic interface between K-Ras4B with PDE6δ) were evaluated. For GOLD, 100 different runs of the Genetic Algorithm were performed and scored using both ChemPLP and Goldscore. The best results from each program were rescored using the other software to compare the outcomes. The best overall score for each pose was selected for subsequent molecular dynamics simulations.

The molecular dynamics (MD) simulations of the wild-type and mutated K-Ras4BWT/PDE6δ–ligand complexes in the presence of C14 and P8 poses with the best binding scores predicted through docking studies were performed using MOE. For the K-Ras4BWT/PDE6δ–ligand complex, a periodic rectangular-shaped box of 48.7 × 73.1 × 60.9 Å was used with TIP3P water model (38–41). Cl^- and Na^+ ions for the protein–ligand system were placed in the model to neutralize the positive or negative charges around the complex at pH 7. Before the MD simulation, the system was minimized through 3,000 steps of steepest descent minimization, followed by 3,000 steps of conjugate gradient minimization. Then, the systems were heated from 0 K to 310 K during 500 picoseconds (ps) of MD with position restraints under an NVT ensemble. Subsequent isothermal, isobaric ensemble (NPT) of MD was carried out for 500 ps to adjust the solvent density followed by 600 ps of constant pressure equilibration at 310 K using the SHAKE algorithm (42) on hydrogen atoms, Langevin dynamics for temperature control, and a 12-Å cutoff for Van der Waals interactions. The equilibration run was followed by 100-ns-long MD simulations without position restraints under periodic boundary conditions using an NPT ensemble at 310 K. The particle mesh Ewald method was utilized to describe the electrostatic term (43). Temperature and pressure were preserved using the weak coupling algorithm (44) with coupling constants τT and τP of 1.0 ps and 0.2 ps, respectively (310 K, 1 atm). The time of the MD simulation was set to 2.0 femtoseconds, and the SHAKE algorithm (42) was used to constrain bond lengths at their equilibrium values. Coordinates were saved for analyses every 50 ps. AmberTools14 was used to examine the MD runs and clustering analysis to identify the most populated conformations during the equilibrated simulation time.

2.2 Calculation of binding free energies

Binding free energies were calculated using the molecular mechanics with a generalized Born and surface area (MMGBSA) approach (45–47) provided in the AMber16 suite (40). A total of 500 snapshots were chosen at time intervals of 100 ps from the last 50 ns of MD simulation using a concentration of 0.1 M and the generalized Born (GB) implicit solvent model (48). The binding free energy of the protein–ligand system was determined as follows:

$$\Delta G_{bind} = \Delta G_{system} - \Delta G_{receptor} - \Delta G_{ligand} \quad (1)$$

$$\Delta G_{bind} = \Delta E_{forcedield} + \Delta G_{solvation} - T\Delta S \quad (2)$$

$\Delta E_{forcefield}$ represents the molecular mechanical force field's total energy, including the electrostatic (ΔEele) and van der Waals (ΔEvdw) interaction energies. $\Delta G_{solvation}$ is the free desolvation energy price upon complex formation estimated from the GB implicit model and solvent-accessible surface area (SASA) calculations yielding ΔGele,sol, and ΔGnpol,sol. TΔS is the solute entropy arising from structural changes in the free solutes' degrees of freedom when forming the protein–ligand complex.

Binding free energies along with their constituent energy components are presented for the complexes based on initially docked conformations, expressed in kcal/mol. The breakdown includes polar contributions (ΔEpolar = ΔEele + ΔGele,sol) and non-polar contributions (ΔEnon-polar = ΔEvwd + ΔGnpol,sol). All energy values have been averaged over 500 snapshots, obtained at 100-ps intervals during the concluding 50 ns of the MD simulations. The average standard error in ΔG_{bind} amounts to 9 kcal/mol.

2.3 Cell culture

The human mammary cancer cell line MDA-MB-231 [HTB-26, American Type Culture Collection (ATCC) (Manassas, VA, USA)] was employed as TNBC cells. In this case, this cell line was selected.

MCF-7 [HTB-22, ATCC] as luminal A model and MCF-10A [CRL-10317, ATCC] as non-tumoral cells. All of them were purchased from the ATCC (Manassas, VA, USA). MDA-MB-231 cells were cultured in Leibovitz's medium supplemented with antibiotics and 10% fetal calf serum (FCS) (Invitrogen, Carlsbad, CA, USA). MCF-7 was cultured in Dulbecco's modified Eagle's medium (DMEM) (Invitrogen) also supplemented with 10% FCS and a mix of antibiotics. MCF-10A was cultivated in DMEM/F12 (Invitrogen) cell media, supplemented with 10% fetal bovine serum (FBS) and a mix of antibiotics. Finally, as radioresistant TNBC cells, the cell line MDA-MB-231RR was employed, which was kindly donated by Professor Elena Arechaga-Ocampo and grown as previously reported (34). All the cell lines were maintained under growth conditions at 37°C and 5% CO_2 in a humidified atmosphere and used between 5 and 10 passage numbers.

2.4 Microscopy assays

Structural characteristics of the cellular models employed were evaluated by confocal microscopy of the F-actin arrangement following the procedure described elsewhere (49). In brief, cells were cultured on coverslips for 24 h. Then, F-actin was stained with phalloidin-rhodamine (Invitrogen) as described above, mounted on slides, and covered with Vectashield as an antifade mounting medium (Invitrogen). All the samples were then visualized in an A1 confocal microscope (NIKON, Tokyo, Japan) at 580-nm excitation and 604-nm emission (50).

2.5 Sequencing of exon 2 of *KRAS* gene

To verify the presence of the mutation c.38G>A in the exon number 2 of *kras* gene, genomic DNA (gDNA) was extracted from MCF-10A, MDA-MB-231, and MDA-MB-231RR cell lines and sequenced. gDNA was purified using the GenElute Mammalian

Genomic DNA (gDNA) miniprep kit (Sigma-Aldrich, St. Louis, MO, USA). Subsequently, quantification of each gDNA sample was performed using NanoDrop 2000 equipment (Thermo Fisher Scientific, Waltham, MA, USA). Then, the integrity of each genomic DNA sample was verified by agarose gel electrophoresis. Both strands of the exon 2 of *kras* gene were sequenced with approximately 60 ng of gDNA as a template and the BigDye Terminator v3.1 Cycle Sequencing Kit (Thermo Fisher Scientific) according to the provider's instructions. The following specific oligonucleotides (10 pM/µl) were employed for this purpose (NCBI Reference Sequence: NM_004985.5):

Forward: RASO1 5′-AAGGCCTGCTGAAAATGAC-3′,

Reverse: RASA2 5′-TGGTCCTGCACCAGTAATATG-3.

Electropherograms obtained were verified using the software ChromasPro 1.7.7 (51).

2.6 Wound-healing migration assay

To determine the cell migration ability of MCF-10A, MDA-MB-231, and MDA-MB-231RR cell lines, wound-healing migration assays were performed. In brief, every cell line was seeded into 6-well culture plates (Corning, New York, NY, USA) and cultured in a medium containing 10% FBS until confluent. Then, a wound was made on the cell monolayer by scratching it with a sterile 200-µl micropipette tip. Any cellular debris that was present was removed by washing with phosphate-buffered saline (PBS). Cells were allowed to migrate at 37°C in 5% CO_2. Images of the wounded areas were taken at 0, 2, 4, and 6 h using a Leica epifluorescence microscope, with a 10× objective (Leica, Wetzlar, Germany). All experiments were performed in triplicate incubations. The images were analyzed with the aid of Leica software (Leica) (52).

2.7 Invasion assay

The invasion ability of MCF-10A, MDA-MB-231, and MDA-MB-231RR cells was evaluated by invasion of Transwell chambers coated with Basement Membrane Matrix Growth Factor Reduce Matrigel (Corning). MCF-10A, MDA-MB-231, and MDA-MB-231RR cells were seeded in the upper chamber of the Transwell at 250,000 cells/100 µl in serum-free media. In the lower chamber, 10% FBS was added as a chemoattractant. As a control, chambers without FCS were employed. Under all conditions, the cells were allowed to migrate to the lower chamber for 24 h at 37°C in 5% CO_2 (53). Each condition was performed in triplicate. After this time of incubation, the non-migrated cells on the upper side of the porous membrane were removed using a cotton swab soaked with PBS. The cells that migrated across the porous membrane were fixed using 4% paraformaldehyde (PFA) and then stained with 0.1% Giemsa stain for cell counting using a Leica epifluorescence microscope with 10× objective (Leica). Afterward, the dye retained in the insert was extracted and transferred to a 96-well microtiter plate to be measured at 560 nm (54).

2.8 Quantitative pseudopodia assay

The number of cellular extensions present in MCF-10A, MDA-MB-231, and MDA-MB-231-RR cells was studied using the Chemicon Quantitative Pseudopodia Assay Kit (Corning). This system allows the insolation and quantification of extending or retracting pseudopodia from the cell body. In brief, porous membranes of Pseudopodia Quantification Inserts were coated with a Basement Membrane Matrix Growth Factor Reduce Matrigel (Corning). Later, the coated plates were incubated for 2 h to allow the gel to polymerize. Then, in the upper chamber of the inserts, 250,000 cells/100 µl of MCF-10A, MDA-MB-231, and MDA-MB-231RR were seeded in serum-free media. In the lower chamber of the inserts, 10% FBS was added as a chemoattractant. As a negative control, cells without chemoattractant were employed. All the samples were maintained for 2 h of incubation to leave an extension of pseudopodia through the pores of the membrane. At the end of the time, every insert was rinsed twice with 1× PBS, and the cell body was removed from the upper membrane surface by wiping with cotton. The cells that extend pseudopodia across the porous membrane were fixed with 4% PFA and then stained with Pseudopodia Stain Solution (Corning). Then, each insert was rinsed with water, and stained Pseudopodia was eluted with Stain Extraction Buffer (Corning). Eluted samples were measured at O.D. 600 nm in a microplate Synergy-HTX microplate reader (BioTek, Winooski, VT, USA). Each condition was performed in triplicate (55).

2.9 Cell viability assay and IC50 determination

In order to evaluate the effect of the C14 and P8 compounds over MCF-10A, MCF-7, MDA-MB-231, and MCF-MB-231-RR cell lines, the IC50 of those molecules was determined. In brief, all the cell lines were seeded at a density of 15,000 cells per well in a 96-well microtiter plate (Corning) in a corresponding growth medium for 24 h. Then, cells were treated with increasing concentrations (from 0 to 200 µM) of the C14 and P8 compounds (Enamine, Kyiv, Ukraine). As a positive control, increased concentrations of cisplatin (from 0 to 200 µM) (Accord, Mexico City, Mexico) were employed. Due to that, dimethyl sulfoxide (DMSO) was used as a vehicle, and its increased concentrations were evaluated as the negative control. All the samples were maintained under growth conditions for 24 h and 48 h. At the end of each time, cell viability was determined using the XTT Cell Proliferation Kit II (Roche Applied Science, Mannheim, Germany) following the manufacturer's protocol. The absorbance was measured in a spectrophotometer Synergy-HTX (BioTek) at a wavelength of 450–500 nm with a reference wavelength of 650 nm. Cell proliferation was expressed as a percentage of viability [(absorbance of treated cells/absorbance of untreated cells × 100)] ± SD. All the assays were performed in triplicate, and

IC50 values for 24 h (IC50-24) and 48 h (IC50-48) of each sample were calculated using the Prism 8 software (GraphPad, La Jolla, CA, USA).

2.10 Apoptosis assay

To determine if the C14 and P8 compounds were able to evoke cell death by apoptosis or necrosis, cell lines MCF-10A, MDA-MB-231, and MDA-MB-231RR were treated at IC50-24 for 24 h. Apoptosis and necrosis were determined using the Apoptosis/Necrosis Detection kit (Abcam, Cambridge, UK) according to the manufacturer's instructions. In brief, approximately 500,000 cells were seeded in 6-well plates (Corning) for 24 h. Then, each cell line was treated with the respective IC50-24 concentrations of C14 and P8. As positive controls, 100 μM cisplatin and 0.5 μM doxorubicin were used as the compounds for 24 h. Cells were harvested and collected by centrifugation. All the samples were analyzed in triplicate using flow cytometry equipment FACSCalibur instrument (BD Biosciences, San Jose, CA, USA) at 530-nm excitation and 575-nm emission. Data analysis was performed using the FlowJo software (Tree Star Inc., Ashland, OR, USA). All experiments were performed in triplicate.

2.11 Clonogenic assay

The principal aim of a clonogenic assay is to evaluate the effect of chemotherapy agents or new drugs by the measurement of their ability to arrest tumor cell division and their ability to develop new colonies after their exposure to these new drugs (56). Therefore, the colony formation ability of the cell lines MCF-10A, MDA-MB-231, and MDA-MB-231RR was evaluated after their exposure to the C14 and P8 compounds. In brief, breast cancer cell lines were cultured in 6-well plates (Corning), seeding 300 cells per well, and incubated at 37°C in 5% CO_2 for 24 h. Compounds C14 and P8 were added at the maximum evaluated concentration IC50-48. As controls, cells without treatment and cells treated in the presence of a vehicle (DMSO at 0.66%) were employed (Sigma-Aldrich). As a positive control, cells treated with conventional chemotherapeutic agents cisplatin (100 μM) and doxorubicin (0.5 μM) were employed. After 10 days of treatment, cells were fixed with 4% PFA and stained with 0.1% crystal violet in citric acid (Sigma-Aldrich) for 15 minutes. Subsequently, the dye present in the cells was extracted using isopropanol and read at 570 nm in a Synergy-HTX microplate reader (BioTek). Each test was performed in triplicate. Data were expressed as % colonies relative to the untreated control (56).

2.12 Ras activation assay

The inactivation of Ras by the C14 and P8 compounds, cisplatin, and doxorubicin was determined by pull-down assays using a Ras activation assay Biochem kit (Cytoskeleton, Denver, CO, USA). The cells were serum-starved for 16 h and pre-treated with C14 and P8 at IC50-48H concentration for 3 h or cisplatin and doxorubicin for 3 h. Subsequently, the cells were stimulated with epidermal growth factor (EGF) (100 ng/ml) for 10 minutes. Lysates (1 mg/ml) were exposed to Ras GTP-binding protein (Raf-RBD), following the manufacturer's instructions. Experiments for each cell type and condition were repeated three times.

2.13 Western blotting assays

To determine the effect of the C14 and P8 compounds over the protein effectors of K-Ras4B, AKT, and ERK, immunoblotting assays were conducted with specific antibodies. In brief, MCF-10A, MDA-MB-231, and MDA-MB-231RR cells were plated in 100-mm culture dishes until 80% of confluents. Cell adhesion was allowed for 24 h. Later, cells were serum-starved for 16 h to be sequentially pre-treated with the IC50-48 of C14 and P8 for 3 h. Additionally, cells were exposed to cisplatin (100 μM) and doxorubicin (0.5 μM) for 3 h. After pre-treatment, cells were stimulated with 100 ng/ml EGF for 10 minutes to promote AKT and ERK activation. Later, the whole-cell extracts were obtained by the lysis of the cells (Cytoskeleton) in the presence of proteases and phosphatase inhibitors. Subsequently, the protein extracts were incubated at 4°C for 40 minutes to be clarified by centrifugation for 10 minutes at 14,000 rpm, at 4°C. The protein concentration of each extract was determined by using the Precision Red Advanced Protein Assay Reagent (Cytoskeleton) Then, approximately 25 μg of protein extract was electrophoresed in 10% sodium dodecyl sulfate–polyacrylamide gel electrophoresis (SDS-PAGE) and transferred to polyvinylidene fluoride (PVDF) membranes (Millipore, Billerica, MA, USA). Blots were probed using the following primary antibodies: Total ERK (Cell Signaling, Danvers, MA, USA), pERK (Cell Signaling), Total AKT (Cell Signaling), pAKT (Cell Signaling), GSK3β (Cell Signaling), and cyclin D1 (Abcam) at a 1:1,000 dilution. As a control, an anti-GAPDH antibody (GeneTex, Irvine, CA, USA) was employed at a 1:100,000 dilution and γ-Tubulin (Invitrogen) 1:5,000. Densitometric analysis of blots was performed using the software ImageJ version 1.45 (National Institutes of Health, Bethesda, MA, USA).

2.14 Cell cycle analysis

MCF-10A, MDA-MB-231, and MDA-MB-231RR cells (1×10^6 cells/well) were either untreated (control group) or treated with C14, P8, cisplatin, and doxorubicin at IC50-48H dose for 3 h. After 3-h incubation, cells were harvested, washed twice in ice-cold PBS, and fixed overnight in 70% ethanol at 4°C. Then, cells were washed in PBS, collected by centrifugation, and stained with staining buffer (PBS with 50 μg/ml propidium iodide and 100 μg/ml RNase A).

2.15 Treatment of orthotopic breast carcinoma xenografts

Female immune-deficient Nu/Nu nude mice at 6–8 weeks of age (CINVESTAV, Mexico City, Mexico) were maintained in

pathogen-free conditions with irradiated chow. The animals were subcutaneously injected in the left 4th mammary gland with 2 × 106 MDA-MB-231RR cells per tumor in 0.1 ml of sterile phosphate-buffered saline. When MDA-MB-231RR cells reached palpable tumors (≥100 mm^3), mice were divided randomly into four groups receiving vehicle (10% DMSO, 0.05% carboxy methyl cellulose, and 0.02% in PBS) (n = 5), C14 at 30 mg/kg (n = 5), P8 at 10 mg/kg (n = 5), or cisplatin at 6 mg/kg (n = 5) intraperitoneally injected daily for 15 days. Body weight and tumor volume were measured every third day. Tumor sizes were calculated using the formula [(length × width2)/2] in mm.

2.16 Immunohistochemistry assays and digital pathology analysis

To determine the impact of C14 and P8 drugs on tumor inhibition, angiogenic, and cell cycle markers in a xenograft model, immunohistochemical assays and digital pathological analysis were conducted. For tissue preparation, 4-µm-thick tumor sections underwent a series of preparations: i) deparaffinization in xylene, ii) antigen retrieval in a sodium citrate buffer at pH 6, iii) blocking of endogenous peroxidase activity using a 10% hydrogen peroxide solution, and iv) non-specific binding blockade for 1 h. For the antibody incubation, the tumor sections were incubated with primary antibodies: Anti-Cyclin D1 (Abcam), Anti-PCNA (Abcam), Anti-CD31 (Abcam), Anti-VEGF (Abcam) at a 1:500 dilution.

The incubation with primary antibodies occurred at room temperature overnight. Subsequently, secondary antibody incubation was conducted. Then, the sections were incubated with horseradish peroxidase (HRP)-conjugated secondary antibody for 30 minutes. Finally, visualization and staining were performed using a diaminobenzidine (DAB) detection system from Vector Laboratories, Inc. (Burlingame, CA, USA). Counterstaining was performed using hematoxylin.

For the mitotic index evaluation, hematoxylin and eosin (H&E) staining was conducted to calculate the mitotic index. From each H&E-stained tumor tissue, 10 random fields were captured at ×40 magnification, and the number of mitotic figures was counted. The average count was used to calculate the mitotic index using the following formula: Mitotic index = Number of mitoses/10.

For digital pathology analysis, the immunohistochemistry (IHC)-stained sections were digitized using an Aperio ScanScope CS2 from Leica Biosystems (Nussloch, Germany), which generated high-resolution ×20 digital images (0.45 µm/pixel). These images were analyzed using ImageScope (Aperio, San Diego, CA, USA) to quantify marker expression. Then, a quantification algorithm was developed for each tissue to assess total and nuclear protein expression. The ImageScope allowed setting thresholds for color saturation and defining upper and lower limits for intensities of weak, moderate, and strong positive pixels. Lastly, the raw data encompassed the number of positive pixels and the intensity of positive pixels, which were normalized to the number of total pixels counted in $µm^2$. Data were presented as total density per $µm^2$.

2.17 Statistical analysis

All data were analyzed using Prism 8 software (GraphPad). Likewise, all of them were expressed as the mean ± standard deviation (SD). Experimental points were gathered for a minimum of three independent experiments. An unpaired Student's t-test was used for the comparison of two groups. A value of $p< 0.05$ was considered significant.

3 Results

3.1 P8 stabilizes the K-Ras4B^{G13D}/PDE6δ system more effectively than C14

As previously shown by our research group, the C14 and P8 compounds belong to the family of molecules that are able to specifically bind to and stabilize the mutated complex of K-Ras4B^{mut}/PDE6δ in G12C, G12V, and G12D K-Ras4B mutant pancreatic cell lines, disrupting its localization, activation, and inhibition of oncogenic Ras signaling in pancreatic cancer cells (33). For this reason, we evaluated if these compounds were also capable of stabilizing the complex formed by the exclusive mutant form of K-Ras4B reported in breast cancer K-Ras4B^{G13D} and this membrane transporter PDE6δ (K-Ras4B^{G13D}/PDE6δ) to inhibit its oncogenic activity.

To evaluate the ability of C14 and P8 to stabilize the mutated complex K-Ras4B^{G13D}/PDE6δ, docking and MD simulations were performed. The lowest binding free energy poses of C14 and P8 within the K-Ras4B^{G13D}–PDE6δ-HVR2 system, which were predicted through docking studies, were used as starting conformers to run 100-ns-long MD simulations. Representative protein-ligand conformations were obtained over the equilibrated simulation time (last 50 ns) using clustering analysis. Structural analysis of the representative conformations showed that C14 within the K-Ras4B^{G13D}–PDE6δ-HVR2 system was bound through hydrophobic interactions by five residues from K-Ras4B^{G13D} (R41, I36, Y64, Y40, and M67) and PDE6δ (F96, F94, F92, L108, and F91) (Figure 1A; Supplementary Table 1). P8 within the K-Ras4B^{G13D}–PDE6δ-HVR2 complex was stabilized through non-polar interactions by the same five residues of K-Ras4B^{G13D} (Supplementary Table 1) observed for the C14 compound and five residues of PDE6δ (F96, F94, F92, L108, and Q106) (Figure 1B; Supplementary Table 1). These results show that both compounds interact with the same amino acid residues, which suggests that the simultaneous binding of the two compounds could indicate a competitive interaction with the K-Ras4B^{G13D} mutant complex. This competition for the binding site was also verified by synergic assay where the cytotoxic effect of both compounds was almost additive but not synergic.

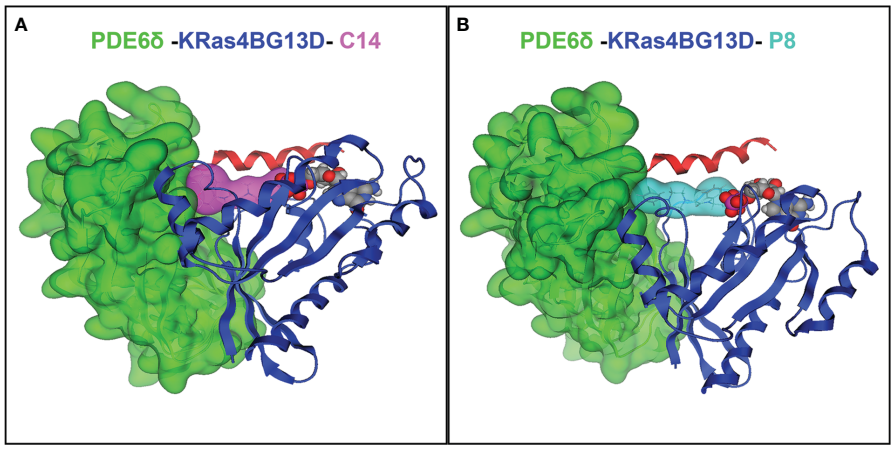

FIGURE 1
Protein–ligand interactions between compounds C14 and P8 and the K-Ras4B^{G13D}–PDE6δ-HVR2 system. **(A)** Complex of K-Ras4B^{G13D}/PDE6δ-HVR2 and C14. **(B)** Complex of K-Ras4B^{G13D}/PDE6δ-HVR2 and P8. The interaction energy between PDE6δ protein and the GTPase K-Ras4B^{G13D} in the complex increases due to the action of compounds C14 and P8. K-Ras4B^{G13D} is shown in blue, PDE6δ-HVR2 protein in green, C14 in purple, and P8 in cyan. Position of GDP nucleotide in the complex (spheres in red, gray, and purple) is observed in the images.

Based on free energy (ΔGbind) data calculated using Equations 1 and 2, for free K-Ras4B^{G13D}/PDE6δ-HVR2, this energy was increased in complexes that contain C14 or P8. Table 1 shows that all the complexes exhibited favorable ΔGbind values, where the non-polar (ΔEnon-polar = ΔEvwd + ΔGnpol,sol) contributions guided the molecular recognition. The ΔGbind values also showed that K-Ras4B^{G13D}–PDE6δ binding was energetically more favorable for P8 (−497.8 kcal/mol) than for C14 (−490.2 kcal/mol). These results showed that the mutant form of KRas4B, KRas4B^{G13D}, improved its affinity for PDE6δ compared with the wild-type system from −406.9 to −484.9 kcal/mol. KRas4B^{G13D} also increased its affinity for PDE6δ when C14 or P8 stabilized the K-Ras4B^{G13D}/PDE6δ system compared with free K-Ras4B^{G13D}/PDE6δ or K-Ras4B^{WT}/PDE6δ systems (Table 1). Comparing compound C14 to P8 revealed that compound P8 may be better capable of stabilizing the K-Ras4B^{G13D}/PDE6δ system.

TABLE 1 Binding free energy components of protein–protein complexes (in kcal/mol units).

System	$\Delta E_{non\text{-}polar}$	ΔE_{polar}	ΔG_{bind}
Protein–protein free and bound wild-type and mutated K-Ras4B^{G13D}–PDE6δ			
K-Ras4B^{WT}/PDE6δ	−80.2	−326.6	**−406.9**
K-Ras4B^{G13D}/PDE6δ	−79.1	−405.8	**−484.9**
K-Ras4B^{G13D}/PDE6δ-C14	−78.8	−411.4	**−490.2**
K-Ras4B^{G13D}/PDE6δ-P8	−60.9	−437.0	**−497.8**

Binding free energies and individual energy terms of complexes starting from docked conformations (kcal/mol). The polar (ΔEpolar = ΔEele + ΔGele,sol) and non-polar (ΔEnon-polar = ΔEvwd + ΔGnpol,sol) contributions are shown. All the energies are averaged over 500 snapshots at time intervals of 100 ps from the last 50-ns-long molecular dynamics (MD) simulations and are in kcal/mol (± standard error of the mean).
The bold values signify Gibbs free energy of interaction between compounds and target proteins, indicating spontaneous interaction efficiency. Negative values indicate an energetically favorable interaction suggesting thermodynamically favorable binding, likely to occur spontaneously under given conditions.

3.2 C14 and P8 compounds decrease cellular viability of TNBC cell lines

According to these results, C14 and P8 may have a cytotoxic effect on breast cancer cells. To validate this hypothesis, we evaluated the effect of both molecules in the cell lines MCF-10A as a control and MDA-MB-231 as TNBC cells that naturally express the mutant form K-Ras4B^{G13D}. TNBC K-Ras mutant has a high propensity for developing resistance to radiation therapy. This resistance often leads to increased cancer recurrence and more aggressive behavior. By using a radioresistant cell line MDA-MB-231RR, we simulated the clinical challenges of treating radioresistant breast cancer, which is crucial for assessing the effectiveness of potential therapeutic agents. We verified the presence of K-Ras4B^{WT} in MCF-10A and MCF-7 as well as K-Ras4B^{G13D} in MDA-MB-231 and MDA-MB-231RR by sequencing of exon 2 (Supplementary Figure 2).

First, we validated the oncogenic potential of the radioresistant cells as a suitable model. The results demonstrated that these cells exhibited a notably high migration and invasion capability (Supplementary Figure 3). Additionally, the radioresistant cells displayed a significantly higher migration velocity compared to their parental counterparts, indicating their heightened aggressiveness (Supplementary Figure 3). Likewise, MDA-MB-231 displayed a spindle-like, metastatic appearance with stress fibers, while MDA-MB-231RR differed by less stress fibers and exhibited numerous vacuoles or villi (Supplementary Figure 4). Thus, these findings establish MDA-MB-231RR cells as a model for radioresistant-TNBC with a heightened oncogenic potential and confirm their preservation of typical markers from their parental cell lineage.

To determine whether C14 and P8 have a cytotoxic effect on breast cancer cell lines, an XTT assay was employed under experimental conditions for 24 h and 48 h. Antiproliferative effects of both compounds on MDA-MB-231 and MDA-MB-

231RR cell lines were clearly observed. In contrast, a diminished cytotoxic effect was observed in the non-tumoral MCF-10A cell line (Figure 2A–C). Likewise, the IC50 values obtained for this cell line were greater than 200 μM at 24 h and 48 h post-treatment. According to statistical analyses using the "Sidak Bonferroni-type multiple comparisons" and "Multiple t-tests Holm–Sidak method", concentrations higher than 100 μM and 150 μM are required to observe any effect of the compounds on cell viability in the control cells for C14 and P8, respectively. In comparison, in the TNBC and radioresistant TNBC cell lines, the compounds began to affect their viability at concentrations starting from 10 μM at 48 h. This suggests that C14 and P8 would not significantly reduce the viability of the non-tumoral cell line (Figure 2A).

In contrast, a significant cytotoxic effect of both compounds was observed on MDA-MB-231 (Figure 2B). Significance was noted from concentrations as low as 10 μM compared to the vehicle (DMSO) at 48 h. A similar pattern was observed in the radioresistant MDA-MB-231RR cell line, where the compounds exhibited a significant inhibitory effect on viability at 48 h, starting from 10 μM and 30 μM for P8 and C14, respectively (Figure 2C). Based on this information, C14 and P8 are able to promote diminution in cell viability of tumoral cells. The aforementioned statistical analyses suggested that the compounds demonstrate greater efficacy against triple-negative breast cancer cell lines with KRAS mutations compared to the non-tumorigenic control line. The improved effect of both compounds for the K-Ras4B^{MUT} form could be explained based on the more favorable ΔGbind values observed for the K-Ras4B^{G13D}/PDE6δ complex. These data propose a preferential impact on aggressive breast cancer cells over non-tumoral cells.

To demonstrate the specific effects of C14 and P8 on cells expressing K-Ras4B^{G13D}, their cytotoxic effect was assessed on the MCF-7 cell line, which expresses the wild-type form of K-Ras4B (27) (Figure 2D). The cytotoxic effect of C14 and P8 on MCF-10A, MDA-MB-231, MDA-MB-231RR, and MCF-7 cell lines was represented by the corresponding IC50 values (Table 2). As observed for MCF-10A cells, there was no significant effect on cell viability by both molecules (C14, IC50-48: 310.2 ± 210.0 μM; P8, IC50-48: 907.1 ± 291.0 μM) (Table 2). This result suggests that the compounds did not affect the growth of non-tumoral breast cells. However, in these control cells, the chemotherapeutic agent cisplatin reduced cellular viability by more than 90% at low concentrations (IC50-48: 5.9 ± 1.6 μM) (Table 2).

In contrast, a cytotoxic effect of both compounds was observed in the triple-negative line MDA-MB-231. The IC50-48H values of 60.0 ± 6.6 μM and 63.2 ± 10.6 μM for C14 and P8, respectively, underscored their similar efficacy in suppressing TNBC cell viability (Table 2). This contrasted with cisplatin, for which an IC50-48 value nearly 40-fold higher was required when compared to MCF-10A cells (296.8 ± 34.8 μM) to achieve a comparable effect (Table 2). Likewise, the radioresistant MDA-MB-231RR cell line exhibited a comparable response to compound C14 with calculated IC50-48 values of 70.6 ± 3.5 μM (Table 2). In the case of P8, there was an effective response but with a higher IC50-48, which was 156.4 ± 28.4

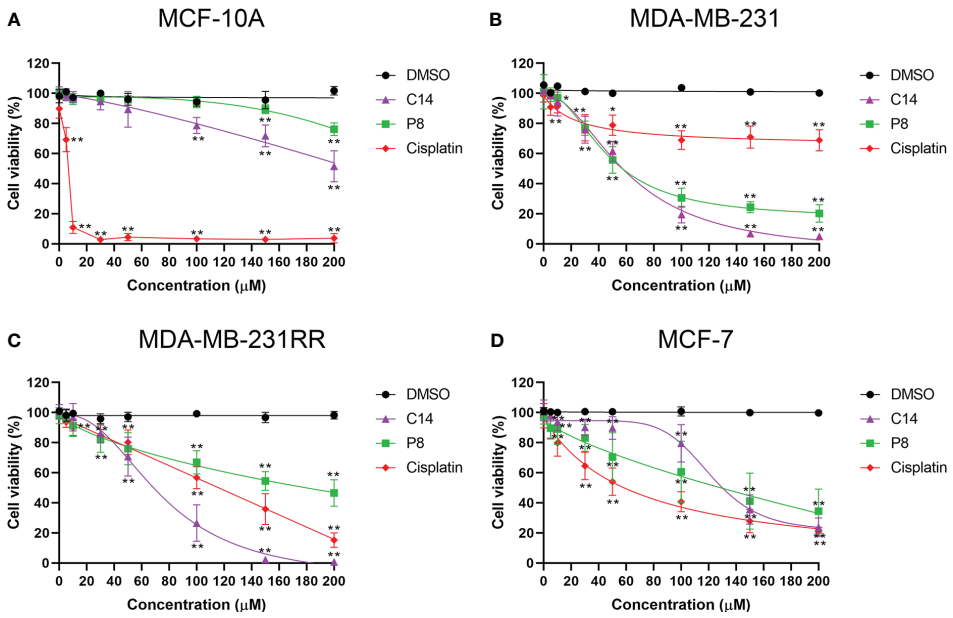

FIGURE 2
Compounds C14 and P8 decrease the cellular viability of breast cancer cells that express K-Ras4B^{G13D}. **(A)** Dose–response curve of non-tumor MCF-10A cells treated with increasing concentrations of C14 and P8 compounds. **(B)** Dose–response curve of K-Ras4B^{G13D} in MDA-MB-231 cells treated with increasing concentrations of C14 and P8 compounds. **(C)** Dose–response curve of radioresistant MDA-MB-231RR cells treated with increasing concentrations of C14 and P8 compounds. **(D)** Dose–response curve of no mutant *KRAS* MCF-7 cells treated with increasing concentrations of C14 and P8 compounds. Concentration–response curves were evaluated after 48 h of exposure with increasing concentrations of C14 and P8 (0 to 200 μM) and show normalized percent activity for the individual doses. Cisplatin (0 to 200 μM) was used as a control, and maximal concentration of the vehicle (dimethyl sulfoxide (DMSO)) was evaluated. The line graph represents the mean means ± SEM from three independent experiments (*p< 0.05, **p< 0.01 compared to vehicle).

TABLE 2 IC50 values were calculated for several compounds in each cell line.

Compound	MCF-10A	MDA-MB-231	MDA-MB-231RR	MCF-7
IC50-24 (μM)				
C14	591.4 ± 210.0	91.1 ± 3.9	128.2 ± 2.6	174.2 ± 19.0
P8	1,146.8 ± 291.0	140.1 ± 33.5	163.3 ± 16.8	185.3 ± 15.3
Cisplatin	12.0 ± 0.0	352.1 ± 41.2	200.0 ± 0.0	150.3 ± 32.1
IC50-48 (μM)				
C14	310.2 ± 10.6	60.0 ± 6.6	70.6 ± 3.5	134.5 ± 10.5
P8	907.1 ± 219.2	63.2 ± 10.6	156.4 ± 28.4	103.6 ± 49.8
Cisplatin	5.9 ± 1.6	296.8 ± 34.8	103.6 ± 8.7	67.3 ± 20.6

IC50 values for 24 h (IC50-24) and 48 h (IC50-48) of each sample were calculated and shown in μM ± standard deviation of the mean.

μM (Table 2). Notably, the IC50-48 value for cisplatin, when evaluated in this context, was 103.6 ± 8.7 μM. Thus, these findings underscore the potential of C14 and P8 in both the parental and radioresistant TNBC cell lines. Their lower IC50-48 values compared to cisplatin suggest their promising role in addressing the challenges posed by drug resistance in TNBC treatment.

In comparison with cells that expressed the mutant form of KRAS gene, a major concentration of C14 was necessary to impact the cell viability of MCF-7 cells. The IC50-48 values obtained for this cell line were 134.5 ± 10.5 μM for C14 and 103.6 ± 49.8 μM for P8 (Table 2). It is important to note that despite this cell line being $KRAS^{wt}$, a cytotoxic effect was observed, but the IC50-48 values were slightly higher than those obtained for mutant cell lines. Finally, MCF-7 cells exhibited more sensitivity to cisplatin with an IC50-48 value of 67.3 ± 20.6 μM (Table 2). Thus, our findings demonstrate that C14 and P8 have the potential to reduce the viability of breast cancer cell lines, with their primary efficacy against triple-negative and radioresistant cells and especially against the K-Ras4B mutant variants.

3.3 C14 and P8 compounds induce apoptosis in breast cancer cell lines

Mechanisms underlying these cytotoxic effects observed in TNBC and radioresistant cell lines were further investigated by flow cytometric assays by determination of percentage (%) of apoptosis cells (Annexin V) or % of necrosis (propidium iodide) following exposure to C14 and P8 being quantified employing the IC50-24 of each compound (Figure 3A). MDA-MB-231 cells showed that compound C14 promoted cell death *via* apoptosis in up to 18.52% of cells, with a minimal necrotic effect at 0.56%. Remarkably, P8 demonstrated even greater apoptotic potential, inducing cell death through apoptosis in 48.5% of cells and necrosis in 4.28% of the same cell line. In comparison, the chemotherapeutic agents cisplatin and doxorubicin promoted cell death *via* apoptosis in a lower percentage, 13.71% and 4.65% of cells, and greater necrosis in 2.14% and 9.20% of cells, respectively, compared to C14 and P8 (Figure 3C).

In the case of the MDA-MB-231RR cell line, C14 promoted cell death primarily through apoptosis in up to 21.62% of cells, with a minimal necrosis of only 0.13%. Compound P8 exhibited a remarkable capability to induce apoptosis in 72% of cells, while necrosis was observed in 1.75% of cells. Conversely, cisplatin induced apoptosis in up to 19.13% of cells, with necrosis in 0.40% of cells. Notably, the efficacy of doxorubicin was limited in radioresistant cells, inducing apoptosis in only 0.61% of cells and necrosis in 1.28% of cells (Figure 3D). According to these data, C14 and P8 reduced the growth of aggressive and radioresistant breast cancer cells, with a strong emphasis on apoptosis as the primary mode of action (57).

In contrast, neither C14 nor P8 induced significant cell death in normal breast MCF-10A cells, with viability at 91.1% and 94.3%, respectively. Conversely, cisplatin promoted apoptosis in over 70% and 5.46% of necrosis in normal breast cells. Doxorubicin also exhibited potent cytotoxic effects, leading to apoptotic cell death in up to 11.54% of cells and a necrotic cell death rate of 5.46% (Figure 3B).

These compelling findings not only reaffirm the cytotoxic potential of C14 and P8 but also shed light on their distinctive mechanisms of action. Particularly, P8 emerges as an inductor of apoptosis, an important pathway in the field of targeted cancer therapy. This revelation not only underscores the promise of C14 and P8 but also adds a significant dimension to their potential therapeutic applications, particularly in the challenging context of radioresistant cancer cells.

3.4 C14 and P8 compounds inhibit colony formation of breast cancer cell line

To assess the presence of cells capable of maintaining their proliferative capacity as colonies following exposure to the C14 and P8 compounds, clonogenic assays were conducted. After a period of 10 to 12 days, it was evident that in the case of MCF-10A, both compounds were not able to significantly impact the rate of growth of these non-tumoral cells. Specifically, C14 reduced the growth of 14% of colonies, and P8 reduced the growth of 48% of colonies (Figure 4A). Cisplatin significantly reduced the growth of 95% of

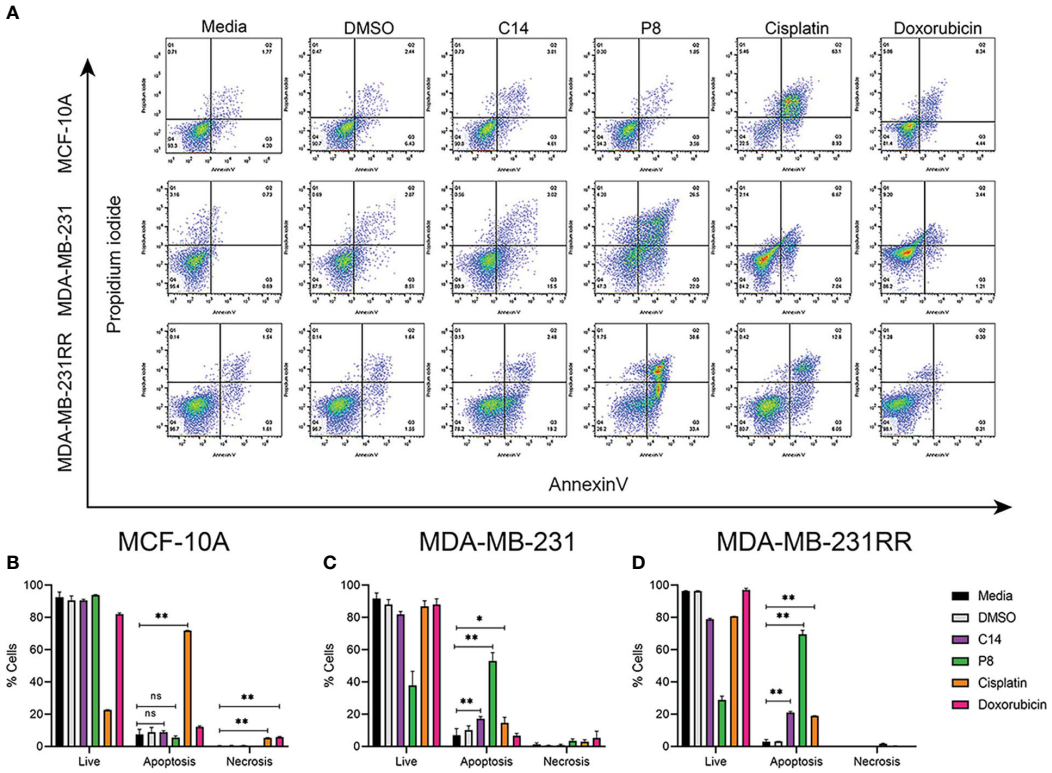

FIGURE 3
C14 and P8 compounds induce apoptosis in breast cancer cell lines. **(A)** Flow cytometric analysis diagram of compounds C14 and P8 for MCF-10A, MDA-MB-231, and MDA-MB-231RR cell lines. Evaluation of apoptosis/necrosis rate was conducted in a 24-h incubation period of compounds C14 and P8 at IC50-24 concentrations and Annexin V−propidium iodide staining. Cells kept in a growth medium or presence of vehicle (dimethyl sulfoxide (DMSO)) were included as control. Chemotherapeutic agents, 100 μM cisplatin and 0.5 μM doxorubicin for 24 h, were included as positive controls. **(B)** Graphical representation of percentage of live cells, apoptotic cells, and necrotic cells of MCF-10A in each condition. **(C)** Graphical representation of percentage of live cells, apoptotic cells, and necrotic cells of MDA-MB-231 in each condition. **(D)** Graphical representation of percentage of live cells, apoptotic cells, and necrotic cells of MDA-MB-231RR in each condition. Graphed results are means ± SEM from three independent experiments (*p< 0.05, **p< 0.01 compared to vehicle).; ns, not significant.

colonies, while doxorubicin reduced the growth of up to 90% of colonies (Figure 4B).

In the case of MDA-MB-231 cells, both C14 and P8 led to an important decrease in colony formation, with reductions of up to 95% observed (Figure 4B). As expected, conventional chemotherapeutic agents, cisplatin and doxorubicin, were able to induce a significant reduction of colony growth (Figure 4B). Notably, P8 demonstrated a potent inhibitory effect on colony formation in MDA-MB-231-RR, with a reduction of up to 99%. In the case of C14, an inhibitory effect on colony formation with a reduction of up to 90% was observed in MDA-MB-231-RR cells (Figure 4C). Likewise, cisplatin (99% reduction in colony formation) and doxorubicin (90% reduction in colony formation) were both able to reduce colony growth (Figure 4C). In summary, the P8 compound efficiently inhibited colony formation in both MDA-MB-231 and the radioresistant cells, MDA-MB-231-RR. Although the C14 compound was effective against MDA-MB-231, nearly 10% of MDA-MB-231-RR colonies persisted.

These results highlight the significant implications of treatment-resistant cells, where C14 and P8 were effective in reducing colony formation in MDA-MB-231, particularly P8, which was the most effective in radioresistant MDA-MB-231-RR cells. In contrast, no significant impact was observed in MCF-10A with the C14 compound. However, P8 exhibited a 40% reduction in colony formation in this cell line. While this effect is less pronounced compared to its impact on cancer cell lines, it may be attributed to the intrinsic chemical characteristics of P8 within the complex K-Ras4B/PDE6δ that make it, in general, a more potent compound.

3.5 Significant reduction in Ras activation observed in the presence of compounds C14 and P8

To further validate whether the specific impact of compounds C14 and P8 on TNBC and radioresistant cell lines is mediated through the reduction of Ras protein activation, pull-down assays were conducted within breast cancer cell lines, as illustrated in Figure 5.

In the MCF-10A cell line, exposure to C14 and P8 resulted in a reduction in Ras-GTP by approximately 40% (Figure 5A). In this

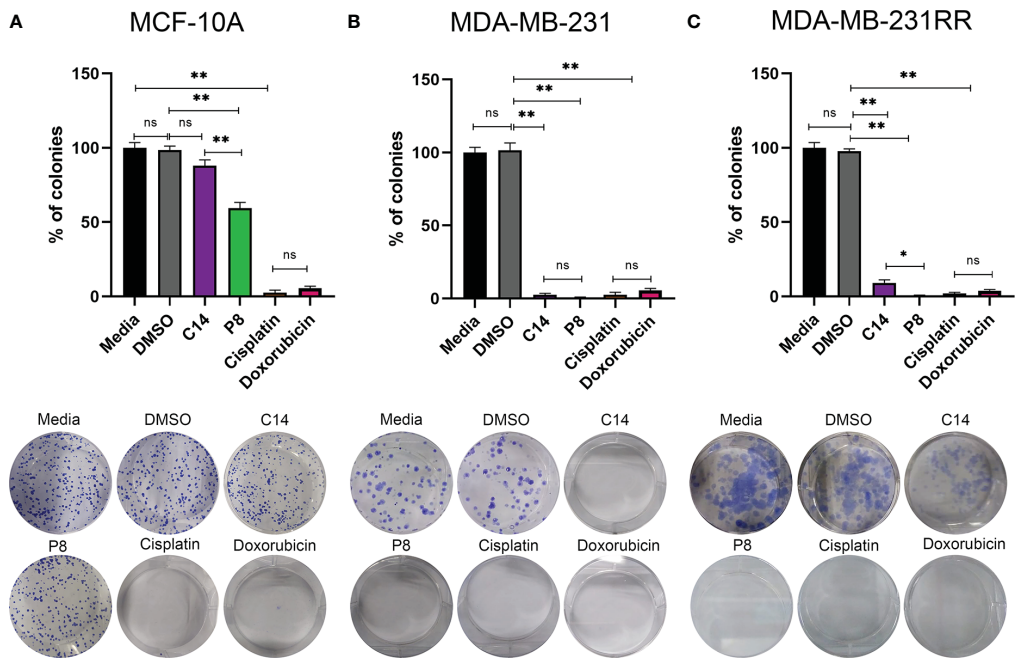

FIGURE 4
P8 inhibits the colony formation capability of triple-negative breast cancer (TNBC) and radioresistant cells. **(A)** Colony formation of MCF-10A cells after exposure to C14 and P8 compounds at IC50-48 value for 10 to 12 days. **(B)** Colony formation of MDA-MB-231 cells after exposure to C14 and P8 compounds at IC50-48 for 10 to 12 days. **(C)** Colony formation of MDA-MB-231RR cells after exposure to C14 and P8 compounds at IC50-48 for 10 to 12 days. Cells without treatment and cells treated with vehicle (dimethyl sulfoxide (DMSO) at 0.66%) were employed as controls. Cells treated with chemotherapeutic agents, 100 μM cisplatin and 0.5 μM doxorubicin, were employed as positive control. Bar charts show the percentage of counted colonies relative to control untreated cells and represent the means ± SEM of three independent experiments (*p< 0.05, **p< 0.01 versus control cells).; ns, not significant.

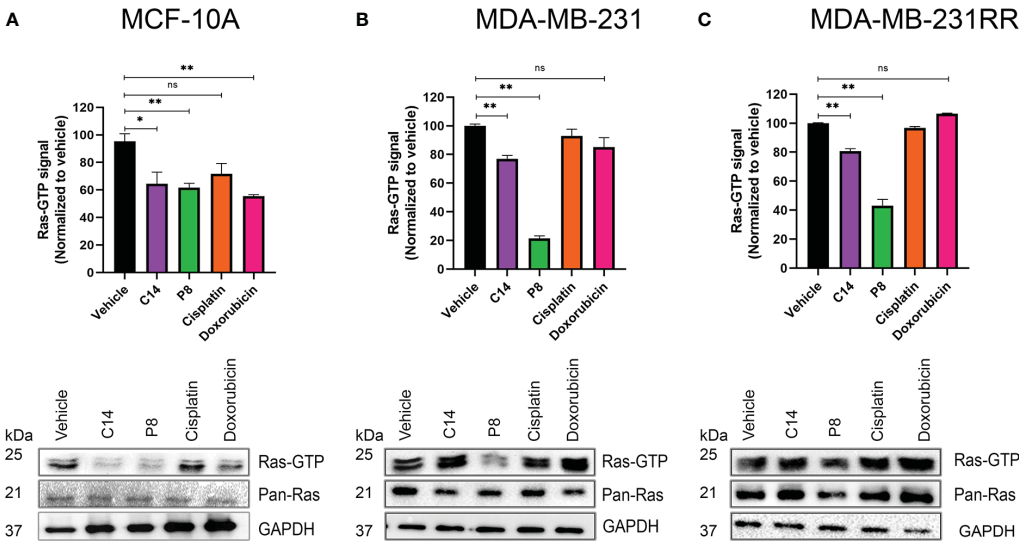

FIGURE 5
Amount of active Ras after cell exposure with C14 and P8. **(A)** MCF-10A cells that express the wild-type isoform of K-RAS4B. **(B)** MDA-MB-231 cells that express the mutant form K-Ras4B^{G13D} were treated with C14 and P8 for 3 h. **(C)** MDA-MB-231RR cells were also observed to have an important reduction of bound-GTP form of Ras, principally with P8 molecule. Dimethyl sulfoxide (DMSO) was employed as vehicle, and cisplatin and doxorubicin were employed as negative controls. Graphics represent the quantitative analysis of three independent assays. In blots, GAPDH was employed as loading control. Graphed results are means ± SEM from three independent experiments (*p< 0.05, **p< 0.01 compared to vehicle).; ns, not significant.

case, also the compound doxorubicin reduced the amount of Ras-GTP by 40%, probably by a non-specific cell death effect. In contrast, cisplatin did not show an effect. Likewise, although the presence of C14 did not lead to a notable reduction in Ras-GTP levels (20%), compound P8 caused a dramatic reduction of over 80% in MDA-MB-231 cells (Figure 5B). These effects persisted in the radioresistant cells, with a decrease of approximately 20% in Ras-GTP levels with C14 and a more significant reduction of over 60% with P8 (Figure 5C).

According to the data shown, compounds C14 and P8 have an effect on the MCF-10A line at short exposure times (3 h). The reduction in K-Ras-GTP activity could be a result of the low activity levels of this molecule in non-tumor cells. On the contrary, compound C14 did not show a substantial effect on K-Ras activity in MDA-MB-231 and MDA-MB-231RR. This apparent lower effectiveness could be explained by two aspects: the abundant activity levels of this GTPase in cancer cell lines and the short exposure time to the compounds. Probably, C14 requires longer periods of time to affect its target. In the case of P8, a potent reduction in Ras-GTP levels is observed in both tumoral cell lines. This could be because this molecule exhibits a more powerful effect in a short time due to its chemical characteristics.

3.6 Compounds C14 and P8 decrease Ras activity and inhibit AKT and ERK phosphorylation in MDA-MB-231 and MDA-MB-231RR cells

Furthermore, it has been widely reported that molecules downstream of K-Ras4B, such as pAKT and pERK, are related to the signaling pathways involved in cell survival and differentiation. In order to ascertain whether the effect of the C14 and P8 compounds on the Ras activation negatively impacts the activation of critical downstream molecules regulated by K-Ras4B^{G13D}, the levels of pAKT and pERK activation in MCF-10A, MDA-MB-231, and MDA-MB-231RR cells were determined by Western blotting (Figure 6). Densitometric analysis of the blots revealed in the graph that in MCF-10A, there was a reduction in the phosphorylation levels of pERK (40%) and pAKT (25%) after exposure to C14 and P8 (Figure 6A, upper and middle panel). In MDA-MB-231, C14 and P8 exhibited a significant impact by diminishing pERK up to 70% with both compounds (Figure 6B, middle panel). Likewise, there was a substantial reduction in the levels of pAKT in these cells treated with P8 (up to 70%) and C14 (up to 60%) (Figure 6B, upper panel). In MDA-MB-231-RR cells,

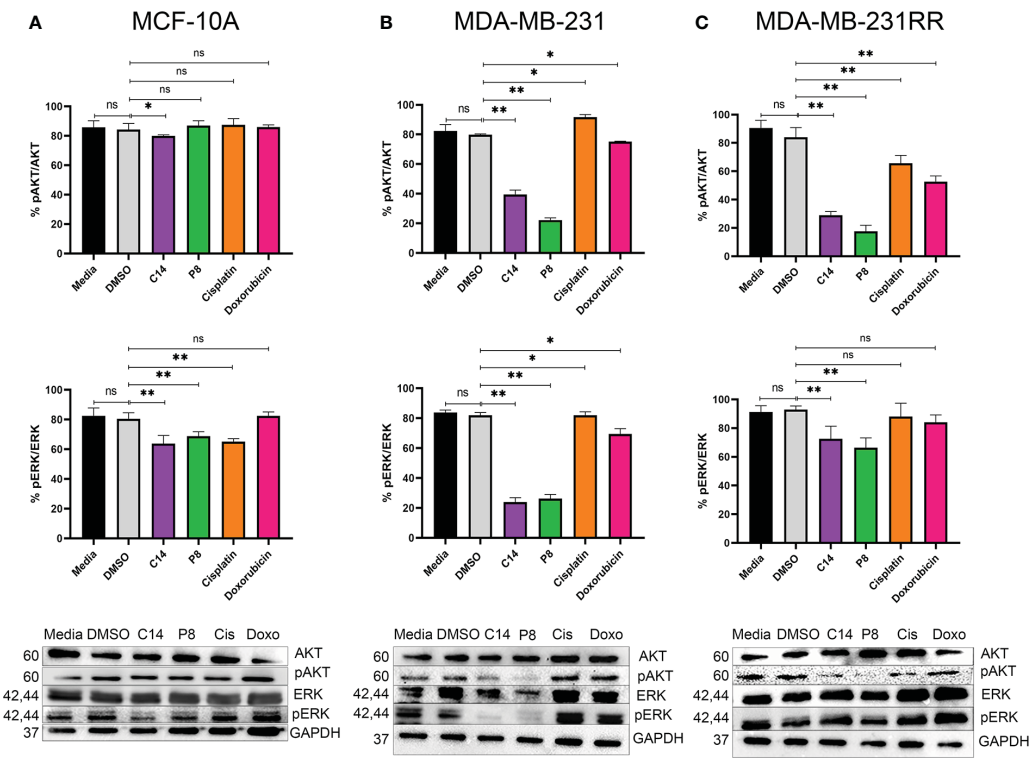

FIGURE 6
Compounds C14 and P8, decrease AKT and ERK phosphorylation. **(A)** Representative immunoblots of whole protein extracts from MCF-10A, plotted against total AKT and ERK proteins and phosphorylated AKT and ERK forms. **(B)** Representative immunoblots of whole protein extracts from MDA-MB-231, plotted against total AKT and ERK proteins and phosphorylated AKT and ERK forms. **(C)** Representative immunoblots of whole protein extracts from MDA-MB-231RR, plotted against total AKT and ERK proteins and phosphorylated AKT and ERK forms. Cells were treated with C14 and P8 at IC50-48, Cisplatin at 100 μM and Doxorubicin at 0.5 μM for 3 h. Cells kept in growth media or media plus vehicle (DMSO), were employed as control. After pre-treatment, cells were stimulated with 100 ng/ml EGF for 10 minutes to promote AKT and ERK activation. GAPDH was plotted with specific antibodies as control. Graphed results are means ± SEM from three independent experiments of pAKT and pERK (*$p < 0.05$, **$p < 0.01$ compared to vehicle).; ns, not significant.

C14 induced a reduction of approximately 30% in pERK, while a 35% reduction in pERK was observed with P8 (Figure 6C, middle panel). However, there was a marked reduction in pAKT levels with both compounds (>70%) (Figure 6C, upper panel).

These findings demonstrate that C14 and P8 reduce the activity of signaling pathways regulated by K-Ras, primarily *via* pAKT, in tumoral and radioresistant breast cancer cell lines. In the case of MDA-MB-231, there was a clear reduction in pERK after exposure to C14 and P8. Conversely, a non-clear effect was observed in MDA-MB-231RR, likely due to its more aggressive genotype. However, the clear impact of both compounds on pAKT suggests their potential use as therapeutic options against TNBC and radioresistant TNBC.

3.7 Radioresistant-related signaling pathway effect and induction of cell cycle arrest in human radioresistant breast cancer cells by compounds

To determine the effects observed of compounds C14 and P8 on the AKT activation on radioresistant cells, the pathway associated with cell proliferation *via* K-Ras4B negatively impacts the radiation resistance acquisition pathways regulated by this kinase, particularly the AKT/GSK3β/cyclin D1 pathway. The protein levels of cyclin D1 and Glycogen Synthase Kinase-3β (GSK3β) were evaluated in MCF-10A, MDA-MB-231, and radioresistant MDA-MB-231RR cell lines.

This method was adopted, considering that human tumor cells develop radioresistance when exposed to fractionated X-ray radiation (FR) (34, 58). Likewise, during this process, cyclin D1 is overexpressed to potentially enhance tumor cell proliferation (59). Densitometric analysis of blots showed that in MCF-10A, there was a 40% reduction in cyclin D1 protein after exposure to C14 and P8, compared to controls (media and DMSO) and chemotherapeutic agents (cisplatin and doxorubicin) (Figure 7A, upper panel). In MDA-MB-231, both molecules reduced the expression of cyclin D1 by 20%. There was no significant effect in controls and doxorubicin. On the contrary, cisplatin reduced the expression of cyclin D1 by 10% (Figure 7B, upper panel). In radioresistant MDA-MB-231-RR cells, there was a significant reduction in cyclin D1 with the C14 compounds (40%). However, P8 diminished the expression of cyclin D1 by 18%. Finally, cisplatin and doxorubicin reduced the presence of cyclin D1 by 20% (Figure 7C, upper panel). According to the results, cyclin D1 levels in tumoral cells were consistently higher than those observed in control cells, and both compounds showed a potent effect. This difference could be attributed to the elevated levels of cyclin D1 in tumor cell lines (60).

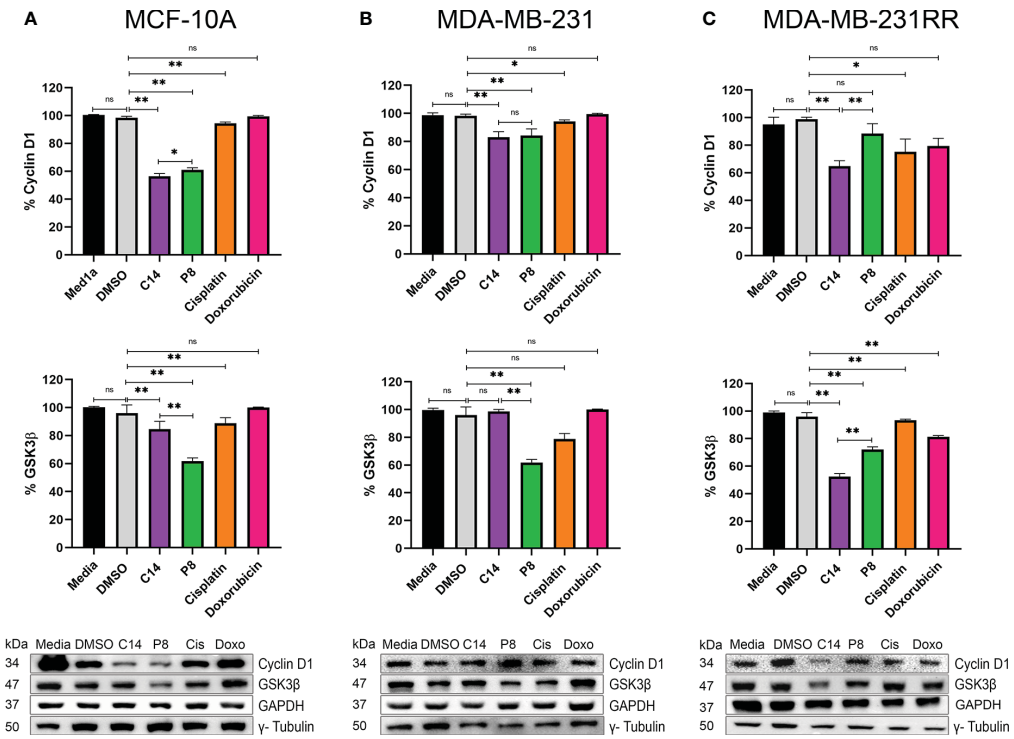

FIGURE 7
Compounds C14 and P8, decrease GSK3β and Cyclin D1. **(A)** Representative immunoblots of whole protein extracts from MCF-10A, plotted against total Cyclin D1 and GSK3β proteins. **(B)** Representative immunoblots of whole protein extracts from MDA-MB-231, plotted against total Cyclin D1 and GSK3β proteins. **(C)** Representative immunoblots of whole protein extracts from MDA-MB-231RR, plotted against total Cyclin D1 and GSK3β proteins. Cells were treated with C14 and P8 at IC50-24, Cisplatin at 100 μM and Doxorubicin at 0.5 μM for 3 h. GAPDH and γ- Tubulin was plotted with specific antibodies as loading control. Quantitative representation of 3 independent immunoblots studies, are shown in the upper and middle graphs, respectively. Graphed results are means ± SEM from three independent experiments of pAKT and pERK (*p < 0.05, **p < 0.01 compared to vehicle).; ns, not significant.

In contrast, although the impact of ionizing radiation on GSK3β is multifaceted, it could be associated with the expression of cyclin D1 (61). In this case, administration of C14 in MCF-10A reduced the amount of GSK3β by 10%. By P8, the reduction was 40% (Figure 7A, middle panel). By MDA-MB-231, C14 did not show an effect on this molecule. In contrast, in this cell line, the P8 compound reduced the expression of GSK3β principally by 40% (Figure 7B, middle panel). Finally, in MDA-MB-231RR, P8 and C14 respectively reduced 25% and 50% the expression of GSK3β (Figure 7C, middle panel). These data suggest that in MDA-MB-231RR cells, C14 principally inhibits the effect of GSK3β/cyclin D1 molecules probably *via* AKT. However, these aspects must be studied in greater depth.

To investigate the mechanism behind the anticancer activity of C14 and P8 and their increased sensitivity in radioresistant breast cancer cells, we analyzed the cell cycle distribution using flow cytometry. As shown in Figure 8, the majority of MCF-10A control cells remained in the G1 phase even after treatments (Figures 8A, B). Treatment with doxorubicin and cisplatin showed a similar number of cells arrested in the S phase (Figures 8A, B). Additionally, we observed that most of the MDA-MB-231 cells were arrested in the G0/G1 phase compared to the control (Figures 8A, C). The percentage of cells in G2/M decreased from 10.0% to 6.4% and 8.2% after treatment with C14 and P8, respectively, but increased after treatment with doxorubicin (Figures 8B, D). MDA-MB-231RR cells were also arrested in the G0/G1 phase compared to the control after treatment and exhibited a decrease in the S phase from 35.6% to 20.7% and 26.4% after treatment with C14 and P8, respectively (Figures 8C, D). Notably, there were no significant changes in the G2/M phase of the MDA-MB-231RR cells following treatment. Additionally, a slight increase in apoptotic cells was observed in the RT group compared to the control.

The arrest of TNBC and radioresistant TNBC cells in the G0/G1 phase and the reduction of cells in the S phase following treatment with the C14 and P8 compounds, principally in the context of MDA-MB-231RR, imply a disruption in the cell cycle progression. It is a mechanism often targeted in cancer therapy to inhibit the uncontrolled growth of cancer cells particularly concerning treatment-resistant cells.

3.8 Inhibition of tumor growth in a radioresistant breast cancer xenograft mouse model by compounds C14 and P8

Based on the effectiveness of C14 and P8 obtained *in vitro*, specifically the reduction in the proliferation and growth of radioresistant cells, the antitumor activity of both molecules was evaluated using an *in vivo* model. To accomplish this, highly aggressive radioresistant cancer cells, MDA-MB-231 RR, were subcutaneously inoculated into female Nu/Nu mice to closely monitor tumor growth. The different treatments were administered *via* intraperitoneal (i.p.) injection daily for 2 weeks

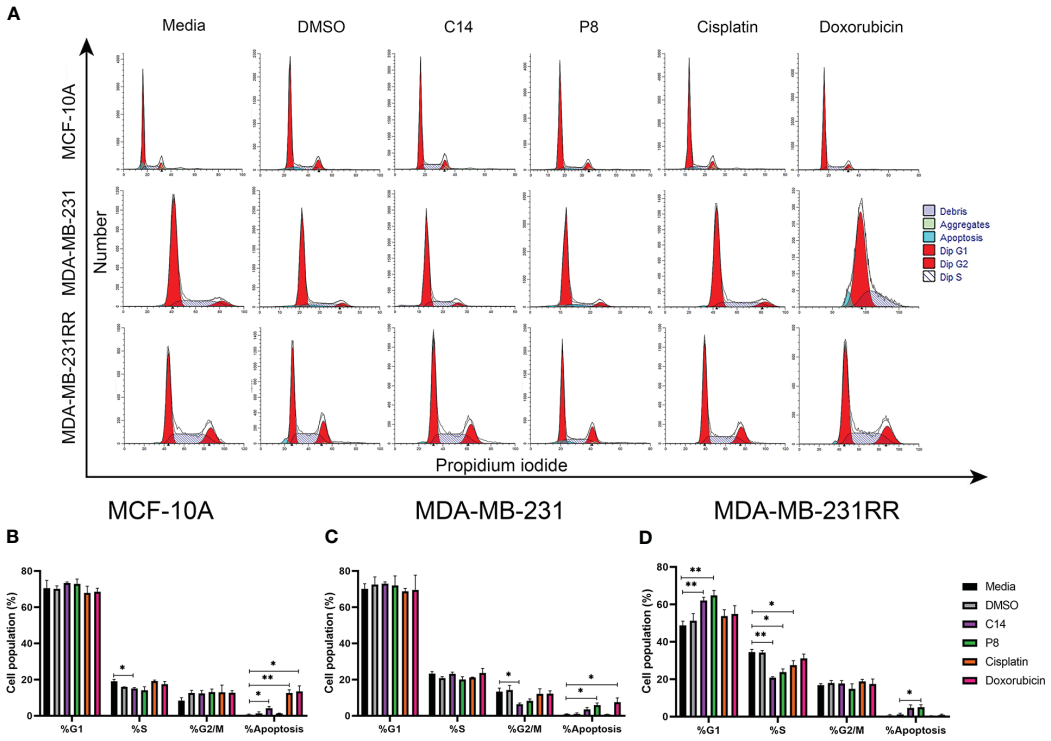

FIGURE 8
Compounds induced G0/G1 cell cycle arrest and apoptosis in radioresistant cells. **(A)** A representative histogram of propidium iodide (PI) staining in breast cancer (BC) cells. **(B)** MCF-10A cell population proportion in each cell cycle phase. **(C)** MDA-MB-23 cell population proportion in each cell cycle phase. **(D)** MDA-MB-231RR cell population proportion in each cell cycle phase. After 3 h of treatment with C14, P8, cisplatin, and doxorubicin. Graphed results are means ± SEM from three independent experiments of pAKT and pERK (*$p< 0.05$, **$p< 0.01$ compared to media).

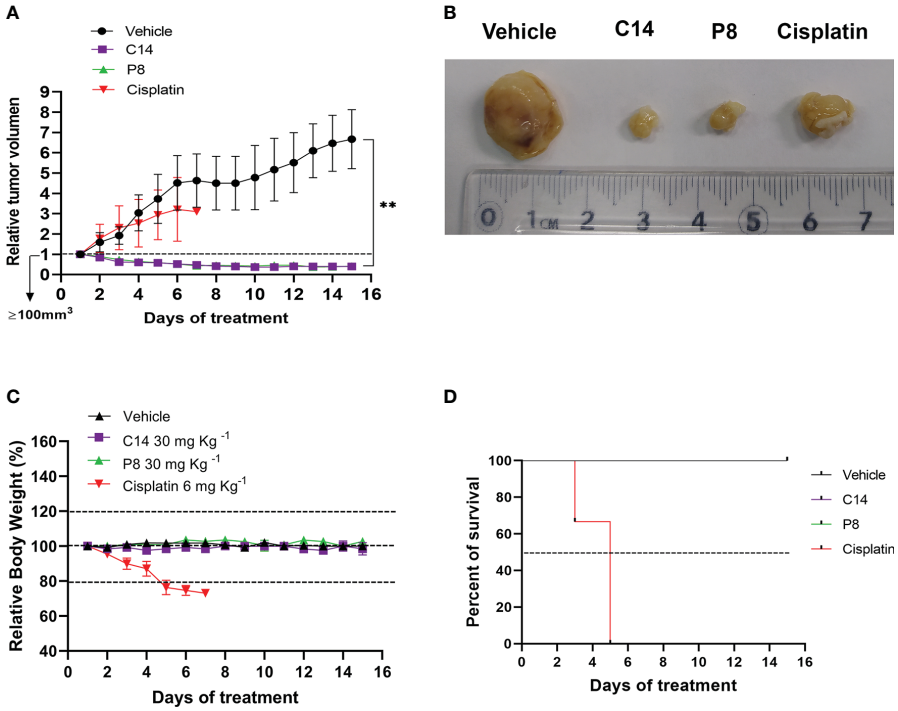

FIGURE 9
Inhibition of tumor growth by compounds C14 and P8 in a xenograft model of radioresistant MDA-MB-231RR cells. **(A)** The relative tumor volume was evaluated over a 15-day treatment period. **(B)** Representative images depicting tumor sizes. **(C)** Body weight measurements of mice were recorded during the treatment period. Nu/Nu mice were treated with the following: vehicle (10% dimethyl sulfoxide (DMSO) and 0.05% carboxy methyl cellulose), C14 and P8 at 30 mg/kg, or cisplatin at 6 mg/kg, administered daily by intraperitoneal injection (n = 5 for DMSO, n = 5 for C14, n = 5 for P8, and n = 5 for cisplatin). Changes in tumor volume are given in relation to the initial volume before treatment (the dotted line indicates the initial size of the tumor ~100 mm^3). **(D)** Survival curve throughout the treatment period. Mice treated with cisplatin at 6 mg/kg did not survive beyond 6 days. The line graph represents the mean and SD (**$p< 0.01$).

(Figure 9A). The results showed a 40.0% reduction in tumor size in mice treated with compound C14 and a 41.6% reduction in those treated with P8. It is crucial to note that these treatments, administered at 30 mg/kg, were well tolerated by the mice, with no weight loss or impact on their overall survival rates observed. Conversely, mice treated with cisplatin (6 mg/kg) experienced over a 20% weight decrease within the first 5 days of treatment, necessitating ethical considerations for the wellbeing of the animals in this group (Figures 9C, D). All data emphasized not only the non-toxic nature of compounds C14 and P8 but also their specific anti-neoplastic effects, especially against breast cancer cells inhibiting tumor growth (Figures 9A, B). Likewise, it highlights the specific effect of these compounds over radioresistant cells.

3.9 Inhibition of proliferation and expression of CD31 by compounds C14 and P8 in a radioresistant TNBC mouse model

According to the data presented above, C14 and P8 have shown effects on cell cycle progression by inducing arrest in the G0/G1 phase. To comprehensively evaluate and support these observations, various markers of proliferation and angiogenesis were assessed using an *in vivo* model through microphotography of IHC of tumor samples (Figure 10). To enhance the quality of the analysis of the images, a digital pathology system was employed. With this system, it was possible to evaluate the expression of proliferation and angiogenesis markers with transparency and consistency. The digital pathological analysis of immunostainings demonstrated the reduction in proliferation markers, indicated by a lower mitotic index in the H&E staining in both C14 and P8 treatment groups when compared to the control group (Figure 10A). Likewise, C14 promotes the inhibition of cyclin D1 (8 μm^2), PCNA (10 μm^2), and VEGF (100 μm^2), highlighting its potential in reducing key markers associated with DNA synthesis during replication and the control of cell cycle progression for proliferation (62). In contrast, P8 and cisplatin also reduced the expression of cyclin D1 (20 μm^2 and 25 μm^2, respectively), PCNA (18 μm^2 and 22 μm^2, respectively), and VEGF (3,000 μm^2 in both cases) (Figures 10B–D). These data support the inhibition of cell cycle progression by C14 and P8 observed in cell lines and mouse models.

Likewise, the expression of CD31, an endothelial protein related to the restoration and maintenance of blood vessels and angiogenesis, was evaluated (63). In this case, both compounds but principally P8 decreased the expression of CD31 (Figure 10E). This finding holds significance, as CD31 plays a crucial role in the formation of fresh blood vessels and functions as an indicator of angiogenesis (64). Taken together, the outcomes indicate that

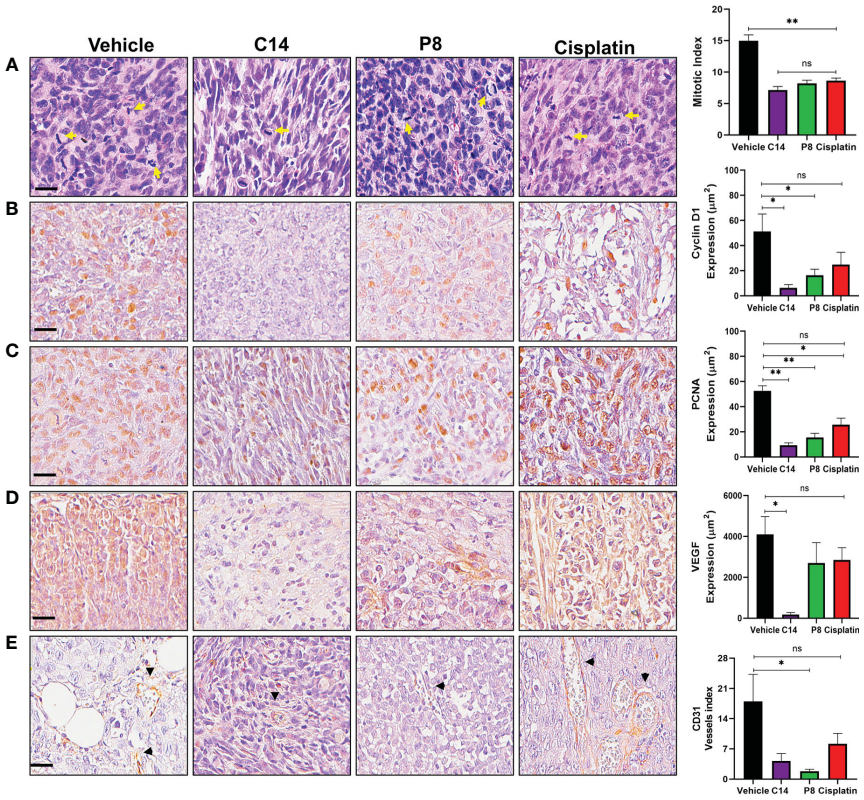

FIGURE 10
Inhibition of proliferation and angiogenesis by compounds C14 and P8 in a radioresistant triple-negative breast cancer (TNBC) mouse model. **(A)** Representative images of breast cancer tumors with H&E staining and evaluation of the mitotic index. Yellow arrows indicate cells undergoing mitosis. **(B)** Immunostaining and analysis of cyclin D1. **(C)** Immunostaining and analysis of PCNA nuclear expression. **(D)** Analysis of VEGF expression assessed *via* immunohistochemistry. **(E)** Quantification of blood vessels using CD31 immunostaining. Black arrowheads represent blood vessels. Scale bar, 20 µM. The data are presented as the mean ± SEM, n = 5 per group (*$p < 0.05$, **$p < 0.01$).; ns, not significant.

compounds C14 and P8 could reduce the expression of molecules related to the formation of new blood vessels in radioresistant TNBC. However, the specific role of both compounds during angiogenesis should be addressed more thoroughly.

4 Discussion

BC is a highly prevalent and deadly disease among women worldwide. Its aggressive nature is characterized by several clinical manifestations, high cellular diversity within tumors, and distinct gene expression patterns. As a result, numerous treatment approaches have been developed to reduce the negative effects of this complex disease. However, TNBC is of particular concern due to limited treatment options, typically limited to chemotherapy or radiotherapy, as it lacks the hormone receptors and targeted therapies effective in other breast cancer subtypes (65). This aggressive nature and resistance to therapies highlight the urgent need for ongoing research and the development of novel treatment strategies to improve outcomes for TNBC or radioresistant TNBC patients and reduce mortality.

To address this need, the focus of the present study is to evaluate the cytotoxic effects of compounds C14 and P8. As mentioned above, to the best of our group's knowledge, there is only one study reporting the specific types of K-Ras4B mutations in patients with BC (24). Also, the unique mutant form of K-Ras4B reported in cellular models of BC is G13D (27). Likewise, few reports have shown a low frequency of mutant forms of K-Ras4B in BC (7%–12%) (29). Based on this information, it is clear that there is a need to carry out a more in-depth evaluation to determine the real type and frequency of K-Ras4B mutations in BC.

To achieve our goal, the cell lines MDA-MB-231 and MDA-MB-231RR were employed. These cell lines are particularly relevant because they exhibit TNBC characteristics and express the K-Ras4B^{G13D} mutation. In this case, clear effectiveness was observed by C14 and P8 as antitumoral agents in TNBC cells that express the mutant form of G13D. This is achieved through the stabilization of the molecular complex of K-Ras4B^{G13D}/PDE6δ and the reduction of associated signaling pathways (31–33, 66).

With this information, we propose that C14 and P8 could be considered as potential therapeutic options for TNBC or for TNBC stages that develop resistance to conventional therapies, especially in cases with a poor prognosis and limited therapeutic alternatives. Additionally, we propose that the effectiveness of both compounds against TNBC is not limited to cells that express the G13D mutation. This observation is supported by previous reports in which the antitumoral effects of C14 and P8 were determined over different mutations of K-RAS4B, such as G12D, G12C, and G12V

(33). The importance of this multiple effect is clear considering the lack of information about the frequency and type of mutation of K-Ras present in TNBC.

Selectivity of C14 and P8 over the mutant forms of K-Ras4B^{G13D} was further demonstrated through *in silico* analysis. These results, as indicated by the binding free energy (ΔGbind), show that both the C14 and P8 compounds enhance the affinity of the mutated K-Ras4B^{G13D} variant for PDE6δ compared to the K-Ras4B^{wt}/PDE6δ counterpart. Furthermore, our predictive modeling indicated a greater efficiency of P8 in stabilizing the K-Ras4B^{G13D}/PDE6δ complex when compared to compound C14. This increased ability to stabilize the complex might potentially result in blocking the abnormal activation of the K-Ras4B^{G13D} signaling pathway, subsequently inducing apoptosis in breast cancer cells (67). These findings align with previous studies, demonstrating that this compound family possesses the ability to stabilize the K-Ras4B^{mut}/PDE6δ complex, irrespective of the aggressiveness state, or the development of resistance against conventional therapies. This underscores their potential for therapeutic application in advanced stages of breast cancer.

Given the distinct nature of K-Ras4B^{G13D}, characterized by heightened affinity and GDP-to-GTP exchange compared to K-Ras4B^{G12D}, where intrinsic GTPase activity remains inhibited, effectively entrapping K-Ras4B in a constitutively active state, we postulate two potential mechanisms underlying the influence of compounds on the K-Ras4B^{G13D}/PDE6δ complex. These mechanisms involve the hindrance of complex dissociation and K-Ras4B anchoring to the plasma membrane. Alternatively, due to the compounds' demonstrated affinity for both K-Ras4B protein and GDP, they might perturb the activity of guanine exchange factor (GEF) proteins, thereby impeding the GDP-to-GTP exchange process (68). In either scenario, the outcome is the inhibition of protein activation and KRAS-dependent signaling pathways through the binding of the K-Ras4B^{MUT}/PDE6δ complex with C14 or P8.

Conversely, it is noteworthy that both compounds exhibit interaction with nearly identical amino acid residues. This observation implies that concurrent administration of C14 and P8 to the complex could lead to the establishment of competitive interactions among the analyzed components. The results of the MD assay predict that the separate use of compounds C14 and P8 should independently stabilize the K-Ras4B^{G13D}/PDE6δ complex, consequently exerting a detrimental impact on the activation of K-Ras signaling pathways within mutant breast cancer cell lines.

The specificity of both compounds for the mutated K-Ras4B^{G13D}/PDE6δ complex, in comparison to the K-Ras4B^{WT}/PDE6δ counterpart, was further demonstrated by cytotoxic assays. In them, significantly higher IC50 values were observed in the non-tumoral MCF-10A cell line compared to TNBC cell lines and the radioresistant TNBC cell line, which showed reduced IC50 values.

In MDA-MB-231RR cells particularly, both molecules C14 and P8 displayed potent cytotoxic effects, indicating their potential to reduce the viability of radioresistant TNBC cell lines. This is particularly significant, considering the highly aggressive phenotype associated with the acquisition of radioresistance (69). Moreover, the unique impact of C14 and P8 on mutant TNBC cell lines compared to non-tumoral cells underscores their potential as selective anticancer treatments, minimizing side effects. In contrast, conventional chemotherapy agents displayed substantial cytotoxicity in non-tumoral cells, emphasizing the potential advantages of C14 and P8 over traditional treatments (70).

This study also validates the distinct influence of these compounds on KRas4B protein function, as evidenced by the reduction in Ras-GTP levels and GTPase effectors observed in breast cancer cells when exposed to C14 and P8. The binding to K-Ras^{G13D}/PDE6δ reduces the activation of Ras proteins, making these compounds good candidates for targeted therapies against breast cancer, particularly in TNBC or in patients that present resistances to conventional therapies, in which dysregulation in the Ras pathway generally occurs and plays a central role in tumorigenesis (14). Another crucial aspect to consider is the mechanism by which these compounds trigger cell death. While both C14 and P8 initiate apoptosis in the TNBC cell line and radioresistant TNBC cells, P8 demonstrates superior effectiveness as mentioned in earlier reports (33). It is also notable that these molecules show reduced necrosis and low cytotoxicity in non-tumoral cells. In contrast, conventional chemotherapy agents led to substantial cell death, including both apoptosis and necrosis, emphasizing the potential of C14 and P8 as therapies for TNBC and radioresistant cells, focusing on apoptosis-driven cell death mechanisms with minimized inflammatory effects.

The apoptosis-driven cell death mechanism elicited by C14 and P8 is associated with their negative impact on Ras activity, which directly impacted K-Ras-dependent pathways, including AKT and ERK (71). These experimental findings suggest that both compounds could be associated with survival, cell cycle progression, and cell growth in MDA-MB-231 and MDA-MB-231RR cells. Likewise, neither molecule causes reduced signaling pathway inhibition in the MCF-10A cell line. Interestingly enough, MDA-MB-231 cells presented more dependency and effectiveness at the ERK pathway, while MDA-MB-231RR presented higher dependency on the AKT pathway. Although these observations highlight the complex interplay between these compounds and the signaling pathways within different cellular contexts, it is important to mention that both molecules do not lose their effectiveness as antitumor agents in advanced stages of breast cancer.

The administration of C14 and P8 resulted in the observed loss of clonogenic capability in MDA-MB-231 cells. Nonetheless, MDA-MB-231RR cells presented a low grade of resistance against C14 but not P8. This observation is important considering that MDA-MB-231RR is a radioresistant cell line with a more aggressive phenotype, such as high proliferation rates and high migration, velocity, and invasion phenotypes. According to previous reports, exposure to ionizing radiation evokes a higher proliferation rate and chemoresistance that can also be attributed to the presence of a small population of cancer stem cells (CSCs) (69, 72). In this case, despite not quantifying the number of CSCs in MDA-MB-231RR, the small number of cells capable of surviving the administration of C14 could be attributed to this kind of cell based on the more aggressive phenotype of MDA-MB-231RR. In contrast, it is important to mention that in the case of compound P8, a total inhibition of the clonogenic capacity of the MDA-MB-231RR cell

line was observed. These data position this compound as a possible molecule capable of inhibiting the effects of CSC. However, it is important to highlight that the C14 and P8 compounds were completely effective in inhibiting the clonogenic ability of MDA-MB-231 cells. This effect could be attributed to the presence of fewer CSCs in this cell line. In conclusion, both molecules are highly effective against TNBC. However, P8 demonstrates greater potency in the context of more aggressive behavior, advanced stages, and resistance states, which could be attributed to its enhanced capability to eradicate CSC. This is associated with its high affinity to inhibit the activity of the K-Ras4B^{G13D}/PDE6δ complex.

According to the information presented in Figures 7C and 10B, C14 reduces the amount of GSK3β/cyclin D1. In this case, it is proposed that this effect is attributable to the inhibition in the activity of the K-Ras4B^{G13D}/PDE6δ complex and its molecular effector AKT. The reduction in this signaling pathway has a direct impact on the acquisition of a radioresistant phenotype. In this context, reports have shown that a fraction dose of ionizing radiation leads to radioresistance. A similar protocol was applied for established long-term FR cells MDA-MB-231RR (34). Thus, the acquired radioresistant phenotype is long-lasting and possibly irreversible as a result of the constitutive activation of AKT/GSK3β/cyclin D1/Cdk4 pathway, which is induced by a positive feedback loop mediated through the cyclin D1 overexpression, which triggers the development of radioresistance in tumor cells (58). Considering this information, it is suggested that C14 could reduce the activity of the AKT/GSK3β/cyclin D1 axis and potentially prevent the acquisition of radioresistance when it is administered before radiotherapy. This hypothesis requires more comprehensive evaluations.

Additionally, cell cycle analysis revealed the impact of the C14 and P8 compounds on the G0/G1 phase. The C14 compound was effective in inhibiting the progression of the S phase, resulting in the inhibition of cell growth and the induction of apoptosis in radioresistant breast cancer cells. Conversely, treatment with P8 resulted in a substantial increase in the number of cells in the G0/G1 phase and a concurrent decrease in the number of cells in the S phase in MDA-MB-231RR cells. These observations highlight the distinctive roles of C14 and P8 in influencing the cell cycle dynamics of breast cancer cells, particularly in the context of radioresistant cells.

Taking into consideration the limited therapeutic alternatives available for TNBC patients who have developed radioresistance, and in addition to the data that have demonstrated compounds C14 and P8 as antitumor molecules, their efficiency was evaluated in an *in vivo* model. The model employed involved female Nu/Nu mice and radioresistant MDA-MB-231RR cells to induce tumors. The treatments with C14 and P8 showed a significant reduction in tumor size, with a 40.0% reduction in C14-treated mice and a 41.6% reduction in P8-treated mice. Importantly, these treatments were well-tolerated and non-toxic, in contrast to cisplatin, which induced significant weight loss. These results underscore the non-toxic nature of C14 and P8 and emphasize their specific antineoplastic properties against breast cancer cells, especially radioresistant cells.

To verify the effects of the C14 and P8 compounds on cell progression in *in vitro* models, the mitotic index was determined in *in vivo* models through H&E staining. This analysis showed that the administration of C14 and P8 resulted in a significant reduction in cell proliferation of radioresistant TNBC cells, supporting the findings observed in *in vitro* models. These results were confirmed by observing a significant reduction in the expression of cyclin D1 and PCNA, which are essential regulators of the cell cycle. Likewise, C14 and P8 were found to influence angiogenesis-related biomarkers, specifically VEGF and CD31, in radioresistant TNBC tumors. A decrease in VEGF levels was observed in the C14-treated group compared to the control. Additionally, CD31, a marker of neo-vascularization, exhibited a reduction in the P8 group. This observation opens the door to exploring the effect of both compounds during the angiogenesis process.

Finally, while the cytotoxic effects of compounds C14 and P8 in TNBC and radioresistant TNBC cells were demonstrated, there are several considerations that must be taken into account for their potential use in the clinical setting. This includes the need for extensive clinical trials to validate the efficacy and safety of these compounds in humans. Long-term studies are essential, focusing on potential resistance development, recurrent tumor growth, and the sustainability of the compounds' efficacy over extended treatment periods. Further investigation into the detailed molecular mechanisms underlying the inhibitory effects of these compounds over K-Ras4B^{G13D} is also required.

In conclusion, the present work shows a comprehensive view of the molecular changes induced by C14 and P8 in TNBC and radioresistant TNBC cells. Both molecules are effective in stabilizing and inhibiting the action of the mutant form of K-Ras4B, K-Ras4B^{G13D}, and its association with its membrane transporter, PDE6δ. The antineoplastic evaluation of these compounds demonstrates that both molecules preferentially affected K-Ras4B mutated forms. Furthermore, C14 and P8 influence critical signaling pathways related principally to cell survival and cell cycle regulation to reduce cell proliferation.

Data availability statement

The authors acknowledge that the data presented in this study must be deposited and made publicly available in an acceptable repository, prior to publication. Frontiers cannot accept an article that does not adhere to our open data policies.

Ethics statement

The animal study was approved by Ethics approval and consent to participate The Center for Research and Advanced Studies (CINVESTAV) fulfill the standards of the Mexican Official Norm (NOM-062-ZOO-1999) "Technical Specifications for the Care and Use of Laboratory Animals" based on the Guide for the Care and Use of Laboratory Animals "The Guide", 2011, NRC, USA with the Federal Register Number # BOO.02.08.01.01.0095/2014, awarded by the National Health Service, Food Safety and Quality (SENASICA) belong to the Animal Health Office of the Minister of Agriculture, Livestock, Rural Development, Fisheries and Food

(SAGARPA), an organization that verifies the state compliance of such NOM in Mexico. The Institutional Animal Care and Use Committee (IACUC) from the CINVESTAV as the regulatory office for the approval of research protocols involving the use of laboratory animals and in fulfillment of the Mexican Official Norm resolved: TO APPROVE THE FOLLOWING RESEARCH PROJECT TITLED: "EVALUATION OF COMPOUNDS C14 AND P8 IN PRECLINICAL STAGES ON MAMMOSPHERES OF RADIORESISTANT AND NON-RADIORESISTANT CELLS". ID Animal use protocol number: 0319-21. The study was conducted in accordance with the local legislation and institutional requirements.

Author contributions

DC: Conceptualization, Formal analysis, Investigation, Methodology, Writing – original draft, Writing – review & editing. AA: Formal analysis, Investigation, Methodology, Resources, Writing – review & editing. SH: Formal analysis, Methodology, Writing – review & editing. MM: Formal analysis, Methodology, Writing – review & editing. MB: Formal analysis, Methodology, Resources, Writing – review & editing. AR: Formal analysis, Investigation, Resources, Software, Writing – review & editing. EA: Investigation, Methodology, Writing – review & editing. PB: Methodology, Writing – review & editing. MM-R: Methodology, Resources, Writing – review & editing. MT: Investigation, Methodology, Resources, Writing – review & editing. RH: Formal analysis, Investigation, Methodology, Writing – review & editing. MV: Conceptualization, Formal analysis, Investigation, Methodology, Project administration, Resources, Supervision, Writing – original draft, Writing – review & editing.

Funding

The author(s) declare financial support was received for the research, authorship, and/or publication of this article. ANR-CONACyT (140364); Research and Postgraduate Secretariat of the National Polytechnic Institute (SIP-IPN 20230344).

Acknowledgments

This work was supported by the Consejo Nacional de Ciencia y Tecnología (CONACyT-México) DC-E is a postgraduate student from the Programa de Doctorado en Biomedicina Molecular, Departamento de Biomedicina Molecular, CINVESTAV, México, and received scholarship No. 935796 from CONACyT. We are also grateful for the excellent technical assistance of Ma de Jesús Almaraz Barrera and we thank veterinarian Benjamin Emmanuel Chávez Álvarez for his excellent technical assistance and help with animal care.

Conflict of interest

The authors declare that the research was conducted in the absence of any commercial or financial relationships that could be construed as a potential conflict of interest.

The author(s) declared that they were an editorial board member of Frontiers, at the time of submission. This had no impact on the peer review process and the final decision.

Publisher's note

Supplementary material

The Supplementary Material for this article can be found online at: https://www.frontiersin.org/articles/10.3389/fonc.2024.1341766/full#supplementary-material

References

1. Lei S, Zheng R, Zhang S, Wang S, Chen R, Sun K, et al. Global patterns of breast cancer incidence and mortality: A population-based cancer registry data analysis from 2000 to 2020. *Cancer Commun* (2021) 41:1183–94. doi: 10.1002/cac2.12207

2. Sung H, Ferlay J, Siegel RL, Laversanne M, Soerjomataram I, Jemal A, et al. Global cancer statistics 2020: GLOBOCAN estimates of incidence and mortality worldwide for 36 cancers in 185 countries. *CA: Cancer J Clin* (2021) 71:209–49. doi: 10.3322/caac.21660

3. Perou CM, Sorlie T, Eisen MB, van de Rijn M, Jeffrey SS, Rees CA, et al. Molecular portraits of human breast tumours. *nature* (2000) 406:747–52. doi: 10.1038/35021093

4. Foulkes WD, Smith IE, Reis-Filho JS. Triple-negative breast cancer. *N Engl J Med* (2010) 363:1938–48. doi: 10.1056/NEJMra1001389

5. Harbeck N, Penault-Llorca F, Cortes J, Gnant M, Houssami N, Poortmans P, et al. Breast cancer. *Nat Rev Dis Primers* (2019) 5:1–31. doi: 10.1038/s41572-019-0111-2

6. Dent R, Trudeau M, Pritchard KI, Hanna WM, Kahn HK, Sawka CA, et al. Triple-negative breast cancer: clinical features and patterns of recurrence. *Clin Cancer Res* (2007) 13:4429–34. doi: 10.1158/1078-0432.CCR-06-3045

7. Andreopoulou E, Kelly CM, McDaid HM. Therapeutic advances and new directions for triple-negative breast cancer. *BreastCare* (2017) 12:20–7. doi: 10.1159/000455821

8. Nedeljković M, Damjanović A. Mechanisms of chemotherapy resistance in triple-negative breast cancer—how we can rise to the challenge. *Cells* (2019) 8:957. doi: 10.3390/cells8090957

9. Lin NU, Claus E, Sohl J, Razzak AR, Arnaout A, Winer EP. Sites of distant recurrence and clinical outcomes in patients with metastatic triple-negative breast cancer: high incidence of central nervous system metastases. *Cancer* (2008) 113:2638–45. doi: 10.1002/cncr.23930

10. Dias Carvalho P, Guimaraes CF, Cardoso AP, Mendonca S, Costa AM, Oliveira MJ, et al. KRAS oncogenic signaling extends beyond cancer cells to orchestrate the microenvironment. *Cancer Res* (2018) 78:7–14. doi: 10.1158/0008-5472.CAN-17-2084

11. Balko JM, Giltnane JM, Wang K, Schwarz LJ, Young CD, Cook RS, et al. Molecular profiling of the residual disease of triple-negative breast cancers after neoadjuvant chemotherapy identifies actionable therapeutic targets. *Cancer Discovery* (2014) 4:232–45. doi: 10.1158/2159-8290.CD-13-0286

12. Chung CH, Lee J, Slebos R, Howard J, Perez J, Kang H, et al. A 3′-UTR KRAS-variant is associated with cisplatin resistance in patients with recurrent and/or metastatic head and neck squamous cell carcinoma. *Ann Oncol* (2014) 25:2230–6. doi: 10.1093/annonc/mdu367

13. Wright KL, Adams JR, Liu JC, Loch AJ, Wong RG, Jo CE, et al. Ras signaling is a key determinant for metastatic dissemination and poor survival of luminal breast cancer patients. *Cancer Res* (2015) 75:4960–72. doi: 10.1158/0008-5472.CAN-14-2992

14. Toulany M, Dittmann K, Krüger M, Baumann M, Rodemann HP. Radioresistance of K-Ras mutated human tumor cells is mediated through EGFR-dependent activation of PI3K-AKT pathway. *Radiother Oncol* (2005) 76:143–50. doi: 10.1016/j.radonc.2005.06.024

15. Poleszczuk J, Luddy K, Chen L, Lee JK, Harrison LB, Czerniecki BJ, et al. Neoadjuvant radiotherapy of early-stage breast cancer and long-term disease-free survival. *Breast Cancer Res Treat* (2017) 19:1–7. doi: 10.1186/s13058-017-0870-1

16. Jančík S, Drábek J, Radzioch D, Hajdúch M. Clinical relevance of KRAS in human cancers. *J Biomed Biotechnol Hindawi Publishing Corporation* (2010) 2010:1–13. doi: 10.1155/2010/150960

17. Santen RJ, Song RX, McPherson R, Kumar R, Adam L, Jeng M-H, et al. The role of mitogen-activated protein (MAP) kinase in breast cancer. *J Steroid Biochem Mol Biol* (2002) 80:239–56. doi: 10.1016/S0960-0760(01)00189-3

18. Karnoub AE, Weinberg RA. Ras oncogenes: split personalities. *Nat Rev Mol Cell Biol* (2008) 9:517–31. doi: 10.1038/nrm2438

19. Paranjape T, Heneghan H, Lindner R, Keane FK, Hoffman A, Hollestelle A, et al. A 3'-untranslated region KRAS variant and triple-negative breast cancer: a case-control and genetic analysis. *Lancet Oncol* (2011) 12:377–86. doi: 10.1016/S1470-2045(11)70044-4

20. Tokumaru Y, Oshi M, Katsuta E, Yan L, Satyananda V, Matsuhashi N, et al. KRAS signaling enriched triple negative breast cancer is associated with favorable tumor immune microenvironment and better survival. *Am J Cancer Res* (2020) 10:897.

21. Pilarski R, Patel DA, Weitzel J, McVeigh T, Dorairaj JJ, Heneghan HM, et al. The KRAS-variant is associated with risk of developing double primary breast and ovarian cancer. *PloS One* (2012) 7. doi: 10.1371/journal.pone.0037891

22. Chandra A, Grecco HE, Pisupati V, Perera D, Cassidy L, Skoulidis F, et al. The GDI-like solubilizing factor PDEδ sustains the spatial organization and signalling of Ras family proteins. *Nat Cell Biol* (2012) 14:148–58. doi: 10.1038/ncb2394

23. Prior IA, Lewis PD, Mattos C. A comprehensive survey of Ras mutations in cancer. *Cancer Res* (2012) 72:2457–67. doi: 10.1158/0008-5472.CAN-11-2612

24. Erdogan G, Ozcan M, Karaveli FS, Pestereli HE. KRAS, EGFR AND PIK3CA mutation in triple negative breast carcinomas. *Int J Med Res Health Sci* (2016) 5:95–104.

25. Timar J, Kashofer K. Molecular epidemiology and diagnostics of KRAS mutations in human cancer. *Cancer Metastasis Rev* (2020) 39:1029–38. doi: 10.1007/s10555-020-09915-5

26. Meng M, Zhong K, Jiang T, Liu Z, Kwan HY, Su T. The current understanding on the impact of KRAS on colorectal cancer. *Biomed Pharmacother* (2021) 140:111717. doi: 10.1016/j.biopha.2021.111717

27. Osborne CK, Hobbs K, Trent JM. Biological differences among MCF-7 human breast cancer cell lines from different laboratories. *Breast Cancer Res Treat* (1987) 9:111–21. doi: 10.1007/BF01807363

28. Huynh MV, Hobbs GA, Schaefer A, Pierobon M, Carey LM, Diehl JN, et al. Functional and biological heterogeneity of KRASQ61 mutations. *Sci Signaling* (2022) 15:eabn2694. doi: 10.1126/scisignal.abn2694

29. Kodaz H, Kostek O, Hacioglu MB, Erdogan B, Kodaz CE, Hacibekiroglu I, et al. Frequency of Ras mutations (Kras, Nras, Hras) in human solid cancer. *Breast Cancer* (2017) 7:1–7. doi: 10.14744/ejmo.2017.22931

30. Prior IA, Hood FE, Hartley JL. The frequency of Ras mutations in cancer. *Cancer Res* (2020) 80:2969–74. doi: 10.1158/0008-5472.CAN-19-3682

31. Casique-Aguirre D, Briseno-Diaz P, Garcia-Gutierrez P, la Rosa CHG, Quintero-Barceinas RS, Rojo-Dominguez A, et al. KRas4B-PDE6delta complex stabilization by small molecules obtained by virtual screening affects Ras signaling in pancreatic cancer. *BMC Cancer* (2018) 18:1299. doi: 10.1186/s12885-018-5142-7

32. Cruz-Nova P, Schnoor M, Correa-Basurto J, Bello M, Briseno-Diaz P, Rojo-Dominguez A, et al. The small organic molecule C19 binds and strengthens the KRAS4b-PDEdelta complex and inhibits growth of colorectal cancer cells in *vitro* and in *vivo*. *BMC Cancer* (2018) 18:1056. doi: 10.1186/s12885-018-4968-3

33. Briseño-Díaz P, Schnoor M, Bello-Ramirez M, Correa-Basurto J, Rojo-Domínguez A, Arregui L, et al. Synergistic effect of antagonists to KRas4B/PDE6 molecular complex in pancreatic cancer. *Life Sci Alliance* (2023) 6:12. doi: 10.26508/lsa.202302019

34. Perez-Añorve IX, Gonzalez-De la Rosa CH, Soto-Reyes E, Beltran-Anaya FO, Del Moral-Hernandez O, Salgado-Albarran M, et al. New insights into radioresistance in breast cancer identify a dual function of miR-122 as a tumor suppressor and oncomiR. *Mol Oncol* (2019) 13:1249–67. doi: 10.1002/1878-0261.12483

35. Jones G, Willett P, Glen R, Leach A, Taylor R. *Development and validation of a genetic algorithm for flexible ligand docking*. Washington, DC 20036: Paper presented at the Abstracts of Papers of the American Chemical Society (1997).

36. Chen F, Liu H, Sun H, Pan P, Li Y, Li D, et al. Assessing the performance of the MM/PBSA and MM/GBSA methods. 6. Capability to predict protein–protein binding free energies and re-rank binding poses generated by protein–protein docking. *Phys Chem Chem Phys* (2016) 18:22129–39. doi: 10.1039/C6CP03670H

37. Weng G, Wang E, Wang Z, Liu H, Zhu F, Li D, et al. HawkDock: a web server to predict and analyze the protein–protein complex based on computational docking and MM/GBSA. *Nucleic Acids Res* (2019) 47:W322–30. doi: 10.1093/nar/gkz397

38. Jorgensen WL, Chandrasekhar J, Madura JD, Impey RW, Klein ML. Comparison of simple potential functions for simulating liquid water. *J Chem Phys* (1983) 79:926–35. doi: 10.1063/1.445869

39. Wang J, Wolf RM, Caldwell JW, Kollman PA, Case DA. Development and testing of a general amber force field. *J Comput Chem* (2004) 25:1157–74. doi: 10.1002/jcc.20035

40. Case DA, Cheatham TE III, Darden T, Gohlke H, Luo R, Merz KM Jr., et al. The Amber biomolecular simulation programs. *J Comput Chem* (2005) 26:1668–88. doi: 10.1002/jcc.20290

41. Cieplak P, Dupradeau F-Y, Duan Y, Wang J. Polarization effects in molecular mechanical force fields. *J Phys: Condensed Matter* (2009) 21:333102. doi: 10.1088/0953-8984/21/33/333102

42. Van Gunsteren W, Berendsen HJ. Algorithms for macromolecular dynamics and constraint dynamics. *Mol Phys* (1977) 34:1311–27. doi: 10.1080/00268977700102571

43. Darden T, York D, Pedersen L. Particle mesh Ewald: An N· log (N) method for Ewald sums in large systems. *J Chem Phys* (1993) 98:10089–92. doi: 10.1063/1.464397

44. Berendsen HJ, Postma JV, Van Gunsteren WF, DiNola A, Haak JR. Molecular dynamics with coupling to an external bath. *J Chem Phys* (1984) 81:3684–90. doi: 10.1063/1.448118

45. Kollman PA, Massova I, Reyes C, Kuhn B, Huo S, Chong L, et al. Calculating structures and free energies of complex molecules: combining molecular mechanics and continuum models. *Accounts Chem Res* (2000) 33:889–97. doi: 10.1021/ar000033j

46. Gohlke H, Case DA. Converging free energy estimates: MM-PB (GB) SA studies on the protein–protein complex Ras–Raf. *J Comput Chem* (2004) 25:238–50. doi: 10.1002/jcc.10379

47. Miller BR III, McGee TD Jr., Swails JM, Homeyer N, Gohlke H, Roitberg AE. MMPBSA. py: an efficient program for end-state free energy calculations. *J Chem Theory Comput* (2012) 8:3314–21. doi: 10.1021/ct300418h

48. Onufriev A, Bashford D, Case DA. Exploring protein native states and large-scale conformational changes with a modified generalized born model. *J Comput Chem* (2004) 55:383–94. doi: 10.1002/prot.20033

49. Menu E, Braet F, Timmers M, Van Riet I, Van Camp B, Vanderkerken K. The F-actin content of multiple myeloma cells as a measure of their migration. *Ann New York Acad Sci* (2002) 973:124–36. doi: 10.1111/j.1749-6632.2002.tb04620.x

50. Paddock SW. *Confocal microscopy: methods and protocols* Vol. Vol. 122. Totowa, New Jersey 07512: Springer Science & Business Media (1999).

51. Franklin WA, Haney J, Sugita M, Bemis L, Jimeno A, Messersmith WA. KRAS mutation comparison of testing methods and tissue sampling techniques in colon cancer. *J Mol Diagnost* (2010) 12:43–50. doi: 10.2353/jmoldx.2010.080131

52. Jonkman JE, Cathcart JA, Xu F, Bartolini ME, Amon JE, Stevens KM, et al. An introduction to the wound healing assay using live-cell microscopy. *Cell Adhes Migr* (2014) 8:440–51. doi: 10.4161/cam.36224

53. Ottoson NC, Pribila JT, Chan AS, Shimizu Y. Cutting edge: T cell migration regulated by CXCR4 chemokine receptor signaling to ZAP-70 tyrosine kinase. *J Immunol* (2001) 167:1857–61. doi: 10.4049/jimmunol.167.4.1857

54. Sharaf H, Matou-Nasri S, Wang Q, Rabhan Z, Al-Eidi H, Al Abdulrahman A, et al. Advanced glycation endproducts increase proliferation, migration and invasion of the breast cancer cell line MDA-MB-231. *Biochim Biophys Acta Mol Basis Dis* (2015) 1852:429–41. doi: 10.1016/j.bbadis.2014.12.009

55. Cho SY, Klemke RL. Purification of pseudopodia from polarized cells reveals redistribution and activation of Rac through assembly of a CAS/Crk scaffold. *J Cell Biol* (2002) 156:725–36. doi: 10.1083/jcb.200111032

56. Franken NA, Rodermond HM, Stap J, Haveman J, Van Bree C. Clonogenic assay of cells in *vitro*. *Nat Protoc* (2006) 1:2315. doi: 10.1038/nprot.2006.339

57. Schlegel R, Williamson P. Phosphatidylserine, a death knell. *Cell Death Differ* (2001) 8:551–63. doi: 10.1038/sj.cdd.4400817

58. Shimura T. Acquired radioresistance of cancer and the AKT/GSK3β/cyclin D1 overexpression cycle. *J Radiat Res* (2011) 52:539–44. doi: 10.1269/jrr.11098

59. Choi YJ, Li X, Hydbring P, Sanda T, Stefano J, Christie AL, et al. The requirement for cyclin D function in tumor maintenance. *Cancer Cell* (2012) 22:438–51. doi: 10.1016/j.ccr.2012.09.015

60. Xie J, Yu H, Song S, Fang C, Wang X, Bai Z, et al. Pu-erh tea water extract mediates cell cycle arrest and apoptosis in MDA-MB-231 human breast cancer cells. *Front Pharmacol* (2017) 8:190. doi: 10.3389/fphar.2017.00190

61. McCubrey JA, Steelman LS, Bertrand FE, Davis NM, Sokolosky M, Abrams SL, et al. GSK-3 as potential target for therapeutic intervention in cancer. *Oncotarget* (2014) 5:2881. doi: 10.18632/oncotarget.2037

62. Zińczuk J, Zaręba K, Guzińska-Ustymowicz K, Kędra B, Kemona A, Pryczynicz A. Expression of chosen cell cycle and proliferation markers in pancreatic intraepithelial neoplasia. *Gastroenterol Rev/Przegląd Gastroenterologiczny* (2018) 13:118–26. doi: 10.5114/pg.2018.75824

63. Lertkiatmongkol P, Liao D, Mei H, Hu Y, Newman PJ. Endothelial functions of PECAM-1 (CD31). *Curr Opin Hematol* (2016) 23:253. doi: 10.1097/MOH.0000000000000239

64. Wang D, Stockard CR, Harkins L, Lott P, Salih C, Yuan K, et al. Immunohistochemistry in the evaluation of neovascularization in tumor xenografts. *Mol Phys* (2008) 83:179–89. doi: 10.1080/10520290802451085

65. Kalimutho M, Parsons K, Mittal D, López JA, Srihari S, Khanna KK. Targeted therapies for triple-negative breast cancer: combating a stubborn disease. *Trends Pharmacol Sci* (2015) 36:822–46. doi: 10.1016/j.tips.2015.08.009

66. Hanker AB, Der CJ. The roles of ras family small GTPases in breast cancer. In: *Handbook of Cell Signaling*. San Francisco, California: Elsevier (2010). p. 2763–72.

67. Siddiqui FA, Alam C, Rosenqvist P, Ora M, Sabt A, Manoharan GB, et al. PDE6D inhibitors with a new design principle selectively block K-Ras activity. *ACS Omega* (2019) 5:832–42. doi: 10.1021/acsomega.9b03639

68. Hunter JC, Manandhar A, Carrasco MA, Gurbani D, Gondi S, Westover KD. Biochemical and structural analysis of common cancer-associated KRAS mutations. *Mol Cancer Res* (2015) 13:1325–35. doi: 10.1158/1541-7786.MCR-15-0203

69. Jameel JK, Rao VS, Cawkwell L, Drew PJ. Radioresistance in carcinoma of the breast. *Breast* (2004) 13:452–60. doi: 10.1016/j.breast.2004.08.004

70. Al-Taweel N, Varghese E, Florea A-M, Büsselberg D. Cisplatin (CDDP) triggers cell death of MCF-7 cells following disruption of intracellular calcium ([Ca2+] i) homeostasis. *J Toxicol Sci* (2014) 39:765–74. doi: 10.2131/jts.39.765

71. Velasco A, Bussaglia E, Pallares J, Dolcet X, Llobet D, Encinas M, et al. PIK3CA gene mutations in endometrial carcinoma. Correlation with PTEN and K-RAS alterations. *Hum Pathol* (2006) 37:1465–72. doi: 10.1016/j.humpath.2006.05.007

72. Barbato L, Bocchetti M, Di Biase A, Regad T. Cancer stem cells and targeting strategies. *Cells* (2019) 8:926. doi: 10.3390/cells8080926

frontiers | Frontiers in Oncology

TYPE Mini Review
PUBLISHED 08 May 2024
DOI 10.3389/fonc.2024.1407511

OPEN ACCESS

EDITED BY
Monica Fedele,
National Research Council (CNR), Italy

REVIEWED BY
Pasquale Pisapia,
University of Naples Federico II, Italy

*CORRESPONDENCE
Alma D. Campos-Parra
almcampos@uv.mx

RECEIVED 26 March 2024
ACCEPTED 16 April 2024
PUBLISHED 08 May 2024

CITATION
Sánchez-Marín D, Silva-Cázares MB, González-Del Carmen M and Campos-Parra AD (2024) Drug repositioning in thyroid cancer: from point mutations to gene fusions. *Front. Oncol.* 14:1407511. doi: 10.3389/fonc.2024.1407511

Drug repositioning in thyroid cancer: from point mutations to gene fusions

David Sánchez-Marín[1], Macrina Beatriz Silva-Cázares[2], Manuel González-Del Carmen[3] and Alma D. Campos-Parra[4]*

[1]Posgrado en Ciencias Biológicas, Facultad de Medicina, Universidad Nacional Autónoma de Mexico (UNAM), Ciudad de Mexico, Mexico, [2]Unidad Académica Multidisciplinaria Región Altiplano, Universidad Autónoma de San Luis Potosí, (UASL), Matehuala, San Luis Potosí, Mexico, [3]Facultad de Medicina, Universidad Veracruzana (UV), Ciudad Mendoza, Veracruz, Mexico, [4]Instituto de Salud Pública, Universidad Veracruzana (UV), Xalapa, Veracruz, Mexico

The diagnosis of thyroid cancer (TC) has increased dramatically in recent years. Papillary TC is the most frequent type and has shown a good prognosis. Conventional treatments for TC are surgery, hormonal therapy, radioactive iodine, chemotherapy, and targeted therapy. However, resistance to treatments is well documented in almost 20% of all cases. Genomic sequencing has provided valuable information to help identify variants that hinder the success of chemotherapy as well as to determine which of those represent potentially druggable targets. There is a plethora of targeted therapies for cancer, most of them directed toward point mutations; however, chromosomal rearrangements that generate fusion genes are becoming relevant in cancer but have been less explored in TC. Therefore, it is relevant to identify new potential inhibitors for genes that are recurrent in the formation of gene fusions. In this review, we focus on describing potentially druggable variants and propose both point variants and fusion genes as targets for drug repositioning in TC.

KEYWORDS

thyroid cancer, variants, repurposed drugs, gene fusions, mutations

Introduction

Thyroid cancer (TC) is the most common malignant tumor of the endocrine system, with 586,202 new cases worldwide in 2020 (1). The overall incidence of TC has increased dramatically in the last 30 years. This increase may be due to overdiagnosis, thanks to improvements made in diagnostic procedures (2). Morphologically and clinically, TC is classified into two main groups: differentiated cancer—comprising papillary and follicular thyroid cancer—and undifferentiated TC, designated anaplastic carcinoma of the thyroid (3). The most prevalent is papillary thyroid cancer (PTC), which accounts for up to 85% and has a good prognosis (5-year survival rate of more than 95%, mainly in patients with

stage I or II disease), as does follicular thyroid cancer (FTC), which is less prevalent, accounting for 15% of all cases (4). Patients with poorly differentiated or anaplastic TC, advanced-stage disease, or distant metastases have higher mortality rates (5). Moreover, about 20% of PTC patients manifest disease recurrence because of drug resistance, suggesting a change in treatment approaches. This points out the need to personalize treatments, including drug repositioning (6). Target therapy can be repositioned and offers greater success since it can be customized according to the patient's genomic alterations. In this review, we highlight therapeutic opportunities for TC, focusing on druggable genes with potential repositioning for personalized therapy.

Classical point mutations in thyroid cancer: windows of opportunity for the use of drug repositioning

Radioactive iodine administration and/or surgery remain the first line of treatment for TC; however, for advanced disease, chemotherapy (CT) becomes the systemic option of treatment available (7). Nevertheless, CT constantly faces resistance and severe secondary effects (8). Therefore, it is necessary to overcome resistance by recognizing drug-susceptible mutations, which may lead to the identification of a broad spectrum of target therapies that could be repositioned in TC (Figure 1).

Next-Generation Sequencing (NGS) has made it possible to sequence the genomes of different types of cancer, which has revealed that around 90% of patients with TC have one or more genetic abnormalities (9). Dysregulation of phosphatidylinositol 3-kinase (*PI3KCA*) and mitogen-activated protein kinase (*MAPK*) signaling pathways is mainly affected by point mutations in target genes such as B-Raf proto-oncogene, serine/threonine kinase (*BRAF*), A-Raf proto-oncogene, serine/threonine kinase (*RAS*), and ret proto-oncogene (*RET*) (10). One of the best-documented and highest prevalence point mutations in PTC is *BRAF* exon 15 p. V600E (45% of all cases), which is associated with poor prognosis and high recurrence (11). The *BRAF* exon 15 p. V600E variant has constitutively active *BRAF* serine–threonine leading to the activation of effectors of the *MAPK* pathway and, consequently, surveillance and proliferation (11). Vemurafenib has shown antitumor activity in patients with *BRAF* exon 15 p. V600E-positive progressive PTC, representing a potential new therapeutic option (12, 13). Ipilimumab, nivolumab, dabrafenib, and trametinib are also approved target therapy options for *BRAF* mutations in melanoma (14) that could be repositioned to TC. In addition, drugs blocking phosphatase and tensin homolog (*PTEN*) and *PI3KCA* homogenize the font of the letter with that of the rest of the text effects (Table 1).

PI3KCA is another gene with several missense mutations in three subtypes of TC: follicular, papillary, and anaplastic. Interestingly, *PI3KCA* mutations are associated with drug resistance in *BRAF* exon 15 p. V600E-positive cases. In this scenario, it is worth looking at how alpelisib can counteract the resistance mechanism by diminishing the EPH receptor B2 (*EPHB2*)-induced signaling (38). Consistent with the latest, *PTEN*, which has a negative regulatory role in the same pathway, has reported variants in TC (39).

KRAS proto-oncogene, GTPase (*KRAS*), is a G protein that plays an important role in the *PI3KCA*/*MAPK* signaling pathway. Point mutations in *KRAS* usually occur at codons 12, 13, and 61 and have been found in FTC and PTC at a frequency of 50% and 20%,

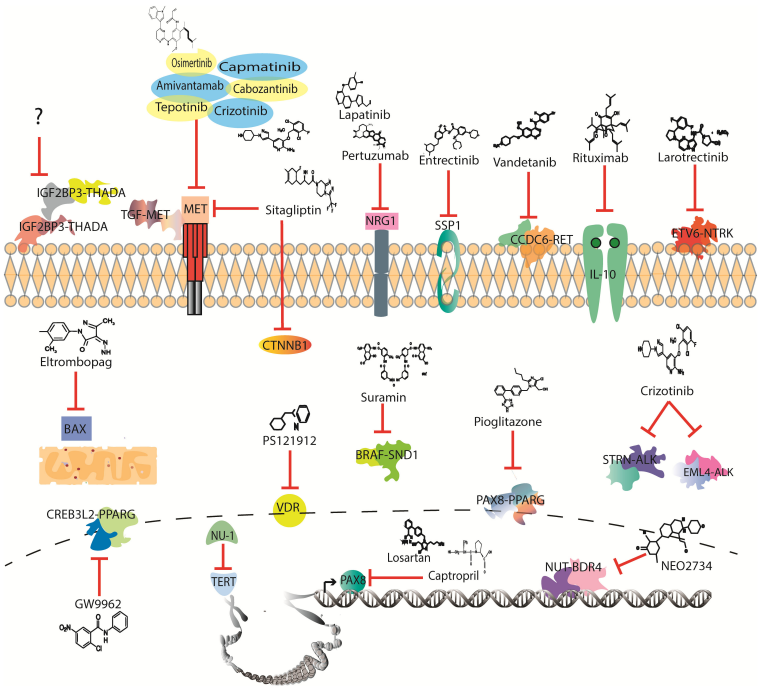

FIGURE 1
Drugs with potential to be investigated in thyroid cancer clinical trials according to mutational profile.

TABLE 1 Variants in potentially druggable genes in thyroid cancer.

Drug	Gene	Variant in thyroid cancer	Cancer	Reference
Ipilimumab, nivolumab, dabrafenib, and trametinib	BRAF	V600E	Melanoma	(14)
Alpelisib	PI3KCA	GAA>AAA, G1564A/ CCA>TCA, C3031T	Breast	(15)
Sotorasib and adagrasib	KRAS	G12C	NSCL	(16)
Vandenitib and cabozantinib	RET	Codons: 609, 611, 618, and 620 Val804Met. S836S	NSCL	(17)
Amivantamab, cabozantinib, capmatinib, crizotinib, osimertinib, tepotinib, and sitagliptin	MET	rs1621 AG	NSCL, thyroid	(18) (19–23), (18)
Sitagliptin	CTNNB1	c.133T>C	Thyroid	(24)
Afatinib, lapatinib, and pertuzumab	NRG1	rs2439302	Colorectal, breast	(25)
Entrectinib	SPP1	rs4754	Cervical	(26)
Eltrombopag	BAX	–248 G>A	---	(27)
PS121912	VDR	(rs2228570) CT/TT	Leukemia	(28)
Rituximab	IL-10	G-1082A	B-cell non-Hodgkin's lymphoma	(29)
Nu-1	TERT	C>T (C228T) and 1,295,250 C>T (C250T)	Lung and colorectal	(30)
Vandetanib	CCDC6-RET	Gene fusion	NSCL	(17)
Larotrectinib	ETV6-NTRK3	Gene fusion	Secretory breast cancer	(31)
Crizotinib, ceritinib, alectinib, brigatinib, and lorlatinib	STRN-ALK	Gene fusion	Lung adenocarcinoma	(32)
Crizotinib, ceritinib, alectinib, brigatinib, and lorlatinib	EML4-ALK	Gene fusion	Lung	(33)
Suramin	BRAF-SND1	Gene fusion	---	(33)
---	IGF2BP3-THADA	Gene fusion	---	(34)
Pioglitazone, GW9662	PAX8-PPARG	Gene fusion	Thyroid	(35)
NEO2734	NUT-BRD4	Gene fusion	NUT midline carcinoma	(36)
Amivantamab, cabozantinib, capmatinib, crizotinib, osimertinib, tepotinib, and sitagliptin	TGF-MET	Gene fusion	Sarcoma, glioma	(37)

respectively. These mutations confer a more aggressive phenotype and increase the risk of mortality (40). Sotorasib and adagrasib are *KRAS* exon 2 p. G12C mutation drugs approved for non-small cell lung cancer (NSCLC) (16, 41). It remains of interest to analyze the effect of these drugs on TC harboring the *KRAS* exon 2 p. G12C mutation. *RET* is another gene commonly mutated in PTC and medullary thyroid cancer (MTC), with both large rearrangements and point mutations reported. *RET* is a receptor tyrosine kinase that regulates growth, survival, migration, and survival, activating multiple intracellular signaling pathways, including *PI3KCA/AKT* serine/threonine kinase 1 (*AKT*), *MAPK*, mitogen-activated protein kinase 8 (*JNK*), and others. Oncogenic activating point mutations can occur mainly in the extracellular domain, particularly in codon C634 of exon 11, in 609, 611, 618, or 620 of exon 10, and in M918 of exon 16, being *RET* exon 16 p. M918T mutation the most common and represents more than 75% of all *RET* somatic mutations found in MTC (42). Selpercatinib and pralsetinib are *RET*-specific inhibitors approved for the MTC variant and have been well tolerated (43–45). Other multitargeted kinase inhibitors used to inhibit the *PI3KCA/AKT*/mechanistic target of the rapamycin kinase (*MTOR*) pathway in MTC are vandenitib and cabozantinib. The first one inhibits *RET* but also inhibits other kinases such as vascular endothelial growth factor receptor 2 (*VEGFR2*), vascular endothelial growth factor receptor 3 (*VEGFR3*), and epidermal growth factor receptor (*EGFR*), while cabozantinib inhibits *RET*, vascular endothelial growth factor (*VEGF*), *MET* proto-oncogene, receptor tyrosine kinase (*MET*), and *ROS* proto-oncogene 1, receptor tyrosine kinase (*ROS1*) (46). Both inhibitors have shown efficacy and improved overall survival in patients harboring *RET* exon 16 p. M918T mutation (47, 48).

MET is a receptor tyrosine kinase that has an oncogene role in promoting angiogenesis due to downstream activation of *RAS*,

PI3KCA, and signal transducer and activator of transcription 3 (*STAT3*) signaling pathways (49). Drugs that inhibit *MET* are amivantamab, cabozantinib, capmatinib, crizotinib, osimertinib, and tepotinib (50). Particularly, *MET* has a reported variant in NSCLC that skips the exon 14 and makes the protein constitutively active (51). In TC, it constitutes an inclusion criterion for thyroid gland medullary carcinoma (52, 53). Currently, therapy targeting *MET*, although only indicated to treat NSCL, represents a potential target in TC. Furthermore, a PTC expression signature has been identified in which three genes are overexpressed, promoting metastasis and being associated with poor prognosis: dipeptidyl peptidase 4 (*DPP4*), *MET*, and catenin beta 1 (*CTNNB1*). The signature is associated with immunosuppression and correlates with tumor infiltration of tumor-associated macrophages, which leads to T-cell exclusion. Interestingly, sitagliptin, an FDA-approved drug to treat diabetes type II, has affinity not only to *DPP4* (diabetes target) but also to *MET* and *CTNNB1* (54–56). Moreover, the affinity for *MET* and *CTNNB1* is even higher than FDA-approved inhibitors specific for each of them, like crizotinib and PNU-74654, respectively. Therefore, sitagliptin represents a multidrug therapy window for TC (18).

Paired box 8 (*PAX8*), a gene implicated in proliferation and migration, is usually overexpressed in TC. Likewise, in high-grade serous ovarian cancer, *PAX8* is upregulated (57). Remarkably, losartan and captopril, which are FDA-approved drugs, have been found effective at inhibiting *PAX8* expression and function. This evidence suggests potential therapeutic opportunities using losartan and captopril, not only for ovarian cancer but also for TC (57).

Besides the variants reported in the above-mentioned genes, there are also polymorphisms associated with TC (58). For instance, neuregulin 1 (*NRG1*) acts as an oncogene through its role as a glycoprotein that mediates cell-to-cell signaling (59). In breast cancer, lapatinib may be used to inhibit *EGFR* and erb-b2 receptor tyrosine kinase 2 (*HER2*) kinases, two receptors of also relevant function in TC. Nonetheless, resistance is acquired and correlates with an increased expression of *NRG1*. By trying to overcome it, adding pertuzumab has shown promising results in decreasing *NRG1*-acquired resistance and tumor progression (25).

Similarly, secreted phosphoprotein 1 (*SPP1*), an integrin-binding glycophosphoprotein overexpressed in TC that promotes tumorigenesis through the inhibition of differentiation factors of thyroid cells, represents an opportunity for drug repositioning (60, 61). Although there are no current FDA drugs approved for inhibiting *SPP1*, a recent publication showed a promising inhibitory drug for cervical cancer: entrectinib (26). This represents a highlight, as entrectinib is an FDA-approved drug for NTRK fusions in solid tumors, including TC (62).

As with *SPP1*, another window of opportunity for targeted treatment is *BCL2*-associated X, apoptosis regulator (*BAX*). This gene participates in mitochondrial regulation of cell death; however, in cancer, it contributes to cell death dysregulation (63). Importantly, in TC, *BAX* has a reported polymorphism positively correlated with PTC, and more importantly, the FDA-approved drug eltrombopag acts as a *BAX* inhibitor, which drives apoptosis induction (64, 65). *SPP1* and *BAX* are not the only genes in which polymorphism is related to TC. *VDR* stands for vitamin D receptor and has been associated with cancer development (66). It is not well established if TC contributes to or attenuates tumor growth; however, two polymorphisms, FokI and TaqI, are associated with a more aggressive type, and the heterozygous FokI to metastasis (67). Remarkably, it has been shown that antagonists of vitamin D have therapeutic effects as they inhibit downstream cell cycle proliferation. There is already an insight into potential therapies using *VDR* as a druggable target. For instance, PS121912 has shown promising therapeutic effects by acting as a selective *VDR* inhibitor (28).

In the immunology context, several profiles have been described causing differential expression and immune cell proliferation among TC subtypes (68). Interleukin-10 (*IL-10*) is one of several dysregulated cytokines in TC associated with immunological and apoptosis evasion and aggressiveness (68). This effect is caused by expression induction of *BCL2* like 1 (*bcl-xL*) and *BCL2* apoptosis regulator (*BcCL2*) and resistance to *CD95*-mediated apoptosis (69, 70). Due to its oncological role, *IL-10* figures as a potential therapeutic target. Rituximab has promising inhibitory effects against *IL-10* through downregulation of *BCL2* and sensitization of B-cell non-Hodgkin's lymphoma to apoptosis (29). However, resistance constitutes a problem due to broad kinase inhibitor activity and toxicity, which may limit their use and encourage the use of more specific inhibitors (71).

Lastly, telomerase reverse transcriptase (*TERT*), an enzyme known to be implicated in cancer, has been described as one of the most frequently mutated genes in TC, particularly in its promoter, which causes its overactivation. *TERT* inhibitors are currently under study, and NU-1 not only sensitizes the cell to chemo- and radiotherapy but also can inhibit proliferation and increase immune activity (30).

From NGS of long DNA fragments, gene fusions have been identified. When two genes conform to a fusion, they either lose or gain function. In cancer, they can contribute to tumor growth due to constitutive activation of an oncogene, such as *BCR-ABL* (72). Remarkably, some gene fusions are considered drivers, while others contribute to generating more genomic instability and disease development. There are gene fusions that are found across various cancers (73). These features of gene fusions represent an unprecedented opportunity to develop target therapies aimed at providing personalized medicine to patients.

Spotlight of novel therapies: gene fusions

Over 50 gene fusions have been identified in TC, which are mainly conformed by the *RET*, neurotrophic receptor tyrosine kinase (*NTRK*), *ALK*, and *BRAF* genes (74). These genes are tyrosine kinase overactivated mainly due to kinase retention and overexpression by transcription factors of the parental genes, making them druggable targets (75). Currently, three drugs are being used in clinics to treat TC-targeting gene fusions: pralsetinib, selpercatinib, and larotrectinib (76). The first two are *RET* inhibitors and were first set as a treatment for both point

mutations and gene fusions; however, selpercatinib shows efficacy in specific *RET* variant genotypes that present pralsetinib resistance. For instance, *BaF4/KIF5B-RET* shows tumor growth despite treatment with pralsetinib, while selpercatinib can effectively inhibit growth (44, 77). However, as with other variants, these gene fusions are not expressed across all subtypes of cancer, while some therapies face drug resistance and lack of treatment for greater, yet untargeted variants (Figure 1).

For *RET*, 19 fusions have been described; however, only therapies consisting of *RET* inhibitors are currently available, leaving the partner genes pharmacologically unexplored (78). This is of great importance as it has been described that the inhibitory sensitivity of several gene fusions varies depending on the partner gene; hence, drug screening should be performed testing not only the most common gene. For instance, the coiled-coil domain containing 6 (*CCDC6*) is a recurrent gene-forming fusion with *RET* in lung cancer, where it has shown potential druggability of *EGFR* inhibitors in combination with *RET* inhibitors, decreasing resistance to *RET* inhibitors while also enhancing sensitivity to *PARP* inhibitors (79). Particularly, the fusion *CCDC6-RET* is more sensitive to vandetanib due to the off-target inhibitory effect and crosstalk with *EGFR* pathway activation (80). Furthermore, this fusion and *ERC1-RET* have not had a response to the *RET* drug, cabozantinib, supporting the idea of focusing on the second gene as well (81).

Larotrectinib targets the *NTRK* genes, which are neurotrophic tyrosine kinase receptors. If binding occurs, the protein phosphorylates itself and activates the *MAPK* pathway. Therefore, as part of a gene fusion, it causes its constitutive activation (82). Several fusions involving *NTRK1*, *NTRK2*, and *NTRK3* have been described in the lung, colon, brain, head and neck, and TC (83). For this reason, it has been a promising targeted therapy, as the same fusions can occur in several tissues. In TC, larotrectinib is administered to patients diagnosed with the anaplastic subtype, and tumor growth continues despite other treatments (82). An example of this is the *ETV6-NTRK3* fusion, which has been described as a driver variant in secretory breast cancer with high efficacy upon larotrectinib treatment (84). However, larotrectinib therapy targets only the *NTRK* gene, while their partner genes remain untargeted. For instance, sequestosome 1 (*SQSTM1)* is a gene that conforms to fusions with both *NTRKs* and plays a role in autophagy, specifically through the *AKT*/protein kinase AMP-activated catalytic subunit alpha 2 (*AMPK*)/*MTOR* signaling reported in PTC (84).

Although only three drugs are being used in TC to target gene fusions, there are several other recurrent genes forming gene fusions that are already targeted in other cancers. On one hand, there is *ALK*, which is widely known for its oncogenic role, especially as part of gene fusions (85). Currently, *ALK* fusions do not have a regimen of treatment for TC, but its potential has already been evaluated. For example, *STRN-ALK* and *EML4-ALK* are promising targets in TC using the FDA-approved drug crizotinib, among other drugs such as ceritinib, alectinib, brigatinib, and lorlatinib (32, 33).

On the other hand, there are *BRAF* fusions, and remarkably, despite *BRAF* having several target drugs, none of them are used to treat TC. Furthermore, among all the gene partners of *BRAF*, staphylococcal nuclease and Tudor domain containing 1 (*SND1*), an oncogene in several types of cancer acts in addition to posttranscriptional modifications (86). This is a highlight for novel therapy, as a small molecule called suramin has been identified to inhibit their protein by impairing its interaction with several microRNAs and sensitizing the response to standard chemotherapy (87).

Interestingly, up to five gene fusions are involved in *THADA* armadillo repeat containing (*THADA*), which stands for thyroid adenoma-associated gene (Table 1) (74). This gene participates in metabolism and energy storage through the calcium pathway. In cancer, not only fusions but also polymorphisms are associated with the disease development (88). Particularly, it has been described that *THADA* is necessary to retain *CD274* in the Golgi for maturation. On the contrary, if suppressed, the immune response is triggered through the infiltration of *CD8* + T cells and increased toxicity (89). In addition to this finding, the *IGF2BP3-THADA* fusion has been demonstrated to cause overexpression of the partner gene *IGF2BP3*, leading to sustained growth and invasion through the activation of PI3KCA and MAPK pathways (34, 90). For its part, insulin-like growth factor 2 mRNA-binding protein 3 (*IGF2BP3*) is associated with a poor prognosis implicated in several mechanisms leading to aberrant metabolism in cancer (91). Currently, there are no inhibitors for *THADA*; however, the data strongly point out *THADA* as a potential therapeutic target in TC.

Another gene found in 30%–35% of FTC is PAX8-*PPARG*, characterized as an oncogene due to its binding to several genomic regions that code for genes related to cell proliferation, apoptosis evasion, and motility (92). Contrary to the case of repurposing losartan to *PAX8* alterations, this fusion promotes tumor progression due to the likely loss of functions of peroxisome proliferator-activated receptor gamma (*PPARG*). When inhibited with pioglitazone, anti-inflammatory effects and growth modulation are observed; however, the function of the gene fusion is not yet fully understood (35). Opposed to this idea, the antitumoral effect of *PPARG* inhibitor GW9662 has also been described, indicating the existence of independent pathways of *PPARG* (93). Remarkably, *PAX8-PPARG* is not the only fusion in TC involving *PPARG*; there is also *CREB3L2-PPARG* (94).

NUT-BDR4 is an oncogenic driver fusion that causes a rare type of cancer named NUT midline carcinoma. Bromodomain-containing protein 4 (*BDR4*) binds to the chromatin, while *NUT* midline carcinoma family member 1 (*NUT*) recruits histone acetyltransferase (*HAT*), promoting the expression of several associated oncogenes (95). This rare fusion has also been described in some TC cases, and it is associated with high expression of *CD274* (96). The prognosis is low, with an estimated overall survival of 10 months, while therapy consists of radiotherapy and standard chemotherapy for large tumors. With no targeted therapy available, it is an urgent matter to start studying potential inhibitors for the treatment of these patients (97). Currently, only one inhibitor has been proposed to target the NUT-*BDR4* fusion. It consists of a dual inhibitor of bromodomain and extra-terminal motif (*BET*) proteins and the p300 bromodomain, named NEO2734, with proven inhibition of tumor growth and improvement of overall survival (36).

Lastly, *MET* not only has point mutations in TC but also a gene fusion. It has been identified that *TGF-MET* fusion is present in sarcoma, glioma, and TC (37, 98). Interestingly, in sarcoma, tumors that have this variant do not fit into a specific subtype,

which is a remarkable finding due to the existence of effective *MET* inhibitors (50, 98).

Conclusions and perspectives

It is relevant to recognize that in the era of personalized medicine, drug repositioning has a major impact on oncology. This is possible due to the identification of new therapeutic targets, which can be shared in different diseases and even between cancers. This opens a whole window of opportunity for the use of a plethora of drugs, reducing the time and costs involved in the production of new drugs, which has a positive impact on patients. In this review, we found that several drugs used in different types of cancer can be repositioned to TC, either by the presence of point mutations or by gene fusions. We found an area of opportunity for 13 genes with missense mutations and 10 for gene fusions. Among all these drugs, 22 are FDA-approved drugs, while the remaining five are inhibitors with proven efficacy in *in vitro* studies, both of which represent a promising area of therapy opportunity. It is the aim of this work to highlight the relevance of the identification of new potential inhibitors for genes that are part of recurrent fusion formation in TC as well as other types of cancer due to the likelihood of their contribution to disease development. Hence, it is of interest to the clinic to elucidate these variants' potential as biomarkers or prognostic or therapeutic targets.

Author contributions

DS-M: Writing – review & editing, Writing – original draft, Conceptualization. MS-C: Investigation, Formal analysis, Writing – original draft. MG-DC: Writing – original draft, Investigation, Formal analysis. AC-P: Writing – review & editing, Supervision, Resources, Project administration, Methodology, Funding acquisition, Conceptualization, Writing – original draft, Investigation.

Funding

The author(s) declare financial support was received for the research, authorship, and/or publication of this article. This research was funded by the Instituto de Salud Pública, Universidad Veracruzana, Xalapa, Veracruz, México.

Conflict of interest

The authors declare that the research was conducted in the absence of any commercial or financial relationships that could be construed as a potential conflict of interest.

The author(s) declared that they were an editorial board member of Frontiers, at the time of submission. This had no impact on the peer review process and the final decision.

Publisher's note

References

1. Pizzato M, Li M, Vignat J, Laversanne M, Singh D, La Vecchia C, et al. The epidemiological landscape of thyroid cancer worldwide: GLOBOCAN estimates for incidence and mortality rates in 2020. *Lancet Diabetes Endocrinol.* (2022) 10:264–72. doi: 10.1016/S2213-8587(22)00035-3

2. Xie Z, Zhou J, Zhang X, Li Z. Clinical potential of microbiota in thyroid cancer therapy. *Biochim Biophys Acta Mol Basis Dis.* (2024) 1870:166971. doi: 10.1016/j.bbadis.2023.166971

3. Cameselle-Teijeiro JM, Sobrinho-Simões M. New WHO classification of thyroid tumors: a pragmatic categorization of thyroid gland neoplasms. *Endocrinol Diabetes Nutr (Engl Ed).* (2018) 65:133–5. doi: 10.1016/j.endinu.2017.11.012

4. Ganly I, Nixon IJ, Wang LY, Palmer FL, Migliacci JC, Aniss A, et al. Survival from differentiated thyroid cancer: what has age got to do with it? *Thyroid.* (2015) 25:1106–14. doi: 10.1089/thy.2015.0104

5. Wan Z, Wang B, Yao J, Li Q, Miao X, Jian Y, et al. Predictive factors and clinicopathological characteristics of outcome in poorly differentiated thyroid carcinoma: a single-institution study. *Front Oncol.* (2023) 13:1102936. doi: 10.3389/fonc.2023.1102936

6. Zhang Y, Xing Z, Liu T, Tang M, Mi L, Zhu J, et al. Targeted therapy and drug resistance in thyroid cancer. *Eur J Med Chem.* (2022) 238:114500. doi: 10.1016/j.ejmech.2022.114500

7. Nguyen QT, Lee EJ, Huang MG, Park YI, Khullar A, Plodkowski RA. Diagnosis and treatment of patients with thyroid cancer. *Am Health Drug Benefits.* (2015) 8:30–40.

8. Al-Malky HS, Al Harthi SE, Osman A-MM. Major obstacles to doxorubicin therapy: Cardiotoxicity and drug resistance. *J Oncol Pharm Pract.* (2020) 26:434–44. doi: 10.1177/1078155219877931

9. Hsiao SJ, Nikiforov YE. Molecular approaches to thyroid cancer diagnosis. *Endocr Relat Cancer.* (2014) 21:T301–313. doi: 10.1530/ERC-14-0166

10. Kimura ET, Nikiforova MN, Zhu Z, Knauf JA, Nikiforov YE, Fagin JA. High prevalence of BRAF mutations in thyroid cancer: genetic evidence for constitutive activation of the RET/PTC-RAS-BRAF signaling pathway in papillary thyroid carcinoma. *Cancer Res.* (2003) 63:1454–7.

11. Abdulhaleem M, Bandargal S, Pusztaszeri MP, Rajab M, Greenspoon H, Krasner JR, et al. The impact of BRAF V600E mutation allele frequency on the histopathological characteristics of thyroid cancer. *Cancers (Basel).* (2023) 16:113. doi: 10.3390/cancers16010113

12. Brose MS, Cabanillas ME, Cohen EEW, Wirth LJ, Riehl T, Yue H, et al. Vemurafenib in patients with BRAF(V600E)-positive metastatic or unresectable papillary thyroid cancer refractory to radioactive iodine: a non-randomised, multicentre, open-label, phase 2 trial. *Lancet Oncol.* (2016) 17:1272–82. doi: 10.1016/S1470-2045(16)30166-8

13. Chen D, Su X, Zhu L, Jia H, Han B, Chen H, et al. Papillary thyroid cancer organoids harboring BRAFV600E mutation reveal potentially beneficial effects of BRAF inhibitor-based combination therapies. *J Transl Med.* (2023) 21:9. doi: 10.1186/s12967-022-03848-z

14. Trojaniello C, Sparano F, Cioli E, Ascierto PA. Sequencing targeted and immune therapy in BRAF-mutant melanoma: lessons learned. *Curr Oncol Rep.* (2023) 25:623–34. doi: 10.1007/s11912-023-01402-8

15. Chang D-Y, Ma W-L, Lu Y-S. Role of alpelisib in the treatment of PIK3CA-mutated breast cancer: patient selection and clinical perspectives. *Ther Clin Risk Manag.* (2021) 17:193–207. doi: 10.2147/TCRM.S251668

16. Hallin J, Engstrom LD, Hargis L, Calinisan A, Aranda R, Briere DM, et al. The KRASG12C inhibitor MRTX849 provides insight toward therapeutic susceptibility of KRAS-mutant cancers in mouse models and patients. *Cancer Discovery*. (2020) 10:54–71. doi: 10.1158/2159-8290.CD-19-1167

17. Lee S-H, Lee J-K, Ahn M-J, Kim D-W, Sun J-M, Keam B, et al. Vandetanib in pretreated patients with advanced non-small cell lung cancer-harboring RET rearrangement: a phase II clinical trial. *Ann Oncol*. (2017) 28:292–7. doi: 10.1093/annonc/mdw559

18. Cheng S-Y, Wu ATH, Batiha GE-S, Ho C-L, Lee J-C, Lukman HY, et al. Identification of DPP4/CTNNB1/MET as a theranostic signature of thyroid cancer and evaluation of the therapeutic potential of sitagliptin. *Biol (Basel)*. (2022) 11:324. doi: 10.3390/biology11020324

19. Grüllich C. Cabozantinib: multi-kinase inhibitor of MET, AXL, RET, and VEGFR2. *Recent Results Cancer Res*. (2018) 211:67–75. doi: 10.1007/978-3-319-91442-8_5

20. Ramesh S, Cifci A, Javeri S, Minne R, Longhurst CA, Nickel KP, et al. MET inhibitor capmatinib radiosensitizes MET exon 14-mutated and MET-amplified non-small cell lung cancer. *bioRxiv*. (2023) 2023:10.26.564232. doi: 10.1101/2023.10.26.564232

21. Shalata W, Yakobson A, Weissmann S, Oscar E, Iraqi M, Kian W, et al. Crizotinib in MET exon 14-mutated or MET-amplified in advanced disease non-small cell lung cancer: A retrospective, single institution experience. *Oncology*. (2022) 100:467–74. doi: 10.1159/000525188

22. Hartmaier RJ, Markovets AA, Ahn MJ, Sequist LV, Han J-Y, Cho BC, et al. Osimertinib + Savolitinib to overcome acquired MET-mediated resistance in epidermal growth factor receptor-mutated, MET-amplified non-small cell lung cancer: TATTON. *Cancer Discovery*. (2023) 13:98–113. doi: 10.1158/2159-8290.CD-22-0586

23. Lyczak A. [Effect of tetanus toxin on the activity of the 5-hydroxytryptaminergic system in the mouse brain]. *Med Dosw Mikrobiol*. (1988) 40:155–60.

24. Cadranel J, Liu SV, Duruisseaux M, Branden E, Goto Y, Weinberg BA, et al. Therapeutic potential of afatinib in NRG1 fusion-driven solid tumors: A case series. *Oncologist*. (2021) 26:7–16. doi: 10.1634/theoncologist.2020-0379

25. Leung W, Roxanis I, Sheldon H, Buffa FM, Li J, Harris AL, et al. Combining lapatinib and pertuzumab to overcome lapatinib resistance due to NRG1-mediated signalling in HER2-amplified breast cancer. *Oncotarget*. (2015) 6:5678–94. doi: 10.18632/oncotarget.3296

26. Poleboyina PK, Alagumuthu M, Pasha A, Ravinder D, Pasumarthi D, Pawar SC. Entrectinib a plausible inhibitor for osteopontin (SPP1) in cervical cancer-integrated bioinformatic approach. *Appl Biochem Biotechnol*. (2023) 195:7766–95. doi: 10.1007/s12010-023-04541-7

27. Chen S-M, Feng J-N, Zhao C-K, Yao L-C, Wang L-X, Meng L, et al. A multi-targeting natural product, aiphanol, inhibits tumor growth and metastasis. *Am J Cancer Res*. (2022) 12:4930–53.

28. Sidhu PS, Teske K, Feleke B, Yuan NY, Guthrie ML, Fernstrum GB, et al. Anticancer activity of VDR-coregulator inhibitor PS121912. *Cancer Chemother Pharmacol*. (2014) 74:787–98. doi: 10.1007/s00280-014-2549-y

29. Alas S, Emmanouilides C, Bonavida B. Inhibition of interleukin 10 by rituximab results in down-regulation of bcl-2 and sensitization of B-cell non-Hodgkin's lymphoma to apoptosis. *Clin Cancer Res*. (2001) 7:709–23.

30. Liu Y, Betori RC, Pagacz J, Frost GB, Efimova EV, Wu D, et al. Targeting telomerase reverse transcriptase with the covalent inhibitor NU-1 confers immunogenic radiation sensitization. *Cell Chem Biol*. (2022) 29:1517–1531.e7. doi: 10.1016/j.chembiol.2022.09.002

31. Shukla N, Roberts SS, Baki MO, Mushtaq Q, Goss PE, Park BH, et al. Successful targeted therapy of refractory pediatric ETV6-NTRK3 fusion-positive secretory breast carcinoma. *JCO Precis Oncol*. (2017) 2017:PO.17.00034. doi: 10.1200/PO.17.00034

32. Su C, Jiang Y, Jiang W, Wang H, Liu S, Shao Y, et al. STRN-ALK fusion in lung adenocarcinoma with excellent response upon alectinib treatment: A case report and literature review. *Onco Targets Ther*. (2020) 13:12515–9. doi: 10.2147/OTT.S282933

33. Mano H. The EML4-ALK oncogene: targeting an essential growth driver in human cancer. *Proc Jpn Acad Ser B Phys Biol Sci*. (2015) 91:193–201. doi: 10.2183/pjab.91.193

34. Panebianco F, Kelly LM, Liu P, Zhong S, Dacic S, Wang X, et al. THADA fusion is a mechanism of IGF2BP3 activation and IGF1R signaling in thyroid cancer. *Proc Natl Acad Sci U.S.A*. (2017) 114:2307–12. doi: 10.1073/pnas.1614265114

35. Giordano TJ, Haugen BR, Sherman SI, Shah MH, Caoili EM, Koenig RJ. Pioglitazone therapy of PAX8-PPARγ Fusion protein thyroid carcinoma. *J Clin Endocrinol Metab*. (2018) 103:1277–81. doi: 10.1210/jc.2017-02533

36. Morrison-Smith CD, Knox TM, Filic I, Soroko KM, Eschle BK, Wilkens MK, et al. Combined targeting of the BRD4-NUT-p300 axis in NUT midline carcinoma by dual selective bromodomain inhibitor, NEO2734. *Mol Cancer Ther*. (2020) 19:1406–14. doi: 10.1158/1535-7163.MCT-20-0087

37. Xu T, Wang H, Huang X, Li W, Huang Q, Yan Y, et al. Gene fusion in Malignant glioma: an emerging target for next-generation personalized treatment. *Transl Oncol*. (2018) 11:609–18. doi: 10.1016/j.tranon.2018.02.020

38. Liu D, Hou P, Liu Z, Wu G, Xing M. Genetic alterations in the phosphoinositide 3-kinase/Akt signaling pathway confer sensitivity of thyroid cancer cells to therapeutic targeting of Akt and mammalian target of rapamycin. *Cancer Res*. (2009) 69:7311–9. doi: 10.1158/0008-5472.CAN-09-1077

39. Colombo C, Pogliaghi G, Tosi D, Muzza M, Bulfamante G, Persani L, et al. Thyroid cancer harboring PTEN and TP53 mutations: A peculiar molecular and clinical case report. *Front Oncol*. (2022) 12:949098. doi: 10.3389/fonc.2022.949098

40. Bikas A, Ahmadi S, Pappa T, Marqusee E, Wong K, Nehs MA, et al. Additional oncogenic alterations in RAS-driven differentiated thyroid cancers associate with worse clinicopathologic outcomes. *Clin Cancer Res*. (2023) 29:2678–85. doi: 10.1158/1078-0432.CCR-23-0278

41. Hong DS, Fakih MG, Strickler JH, Desai J, Durm GA, Shapiro GI, et al. KRASG12C inhibition with sotorasib in advanced solid tumors. *N Engl J Med*. (2020) 383:1207–17. doi: 10.1056/NEJMoa1917239

42. Ciampi R, Romei C, Pieruzzi L, Tacito A, Molinaro E, Agate L, et al. Classical point mutations of RET, BRAF and RAS oncogenes are not shared in papillary and medullary thyroid cancer occurring simultaneously in the same gland. *J Endocrinol Invest*. (2017) 40:55–62. doi: 10.1007/s40618-016-0526-5

43. Hadoux J, Elisei R, Brose MS, Hoff AO, Robinson BG, Gao M, et al. Phase 3 trial of selpercatinib in advanced RET-mutant medullary thyroid cancer. *N Engl J Med*. (2023) 389:1851–61. doi: 10.1056/NEJMoa2309719

44. Wirth LJ, Robinson B, Boni V, Tan DSW, McCoach C, Massarelli E, et al. Patient-reported outcomes with selpercatinib treatment among patients with RET-mutant medullary thyroid cancer in the phase I/II LIBRETTO-001 trial. *Oncologist*. (2022) 27:13–21. doi: 10.1002/onco.13977

45. Subbiah V, Hu MI, Wirth LJ, Schuler M, Mansfield AS, Curigliano G, et al. Pralsetinib for patients with advanced or metastatic RET-altered thyroid cancer (ARROW): a multi-cohort, open-label, registrational, phase 1/2 study. *Lancet Diabetes Endocrinol*. (2021) 9:491–501. doi: 10.1016/S2213-8587(21)00120-0

46. Gentile C, Martorana A, Lauria A, Bonsignore R. Kinase inhibitors in multitargeted cancer therapy. *Curr Med Chem*. (2017) 24:1671–86. doi: 10.2174/0929867324666170112112734

47. Fallahi P, Ferrari SM, Elia G, Ragusa F, Paparo SR, Ruffilli I, et al. Evaluating vandetanib in the treatment of medullary thyroid cancer: patient-reported outcomes. *Cancer Manag Res*. (2019) 11:7893–907. doi: 10.2147/CMAR.S127848

48. Cabanillas ME, de Souza JA, Geyer S, Wirth LJ, Menefee ME, Liu SV, et al. Cabozantinib as salvage therapy for patients with tyrosine kinase inhibitor-refractory differentiated thyroid cancer: results of a multicenter phase II international thyroid oncology group trial. *J Clin Oncol*. (2017) 35:3315–21. doi: 10.1200/JCO.2017.73.0226

49. You W-K, McDonald DM. The hepatocyte growth factor/c-Met signaling pathway as a therapeutic target to inhibit angiogenesis. *BMB Rep*. (2008) 41:833–9. doi: 10.5483/bmbrep.2008.41.12.833

50. Dong Y, Xu J, Sun B, Wang J, Wang Z. MET-targeted therapies and clinical outcomes: A systematic literature review. *Mol Diagn Ther*. (2022) 26:203–27. doi: 10.1007/s40291-021-00568-w

51. Fujino T, Suda K, Mitsudomi T. Lung cancer with MET exon 14 skipping mutation: genetic feature, current treatments, and future challenges. *Lung Cancer (Auckl)*. (2021) 12:35–50. doi: 10.2147/LCTT.S269307

52. Garcia C, Buffet C, El Khattabi L, Rizk-Rabin M, Perlemoine K, Ragazzon B, et al. MET overexpression and activation favors invasiveness in a model of anaplastic thyroid cancer. *Oncotarget*. (2019) 10:2320–34. doi: 10.18632/oncotarget.26798

53. Ning L, Yu Y, Liu X, Ai L, Zhang X, Rao W, et al. Association analysis of MET gene polymorphism with papillary thyroid carcinoma in a chinese population. *Int J Endocrinol*. (2015) 2015:405217. doi: 10.1155/2015/405217

54. Enz N, Vliegen G, De Meester I, Jungraithmayr W. CD26/DPP4 - a potential biomarker and target for cancer therapy. *Pharmacol Ther*. (2019) 198:135–59. doi: 10.1016/j.pharmthera.2019.02.015

55. Yang X, Liao H-Y, Zhang H-H. Roles of MET in human cancer. *Clin Chim Acta*. (2022) 525:69–83. doi: 10.1016/j.cca.2021.12.017

56. Shang S, Hua F, Hu Z-W. The regulation of β-catenin activity and function in cancer: therapeutic opportunities. *Oncotarget*. (2017) 8:33972–89. doi: 10.18632/oncotarget.15687

57. Salvi A, Hardy LR, Heath KN, Watry S, Pergande MR, Cologna SM, et al. PAX8 modulates the tumor microenvironment of high grade serous ovarian cancer through changes in the secretome. *Neoplasia*. (2023) 36:100866. doi: 10.1016/j.neo.2022.100866

58. Guo Y, Zhang W, He R, Zheng C, Liu X, Ge M, et al. Investigating the association between rs2439302 polymorphism and thyroid cancer: A systematic review and meta-analysis. *Front Surg*. (2022) 9:877206. doi: 10.3389/fsurg.2022.877206

59. Talmage DA. Mechanisms of neuregulin action. *Novartis Found Symp*. (2008) 289:74–84. doi: 10.1002/9780470751251.ch6

60. Wei T, Bi G, Bian Y, Ruan S, Yuan G, Xie H, et al. The significance of secreted phosphoprotein 1 in multiple human cancers. *Front Mol Biosci*. (2020) 7:565383. doi: 10.3389/fmolb.2020.565383

61. Ma J, Huang X, Xu J, Li Z, Lai J, Shen Y, et al. SBP1 promotes tumorigenesis of thyroid cancer through TXN/NIS pathway. *Mol Med*. (2023) 29:121. doi: 10.1186/s10020-023-00700-y

62. Damásio I, Simões-Pereira J, Donato S, Horta M, Cavaco BM, Rito M, et al. Entrectinib in the neoadjuvant setting of anaplastic thyroid cancer: a case report. *Eur Thyroid J*. (2023) 12:e220179. doi: 10.1530/ETJ-22-0179

63. Huska JD, Lamb HM, Hardwick JM. Overview of BCL-2 family proteins and therapeutic potentials. *Methods Mol Biol*. (2019) 1877:1–21. doi: 10.1007/978-1-4939-8861-7_1

64. Cardoso-Duarte LCA, Fratelli CF, Pereira ASR, de Souza JNG, de S Freitas R, de Morais RM, et al. BAX gene (-248 G > A) polymorphism in a sample of patients diagnosed with thyroid cancer in the Federal District, Brazil. *Int J Biol Markers*. (2021) 36:21–6. doi: 10.1177/17246008211057576

65. Spitz AZ, Zacharioudakis E, Reyna DE, Garner TP, Gavathiotis E. Eltrombopag directly inhibits BAX and prevents cell death. *Nat Commun*. (2021) 12:1134. doi: 10.1038/s41467-021-21224-1

66. Campbell MJ, Trump DL. Vitamin D receptor signaling and cancer. *Endocrinol Metab Clin North Am*. (2017) 46:1009–38. doi: 10.1016/j.ecl.2017.07.007

67. Cocolos A-M, Muresan A, Caragheorgheopol A, Ghemigian M, Ioachim D, Poiana C. Vitamin D status and VDR polymorphisms as prognostic factors in differentiated thyroid carcinoma. *In Vivo*. (2022) 36:2434–41. doi: 10.21873/invivo.12977

68. Cunha LL, Domingues GAB, Morari EC, Soares FA, Vassallo J, Ward LS. The immune landscape of the microenvironment of thyroid cancer is closely related to differentiation status. *Cancer Cell Int*. (2021) 21:387. doi: 10.1186/s12935-021-02084-7

69. Stassi G, Todaro M, Zerilli M, Ricci-Vitiani L, Di Liberto D, Patti M, et al. Thyroid cancer resistance to chemotherapeutic drugs *via* autocrine production of interleukin-4 and interleukin-10. *Cancer Res*. (2003) 63:6784–90.

70. Todaro M, Zerilli M, Ricci-Vitiani L, Bini M, Perez Alea M, Maria Florena A, et al. Autocrine production of interleukin-4 and interleukin-10 is required for survival and growth of thyroid cancer cells. *Cancer Res*. (2006) 66:1491–9. doi: 10.1158/0008-5472.CAN-05-2514

71. Ghrenassia E, Mariotte E, Azoulay E. Rituximab-related Severe Toxicity. In: Vincent J-L, editor. *Annual Update in Intensive Care and Emergency Medicine 2018. Annual Update in Intensive Care and Emergency Medicine*. Springer International Publishing, Cham (2018). p. 579–96. doi: 10.1007/978-3-319-73670-9_43

72. Mertens F, Johansson B, Fioretos T, Mitelman F. The emerging complexity of gene fusions in cancer. *Nat Rev Cancer*. (2015) 15:371–81. doi: 10.1038/nrc3947

73. Yu Y-P, Liu P, Nelson J, Hamilton RL, Bhargava R, Michalopoulos G, et al. Identification of recurrent fusion genes across multiple cancer types. *Sci Rep*. (2019) 9:1074. doi: 10.1038/s41598-019-38550-6

74. Yakushina VD, Lerner LV, Lavrov AV. Gene fusions in thyroid cancer. *Thyroid*. (2018) 28:158–67. doi: 10.1089/thy.2017.0318

75. Stransky N, Cerami E, Schalm S, Kim JL, Lengauer C. The landscape of kinase fusions in cancer. *Nat Commun*. (2014) 5:4846. doi: 10.1038/ncomms5846

76. Nacchio M, Pisapia P, Pepe F, Russo G, Vigliar E, Porcelli T, et al. Predictive molecular pathology in metastatic thyroid cancer: the role of RET fusions. *Expert Rev Endocrinol Metab*. (2022) 17:167–78. doi: 10.1080/17446651.2022.2060819

77. Wu Y, Yan Z, Pan J, Chang X, Huang B, Luo D, et al. Nie X. Partial response to pralsetinib in an advanced pulmonary sarcomatoid carcinoma patient harboring a KIF5B-RET rearrangement: a case report. *World J Surg Oncol*. (2022) 20:386. doi: 10.1186/s12957-022-02848-z

78. Vodopivec DM, Hu MI. RET kinase inhibitors for RET-altered thyroid cancers. *Ther Adv Med Oncol*. (2022) 14:17588359221101691. doi: 10.1177/17588359221101691

79. Chang H, Sung JH, Moon SU, Kim HS, Kim JW, Lee JS. EGF induced RET inhibitor resistance in CCDC6-RET lung cancer cells. *Yonsei Med J*. (2017) 58:9–18. doi: 10.3349/ymj.2017.58.1.9

80. Levinson S, Cagan RL. Drosophila cancer models identify functional differences between ret fusions. *Cell Rep*. (2016) 16:3052–61. doi: 10.1016/j.celrep.2016.08.019

81. Drilon A, Rekhtman N, Arcila M, Wang L, Ni A, Albano M, et al. Cabozantinib in patients with advanced RET-rearranged non-small-cell lung cancer: an open-label, single-centre, phase 2, single-arm trial. *Lancet Oncol*. (2016) 17:1653–60. doi: 10.1016/S1470-2045(16)30562-9

82. Cocco E, Scaltriti M, Drilon A. NTRK fusion-positive cancers and TRK inhibitor therapy. *Nat Rev Clin Oncol*. (2018) 15:731–47. doi: 10.1038/s41571-018-0113-0

83. O'Haire S, Franchini F, Kang Y-J, Steinberg J, Canfell K, Desai J, et al. Systematic review of NTRK 1/2/3 fusion prevalence pan-cancer and across solid tumours. *Sci Rep*. (2023) 13:4116. doi: 10.1038/s41598-023-31055-3

84. Yu F, Ma R, Liu C, Zhang L, Feng K, Wang M, et al. SQSTM1/p62 promotes cell growth and triggers autophagy in papillary thyroid cancer by regulating the AKT/AMPK/mTOR signaling pathway. *Front Oncol*. (2021) 11:638701. doi: 10.3389/fonc.2021.638701

85. He Y, Cao L, Wang L, Liu L, Huang Y, Gong X. Metformin inhibits proliferation of human thyroid cancer TPC-1 cells by decreasing LRP2 to suppress the JNK pathway. *Onco Targets Ther*. (2020) 13:45–50. doi: 10.2147/OTT.S227915

86. Chu Y-H, Wirth LJ, Farahani AA, Nosé V, Faquin WC, Dias-Santagata D, et al. Clinicopathologic features of kinase fusion-related thyroid carcinomas: an integrative analysis with molecular characterization. *Mod Pathol*. (2020) 33:2458–72. doi: 10.1038/s41379-020-0638-5

87. Lehmusvaara S, Haikarainen T, Saarikettu J, Martinez Nieto G, Silvennoinen O. Inhibition of RNA binding in SND1 increases the levels of miR-1-3p and sensitizes cancer cells to navitoclax. *Cancers (Basel)*. (2022) 14:3100. doi: 10.3390/cancers14133100

88. Moraru A, Cakan-Akdogan G, Strassburger K, Males M, Mueller S, Jabs M, et al. THADA regulates the organismal balance between energy storage and heat production. *Dev Cell*. (2017) 41:72–81.e6. doi: 10.1016/j.devcel.2017.03.016

89. Li C, Chi H, Deng S, Wang H, Yao H, Wang Y, et al. THADA drives Golgi residency and upregulation of PD-L1 in cancer cells and provides promising target for immunotherapy. *J Immunother Cancer*. (2021) 9:e002443. doi: 10.1136/jitc-2021-002443

90. Gubbiotti MA, Andrianus S, Baloch Z. THADA-IGF2BP3 fusions detected in fine-needle aspiration specimens of thyroid nodules: An institutional experience. *Diagn Cytopathol*. (2023) 51:349–55. doi: 10.1002/dc.25113

91. Liu X, Chen J, Chen W, Xu Y, Shen Y, Xu X. Targeting IGF2BP3 in cancer. *Int J Mol Sci*. (2023) 24:9423. doi: 10.3390/ijms24119423

92. Raman P, Koenig RJ. Pax-8-PPAR-γ fusion protein in thyroid carcinoma. *Nat Rev Endocrinol*. (2014) 10:616–23. doi: 10.1038/nrendo.2014.115

93. Seargent JM, Yates EA, Gill JH. GW9662, a potent antagonist of PPARgamma, inhibits growth of breast tumour cells and promotes the anticancer effects of the PPARgamma agonist rosiglitazone, independently of PPARgamma activation. *Br J Pharmacol*. (2004) 143:933–7. doi: 10.1038/sj.bjp.0705973

94. Lui W-O, Zeng L, Rehrmann V, Deshpande S, Tretiakova M, Kaplan EL, et al. CREB3L2-PPARgamma fusion mutation identifies a thyroid signaling pathway regulated by intramembrane proteolysis. *Cancer Res*. (2008) 68:7156–64. doi: 10.1158/0008-5472.CAN-08-1085

95. Lauer UM, Hinterleitner M, Horger M, Ohnesorge PV, Zender L. NUT carcinoma-an underdiagnosed Malignancy. *Front Oncol*. (2022) 12:914031. doi: 10.3389/fonc.2022.914031

96. Zhou J, Duan M, Jiao Q, Chen C, Xing A, Su P, et al. Primary thyroid NUT carcinoma with high PD-L1 expression and novel massive IGKV gene fusions: A case report with treatment implications and literature review. *Front Oncol*. (2021) 11:778296. doi: 10.3389/fonc.2021.778296

97. Wang S, Li J, Tong W, Li H, Feng Q, Teng B. Advances in the pathogenesis and treatment of nut carcinoma: a narrative review. *Transl Cancer Res*. (2020) 9:6505–15. doi: 10.21037/tcr-20-1884

98. Flucke U, van Noesel MM, Wijnen M, Zhang L, Chen C-L, Sung Y-S, et al. TFG-MET fusion in an infantile spindle cell sarcoma with neural features. *Genes Chromosomes Cancer*. (2017) 56:663–7. doi: 10.1002/gcc.22470

frontiers | Frontiers in Oncology

TYPE Original Research
PUBLISHED 22 May 2024
DOI 10.3389/fonc.2024.1382276

OPEN ACCESS

EDITED BY
Alma D. Campos-Parra,
Universidad Veracruzana, Mexico

REVIEWED BY
Dorian Yarih Garcia-Ortega,
National Institute of Cancerology (INCAN), Mexico
Gerardo Cuamani-Mitznahuatl,
ABC Medical Center, Mexico
Macrina Beatriz Silva Cázares,
Autonomous University of San Luis Potosí, Mexico

*CORRESPONDENCE
Jingnan Shen
shenjn@mail.sysu.edu.cn
Junqiang Yin
yinjunq@mail.sysu.edu.cn

†These authors have contributed equally to this work

RECEIVED 05 February 2024
ACCEPTED 19 April 2024
PUBLISHED 22 May 2024

CITATION
Zou C, Huang R, Lin T, Wang Y, Tu J, Zhang L, Wang B, Huang J, Zhao Z, Xie X, Huang G, Wang K, Yin J and Shen J (2024) Age-dependent molecular variations in osteosarcoma: implications for precision oncology across pediatric, adolescent, and adult patients. *Front. Oncol.* 14:1382276. doi: 10.3389/fonc.2024.1382276

Age-dependent molecular variations in osteosarcoma: implications for precision oncology across pediatric, adolescent, and adult patients

Changye Zou[1†], Renxuan Huang[1†], Tiao Lin[1†], Yaxian Wang[2†], Jian Tu[1], Liwen Zhang[2], Bo Wang[1], Jintao Huang[2], Zhiqiang Zhao[1], Xianbiao Xie[1], Gang Huang[1], Kai Wang[2], Junqiang Yin[1*] and Jingnan Shen[1*]

[1]Department of Musculoskeletal Oncology Center, The First Affiliated Hospital of Sun Yat-sen University, Guangzhou, China, [2]OrigiMed, Shanghai, China

Background: Osteosarcoma is a leading subtype of bone tumor affecting adolescents and adults. Comparative molecular characterization among different age groups, especially in pediatric, adolescents and adults, is scarce.

Methods: We collected samples from 194 osteosarcoma patients, encompassing pediatric, adolescent, and adult cohorts. Genomic analyses were conducted to reveal prevalent mutations and compare molecular features in pediatric, adolescent, and adult patients.

Results: Samples from 194 osteosarcoma patients across pediatric to adult ages were analyzed, revealing key mutations such as TP53, FLCN, NCOR1, and others. Children and adolescents showed more gene amplifications and HRD mutations, while adults had a greater Tumor Mutational Burden (TMB). Mutations in those over 15 were mainly in cell cycle and PI3K/mTOR pathways, while under 15s had more in cell cycle and angiogenesis with higher VEGFA, CCND3, TFEB mutations. CNV patterns varied with age: VEGFA and XPO5 amplifications more in under 25s, and CDKN2A/B deletions in over 25s. Genetic alterations in genes like MCL1 and MYC were associated with poor prognosis, with VEGFA mutations also indicating worse outcomes. 58% of patients had actionable mutations, suggesting opportunities for targeted therapies. Age-specific patterns were observed, with Multi-TKI mutations more common in younger patients and CDK4/6 inhibitor mutations in adults, highlighting the need for personalized treatment approaches in osteosarcoma. In a small group of patients with VEGFR amplification, postoperative treatment with multi-kinase inhibitors resulted in a PR in 3 of 13 cases, especially in patients under 15. A significant case involved a 13-year-old with a notable tumor size reduction achieving PR, even with other genetic alterations present in some patients with PD.

Conclusion: This study delineates the molecular differences among pediatric, adolescent, and adult osteosarcoma patients at the genomic level, emphasizing the necessity for precision diagnostics and treatment strategies, and may offer novel prognostic biomarkers for patients with osteosarcoma. These findings provide a significant scientific foundation for the development of individualized treatment approaches tailored to patients of different age groups.

KEYWORDS

osteosarcoma, pediatrics, adolescents, adults, genomic alteration, next generation sequencing

1 Introduction

Osteosarcoma, a relatively uncommon malignancy, manifests a distinct incidence pattern characterized by a significant surge during the growth phase of adolescence. The rarity of this disease poses substantial challenges for conducting broad research initiatives, rendering large-scale studies especially crucial (1, 2). Despite significant advances in limb-salvage surgery and multimodal chemotherapy, the long-term survival for non-metastatic osteosarcoma has stagnated around 70% for the past few decades, while patients presenting with metastatic disease at diagnosis have an even poorer prognosis, with survival rates hovering around 20-30% (3, 4). Moreover, the high-dose chemotherapeutic regimens necessary for treatment are associated with considerable acute and long-term morbidity (5, 6).

The complexity of osteosarcoma is underscored by its clinical and molecular heterogeneity, which poses a challenge for the identification of prognostic markers and therapeutic targets. Clinical prognosticators, including tumor size, site, and response to chemotherapy, have been well-documented (7). In multivariate analysis, proximal position within the limb was independently associated with worse overall survival of patients with osteosarcoma (8). Previous study showed that the prognosis of male osteosarcoma is slightly worse than that of female patients (9). Age is generally considered to be an independent factor of osteosarcoma. Due to the onset characteristics of osteosarcoma, that is, patients with osteosarcoma show a bimodal distribution according to age, with the highest proportion of 15-19 years old, followed by 75-79 years old, and then 25-59 years old (10). The study found that in adolescent patients with osteosarcoma, the younger the age, the worse the prognosis (7). However, the impact of age on disease characteristics and outcomes has become a focal point of recent research, with studies suggesting that older age may correlate with a higher frequency of adverse histologic response to chemotherapy and inferior survival (11, 12).

Advancements in high-throughput sequencing technologies have revolutionized our understanding of osteosarcoma biology, revealing a multitude of genetic alterations with potential prognostic and therapeutic implications (13). Unlike other solid tumors, osteosarcoma has a low proportion of common driver gene mutations and depends more on the activation of signal pathways caused by gene amplification or overexpression, such as PI3K/mTOR (14), IGF1 (15), VEGF (16), and PDGF (17), etc. Clinical trials of molecular typing and targeted therapy of osteosarcoma based on gene mutations are particularly necessary to improve the prognosis of patients with osteosarcoma. Due to the low incidence rate of osteosarcoma and the heterogeneity of osteosarcoma, it is difficult to carry out large-scale clinical trials. The clinical characteristics of osteosarcoma in young and elderly patients have been reported to differ, along with correlations between clinical features and prognosis (7, 18–20). A few studies have also depicted the distinct genomic profiles of osteosarcomas in different age groups, revealing age-specific mutation patterns and alterations in signaling pathways (14, 15). These findings underline the significance of age as a biological variable in osteosarcoma and may pave the way for age-specific treatment strategies. In a glioma study, age groups defined by 15 and 25 years - children (<15 years), adolescents (15-25 years), and adults (>25 years) - were found to have distinct molecular features, such as differences in the proportion of IDH1,BRAF and H3G34 mutations (21).

Studies have shown that in untreated osteosarcoma, the presence of Vascular Endothelial Growth Factor (VEGF) serves as a prognostic indicator for the likelihood of pulmonary metastasis and unfavorable outcomes in patients undergoing intensive therapy (22). Additionally, a notable discovery is that patients who are very young exhibit a substantially increased incidence of capillary hemangioma-like histological features (10.2% compared to 2.9%; $P = 0.017$) (23). These insights provide a crucial foundation for devising therapeutic approaches that concentrate on the vascular growth properties of osteosarcoma and may also prompt a reconsideration of age ranges for the inclusion of subjects in clinical trials for emerging therapeutics.

This study is designed to conduct a comprehensive analysis of the molecular mutation characteristics in osteosarcoma patients across various age groups, with the intent of identifying unique molecular markers that could enable personalized treatment approaches. By delving into the age-specific mutation patterns and signaling pathway alterations as previously reported, and

utilizing advanced genomic data, our goal is to enhance the current understanding of the complex molecular landscape of osteosarcoma. Ultimately, this research aims to contribute to precision medicine efforts, and thereby improve clinical outcomes for osteosarcoma patients of all ages.

2 Patients and methods

2.1 Patients and samples

From June 2017 to April 2023, we have gathered a cohort of 194 osteosarcoma patients from The First Affiliated Hospital of Sun Yat-sen University. These patients were selected based on their visits to our institution for treatment, during which they also underwent genetic testing. These patients were stratified into three age groups for analysis: pediatric patients (under 15 years), adolescent and young adult patients (15 - 25 years), and adult patients (over 25 years). Samples included fresh surgical/biopsy tissues or formalin-fixed, paraffin-embedded (FFPE) tumor tissues, along with matched blood samples, which were collected to detect genomic alterations (GAs). Genomic DNA was prepared by using QIAamp DNA FFPE Tissue Kit and QIAamp DNA Blood Midi Kit (Qiagen, Hilden, Germany) according to the manufacturer's instructions. The concentration of DNA was measured and normalized to 20–50 ng/μL. The study was approved by the Ethics Committee of The First Affiliated Hospital of Sun Yat-sen University, and all patients signed an informed consent form.

2.2 Genomic alterations identification

The DNA samples were detected by using the NGS-based Yuansu 450 gene panel or whole exon sequencing (WES) (OrigiMed, Shanghai, China). Yuansu 450gene panel covers all the coding exons of 450 tumor-related genes, the genes were captured and sequenced with a mean depth of 1000×. WES libraries were prepared and captured using the SureSelect Human All Exon V6 kit (Agilent Technologies) following manufacturer's instructions and sequenced with a mean coverage depth of 300X. All these experiments were performed on Illumina Novaseq 6000 system (Illumina, Inc., CA). Resultant sequences were further analyzed for genomic alterations compared with normal genomic DNA, including single nucleotide variants, short and long insertions/deletions (indels), copy number variations, and structural variants of gene rearrangement/fusion. The tumor mutational burden (TMB) was estimated by analyzing somatic mutations, including coding base substitution and INDELs, per mega-base of the panel sequences examined.

2.3 Mutational signature analysis

According to the number of different types of point mutations such as C > A/G > T, C > G/G > C, C > T/G > A, T > A/A > T, T > C/A > G, and T > G/A > C, a cluster analysis was performed in order to observe similarity in tumor samples. Extracted mutational features were compared with the pan-cancer catalogue for 94 known features cited in the cancer somatic mutation catalogue (COSMIC) database (https://cancer.sanger.ac.uk/signatures/) using Mutational Patterns packages (3.6.0) (24). The similarity of mutational features was assessed based on a cosine similarity > 0.85, which indicated common features.

2.4 Function enrichment analyses

To explore the biological functions of somatic mutations, gene ontology (GO) and a Kyoto Encyclopedia of Genes and Genomes (KEGG) enrichment analysis were conducted using the ClusterProfiler (v.3.10.1) in the R software.

2.5 Statistical analysis

Statistical analysis was conducted using the R statistical software package (R Foundation for Statistical Computing, Vienna, Austria). Categorical variables are expressed as in frequency and percentages; Continuous variables was presented with medians and percentiles. Wilcoxon rank test was used for comparing two continuous data and Fisher's exact tests were used for comparing two categorical data. $P < 0.05$ was considered statistically significant.

3 Results

3.1 Characterization of osteosarcoma patients

A total of 194 osteosarcoma patients were enrolled in this study. There were 127 males and 67 females. The median age was 16 Years old, ranged from 5-73 years old. Osteosarcoma is predominantly seen in adolescents, with about 75% of cases occurring between the ages of 15 and 25. Therefore, we categorize patients aged younger 15 as pediatric patients, those between 15 to 25 years as adolescent & young adult patients, and those over 25 years as adult patients. Our cohort includes 81 pediatric patients, 85 adolescent patients, and 28 adult patients. Based on pathological staging records, there were 2 cases of Stage I tumors, 136 cases of Stage II tumors, 2 cases of Stage III tumors, and 43 cases of Stage IV tumors. Additionally, there were 11 cases of pelvic and spinal bone tumors for which the AJCC staging criteria were not applicable. Within this cohort, the YuanSu450 gene panel and WES (Whole Exome Sequencing) (OrigiMed, Shanghai, China) were utilized to test samples from 110 and 84 patients, respectively. In this cohort, 177 underwent immunohistochemistry testing for PD-L1 expression, there were 44 PD-L1 positive patients and 133 negative patients. The majority of patients (193/194, 99.5%) were characterized as having Microsatellite Stable (MSS) tumors (Table 1).

TABLE 1 Patient characteristics.

Characteristics	Total (n = 194)
Age,n(%), median(min-max)	16(5-73)
Age<15	81 (42)
15≤Age≤25	85 (44)
Age>25	28 (14)
Gender, n (%)	Total (n = 194)
Female	66 (34)
Male	128 (66)
Stage, n (%)	Total (n = 194)
IA	1 (0.5)
IB	1 (0.5)
IIA	44 (23)
IIB	92 (47)
III	2 (1)
IVA	43 (22)
/	11 (6)
Histologic subtypes	Total (n = 194)
Parosteal osteosarcoma	3 (1.5)
Small cell osteosarcoma	1 (0.5)
Conventional osteosarcoma	190 (98)
grading	Total (n = 194)
G1	2 (1)
G2	192 (99)
therapy	Total (n = 194)
Neoadjuvant + surgery + adjuvant	164 (85)
surgery + adjuvant	30 (15)
MSI, n (%)	Total (n = 194)
MSS	193 (99)
MSI-H	1 (1)
PD-L1 (≥1=positive)	Total (n = 177)
Positive	44 (25)
Negative	133 (75)

In staging patients, the AJCC (American Joint Committee on Cancer) system is utilized. However, it should be noted that for pelvic and spinal bone tumors (n=11), the AJCC staging criteria are not applicable, as indicated by the "/" symbol, according to the Bone Cancer NCCN Guidelines 2024, Version 2.

3.2 Mutational profile of osteosarcomas

In this research, a total of 23,951 gene mutations were detected among 194 osteosarcoma patients. Gene panel testing yielded 1,066 mutations in 110 patients, while whole-exome sequencing (WES) detected 22,885 mutations in 84 patients. We found that the most prevalent mutation type in osteosarcomas was gene amplification (71.8%), followed by substitutions/deletions (19.7%), gene fusions (3.8%), homozygous deletions (2.6%), and truncating mutations (2.1%) (Supplementary Figure S1).

To illustrate the genomic landscape based on a large cohort, we integrated the results of WES and panel testing by filtering the WES data for panel probe sites. The results revealed that the most frequent mutations in osteosarcomas were in *TP53* (39%), *FLCN* (22%), *NCOR1* (21%), *VEGFA* (16%), *CCND3* (15%), *RB1* (14%), *TFEB* (12%), and *MAP2K4* (11.8%) (Figure 1A). *TP53* mutations were predominantly of the substitution/indel type and concentrated in the p53 protein's DNA-binding domain (Figure 1B).

3.3 Comparison of mutation characteristics between pediatric, adolescent and adult osteosarcoma patients

In this study, osteosarcoma patients under the age of 15 were categorized as pediatric patients, those aged 15-25 as adolescent patients, and those over the age of 25 as adult patients. Our findings indicate that pediatric and then adolescent patients have a higher frequency of gene amplification compared to adult patients, while substitution/Indel mutation types are less frequent than in adult osteosarcoma patients (Figure 1C). Enrichment analysis indicates that gene mutations in patients older than 15 years are mainly enriched in the cell cycle and PI3K/mTOR signaling pathways, while gene mutations in patients younger than 15 years are primarily enriched in the cell cycle and angiogenesis signaling pathways. Additionally, we compared Homologous Recombination Deficiency (HRD) mutated genes. The results showed that the frequency of HRD mutations in pediatric and adolescent patients was higher than in adult patients (17.5% vs. 16.5% vs. 7.7%) (Figures 2A, B). We also compared the Tumor Mutational Burden (TMB) distribution among pediatric, adolescent, and adult patients. It was found that the TMB in adult patients was higher than in pediatric patients, with a statistically significant difference ($p = 0.04$) (Figure 2C). Compared with adult patients, the mutation frequency of *VEGFA* ($P < 0.001$), CCND3 ($P = 0.016$) and *TEEB* ($P = 0.0016$) were significantly higher in pediatrics and adolescents (Figure 2D). The co-mutation analysis revealed that *VEGFA*, *CCND3*, and *TEEB* are the most commonly co-mutated genes. In addition, *XPO5* is frequently co-mutated with *VEGFA*, *CCND3*, and *TEEB*, while *AURKB* is commonly co-mutated with *FLCN*, *NCOR1*, *CCND1*, *TFEB*, and *MAP2K4* (Figure 2E).

3.4 Analysis of CNV distribution of osteosarcoma in different age groups

In our study, we identified a total of 1,156 copy number variation (CNV) variants across a cohort of 194 patients with osteosarcoma. Among all CNVs, amplifications of *VEGFA* and *XPO5* were primarily found in patients under the age of 25, while

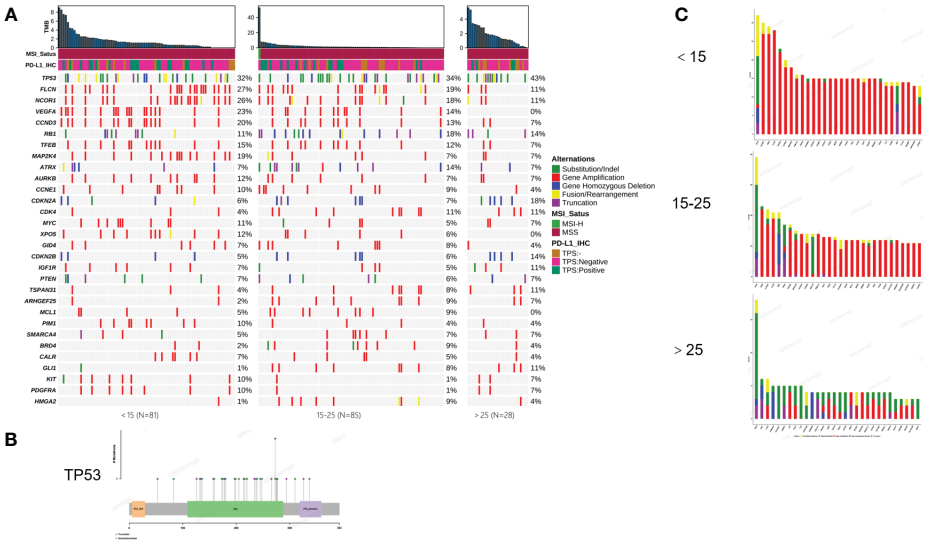

FIGURE 1
Mutational characterization of this cohort. **(A)** Mutational landscape of 194 osteosarcoma patients (<15, 15-25, >25, respectively). **(B)** Distribution of TP53 mutation sites. **(C)** Amplification statistics of patients in different age groups (< 15, 15-25, > 25, respectively). Green represents substitution/Indel mutations, red represents gene amplification mutations, blue represents gene homozygous deletion mutations, yellow represents fusion/rearrangement mutations, and purple represents truncation mutations.

amplifications of *DAXX* and *DDR1* were concentrated in patients under the age of 15. Conversely, deletions of *CDKN2A* and *CDKN2B* were more prevalent in the age group over 25 years old (Figure 3A). Additionally, within a subset of 75 osteosarcoma patients who underwent whole-exome sequencing (WES), we detected 668 CNV variants. The most frequent CNV include 17p11.2, 19q12, 6q21.1 and 12q12.1 amplification. In 31 pediatric patients, 258 CNVs we detected including 247 amplifications and 11 gene homozygous deletions, and the most frequent CNVs included 6p21.1 amplification, 17p12 amplification, 19q12 amplification, 16p13.3 deletion and 17p13.1 deletion; In 30 pediatric patients, 292 CNVs we detected including 277 amplifications and 15 gene homozygous deletions, and the most frequent CNVs included 1p36.13 amplification, 6p21.1 amplification, 12q14.1 amplification, and 17p11.2 amplification; In 14 adult patients, 118 CNVs were detected including 102 amplifications and 16 gene homozygous deletions, and the most common CNVs included 8p12 deletion, 9p21.3 deletion, 13q13.3 deletion, 15q15.1 deletion, and 16p13.3 deletion (Figure 3B).

3.5 Signature analysis

We observed similar trends across all six possible point mutation types in the three groups. C>T mutations were the most abundant types, followed by C>A and C>G. Upon conducting a comprehensive Signature analysis, underscores the importance of age as a factor in mutational processes. The differential signature analysis indicates that mutations characteristic of BRCA1/2 and Aristolochic acid are more pronounced in adults. The individual distribution of these signatures was shown in Figure 4 and Table S1.

3.6 Prognosis analysis of osteosarcoma patients

Based on the genomic alteration, we evaluated the prognostic significance of specific genetic alterations in a cohort of patients. We collected the effective overall survival (OS) information of 74 patients, including 39 pediatric, 31 adolescents and 4 adult patients. The overall median DFS was 24 months. Notably, mutations in the genes *MCL1*, *MYC*, *TFEB*, *CCND3*, *AURKB*, and *ALOX12B* were associated with a significantly worse prognosis, with p-values less than 0.05, underscoring their potential role as markers for aggressive disease courses. On the other hand, mutations in VEGFA were also correlated with a poorer prognosis, with p-values approaching the threshold of significance (near 0.05), suggesting a trend that warrants further investigation for definitive conclusions (Figure 5 and Table S2).

3.7 Available drug mutations in osteosarcoma

Actionable drug mutations were detected in 58% (113 out of 194) of patients, encompassing 185 mutations across 35 target genes, with *VEGFA* being the most frequently mutated gene associated with drug responsiveness. About 25% (49/194) of patients harbored the mutations of angiogenesis related gene amplification, such as *VEGFA*, *KIT*, *KDR*, *PDGFRA*, *ARAF*, *FGFR1*, *VHL*, and *TFE3*, and 18% (34/194) patients were harbored CDK4/6 inhibition related mutations. These results suggested the potential targeted treatment of osteosarcomas. In pediatric adolescent patients, 86 available drug mutations from 23 targeted genes were detected in 49 osteosarcoma patients. In

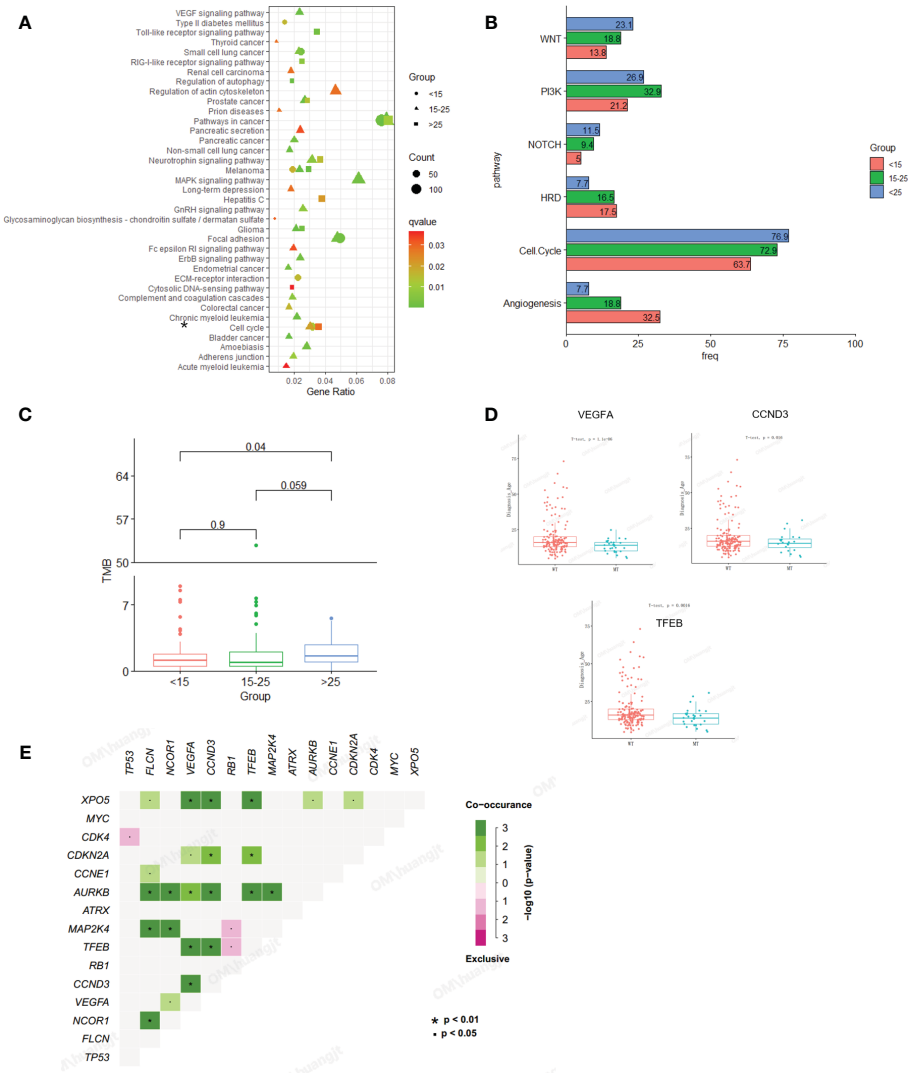

FIGURE 2
Comparison of mutation characteristics between osteosarcoma subgroups (pediatric, adolescent and adult). **(A)** Enrichment analysis of mutated pathways in adult osteosarcoma group and adolescent osteosarcoma group. From blue to red represents the gradually decreased p value, circle size represents the count of mutations in each pathway. **(B)** Enrichment differences in signaling pathways across age groups. **(C)** Association analysis between TMB and osteosarcoma subgroup (pediatric, adolescent and adult). **(D)** Correlation analysis between genetic variation and age. **(E)** Co-mutation analysis of genes.

adolescent patients, 66 available drug mutations from 25 targeted genes were detected in 49 osteosarcoma patients, and in adult patients, 25 available drug mutations from 15 targeted genes were detected in 15 osteosarcoma patients. The most common available drug mutated genes include *VEGFA* in pediatric and adolescent patients, *CDK4* in adolescent patients, and *CDKN2A*, and *CDKN2B* in adult patients. According to the drug type, the drug available mutations were divided into Anti-PD-1/PD-L1 related mutations such as *CD274* and *PDCD1LG2*, *CDK4/6* inhibitor related mutations such as *CDKN2A*, *CDKN2B*, *CCND1*, and *CDK4*, mTOR inhibitor related mutations such as *PTEN*, *MTOR*, *FBXW7*, *PIK3CA*, and *STK11*, Multi-TKI related mutations such as *VEGFA*, *KIT*, *KDR*, *PDGFRA*, *ARAF*, *FGFR1*, *VHL*, and *TFE3*, *VEGFA*, *KIT*, *KDR*, *PDGFRA*, *ARAF*, *FGFR1*, *VHL*, and TFE3, and PARP inhibitor related mutations such as *ATM*, *BRCA2*, and *BRCA1*, and TKI related mutations such as *ALK*, *KRAS*, *NRAS*, *ROS1*, *MET*, *BRAF*, *EGFR*, and *MET*. We found that the frequency of Multi-TKI related mutations was significantly higher in pediatric and adolescent patients than that in adult patients (34.57% vs 21.18% vs 10.71%, P =0.02), while the frequency of CDK4/6 inhibitor related mutations was significantly higher in adult patients than that of pediatric and adolescent patients (32.14% vs 18.82 vs 11.11%, P= 0.04) (Figure 6).

In the cohort of patients with *VEGFR* amplification, 13 individuals underwent adjuvant therapy with multi-kinase inhibitors post-surgery, including agents such as anlotinib, apatinib, and recombinant human vascular endothelial inhibitors. The median duration of follow-up was 3 months (1-20 months). Within this subgroup, 3 patients achieved a Partial Response (PR), all of whom were younger than 15 years. Furthermore, 4 patients maintained Stable Disease (SD), and 6 patients experienced Progressive Disease (PD). Notably, among the patients with PD, 4

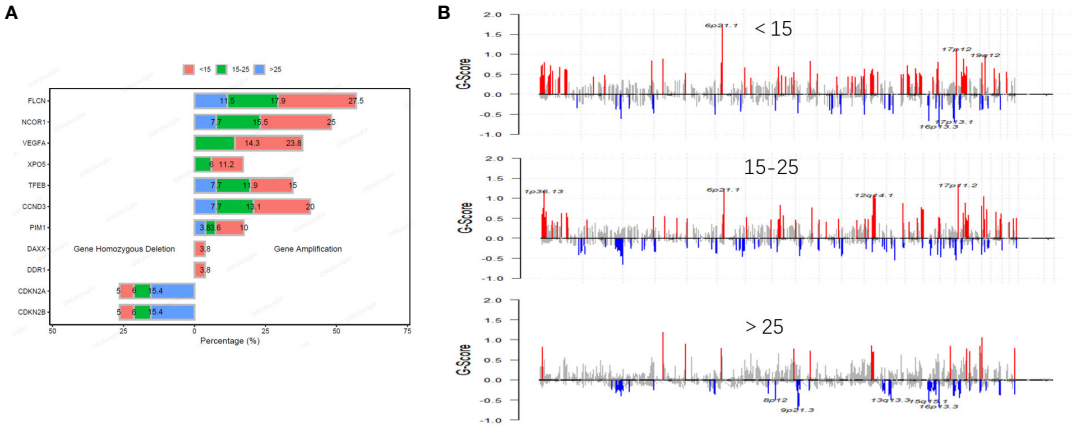

FIGURE 3
Distribution and frequency of CNVs in osteosarcoma across different age groups. The frequency of common CNV in osteosarcoma is different in different age groups **(A)**. Distribution of CNVs in osteosarcoma across different age groups **(B)**.

exhibited additional genetic alterations: 2 cases with *CDK4* amplification, 1 with *PIK3CA* amplification, and 1 with a *PTEN* mutation.

One notable case of PR was a 13-year-old patient diagnosed with proximal tibial osteosarcoma, which demonstrated *VEGFR* amplification. The patient underwent a successful surgical resection of the tumor on December 18, 2018, which was classified as Stage IIB by postoperative pathology. Between January 14, 2019, and February 22, 2019, the patient received two cycles of adjuvant chemotherapy using pirarubicin and cisplatin. Subsequent treatment from April 2019 to January 2020 included the oral *VEGFR* inhibitor anlotinib hydrochloride (Focilex).

To assess treatment response, a baseline imaging study was obtained before the initiation of anlotinib, which identified multiple lung nodules. According to RECIST criteria, target lesions were defined, with the largest nodule in the lingular segment of the left upper lobe measuring 10mm in diameter (considered as the target lesion). Follow-up CT scans were performed to evaluate the

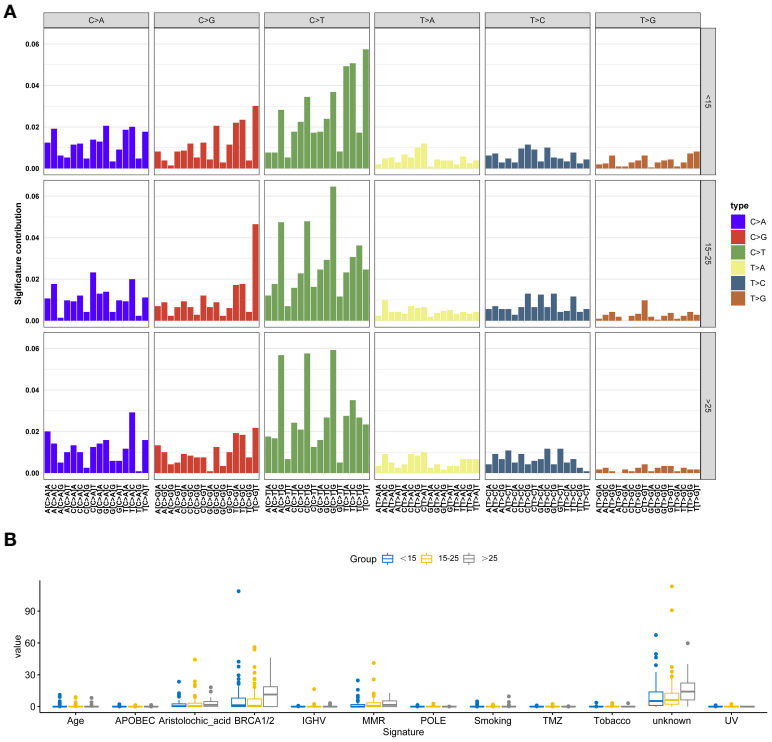

FIGURE 4
Signature analysis of this cohort. **(A)** The most significant signatures in adolescent osteosarcoma patients. **(B)** The most significant signatures in adult osteosarcoma patients.

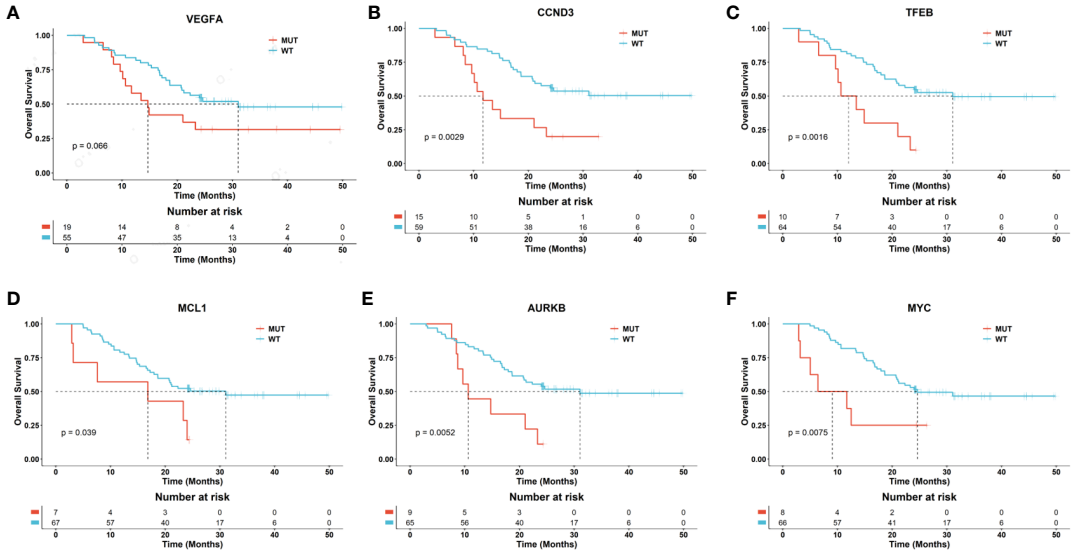

FIGURE 5
Potential biomarkers related to the prognosis of osteosarcoma patients. The Kaplan-Meier curves separately depict the overall survival (OS) for patients with and without mutations in the genes VEGFA **(A)**, CCND3 **(B)**, TFEB **(C)**, MCL1 **(D)**, AURKB **(E)**, and MYC **(F)**. The p-values between the risk groups were calculated using the log-rank test.

response at regular intervals. On July 1, 2019, the size of the target lesion had decreased to 5mm, and by September 20, 2019, it had further reduced to 4mm. Comparative imaging on December 19, 2019, showed continued reduction in the size of the target lesion as well as non-target lesions. As of March 18, 2020, the target lesions have further reduced in size. Based on the RECIST criteria, this patient achieved a Partial Response (PR), with a significant reduction in the size of the target lesion and overall tumor burden (Figure 7).

4 Discussion

With the development of molecular biology and next-generation sequencing technology, the genomic variation information of many cancer types has been revealed and applied to targeted therapy. In osteosarcoma, due to the lack of osteosarcoma samples and extensive genomic heterogeneity, the determination of its somatic therapeutic targets is particularly challenging. Although germline genetic variation is an important risk factor associated with osteosarcoma, many studies are still aiming to explore new treatments by identifying osteosarcoma related biologically important pathways (1, 25, 26). In this study, we collected 194 osteosarcoma patients, grouped them according to their age, and analyzed the mutation characteristics of pediatric, adolescent and adult osteosarcoma patients.

Previous studies have shown that the common mutant genes in osteosarcoma include *TP53*, *RB1*, *MYC* (6, 7), however, there are few studies on the mutation characteristics of osteosarcoma patients based on large samples. Our results showed that not only identified the high-frequency mutations of *TP53* and *RB1*, but also revealed high-frequency mutations in *FLCN*, *NCOR1*, *VEGFA*, *CCND3*, *TFEB*, *MAP2K4*, and *ATRX* in osteosarcoma. Mutations in *FLCN* gene are associated with Birt-Hogg-Dube syndrome, which is characterized by fibrofolliculomas, renal tumors, lung cysts, and pneumothorax (https://www.ncbi.nlm.nih.gov/gene/201163). The

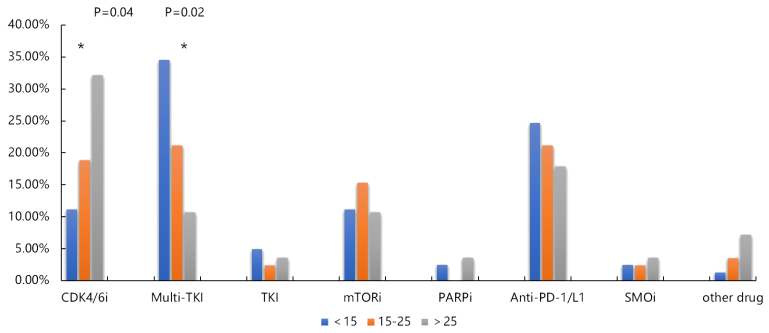

FIGURE 6
Comparison of available drug mutation distribution in pediatric, adolescent and adult osteosarcoma group. * $p < 0.05$.

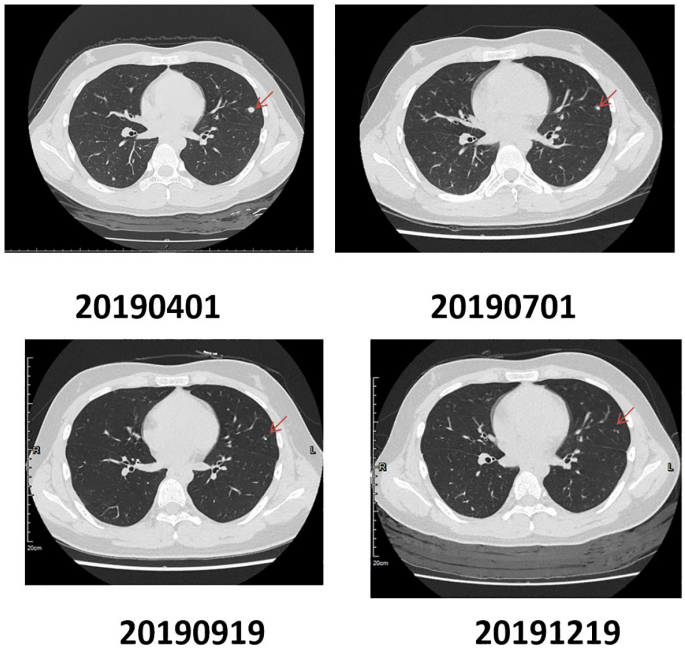

FIGURE 7
Computed Tomography (CT) imaging changes in tumor size during patient medication regimen.

FLCN gene is commonly observed in patients diagnosed with both primary and metastatic osteosarcoma (27), with a higher frequency of alterations seen in pediatric cases compared to those in adults (28). *NCOR1* is a tumor suppressor gene. According to AACR Genie cases, *NCOR1* amplification is frequently occurred proportion in osteosarcoma, which only less frequent than leiomyosarcoma (29) (https://www.mycancergenome.org/content/gene/ncor1/). *NCOR1* has been reported to be associated with prognosis in many cancer type (30, 31). In bladder cancer, *NCOR1* mutation is associated with immune biomarker such as TMB, suggesting that it may be used as biomarker for immunotherapy (32). Therefore, *NCOR1* has great potential for clinical application. Its high frequency amplification mutation in osteosarcoma may become a potential biomarker for guiding the treatment. *ATRX* deficiency can promote tumorigenesis, including enhanced cell movement of glioma cells and *TGF* in hepatoma cells-β Activation and *CDH1* (E-cadherin) down-regulation (33–35). In osteosarcoma, *ATRX* deficiency also can promote tumor formation, growth, infection and metastasis (36). In this study, there was no significant difference in the proportion of *ATRX* mutations between pediatric, adolescents and adults.

The onset characteristics of osteosarcoma are related to the age of patients. The first peak of osteosarcoma is in adolescence, which indicates that there is a close relationship between adolescent growth spurt and osteosarcoma; The second peak of osteosarcoma occurs in adults over 65 years old, which may be related to the accumulation of mutations and the occurrence of diseases (37). However, little is known about the mutation characteristics of pediatric, adolescent and adult patients with osteosarcoma. The comparison of mutation characteristics between the three groups suggested that pediatric, adolescents are more prone to gene amplification / deletion and fusion than adults, and adults may accumulate more point mutations over time. The differential signature analysis indicates that mutations characteristic of *BRCA1/2* and Aristolochic acid are more pronounced in adults, and homologous recombination deficiency associated signature may lead to the accumulation of DNA damage and genomic instability (38). These results suggested the special molecular characteristics of pediatric, adolescent and adult osteosarcoma patients. Compared to adult patients with osteosarcoma, we observed that the amplification frequencies of *NCOR1*, *VEGFA*, *CCND3*, and *TEEB* were higher in pediatric and adolescent patients. In contrast, the amplification frequencies of *CDK4*, *TSPAN31*, *GLI1*, *MDM2*, and *FRS2* were highest in adult patients with osteosarcoma, followed by adolescents, and lowest in pediatric patients. There have been few reports on mutations of *TEEB*, *GLI1*, *MDM2*, and *FRS2* in osteosarcoma. This suggests that the genetic mutation characteristics of osteosarcoma are age-related, and the pathogenesis of osteosarcoma may differ across various age groups. The *CCND3* encodes a highly conserved cell cycle regulatory protein, and the expression of cyclin is characterized by cyclicity. The fusion of *KCNMB4-CCND3* was ever detected in osteosarcoma and promoted the migration of osteosarcoma cell line SAOS-2 (39). The overexpression of *VEGFA* in various human tumors is associated with tumor cell invasion, increased vascular density, tumor metastasis, tumor recurrence and poor prognosis (40). The amplification of *VEGFA* may elevate their respective proteins in osteosarcoma (41). In this study, we grouped osteosarcoma patients by their age and suggested that high frequency *VEGFA* and *CCND3* amplification may be the

molecular characteristics of adolescent osteosarcoma patients. There has been an increasing interest in exploring the role of *TSPAN31* in cancerous diseases. Earlier studies have discovered a significant rise in *TSPAN31* levels in osteosarcoma, hinting at its possible link to the expansion and dissemination of the tumor. It is also important to point out that *TSPAN31* acts as a natural antisense transcript to *CDK4*. Investigations have demonstrated that *TSPAN31* plays a role in the advancement of tumors by controlling the expression of *CDK4*, with evidence from research on cervical and liver cancer cases (42–44). *FRS2* and *MDM2* are close to each other on chromosomes and are often detected in the form of co-amplification. Previous study had shown that the amplification of *FRS2* and *MDM2* occurs frequently in low-grade osteosarcoma (95%, 21/22), and only one of these patients is younger than 20 years old (45). Our research underscores the high amplification frequency of MDM2 within the adult patient population, particularly considering MDM2's role in the negative regulation of the p53 pathway—a pivotal aspect of tumor biology. The amplification of MDM2 correlates with increased protein levels capable of inhibiting p53, thereby promoting tumor progression and potentially exerting a detrimental effect on patient outcomes. The age-specific prevalence of MDM2 amplification identified in our study positions it as a valuable biomarker for the diagnosis and prognosis of adult osteosarcoma. It may also signal the need for more aggressive therapeutic approaches in this demographic group. Furthermore, the potential for targeted therapy against MDM2, with inhibitors that are already undergoing clinical trials for other cancers, presents an optimistic path for personalized treatment strategies. Recognizing the necessity for additional validation, we propose further research to solidify the predictive and prognostic utility of MDM2 amplification. This would involve larger patient cohorts and an analysis of clinical outcomes, such as treatment response, disease progression, and survival rates. Other studies have shown that higher TMB is more distributed in older patients (46). Similar results have been obtained in our study. The TMB of adult patients is higher than that of pediatric patients, which may be related to the long-term accumulation of point mutations. This also supports our previous conjecture to properly explain the age characteristics of osteosarcoma patients. A significant role of NGS in cancer precision medicine is to detect potential available targets (47). *PDGFRA* and *KIT* mutations are common in gastrointestinal stromal tumors (48). Our results suggest that these two mutations are also common in patients with osteosarcoma. Sunitinib, regorafenib, and imatinib have kinase inhibitory activities of *KIT* and *PDGFRA* (49). Studies have shown that regorafenib is also active in osteosarcoma (50). However, we did not find any difference in the frequency of these gene mutations between adolescent and adult osteosarcoma patients.

Osteosarcomas are genetically defined by significant genomic instability, which is manifested through extensive aneuploidy, the existence of imbalanced chromosomal rearrangements, and the frequent amplification or deletion of various genomic segments. Previous studies have indicated that amplifications in osteosarcoma are commonly concentrated in specific regions such as regions 6p12-p21, 8q24, and 17p11.2-p12 (51–53). However, differences in amplification regions among patients of varying age groups have not yet been reported. Our genomic analysis identified a chromosomal hotspot harboring high-frequency mutations at the 6p21 locus, particularly involving the *TFEB*, *CCND3*, and *VEGFA* genes. This region is known to be critical during pediatric and adolescence, and the presence of mutations in this area may indicate a predisposition to certain malignancies in younger populations. These results indicate the unique prognosis molecular indicators of osteosarcoma patients in different age groups.

Previous studies have indicated that the loss of *RB1*, amplification of *MYC*, and amplification of *VEGFA* are molecular characteristics that can identify high-risk patients. However, these risk factors have not been fully validated and cannot yet serve as the basis for clinical risk stratification (54). Our research findings suggest that in addition to *MYC*, mutations in the genes *MCL1*, *TFEB*, *CCND3*, *AURKB*, and *ALOX12B* are also significantly associated with poor prognosis. Additionally, mutations in the *VEGFA* gene have shown a trend towards association with poor prognosis, although the p-value is close to the significance threshold and has not yet reached statistical significance. Given the critical role of *VEGFA* in angiogenesis, this trend suggests that the gene might play a role in vascular supply and tumor microenvironment formation in osteosarcoma. These findings prompt us to further investigate the specific role of *VEGFA* in the development of osteosarcoma and to explore its potential as a therapeutic target.

VEGFA can bind to vascular endothelial growth factor receptor on the surface of cell membrane, produce biological effects through a series of signal pathways, and finally lead to angiogenesis (55), and plays a role in regulating vascular development and is the target of targeted drugs to inhibit angiogenesis (56). VEGF/VEGFR can be used as a target to inhibit angiogenesis (57–59). The most common CNV of osteosarcoma includes *VEGFA*, which suggested the potential opportunity to benefit from anti-angiogenic agent (60). In our cohort, we stratified the patients and found that 100% of patients with *VEGFA* mutations belong to pediatric and adolescent patients. The *VEGFA* variations correspond to Multi-TKI, and the high proportion of *VEGFA* variants in pediatric and adolescents may result in the more opportunities to benefit from Multi-TKI treatment than adults. This also showed that it is necessary to stratify patients with osteosarcoma according to their age and provide accurate medical treatment.

The CDK4/6 inhibitor related gene include *CDKN2A/B*, *CCND1*, and *CDK4*, and the variations frequency of these genes increase with age (61). Research has indicated that elevated levels of *CDK4* expression and its amplification in tumors serve as predictive biomarkers for resistance to standard chemotherapy in osteosarcoma (OS) patients, suggesting that palbociclib holds potential as an effective treatment option for this clinically challenging group (62). Our study findings confirm the same trend, with higher frequencies of *CDKN2A/B*, *CCND1*, and *CDK4* gene mutations observed in adults. This indicates that with the growth of age, adult osteosarcoma patients are more likely to accumulate age-related gene mutations, including *CDKN2A/B*, *CCND1*, and *CDK4*, which supports that adult osteosarcoma patients may have more opportunities to benefit from CDK4/6 inhibitors.

Additionally, our study found that the number of patients under the age of 15 (81 cases) closely matches those aged 15-25 (85 cases),

with their molecular differences predominantly centralized in variations in enriched signaling pathways. In patients older than 15, gene mutations are mainly enriched in the cell cycle and PI3K/mTOR signaling pathways. In contrast, patients younger than 15 exhibit gene mutations largely concentrated in the cell cycle and angiogenesis signaling pathways. CDK4 mutations are more frequently observed in adolescent patients. Furthermore, all patients who achieved partial remission with multitargeted kinase inhibitor therapy were under the age of 15. There are also mutual molecular features; mutations in VEGFA, CCND3, and TFEB are significantly present in both children and adolescents. The amplification rates of VEGFA and XPO5 are high in pediatric and adolescent patients as well, whereas mutations in CDKN2A and CDKN2B are more common in adults, underscoring the stark differences between pediatric/adolescent and adult patients. Adolescent patients may represent a transitional state in terms of molecular characteristics and treatment responses, falling between children and adults.

The study examining molecular distinctions among pediatric, adolescent, and adult patients with osteosarcoma is subject to several limitations: It encompasses a modest patient population of 194 cases, potentially curtailing the power to discern differences and possibly not reflecting the wider osteosarcoma demographic. Although the research indicates potential associations between certain mutations and poorer outcomes, these findings do not confirm causality or establish definitive prognostic indicators without additional substantiation. Consequently, while the study sheds valuable light on the molecular landscape of osteosarcoma across various age groups, the results warrant cautious interpretation and require corroboration via more extensive, prospective, multicentered studies with prolonged follow-up periods and randomized clinical trials to determine the true clinical relevance of the molecular markers identified. Another limitation of our study is that 28 of 194 patients who were enrolled had tissue samples obtained from needle biopsies, and tumor heterogeneity poses substantial challenges. This heterogeneity implies that distinct molecular profiles may be present in different tumor areas, making genetic data interpretation complex. Biopsy samples inherently offer a limited snapshot of the entire tumor since they are typically obtained from a single region. This selective sampling might render an incomplete or potentially misleading picture of the tumor's genetic makeup. The impact of tumor heterogeneity on study outcomes is significant; it may lead to overrepresentation of genetic alterations that are prevalent in the sampled region but not indicative of the whole tumor. Conversely, crucial mutations in other tumor parts may be overlooked. Such omissions could profoundly affect our conclusions on the correlation between genetic mutations and clinical outcomes, as they might not accurately reflect the mutational burden of the entire tumor. To mitigate the potential biases introduced by tumor heterogeneity in biopsy samples, future studies should consider incorporating multiple biopsy samples from diverse tumor regions when possible. Additionally, the comparison of genetic data from biopsy samples with that from complete tumor resections could yield a more holistic view of the molecular changes in osteosarcoma. Employing standardized methods for sample collection and DNA sequencing, as well as including larger patient cohorts from various demographics, is essential for future research. These steps will help lessen the effects of heterogeneity and enhance the generalizability of the study's findings to a broader osteosarcoma patient population. In this study, the majority of the specimens were surgical samples obtained after 2 to 3 cycles of neoadjuvant chemotherapy. We acknowledge that neoadjuvant chemotherapy may impact the genomic analysis of the surgical tissue. The potential effects include a significant reduction in the number of detectable tumor cells, which could affect genetic analyses that require a sufficient quantity of tumor cells. Chemotherapy might selectively eliminate tumor cell populations that are sensitive to the drugs, leaving behind resistant populations, which could result in altered genetic characteristics of the tumor. Furthermore, chemotherapy could influence the gene expression patterns within tumor cells, leading to the upregulation or downregulation of certain genes, thereby affecting the outcomes of genetic testing.

In this study, we examined the molecular characteristics of osteosarcoma across pediatric, adolescent, and adult patients, highlighting differences in the molecular mechanisms of the disease between adolescents and adults, and investigated biomarkers that could specifically predict the prognosis of adolescent osteosarcoma patients. Furthermore, we identified the importance of age in the distribution of copy number variations (CNVs) and point mutations, revealing age-related pathogenic differences and the potential influence of certain genetic variations on patient outcomes. Notably, younger patients with VEGFR-amplified osteosarcoma who received adjuvant multi-kinase inhibitor therapy achieved partial remission or disease stabilization, emphasizing the necessity for personalized treatment approaches. These insights contribute to a deeper understanding of the genetic heterogeneity in osteosarcoma and support the development of precise diagnostic and treatment strategies that are tailored to the individual needs of patients from different age cohorts.

Data availability statement

The authors acknowledge that the data presented in this study must be deposited and made publicly available in an acceptable repository, prior to publication. Frontiers cannot accept an article that does not adhere to our open data policies.

Ethics statement

The studies involving humans were approved by The Clinical Research and Laboratory Animal Ethics Committee of the First Affiliated Hospital of Sun Yat-sen University. The studies were conducted in accordance with the local legislation and institutional requirements. The human samples used in this study were acquired from Tissue samples are the remaining samples for pathological diagnosis, which will not affect the subject's diagnosis. The studies were conducted in accordance with the local legislation and institutional requirements. The human samples used in this study were obtained in compliance with ethical standards. Written informed consent for participation was not required from the participants or the participants' legal guardians/next of kin in

accordance with the national legislation and institutional requirements. Written informed consent was obtained from the minor(s)' legal guardian/next of kin for the publication of any potentially identifiable images or data included in this article.

Author contributions

JS: Funding acquisition, Project administration, Resources, Supervision, Writing – review & editing. CZ: Data curation, Funding acquisition, Writing – review & editing. RH: Conceptualization, Data curation, Investigation, Writing – original draft. TL: Investigation, Supervision, Writing – review & editing. YW: Formal analysis, Writing – original draft. JT: Resources, Supervision, Writing – review & editing. LZ: Formal analysis, Visualization, Writing – review & editing. BW: Investigation, Methodology, Writing – review & editing. JH: Formal analysis, Methodology, Writing – review & editing. ZZ: Resources, Validation, Writing – review & editing. XX: Resources, Supervision, Writing – review & editing. GH: Data curation, Resources, Writing – review & editing. KW: Resources, Writing – review & editing. JY: Project administration, Resources, Supervision, Validation, Writing – review & editing.

Funding

The author(s) declare financial support was received for the research, authorship, and/or publication of this article. This work is supported by grants from the National Natural Science Foundation of China (NSFC) -General Program (82072964, 81972507 and 82273413).

Acknowledgments

The authors are grateful to all the study participants, patients, and their family members for their contributions and support.

Conflict of interest

Authors YW, LZ, JH, and KW were employed by OrigiMed.

The authors declare that the research was conducted in the absence of any commercial or financial relationships that could be construed as a potential conflict of interest.

Publisher's note

Supplementary material

The Supplementary Material for this article can be found online at: https://www.frontiersin.org/articles/10.3389/fonc.2024.1382276/full#supplementary-material

SUPPLEMENTARY FIGURE 1
Distribution of mutation types in osteosarcoma patients.

References

1. Whelan JS, Davis LE. Osteosarcoma, chondrosarcoma, and chordoma. *J Clin Oncol*. (2018) 36:188–93. doi: 10.1200/JCO.2017.75.1743

2. Mirabello L, Troisi RJ, Savage SA. Osteosarcoma incidence and survival rates from 1973 to 2004: data from the Surveillance, Epidemiology, and End Results Program. *Cancer: Interdiscip Int J Am Cancer Soc*. (2009) 115:1531–43. doi: 10.1002/cncr.24121

3. Bielack SS, Kempf-Bielack B, Delling G, Exner GU, Flege S, Helmke K, et al. Prognostic factors in high-grade osteosarcoma of the extremities or trunk: an analysis of 1,702 patients treated on neoadjuvant cooperative osteosarcoma study group protocols. *J Clin Oncol*. (2002) 20:776–90. doi: 10.1200/JCO.20.3.776

4. Kager L, Zoubek A, Poütschger U, Kastner U, Flege S, Kempf-Bielack B, et al. Primary metastatic osteosarcoma: presentation and outcome of patients treated on neoadjuvant Cooperative Osteosarcoma Study Group protocols. *J Clin Oncol*. (2003) 21:2011–8. doi: 10.1200/JCO.2003.08.132

5. Lewis IJ, Nooij MA, Whelan J, Sydes MR, Grimer R, Hogendoorn PC, et al. Improvement in histologic response but not survival in osteosarcoma patients treated with intensified chemotherapy: a randomized phase III trial of the European Osteosarcoma Intergroup. *J Natl Cancer Institute*. (2007) 99:112–28. doi: 10.1093/jnci/djk015

6. Wachtel M, Schäfer BW. Targets for cancer therapy in childhood sarcomas. *Cancer Treat Rev*. (2010) 36:318–27. doi: 10.1016/j.ctrv.2010.02.007

7. Jiang Y, Wang T, Wei Z. Construction and validation of nomograms for predicting the prognosis of juvenile osteosarcoma: a real-world analysis in the SEER database. *Technol Cancer Res Treat*. (2020) 19:1533033820947718. doi: 10.1177/1533033820947718

8. Morsy AM, Ahmed BM, Rezk KM, Ramadan IK, Aboelgheit AM, Eltyb HA, et al. Age and tumor location predict survival in nonmetastatic osteosarcoma in upper Egypt. *J Pediatr Hematology/Oncology*. (2020) 42:e66–78. doi: 10.1097/MPH.0000000000001506

9. Ding WZ, Liu K, Li Z, Chen SR. A meta-analysis of prognostic factors of osteosarcoma. *Eur Rev Med Pharmacol Sci*. (2020) 24:4103–12. doi: 10.26355/eurrev_202004_20989

10. Savage SA, Mirabello L. Using epidemiology and genomics to understand osteosarcoma etiology. *Sarcoma*. (2011) 2011:548151. doi: 10.1155/2011/548151

11. Ferrari S, Bielack SS, Smeland S, Longhi A, Egerer G, Sundby Hall K, et al. EURO-BOSS: A European study on chemotherapy in bone-sarcoma patients aged over 40: Outcome in primary high-grade osteosarcoma. *Tumori J*. (2018) 104:30–6. doi: 10.5301/tj.5000696

12. Grimer RJ, Cannon SR, Taminiau AM, Bielack S, Kempf-Bielack B, Windhager R, et al. Osteosarcoma over the age of forty. *Eur J Cancer*. (2003) 39:157–63. doi: 10.1016/S0959-8049(02)00478-1

13. Chen X, Bahrami A, Pappo A, Easton J, Dalton J, Hedlund E, et al. Recurrent somatic structural variations contribute to tumorigenesis in pediatric osteosarcoma. *Cell Rep*. (2014) 7:104–12. doi: 10.1016/j.celrep.2014.03.003

14. Hu K, Dai HB, Qiu ZL. mTOR signaling in osteosarcoma: Oncogenesis and therapeutic aspects. *Oncol Rep*. (2016) 36:1219–25. doi: 10.3892/or.2016.4922

15. Li Y, Liu Q, He HB, Luo W. The possible role of insulin-like growth factor-1 in osteosarcoma. *Curr Problems Cancer*. (2019) 43:228–35. doi: 10.1016/j.currproblcancer.2018.08.008

16. Assi T, Watson S, Samra B, Rassy E, Le Cesne A, Italiano A, et al. Targeting the VEGF pathway in osteosarcoma. *Cells*. (2021) 10:1240. doi: 10.3390/cells10051240

17. Xu J, Xie L, Guo W. PDGF/PDGFR effects in osteosarcoma and the "add-on" strategy. *Clin Sarcoma Res*. (2018) 8:1–9. doi: 10.1186/s13569-018-0102-1

18. Tsuchie H, Emori M, Nagasawa H, Miyakoshi N, Murahashi Y, Shimizu J, et al. Prognosis of primary osteosarcoma in elderly patients: a comparison between young and elderly patients. *Med Principles Pract*. (2019) 28:425–31. doi: 10.1159/000500404

19. Vasquez L, Silva J, Chavez S, Zapata A, Diaz R, Tarrillo F, et al. Prognostic impact of diagnostic and treatment delays in children with osteosarcoma. *Pediatr Blood Cancer*. (2020) 67:e28180. doi: 10.1002/pbc.28180

20. Pan Y, Chen D, Hu T, Lv G, Dai Z. Characteristics and prognostic factors of patients with osteosarcoma older than 60 years from the SEER database. *Cancer Control*. (2019) 26:1073274819888893. doi: 10.1177/1073274819888893

21. Roux A, Pallud J, Saffroy R, Edjlali-Goujon M, Debily MA, Boddaert N, et al. High-grade gliomas in adolescents and young adults highlight histomolecular differences from their adult and pediatric counterparts. *Neuro-oncology*. (2020) 22:1190–202. doi: 10.1093/neuonc/noaa024

22. Kaya M, Wada T, Akatsuka T, Kawaguchi S, Nagoya S, Shindoh M, et al. Vascular endothelial growth factor expression in untreated osteosarcoma is predictive of pulmonary metastasis and poor prognosis. *Clin Cancer Res*. (2000) 6:572–7.

23. Worch J, Matthay KK, Neuhaus J, Goldsby R, DuBois SG. Osteosarcoma in children 5 years of age or younger at initial diagnosis. *Pediatr Blood Cancer*. (2010) 55:285–9. doi: 10.1002/pbc.22509

24. Blokzijl F, Janssen R, Van Boxtel R, Cuppen E. MutationalPatterns: comprehensive genome-wide analysis of mutational processes. *Genome Med*. (2018) 10:1–11. doi: 10.1186/s13073-018-0539-0

25. Friebele JC, Peck J, Pan X, Abdel-Rasoul M, Mayerson JL. Osteosarcoma: a meta-analysis and review of the literature. *Am J Orthop*. (2015) 44:547–53.

26. Meyers PA, Heller G, Healey JH, Huvos A, Applewhite A, Sun M, et al. Osteogenic sarcoma with clinically detectable metastasis at initial presentation. *J Clin Oncol*. (1993) 11:449–53. doi: 10.1200/JCO.1993.11.3.449

27. Zou C, Zhao Z, Xu M, Guo W, Huang J, Zhang X, et al. Deciphering possible mechanisms of action in pathophysiology of osteosarcoma: PI3K-Akt/MAPK pathways contribute to tumorigenesis versus FoxO/mTOR/HIF-1 pathways involved in metastasis. *J Clin Oncol*. (2022) 40:e23515–e23515. doi: 10.1200/JCO.2022.40.16_suppl.e23515

28. Seeber A, Elliott A, Modiano J, Untergasser G, von Mehren M, Rosenberg AE, et al. Age as a factor in the molecular landscape and the tumor-microenvironmental signature of osteosarcoma. *J Clin Oncol*. (2022) 40. doi: 10.1200/JCO.2022.40.16_suppl.11525

29. André F, Arnedos M, Baras AS, Baselga J, Bédard PL, Berger MF, et al. AACR Project GENIE: powering precision medicine through an international consortium. *Cancer Discovery*. (2017) 7:818–31. doi: 10.1158/2159-8290.cd-17-0151

30. Noblejas-López MM, Morcillo-Garcia S, Nieto-Jiménez C, Nuncia-Cantarero M, Győrffy B, Galan-Moya EM, et al. Evaluation of transcriptionally regulated genes identifies NCOR1 in hormone receptor negative breast tumors and lung adenocarcinomas as a potential tumor suppressor gene. *PloS One*. (2018) 13:e0207776. doi: 10.1371/journal.pone.0207776

31. Tang L, Zhang L, Liu L, Dong L, Dong Y, Zhu W, et al. NCOR1 may be a potential biomarker of a novel molecular subtype of prostate cancer. *FEBS Open Bio*. (2020) 10:2678–86. doi: 10.1002/2211-5463.13004

32. Lin A, Qiu Z, Zhang J, Luo P. Effect of NCOR1 mutations on immune microenvironment and efficacy of immune checkpoint inhibitors in patient with bladder cancer. *Front Immunol*. (2021) 12:630773. doi: 10.3389/fimmu.2021.630773

33. Danussi C, Bose P, Parthasarathy PT, Silberman PC, Van Arnam JS, Vitucci M, et al. Atrx inactivation drives disease-defining phenotypes in glioma cells of origin through global epigenomic remodeling. *Nat Commun*. (2018) 9:1057. doi: 10.1038/s41467-018-03476-6

34. Haase S, Garcia-Fabiani MB, Carney S, Altshuler D, Núñez FJ, Méndez FM, et al. Mutant ATRX: uncovering a new therapeutic target for glioma. *Expert Opin Ther Targets*. (2018) 22:599–613. doi: 10.1080/14728222.2018.1487953

35. Liang J, Liu H, Li G, Qian J, Gao R, Zhou Y, et al. Global changes in chromatin accessibility and transcription following ATRX inactivation in human cancer cells. *FEBS Lett*. (2020) 594:67–78. doi: 10.1002/1873-3468.13549

36. DeWitt SB, Plumlee SH, Brighton HE, Sivaraj D, Martz EJ, Zand M, et al. Loss of ATRX promotes aggressive features of osteosarcoma with increased NF-κB signaling and integrin binding. *JCI Insight*. (2022) 7:e15158. doi: 10.1172/jci.insight.151583

37. Ottaviani G, Jaffe N. The epidemiology of osteosarcoma. *Pediatr Adolesc osteosarcoma*. (2010), 3–13. doi: 10.1093/annonc/mdx709

38. Hoppe MM, Sundar R, Tan DSP, Jeyasekharan AD. Biomarkers for homologous recombination deficiency in cancer. *JNCI: J Natl Cancer Institute*. (2018) 110:704–13. doi: 10.1093/jnci/djy085

39. Yang J, Annala M, Ji P, Wang G, Zheng H, Codgell D, et al. Recurrent LRP1-SNRNP25 and KCNMB4-CCND3 fusion genes promote tumor cell motility in human osteosarcoma. *J Hematol Oncol*. (2014) 7:1–10. doi: 10.1186/s13045-014-0076-2

40. Kerbel RS. Tumor angiogenesis. *New Engl J Med*. (2008) 358:2039–49. doi: 10.1056/NEJMra0706596

41. Yang J, Zhao L, Tian W, Liao Z, Zheng H, Wang G, et al. Correlation of WWOX, RUNX2 and VEGFA protein expression in human osteosarcoma. *BMC Med Genomics*. (2013) 6:1–8. doi: 10.1186/1755-8794-6-56

42. Ragazzini P, Gamberi G, Pazzaglia L, Serra M, Magagnoli G, Ponticelli F, et al. Amplification of CDK4, MDM2, SAS and GLI genes in leiomyosarcoma, alveolar and embryonal rhabdomyosarcoma. *Histol Histopathology*. (2004) 19(2):401–11. doi: 10.14670/hh-19.401

43. Xia Y, Deng Y, Zhou Y, Li D, Sun X, Gu L, et al. TSPAN31 suppresses cell proliferation in human cervical cancer through down-regulation of its antisense pairing with CDK4. *Cell Biochem Funct*. (2020) 38:660–8. doi: 10.1002/cbf.3526

44. Wang J, Zhou Y, Li D, Sun X, Deng Y, Zhao Q. TSPAN 31 is a critical regulator on transduction of survival and apoptotic signals in hepatocellular carcinoma cells. *FEBS Lett*. (2017) 591:2905–18. doi: 10.1002/1873-3468.12737

45. He X, Pang Z, Zhang X, Lan T, Chen H, Chen M, et al. Consistent amplification of FRS2 and MDM2 in low-grade osteosarcoma. *Am J Surg Pathol*. (2018) 42:1143–55. doi: 10.1097/PAS.0000000000001125

46. Wang L, Pan S, Zhu B, Yu Z, Wang W. Comprehensive analysis of tumour mutational burden and its clinical significance in prostate cancer. *BMC Urol*. (2021) 21:1–10. doi: 10.1186/s12894-021-00795-7

47. Strom SP. Current practices and guidelines for clinical next-generation sequencing oncology testing. *Cancer Biol Med*. (2016) 13:3. doi: 10.20892/j.issn.2095-3941.2016.0004

48. Lasota J, Miettinen M. KIT and PDGFRA mutations in gastrointestinal stromal tumors (GISTs). *Semin Diagn Pathol*. (2006) 23:91–102. doi: 10.1053/j.semdp.2006.08.006

49. Demetri GD, Reichardt P, Kang YK, Blay JY, Rutkowski P, Gelderblom H, et al. Efficacy and safety of regorafenib for advanced gastrointestinal stromal tumours after failure of imatinib and sunitinib (GRID): an international, multicentre, randomised, placebo-controlled, phase 3 trial. *Lancet*. (2013) 381:295–302. doi: 10.1016/S0140-6736(12)61857-1

50. Davis LE, Bolejack V, Ryan CW, Ganjoo KN, Loggers ET, et al. Randomized double-blind phase II study of regorafenib in patients with metastatic osteosarcoma. *J Clin Oncol*. (2019) 37:1424. doi: 10.1200/JCO.18.02374

51. Forus A, Weghuis DO, Smeets D, Fodstad O, Myklebost O, Geurts van Kessel A. Comparative genomic hybridization analysis of human sarcomas: II. Identification of novel amplicons at 6p and 17p in osteosarcomas. *Genes Chromosomes Cancer*. (1995) 14:15–21. doi: 10.1002/gcc.2870140104

52. Lau CC, Harris CP, Lu XY, Perlaky L, Gogineni S, Chintagumpala M, et al. Frequent amplification and rearrangement of chromosomal bands 6p12-p21 and 17p11. 2 in osteosarcoma. *Genes Chromosomes Cancer*. (2004) 39:11–21. doi: 10.1002/gcc.10291

53. Selvarajah S, Yoshimoto M, Ludkovski O, Park PC, Bayani J, Thorner P, et al. Genomic signatures of chromosomal instability and osteosarcoma progression detected by high resolution array CGH and interphase FISH. *Cytogenetic Genome Res*. (2008) 122:5–15. doi: 10.1159/000151310

54. Beird HC, Bielack SS, Flanagan AM, Gill J, Heymann D, Janeway KA, et al. Osteosarcoma. *Nat Rev Dis Primers*. (2022) 8:77. doi: 10.1038/s41572-022-00409-y

55. Holmes DIR, Zachary I. The vascular endothelial growth factor (VEGF) family: angiogenic factors in health and disease. *Genome Biol*. (2005) 6(2):209. doi: 10.1186/gb-2005-6-2-209

56. Eswarappa SM, Fox PL. Antiangiogenic VEGF-Ax: a new participant in tumor angiogenesis. *Cancer Res*. (2015) 75:2765–9. doi: 10.1158/0008-5472.CAN-14-3805

57. Cao G, Li X, Qin C, Li J. Prognostic value of VEGF in hepatocellular carcinoma patients treated with sorafenib: a meta-analysis. *Med Sci monitor: Int Med J Exp Clin Res*. (2015) 21:3144. doi: 10.12659/MSM.894617

58. Peng H, Zhang Q, Li J, Zhang N, Hua Y, Xu L, et al. Apatinib inhibits VEGF signaling and promotes apoptosis in intrahepatic cholangiocarcinoma. *Oncotarget*. (2016) 7:17220. doi: 10.18632/oncotarget.v7i13

59. Amano T, Iijima H, Shinzaki S, Tashiro T, Iwatani S, Tani M, et al. Vascular endothelial growth factor-A is an Immunohistochemical biomarker for the efficacy of bevacizumab-containing chemotherapy for duodenal and jejunal adenocarcinoma. *BMC Cancer*. (2021) 21:978. doi: 10.1186/s12885-021-08724-5

60. Suehara Y, Alex D, Bowman A, Middha S, Zehir A, Chakravarty D, et al. Clinical genomic sequencing of pediatric and adult osteosarcoma reveals distinct molecular subsets with potentially targetable alterations. *Clin Cancer Res*. (2019) 25:6346–56. doi: 10.1158/1078-0432.CCR-18-4032

61. Chatsirisupachai K, Lesluyes T, Paraoan L, Van Loo P, de Magalhães JP. An integrative analysis of the age-associated multi-omic landscape across cancers. *Nat Commun*. (2021) 12:2345. doi: 10.1038/s41467-021-22560-y

62. Iwata S, Tatsumi Y, Yonemoto T, Araki A, Itami M, Kamoda H, et al. CDK4 overexpression is a predictive biomarker for resistance to conventional chemotherapy in patients with osteosarcoma. *Oncol Rep*. (2021) 46:1–11. doi: 10.3892/or

frontiers | Frontiers in Oncology

TYPE Review
PUBLISHED 08 October 2024
DOI 10.3389/fonc.2024.1441460

OPEN ACCESS

EDITED BY
Teresita Padilla-Benavides,
Wesleyan University, United States

REVIEWED BY
Mario Chiariello,
Italian National Research Council, Italy
Lisa Gherardini,
National Research Council (CNR), Italy

*CORRESPONDENCE
Ahmad Daher
adaher@uic.edu

RECEIVED 31 May 2024
ACCEPTED 23 September 2024
PUBLISHED 08 October 2024

CITATION
Bae WH, Maraka S and Daher A (2024) Challenges and advances in glioblastoma targeted therapy: the promise of drug repurposing and biomarker exploration. *Front. Oncol.* 14:1441460. doi: 10.3389/fonc.2024.1441460

Challenges and advances in glioblastoma targeted therapy: the promise of drug repurposing and biomarker exploration

William Han Bae[1], Stefania Maraka[2] and Ahmad Daher[2*]

[1]Division of Hematology/Oncology, Department of Internal Medicine, University of Illinois Chicago, Chicago, IL, United States, [2]Department of Neurology and Rehabilitation, University of Illinois Chicago, Chicago, IL, United States

Glioblastoma remains the most prevalent and aggressive primary malignant brain tumor in adults, characterized by limited treatment options and a poor prognosis. Previous drug repurposing efforts have yielded only marginal survival benefits, particularly those involving inhibitors targeting receptor tyrosine kinase and cyclin-dependent kinase-retinoblastoma pathways. This limited efficacy is likely due to several critical challenges, including the tumor's molecular heterogeneity, the dynamic evolution of its genetic profile, and the restrictive nature of the blood-brain barrier that impedes effective drug delivery. Emerging diagnostic tools, such as circulating tumor DNA and extracellular vesicles, offer promising non-invasive methods for real-time tumor monitoring, potentially enabling the application of targeted therapies to more selected patient populations. Moreover, innovative drug delivery strategies, including focused ultrasound, implantable drug-delivery systems, and engineered nanoparticles, hold potential for enhancing the bioavailability and therapeutic efficacy of treatments.

KEYWORDS

glioblastoma, targeted therapy, drug repurposing, liquid biopsy, extracellular vesicle (EV), ctDNA

1 Introduction

Glioblastoma (GB) is the most common and aggressive adult primary malignant brain tumor. First-line FDA-approved treatment relies on a multimodal approach of surgery, radiation, temozolomide (TMZ) chemotherapy, and tumor-treating fields. Unfortunately, the prognosis remains poor, with a median overall survival (mOS) of 20.9 months and a median progression-free survival (mPFS) of 6.7 months (1). The therapeutic outcomes are even less favorable in recurrent disease, where there is no standard of care, and the mOS from the first recurrence is around 6.5 months (2). Currently, there are only limited FDA-approved drugs for GB, such as TMZ, Bevacizumab, CCNU, and BiCNU, highlighting the urgent need for

new treatment options for GB. One of the most promising approaches in cancer therapy is implementing next-generation sequencing (NGS) techniques to uncover actionable mutations that can be targeted in a tissue-agnostic fashion. In that regard, repurposing existing anticancer medications offers a potentially efficient and effective tool to discover new therapeutic agents for GB.

Here, we will discuss the previously explored repurposing efforts in the treatment of GB based on targeting two of the three most altered signal transduction pathways in GB: Receptor tyrosine kinase (RTK) and cyclin-dependent kinase (CDK)-retinoblastoma (Rb) (3). Approximately 57-60% of glioblastomas exhibit alterations in the RTK/PI3K pathway, with EGFR amplification or mutation being the most common, occurring in about 40-50% of cases (3). The CDK-Rb pathway is also frequently altered, with aberrations occurring in about 78-80% of cases, often involving the loss of CDKN2A, amplification of CDK4 or CDK6, and/or inactivation of the Rb1 protein. There are no validated targeted therapeutics for the murine double minute 2 (MDM2)-p53 pathway, the third commonly altered pathway in GB or other malignancies, primarily due to its crucial role in normal cell functions (4).

Despite an increased understanding of GB tumor biology with discoveries of potential targets, the unique challenges posed by this aggressive tumor continue to thwart treatment benefits. The tumor microenvironment (TME) of GB is highly heterogeneous and exceptionally dynamic, creating a landscape where cancer cells can evade therapies and rapidly adapt to treatment pressures. Compounding this complexity is the formidable blood-brain barrier (BBB), which acts as a gatekeeper, severely limiting the delivery of therapeutic agents to the tumor bed. Moreover, the inherent risk and challenges with accessing GB tissue at recurrence further hamper the ability to tailor treatments to individual patients, making it difficult to combat this relentless disease.

However, hope lies in innovative approaches designed to overcome these barriers. Cutting-edge techniques aimed at enhancing the detection of cancer biomarkers are on the horizon, offering the potential for more precise targeting of GB. Additionally, novel drug delivery vehicles, such as nanoparticles (NPs), are being developed to penetrate the BBB and deliver therapies directly to the tumor site. These advancements not only hold promise for improving treatment outcomes but also represent a bold step forward in the fight against GB.

2 RTK pathway inhibitors

2.1 Epidermal growth factor receptor-targeted agents

Anti-EGFR tyrosine kinase inhibitors (TKIs) have been a focal point in GB treatment trials due to the high rates of EGFR alterations, reaching ~60% in GB (5). Gefitinib was the first anti-EGFR TKI tested in GB. Various trials evaluated the role of gefitinib monotherapy in recurrent glioblastoma (rGB) treatment, showing good safety data but without promising efficacy (6, 7). The use of gefitinib with other RTK pathway inhibitors (8) and in newly diagnosed GB (nGB) treatment (9) was similarly inefficacious.

Erlotinib demonstrated limited efficacy in the treatment of GB. Early clinical trials indicated minimal activity, primarily because the drug couldn't penetrate the blood-brain barrier (BBB) effectively and because the tumor growth wasn't largely dependent on the targeted pathway (10). Subsequent trials exploring combinations of erlotinib with various chemotherapeutic agents, such as carboplatin, failed to yield significant improvements in PFS or OS in rGB (11). Additionally, while the addition of receptor tyrosine kinase (RTK) pathway inhibitor sirolimus, the mammalian target of rapamycin (mTOR) inhibitor temsirolimus, Ras/Raf/mitogen-activated protein kinase (MAPK) inhibitor sorafenib, and the anti-angiogenic agent bevacizumab was well tolerated, these combinations did not translate into clinically meaningful survival benefits (12–15). Furthermore, erlotinib demonstrated limited efficacy in treating newly diagnosed glioblastoma (nGB) (16).

Lapatinib, a dual inhibitor of EGFR and human epidermal growth factor receptor 2 (HER2), is the most frequently tested EGFR inhibitor in GB trials. However, its activity has been minimal when used as alone (17) and in combination with TMZ (18) or with pazopanib in rGB (19). In the nGB setting, pulsatile dosing of lapatinib in conjunction with TMZ chemoradiation was well-tolerated and showed promise in a phase 2 study, although further clinical data is currently lacking to establish its efficacy (20). The anti-EGFR monoclonal antibody cetuximab has not consistently outperformed existing GB therapies (21, 22). Nevertheless, a subgroup analysis from a phase 2 trial involving rGB patients with EGFR mutations revealed that tumors with EGFR amplification but without the EGFR variant III mutation experienced a statistically significant increase in progression-free survival (PFS) of 3.03 months compared to 1.63 months ($p = 0.006$), with a trend toward improved overall survival (OS) of 5.56 months versus 3.97 months ($p = 0.12$) (22). This suggests that certain EGFR mutations may confer a selective advantage in anti-EGFR treatment for GB.

Nimotuzumab is another anti-EGFR monoclonal antibody that has shown some promise, particularly when combined with radiation or TMZ chemoradiation. A phase 2 study reported an improved median overall survival (mOS) when nimotuzumab was combined with radiation in patients with high-grade glioma, showing a mOS of 17.76 months compared to 12.63 months in the placebo plus radiation group (23). Another phase 2 trial yielded similar positive outcomes with nimotuzumab (24). However, a subsequent phase 3 trial that combined nimotuzumab with TMZ chemoradiation did not replicate these survival benefits (25), suggesting a nuanced potential for monoclonal antibodies in targeted GB therapy, dependent on specific patient genetic profiles.

Recent preclinical studies utilizing *in vitro* glioblastoma stem cells (GCS) models and GB orthotopic xenograft model with EGFR variant III showed antitumor activity along with inhibition of EGFR downstream signaling pathway for the third-generation EGFR inhibitor osimertinib (26). Initial clinical studies of osimertinib in GB treatment are promising. Two small retrospective studies on rGB patients with EGFR mutations showed some benefit when used as monotherapy (27) and in combination with bevacizumab (28). These promising findings indicate that osimertinib's primary advantage over earlier generations of EGFR inhibitors in GB therapy lies in its superior ability to penetrate BBB.

2.2 Platelet-derived growth factor receptor-targeted agents

Imatinib, a drug primarily approved for leukemia, has been explored for its potential in treating rGB with mixed outcomes. An initial phase 2 study combining imatinib with hydroxyurea demonstrated some antitumor activity, with a median PFS of 14.4 weeks and 9% of patients achieving radiographic responses (29). However, subsequent trials found no significant clinical benefit with imatinib, either as a monotherapy or in combination with hydroxyurea (30–32). Similarly, other early-phase trials that combined imatinib with TMZ (33) or the vascular endothelial growth factor receptor (VEGFR) inhibitor vatalanib (34) reported minimal clinical activity. While neoadjuvant administration of imatinib resulted in detectable drug levels in brain tissue, it had a limited impact on tumor proliferation and patient survival (35, 36), highlighting the drug's limited efficacy in this context.

Dasatinib, another leukemia-approved drug, was tested in rGB with minimal success. A retrospective study combining dasatinib with bevacizumab showed little activity (37), and further trials involving dasatinib with CCNU highlighted significant hematologic toxicities (38), curtailing additional studies with this combination. More focused clinical trials on rGB harboring activation or overexpression mutations of dasatinib targets, such as SRC, c-kit, EPHA, and PDGFR, also indicated insufficient clinical benefits, even with pulse-dosing strategies combined with bevacizumab (39).

Ripretinib (DCC-2618), an innovative type 2 tyrosine switch control inhibitor of the KIT and PDGFRA activating mutations, showed some potential in an early-phase study in which five high-grade glioma patients were enrolled. One of the two GB patients carrying triple amplification of PDGFRA, KIT, and KDR (4q12 amplicon) showed a remarkable 94% tumor reduction and survived through over 20 cycles. However, larger-scale evidence is still lacking (40).

Despite the theoretical promise based on their successful oncological applications elsewhere, none of those above PDGFR-targeted agents demonstrated substantial benefits in GB, particularly in recurrent settings.

2.3 VEGFR-targeted agents

Cabozantinib, a multikinase inhibitor targeting targets Met, VEGFR, and Axl, has been approved for different cancers. It has been tested in rGBs with mixed results. In large phase 2 trials, cabzantinib demonstrated reasonable tolerance and some clinical activity in rGB patients who were naïve to antiangiogenic therapy (41) or those previously exposed to an antiangiogenic agent (42).

Another multi-kinase inhibitor, Sunitinib, showed limited antitumor activity across several GB trials. Its use with irinotecan resulted in moderate toxicities and insufficient clinical effectiveness (43, 44), leading to the early termination of a subsequent phase 2 trial (45). Another phase 2 trial using sunitinib monotherapy in non-resectable nGB also failed to show antitumor activity (46). Despite these setbacks, interest in sunitinib continues with ongoing trials exploring different dosing strategies in the rGB setting.

Pazopanib, approved for sarcoma, is also a multikinase inhibitor targeting VEGFR and PDGFR. It has similarly struggled to demonstrate efficacy in GB. An initial trial using pazopanib monotherapy in rGB failed to prolong PFS, and a subsequent trial combining pazopanib with lapatinib in rGB yielded questionable antitumor activity with 0% and 15% PFS rates in PTEN/EGFRvIII-positive and PTEN/EGFRvIII- negative cohorts respectively (19). A complex combination therapy trial combining pazopanib and four other drugs showed promising clinical response rates: complete response (CR) in 18.2.%, partial response (PR) in 36.3%, and stable disease (SD) in 27.3% of patients. However, issues with patient compliance halted further exploration of this regimen (47). Additional studies pairing pazopanib with topotecan and bevacizumab also did not meet the anticipated outcomes, recording poor mPFS and mOS rates compared to historical controls, as reported in preliminary results on clinicaltrials.gov (48).

2.4 Fibroblast growth factor receptor-targeted agents

The frequency of FGFR mutations in GB is relatively low, resulting in limited use of FGFR inhibitors in this disease. However, various preclinical studies showed that FGFR signaling has a significant impact on GB progression (49).

Infigratinib monotherapy was tested on twenty-six rGB patients in a phase 2 trial, and it showed limited efficacy overall. However, durable disease control was observed in subgroups of patients harboring FGFR1 or FGFR3 point mutations or with FGFR3-TACC fusion mutation (50).

Two separate FGFR-mutated solid malignancy basket trials with erdafitnib (51) and pemigitinib (52), including thirty-two and twelve glioma patients, respectively, showed promising clinical benefits that have not been verified in subsequent trials yet.

2.5 PIK/Akt/mTOR pathway inhibitors

The PI3K/Akt/mTOR pathway, mutated in approximately 45.6% of GB cases, has been one of the key pathways implicated in tumorigenesis.

Paxslisib is a selective small-molecule PI3K inhibitor used in two glioma trials. A phase 1 study on forty-seven recurrent high-grade glioma patients showed reasonable safety and promising efficacy, with 40% having SD (53). A subsequent multi-center phase 2 study on thirty patients with O^6-methylguanine-DNA methyltransferase (MGMT) promoter unmethylated nGB showed encouraging survival data with median PFS and OS of 8.6 months and 15.7 months, respectively (54).

Buparlisib, a pan-PI3K inhibitor, has been the focus of several clinical trials in GB. Although it showed good brain penetrance and tolerability in a phase 2 trial for rGB with PI3K pathway activation mutations, its efficacy was limited, with only a small fraction of patients achieving PFS at six months (55). Subsequent trials combining buparlisib with other therapies like bevacizumab, carboplatin (56), or the c-met inhibitor capmatinib (57) did not

demonstrate superior efficacy over monotherapy or existing treatments.

Another therapeutic approach involved the mTOR inhibitors temsirolimus and everolimus, both of which have been extensively evaluated in GB in various clinical settings. An early phase trial using temsirolimus in rGB showed promising results, with 36% of participants showing radiographic responses and significantly longer time to progression than non-responders (58). However, the drug failed to meet efficacy endpoints in subsequent studies, including combinations with TMZ chemoradiation (59) and sorafenib (60). These combinations often resulted in increased toxicity, most notably severe hematologic toxicity, and increased infection risk (61).

Everolimus use with TMZ and radiation in nGB has shown reasonable tolerability in phase 1 trials (62–64). However, subsequent phase 2 trials did not demonstrate a significant survival benefit over historical controls (65) or over TMZ arm in a randomized trial (66). A phase 2 study for nGB treatment with concurrent TMZ, bevacizumab and radiation therapy followed by adjuvant treatment with bevacizumab/everolimus showed a favorable response with median PFS of 11.3 months but not mOS benefit compared to historical control. Additionally, the radiographic objective response rate (ORR) of 61% could have been influenced by the use of bevacizumab, considering its known radiographic effects (67).

2.6 Pan-kinase inhibitors

Anlotinib is a multi-kinase inhibitor targeting VEGFR, PDGFR, and FGFR. In a phase 2 study involving 21 patients with recurrent rGB, anlotinib combined with temozolomide demonstrated efficacy, achieving a median progression-free survival (PFS) of 7.3 months and a median overall survival (OS) of 16.9 months (68). Additionally, anlotinib showed promising activity in patients with MGMT promoter-unmethylated nGB when used in place of temozolomide in a phase 2 study of 32 patients (69).

Regorafinib, a pankinase inhibitor, was initially tested as monotherapy on rGB patients in a phase 2 trial, which showed a survival benefit when compared to CCNU (70). Recently, a large multi-center prospective observational trial on 190 rGB patients showed similar promising mOS and better drug tolerability compared to that seen by Lombardi et al. (71).

3 CDK-Rb targeting agents

Targeting this pathway in oncology has been primarily limited to CDK4/6 inhibitors.

Abemaciclib activity in rGB was assessed in a basket trial involving seventeen GB patients and showed limited effectiveness. A subsequent phase 2 trial on thirty-two rGB with documented CDK mutations showed SD in 35.5% and PR in 3.2% of the patients (72). More recently, abemaciclib was tested on seventy-three nGB patients in a phase 2 study, resulting in improved PFS compared to standard of care (HR 0.72; one-sided p =0.046), suggesting some potential for this drug in specific GB populations, but it failed to demonstrate significant overall survival (OS) benefit (73).

Palbociclib role in GB has been less encouraging. A phase 2 trial on heavily pretreated rGB patients noted adequate pharmacokinetics but ultimately showed limited efficacy, leading to the trial's termination (74). No further studies are currently investigating its role in GB.

Ribociclib, another CDK4/6 inhibitor, also displayed minimal clinical activity in a phase 0/2 surgical trial on rGB patients (75). The trial identified upregulation of the mTOR pathway as a potential resistance mechanism, suggesting the addition of mTOR inhibitor as a potential strategy to enhance ribociclib effectiveness in GB treatment.

4 Repurposing targeted drugs in GB: challenges and solutions

Below described are the main barriers to GB targeted therapy, which is a field largely dependent on repurposed drugs, with a few exceptions outside the scope of this review.

4.1 Complexity of GB biology

Intra-tumoral heterogeneity, which has also been previously described in GB using single-cell RNA-seq profiling (76), complicates accurate targeted therapy in several ways. Different regions within the tumor exhibit distinct genetic, epigenetic, and transcriptional profiles. As a result, tissue samples, particularly those obtained through biopsy, may not capture the full spectrum of mutations within the tumor, leading to suboptimal treatment strategies that fail to target all tumor cell populations. Furthermore, this variability complicates the identification of reliable therapeutic targets, as a target found in one tumor region may be absent in another, increasing the likelihood of treatment failure. Resistance mechanisms also play a critical role, with certain cell populations potentially being resistant to specific therapies due to their unique genetic or epigenetic characteristics. This resistance can lead to disease progression and recurrence, especially as therapy may select for these resistant clones over time. While single-cell RNA-seq provides valuable insights into tumor heterogeneity, its application in clinical practice is limited by the complexity and resources required for its clinical use.

Redundant signaling pathways in gliomagenesis limit the effectiveness of targeted therapies that focus on a single gene or pathway, even when the tumor's complete molecular profile is known. Combination strategies that target multiple actionable mutations within a tumor could potentially enhance the efficacy of targeted therapies for GB. However, the potential benefits of such approaches must be carefully weighed against the risk of cumulative toxicities associated with combination treatments. Additionally, our understanding of the role of downstream mutations within gliomagenesis signaling pathways remains incomplete. For example, PTEN mutations, which occur downstream of EGFR

signaling, have been identified as a resistance factor in anti-EGFR therapy for GB, highlighting the complexity of these pathways and the challenges in developing effective targeted treatments (77). Figure 1 further illustrates the intricate and overlapping signaling cascades within the RTK pathway, emphasizing the complexity involved in the context of the various targeted therapeutics discussed above.

Another challenge is the lack of a consensus on what level of increased expression is considered significant enough to influence clinical decisions. NGS platforms routinely provide the percentage of overexpression of an amplified gene, but there are no studies that have stratified clinical response to a drug by the fold-increase of its target. Retrospective analysis of clinical trial data using targeted therapeutics based on survival by target fold-increase may help refine personalized therapies.

Reliance on a single molecular profiling platform, such as NGS, can diminish the importance of other platforms in identifying personalized treatment response signatures. For instance, methylation profiling of GB specimens is currently the only sequencing method that can identify a subset of IDH-wild type gliomas. This subset represents a negative prognostic marker that is sufficient to diagnose GB in a glioma, regardless of its histopathological grade (78). On the other hand, methylation of MGMT gene promoter is associated with a more favorable prognosis (79). High-throughput drug screening combined with pan-omic molecular profiling of response can help generate relevant predictive biomarker libraries (80), resulting in a more nuanced approach to targeted therapy, one that is not single actionable mutation-based. Such efforts can also help inform future clinical trial design.

4.2 Dynamic evolution of the tumor

GB is a dynamic tumor that continuously evolves in response to therapeutic interventions like radiation and chemotherapy. This evolution is driven by clonal diversity within the tumor, where different cell populations harbor distinct genetic mutations. As treatments impose selective pressures, sensitive clones are eliminated, while resistant clones survive and proliferate. For example, radiation and chemotherapy, such as alkylating agents, work by imposing lethal DNA damage. However, clones with efficient DNA repair mechanisms can selectively survive through radiochemical stress and flourish in less competitive environments. On the other hand, the increased mutation burden from radiation or chemotherapy can potentially lead to the emergence of new mutations that confer resistance to the therapy (81). This dynamic nature means that the tumor's mutational profile at recurrence differs from its profile at diagnosis, and the problem is exacerbated by limited access to GB tissue at recurrence, as re-resection is not always safe or preferred. The failure of most targeted therapy trials for rGB can be attributed to their focus on the tumor's initial mutational profile, which may not reflect the tumor's current genetic state due to its evolution over time. Advances in liquid

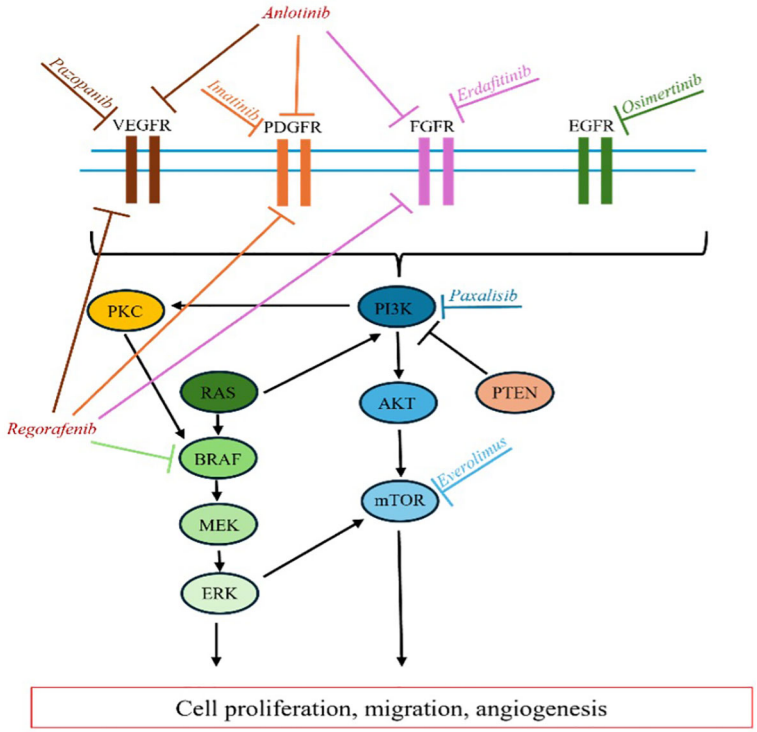

FIGURE 1
RTK Pathway. Overview of targeted inhibition of various RTK signaling enzymes.

biopsy techniques for non-invasive profiling of GB can help to overcome this challenge and will be discussed in more detail in the next section.

For nGB, the presence of FDA-approved standard chemotherapy (TMZ) limits the application of new therapies and delays the approval of new drugs for nGB. Advances in clinical trial design for these patients fall under one of three categories:

1. Combining the experimental drug with TMZ so as not to deprive patients of standard of care treatment.
2. Using an experimental drug instead of TMZ in the setting of unmethylated MGMT promoter which results in high expression of the DNA-repair enzyme MGMT. Overexpression of MGMT results in decreased response to alkylating agents such as TMZ, as evidenced by the significantly improved survival outcomes in the MGMT promotor methylated group (Median PFS 19 mo *vs*. 6 months; p=.014) when adjuvant TMZ, lomustine, and radiation therapy was used (82).
3. Utilizing adaptive trial platforms to accelerate drug discovery in an efficient and cost-effective manner. This approach involves continuously adjusting multiple treatment arms, including adding new ones and terminating others early based on emerging data, all within a single master protocol. Response-adaptive randomization allows trials to progress through different phases more quickly and facilitates the rapid identification of promising therapies and response biomarkers. Currently, two major adaptive trials in GB, AGILE and INSIGhT, have successfully increased enrollment rates by leveraging this methodology (83)

Lastly, the frequency of an actionable mutation within a tumor, as indicated by variant allele frequency (VAF) in NGS reports, varies between different GB specimens. However, targeted therapy trials almost never include a VAF cutoff as an eligibility criterion. Consequently, these trials' perceived low response rate may be diluted by a subset of patients with low VAF, highlighting the need for detailed subgroup analysis upon trial completion.

4.3 GB microenvironment

4.3.1 BBB

BBB is a critical and complex structure that serves as a dynamic interface between the bloodstream and the CNS. It is primarily composed of endothelial cells, basement membrane, pericyte, and astrocyte. The endothelial cells are tightly connected by intracellular junctions that play a crucial role in maintaining the highly selective permeability of the BBB, allowing it to regulate the movement of ions, molecules, and cells between the blood and the neural tissue (84, 85). This selective permeability is essential for maintaining CNS homeostasis, protecting the brain from toxins, pathogens, and immune cells, and regulating the influx and efflux of nutrients and other compounds necessary for brain function. The BBB's integrity is hallmarked by its high transendothelial electrical resistance (TEER), which restricts the passage of most water-soluble compounds, including polar drugs (86). Only small, lipophilic molecules, such as oxygen and carbon dioxide, can passively diffuse across the BBB. Additionally, specific transporters and receptors on the endothelial cells facilitate the selective transport of essential molecules like glucose, amino acids, and nucleosides, while actively effluxing potentially harmful substances, including many therapeutic drugs, back into the bloodstream.

This highly selective and regulated nature of the BBB presents a significant challenge in the treatment of GB. The barrier limits the delivery of therapeutic agents, particularly large or hydrophilic molecules, into the brain. Most anti-neoplastic drugs, which are often hydrophilic and large, cannot cross the BBB efficiently due to their size and polarity (87, 88). Furthermore, the presence of active efflux transporters like P-glycoproteins exacerbates this challenge by pumping out drugs that manage to penetrate the endothelial cells (89). Moreover, the BBB's integrity is not uniform throughout the GB tumor (90). While the BBB may be compromised in some regions of the tumor, allowing partial drug penetration, other areas may still have an intact barrier, further complicating effective drug delivery. This heterogeneity in BBB disruption within GB tumors means that even if a therapeutic agent reaches some parts of the tumor, it may not reach all areas, leading to incomplete treatment and potential recurrence. Consequently, innovative strategies are required to either bypass or transiently disrupt the BBB to improve drug delivery and therapeutic efficacy in GB treatment. One strategy involves incorporating a window-of-opportunity component into surgical clinical trials. In this approach, patients receive the experimental drug before the tumor resection. Pharmacodynamic studies on the resected tumor can then determine whether the drug crossed the blood-brain barrier (BBB) and performed its expected function. This helps differentiate between a mechanistic failure and a delivery failure of the experimental drug (91). BBB disruption is another strategy that will be discussed in more detail below.

4.3.2 Hypoxia

GB TME features a necrotic core primarily formed due to high cell density or vaso-occlusive events leading to hypoxia, a pervasive feature in GB. The hypoxic niches contribute to the development of therapy resistance to conventional chemotherapy, which often relies on oxygen to generate reactive oxygen species (ROS) that damage cancer cells. This results in increased expression of hypoxia-inducible factors (HIFs), which promote angiogenesis (via VEGF upregulation) and invasion (92, 93). In the context of radiotherapy, hypoxic tumor cells exhibit increased resistance due to their impaired ability to produce damaging oxygen radicals upon irradiation (94). Additionally, HIFs help mitigate the DNA damage caused by radiotherapy, further reducing its effectiveness (95).

4.3.3 Acidosis

Tumor acidosis crucially impacts the effectiveness of various therapeutic interventions by modulating the TME and promoting oncogenesis. It enhances the expression of glioma stem cell (GSC) markers, fostering tumor growth through paracrine actions that

involve angiogenic factors controlled by HIFs, particularly HIF-2α (96). Acidosis also heightens autophagic activity linked to the maintenance and aggressiveness of GSCs (97). Additionally, it supports tumor invasion by activating cathepsin L, which converts plasminogen into plasmin, leading to the degradation of key extracellular matrix proteins and activation of latent matrix metalloproteinases (98). It also compromises the efficacy of chemotherapeutics, particularly weak base drugs like doxorubicin and vincristine, through ion trapping that reduces their intracellular concentration and by increasing the efflux activity of the p-glycoprotein (99–101). Moreover, acidosis facilitates tumor immune escape and resistance to immunotherapy by impairing CD8+ T lymphocytes, reducing their cytokine secretion and expression of critical receptors, thus dampening key immune signaling pathways (102, 103). It also lowers the production of vital immune effectors by T cells and monocytes, enhances the number of myeloid-derived suppressor cells (MDSCs), and inhibits the cytotoxic functions of NK and NKT cells (104).

4.3.4 Glutathione

Elevated glutathione levels in GB lead to reduced oxidative stress which is crucial for disease progression (105). Although increased glutathione protects healthy cells from oxidative stress, it concurrently promotes resistance to many chemotherapeutics which exert their cancer killing properties by ROS production. This is further highlighted by studies showing that resistant cells had higher levels of glutathione and lower levels of ROS than TMZ-sensitive cells (106, 107).

4.3.5 Altered drug mechanism of action

Repurposed drugs may exert their effect on the CNS tumor differently from their actions in the originally FDA-approved tumor type (108, 109). Many drugs repurposed for GB treatment, like cabozantinib, inhibit multiple pathways. While they are primarily known as VEGF inhibitors, their role as multi-targeted tyrosine kinase inhibitors can lead to a range of effects, resulting in a broader range of biological effects. This variability in drug action within the unique CNS tumor microenvironment further complicates the therapeutic efficacy and predictability of these agents (110).

The cumulative effect of all these features is a selective pressure favoring the growth of resistant clones, complicating future therapies, whether targeted or otherwise.

5 Emerging diagnostic tools: liquid biopsy

As previously mentioned, the failure of drug repurposing efforts in GB can be attributed to several factors. Tumor heterogeneity, characterized by the presence of multiple clones, increases the likelihood of drug-resistant clones, resulting in treatment failure or recurrence. Even if the tumor initially responds to treatment, tumor cells may evolve into different phenotypes with new mechanisms of therapeutic resistance. In clinical practice, disease monitoring predominantly relies on imaging modalities, limiting the ability to observe real-time tumor dynamics and variations in biomarkers. While tumor biopsy at recurrence is an option, it is infrequently performed due to its morbidity risks and the lack of clear benefit. It remains uncertain whether molecular characterization of recurrent tumors provides a definitive survival advantage in patients treated with targeted therapies. In that regard, liquid biopsy rapidly emerges as a promising non-invasive diagnostic tool, showing encouraging results.

By analyzing molecular biomarkers in bodily fluids, liquid biopsies provide a real-time snapshot of the tumor's genetic landscape without the need for invasive surgical procedures. This approach can detect changes in the tumor's mutational profile over time, allowing for more precise and adaptive treatment strategies that respond to the tumor's evolving nature. Liquid biopsies offer a promising tool to enhance the effectiveness of targeted therapies and improve the prognosis for GB patients by enabling continuous monitoring and timely adjustments to therapeutic interventions.

While the field of liquid biopsy in GB began with studies on circulating tumor cells, there are no validated or reproducible studies on isolating them. Therefore, we will focus here on the three main molecular markers studied in liquid biopsy (Figure 2).

5.1 ctDNA

The detection of circulating tumor DNA (ctDNA) in glioma patients varies significantly between blood and cerebrospinal fluid (CSF). The BBB limits ctDNA detection in blood to less than 10% of glioma patients, primarily due to ctDNA's inability to effectively penetrate the BBB (111). In contrast, ctDNA levels in CSF are generally higher (112, 113), as it is directly shed into the CSF from the tumor. However, monitoring treatment response by serial CSF ctDNA measurements requires repeated lumbar punctures and exposes patients to potentially unjustified morbidities.

Peripheral blood is a less invasive option for serial monitoring, facilitating longitudinal monitoring studies, but it presents several challenges. The rapid clearance of ctDNA with a half-life of about 1.5h (114) and the small size of ctDNA fragments, which may not include relevant genetic alterations, contribute to plasma ctDNA's low sensitivity. However, recent advances in NGS have increased the sensitivity of their detection. According to Piccioni et al., the NGS panel could detect ctDNA mutation in blood from 50% of all brain tumor patients and 55% of GB patients (115), allowing for measurement of GB's mutational profile evolution during treatment. A more recent pilot study enrolling ten glioma patients utilizing the CAPP-seq-based NGS technique reported a detection rate of up to 93.8% plasma samples with successful tracking of change in mutation profiles (116). The serial ctDNA analyses detected an emergence of mismatch repair gene *MSH2* and *MSH6* gene mutations, which is associated with hypermutation and potential development of TMZ resistance during treatment with TMZ. Another study utilizing a droplet digital PCR technique reliably detected the IDH1 mutation with 84% sensitivity in cross-comparison with tissue mutations (117). TERTp C228T

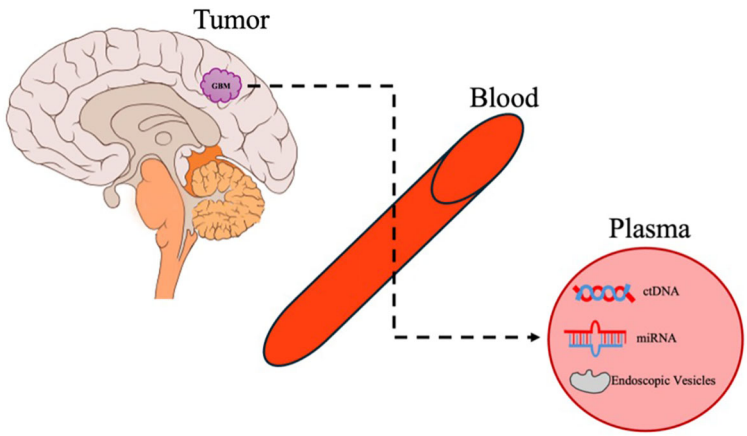

FIGURE 2
Liquid biopsy. An overview of the release of GB molecular biomarkers and cargo into the systemic circulation and its detection in plasma.

mutation was detected in 88% of patients, and EGFRvIII mutation was detected in 71% of patients.

5.2 miRNA

There have been several studies exploring the role of circulating miRNA in GB. Differentially expressed miRNAs were identified in several studies comparing the plasma of GB patients to that of healthy controls (118–120). Circulating miRNAs can also serve as biomarkers correlating with OS and PFS in GB patients (121, 122). However, the clinical implications of these findings in relation to treatment strategies warrant further exploration.

5.3 Extracellular vesicles

Extracellular vesicles (EVs) are small membrane-bound vesicles released by cells under both normal and abnormal conditions, playing a crucial role in cell-to-cell communication. These vesicles transport genetic materials like DNA, mRNA, and miRNA across the body, influencing the behavior and phenotype of distant cells, including endothelial cells (123, 124).

EVs originating from gliomas or other cells in the tumor microenvironment appear to play crucial roles in tumor cell proliferation, invasion, malignancy, and drug resistance (125). Cancer cells release a greater number of EVs with differing protein and RNA contents, compared to non-malignant cells (126). These EVs facilitate communication with surrounding cells to alter the TME by influencing the behavior of local and recruited stromal cells, contributing to the creation of a tumor-supportive environment that enhances angiogenesis, immunosuppression, and the malignant transformation of cancer cells (127). Tumor-derived EVs can also enter into the circulation and prepare distant organs for metastasis by creating favorable conditions for tumor cell growth (128). This process, known as pre-metastatic niche formation, involves steps such as inducing vascular leakiness, altering stromal components, and suppressing the immune system. These interactions underscore the significance of EVs in the progression and maintenance of cancer.

From a diagnostic standpoint, EVs are increasingly recognized for their potential in identifying tumor molecular signatures, particularly due to their ability to traverse an intact BBB (129). Manda et al. reported that variant EGFR RNA transcripts were detected with similar frequency in GB tissue (39.5%) and their matched serum exosomes (44.7%). The presence of circulating exosomal EGFRvIII variants correlated with poor outcomes (130). Studies on miRNA contents of EVs revealed that the exosomal levels and types of miRNA within the EVs were associated with the aggressive potentials of the GB (131). For example, an *in vitro* functional study using glioma cell lines has indicated that miR-221 silencing can reduce cell proliferation, migratory potential, and resistance to temozolomide (132). In addition, exosomal levels of miR-221 were increased in parallel with glioma grades. Another study reported that syndecan-1 plasma EVs could distinguish between low-grade and high-grade gliomas with a sensitivity and specificity greater than 70% (133).

However, challenges remain. We still lack an understanding of the mechanisms that drive the RNA incorporation into EVs of various sizes and types in different RNA concentrations. The technical challenges of isolating purified tumor-specific EVs of different sizes in high-yield continue to complicate the interpretation and utility of these biomarkers in clinical settings.

Liquid biopsy offers significant potential in enhancing the management of GB by providing a non-invasive method to monitor treatment response in real-time, tracking changes in tumor-derived biomarkers. By identifying specific genetic mutations and alterations, liquid biopsies can guide targeted therapies, facilitating more personalized and effective treatment strategies. However, the clinical implementation of liquid biopsy in GB is still in its early stages. There is a need for standardized methodologies across laboratories to ensure consistent and reliable results. Larger prospective studies are required to validate the clinical utility of liquid biopsy biomarkers in GB.

6 Strategies to improve drug delivery to GB

Effective drug delivery to the CNS is significantly hindered by the BBB, posing a substantial challenge in GB treatment. The BBB is a multi-layered cellular physical barrier composed of endothelial cells, astrocytes, and pericytes, which effectively prevent the diffusion of small molecules. It facilitates the exchange of essential nutrients and metabolites through a selective transport system. Even if small molecules manage to penetrate the BBB, they are often actively transported back out via efflux pumps (134). Overcoming this barrier to enhance bioavailability is a critical area of ongoing research.

6.1 Focused ultra-sound

FUS has been investigated as a method to transiently and non-invasively increase the permeability of the BBB, thereby enhancing the delivery of therapeutic agents to GB tissue. This technique involves the use of pulsed ultrasound waves in conjunction with microbubbles, which oscillate and cause transient disruption of the BBB. Preclinical studies have demonstrated that FUS can improve the concentration of chemotherapeutic agents such as TMZ in brain tissue, leading to prolonged survival in animal models (135, 136). Adding MRI to FUS (MR-guided FUS) further improves the precision of the drug delivery, thus minimizing damage to healthy tissue. Clinical trials have begun to explore the safety and efficacy of FUS in humans, with early results indicating that FUS can be safely performed and may improve drug delivery and patient survival (137, 138).

Animal studies have shown that FUS can improve the penetration of immunotherapy into brain tumors, the immune response against the cancer cells, and survival outcomes (139, 140). The clinical use of immunotherapy in GB treatment is currently not validated with debatable early study outcomes.

FUS is actively investigated for its use in direct tumor ablation by delivering high-energy ultrasound waves. Initial clinical studies using MR-guided FUS demonstrated precise ablation of brain tumors after craniotomy (141). However, significant attenuation of ultrasound waves by the skull, significant damage to healthy brain tissue, and lack of clinical validity currently limit its use.

6.2 Implantable drug-delivery systems

The development of new extended-release drug-delivery vehicles led to several promising strategies for improving patient outcomes after tumor resection.

The pioneering work of Langer's group in the 1980s led to the development of localized controlled-release therapies for GB, culminating in the FDA approval of the first implantable intra-cavity wafer, Gliadel, in 1996 (142). Gliadel, a polyanhydride-based wafer containing carmustine (BCNU), is designed for optimal drug release, achieving substantial polymer degradation within three weeks of implantation. Clinical trials demonstrated survival benefits for patients receiving Gliadel compared to placebo (13.8 months *vs* 11.6 months; p=0.018) (25). On the other hand, implantation is associated with several negative side effects, including seizures, vasogenic edema, meningitis, and impaired wound healing (143). It can also dislodge and cause micro-tears (144). Also, its content (BCNU) has a low diffusion rate (145). Therefore, it is no longer commonly used in clinical practice.

Following Gliadel's approval, there has been a surge in the development of locally administered chemotherapeutic devices. Sheleg et al. explored a biodegradable polymer device loaded with cisplatin (146). Twenty 1.5 x 1.5cm polymer plates loaded with cisplatin with a drug density of 1mg/cm2 were implanted in the surgical bed after subtotal removal of GB. This strategy resulted in extended OS when administered with radiation therapy compared to radiation alone (427.5 *vs* 211.0 days; p = 0.00001) (146). Similarly, Di Mascolo et al. developed microfabricated PLGA meshes loaded with diclofenac and docetaxel, which effectively prevented tumor recurrence and significantly extended survival in orthotopic brain tumor mouse models, emphasizing the advantage of the meshes' flexibility over solid films (147).

Technological advancement led to different designs of implantable drug-delivery systems, including hydrogel and microparticles. Hydrogel is a hydrophilic polymer network with high water contents that can be loaded with water-soluble biomacromolecules such as small molecules and NPs. For example, OncoGel, a type of thermoresponsive PLGA-PEG matrix hydrogel loaded with paclitaxel, transitions to a semisolid state at the body temperature once applied to the tumor bed and maintains drug release over six weeks (148). PLGA microparticles have been studied extensively, offering controlled release of anticancer drugs like 5-fluorouracil (149), which has shown to work synergistically with radiotherapy in enhancing survival in animal models (150).

There are no implantable targeted drug-delivery systems, likely due to cost considerations. However, as this technology advances and shows more promising data, it can potentially be applied to targeted therapeutics.

In the context of targeted therapy, only EGFR-targeting nanoparticles have been investigated in human studies. The first was a phase 1/2 trial involving fourteen patients with rGB. In this study, doxorubicin-loaded nanoparticles targeting EGFR were used to deliver the chemotherapeutic agent into GB tumor cells (155). While the maximum tolerated dose (MTD) was determined, the trial was prematurely terminated by the sponsor, leaving efficacy data unavailable. Similarly, a phase 1 study utilizing anti-EGFR doxorubicin-loaded immunoliposomes was conducted in nine rGB patients with EGFR amplification (155). This study confirmed the successful delivery of nanoliposomes to GB tissue; however, the small sample size and absence of a control group limited the assessment of therapeutic efficacy.

6.3 Nanoparticles

NPs can be engineered specifically to cross the BBB and target tumor cells directly, minimizing side effects. NPs, with their tunable

physicochemical properties, can be loaded with various therapeutic agents to deliver the intended targets. The NPs can be tailored to have specific intrinsic (electronic, optical, and magnetic) and extrinsic (size, surface-to-volume ratio, or surface energy) characteristics to increase delivery efficiency, decrease off-target effects, and improve drug kinetics. These NPs act as "Trojan horses," facilitating the delivery of drugs like doxorubicin and paclitaxel and biological molecules such as antibodies, DNA, and peptides directly to GB cells.

The surface of NPs can be modified with specific ligands that recognize and bind to receptors on endothelial cells lining the brain, facilitating their entry into the brain through mechanisms like receptor-mediated transcytosis. For example, the transferrin receptor (TfR) and low-density lipoprotein receptor (LRP1) are common targets on brain endothelial cells that NPs exploit to achieve transcytosis (151, 152). These receptors allow NPs to bypass the typical barriers posed by the BBB, improving the delivery efficiency of chemotherapeutics into the brain. Since the brain uptakes glucose via like the glucose transporter-1 (GLUT1), Anraku et al. utilized glycosylated micelles to transport bioactive substances via the GLUT1 transporter. The precisely calculated glucose density on the surface of the NP allowed the regulation of its distribution within the brain, thus successfully increasing the number of nanocarriers within the brain (153). Further, PEGylation of these NPs further prolongs their circulation time in the bloodstream, reducing protein interactions and enhancing their therapeutic efficacy (154).

In the context of targeted therapy, only EGFR-targeting nanoparticles have been investigated in human studies. The first was a phase 1/2 trial involving fourteen patients with rGB. In this study, doxorubicin-loaded nanoparticles targeting EGFR were used to deliver the chemotherapeutic agent into GB tumor cells (155). While the maximum tolerated dose (MTD) was determined, the trial was prematurely terminated by the sponsor, leaving efficacy data unavailable. Similarly, a phase 1 study utilizing anti-EGFR doxorubicin-loaded immunoliposomes was conducted in nine rGB patients with EGFR amplification (156). This study confirmed the successful delivery of nanoliposomes to GB tissue; however, the small sample size and absence of a control group limited the assessment of therapeutic efficacy.

7 Conclusions/future directions

Treatment of GB remains a formidable challenge with limited treatment options, particularly in recurrent settings. Many past attempts to employ targeted therapy, including clinical trials selecting patients whose tumors possess the actionable mutation of interest, have not resulted in substantial clinical benefits. This is largely due to the unique biological and clinical characteristics of GB, including dynamic evaluation of the tumor, its highly heterogeneous tumor microenvironment, and poor drug penetration through BBB, as illustrated in Figure 3. These obstacles underscore the need for innovative approaches to improve the understanding and monitoring of tumor biology.

Emerging diagnostic tools such as liquid biopsy offer promising, non-invasive methods to monitor GB. Liquid biopsies using ctDNA provide real-time snapshots of the tumor's genetic landscape,

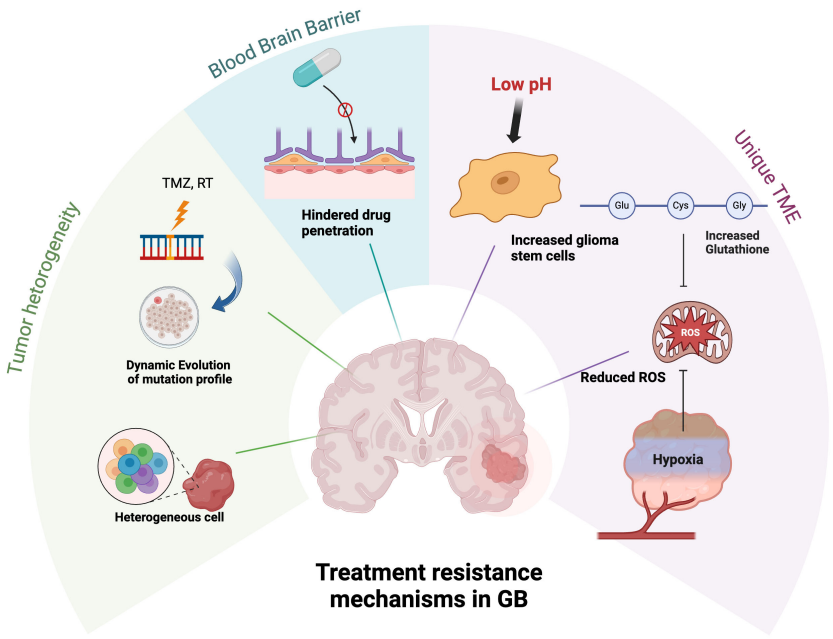

FIGURE 3
Treatment resistance mechanisms of GB. The tumor cells continuously evolve and diversify the tumor's genetic profile. Targeted treatment strategies face additional challenges due to poor drug penetration across the BBB. The unique biochemical environment of GB TME, characterized by low pH, hypoxia, and elevated glutathione levels, promotes the proliferation of glioma stem cells and reduces ROS, thereby diminishing the efficacy of anti-neoplastic therapies.

allowing for adaptive treatment strategies that respond to the tumor's evolving nature. Although ctDNA detection in blood is limited by the BBB, advances in NGS have improved sensitivity. The regulatory role of miRNA sets them apart as particularly promising biomarkers in liquid biopsy. Further validation of the role of plasma miRNA in GB may result in the identification of GB-specific miRNAs that can be used in lieu of surgery for some patients. EVs can traverse an intact BBB and are valuable in identifying tumor molecular signatures and monitoring treatment response with increased sensitivity. There are other uses of plasma from GB patients. A recent study identified unique metabolomic signatures in the plasma of GB patients at diagnosis and recurrence (157). We believe that serial plasma collection from GB patients during their treatment, along with multi-platform profiling at clinically relevant endpoints (*e.g.*, pre-surgery, post-surgery, recurrence, tissue-proven radionecrosis), can further revolutionize this field and be an extremely valuable diagnostic tool for GB patients.

Recent innovative strategies have shown potential in overcoming GB treatment challenges and enhancing therapeutic agents' delivery and efficacy. NPs can be engineered to cross the BBB and deliver drugs directly to the tumor site, leveraging mechanisms like receptor-mediated transcytosis. Additionally, MRgFUS can transiently disrupt the BBB, allowing therapeutic agents to penetrate the brain more effectively. Combining this with implantable drug delivery systems, which provide sustained and localized release of therapeutic agents directly to the tumor bed following surgical resection, shows promise. Innovations such as hydrogel-based delivery systems and biodegradable polymer devices have demonstrated efficacy in preclinical models, offering prolonged drug release and improved survival outcomes. These technologies collectively enhance drug delivery efficiency, reduce off-target effects, and improve therapeutic efficacy.

In summary, while the treatment of GB has faced significant difficulties, new strategies such as NPs, FUS, implantable drug delivery systems, liquid biopsy, and adaptive trial platforms offer promising solutions. Continued research and clinical trials are essential to fully realize the potential of these innovative therapies, ultimately improving the prognosis for patients with this aggressive and devastating disease.

Author contributions

WB: Writing – original draft, Writing – review & editing. SM: Supervision, Writing – review & editing. AD: Conceptualization, Supervision, Writing – original draft, Writing – review & editing.

Funding

The author(s) declare that no financial support was received for the research, authorship, and/or publication of this article.

Conflict of interest

The authors declare that the research was conducted in the absence of any commercial or financial relationships that could be construed as a potential conflict of interest.

Publisher's note

References

1. Stupp R, Hegi ME, Mason WP, van den Bent MJ, Taphoorn MJ, Janzer RC, et al. Effects of radiotherapy with concomitant and adjuvant temozolomide versus radiotherapy alone on survival in glioblastoma in a randomised phase III study: 5-year analysis of the EORTC-NCIC trial. *Lancet Oncol.* (2009) 10:459–66. doi: 10.1016/S1470-2045(09)70025-7

2. van Linde ME, Brahm CG, de Witt Hamer PC, Reijneveld JC, Bruynzeel AME, Vandertop WP, et al. Treatment outcome of patients with recurrent glioblastoma multiforme: A retrospective multicenter analysis. *J Neurooncol.* (2017) 135:183–92. doi: 10.1007/s11060-017-2564-z

3. Cancer Genome Atlas Research N. Comprehensive genomic characterization defines human glioblastoma genes and core pathways. *Nature.* (2008) 455:1061–8. doi: 10.1038/nature07385

4. Alaseem AM. Advancements in MDM2 inhibition: clinical and pre-clinical investigations of combination therapeutic regimens. *Saudi Pharm J.* (2023) 31:101790. doi: 10.1016/j.jsps.2023.101790

5. Xu H, Zong H, Ma C, Ming X, Shang M, Li K, et al. Epidermal growth factor receptor in glioblastoma. *Oncol Lett.* (2017) 14:512–6. doi: 10.3892/ol.2017.6221

6. Rich JN, Reardon DA, Peery T, Dowell JM, Quinn JA, Penne KL, et al. Phase II trial of gefitinib in recurrent glioblastoma. *J Clin Oncol.* (2004) 22:133–42. doi: 10.1200/JCO.2004.08.110

7. Hegi ME, Diserens AC, Bady P, Kamoshima Y, Kouwenhoven MC, Delorenzi M, et al. Pathway analysis of glioblastoma tissue after preoperative treatment with the EGFR tyrosine kinase inhibitor gefitinib–a phase II trial. *Mol Cancer Ther.* (2011) 10:1102–12. doi: 10.1158/1535-7163.MCT-11-0048

8. Kreisl TN, Lassman AB, Mischel PS, Rosen N, Scher HI, Teruya-Feldstein J, et al. A pilot study of everolimus and gefitinib in the treatment of recurrent glioblastoma (Gbm). *J Neurooncol.* (2009) 92:99–105. doi: 10.1007/s11060-008-9741-z

9. Chakravarti A, Wang M, Robins HI, Lautenschlaeger T, Curran WJ, Brachman DG, et al. RTOG 0211: A phase 1/2 study of radiation therapy with concurrent gefitinib for newly diagnosed glioblastoma patients. *Int J Radiat Oncol Biol Phys.* (2013) 85:1206–11. doi: 10.1016/j.ijrobp.2012.10.008

10. van den Bent MJ, Brandes AA, Rampling R, Kouwenhoven MC, Kros JM, Carpentier AF, et al. Randomized phase II trial of erlotinib versus temozolomide or carmustine in recurrent glioblastoma: eortc brain tumor group study 26034. *J Clin Oncol.* (2009) 27:1268–74. doi: 10.1200/JCO.2008.17.5984

11. de Groot JF, Gilbert MR, Aldape K, Hess KR, Hanna TA, Ictech S, et al. Phase II study of carboplatin and erlotinib (Tarceva, OSI-774) in patients with recurrent glioblastoma. *J Neurooncol.* (2008) 90:89–97. doi: 10.1007/s11060-008-9637-y

12. Reardon DA, Desjardins A, Vredenburgh JJ, Gururangan S, Friedman AH, Herndon JE 2nd, et al. Phase 2 trial of erlotinib plus sirolimus in adults with recurrent glioblastoma. *J Neurooncol.* (2010) 96:219–30. doi: 10.1007/s11060-009-9950-0

13. Wen PY, Chang SM, Lamborn KR, Kuhn JG, Norden AD, Cloughesy TF, et al. Phase I/II study of erlotinib and temsirolimus for patients with recurrent Malignant gliomas: north American brain tumor consortium trial 04-02. *Neuro Oncol.* (2014) 16:567–78. doi: 10.1093/neuonc/not247

14. Peereboom DM, Ahluwalia MS, Ye X, Supko JG, Hilderbrand SL, Phuphanich S, et al. Nabtt 0502: A phase II and pharmacokinetic study of erlotinib and sorafenib for patients with progressive or recurrent glioblastoma multiforme. *Neuro Oncol.* (2013) 15:490–6. doi: 10.1093/neuonc/nos322

15. Sathornsumetee S, Desjardins A, Vredenburgh JJ, McLendon RE, Marcello J, Herndon JE, et al. Phase II trial of bevacizumab and erlotinib in patients with recurrent Malignant glioma. *Neuro Oncol.* (2010) 12:1300–10. doi: 10.1093/neuonc/noq099

16. Peereboom DM, Shepard DR, Ahluwalia MS, Brewer CJ, Agarwal N, Stevens GH, et al. Phase II trial of erlotinib with temozolomide and radiation in patients with newly diagnosed glioblastoma multiforme. *J Neurooncol.* (2010) 98:93–9. doi: 10.1007/s11060-009-0067-2

17. Thiessen B, Stewart C, Tsao M, Kamel-Reid S, Schaiquevich P, Mason W, et al. A phase I/II trial of GW572016 (Lapatinib) in recurrent glioblastoma multiforme: clinical outcomes, pharmacokinetics and molecular correlation. *Cancer Chemother Pharmacol.* (2010) 65:353–61. doi: 10.1007/s00280-009-1041-6

18. Karavasilis V, Kotoula V, Pentheroudakis G, Televantou D, Lambaki S, Chrisafi S, et al. A phase I study of temozolomide and lapatinib combination in patients with recurrent high-grade gliomas. *J Neurol.* (2013) 260:1469–80. doi: 10.1007/s00415-012-6812-z

19. Reardon DA, Groves MD, Wen PY, Nabors L, Mikkelsen T, Rosenfeld S, et al. A phase I/II trial of pazopanib in combination with lapatinib in adult patients with relapsed Malignant glioma. *Clin Cancer Res.* (2013) 19:900–8. doi: 10.1158/1078-0432.CCR-12-1707

20. Yu A, Faiq N, Green S, Lai A, Green R, Hu J, et al. Report of safety of pulse dosing of lapatinib with temozolomide and radiation therapy for newly-diagnosed glioblastoma in a pilot phase II study. *J Neurooncol.* (2017) 134:357–62. doi: 10.1007/s11060-017-2533-6

21. Hasselbalch B, Eriksen JG, Broholm H, Christensen IJ, Grunnet K, Horsman MR, et al. Prospective evaluation of angiogenic, hypoxic and EGFR-related biomarkers in recurrent glioblastoma multiforme treated with cetuximab, bevacizumab and irinotecan. *APMIS.* (2010) 118:585–94. doi: 10.1111/j.1600-0463.2010.02631.x

22. Lv S, Teugels E, Sadones J, De Brakeleer S, Duerinck J, Du Four S, et al. Correlation of EGFR, IDH1 and PTEN status with the outcome of patients with recurrent glioblastoma treated in a phase II clinical trial with the EGFR-blocking monoclonal antibody cetuximab. *Int J Oncol.* (2012) 41:1029–35. doi: 10.3892/ijo.2012.1539

23. Solomon MT, Selva JC, Figueredo J, Vaquer J, Toledo C, Quintanal N, et al. Radiotherapy plus nimotuzumab or placebo in the treatment of high grade glioma patients: results from a randomized, double blind trial. *BMC Cancer.* (2013) 13:299. doi: 10.1186/1471-2407-13-299

24. Du XJ, Li XM, Cai LB, Sun JC, Wang SY, Wang XC, et al. Efficacy and safety of nimotuzumab in addition to radiotherapy and temozolomide for cerebral glioblastoma: A phase II multicenter clinical trial. *J Cancer.* (2019) 10:3214–23. doi: 10.7150/jca.30123

25. Westphal M, Heese O, Steinbach JP, Schnell O, Schackert G, Mehdorn M, et al. A randomised, open label phase III trial with nimotuzumab, an anti-epidermal growth factor receptor monoclonal antibody in the treatment of newly diagnosed adult glioblastoma. *Eur J Cancer.* (2015) 51:522–32. doi: 10.1016/j.ejca.2014.12.019

26. Chagoya G, Kwatra SG, Nanni CW, Roberts CM, Phillips SM, Nullmeyergh S, et al. Efficacy of osimertinib against EGFRvIII+ Glioblastoma. *Oncotarget.* (2020) 11:2074–82. doi: 10.18632/oncotarget.27599

27. Abousaud M, Faroqui NM, Lesser G, Strowd RE, Ramkissoon SH, Kwatra M, et al. Clinical experience using osimertinib in patients with recurrent Malignant gliomas containing EGFR alterations. *J Cancer Sci Clin Ther.* (2021) 5:210–20. doi: 10.26502/jcsct.5079114

28. Cardona AF, Jaramillo-Velasquez D, Ruiz-Patino A, Polo C, Jimenez E, Hakim F, et al. Efficacy of osimertinib plus bevacizumab in glioblastoma patients with simultaneous EGFR amplification and EGFRvIII mutation. *J Neurooncol.* (2021) 154:353–64. doi: 10.1007/s11060-021-03834-3

29. Reardon DA, Egorin MJ, Quinn JA, Rich JN, Gururangan S, Vredenburgh JJ, et al. Phase II study of imatinib mesylate plus hydroxyurea in adults with recurrent glioblastoma multiforme. *J Clin Oncol.* (2005) 23:9359–68. doi: 10.1200/JCO.2005.03.2185

30. Hassler MR, Vedadinejad M, Flechl B, Haberler C, Preusser M, Hainfellner JA, et al. Response to imatinib as a function of target kinase expression in recurrent glioblastoma. *Springerplus.* (2014) 3:111. doi: 10.1186/2193-1801-3-111

31. Dresemann G, Weller M, Rosenthal MA, Wedding U, Wagner W, Engel E, et al. Imatinib in combination with hydroxyurea versus hydroxyurea alone as oral therapy in patients with progressive pretreated glioblastoma resistant to standard dose temozolomide. *J Neurooncol.* (2010) 96:393–402. doi: 10.1007/s11060-009-9976-3

32. Raymond E, Brandes AA, Dittrich C, Fumoleau P, Coudert B, Clement PM, et al. Phase II study of imatinib in patients with recurrent gliomas of various histologies: A European organisation for research and treatment of cancer brain tumor group study. *J Clin Oncol.* (2008) 26:4659–65. doi: 10.1200/JCO.2008.16.9235

33. Reardon DA, Desjardins A, Vredenburgh JJ, Sathornsumetee S, Rich JN, Quinn JA, et al. Safety and pharmacokinetics of dose-intensive imatinib mesylate plus temozolomide: phase 1 trial in adults with Malignant glioma. *Neuro Oncol.* (2008) 10:330–40. doi: 10.1215/15228517-2008-003

34. Reardon DA, Egorin MJ, Desjardins A, Vredenburgh JJ, Beumer JH, Lagattuta TF, et al. Phase I pharmacokinetic study of the vascular endothelial growth factor receptor tyrosine kinase inhibitor vatalanib (Ptk787) plus imatinib and hydroxyurea for Malignant glioma. *Cancer.* (2009) 115:2188–98. doi: 10.1002/cncr.24213

35. Holdhoff M, Supko JG, Gallia GL, Hann CL, Bonekamp D, Ye X, et al. Intratumoral concentrations of imatinib after oral administration in patients with glioblastoma multiforme. *J Neurooncol.* (2010) 97:241–5. doi: 10.1007/s11060-009-0008-0

36. Razis E, Selviaridis P, Labropoulos S, Norris JL, Zhu MJ, Song DD, et al. Phase II study of neoadjuvant imatinib in glioblastoma: evaluation of clinical and molecular effects of the treatment. *Clin Cancer Res.* (2009) 15:6258–66. doi: 10.1158/1078-0432.CCR-08-1867

37. Lu-Emerson C, Norden AD, Drappatz J, Quant EC, Beroukhim R, Ciampa AS, et al. Retrospective study of dasatinib for recurrent glioblastoma after bevacizumab failure. *J Neurooncol.* (2011) 104:287–91. doi: 10.1007/s11060-010-0489-x

38. Franceschi E, Stupp R, van den Bent MJ, van Herpen C, Laigle Donadey F, Gorlia T, et al. EORTC 26083 phase I/II trial of dasatinib in combination with CCNU in patients with recurrent glioblastoma. *Neuro Oncol.* (2012) 14:1503–10. doi: 10.1093/neuonc/nos256

39. Lassman AB, Pugh SL, Gilbert MR, Aldape KD, Geinoz S, Beumer JH, et al. Phase 2 trial of dasatinib in target-selected patients with recurrent glioblastoma (Rtog 0627). *Neuro Oncol.* (2015) 17:992–8. doi: 10.1093/neuonc/nov011

40. de Groot J, George S, Razak A, Gordon M, Janku F, Ligon K, et al. ACTR-02. DCC-2618, a novel pan-KIT and PDGFRa kinase switch control inhibitor, shows encouraging signal in a patient (PT) with glioblastoma (GBM). *Neuro-Oncology.* (2017) 19:vi1. doi: 10.1093/neuonc/nox168.002

41. Wen PY, Drappatz J, de Groot J, Prados MD, Reardon DA, Schiff D, et al. Phase II study of cabozantinib in patients with progressive glioblastoma: subset analysis of patients naive to antiangiogenic therapy. *Neuro Oncol.* (2018) 20:249–58. doi: 10.1093/neuonc/nox154

42. Cloughesy TF, Drappatz J, de Groot J, Prados MD, Reardon DA, Schiff D, et al. Phase II study of cabozantinib in patients with progressive glioblastoma: subset analysis of patients with prior antiangiogenic therapy. *Neuro Oncol.* (2018) 20:259–67. doi: 10.1093/neuonc/nox151

43. Hutterer M, Nowosielski M, Haybaeck J, Embacher S, Stockhammer F, Gotwald T, et al. A single-arm phase II Austrian/German multicenter trial on continuous daily sunitinib in primary glioblastoma at first recurrence (Surge 01-07). *Neuro Oncol.* (2014) 16:92–102. doi: 10.1093/neuonc/not161

44. Reardon DA, Vredenburgh JJ, Coan A, Desjardins A, Peters KB, Gururangan S, et al. Phase I study of sunitinib and irinotecan for patients with recurrent Malignant glioma. *J Neurooncol.* (2011) 105:621–7. doi: 10.1007/s11060-011-0631-4

45. Grisanti S, Ferrari VD, Buglione M, Agazzi GM, Liserre R, Poliani L, et al. Second line treatment of recurrent glioblastoma with sunitinib: results of a phase II study and systematic review of literature. *J Neurosurg Sci.* (2019) 63:458–67. doi: 10.23736/S0390-5616.16.03874-1

46. Balana C, Gil MJ, Perez P, Reynes G, Gallego O, Ribalta T, et al. Sunitinib administered prior to radiotherapy in patients with non-resectable glioblastoma: results of a phase II study. *Target Oncol.* (2014) 9:321–9. doi: 10.1007/s11523-014-0305-1

47. Stanislaw R, Burzynski TJ, Burzynski GS, Brookman S. Preliminary findings on the use of targeted therapy with pazopanib and other agents in combination with sodium phenylbutyrate in the treatment of glioblastoma multiforme. *J Cancer Ther.* (2014) 5:1423–37. doi: 10.4236/jct.2014.514144

48. Gilbert M. Oral Pazopanib Plus Oral Topotecan Metronomic Antiangiogenic Therapy for Recurrent Glioblastoma Multiforme (a) without Prior Bevacizumab Exposure and (B) after Failing Prior Bevacizumab. National Cancer Institute (NCI), Bethesda, USA: ClinicalTrials.gov (2020). Available at: https://clinicaltrials.gov/study/NCT01931098?tab=results#outcome-measures.

49. Jimenez-Pascual A, Siebzehnrubl FA. Fibroblast growth factor receptor functions in glioblastoma. *Cells.* (2019) 8. doi: 10.3390/cells8070715

50. Lassman AB, Sepulveda-Sanchez JM, Cloughesy TF, Gil-Gil MJ, Puduvalli VK, Raizer JJ, et al. Infigratinib in patients with recurrent gliomas and FGFR alterations: A multicenter phase II study. *Clin Cancer Res.* (2022) 28:2270–7. doi: 10.1158/1078-0432.CCR-21-2664

51. Pant S, Schuler M, Iyer G, Witt O, Doi T, Qin S, et al. Erdafitinib in patients with advanced solid tumours with FGFR alterations (RAGNAR): an international, single-arm, phase 2 study. *Lancet Oncol.* (2023) 24:925–35. doi: 10.1016/S1470-2045(23)00275-9

52. Rodon J, Damian S, Furqan M, Garcia-Donas J, Imai H, Italiano A, et al. Pemigatinib in previously treated solid tumors with activating FGFR1-FGFR3 alterations: phase 2 fight-207 basket trial. *Nat Med.* (2024) 30:1645–54. doi: 10.1038/s41591-024-02934-7

53. Wen PY, Cloughesy TF, Olivero AG, Morrissey KM, Wilson TR, Lu X, et al. First-in-human phase I study to evaluate the brain-penetrant PI3K/mtor inhibitor GDC-0084 in patients with progressive or recurrent high-grade glioma. *Clin Cancer Res.* (2020) 26:1820–8. doi: 10.1158/1078-0432.CCR-19-2808

54. Wen PY, de Groot J, Battiste J, Goldlust S, Damek D, Ellingson B, et al. CTNI-27. Multi-center, phase 2 study evaluating the pharmacokinetics, safety and preliminary efficacy of paxalisib in newly diagnosed adult patients with unmethylated glioblastoma (GBM). *Neuro-Oncology.* (2022) 24:vii76–vii7. doi: 10.1093/neuonc/noac209.292

55. Wen PY, Touat M, Alexander BM, Mellinghoff IK, Ramkissoon S, McCluskey CS, et al. Buparlisib in patients with recurrent glioblastoma harboring

phosphatidylinositol 3-kinase pathway activation: an open-label, multicenter, multi-arm, phase II trial. *J Clin Oncol*. (2019) 37:741–50. doi: 10.1200/JCO.18.01207

56. Rosenthal M, Clement PM, Campone M, Gil-Gil MJ, DeGroot J, Chinot O, et al. Buparlisib plus carboplatin or lomustine in patients with recurrent glioblastoma: A phase Ib/II, open-label, multicentre, randomised study. *ESMO Open*. (2020) 5. doi: 10.1136/esmoopen-2020-000672

57. van den Bent M, Azaro A, De Vos F, Sepulveda J, Yung WKA, Wen PY, et al. A phase Ib/II, open-label, multicenter study of INC280 (Capmatinib) alone and in combination with buparlisib (BKM120) in adult patients with recurrent glioblastoma. *J Neurooncol*. (2020) 146:79–89. doi: 10.1007/s11060-019-03337-2

58. Galanis E, Buckner JC, Maurer MJ, Kreisberg JI, Ballman K, Boni J, et al. Phase II trial of temsirolimus (CCI-779) in recurrent glioblastoma multiforme: A north central cancer treatment group study. *J Clin Oncol*. (2005) 23:5294–304. doi: 10.1200/JCO.2005.23.622

59. Wick W, Gorlia T, Bady P, Platten M, van den Bent MJ, Taphoorn MJ, et al. Phase II study of radiotherapy and temsirolimus versus radiochemotherapy with temozolomide in patients with newly diagnosed glioblastoma without MGMT promoter hypermethylation (EORTC 26082). *Clin Cancer Res*. (2016) 22:4797–806. doi: 10.1158/1078-0432.CCR-15-3153

60. Lee EQ, Kuhn J, Lamborn KR, Abrey L, DeAngelis LM, Lieberman F, et al. Phase I/II study of sorafenib in combination with temsirolimus for recurrent glioblastoma or gliosarcoma: north American brain tumor consortium study 05-02. *Neuro Oncol*. (2012) 14:1511–8. doi: 10.1093/neuonc/nos264

61. Sarkaria JN, Galanis E, Wu W, Dietz AB, Kaufmann TJ, Gustafson MP, et al. Combination of temsirolimus (CCI-779) with chemoradiation in newly diagnosed glioblastoma multiforme (GBM) (NCCTG trial N027D) is associated with increased infectious risks. *Clin Cancer Res*. (2010) 16:5573–80. doi: 10.1158/1078-0432.CCR-10-1453

62. Sarkaria JN, Galanis E, Wu W, Peller PJ, Giannini C, Brown PD, et al. North central cancer treatment group phase I trial N057k of everolimus (Rad001) and temozolomide in combination with radiation therapy in patients with newly diagnosed glioblastoma multiforme. *Int J Radiat Oncol Biol Phys*. (2011) 81:468–75. doi: 10.1016/j.ijrobp.2010.05.064

63. Chinnaiyan P, Won M, Wen PY, Rojiani AM, Wendland M, Dipetrillo TA, et al. RTOG 0913: A phase 1 study of daily everolimus (RAD001) in combination with radiation therapy and temozolomide in patients with newly diagnosed glioblastoma. *Int J Radiat Oncol Biol Phys*. (2013) 86:880–4. doi: 10.1016/j.ijrobp.2013.04.036

64. Mason WP, Macneil M, Kavan P, Easaw J, Macdonald D, Thiessen B, et al. A phase I study of temozolomide and everolimus (RAD001) in patients with newly diagnosed and progressive glioblastoma either receiving or not receiving enzyme-inducing anticonvulsants: an NCIC CTG study. *Invest New Drugs*. (2012) 30:2344–51. doi: 10.1007/s10637-011-9775-5

65. Ma DJ, Galanis E, Anderson SK, Schiff D, Kaufmann TJ, Peller PJ, et al. A phase II trial of everolimus, temozolomide, and radiotherapy in patients with newly diagnosed glioblastoma: NCCTG N057k. *Neuro Oncol*. (2015) 17:1261–9. doi: 10.1093/neuonc/nou328

66. Chinnaiyan P, Won M, Wen PY, Rojiani AM, Werner-Wasik M, Shih HA, et al. A randomized phase II study of everolimus in combination with chemoradiation in newly diagnosed glioblastoma: results of NRG oncology RTOG 0913. *Neuro Oncol*. (2018) 20:666–73. doi: 10.1093/neuonc/nox209

67. Hainsworth JD, Shih KC, Shepard GC, Tillinghast GW, Brinker BT, Spigel DR. Phase II study of concurrent radiation therapy, temozolomide, and bevacizumab followed by bevacizumab/everolimus as first-line treatment for patients with glioblastoma. *Clin Adv Hematol Oncol*. (2012) 10:240–6.

68. Xu Q, Huang K, Meng X, Weng Y, Zhang L, Bu L, et al. Safety and efficacy of anlotinib hydrochloride plus temozolomide in patients with recurrent glioblastoma. *Clin Cancer Res*. (2023) 29:3859–66. doi: 10.1158/1078-0432.CCR-23-0388

69. Yang K, Wu B, Zhang Z, Peng G, Huang J, Hong X, et al. Anlotinib for patients with newly diagnosed glioblastoma with unmethylated mgmt promoter: an open-label, single-center, phase 2 clinical trial. *J Clin Oncol*. (2023) 41:e14039–e. doi: 10.1200/JCO.2023.41.16_suppl.e14039

70. Lombardi G, De Salvo GL, Brandes AA, Eoli M, Ruda R, Faedi M, et al. Regorafenib compared with lomustine in patients with relapsed glioblastoma (Regoma): A multicentre, open-label, randomised, controlled, phase 2 trial. *Lancet Oncol*. (2019) 20:110–9. doi: 10.1016/S1470-2045(18)30675-2

71. Caccese M, Desideri I, Villani V, Simonelli M, Buglione M, Chiesa S, et al. Regoma-oss: A large, italian, multicenter, prospective, observational study evaluating the efficacy and safety of regorafenib in patients with recurrent glioblastoma. *ESMO Open*. (2024) 9:102943. doi: 10.1016/j.esmoop.2024.102943

72. Lee E, Muzikansky A, Arrillaga-Romany I, Chukwueke U, Cloughesy T, Colman H, et al. CTNI-47. Phase II study of abemaciclib in recurrent GBM patients with CDKN2A/B loss and intact RB. *Neuro-Oncology*. (2020) 22:ii53. doi: 10.1093/neuonc/noaa215.213

73. Rahman R, Trippa L, Lee EQ, Arrillaga-Romany I, Fell G, Touat M, et al. Inaugural results of the individualized screening trial of innovative glioblastoma therapy: A phase II platform trial for newly diagnosed glioblastoma using bayesian adaptive randomization. *J Clin Oncol*. (2023) 41:5524–35. doi: 10.1200/JCO.23.00493

74. Taylor JW, Parikh M, Phillips JJ, James CD, Molinaro AM, Butowski NA, et al. Phase-2 trial of palbociclib in adult patients with recurrent RB1-positive glioblastoma. *J Neurooncol*. (2018) 140:477–83. doi: 10.1007/s11060-018-2977-3

75. Tien AC, Bao X, Derogatis A, Kim S, Mehta S, Li J, et al. ACTR-45. Phase 0/2 study of ribociclib in patients with recurrent glioblastoma. *Neuro-Oncology*. (2018) 20:vi21. doi: 10.1093/neuonc/noy148.077

76. Patel AP, Tirosh I, Trombetta JJ, Shalek AK, Gillespie SM, Wakimoto H, et al. Single-cell RNA-seq highlights intratumoral heterogeneity in primary glioblastoma. *Science*. (2014) 344:1396–401. doi: 10.1126/science.1254257

77. Mellinghoff IK, Cloughesy TF, Mischel PS. Pten-mediated resistance to epidermal growth factor receptor kinase inhibitors. *Clin Cancer Res*. (2007) 13:378–81. doi: 10.1158/1078-0432.CCR-06-1992

78. Louis DN, Perry A, Wesseling P, Brat DJ, Cree IA, Figarella-Branger D, et al. The 2021 who classification of tumors of the central nervous system: A summary. *Neuro Oncol*. (2021) 23:1231–51. doi: 10.1093/neuonc/noab106

79. Ceccarelli M, Barthel FP, Malta TM, Sabedot TS, Salama SR, Murray BA, et al. Molecular profiling reveals biologically discrete subsets and pathways of progression in diffuse glioma. *Cell*. (2016) 164:550–63. doi: 10.1016/j.cell.2015.12.028

80. Daher A, de Groot J. Rapid identification and validation of novel targeted approaches for glioblastoma: A combined ex vivo-in vivo pharmaco-omic model. *Exp Neurol*. (2018) 299:281–8. doi: 10.1016/j.expneurol.2017.09.006

81. Gerlinger M, Rowan AJ, Horswell S, Math M, Larkin J, Endesfelder D, et al. Intratumor heterogeneity and branched evolution revealed by multiregion sequencing. *N Engl J Med*. (2012) 366:883–92. doi: 10.1056/NEJMoa1113205

82. Herrlinger U, Rieger J, Koch D, Loeser S, Blaschke B, Kortmann RD, et al. Phase II trial of lomustine plus temozolomide chemotherapy in addition to radiotherapy in newly diagnosed glioblastoma: UKT-03. *J Clin Oncol*. (2006) 24:4412–7. doi: 10.1200/JCO.2006.06.9104

83. Cho NS, Wong WK, Nghiemphu PL, Cloughesy TF, Ellingson BM. The future glioblastoma clinical trials landscape: early phase 0, window of opportunity, and adaptive phase I-III studies. *Curr Oncol Rep*. (2023) 25:1047–55. doi: 10.1007/s11912-023-01433-1

84. Tietz S, Engelhardt B. Brain barriers: crosstalk between complex tight junctions and adherens junctions. *J Cell Biol*. (2015) 209:493–506. doi: 10.1083/jcb.201412147

85. Vorbrodt AW, Dobrogowska DH. Molecular anatomy of intercellular junctions in brain endothelial and epithelial barriers: electron microscopist's view. *Brain Res Brain Res Rev*. (2003) 42:221–42. doi: 10.1016/s0165-0173(03)00177-2

86. Butt AM, Jones HC, Abbott NJ. Electrical resistance across the blood-brain barrier in anaesthetized rats: A developmental study. *J Physiol*. (1990) 429:47–62. doi: 10.1113/jphysiol.1990.sp018243

87. Abbott NJ, Patabendige AA, Dolman DE, Yusof SR, Begley DJ. Structure and function of the blood-brain barrier. *Neurobiol Dis*. (2010) 37:13–25. doi: 10.1016/j.nbd.2009.07.030

88. Agarwal S, Sane R, Oberoi R, Ohlfest JR, Elmquist WF. Delivery of molecularly targeted therapy to Malignant glioma, a disease of the whole brain. *Expert Rev Mol Med*. (2011) 13:e17. doi: 10.1017/S1462399411001888

89. Arvanitis CD, Ferraro GB, Jain RK. The blood-brain barrier and blood-tumour barrier in brain tumours and metastases. *Nat Rev Cancer*. (2020) 20:26–41. doi: 10.1038/s41568-019-0205-x

90. Zhang F, Xu CL, Liu CM. Drug delivery strategies to enhance the permeability of the blood-brain barrier for treatment of glioma. *Drug Des Devel Ther*. (2015) 9:2089–100. doi: 10.2147/DDDT.S79592

91. Srinivasan VM, Ene C, Kerrigan BP, Lang FF. Window of opportunity clinical trials to evaluate novel therapies for brain tumors. *Neurosurg Clin N Am*. (2021) 32:93–104. doi: 10.1016/j.nec.2020.09.002

92. Jensen RL, Ragel BT, Whang K, Gillespie D. Inhibition of hypoxia inducible factor-1alpha (HIF-1alpha) decreases vascular endothelial growth factor (VEGF) secretion and tumor growth in Malignant gliomas. *J Neurooncol*. (2006) 78:233–47. doi: 10.1007/s11060-005-9103-z

93. Cassavaugh J, Lounsbury KM. Hypoxia-mediated biological control. *J Cell Biochem*. (2011) 112:735–44. doi: 10.1002/jcb.22956

94. Burroughs SK, Kaluz S, Wang D, Wang K, Van Meir EG, Wang B. Hypoxia inducible factor pathway inhibitors as anticancer therapeutics. *Future Med Chem*. (2013) 5:553–72. doi: 10.4155/fmc.13.17

95. Osuka S, Van Meir EG. Overcoming therapeutic resistance in glioblastoma: the way forward. *J Clin Invest*. (2017) 127:415–26. doi: 10.1172/JCI89587

96. Hjelmeland AB, Wu Q, Heddleston JM, Choudhary GS, MacSwords J, Lathia JD, et al. Acidic stress promotes a glioma stem cell phenotype. *Cell Death Differ*. (2011) 18:829–40. doi: 10.1038/cdd.2010.150

97. Peppicelli S, Andreucci E, Ruzzolini J, Laurenzana A, Margheri F, Fibbi G, et al. The acidic microenvironment as a possible niche of dormant tumor cells. *Cell Mol Life Sci*. (2017) 74:2761–71. doi: 10.1007/s00018-017-2496-y

98. Mignatti P, Rifkin DB. Plasminogen activators and matrix metalloproteinases in angiogenesis. *Enzyme Protein*. (1996) 49:117–37. doi: 10.1159/000468621

99. Gerweck LE, Vijayappa S, Kozin S. Tumor pH controls the in vivo efficacy of weak acid and base chemotherapeutics. *Mol Cancer Ther*. (2006) 5:1275–9. doi: 10.1158/1535-7163.MCT-06-0024

100. Daniel C, Bell C, Burton C, Harguindey S, Reshkin SJ, Rauch C. The role of proton dynamics in the development and maintenance of multidrug resistance in cancer. *Biochim Biophys Acta*. (2013) 1832:606–17. doi: 10.1016/j.bbadis.2013.01.020

101. Thews O, Gassner B, Kelleher DK, Schwerdt G, Gekle M. Impact of extracellular acidity on the activity of P-glycoprotein and the cytotoxicity of chemotherapeutic drugs. *Neoplasia*. (2006) 8:143–52. doi: 10.1593/neo.05697

102. Fischer K, Hoffmann P, Voelkl S, Meidenbauer N, Ammer J, Edinger M, et al. Inhibitory effect of tumor cell-derived lactic acid on human T cells. *Blood*. (2007) 109:3812–9. doi: 10.1182/blood-2006-07-035972

103. Dietl K, Renner K, Dettmer K, Timischl B, Eberhart K, Dorn C, et al. Lactic acid and acidification inhibit TNF secretion and glycolysis of human monocytes. *J Immunol*. (2010) 184:1200–9. doi: 10.4049/jimmunol.0902584

104. Vaupel P, Multhoff G. Accomplices of the hypoxic tumor microenvironment compromising antitumor immunity: adenosine, lactate, acidosis, vascular endothelial growth factor, potassium ions, and phosphatidylserine. *Front Immunol*. (2017) 8:1887. doi: 10.3389/fimmu.2017.01887

105. Ogunrinu TA, Sontheimer H. Hypoxia increases the dependence of glioma cells on glutathione. *J Biol Chem*. (2010) 285:37716–24. doi: 10.1074/jbc.M110.161190

106. Rocha CR, Garcia CC, Vieira DB, Quinet A, de Andrade-Lima LC, Munford V, et al. Glutathione depletion sensitizes cisplatin- and temozolomide-resistant glioma cells in vitro and in vivo. *Cell Death Dis*. (2014) 5:e1505. doi: 10.1038/cddis.2014.465

107. Zhu Z, Du S, Du Y, Ren J, Ying G, Yan Z. Glutathione reductase mediates drug resistance in glioblastoma cells by regulating redox homeostasis. *J Neurochem*. (2018) 144:93–104. doi: 10.1111/jnc.14250

108. Pardridge WM. Drug transport across the blood-brain barrier. *J Cereb Blood Flow Metab*. (2012) 32:1959–72. doi: 10.1038/jcbfm.2012.126

109. Banks WA. From blood-brain barrier to blood-brain interface: new opportunities for CNS drug delivery. *Nat Rev Drug Discovery*. (2016) 15:275–92. doi: 10.1038/nrd.2015.21

110. Wen PY, Kesari S. Malignant gliomas in adults. *N Engl J Med*. (2008) 359:492–507. doi: 10.1056/NEJMra0708126

111. Bettegowda C, Sausen M, Leary RJ, Kinde I, Wang Y, Agrawal N, et al. Detection of circulating tumor DNA in early- and late-stage human Malignancies. *Sci Transl Med*. (2014) 6:224ra24. doi: 10.1126/scitranslmed.3007094

112. Wang Y, Springer S, Zhang M, McMahon KW, Kinde I, Dobbyn L, et al. Detection of tumor-derived DNA in cerebrospinal fluid of patients with primary tumors of the brain and spinal cord. *Proc Natl Acad Sci U.S.A*. (2015) 112:9704–9. doi: 10.1073/pnas.1511694112

113. Wang Z, Jiang W, Wang Y, Guo Y, Cong Z, Du F, et al. MGMT promoter methylation in serum and cerebrospinal fluid as a tumor-specific biomarker of glioma. *BioMed Rep*. (2015) 3:543–8. doi: 10.3892/br.2015.462

114. Diehl F, Schmidt K, Choti MA, Romans K, Goodman S, Li M, et al. Circulating mutant DNA to assess tumor dynamics. *Nat Med*. (2008) 14:985–90. doi: 10.1038/nm.1789

115. Piccioni DE, Achrol AS, Kiedrowski LA, Banks KC, Boucher N, Barkhoudarian G, et al. Analysis of cell-free circulating tumor DNA in 419 patients with glioblastoma and other primary brain tumors. *CNS Oncol*. (2019) 8:CNS34. doi: 10.2217/cns-2018-0015

116. Jones JJ, Jones KL, Wong SQ, Whittle J, Goode D, Nguyen H, et al. Plasma ctdna enables early detection of temozolomide resistance mutations in glioma. *Neurooncol Adv*. (2024) 6:vdae041. doi: 10.1093/noajnl/vdae041

117. Jones JJ, Nguyen H, Wong SQ, Whittle J, Iaria J, Stylli S, et al. Plasma ctdna liquid biopsy of IDH1, TERTp, and EGFRvIII mutations in glioma. *Neurooncol Adv*. (2024) 6:vdae027. doi: 10.1093/noajnl/vdae027

118. Roth P, Wischhusen J, Happold C, Chandran PA, Hofer S, Eisele G, et al. A specific miRNA signature in the peripheral blood of glioblastoma patients. *J Neurochem*. (2011) 118:449–57. doi: 10.1111/j.1471-4159.2011.07307.x

119. Wang Q, Li P, Li A, Jiang W, Wang H, Wang J, et al. Plasma specific mirnas as predictive biomarkers for diagnosis and prognosis of glioma. *J Exp Clin Cancer Res*. (2012) 31:97. doi: 10.1186/1756-9966-31-97

120. Geczi D, Nagy B, Szilagyi M, Penyige A, Klekner A, Jenei A, et al. Analysis of circulating miRNA profile in plasma samples of glioblastoma patients. *Int J Mol Sci*. (2021) 22. doi: 10.3390/ijms22105058

121. Swellam M, Ezz El Arab L, Al-Posttany AS, Said SB. Clinical impact of circulating oncogenic miRNA-221 and miRNA-222 in glioblastoma multiform. *J Neurooncol*. (2019) 144:545–51. doi: 10.1007/s11060-019-03256-2

122. Zhao H, Shen J, Hodges TR, Song R, Fuller GN, Heimberger AB. Serum microrna profiling in patients with glioblastoma: A survival analysis. *Mol Cancer*. (2017) 16:59. doi: 10.1186/s12943-017-0628-5

123. Shankar GM, Balaj L, Stott SL, Nahed B, Carter BS. Liquid biopsy for brain tumors. *Expert Rev Mol Diagn*. (2017) 17:943–7. doi: 10.1080/14737159.2017.1374854

124. Kahlert C, Kalluri R. Exosomes in tumor microenvironment influence cancer progression and metastasis. *J Mol Med (Berl)*. (2013) 91:431–7. doi: 10.1007/s00109-013-1020-6

125. Balakrishnan A, Roy S, Fleming T, Leong HS, Schuurmans C. The emerging role of extracellular vesicles in the glioma microenvironment: biogenesis and clinical relevance. *Cancers (Basel)*. (2020) 12. doi: 10.3390/cancers12071964

126. Matarredona ER, Pastor AM. Extracellular vesicle-mediated communication between the glioblastoma and its microenvironment. *Cells*. (2019) 9. doi: 10.3390/cells9010096

127. Bebelman MP, Smit MJ, Pegtel DM, Baglio SR. Biogenesis and function of extracellular vesicles in cancer. *Pharmacol Ther*. (2018) 188:1–11. doi: 10.1016/j.pharmthera.2018.02.013

128. Peinado H, Aleckovic M, Lavotshkin S, Matei I, Costa-Silva B, Moreno-Bueno G, et al. Melanoma Exosomes Educate Bone Marrow Progenitor Cells toward a Pro-Metastatic Phenotype through Met. *Nat Med*. (2012) 18:883–91. doi: 10.1038/nm.2753

129. Garcia-Romero N, Carrion-Navarro J, Esteban-Rubio S, Lazaro-Ibanez E, Peris-Celda M, Alonso MM, et al. DNA sequences within glioma-derived extracellular vesicles can cross the intact blood-brain barrier and be detected in peripheral blood of patients. *Oncotarget*. (2017) 8:1416–28. doi: 10.18632/oncotarget.13635

130. Manda SV, Kataria Y, Tatireddy BR, Ramakrishnan B, Ratnam BG, Lath R, et al. Exosomes as a biomarker platform for detecting epidermal growth factor receptor-positive high-grade gliomas. *J Neurosurg*. (2018) 128:1091–101. doi: 10.3171/2016.11.JNS161187

131. Khayamzadeh M, Niazi V, Hussen BM, Taheri M, Ghafouri-Fard S, Samadian M. Emerging role of extracellular vesicles in the pathogenesis of glioblastoma. *Metab Brain Dis*. (2023) 38:177–84. doi: 10.1007/s11011-022-01074-6

132. Yang JK, Yang JP, Tong J, Jing SY, Fan B, Wang F, et al. Exosomal miR-221 targets DNM3 to induce tumor progression and temozolomide resistance in glioma. *J Neurooncol*. (2017) 131:255–65. doi: 10.1007/s11060-016-2308-5

133. Indira Chandran V, Welinder C, Mansson AS, Offer S, Freyhult E, Pernemalm M, et al. Ultrasensitive immunoprofiling of plasma extracellular vesicles identifies syndecan-1 as a potential tool for minimally invasive diagnosis of glioma. *Clin Cancer Res*. (2019) 25:3115–27. doi: 10.1158/1078-0432.CCR-18-2946

134. Mason WP. Blood-brain barrier-associated efflux transporters: A significant but underappreciated obstacle to drug development in glioblastoma. *Neuro Oncol*. (2015) 17:1181–2. doi: 10.1093/neuonc/nov122

135. Liu HL, Huang CY, Chen JY, Wang HY, Chen PY, Wei KC. Pharmacodynamic and therapeutic investigation of focused ultrasound-induced blood-brain barrier opening for enhanced temozolomide delivery in glioma treatment. *PloS One*. (2014) 9:e114311. doi: 10.1371/journal.pone.0114311

136. Wei HJ, Upadhyayula PS, Pouliopoulos AN, Englander ZK, Zhang X, Jan CI, et al. Focused ultrasound-mediated blood-brain barrier opening increases delivery and efficacy of etoposide for glioblastoma treatment. *Int J Radiat Oncol Biol Phys*. (2021) 110:539–50. doi: 10.1016/j.ijrobp.2020.12.019

137. Park SH, Kim MJ, Jung HH, Chang WS, Choi HS, Rachmilevitch I, et al. One-year outcome of multiple blood-brain barrier disruptions with temozolomide for the treatment of glioblastoma. *Front Oncol*. (2020) 10:1663. doi: 10.3389/fonc.2020.01663

138. Carpentier A, Stupp R, Sonabend AM, Dufour H, Chinot O, Mathon B, et al. Repeated blood-brain barrier opening with a nine-emitter implantable ultrasound device in combination with carboplatin in recurrent glioblastoma: A phase I/II clinical trial. *Nat Commun*. (2024) 15:1650. doi: 10.1038/s41467-024-45818-7

139. Hersh AM, Bhimreddy M, Weber-Levine C, Jiang K, Alomari S, Theodore N, et al. Applications of focused ultrasound for the treatment of glioblastoma: A new frontier. *Cancers (Basel)*. (2022) 14. doi: 10.3390/cancers14194920

140. Ye D, Yuan J, Yue Y, Rubin JB, Chen H. Focused ultrasound-enhanced delivery of intranasally administered anti-programmed cell death-ligand 1 antibody to an intracranial murine glioma model. *Pharmaceutics*. (2021) 13. doi: 10.3390/pharmaceutics13020190

141. Ram Z, Cohen ZR, Harnof S, Tal S, Faibel M, Nass D, et al. Magnetic resonance imaging-guided, high-intensity focused ultrasound for brain tumor therapy. *Neurosurgery*. (2006) 59:949–55. doi: 10.1227/01.NEU.0000254439.02736.D8

142. Tamada J, Langer R. The development of polyanhydrides for drug delivery applications. *J Biomater Sci Polym Ed*. (1992) 3:315–53. doi: 10.1163/156856292x00402

143. Perry J, Chambers A, Spithoff K, Laperriere N. Gliadel wafers in the treatment of Malignant glioma: A systematic review. *Curr Oncol*. (2007) 14:189–94. doi: 10.3747/co.2007.147

144. Xing WK, Shao C, Qi ZY, Yang C, Wang Z. The role of gliadel wafers in the treatment of newly diagnosed GBM: A meta-analysis. *Drug Des Devel Ther*. (2015) 9:3341–8. doi: 10.2147/DDDT.S85943

145. Fleming AB, Saltzman WM. Pharmacokinetics of the carmustine implant. *Clin Pharmacokinet*. (2002) 41:403–19. doi: 10.2165/00003088-200241060-00002

146. Sheleg SV, Korotkevich EA, Zhavrid EA, Muravskaya GV, Smeyanovich AF, Shanko YG, et al. Local chemotherapy with cisplatin-depot for glioblastoma multiforme. *J Neurooncol*. (2002) 60:53–9. doi: 10.1023/a:1020288015457

147. Di Mascolo D, Palange AL, Primavera R, Macchi F, Catelani T, Piccardi F, et al. Conformable hierarchically engineered polymeric micromeshes enabling combinatorial therapies in brain tumours. *Nat Nanotechnol*. (2021) 16:820–9. doi: 10.1038/s41565-021-00879-3

148. Elstad NL, Fowers KD. Oncogel (Regel/paclitaxel)–clinical applications for a novel paclitaxel delivery system. *Adv Drug Delivery Rev*. (2009) 61:785–94. doi: 10.1016/j.addr.2009.04.010

149. Boisdron-Celle M, Menei P, Benoit JP. Preparation and characterization of 5-fluorouracil-loaded microparticles as biodegradable anticancer drug carriers. *J Pharm Pharmacol*. (1995) 47:108–14. doi: 10.1111/j.2042-7158.1995.tb05760.x

150. Roullin VG, Mege M, Lemaire L, Cueyssac JP, Venier-Julienne MC, Menei P, et al. Influence of 5-fluorouracil-loaded microsphere formulation on efficient rat glioma

radiosensitization. *Pharm Res*. (2004) 21:1558–63. doi: 10.1023/b:pham.0000041448.22771.48

151. Wiley DT, Webster P, Gale A, Davis ME. Transcytosis and brain uptake of transferrin-containing nanoparticles by tuning avidity to transferrin receptor. *Proc Natl Acad Sci U.S.A*. (2013) 110:8662–7. doi: 10.1073/pnas.1307152110

152. Tian X, Leite DM, Scarpa E, Nyberg S, Fullstone G, Forth J, et al. On the shuttling across the blood-brain barrier *via* tubule formation: mechanism and cargo avidity bias. *Sci Adv*. (2020) 6. doi: 10.1126/sciadv.abc4397

153. Anraku Y, Kuwahara H, Fukusato Y, Mizoguchi A, Ishii T, Nitta K, et al. Glycaemic control boosts glucosylated nanocarrier crossing the BBB into the brain. *Nat Commun*. (2017) 8:1001. doi: 10.1038/s41467-017-00952-3

154. Roberts MJ, Bentley MD, Harris JM. Chemistry for peptide and protein pegylation. *Adv Drug Delivery Rev*. (2002) 54:459–76. doi: 10.1016/s0169-409x(02)00022-4

155. Whittle JR, Lickliter JD, Gan HK, Scott AM, Simes J, Solomon BJ, et al. First in human nanotechnology doxorubicin delivery system to target epidermal growth factor receptors in recurrent glioblastoma. *J Clin Neurosci*. (2015) 22:1889–94. doi: 10.1016/j.jocn.2015.06.005

156. Kasenda B, Konig D, Manni M, Ritschard R, Duthaler U, Bartoszek E, et al. Targeting immunoliposomes to EGFR-positive glioblastoma. *ESMO Open*. (2022) 7:100365. doi: 10.1016/j.esmoop.2021.100365

157. Liu A, Aboud O, Dahabiyeh LA, Bloch O, Fiehn O. A pilot study on metabolomic characterization of human glioblastomas and patient plasma. *Res Sq*. (2023). doi: 10.21203/rs.3.rs-2662020/v1

frontiers | Frontiers in Oncology

TYPE Brief Research Report
PUBLISHED 15 November 2024
DOI 10.3389/fonc.2024.1504514

OPEN ACCESS

EDITED BY
Alma D. Campos-Parra,
Universidad Veracruzana, Mexico

REVIEWED BY
Alessandro De Vita,
Scientific Institute of Romagna for the Study and Treatment of Tumors (IRCCS), Italy
Gerardo Cuamani-Mitznahuatl,
ABC Medical Center, Mexico

*CORRESPONDENCE
Leslie A. Caromile
caromile@uchc.edu

RECEIVED 30 September 2024
ACCEPTED 24 October 2024
PUBLISHED 15 November 2024

CITATION
McAllister BC, Mesbahi N, Dodson EE, Abdulsalam S, Berkman CE and Caromile LA (2024) Repurposing of PSMA-targeted diagnostic and therapeutic agents for the detection and treatment of giant cell tumors of bone.
Front. Oncol. 14:1504514.
doi: 10.3389/fonc.2024.1504514

Repurposing of PSMA-targeted diagnostic and therapeutic agents for the detection and treatment of giant cell tumors of bone

Brenna C. McAllister[1], Nooshin Mesbahi[2], Esther E. Dodson[2], Sakinah Abdulsalam[3], Clifford E. Berkman[2] and Leslie A. Caromile[1]*

[1]Center for Vascular Biology, University of Connecticut Health Center, Farmington, CT, United States, [2]Department of Chemistry, Washington State University, Pullman, WA, United States, [3]Department of Neuroscience, University of Connecticut Health Center, Farmington, CT, United States

Giant cell tumor of bone (GCTB) is a rare bone tumor often necessitating surgical intervention, radiation therapy, or treatment with bisphosphonates or denosumab. ^{99m}Tc-MDP bone scintigraphy for GCTB has limited specificity, and the relatively high uptake of ^{18}F-FDG in GCTB makes it challenging to differentiate it from other benign bone tumors. More specific detection and treatment modalities for GCTB are needed to enhance patient monitoring and outcomes. Prostate Specific Membrane Antigen (PSMA) is present in the neovasculature of various tumors, yet unexplored in GCTB. PSMA-targeted imaging and radiotherapeutic agents Locametz and Pluvicto are a powerful theranostic pair for detecting and treating PSMA-positive metastatic tumors, including those in bone, and thus have considerable potential to be repurposed for GCTB. This study aimed to determine if the vasculature of GCTB was PSMA-positive and whether targeting it with PSMA-specific agents was feasible. Using bone core samples from 28 GCTB patients and 9 negative controls, we present the first robust detection of PSMA on the tumor vasculature of GCTB. To demonstrate the potential repurposed use of PSMA-targeted agents in detecting and treating GCTB, we used a PSMA-specific fluorescent probe (FAM-C6-1298) as a model for these radiopharmaceutical agents. Incubation of fresh GCTB tissue samples with FAM-C6-1298 showed increased fluorescence intensity compared to controls, indicating successful targeting of PSMA in GCTB tissue. In conclusion, our data established that PSMA is not only present in the tumor vasculature of GCTB patient tissue but can be effectively targeted with repurposed PSMA-specific radiopharmaceuticals for diagnosis and therapy.

KEYWORDS

prostate specific membrane antigen (PSMA), repurposable drugs, Pluvicto, Locametz, giant cell tumor of bone (GCTB)

Introduction

Giant cell tumor of bone (GCTB) is primary osteolytic neoplasm that accounts for approximately 5-6% of all primary bone tumors and about 20% of benign bone tumors (1). GCTB progression is driven, in part, by the overactivity of the receptor activator of nuclear factor-kappa β ligand (RANKL) (2) and typically affects the (3) decade of life (median age 20-40 years) (1, 4). The World Health Organization's classification of soft tissue and bone tumors categorized GCTB as an intermediate malignant tumor with locally aggressive behavior and a high recurrence rate (5). GCTB has been observed to metastasize to the lungs in up to 6% of cases and can also undergo a malignant transformation in 2.4% of cases (6). The clinical presentation of GCTB includes local swelling, pain, and limitations in joint movement (7, 8). While ^{99m}Tc-methyl diphosphonate (^{99m}Tc-MDP) bone scintigraphy is routinely used for evaluating GCTB skeletal involvement, its utility is limited by reduced specificity (9). Additionally, ^{18}F-fluorodeoxyglucose (FDG) uptake in GCTB, as measured by positron emission tomography/computed tomography (PET/CT), is comparatively higher than in other benign bone tumors due to the increased metabolic activity of osteoclasts (10, 11) making it difficult to differentiate between benign and malignant bone tumors. Unfortunately, a bone biopsy for histological examination is necessary for a final diagnosis of GCTB.

Due to the absence of randomized clinical trials (<50), treatment methods for GCTB have not significantly changed in the past three decades (12). The preferential treatment is curettage and high-speed drilling with local adjuvants and filling with polymethylmethacrylate (PMMA), bone allografts, and hydroxyapatite, often resulting in recurrence rates of 45% (1, 13–17). Where joint salvage is impossible, resection and reconstruction are favored. While joint replacements result in lower GCTB recurrence, they have higher complication rates and less favorable functional outcomes (18, 19). GCTBs that are inoperable, such as in the pelvis or spine, or cause severe dysfunction even after resection are treated with radiation therapy or antiresorptive drugs such as bisphosphonates and/or the human anti-RANKL antibody (denosumab). Bisphosphonates, such as zoledronic acid, function by inhibiting farnesyl pyrophosphate synthase, which is vital in promoting the attachment of the osteoclast to the bone. As a result, the osteoclast detaches from the bone surface, inhibiting bone resorption (20). Furthermore, Bisphosphonates inhibit osteoclast-like giant cell formation from immature precursors and induce apoptosis in mature osteoclasts. Though some literature supports the efficacy of bisphosphonates, the side effects are not trivial. In 15% - 30% of cases, patients experience nausea, fatigue, bone pain, hypotension, atrial fibrillation, anemia, and alopecia, to name a few. More severe cases include osteonecrosis of the jaw (3).

Denosumab is a human monoclonal antibody that binds the cytokine RANKL, an essential factor initiating bone turnover. RANKL inhibits monocyte activation and osteoclastogenesis, thus reducing bone resorption (21, 22). The response rate to denosumab, defined as more than a 90% depletion of multinucleated giant cells on histopathologic examination, is approximately 72% (23, 24). However, caution is employed since upwards of 40% of recurrent GCTB that transform into malignant sarcomas are found in patients who received denosumab administration before curettage for their initial benign lesion (25, 26). Additionally, denosumab cessation carries a risk of relapse, thus requiring long-term treatment resulting in serious adverse effects (25, 27–29). Therefore, despite efforts, there is a lack of specific detection and treatment methods to improve patient monitoring and reduce bone-related events for GCTB patients. However, if a clinically relevant biomarker for other indications could be identified in GCTB cells, it could support the feasibility of repurposing relevant drugs targeted to such a biomarker.

Prostate-Specific Membrane Antigen (PSMA) is the hallmark enzyme-biomarker for prostate cancer as it is expressed in the epithelium of nearly all prostate cancers, and increased expression correlates with progression to castration resistance and metastatic disease (30–32). PSMA is a type II transmembrane protein with glutamate-carboxypeptidase activity and known substrates. Upon ligand binding, the cytoplasmic domain of PSMA contains an *N*-terminal motif that signals the internalization of PSMA via clathrin-coated pits (33, 34), resulting in the transportation of bound ligands into the cell. Clinical technologies utilize this signaling pathway to enhance tumor detection and management of prostate cancer through the delivery of radiopharmaceuticals into primary and metastatic prostate tumors, with PSMA-targeted PET ([^{68}Ga] Ga-PSMA-11 (Locametz)) and ([^{177}Lu] Lu-PSMA-617 (Pluvicto)) leading the way (35–45). Tumor vascularity significantly impacts tumor growth and drug responsiveness concerning tumor oxygenation and permeability of imaging agents and chemotherapeutics (46–49). In addition to its unique expression in prostate cancer, PSMA is known to be expressed on the endothelial cells of neovasculature in both prostatic and non-prostatic tumors (e.g., renal cell carcinoma, and breast, lung, gastric, colorectal, pancreatic, and bladder cancers) (44, 50–52). However, to date, there have been no reports on the expression of PSMA in the vasculature of GCTB nor any on PSMA-based detection or treatments regarding this disease. If the vasculature of GCTB was similarly characterized by PSMA expression, there would be sufficient rationale for pursuing the repurposing of clinical PSMA-targeted diagnostic and therapeutic agents such as Locametz and Pluvicto.

Drug repurposing involves identifying new therapeutic uses for existing drugs initially developed for other indications. A drug's specific pharmacological action frequently gives rise to a spectrum of side effects, which may exhibit secondary therapeutic uses. Drug repurposing has several advantages over developing new drugs, including a lower risk of failure due to established safety profiles, reduced development time, and lower investment requirements (53–57). Repurposable drugs include generic (off-patent) medications currently available on the market, on-patent medications such as Locametz and Plavicto, including those still undergoing clinical trials, and failed drugs initially intended for a different purpose. New potential medication applications are often uncovered through pre-clinical *in vitro and in vivo* experiments, mathematical modeling, AI-driven network simulations, and clinical trials (58, 59). This strategic approach has primarily targeted chronic conditions such as diabetes, cancer, and rare diseases.

Our aim in this study was to determine if the vasculature of GCTB was positive for PSMA and, if so, whether it would be feasible to target it with PSMA-specific small-molecule fluorescent probe (45). In our analysis of samples obtained from patients clinically

diagnosed with GCTB, we detected a significant presence of PSMA on the endothelial cells of tumor vasculature compared to the control. Furthermore, our results demonstrated the effective internalization and trafficking of a model PSMA-targeted agent into a PSMA (+) human cell line and the targeting of PSMA in GCTB patient tissue. This finding is of substantial clinical importance, especially given the recent availability of the PSMA-targeted radiopharmaceuticals Pluvicto and Locametz and their broader applicability for indications other than prostate cancer. This proof-of-concept paper supports the feasibility of initiating preclinical studies and randomized clinical trials focusing on the repurposing of commercially available PSMA-targeted diagnostic and therapeutic agents for the detection and treatment of GCTB.

Materials and methods

Cells

The immortalized human prostate cancer cell line C4-2B (ATCC, Manassas, VA) used in this study was maintained in RPMI 1640 medium (Thermo Fisher, Waltham, MA), supplemented with 10% fetal bovine serum, 100 µg/ml antibiotic-antimycotic (Thermo Fisher), and insulin-transferrin-selenium (Thermo Fisher) in a humid atmosphere containing 5% CO_2 at 37°C.

Immunohistochemistry

Clinically diagnosed, deidentified, and coded GCTB patient bone core formalin-fixed paraffin-embedded (FFPE) slides were obtained commercially from TissueArray.com (catalog numbers BO801, BO601, and T261b). An in-house pathologist from TissueArray.com and/or the clinical source verified the clinical diagnosis of GCTB using H&E staining and IHC with Anti-S-100 and H3.3. Slides were deparaffinized and rehydrated. Antigen retrieval was conducted at 95°C using 10 mM sodium citrate buffer (pH 6.0, EMD Millipore Corp. Burlington, MA) in a steamer. Endogenous peroxidase activity was quenched by incubating slides for 15 mn in a peroxidase suppressor (Thermo Fisher). Slides were blocked in 10% normal goat serum in PBS for 60 mn at room temperature in a humidified chamber and then incubated with PSMA rabbit monoclonal antibody (Cell Signaling Technology, Danvers, MA) or a CD31 mouse monoclonal antibody (Cell Signaling Technology) 1% normal goat serum, and 1X PBS overnight at 4°C in a humidified chamber. Slides were washed in PBS, and VECTASTAIN Elite ABC Universal PLUS Peroxidase Kit (anti-mouse/rabbit IgG) (Vector Laboratories, Newark, CA) was used according to the manufacturer's instructions. Slides were developed using 3,3'-diaminobenzidine. Slides were counterstained in Hematoxylin Gill's Formula (Vector Laboratories), differentiated in a 1% acetic acid rinse, followed by a bluing solution, and then rehydrated and mounted under Cytoseal 60 (Epredia, Kalamazoo, MI). Images were acquired using a Zeiss LSM510 META based on an Axiovert 200 microscope and processed using the Zeiss Zen software v3.6. Representative H&E images for each patient can be found on the TissueArray.com website.

Immunofluorescence staining

Commercial clinically diagnosed, deidentified, and coded FFPE bone core slides (TissueArray.com, catalog #BO601, #BO801, and #T261b) were deparaffinized and rehydrated. Antigen retrieval was conducted at 95°C using 10 mM sodium citrate buffer, pH 6.0 (EMD Millipore Corp) in a steamer. Slides were blocked and permeabilized in 0.01% Triton X-100 and 10% normal goat serum (Sigma Aldrich, St. Louis, MO) for 1 h and then incubated with a PSMA rabbit monoclonal antibody (Cell Signaling Technology) and a CD31 mouse monoclonal antibody (Cell Signaling Technology), in 1% normal goat serum overnight in humidity chamber 4°C. Slides were washed in PBS and incubated with Alexa Fluor 488 goat anti-mouse (Thermo Fisher Scientific) and Alexa Fluor 546 goat anti-rabbit (Thermo Fisher Scientific) for 1 h. Slides were washed in PBS, and autofluorescence was quenched with Vector TrueVIEW (Vector Laboratories). Slides were washed in PBS and mounted in VECTASHIELD Hardset Antifade Mounting Medium with DAPI (Vector Laboratories.). Images were acquired using a Zeiss LSM510 META based on an Axiovert 200 microscope and processed using the Zeiss Zen software v3.6.

FAM-C6-1298 synthesis

The synthetic methods for preparing FAM-C6-1298 are detailed in the Supplementary Information. DBCO-C6-1298 was available from a prior study (60) and 5-FAM-azide was purchased from Lumiprobe Corporation. All other reagents and general solvents were of commercial quality (Fisher Scientific, Sommerville, NJ) or (Sigma-Aldrich, St. Louis, MO) and were used without further purification. Anhydrous solvents used in reactions were obtained from commercial sources or freshly distilled over calcium hydride. ^{1}H, ^{13}C, and ^{31}P NMR spectra were recorded on a Varian 400, Brucker Avance Neo 500, or Varian 600 MHz spectrometer. ^{1}H NMR chemical shifts are relative to $CDCl_3$ (δ = 7.26 ppm), CD_3OD (δ = 3.31 ppm) or D_2O (δ = 4.79 ppm). ^{13}C NMR chemical shifts were relative to $CDCl_3$ (δ = 77.23 ppm) or CD_3OD (δ = 49.15 ppm). ^{31}P chemical shifts were relative to triphenylphosphine oxide (TPPO, δ = 27.00 ppm). High-resolution mass spectrometry (HRMS) spectra were obtained on an Applied Biosystems 4800 MALDI-TOF/TOF mass spectrometer (Applied Biosystems, Foster City, CA).

Fluorescent cell imaging

Cells were plated onto coverslips at a density of 1×10^5 cells/well in growth medium and allowed to attach for 48 h. Cells were then incubated for 30 min with either 100µM DBCO-C6-1298 or a control growth medium, followed by 30 min with 10µM FAM-C6-1298 at 37°C. For imaging, coverslips were set on ice, rinsed three times in ice-cold phosphate-buffered saline (PBS), fixed in ice-cold 10% neutral buffered formalin solution for 15 min, rinsed again with PBS, and mounted in VECTASHIELD Hardset Antifade Mounting Medium with DAPI (Vector Laboratories).

Fluorescent co-localization cell imaging

Cells were plated onto coverslips at a concentration of 1×10^5 cells/well in 1 mL of growth medium and allowed to attach overnight. Cells were starved for 2 h in fetal bovine serum (FBS)-free RPMI and then incubated for 60 min with 1μM FAM-C6-1298. Coverslips were set on ice, rinsed twice in ice-cold phosphate-buffered saline (PBS), and fixed in ice-cold 10% neutral buffered formalin solution for 15 min. Coverslips were blocked and permeabilized in 0.01% Triton X-100 and10% normal goat serum (Sigma) for 1 h and then incubated with PSMA antibody (D718E, Cell Signaling Technology) in 1% normal goat serum overnight in a humidity chamber 4°C. Coverslips were washed in PBS and incubated with Alexa Fluor 546 goat anti-rabbit (Thermo Fisher Scientific) for 1 h. Slides were washed in PBS and mounted in VECTASHIELD Hardset Antifade Mounting Medium with DAPI (Vector Laboratories).

Ex vivo whole-tissue fluorescence measurements

Frozen tissue blocks from clinically diagnosed GCTB deidentified and coded patients were purchased commercially from OriGene (OriGene, catalog number CB499383, CB649405), divided into two sections, and washed in DPBS at 37°C for 10 mn and then HEPES at 37°C for 10 mn. Tissue blocks were then incubated with either 10μM FAM-C6-1298 in HEPES for 60 min or with 100μM DBCO-C6-1298 in HEPES for 60 min, followed by a 60 min incubation with 10μM FAM-C6-1298 in HEPES at 37°C. The tissue was washed three times in DPBS, placed in 60mm plates, and analyzed for fluorescence using the IVIS Spectrum 2 Imaging System (Revvity). The fluorophore of FAM-C6-1298 was excited at 495 nm and detected at 517 nm. Data was collected as radiant efficiency (photons/sec/cm^2/steradian/μW/cm^2) using Living Image software v4.8.2. To mitigate the effects of arbitrary autofluorescence, the software computes the background-corrected intensity signal using the following formula:

$$Background\ \ corrected\ \ intensity = ROI\ \ intensity - Average\ \ background\ \ ROI\ \ intensity$$

Reagents

All reagents used in this project can be found in the Supplementary Materials.

Ethical statement

All patient samples used in this study were purchased commercially from TissueArray.com (Derwood, MD) and OriGene (Rockville, MD). The following links provide information on the HIPPA-compliant tissue collection procedures and ethical standards followed by these companies:

https://www.tissuearray.com/FAQs#q10

https://www.origene.com/products/tissues/tissue-qc

Statistical analysis

Differences between means were analyzed using either the two-tailed Student's t-test or analysis of variance (ANOVA), where appropriate, and significance was set at p ¾ 0.05. NIH/FIJI was used to analyze IF co-localization staining. The Zeiss Zen software v3.6 co-localization function determined the Pearson correlation coefficient (ρ).

Results

In this study, we aimed to determine if the vasculature of GCTB was positive for PSMA and, if so, whether it would be feasible to target it with a PSMA-specific small-molecule fluorescent probe (45). Deidentified and coded GCTB patient samples were obtained commercially from TissueArray.com. The in-house pathologist from the company and/or the clinical source verified the clinical diagnosis of GCTB using hematoxylin and eosin staining (Figures 1A, B) and IHC with Anti-S-100 and/or H3.3 (not provided). Multinucleated giant cells can be identified within the tumor tissue by hematoxylin and eosin counterstaining, which is a key characteristic of GCTB (61). For our analysis, GCTB patients were chosen to represent a wide range of ages to assess the broad applicability of PSMA agents for GCTB and prevent sampling bias. Therefore, in our immunohistochemical examination of FFPE bone core samples from 28 patients (12 female, 16 males, ages 17y-75y) clinically diagnosed with GCTB and 9 negative control FFPE patient bone core samples from cancer adjacent normal bone (NAT) of rib (five female, four male, ages 50y-68y) (Table 1), we present the first robust detection of PSMA on the tumor vasculature of GCTB compared to NAT control (Figures 1C, D). Additionally, to validate that PSMA was restricted to the endothelial cells of the GCTB vasculature, we co-incubated the FFPE bone core samples with the vascular endothelial cell marker CD31 and PSMA. Using a previously published Pearson correlation coefficient (ρ) scale where a correlation of <0.20 is very weak, a correlation between 0.20-0.39 is weak, correlations between 0.40-0.59 are moderate, correlations between 0.60-0.79 are strong, and correlations >0.80 as very strong (62), we found that 71.4% of GCTB samples exhibited a strong to moderate positive fluorescent co-localization (ρ = 0.5 to 0.7) of CD31 and PSMA compared to control NAT samples (Figures 1E, G, H), thus confirming that PSMA was restricted to the endothelial cells of the GCTB vasculature. The linear relationship between PSMA and CD31 fluorescent co-localization was verified through a scatterplot (Figure 1F). Due to section variability and random vasculature location within the tumor, the Pearson correlation analysis was measured within a specified boxed area on the image. However, the Pearson correlation coefficient cut-offs are set arbitrarily to refer to

10.3389/fonc.2024.1504514

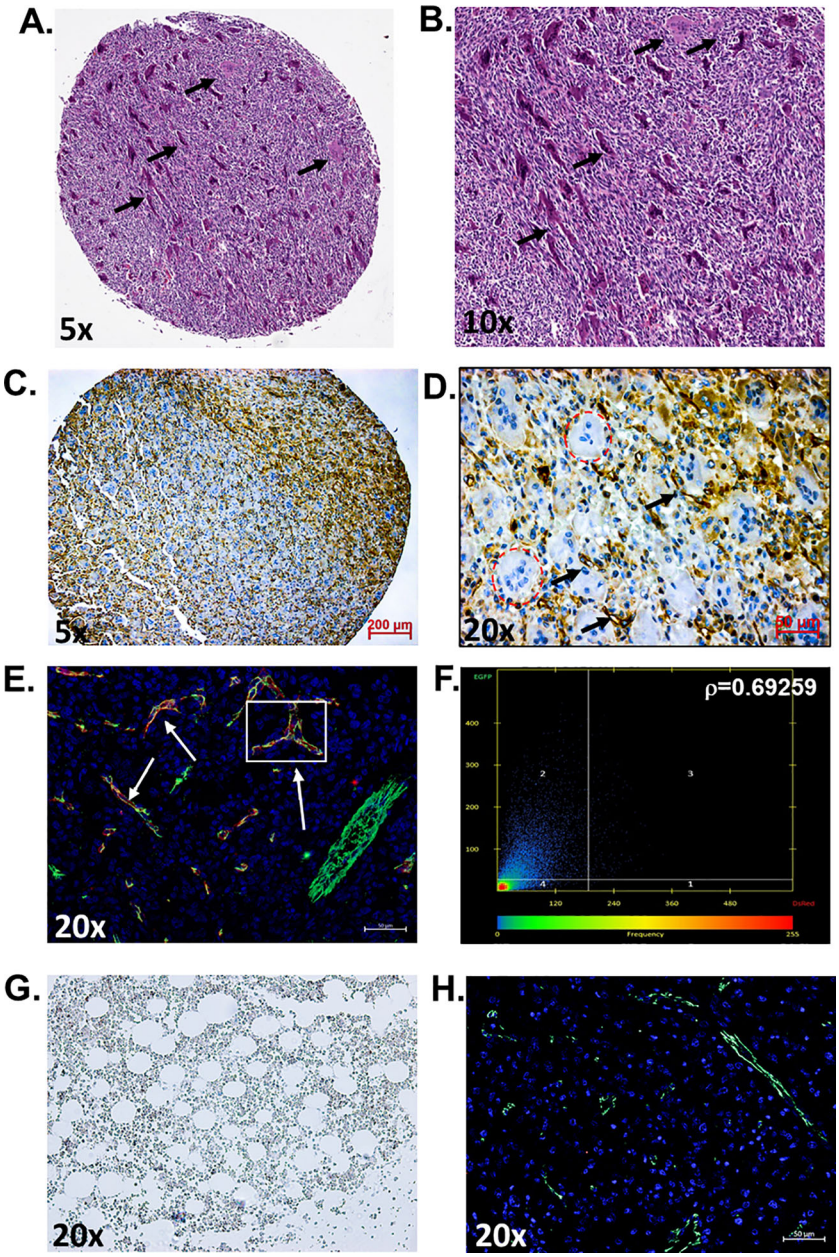

FIGURE 1
PSMA is detected on the vasculature of GCTB. **(A, B)** Representative hematoxylin and eosin staining of an FFPE bone biopsy core from a 20-year-old male with clinically diagnosed GCTB. Arrows point to multinucleated giant cells that are a hallmark of GCTB (black arrows). **(C, D)** IHC of an FFPE bone biopsy from a 20-year-old male with GCTB is positive for PSMA, as visualized by the brown precipitate and black arrows. Multinucleated giant cells counterstained with hematoxylin can be identified within the section (circled in red). **(E)** IF staining of PSMA (red), CD31 (green), and the nucleus (blue, DAPI). White arrows indicate examples of Co-localization. **(F)** Pearson correlation coefficient (r) as measured by Zeiss Zen software. The intensity of a given pixel in the CD31 image is used as the y-coordinate of the scatter plot, and the intensity of the corresponding pixel in the PSMA is the x-coordinate. **(G)** Cancer adjacent normal bone and bone marrow tissue (NAT) of rib containing a layer of adipocytes adjacent to bony trabeculae and red blood cells were used as negative controls and is void of PSMA staining. **(H)** IF staining of NAT negative control for PSMA (red) and CD31 (green), nuccleus (blue, DAPI) (20x, scale bar = 50µM). N=28 GCTB patient bone core samples, N=9 NAT controls. The immunofluorescence and immunohistochemistry images, as well as the co-localization information for all 28 patients and negative controls, can be found in Supplementary Figures 1–3. All tissue in this figure was purchased from MicroArray.Com, and further information about the tissue can be found in Materials and Methods. Hematoxylin and eosin images are from TissueArray.Com.

linear associations, which do not always exist (62). Therefore, to validate our data further and obtain a more accurate measurement of co-localization throughout the entire section, we used FIJI/Image J to calculate the area of PSMA co-2localization as a percentage of the area of CD31 staining using 10% as our cutoff for PSMA positive staining (Table 1; Supplementary Table 1). We found tissue sections with positive PSMA staining in the vasculature, and their corresponding ρ-values aligned with percentages greater than 10%. Two patient samples displayed disagreement between the Pearson coefficient and percent area, highlighting the influence that section

10.3389/fonc.2024.1504514

TABLE 1 Patient biopsy information and GCTB PSMA vasculature staining status.

	Age	Sex	Organ	Site	Pathology Diagnosis	Grade	PSMA Staining	ρ	Percent Area
Female									
1	17	F	Bone	Left femur	GCTB	I	+	0.68695	52.33
2	24	F	Bone	Right humerus	GCTB	I	+	0.64367	44.51
3	32	F	Bone	Inferior left femur	GCTB	I	-	0.17155	2.14
4	33	F	Bone	Right femur	GCTB	I	-	0.27750	2.58
5	36	F	Bone	Right Femur	GCTB	II	+	0.62276	10.11
6	37	F	Bone	Ilium	GCTB	I	+	0.64784	17.91
7	38	F	Bone	Right humerus	GCTB	I	+	0.63026	19.83
8	38	F	Bone	Left wrist	GCTB	I	+	0.73253	50.55
9	40	F	Bone	Distal radius	GCTB	I	-	0.13626	3.95
10	42	F	Bone	Humerus	GCTB	I	-	0.20002	2.35
11	45	F	Bone	Left tibia	GCTB	I	-	0.28878	3.22
12	48	F	Bone	Left femur	GCTB	I	-	0.10619	4.97
Male									
1	20	M	Bone	Right femur inferior	GCTB	I	+	0.69259	15.41
2	20	M	Bone	Left fibula	GCTB	I	-	0.17428	1.37
3	22	M	Bone	Left femur	GCTB	II	+	0.55392	9.23**
4	28	M	Bone	Left femur/clavicle	GCTB	II	+	0.68700	31.19
5	30	M	Bone	Inferior right tibia	GCTB	I	+	0.68068	12.65
6	32	M	Bone	Inferior right femur	GCTB	I	+	0.64174	18.16
7	32	M	Bone	Left tibia superior	GCTB	I	-	0.49351	3.82**
8	32	M	Bone	Bone	GCTB	I	+	0.70681	16.99
9	32	M	Bone	Superior left tibia	GCTB	I	+	0.64874	16.35
10	33	M	Bone	Right humerus	GCTB	I	+	0.67971	58.14
11	33	M	Bone	Right humerus	GCTB (necrosis)	*	+	0.61930	58.39
12	34	M	Bone	Right femur and sacrum	GCTB	II	+	0.67971	56.99
13	34	M	Bone	Right leg	GCTB	II	+	0.62412	12.66
14	47	M	Bone	Left tibia superior	GCTB	I	+	0.65317	14.85
15	50	M	Bone	Right femur inferior	GCTB	I	+	0.65802	25.24
16	75	M	Bone	Left distal radius	GCTB	I	+	0.64481	38.49
Negative Controls									
1	50	F	Bone	Rib	NAT		-	NA	NA
2	50	F	Bone	Rib	NAT		-	NA	NA
3	56	F	Bone	Rib	NAT		-	NA	NA
4	68	F	Bone	Rib	NAT		-	NA	NA
5	68	F	Bone	Rib	NAT		-	NA	NA
6	56	M	Bone	Rib	NAT		-	NA	NA
7	60	M	Bone	Rib	NAT		-	NA	NA

(Continued)

TABLE 1 Continued

	Age	Sex	Organ	Site	Pathology Diagnosis	Grade	PSMA Staining	ρ	Percent Area
Negative Controls									
8	63	M	Bone	Rib	NAT		-	NA	NA
9	66	M	Bone	Rib	NAT		-	NA	NA

Grade as measured by the Campanacci grading system: Grade I: A latent lesion with a well-defined margin and an intact cortex; Grade II: An active lesion with a relatively well-defined margin but no radiopaque rim; Grade III: An aggressive lesion with indistinct borders and cortical destruction (13). *Indicates no grading scale. ρ = Pearson correlation coefficient: Correlations <0.20 as very weak, correlations between 0.20-0.39 as weak, correlations 0.40-0.59 as moderate, correlations 0.60-0.79 as strong, and correlations >0.80 as very strong (62). The percent area co-localization was determined using the color threshold function in ImageJ/Fiji. The area of PSMA co-localization was reported as a percentage of the area of CD31 staining, and the average percentage was reported from serial sections. If >10% PSMA positive (+) staining. **Indicates disagreement between the percent area and r correlation coefficient due to section variability. Cancer adjacent normal bone and bone marrow of rib (NAT) were used as negative controls.
NA, Not Applicable.

variability and vasculature location within the GCTB have on these measurements. Taken together, analysis (visual assessment, Pearson correlation coefficient, and percentage) confirms that PSMA-positive staining is restricted to the vasculature of GCTB. The immunofluorescence and immunohistochemistry images, as well as the co-localization information for all 28 patients and negative controls, can be found in Supplementary Figures 1–3. When patient samples were stratified by biological sex, 87.5% of males were positive for PSMA tumor vasculature staining, compared to 50.0% of female samples (Table 1). While intriguing, additional validation is required to formulate any definitive conclusions.

To illustrate the potential use of PSMA-targeted therapeutics in detecting and treating GCTB, we utilized a PSMA-specific small-molecule fluorescent probe, FAM-C6-1298, as a model. The structure of FAM-C6-1298 is derived from CTT1298 (developed by our lab), which binds *irreversibly* to enzymatically active PSMA and rapidly internalizes into PSMA (+) cells (36, 63). When derivatized, CTT1298 and its congeners possess nanomolar affinity and can deliver a diverse array of payloads (MMAE, SN38, doxorubicin, therapeutic radionuclides, therapeutic enzymes) into the cell (42, 64–74). The specificity and affinity of FAM-C6-1298 are analogous to that of the radiopharmaceuticals Locametz and Pluvictor. Here, we used FAM-C6-1298 as a model PSMA-targeting agent due to its ease in microscopic visualization (Supplementary Figure 4). After binding to extracellular PSMA, CTT1298-based conjugates rapidly traffic to endosomes/lysosomes through the internalization of the PSMA-conjugate complex (42, 45, 69–71, 75). We have previously confirmed that CTT1298 derivatives are internalized 99% in PSMA (+) cells within 4 h (38, 39).

To specifically establish that FAM-C6-1298 was suitable for addressing our experimental question, we confirmed that FAM-C6-1298 could bind to the cell surface PSMA of a PSMA-positive cell line and that the PSMA-bound FAM-C6-1298 could be internalized into the cell through the endosome-lysosome pathway. Using our previously described PSMA CRISPR knockout human prostate cancer C42B cell line (45), we treated C42B-CRISPR-PSMA^{scramble} and C42B-CRISPR-PSMA^{knockout} with 10μM FAM-C6-1298 for 30 min. Fluorescence microscopy indicated that FAM-C6-1298 bound to cell surface PSMA of the C42B-CRISPR-PSMA^{Scramble} cells and not C42B-CRISPR-PSMA^{knockout} (Figures 2A, B). Positive co-localization of FAM-C6-1298 and a PSMA antibody (52.16%) (Figure 2C) was comparable (64.55%) to our previously published PSMA-targeted probe 5FAM-X-FPO-42, which served as the positive control (Figure 2D) (45), further supporting the specificity of current PSMA-targeted imaging probe FAM-C6-1298. Additionally, fluorescence microscopy of C42B-Crispr-PSMA^{Scramble} cells indicated that the PSMA-FAM-C6-1298 complex co-localized with 10.49% of the early endosomal marker, EEA1, and the 55.04% with the lysosomal marker LAMP-1, providing evidence that the PSMA-FAM-C6-1298 complex was internalized into the cell (Figures 2E, F). The results of the percent co-localization measurements can be found in Supplementary Table 2.

To confirm that FAM-C6-1298 bound solely to cell surface PSMA, we first treated both C42B-CRISPR-PSMA^{scramble} and C42B-CRISPR-PSMA^{knockout} with 100μM of a previously published non-fluorescent PSMA-blocking ligand (DBCO-C6-1298) (76). This peptide binds exclusively to and blocks the enzymatic domain of extracellular, membrane-bound PSMA. After a 30-minute incubation with the blocking peptide, we further incubated the cells with 10μM FAM-C6-1298 for an additional 30 min. As predicted, no binding of FAM-C6-1298 was detected by fluorescent microscopy (Figure 2G). Therefore, the PSMA-targeted small-molecule fluorescent analog of Pluvicto and Locametz, FAM-C6-1298, demonstrated specific binding to PSMA, and the PSMA-FAM-C6-1298 complex was internalized and trafficked through the endosomal-lysosomal pathway, indicating its suitability as a therapeutic model for addressing our experimental question.

For proof of the *in vitro* applicability of a PSMA-targeted therapeutic in detecting and targeting GCTB, we commercially obtained fresh frozen tissue samples from patients clinically diagnosed with GCTB from OriGene (patient information in Supplementary Figure 5) and incubated them with either 10μM of our model PSMA-specific small-molecule fluorescent probe (FAM-C6-1298) alone or with 100μM of the PSMA-blocking ligand DBCO-C6-1298, followed by incubation with 10μM FAM-C6-1298. Tissue samples incubated with the combination of the PSMA-blocking peptide and FAM-C6-1298 displayed drastically decreased radiant efficiency ($9.25x10^9$ photons/sec/cm^2/str/μW/cm^2) (Figure 3B), as measured by IVIS compared to those treated with the FAM-C6-1298 alone ($1.66x10^{10}$ photons/sec/cm^2/str/μW/cm^2) (Figure 3A). Data for additional samples can be found in Supplementary Figure 6. Taken together, our data indicate successful targeting specificity and uptake of the model PSMA-targeted agent in GCTB tissue.

10.3389/fonc.2024.1504514

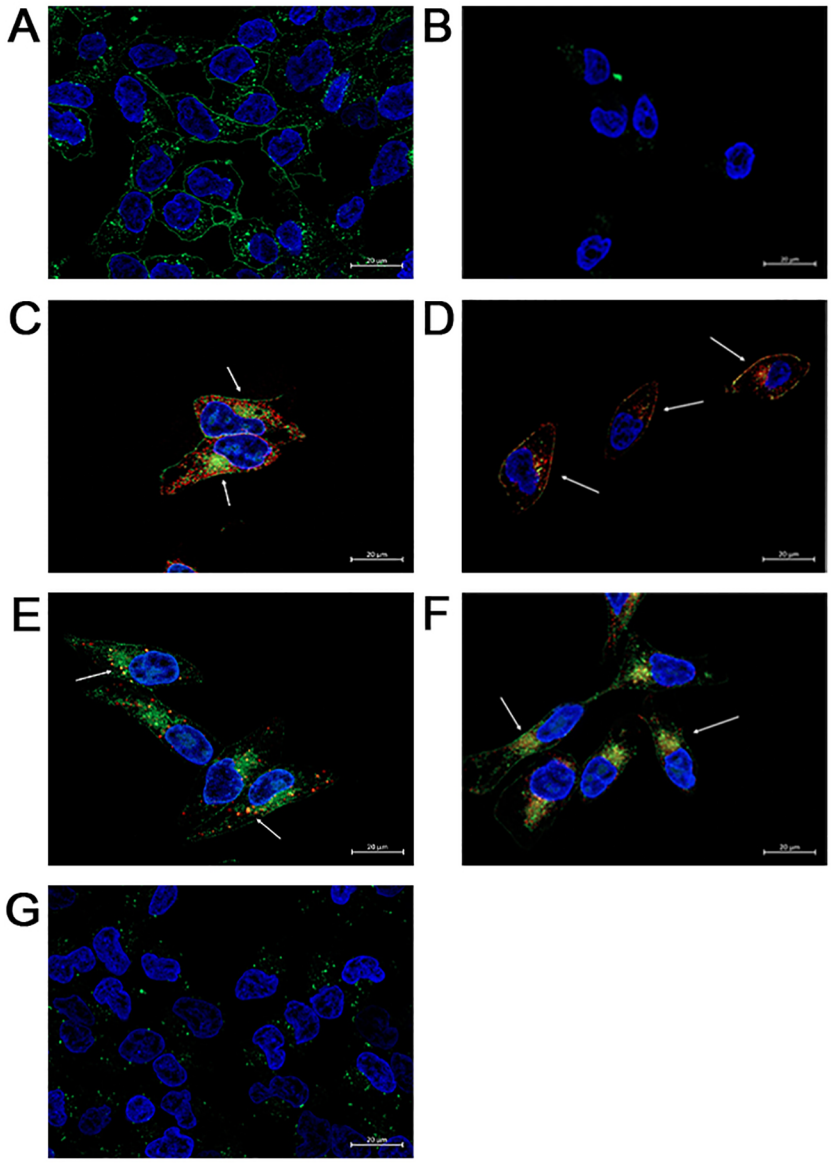

FIGURE 2
FAM-C6-1298 can bind to the cell surface PSMA of C42B cells and be internalized. **(A, B)** C42B-CRISPR-PSMA^{scramble} and C42B-CRISPR-PSMA^{knockout} cells incubated with 10mM FAM-C6-1298 for 30 mn. **(C)** Co-localization of FAM-C6-1298 (green) and PSMA (red) in C42B cells. **(D)** IF staining of positive control PSMA (red) and 5FAM-X-FPO-42 (green). White arrows point to areas of co-localization. **(E)** Co-localization of FAM-C6-1298 (green) and EEA1 (red) in C42B cells **(F)** Co-localization of FAM-C6-1298 (green) and LAMP-1 (red) in C42B cells. **(G)** C42B cells were incubated with 100µM DBCO-C6-1298 PSMA blocking peptide for 30 mn and then 10µM FAM-C6-1298 for 30 mn. 63x oil, scale bar = 20µM. The cell nucleus is stained with DAPI in all images. All experiments were repeated for at least three independent experiments.

Discussion

Drug discovery and development are critical processes in improving human health. The conventional drug development process typically involves several stages, including target identification, compound screening, preclinical studies, clinical trials, and regulatory approval. Unfortunately, this process is often slow, costly, and has high failure rates due to safety or efficacy issues. The average investment for developing a new drug is more than $2.5 billion, and it takes 10-15 years (53, 54) for a new product to be developed, with less than 10% of Phase I candidates receiving FDA approval (55, 56). An alternative strategy known as "drug repurposing" has gained traction to address these challenges and accelerate the discovery of new treatments. Because a drug already has an established safety profile, drug repurposing often skips Phase 1, advancing to Phases 2 and 3 with fewer pharmacokinetic uncertainties, thus significantly reducing the time and costs associated with the drug development process (56, 57). This ultimately results in improved patient outcomes.

Interestingly, in June 2010, denosumab - a treatment for GCTB - was initially approved by the FDA for non-cancer use in postmenopausal women with the risk of osteoporosis under the name Prolia (77), and repurposed in November 2010 as Xgeva for the prevention of skeleton-related events in patients with bone

10.3389/fonc.2024.1504514

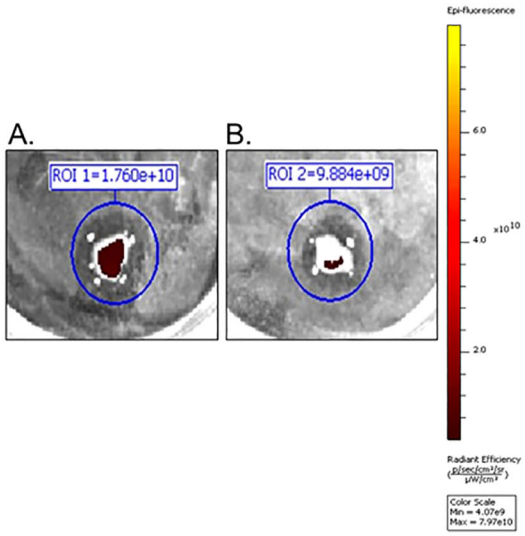

ROI	Total Radiant Efficiency (photon/s/cm²/sr/µW/cm²)	Average Radiant Efficiency (photon/s/cm²/sr/µW/cm²)	Background Corrected Intensity (photon/s/cm²/sr/µW/cm²)
1	1.76 x10^{10}	9.91 x10^{8}	1.66 x10^{10}
2	9.88 x10^{9}	6.25 x10^{8}	9.25 x10^{9}

FIGURE 3
FAM-C6-1298 can successfully target PSMA in GCTB tissue. *Ex vivo* whole-tissue fluorescence measurements of fresh tissue from the tibia of a 23-year-old female with GCTB (OriGene, catalog number CB499383) incubated with **(A)** 10µM PSMA-targeted fluorescent probe, FAM-C6-1298. **(B)** 100µM PSMA blocking peptide DBCO-C6-1298, followed by incubation with 10µM FAM-C6-1298. Data was collected by IVIS as radiant efficiency (photons/sec/cm^2/steradian/µW/cm^2) using Living Image software v4.8.2 and presented as a background-corrected intensity signal in the chart. N=2. Information for sample 2 is in Supplementary Figure 6. All tissue in this figure was purchased from OriGene, and further information about the tissue can be found in Materials and Methods.

metastases from solid tumors, including prostate cancer (78, 79). In the summer of 2011, clinical trials investigated the safety and efficacy of denosumab in giant cell tumors, multiple myeloma with bone metastases, and hypercalcemia of malignancy (24, 26, 80). In June 2013, the FDA expanded the approved use of Xgeva to treat adults and some adolescents with GCTB. While denosumab's efficacy in treating advanced and unresectable tumors is well-established, its role in managing surgically resectable disease is a topic of ongoing debate (22).

GCTB is prone to several factors that can impede successful treatment. Research has indicated that delayed diagnosis and treatment of GCTB are associated with increased tumor size, heightened recurrence rates, and elevated incidences of local complications. Moreover, patients experiencing delayed diagnosis or treatment are more likely to require aggressive interventions such as amputation or chemotherapy (81). In terms of location, sacral GCTB warrants special attention. Despite being one of the commonly affected bones, the treatment for sacral GCTB remains challenging, as sacrificing sacral nerve roots is associated with severe morbidity, such as the disturbance of gait and foot plantar flexion, as well as bowel and bladder dysfunction. Even after successful nerve-sparing surgery, the high recurrence rate (25-35% in most cases and up to 50% in some studies) often demands additional therapy (82, 83). Thus, there is an urgent clinical need to identify and develop novel therapeutic strategies for these patients.

PSMA-targeted radiopharmaceuticals, such as Pluvicto and Locametz, represent a potentially powerful theranostic combination for the detection and selective treatment of PSMA-positive GCTB vasculature. By leveraging the high expression of PSMA in the surrounding tumor vasculature, it is expected that these agents can precisely pinpoint and deliver therapeutic payloads to PSMA-expressing tumor vascular endothelial cells. Therefore, PSMA-targeted treatment in combination with traditional or surgical intervention (where possible) could be highly effective compared to a single therapeutic approach.

Through the use of a PSMA-targeted small-molecule fluorescent analog of Pluvicto and Locametz, we showed that PSMA-targeted agents offer a potential alternative to the detection and treatment of tumor vasculature in GCTB. One limitation of this study is the small sample size of 28 GCTB patients. Consequently, it is imperative to conduct further studies with sufficiently large sample sizes to ensure the replicability and generalizability of our findings. However, we still believe that this finding is timely and of substantial clinical importance, especially given the recent availability of Pluvicto and Locametz and their broader applicability for indications other than prostate cancer. While others are currently working on the identification of biomarkers as potential predictive indicators or druggable targets to improve management of GCTB (84), to date, there have been no reports on the expression of PSMA in the vasculature of GCTB or in any other primary bone cancer, such as osteosarcoma, Ewing sarcoma, chondrosarcoma, or chordoma. Indeed, Heitkötter et al. used immunohistochemistry to show that PSMA was present in Ewing sarcoma tumors. However, they did not convincingly establish that

PSMA co-localized with endothelial cells of the tumor vasculature (85). While Parihar et al. demonstrated that Ga-PSMA-HBED-CC PET/CT described high radiotracer activity in the iliac bone of a single Ewing sarcoma patient (86) and Can et al. reported high radiotracer activity of ^{68}Ga PSMA PET/CT in the primary tumor and metastatic lesions of a 75-year-old man with osteosarcoma of the sternum (87), neither established that PSMA was present on the endothelial cells of the tumor vasculature of these primary bone tumors.

In conclusion, there is potential for repurposing the current commercially available clinical PSMA-targeted agents for the detection and treatment of GCTB, as well as other primary bone tumors, if PSMA expression is found in its vasculature. This proof-of-concept study supports the justification and feasibility for the use of Pluvicto and Locametz in preclinical studies and randomized clinical trials focusing on the repurposing of commercially available PSMA-targeted diagnostic and therapeutic agents for the detection and treatment of GCTB and beyond.

Data availability statement

The raw data supporting the conclusions of this article will be made available by the authors, without undue reservation.

Ethics statement

Ethical approval was not required for the studies on humans in accordance with the local legislation and institutional requirements because only commercially available deidentified patient tissue and established cell lines were used.

Author contributions

BM: Formal analysis, Methodology, Writing – review & editing, Data curation, Validation, Visualization. NM: Data curation, Formal analysis, Visualization, Writing – review & editing. ED: Data curation, Visualization, Writing – review & editing. SA: Writing – review & editing. CB: Writing – review & editing, Conceptualization, Methodology, Supervision. LC: Conceptualization, Methodology, Supervision, Writing – review & editing, Formal analysis, Funding acquisition, Project administration, Resources, Writing – original draft.

Funding

The author(s) declare financial support was received for the research, authorship, and/or publication of this article. This study was supported by NIH/NCI R21CA282396, NIH/NCI R21CA256382, NIH/NIDCR T90DE033006-01.

Acknowledgments

The authors extend their gratitude for technical assistance to the WSU Center for NMR Spectroscopy and Dr. Gerhard Munske (WSU Laboratory of Biotechnology and Bioanalysis).

Conflict of interest

The authors declare that the research was conducted in the absence of any commercial or financial relationships that could be construed as a potential conflict of interest.

Publisher's note

Supplementary material

The Supplementary Material for this article can be found online at: https://www.frontiersin.org/articles/10.3389/fonc.2024.1504514/full#supplementary-material

References

1. Klenke FM, Wenger DE, Inwards CY, Rose PS, Sim FH. Giant cell tumor of bone: risk factors for recurrence. *Clin Orthopaedics Related Research®*. (2011) 469:591–9. doi: 10.1007/s11999-010-1501-7

2. Noh B-J, Park Y-K. Giant cell tumor of bone: updated molecular pathogenesis and tumor biology. *Hum pathology*. (2018) 81:1–8. doi: 10.1016/j.humpath.2018.06.017

3. Gouin F, Rochwerger AR, Di Marco A, Rosset P, Bonnevialle P, Fiorenza F, et al. Adjuvant treatment with zoledronic acid after extensive curettage for giant cell tumours of bone. *Eur J Cancer*. (2014) 50:2425–31. doi: 10.1016/j.ejca.2014.06.003

4. Amelio JM, Rockberg J, Hernandez RK, Sobocki P, Stryker S, Bach BA, et al. Population-based study of giant cell tumor of bone in Sweden (1983–2011). *Cancer Epidemiol*. (2016) 42:82–9. doi: 10.1016/j.canep.2016.03.014

5. WHO Classification of Tumours. *In Soft Tissue and Bone, 5th ed*. (2020) IARC Press: Lyon, France. 3:368.

6. Palmerini E, Picci P, Reichardt P, Downey G. Malignancy in giant cell tumor of bone: a review of the literature. *Technol Cancer Res Treat*. (2019) 18:1533033819840000. doi: 10.1177/1533033819840000

7. Sahito B, Ali SME, Kumar D, Kumar J, Hussain N, Lakho T. Role of denosumab before resection and reconstruction in giant cell tumors of bone: A single-centered retrospective cohort study. *Eur J Orthopaedic Surg Traumatology*. (2022) 32:567–74. doi: 10.1007/s00590-021-03012-1

8. Perrin DL, Visgauss JD, Wilson DA, Griffin AM, Razak ARA, Ferguson PC, et al. The role of denosumab in joint preservation for patients with giant cell tumour of bone. *Bone Joint J*. (2021) 103:184–91. doi: 10.1302/0301-620X.103B1.BJJ-2020-0274.R1

9. Hudson T, Schiebler M, Springfield D, Enneking W, Hawkins I, Spanier S. Radiology of giant cell tumors of bone: computed tomography, arthro-tomography, and scintigraphy. *Skeletal Radiology*. (1984) 11:85–95. doi: 10.1007/BF00348795

10. Aoki J, Watanabe H, Shinozaki T, Takagishi K, Ishijima H, Oya N, et al. FDG PET of primary benign and Malignant bone tumors: standardized uptake value in 52 lesions. *Radiology*. (2001) 219:774–7. doi: 10.1148/radiology.219.3.r01ma08774

11. Park HL, Yoo IR, Lee Y, Park SY, Jung CK. Giant cell tumor of the rib: two cases of F-18 FDG PET/CT findings. *Nucl Med Mol Imaging*. (2017) 51:182–5. doi: 10.1007/s13139-016-0442-9

12. NCBI. ClinicalTrials.gov(2024). Available online at: https://clinicaltrials.gov/ (accessed July 24, 2024).

13. Campanacci M, Baldini N, Boriani S, Sudanese A. Giant-cell tumor of bone. *JBJS*. (1987) 69:106–14. doi: 10.2106/00004623-198769010-00018

14. Errani C, Ruggieri P, Asenzio MAN, Toscano A, Colangeli S, Rimondi E, et al. Giant cell tumor of the extremity: a review of 349 cases from a single institution. *Cancer Treat Rev*. (2010) 36:1–7. doi: 10.1016/j.ctrv.2009.09.002

15. Van der Heijden L, Dijkstra PS, van de Sande MA, Kroep JR, Nout RA, van Rijswijk CS, et al. The clinical approach toward giant cell tumor of bone. *oncologist*. (2014) 19:550–61. doi: 10.1634/theoncologist.2013-0432

16. Knochentumoren A. Local recurrence of giant cell tumor of bone after intralesional treatment with and without adjuvant therapy. *JBJS*. (2008) 90:1060–7. doi: 10.2106/JBJS.D.02771

17. Balke M, Schremper L, Gebert C, Ahrens H, Streitbuerger A, Koehler G, et al. Giant cell tumor of bone: treatment and outcome of 214 cases. *J Cancer Res Clin Oncol*. (2008) 134:969–78. doi: 10.1007/s00432-008-0370-x

18. Lausten G, Jensen P, Schiødt T, Lund B. Local recurrences in giant cell tumour of bone: long-term follow up of 31 cases. *Int Orthopaedics*. (1996) 20:172–6. doi: 10.1007/s002640050057

19. Turcotte RE, Wunder JS, Isler MH, Bell RS, Schachar N, Masri BA, et al. Giant cell tumor of long bone: a Canadian Sarcoma Group study. *Clin Orthopaedics Related Research®*. (2002) 397:248–58. doi: 10.1097/00003086-200204000-00029

20. Ganesan K GA, Roane D. *Bisphosphonate*. Treasure Island, FL: StatPearls Publishing (2023). Available at: https://www.ncbi.nlm.nih.gov/books/NBK470248/.

21. Nagano A, Urakawa H, Tanaka K, Ozaki T. Current management of giant-cell tumor of bone in the denosumab era. *Japanese J Clin Oncol*. (2022) 52:411–6. doi: 10.1093/jjco/hyac018

22. Borkowska AM, Szumera-Cieckiewicz A, Szostakowski B, Pienkowski A, Rutkowski PL. Denosumab in giant cell tumor of bone: multidisciplinary medical management based on pathophysiological mechanisms and real-world evidence. *Cancers (Basel)*. (2022) 14(9):2290. doi: 10.3390/cancers14092290

23. Chawla S, Henshaw R, Seeger L, Choy E, Blay J-Y, Ferrari S, et al. Safety and efficacy of denosumab for adults and skeletally mature adolescents with giant cell tumour of bone: interim analysis of an open-label, parallel-group, phase 2 study. *Lancet Oncol*. (2013) 14:901–8. doi: 10.1016/S1470-2045(13)70277-8

24. Rutkowski P, Ferrari S, Grimer RJ, Stalley PD, Dijkstra SP, Pienkowski A, et al. Surgical downstaging in an open-label phase II trial of denosumab in patients with giant cell tumor of bone. *Ann Surg Oncol*. (2015) 22:2860–8. doi: 10.1245/s10434-015-4634-9

25. Errani C, Tsukamoto S, Leone G, Righi A, Akahane M, Tanaka Y, et al. Denosumab may increase the risk of local recurrence in patients with giant-cell tumor of bone treated with curettage. *JBJS*. (2018) 100:496–504. doi: 10.2106/JBJS.17.00057

26. Traub F, Singh J, Dickson BC, Leung S, Mohankumar R, Blackstein ME, et al. Efficacy of denosumab in joint preservation for patients with giant cell tumour of the bone. *Eur J cancer*. (2016) 59:1–12. doi: 10.1016/j.ejca.2016.01.006

27. Agarwal MG, Gundavda MK, Gupta R, Reddy R. Does denosumab change the giant cell tumor treatment strategy? Lessons learned from early experience. *Clin Orthopaedics Related Research®*. (2018) 476:1773–82. doi: 10.1007/s11999.0000000000000243

28. Chinder PS, Hindiskere S, Doddarangappa S, Pal U. Evaluation of local recurrence in giant-cell tumor of bone treated by neoadjuvant denosumab. *Clinics Orthopedic Surgery*. (2019) 11:352. doi: 10.4055/cios.2019.11.3.352

29. Chen Z, Yang Y, Guo W, Yang R, Tang X, Yan T, et al. Therapeutic benefits of neoadjuvant and post-operative denosumab on sacral giant cell tumor: a retrospective cohort study of 30 cases. *J BU ON*. (2018) 23:453–9.

30. Ghosh A, Heston WD. Tumor target prostate specific membrane antigen (PSMA) and its regulation in prostate cancer. *J Cell Biochem*. (2004) 91:528–39. doi: 10.1002/jcb.10661

31. Murphy GP, Su S, Jarisch J, Kenny GM. Serum levels of PSMA. *Prostate*. (2000) 42:318–9. doi: 10.1002/(SICI)1097-0045(20000301)42:4<318::AID-PROS10>3.0.CO;2-L

32. Bacich DJ, Pinto JT, Tong WP, Heston WD. Cloning, expression, genomic localization, and enzymatic activities of the mouse homolog of prostate-specific membrane antigen/NAALADase/folate hydrolase. *Mamm Genome*. (2001) 12:117–23. doi: 10.1007/s003350010240

33. Rajasekaran AK, Anilkumar G, Christiansen JJ. Is prostate-specific membrane antigen a multifunctional protein? *Am J Physiol Cell Physiol*. (2005) 288:C975–81. doi: 10.1152/ajpcell.00506.2004

34. Liu H, Rajasekaran AK, Moy P, Xia Y, Kim S, Navarro V, et al. Constitutive and antibody-induced internalization of prostate-specific membrane antigen. *Cancer Res*. (1998) 58:4055–60. doi: 10.7150/thno.14744

35. Chatalic KL, Heskamp S, Konijnenberg M, Molkenboer-Kuenen JD, Franssen GM, Clahsen-van Groningen MC, et al. Towards personalized treatment of prostate cancer: PSMA I&T, a promising prostate-specific membrane antigen-targeted theranostic agent. *Theranostics*. (2016) 6:849–61. doi: 10.7150/thno.14744

36. Ganguly T, Dannoon S, Hopkins MR, Murphy S, Cahaya H, Blecha JE, et al. A high-affinity [(18)F]-labeled phosphoramidate peptidomimetic PSMA-targeted inhibitor for PET imaging of prostate cancer. *Nucl Med Biol*. (2015) 42:780–7. doi: 10.1016/j.nucmedbio.2015.06.003

37. Haberkorn U, Eder M, Kopka K, Babich JW, Eisenhut M. New strategies in prostate cancer: prostate-specific membrane antigen (PSMA) ligands for diagnosis and therapy. *Clin Cancer Res*. (2016) 22:9–15. doi: 10.1158/1078-0432.CCR-15-0820

38. Choy CJ, Ling X, Geruntho JJ, Beyer SK, Latoche JD, Langton-Webster B, et al. 177Lu-labeled phosphoramidate-based PSMA inhibitors: the effect of an albumin binder on biodistribution and therapeutic efficacy in prostate tumor-bearing mice. *Theranostics*. (2017) 7:1928–39. doi: 10.7150/thno.18719

39. Ling X, Latoche JD, Choy CJ, Kurland BF, Laymon CM, Wu Y, et al. Preclinical dosimetry, imaging, and targeted radionuclide therapy studies of Lu-177-labeled albumin-binding, PSMA-targeted CTT1403. *Mol Imaging Biology: MIB*. (2019) 22 (2):274–284. doi: 10.1007/s11307-019-01404-8

40. Nedrow-Byers JR, Moore AL, Ganguly T, Hopkins MR, Fulton MD, Benny PD, et al. PSMA-targeted SPECT agents: mode of binding effect on in *vitro* performance. *Prostate*. (2013) 73:355–62.

41. Nedrow-Byers JR, Jabbes M, Jewett C, Ganguly T, He H, Liu T, et al. A phosphoramidate-based prostate-specific membrane antigen-targeted SPECT agent. *Prostate*. (2012) 72:904–12. doi: 10.1002/pros.22575

42. Liu T, Wu LY, Kazak M, Berkman CE. Cell-Surface labeling and internalization by a fluorescent inhibitor of prostate-specific membrane antigen. *Prostate*. (2008) 68:955–64. doi: 10.1002/pros.20753

43. Choy CJ, Geruntho JJ, Davis AL, Berkman CE. Tunable pH-sensitive linker for controlled release. *Bioconjugate Chem*. (2016) 27:824–30. doi: 10.1021/acs.bioconjchem.6b00027

44. Choy CJ, Ley CR, Davis AL, Backer BS, Geruntho JJ, Clowers BH, et al. Second-generation tunable pH-sensitive phosphoramidate-based linkers for controlled release. *Bioconjugate Chem*. (2016) 27:2206–13. doi: 10.1021/acs.bioconjchem.6b00422

45. Olatunji FP, Savoy EA, Panteah M, Mesbahi N, Abbasi A, Talley CM, et al. Prostate-specific membrane antigen-targeted turn-on probe for imaging cargo release in prostate cancer cells. *Bioconjugate Chem*. (2021) 32:2386–96. doi: 10.1021/acs.bioconjchem.1c00435

46. Bostwick DG. The pathology of early prostate cancer. *CA Cancer J Clin*. (1989) 39:376–93. doi: 10.3322/canjclin.39.6.376

47. Hasan J, Byers R, Jayson GC. Intra-tumoural microvessel density in human solid tumours. *Br J cancer*. (2002) 86:1566–77. doi: 10.1038/sj.bjc.6600315

48. Sharma S, Sharma MC, Sarkar C. Morphology of angiogenesis in human cancer: a conceptual overview, histoprognostic perspective and significance of neoangiogenesis. *Histopathology*. (2005) 46:481–9. doi: 10.1111/j.1365-2559.2005.02142.x

49. Lissbrant IF, Stattin P, Damber JE, Bergh A. Vascular density is a predictor of cancer-specific survival in prostatic carcinoma. *Prostate*. (1997) 33:38–45. doi: 10.1002/(SICI)1097-0045(19970915)33:1<38::AID-PROS7>3.0.CO;2-5

50. Chang SS, O'Keefe DS, Bacich DJ, Reuter VE, Heston WD, Gaudin PB. Prostate-specific membrane antigen is produced in tumor-associated neovasculature. *Clin Cancer Res*. (1999) 5:2674–81.

51. Chang SS, Reuter VE, Heston WD, Gaudin PB. Comparison of anti-prostate-specific membrane antigen antibodies and other immunomarkers in metastatic prostate carcinoma. *Urology*. (2001) 57:1179–83. doi: 10.1016/S0090-4295(01)00983-9

52. Grant CL, Caromile LA, Durrani K, Rahman MM, Claffey KP, Fong G-H, et al. Prostate specific membrane antigen (PSMA) regulates angiogenesis independently of VEGF during ocular neovascularization. *PloS One*. (2012) 7:e41285. doi: 10.1371/journal.pone.0041285

53. Paul SM, Mytelka DS, Dunwiddie CT, Persinger CC, Munos BH, Lindborg SR, et al. How to improve R&D productivity: the pharmaceutical industry's grand challenge. *Nat Rev Drug discovery*. (2010) 9:203–14. doi: 10.1038/nrd3078

54. Adams CP, Brantner VV. Estimating the cost of new drug development: is it really $802 million? *Health Affairs*. (2006) 25:420–8. doi: 10.1377/hlthaff.25.2.420

55. Nosengo N. Can you teach old drugs new tricks? *Nature*. (2016) 534:314–6. doi: 10.1038/534314a

56. Smietana K, Siatkowski M, Moller M. Trends in clinical success rates. *Nat Rev Drug Discovery*. (2016) 15:379–80. doi: 10.1038/nrd.2016.85

57. Armando RG, Mengual Gómez DL, Gomez DE. New drugs are not enough –drug repositioning in oncology: An update. *Int J Oncol*. (2020) 56:651–84. doi: 10.3892/ijo.2020.4966

58. Parvathaneni V, Kulkarni NS, Muth A, Gupta V. Drug repurposing: a promising tool to accelerate the drug discovery process. *Drug Discovery Today*. (2019) 24:2076–85. doi: 10.1016/j.drudis.2019.06.014

59. Pritchard JE, O'Mara TA, Glubb DM. Enhancing the promise of drug repositioning through genetics. *Front Pharmacol*. (2017) 8:896. doi: 10.3389/fphar.2017.00896

60. Dhull A, Wei J, Pulukuri AJ, Rani A, Sharma R, Mesbahi N, et al. PSMA-targeted dendrimer as an efficient anticancer drug delivery vehicle for prostate cancer. *Nanoscale*. (2024) 16:5634–52. doi: 10.1039/D3NR06520K

61. Moch H. *Soft tissue and bone tumours WHO classification of tumours/volume 3* Vol. 3. WHO classification of tumours (2020).

62. Papageorgiou SN. On correlation coefficients and their interpretation. *J Orthod*. (2022) 49:359–61. doi: 10.1177/14653125221076142

63. Dannoon S, Ganguly T, Cahaya H, Geruntho JJ, Galliher MS, Beyer SK, et al. Structure-activity relationship of (18)F-labeled phosphoramidate peptidomimetic prostate-specific membrane antigen (PSMA)-targeted inhibitor analogues for PET imaging of prostate cancer. *J Med Chem*. (2016) 59:5684–94. doi: 10.1021/acs.jmedchem.5b01850

64. Lapi SE, Wahnishe H, Pham D, Wu LY, Nedrow-Byers JR, Liu T, et al. Assessment of an 18F-labeled phosphoramidate peptidomimetic as a new prostate-specific membrane antigen-targeted imaging agent for prostate cancer. *J Nucl Med*. (2009) 50:2042–8. doi: 10.2967/jnumed.109.066589

65. Liu T, Jabbes M, Nedrow-Byers JR, Wu LY, Bryan JN, Berkman CE. Detection of prostate-specific membrane antigen on HUVECs in response to breast tumor-conditioned medium. *Int J Oncol*. (2011) 38(5):1349–55. doi: 10.3892/ijo.2011.946

66. Liu T, Nedrow-Byers JR, Hopkins MR, Berkman CE. Spacer length effects on in *vitro* imaging and surface accessibility of fluorescent inhibitors of prostate specific membrane antigen. *Bioorganic Medicinal Chem Letters*. (2011) 21:7013–6. doi: 10.1016/j.bmcl.2011.09.115

67. Liu T, Wu LY, Berkman CE. Prostate-specific membrane antigen-targeted photodynamic therapy induces rapid cytoskeletal disruption. *Cancer letters*. (2010) 296:106–12. doi: 10.1016/j.canlet.2010.04.003

68. Liu T, Wu LY, Choi JK, Berkman CE. *In vitro* targeted photodynamic therapy with a pyropheophorbide–a conjugated inhibitor of prostate-specific membrane antigen. *Prostate*. (2009) 69:585–94. doi: 10.1002/pros.20909

69. Liu T, Wu LY, Choi JK, Berkman CE. Targeted photodynamic therapy for prostate cancer: inducing apoptosis via activation of the caspase-8/-3 cascade pathway. *Int J Oncol*. (2010) 36:777–84. doi: 10.3892/ijo_00000553

70. Liu T, Wu LY, Hopkins MR, Choi JK, Berkman CE. A targeted low molecular weight near-infrared fluorescent probe for prostate cancer. *Bioorganic Medicinal Chem Letters*. (2010) 20:7124–6. doi: 10.1016/j.bmcl.2010.09.057

71. Nedrow-Byers JR, Jabbes M, Jewett C, Ganguly T, He H, Liu T, et al. A phosphoramidate-based prostate-specific membrane antigen-targeted SPECT agent. *Prostate*. (2011) 72:904–12. doi: 10.1002/pros.21493

72. Wu LY, Liu T, Grimm AL, Davis WC, Berkman CE. Flow cytometric detection of prostate tumor cells using chemoaffinity labels. *Prostate*. (2011) 71:52–61. doi: 10.1002/pros.21221

73. Lee J, Chen H, Liu T, Berkman CE, Reilly PT. High resolution time-of-flight mass analysis of the entire range of intact singly-charged proteins. *Analytical Chem*. (2011) 83:9406–12. doi: 10.1021/ac202001z

74. Martin SE, Ganguly T, Munske GR, Fulton MD, Hopkins MR, Berkman CE, et al. Development of inhibitor-directed enzyme prodrug therapy (IDEPT) for prostate cancer. *Bioconjugate Chem*. (2014) 25:1752–60. doi: 10.1021/bc500362n

75. Liu T, Toriyabe Y, Kazak M, Berkman CE. Pseudoirreversible inhibition of prostate-specific membrane antigen by phosphoramidate peptidomimetics. *Biochemistry*. (2008) 47:12658–60. doi: 10.1021/bi801883v

76. Yoon H, Savoy EA, Mesbahi N, Hendricksen AT, March GL, Fulton MD, et al. A PSMA-targeted doxorubicin small-molecule drug conjugate. *Bioorg Med Chem Lett*. (2024) 104:129712. doi: 10.1016/j.bmcl.2024.129712

77. Bone HG, Wagman RB, Brandi ML, Brown JP, Chapurlat R, Cummings SR, et al. 10 years of denosumab treatment in postmenopausal women with osteoporosis: results from the phase 3 randomised FREEDOM trial and open-label extension. *Lancet Diabetes Endocrinology*. (2017) 5:513–23. doi: 10.1016/S2213-8587(17)30138-9

78. Smith MR, Egerdie B, Toriz NH, Feldman R, Tammela TL, Saad F, et al. Denosumab in men receiving androgen-deprivation therapy for prostate cancer. *New Engl J Med*. (2009) 361:745–55. doi: 10.1056/NEJMoa0809003

79. Henry DH, Costa L, Goldwasser F, Hirsh V, Hungria V, Prausova J, et al. Randomized, double-blind study of denosumab versus zoledronic acid in the treatment of bone metastases in patients with advanced cancer (excluding breast and prostate cancer) or multiple myeloma. *J Clin Oncol*. (2011) 29:1125–32. doi: 10.1200/JCO.2010.31.3304

80. Thomas D, Henshaw R, Skubitz K, Chawla S, Staddon A, Blay J-Y, et al. Denosumab in patients with giant-cell tumour of bone: an open-label, phase 2 study. *Lancet Oncol*. (2010) 11:275–80. doi: 10.1016/S1470-2045(10)70010-3

81. Becker RG, Galia CR, Pestilho J, Antunes BP, Baptista AM, Guedes A. Giant cell tumor of bone: a multicenter epidemiological study in Brazil. *Acta Ortop Bras*. (2024) 32:e273066. doi: 10.1590/1413-785220243201e273066

82. Lipplaa A, Kroep JR, van der Heijden L, Jutte PC, Hogendoorn PC, Dijkstra S, et al. Adjuvant zoledronic acid in high-risk giant cell tumor of bone: a multicenter randomized phase II trial. *oncologist*. (2019) 24:889–e421. doi: 10.1634/theoncologist.2019-0280

83. Lau CP, Huang L, Wong KC, Kumta SM. Comparison of the anti-tumor effects of denosumab and zoledronic acid on the neoplastic stromal cells of giant cell tumor of bone. *Connective Tissue Res*. (2013) 54:439–49. doi: 10.3109/03008207.2013.848202

84. De Vita A, Vanni S, Miserocchi G, Fausti V, Pieri F, Spadazzi C, et al. A Rationale for the activity of bone target therapy and tyrosine kinase inhibitor combination in giant cell tumor of bone and desmoplastic fibroma: translational evidences. *Biomedicines*. (2022) 10(2):372. doi: 10.3390/biomedicines10020372

85. Heitkötter B, Trautmann M, Grünewald I, Bögemann M, Rahbar K, Gevensleben H, et al. Expression of PSMA in tumor neovasculature of high grade sarcomas including synovial sarcoma, rhabdomyosarcoma, undifferentiated sarcoma and MPNST. *Oncotarget*. (2017) 8:4268–76. doi: 10.18632/oncotarget.13994

86. Parihar AS, Sood A, Mittal BR, Kumar R, Singh H, Dhatt SS. 68Ga-PSMA-HBED-CC PET/CT and 18F-FDG PET/CT in Ewing sarcoma. *Clin Nucl Med*. (2020) 45:e57–e8. doi: 10.1097/RLU.0000000000002764

87. Can C, Gündoğan C, Kömek H. Is 68Ga-prostate-specific membrane antigen PET/CT superior than 18F-FDG PET/CT for evaluation of metastatic osteosarcoma? *Clin Nucl Med*. (2021) 46:e233–e5. doi: 10.1097/RLU.0000000000003320

frontiers | Frontiers in Oncology

TYPE Review
PUBLISHED 14 January 2025
DOI 10.3389/fonc.2024.1514120

OPEN ACCESS

EDITED BY
Tinghe Yu,
Chongqing Medical University, China

REVIEWED BY
Eswari Dodagatta-Marri,
University of California, San Francisco, United States
Paula Rezende-Teixeira,
University of São Paulo, Brazil

*CORRESPONDENCE
Laura Itzel Quintas-Granados
itzel.quintas@uacm.edu.mx
Gabriela Figueroa-González
gabriela.figueroa@zaragoza.unam.mx

†These authors have contributed equally to this work and share first authorship

RECEIVED 20 October 2024
ACCEPTED 23 December 2024
PUBLISHED 14 January 2025

CITATION
Villegas-Vazquez EY, Marín-Carrasco FP, Reyes-Hernández OD, Báez-González AS, Bustamante-Montes LP, Padilla-Benavides T, Quintas-Granados LI and Figueroa-González G (2025) Revolutionizing ovarian cancer therapy by drug repositioning for accelerated and cost-effective treatments. *Front. Oncol.* 14:1514120. doi: 10.3389/fonc.2024.1514120

Revolutionizing ovarian cancer therapy by drug repositioning for accelerated and cost-effective treatments

Edgar Yebran Villegas-Vazquez[1†], Francisco Pável Marín-Carrasco[1†], Octavio Daniel Reyes-Hernández[1†], Andrea S. Báez-González[2], Lilia Patricia Bustamante-Montes[3], Teresita Padilla-Benavides[2], Laura Itzel Quintas-Granados[4*] and Gabriela Figueroa-González[1*]

[1]Laboratorio de Farmacogenética, UMIEZ, Facultad de Estudios Superiores Zaragoza, Universidad Nacional Autónoma de México, Ciudad de México, Mexico, [2]Department of Molecular Biology and Biochemistry, Wesleyan University, Middletown, CT, United States, [3]Coordinación de Investigación, Centro Universitario siglo XXI, Estado de México, Toluca, Mexico, [4]Colegio de Ciencias y Humanidades, Plantel Cuautepec, Universidad Autónoma de la Ciudad de México, Ciudad de México, Mexico

Drug repositioning, the practice of identifying novel applications for existing drugs beyond their originally intended medical indications, stands as a transformative strategy revolutionizing pharmaceutical productivity. In contrast to conventional drug development approaches, this innovative method has proven to be exceptionally effective. This is particularly relevant for cancer therapy, where the demand for groundbreaking treatments continues to grow. This review focuses on drug repositioning for ovarian cancer treatment, showcasing a comprehensive exploration grounded in thorough *in vitro* experiments across diverse cancer cell lines, which are validated through preclinical *in vivo* models. These insights not only shed light on the efficacy of these drugs but also expand in potential synergies with other pharmaceutical agents, favoring the development of cost-effective treatments for cancer patients.

KEYWORDS

cancer, ovarian cancer, conventional treatment, drug repositioning, cancer hallmarks

Introduction

Drug repositioning, also known as drug repurposing, is a strategy that involves identifying new therapeutic uses for existing drugs beyond their original indications. This approach has gained the attention of the scientific community due to its potential to

expedite the drug development process, reduce costs, and maximize the utility of existing pharmaceutical agents (Figure 1). Drug repositioning possesses multiple advantages, as it presents increased efficiency by shortening the drug development timeline, as existing drugs have already endured various stages of testing for safety and efficacy. It capitalizes on the existing safety, toxicity, and pharmacokinetic data of approved drugs, significantly reducing the time and financial investment compared to *de novo* drug discovery. This approach has been especially valuable in addressing unmet medical needs, such as rare diseases and conditions lacking effective treatments. Thus, repurposing of drugs often results in a more cost-effective process than developing entirely new compounds, as it bypasses the extensive research and development phases, as repositioned drugs usually have established safety profiles, minimizing the risks associated with introducing entirely new substances. In fact, in recent years, the introduction of new drugs to the market has seen a decline owing to the adverse outcomes witnessed in medical trials and challenges in pharmacokinetics (1). However, significant progress in computational sciences, including bioinformatics, machine learning and computational chemistry, coupled with advancements in -omics sciences and high-throughput screening technologies, has enabled the exploration of drugs with multiple target molecules. These have broadened their potential applications and pharmacological benefits (2).

Drug repurposing has multiple applications in cancer treatment. For instance, repositioned drugs offer the opportunity to target specific pathways or mechanisms relevant to cancer, potentially introducing alternative treatment options. In addition, this strategy allows the identification of synergies between repositioned drugs and existing cancer treatments, which can lead to the development of more effective combination therapies. However, there are limitations associated with drug repurposing, such as patent protection for the original application of the drugs, which may pose challenges for repositioning efforts. Ultimately, administration of repurposed drugs in patients may also require adjustments and further investigation of the pharmacological conditions through *in vitro, in vivo* and clinical studies. Thus, designing appropriate clinical trials for repositioned drugs requires careful consideration of the new therapeutic context and side effects, as well as dosing regimens and possible coadjuvant treatments must also be considered when treating patients. Despite these limitations, since the safety and pharmacokinetic parameters of many drugs are well known, the increasing interest in drug repositioning is helping to determine new favorable outcomes of these drugs. Emerging approaches, such as molecular docking studies and other computer-aided methods, are helping to model novel ligand-targeting strategies and to help drug repositioning take a better landscape in cancer therapy and unlocking the potential of already existed drugs.

In addition, combination therapies that integrate repurposed drugs with existing pharmaceutical agents hold significant promise for enhancing treatment efficacy in cancer and other malignancies. These synergies can target multiple pathways simultaneously, overcoming limitations such as drug resistance and heterogeneity within tumors, as discussed in specific cases below. However, the complexity of drug-drug interactions in combination therapies poses challenges. In this regard, additional limitations of drug repurposing combined with existing therapies include variations in pharmacokinetics, off-target effects, and potential antagonistic interactions. Moreover, the tumor microenvironment, patient-

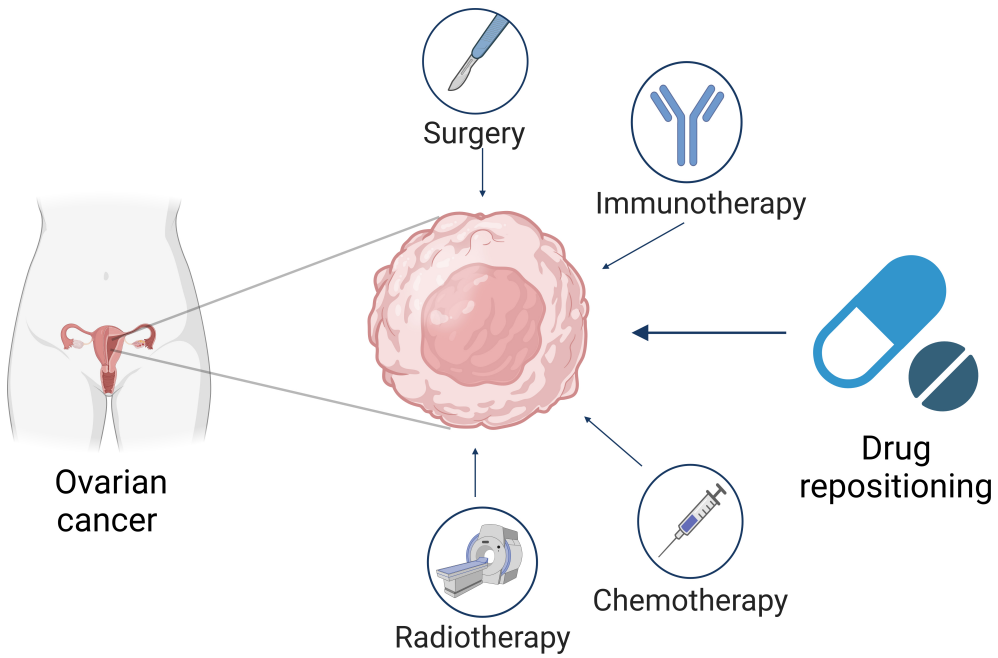

FIGURE 1
Schematic representation of ovarian cancer treatments. This diagram illustrates the general approach to ovarian cancer therapy. Outline the importance of drug repositioning besides surgery, immunotherapy, chemotherapy, and radiotherapy (Figure created with Biorender).

specific genetic factors, and dosage optimization add further layers of complexity. Thus, in order to utilize this strategy in the clinic, it is essential to perform rigorous preclinical and clinical studies, to avoid adverse effects in patients.

This review offers a comprehensive analysis of drug repositioning in ovarian cancer (OC) therapy, synthesizing findings from *in vitro* and preclinical models while also acknowledging the limited data from clinical studies. Despite inherent limitations, the contributions of these models are invaluable for advancing our understanding of potential treatments. *In vitro* studies, particularly with cancer cell lines, continue to be essential tools in screening and identifying promising drug candidates. Although these models cannot fully mimic the complexities of human tumors, they provide controlled environments that allow for detailed investigation of drug effects on cancer cell biology, offering critical insights into drug responses, mechanisms of action, and preliminary efficacy (3–5). These findings can then be validated through more sophisticated *in vivo* models. Preclinical mouse models, for example, provide vital data on the pharmacokinetics, pharmacodynamics, and toxicity of repositioned drugs. These models allow for a comprehensive evaluation of drug responses within the context of tumor microenvironments, immune responses, and metabolism, even though they do not perfectly replicate human disease (6–8). Preclinical models thus serve as an important bridge between *in vitro* assays and clinical applications, often informing the design of clinical trials. Clinical translation remains a significant challenge, but the few studies conducted on repurposed drugs for OC in patients have demonstrated encouraging results. These trials, although limited in scale, provide critical insights into the pharmacokinetic properties, dosing regimens, and side effect profiles of repositioned drugs, underscoring the importance of further research to confirm their clinical efficacy. However, the current focus on short-term experimental models limits our understanding of the long-term therapeutic benefits and safety of these drugs. Longitudinal clinical studies are crucial to fully evaluate their sustained effectiveness and potential side effects, paving the way for the future of OC therapy.

Ovarian cancer

Epithelial ovarian cancer is the rapid growth of cells with abnormal function and structure with the potential to invade and destroy other healthy tissues (9). Among gynecological cancers, OC has a superior mortality rate because of its difficult early diagnosis resulting widely metastatic within the abdomen (10), placing OC as the 3rd most common gynecological cancer around the world in 2020 (11). Low- and middle-income countries presented the highest mortality rates of OC but its incidence was highest in high-income countries (12).

The nomenclature for OC subclassification includes five main histological types: high-grade serous (HGSOC), low-grade serous (LGSOC), endometrioid (ENOC), clear cell (CCOC), and mucinous (MOC) (13–15). HGSOC tumors are solid masses of cells characterized by slit-like fenestrations and structured with papillary, glandular or cribriform architecture (16). LGSOC tumors are distinguished by a monotonous proliferation of cuboidal, low columnar cells, mild to moderate atypia without nuclear pleomorphism, a mitotic index reaching up to 12 mitoses per 10 high-power fields (HPF) and invasion (17–19). Histopathological distinction of ENOC tumors from HGSOC is challenging, but the use of some discriminatory immunohistochemistry tools such as Wilms' tumor 1 (WT1) lead to better tumor classification. ENOC tumors generally lack WT1 expression, whereas HGSOC tumors overwhelmingly exhibit WT1 positivity. In addition, ENOC is positive for the estrogen receptor (ER) in ≥75% of cases and for the progesterone receptor (PR) in over 60% of cases, with the majority (80%) of patients being also positive for wild-type Tumor Protein p53 (*TP53*) (20–23). Immunohistochemical markers, including WT1, Napsin A, hepatocyte nuclear factor-1-beta (HNF-1β), ER, and PR, are employed to distinguish CCOC from HGSOC and ENOC tumors. CCOC tumors are WT1 negative, Napsin A/HNF-1β positive, and EP/PR negative (22–24). MOC tumors are large, unilateral mucinous growths that negative for the WT1 and Napsin A markers, and approximately 60% of cases express a mutant version of p53 (23, 25).

Ovarian tumors are histopathologically heterogeneous, resulting genetic mutations specific for each epithelial OC subtype, which can be used as targets of treatment (10). For instance, near-ubiquitous mutations of p53, Breast Cancer Gene 1/2 (*BRCA1/2*), Neurofibromin 1 (*NF1*), and Cyclin-Dependent Kinase 12 (*CDK12*) are characteristic of HGSOC subtype (10, 26). LGSOC subtype is characterized by mutations in Kirsten Rat Sarcoma Viral Oncogene Homolog (*KRAS*), B-Raf Proto-Oncogene, Serine/Threonine Kinase (*BRAF*), Neuroblastoma RAS Viral Oncogene Homolog (*NRAS*), and Erb-B2 Receptor Tyrosine Kinase 2 (*ERBB2*, also known as HER2) mutations, while Phosphatidylinositol-4,5-Bisphosphate 3-Kinase Catalytic Subunit α (PI3KCA), Phosphatase and Tensin Homolog (*PTEN*), AT-Rich Interaction Domain 1A (*ARID1A*), and Protein Phosphatase 2 Scaffold Subunit α (*PPP2R1A*) mutations are present in ENOC subtypes. Moreover, mutations in *PI3KCA*, *ARID1A*, Catenin β1 (*CTNNB1*), *PTEN*, and *PP2R1A* are also found in the CCOC subtype. Finally, the MOC subtype is characterized by *KRAS* and *ERBB2* mutations (10). Changes in DNA methylation patterns also contribute to the development of OC, being the hypermethylation of the *BRCA* promoter a common example detected in 15-30% of patients (27–30). Figure 2 shows the recorded percentage of cases where mutations on the genes outlined here, as reported by the Integrated Genomic Analyses of Ovarian Carcinoma (Figure 2A) and the Comprehensive and Integrated Genomic Characterization of Adult Soft Tissue Sarcomas (Figure 2B) from The Cancer Genome Atlas (TGCA) Human Cancer Models Initiative (HCMI) Cancer Model Development Center (Figure 2C). This information highlights the relevance of the presence of the mutations described above in the development of OC.

Ovarian cancer staging is determined by the severity of the disease, considering factors such as tumor size, spread to nearby tissues, and the presence of distant metastasis (Figure 3). The International Federation of Gynecology and Obstetrics (FIGO)

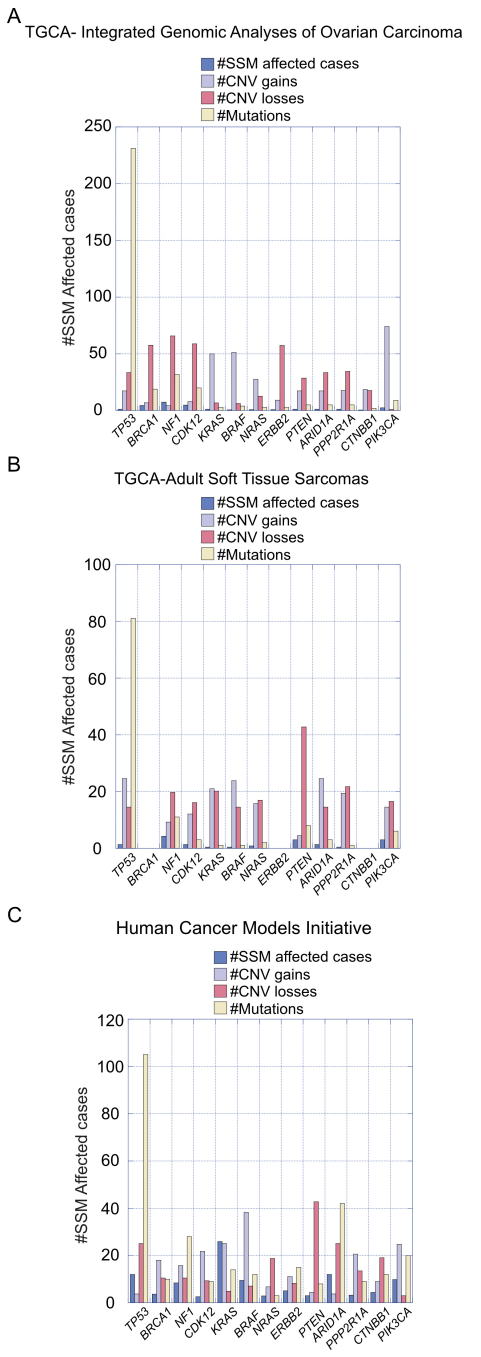

FIGURE 2
Recorded percentage of cases with mutations in specified genes relevant to ovarian carcinoma development. **(A)** Data presented are from the Integrated Genomic Analyses of Ovarian Carcinoma and **(B)** from the Comprehensive and Integrated Genomic Characterization of Adult Soft Tissue Sarcomas, sourced from The Cancer Genome Atlas (TCGA). **(C)** Information on relevant genes was obtained from the Human Cancer Models Initiative (HCMI) Cancer Model Development Center.

system is commonly used for ovarian cancer staging. Stage I is when cancer is confined to one or both ovaries, being sub-stage IA limited to one ovary, no tumor on the external surface; no ascites (fluid in the peritoneal cavity) present containing malignant cells, and substage IB when both ovaries are affected but no tumor is found on the external surfaces; no ascites containing malignant cells. Stage II is when cancerous tissue is found in one or both ovaries with pelvic extension. Substage IIA includes an extension to the uterus and/or fallopian tubes with no evident tumor on the external surfaces and neither ascites containing malignant cells. Substage IIB is when malignant tissue is extended to other pelvic tissues, but no tumor is found on the external surfaces and there are still no ascites containing malignant cells. Stage III OC involves one or both ovaries, the tumor may be spread to the peritoneum outside the pelvis and/or metastasis to the retroperitoneal lymph nodes and/or the omentum. Patients in stage III can be further classified in three substages according to the severity of metastasis. For instance, substage IIIA is determined by microscopic peritoneal metastasis beyond the pelvis; substage IIIB involves macroscopic peritoneal metastasis beyond the pelvis less than 2 cm in size; and substage IIIC includes abdominal metastasis greater than 2 cm in size and/or positive retroperitoneal lymph nodes. Finally, stage IV is diagnosed once malignant cancer cells have spread to distant organs or tissues, being predominant in the pleural fluid (substage IVA) and in the parenchyma of the liver and other distant organs (Substage IVB) (31–33).

Etiology of ovarian cancer

Ovarian cancer is a complex disease with multifactorial etiology, and its development involves a combination of genetic, hormonal, and environmental factors. Risk increases with age and genetic factors such as *BRCA* mutations (34, 35). Mutations in essential genes for DNA repair, such as MutL Homolog 1 (*MLH1*) and MutS Homolog 2 (*MSH2*), which are also predominant in Lynch syndrome patients, also increase the risk of ovarian cancer (36). Having descendants at an early or advanced age, nulliparity, and absence of full-term pregnancy are classic risk factors of OC (37). Long-term use of estrogen-only hormone replacement therapy, without progesterone, has also been linked to an increased risk of OC (38). Recently, an increase between 7 and 28% of OC incidence in women ranging from 15-40 years of age has been detected, likely due to the "normalization" of unhealthy lifestyles such as overweight and obesity (12). In addition, social determinants included the human development index and highest gross domestic product per capita and lifestyle characteristics such as physical inactivity, alcohol use, and prevalence of smoking (39). Some studies have suggested a potential link between the use of talcum powder in the genital area and an increased risk of OC as well (40). Pre-existing conditions such as lipid disorders, hypertension, diabetes, estrogen exposure, and metabolic syndrome are also associated with high OC incidence rates (12, 41–46). Evidence has also pointed to immune responses as potential contributors to OC, such as general dysregulation of the immune system and impaired immune surveillance (47), as well as chronic inflammation in the pelvic region (48).

OC incidence varies by race and ethnicity, with differences observed in the rates of diagnosis and outcomes, which in many instances correlate with the socioeconomic background. White females are the largest population affected, with 14.1 cases per

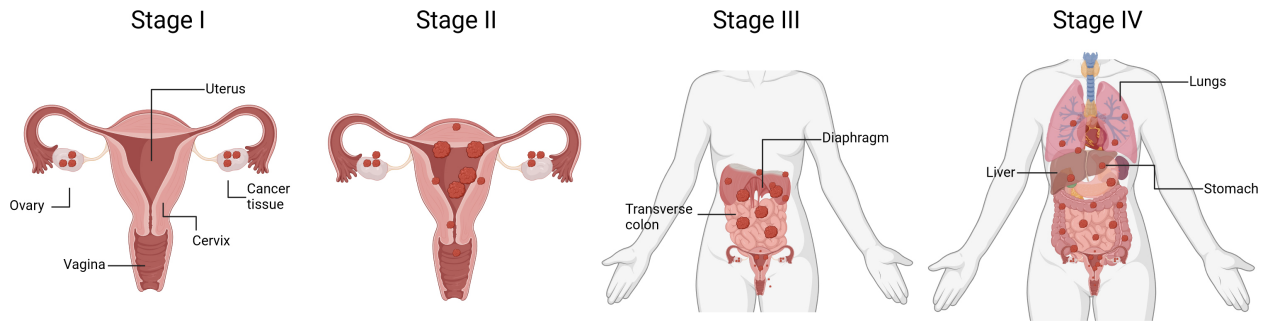

FIGURE 3
Schematic representation of ovarian cancer progression. The diagram outlines the four stages of OC, ranging from Stage I to Stage IV. Stage I signifies cancer that is confined to one or both ovaries. Stage II indicates cancer that has spread beyond the ovaries but is still within the pelvis. Stage III represents cancer that has advanced beyond the pelvis and has spread to the abdominal lining or nearby lymph nodes. Stage IV denotes cancer that has metastasized to distant organs beyond the abdominal cavity, such as the liver or lungs. Understanding the stage of OC is crucial for determining treatment options and predicting prognosis. (Figure created with Biorender).

100,000 women. Then the next highest ethnicity incidence is in (Hispanic females, with a rate of 9.8 affected women per 100,000 individuals. This is followed by Asian/Pacific Islanders, African Americans, and American Indian/Alaska natives, whose incident rates are 9.0, 8.5, and 7.9 patients, respectively, per 100,000 women (49–51). Mortality rates are also dependent on different racial and ethnic groups. African American women often experience lower survival rates compared to non-Hispanic white women. This is largely due to limited access to healthcare and socioeconomic factors, which contribute to these important health disparities. The age at diagnosis and access to screening are also a relevant concern for appropriate treatment and survival, as the age at which OC is diagnosed may also vary by race and ethnicity. Some studies suggest that African American women may be diagnosed at a younger age compared to non-Hispanic white women (52–54).

Prognosis of ovarian cancer

Different histological subtypes of OC may have distinct prognoses. For example, HGSOC, the most common subtype, tends to be more aggressive. Overall, poor prognosis of OC is associated with the age and stage of disease at diagnosis (10, 55). Younger patients, particularly those diagnosed at premenopausal ages, may have a more favorable prognosis.; and the patient's overall health and ability to tolerate treatment can also influence prognosis. In terms of disease stage, for stages I, II, III and IV, the 5-year relative survival rate after diagnosis is estimated at 89%, 70%, 36% and 17%, respectively; while the 10-year-relative survival rate was 84%, 59%, 23% and 8%, for those stages. In general, the overall relative survival rate at 2, 5 and 10 years after diagnosis was 65%, 44% and 36%, respectively (56). Thus, survival rate in women diagnosed at stage I in 5-year is 90% (55, 57). The five-year survival rate is about 80% in patients with disseminated disease to adjacent tissues. In metastatic patients the survival rate is 25% (55, 57). Unfortunately, the 5-year survival rate is less than 50% in patients diagnosed at an advanced OC stage (58–60). In 12-24 months, most patients relapse and die from progressive chemotherapy-resistant tumors (61).

Current therapies for OC treatment

The first-line treatments for OC are surgery, radiotherapy, and chemotherapy. Surgery is performed to remove the tumor tissue in its entirety. Surgery is also useful for histopathological diagnosis and staging of the tumor, according to the International FIGO (10). Surgical procedures include bilateral salpingo-oophorectomy, tumor debulking, total hysterectomy, and omentectomy (62). In addition, different trials used preoperative chemotherapy when interval debulking surgery is performed. Trials reported a reduction in postoperative morbidity (63, 64). Therefore, no difference in survival was observed when a second surgical procedure to complete tumor debulking (10).

For treatment of early-stage OC, cytotoxic chemotherapy improves survival (8%) (63, 64). Treatments with platinum (carboplatin or cisplatin) have been used as the first-line treatment (10). Cisplatin is a platinum-containing chemotherapy drug that is commonly used in the treatment of OC as it binds covalently to DNA in cancer cells, blocking replication and transcription (65, 66). Regimens with two cytotoxic agents improve survival, thus the standard treatment for OC is a combinatory therapy of paclitaxel or docetaxel with platinum-containing drugs (67–69). Rucaparib olaparib, niraparib, and talazoparib are poly(ADP-ribose) polymerase inhibitors (PARPi) that have been accepted by the FDA as chemotherapeutic drugs for OC treatment (70). However, platinum-containing drugs, paclitaxel, olaparib, niraparib, and bevacizumab, cause drug resistance in some OC patients (70).

Novel treatments for OC management employed several strategies (71) that include *i*) target morphomolecular OC types by using PARPi for HGSOC subtype, or the use of inhibitors of the Mitogen-activated protein kinase kinase (MEK) or aromatase inhibitors for LGSOC subtype (72, 73). *ii*) new clinical trial designs, such as umbrella and baskets studies (74, 75). *iii*) new inhibitors (ATRi) against the Ataxia telangiectasia and Rad-3 related kinase (ATR), such as prexasertib, adavosertib (76–82). *iv*) synergistic therapies combining drugs targeting both the tumor and its microenvironment, such as antiangiogenic compounds (e.g., bevacizumab, cediranib),

immunotherapy, and chemotherapy (83–89). *v*) enhanced therapeutic delivery using antibody-directed conjugates or targeted radiotherapy (90–94). Among these, ATR serves as a promising target in cancer due to its role in signaling DNA lesions, replication stress, and regulating the S and G2/M checkpoints, offering potential for exploiting dysregulated DNA damage responses (95). Drugs that interfere with DNA repair, such as PARP inhibitors (Olaparib), are used particularly in patients with BRCA mutations (96).

Novel strategies to overcome drug resistance challenges against OC include the use of monoclonal antibodies. Specifically, the humanized IgG1 monoclonal antibody bevacizumab is directed against Vascular Endothelial Growth Factor (VEGF), and it is currently used for OC therapy (97). Immunotherapy is also an emerging strategy to overcome drug resistance. In this case, immune checkpoint inhibitors, such as pembrolizumab, are being investigated in clinical trials to boost the immune system to target cancer cells (98).

Treating OC presents significant challenges, including late diagnosis, chemoresistance, and the limited efficacy of available therapies. Thus, there is still a need to consider and develop alternative mechanisms to combat OC progression. In this regard, drug repositioning represents an excellent alternative therapy for patients who have developed drug resistance, which may result in failure to prevent recurrence, particularly in advanced stages. Moreover, the tumor microenvironment and genetic heterogeneity of OC further complicate treatment development. Drug repurposing offers a promising avenue to address these challenges by leveraging existing drugs with known safety profiles for new therapeutic uses. In consequence, these emerging approaches can expedite treatment availability and reduce development costs while exploring combinatorial strategies for enhanced efficacy. Drug repurposing studies hold promise as a bridge to personalized medicine, improving outcomes for OC patients.

Drug repositioning for OC treatment

Amid the evolving landscape of OC treatment, the exploration of innovative therapeutic strategies becomes imperative. Drug repositioning, a promising approach, involves repurposing existing drugs to uncover novel and effective treatments for this disease. As indicated above, this strategy harnesses the potential of compounds already approved for other indications, accelerating the development of cost-effective and targeted therapeutic options. In this review, we provide insights into drug repositioning specifically for OC, exploring its challenges, successes, and transformative therapeutic impact. Main highlights and structure of the compounds presented here are summarized in Table 1 and Figure 4.

Among relevant chemical compounds being repurposed towards treatment of OC, statins are medications commonly prescribed to lower cholesterol levels in the blood. Statins inhibit an enzyme involved in the production of cholesterol in the liver. By reducing cholesterol levels, statins help lower the risk of cardiovascular events such as heart attacks and strokes. Strategies to inhibit the mevalonate pathway have also been applied to dyslipidemic diseases. Statins reduce the hydroxymethylglutaryl coenzyme A (HMG-CoA) reductase activity, which is enzymatically essential in the upstream part of the mevalonate pathway, resulting in a reduction in cholesterol levels in blood (99). Thus, considering the mechanism of action of statins related to mevalonate pathway inhibition, they are used to treat hypercholesterolemia (100). However, recent findings suggested that these molecules have antitumoral activities by causing apoptosis in tumor cells (101). For instance, atorvastatin (ATO) inhibits cell proliferation and invasion, while decreasing cell adhesion of cultured OC cells. Besides, ATO induces cellular stress, autophagy, apoptosis, and arrest cell cycle at G1 phase through Akt/mTOR pathway inhibition and MAPK pathway activation (102, 103). ATO also decreased the expression of *VEGF*, matrix-metalloproteinase-9 (*MMP9*), and the proto-oncogene cellular myelocytomatosis (*c-Myc*) in Hey and SKOV3 cultured OC cellular models (102). Experiments using the JQ1 selective inhibitor of bromodomain-containing proteins in Hey and SKOV3 OC cells also increased their sensitivity to the anti-proliferative activity of ATO (102). Another statin example that can be repurposed towards OC treatment is Lovastatin. This is another HMG-CoA reductase inhibitor that has been effective in reducing the proliferation of OC Hey and SKOV3 cells *in vitro* and *in vivo* murine models. Lovastatin delays tumorigenesis, proliferation, and cell cycle progression and suppresses tumor growth by influencing the cholesterol biosynthetic pathway (104, 105). Simvastatin, another HMG-CoA reductase inhibitor, reduces the production of cholesterol in the liver, thus lowering the levels of total cholesterol and low-density lipoprotein (LDL) cholesterol in the bloodstream. Simvastatin reduces the risk of cardiovascular events and has been shown to possess anti-metastatic and anti-tumorigenic effects in OC treatment. For instance, ID8, 28-2, and 30-2 cells treated with simvastatin had increased expression of apoptotic markers starting at 10 μM in 28-2 and 30-2 cells, and 50 μM for ID8 cell lines, suggesting that simvastatin induced cell death and decreased cell viability. Simvastatin was further shown to inhibit OC cell proliferation in a dose-dependent manner as measured by 3-[4,5-dimethylthiazol-2-yl]-2,5 diphenyl tetrazolium bromide (MTT) assay in Hey and SKOV3 OC cells (106, 107). Other inhibitors of mevalonate pathway have been shown to promote autophagic responses. Examples of this are 6-fluoromevalonate, YM-53601, lonafarnib, and GGTI-298. These compounds can induce the expression of autophagy biomarkers such as LC3A (human microtubule-associated protein 1 light chain 3 gene LC3A and LC3B (human microtubule-associated protein 1 light chain 3 gene LC3B) and inhibit cell proliferation in a dose-dependent manner (108). Specifically, Lonafarnib inhibits the enzyme farnesyltransferase, which plays an important role in post-translational modification of proteins. Its primary function is to add a farnesyl group to specific proteins, in a process known as farnesylation.

Lonafarnib also inhibits protein prenylation in the mevalonate pathway, inhibiting cell proliferation with higher efficiency than 6-fluoromevalonate and YM-53601 (108). Besides, lonafarnib induces the expression of *LC3A* and *LC3B* genes, suggesting that the activation of autophagy impairs cell proliferation (108).

Bisphosphonates, such as alendronate, are anti-osteoporotic drugs that also inhibit the mevalonate pathway. Bisphosphonates delayed tumor formation and decreased tumor cell proliferation in

TABLE 1 Drug repositioned for ovarian cancer treatment.

Drug	Original target	*In vivo/in vitro* study model	Mechanism of action or target molecule in OC treatment	Relevant hallmark involved	Concentration/ Dosage	Ref
Atorvastatin	Cardiovascular diseases prevention	*In vitro* cell lines Hey and SKOV3	Inhibit the biosynthesis of the cholesterol enzyme mevalonate, inhibiting difosfatfarnesyl and diphosphategeranylgeranyl	Induction of apoptosis	1 µM, 50 µM, 150 µM	(102)
Lovastatin	Cholesterol treatment	*In vivo* cell lines SKOV-3, OVCAR-5 xenograft in mice	Synthesis disruption of acetyl Co-A in the endoplasmic reticulum	Growth suppression and apoptosis	12.5 mg/kg	(104)
Lonafarnib	Progeria treatment	*In vitro* cell lines SKOV-3, OVCAR-5	Inhibit the biosynthesis of the lipids of the RAS protein in the farnesyl chain for the structuring of the cell membrane	Induction of apoptosis	From 10 nM to10 µM	(108)
Alendronate	Osteoporosis treatment	*In vivo* xenograft cells SKOV3, OVCAR5 in mice models mogp-Tag	Inhibit cholesterol biosynthesis by blocking farnesyl pyrophosphate synthase	Induction of apoptosis	15 mg/kg	(108)
Zoledronic acid	Osteoporosis treatment	*In vitro* cell lines OVCAR-3 and MDAH-2774	Inhibit cholesterol biosynthesis by blocking farnesyl pyrophosphate synthase	Induction of apoptosis	5 µM	(115)
		In vitro extracted samples of ovarian tissue from human patients	Inhibit cholesterol biosynthesis by blocking farnesyl pyrophosphate synthase	Induction of apoptosis	From 2.2 to 69 µM	(117)
Azithromycin	Antibiotic	*In vitro* cell lines SKOV3, Tov21G, ES2	Inhibits protein synthesis by binding to the 30s ribosome subunit and inhibiting peptide translocation.	Deregulating cellular energetics, suppressing proliferation and induction of apoptosis	250 µM	(119)
Doxycycline	Antibiotic	*In vitro* cell lines Tov21G, ES2	Inhibits protein synthesis by binding to the 30S ribosomal subunit	Deregulating cellular energetics, suppressing proliferation and induction of apoptosis	50 µM	(119)
Glycylcyclines	Antibiotic	*In vitro* ovarian cancer cell lines SKOV3, Tov21G, ES2	Inhibits protein synthesis by binding to the 28s ribosome subunit and inhibiting peptide translocation.	Induction of apoptosis	From 10 nM to10 µM	(119)
Tetracycline	Antibiotic	*In vitro* ovarian cancer cell lines SKOV3, Tov21G, ES2	Binding to the subunit 28S small mitoribosome then inhibiting mitochondrial anabolism	Deregulating cellular energetics, suppressing proliferation and induction of apoptosis	From 1 µM to 250 µM	(119)
Pyrvinium pamoate	Anthelmintic	*In vitro* cell lines SKOV3, Tov21G, ES2	Suppression of the mitochondrial activity complex and dysregulation of STAT transcription over the Mito OXPHOS	Deregulating cellular energetics, suppressing proliferation and induction of apoptosis	250 nM, 500 nM	(119)
Tigecycline	Antibiotic	*In vitro* cell lines SKOV3, Tov21G, ES2	It inhibits protein transduction by binding to the 30S ribosomal subunit and blocking the entry of aminoacyl tRNA (transfer	Deregulating cellular energetics, suppressing proliferation	50 µM	(119)

(Continued)

TABLE 1 Continued

Drug	Original target	*In vivo/in vitro* study model	Mechanism of action or target molecule in OC treatment	Relevant hallmark involved	Concentration/ Dosage	Ref
			RNA) molecules into the ribosomal site	and induction of apoptosis		
Monensin	Antibiotic	*In vitro* cell lines SK-OV-3, A2780, OVCAR3, CAOV-3	Decrease in phosphorylated ERK and MEK proteins by activation of E-cadherin and claudin, participating in the epithelial-mesenchymal transition	Inhibition of growth and prevention of cell differentiation	0.2 μM, 1 μM, 5 μM	(61)
Bithionol	Antiparasitic and anthelmintic	*In vivo* xenograft cancer cells SKOV-3-luc-D3 in mice Foxn1	Dysregulation of the cell cycle by ROS generation and NF-kB inhibition	Induction of apoptosis	30 mg/kg, 60 mg/kg, 120 mg/kg, 240 mg/kg	(151)
Itraconazole	Antifungal	*In vivo* humans	Antiangiogenic function by inhibition of growth receptor 2 VEGFR2 and phosphorylation of ERK, hedgehog, and TOR pathways	Antiangiogenic and growth suppression	From 400 to 600 mg	(157)
		In vivo xenograft cancer cells in mice, endothelial human cancer cells	Antiangiogenic function by inhibition of growth receptor 2 VEGFR2 and phosphorylation of ERK, hedgehog, and TOR pathways	Antiangiogenic and growth suppression	From 100 to 600 mg	(156)
Ivermectin	Antiparasitic and anthelmintic	*In vitro* cell line SKOV-3	Induction of stop cell cycle in G0-G1 by modulation of growth factor proteins by kinase PAK-1 inhibiting	Growth suppression	5 μM	(163)
		In vitro cell lines TYK-nu, KOC7c, SKOV3 and MRUG-S	Induction of stop cell cycle in G0-G1 by modulation of growth factor proteins by kinase PAK-1 inhibiting	Growth suppression	5 μM, 20 μM	(160)
Mebendazole	Antiparasitic and anthelmintic	*In vivo* xenograft in mice ovarian cancer cell lines: MES-OV (p53 R282W), ES2 (p53 S241F), A2780 (p53 wild type), SKOV3 parental (p53 null)	Block tubulin polymerization that generates dysfunctional microtubules and difficult cytoskeleton structural functions	Deregulating cellular energetics, suppressing proliferation and induction of apoptosis	50 mg/kg	(172)
		In vitro lines OVCAR8CR and SKOV3CR	Inhibits the sign ways ELK/SRF, NFKB, MYC/MAX y E2F/DP1	Deregulating cellular energetics, suppressing proliferation and induction of apoptosis	From 0 μM to 4 μM	(176)
Ciglitazone	Type 2 diabetes, atherosclerosis	female nu/nu mice xenografted with subcutaneous OVCAR-3 tumors	Inhibits cell growth by causing cell cycle arrest and apoptosis in ovarian cancer cells. Reduce prostaglandin E2 (PGE2) in a COX-2-independent manner, induce apoptosis, inhibit angiogenesis, and inhibit tumor progression.	Inhibit cell cycle and tumor progression induction of apoptosis, inhibit angiogenesis	15 mg/kg intraperitoneally once a week	(183, 184, 275, 276)
Clofibric acid	Hyperlipidemia	OVCAR-3 cells and female BALB/c nu/nu mice model	Inducing carbonyl reductase, which promotes the conversion of PGE2 to PGF2α	Suppression of cell proliferation and increasing apoptosis	500 μmol/L	(190)

(Continued)

TABLE 1 Continued

Drug	Original target	*In vivo/in vitro* study model	Mechanism of action or target molecule in OC treatment	Relevant hallmark involved	Concentration/ Dosage	Ref
Disulfiram	Alcoholism treatment	*In vitro* cell lines OVCAR-3, SKOV3, OV-MZ-30, OV-MZ-31, OV-MZ-37, and OV-MZ-38	Irreversible structural cell damage through oxidized disulfide bonds in paranuclear proteins	Induction of apoptosis	From 0 μM to 5 μM	(196)
Fluphenazine	Antipsychotic	*In vitro* cell line OVCAR-3	Oligonucleosomal cleavage of genomic DNA and caspase substrate polyadenosine diphosphate ribose suggest induces caspase-dependent apoptotic cell death	Induction of apoptosis	3.84 μM	(202)
Metformin	Regulate the amount of sugar in the blood	*In vitro* cells Hey and SKOV3ip1	Inhibits mitochondrial complex I (NADH dehydrogenase) activity and cellular respiration of electrons transported by glucose deprivation, stopping Krebs cycle function	Induction of apoptosis	From 10 mM to 40 mM	(204)
Naftopidil	Prostatic hyperplasia treatment	*In vitro* cell lines IGROV1-R10, SKOV3	Increased expression of Bim, Puma, and Noxa proteins, which affect mitochondria and induce apoptosis	Induction of apoptosis	0 μM, 25μM, 50 μM	(214)
Nelfinavir	Antiretroviral	*In vitro* cell lines PEO1/ PEO4/PEO6 y PEO14/PEO23	Inhibits phosphorylation in AKT and ERK, causing damage to nuclear DNA and endoplasmic reticulum	Suppress proliferation and induce apoptosis	From 1 μM to 50 μM	(215)
Ritonavir	Antiretroviral	*In vitro* cell lines MDH-2774 and SKOV-3	Apoptosis induction by phosphorylation of AKT that inhibits the PI3K/Akt	Antiangiogenic, growth suppression, and apoptosis	20 μM	(217–219)
Sertraline	Antidepressant	*In vivo*, cell lines OVCAR-8, human ovarian adenocarcinoma NCI-ADR/RES (NAR) xenografts in mice	Interferes with cellular pathways of TNF-MAP4K4-JNK, the antiapoptotic PI3K/Akt/mTOR, AMPK/mTOR axis, and TCTP/ P53 feedback loop and with the cytosolic Ca2+ levels	Induction of apoptosis	1 μM	(227)
Ormeloxifene	Contraceptive	*In vitro* cell lines A2780, A2780-CP and SKOV-3	Phosphorylation of p53 and the Akt pathway, increasing cell cycle inhibitors p21 and p27 and inhibition of Bcl-xl on mitochondrial function, generating apoptosis	Growth suppression and apoptosis	10 μM, 20 μM	(256)
Thalidomide	Anti-emetic	*In vitro* SKOV-3 cells	Decreases the TNF-α, MMP-9 and MMP-2 secretion	Did not have a significant effect on cell proliferation and growth	(4×10^{-7} - 2×10^{-5} M)	(237)
Dasatinib	Philadelphia chromosome-positive acute lymphoblastic leukemia or chronic myeloid leukemia	SKOV-3 and Hey cells Hey xenograft model	Reduced the phosphorylation of AKT, mTOR, p70S6K, and S6 kinase expression.	Autophagic cell death	300 nM for SKOv3 cells and 150 nM for HEY cells	(243)
Imatinib	Chronic myelogenous leukemia and gastrointestinal stromal tumors	*In vitro* cell lines: C272-hTert/E7, C889/hTert, CSOC848, CSOC908, and CSOC918	Inhibits phosphorylation of PDGFRα and Akt in PDGFRα-specific manner	Inhibition growth and cell cycle progression in a PDGFRα-specific manner	IC50 < 1 μm	(246).

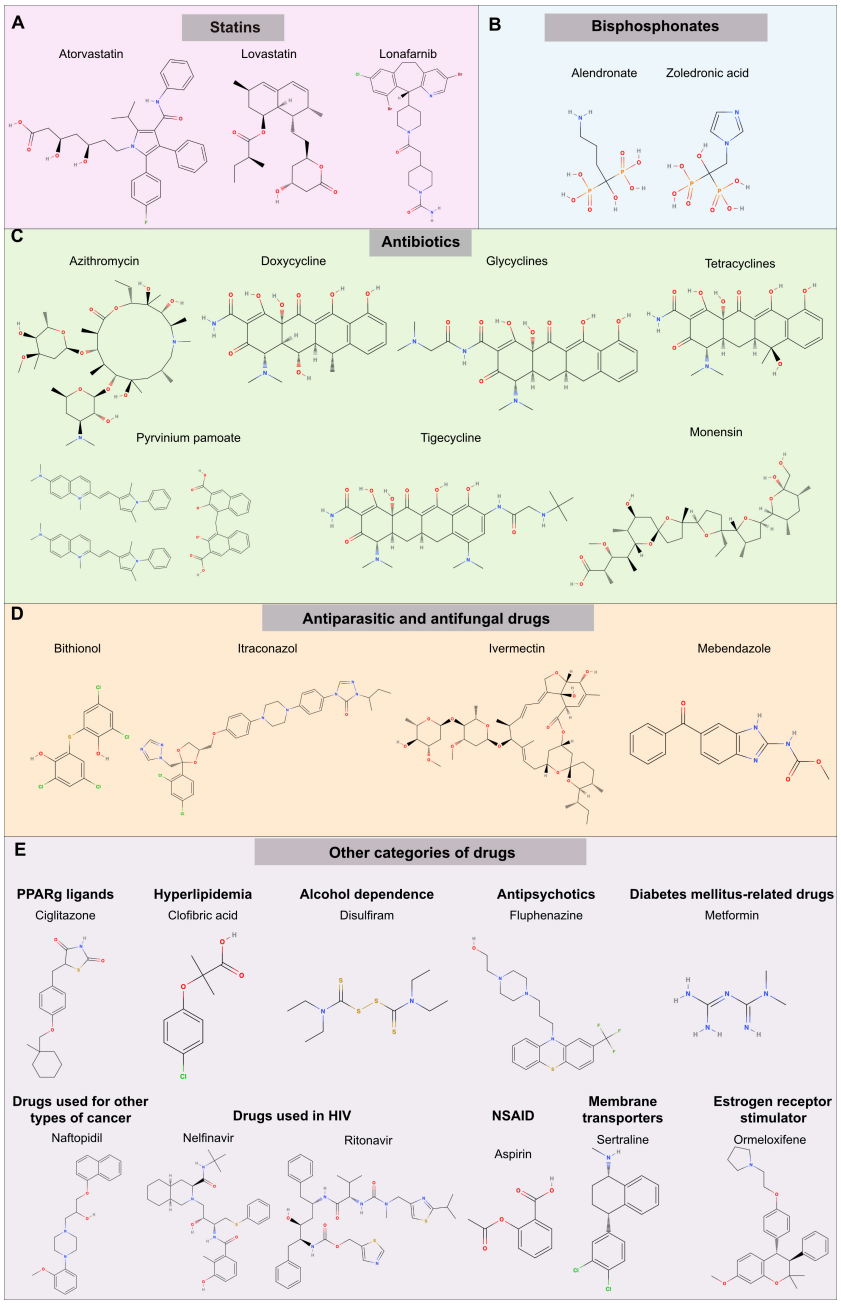

FIGURE 4
Chemical structure of potential drugs to be repurposed against ovarian cancer. The diagram illustrates potential drug candidates for repurposing in the treatment of OC. Various pharmaceutical agents target different pathways; see Table 1 for a summary of mechanisms. The groups represented are **(A)** statins, **(B)** bisphosphonates, **(C)** antibiotics **(D)** antiparasitic and antifungal drugs, **(E)** other categories of drugs including PPARγ inhibitors, compounds used to treat hyperlipidemia, alcoholism, and mental disorders, diabetes, other types of cancer (prostate), HIV infection, Non-steroidal anti-inflammatory drugs (NSAIDs), membrane transporters and estrogen receptors. Each drug offers a unique mode of action that could potentially enhance therapeutic outcomes in OC management.

a murine model of OC (108). Alendronate inhibits proliferation in OC SKOV3 and chemoresistant OVCAR5 cell lines *in vitro*. It induces the expression of *LC3A* and *LC3B* genes, indicating autophagy activation. In a transgenic OC mouse model (mogp-TAg), alendronate reduces total tumor mass, suggesting suppression of tumor initiation, and implies a potential chemo-preventive effect in OC development (108). In addition, alendronate reduces Rho activation by inhibiting the mevalonate pathway, resulting in the inhibition of cell migration in Caov-3, OC cells (109). Furthermore, the alendronate treatment (1mg/kg/d) reduced the tumor burden by ~88% in female nude mice (BALB-c *nu/nu*) injected with Caov-3 (110). Together, *in vitro* and *in vivo* evidence strongly suggested findings that alendronate had potential as a drug for OC treatment (108–110).

Zoledronic acid is another example of a bisphosphonate drug, mainly prescribed for bone-related conditions like osteoporosis and

cancer-induced bone complications. This drug inhibits bone resorption, promoting bone strengthening (111, 112). Specifically, zoledronic acid inhibits the activity of osteoclasts, the cells responsible for breaking down bone tissue, helping to maintain bone density and strength. It has also been used for the treatment of multiple myeloma and metastatic breast cancer and to treat hypercalcemia (high levels of calcium in the blood) associated with malignancy (113, 114). Zoledronic acid has been used in combination with gossypol, a natural polyphenolic compound used as a male contraceptive and with demonstrated anticancer properties in prostate cancer and leukemia. Combined, these two drugs render a synergistic cytotoxic and apoptotic effect in OC OVCAR-3 and MDAH-2774 cell lines (115). This combined treatment repressed the transcriptional expression of angiogenic molecules such as the inhibitor of differentiation or DNA binding (ID-1), EPH (Ephrin) receptors B2 and B4 (EPHB2/B4), laminin α-5 (LAMA-5), the fibroblastic growth factor (FGF2) and FGF receptor-3 (FGFR3), midkine (MDK), thymidine phosphorylase (TP), platelet-derived growth factor A (PDGF-A), and the cytokine CXCL-1, which plays a pivotal role in angiogenesis (115). Furthermore, experiments where NCI-H929, OPM-2, U266 and RPMI-8226 myeloma cell lines were pre-treated with simvastatin and then combined with antimyeloma drugs resulted in the apoptotic cascade (116). The combination of fluvastatin with zoledronic acid enhanced the chemosensitivity to the ATP-based tumor assay (ATP-TCA) in twenty-two pre-treated (mostly with platinum-based chemotherapy) ovarian carcinomas. Sequential drug experiments showed that pretreatment of tumor cells dissociated from solid carcinomas with fluvastatin resulted in decreased sensitivity to zoledronic acid (117). Mechanistically, zoledronic acid and fluvastatin treatment enhance the effects that involved Ras prenylation. Thus, implying that prior to bisphosphonate administration, statins would be expected to block the entry of mevalonate into the pathway, reducing the substrate concentration for the step that is blocked by zoledronic acid, potentially enhancing the effectiveness of the combination (117).

Research has suggested cancer could be managed as an infectious disease, in other words, by taking advantage of antibiotics that inhibit mitochondrial biogenesis, which is essential for clonal expansion and survival of cancer stem cells (118). This idea arose from the anabolic nature of cancer stem cells, which require mitochondrial biogenesis for proliferation and survival (118). Thus, targeting mitochondrial biogenesis is an alternative avenue that might render anti-tumorigenic effects useful against cancer treatment. Examples of antibiotics that impair mitochondrial biogenesis as a side effect are pyrvinium pamoate, doxycycline, azithromycin, tigecycline, and chloramphenicol, which make these compounds potential candidates in the treatment of OC (119). Mechanistically, antibiotics such as erythromycin, chloramphenicol, tetracyclines, glycylcyclines and pyrvinium pamoate target three main mitochondrial molecules. These are the mitochondrial 39S/large and the 28S/small ribosome subunits and mitochondrial oxidative phosphorylation proteins (OXPHOS), such as complex I of the electron transport chain (119–121). Azithromycin was shown to inhibit the tumor-sphere formation of OC SKOV3, ES2 and Tov21G cells, demonstrating the potential for cancer management (119). Conventionally, doxycycline has been used in the treatment of prostatitis, urinary tract infections and acne due to its anti-inflammatory properties (122–124). Doxycycline also inhibits cell proliferation, migration and matrix metalloproteinase 2 (MMP-2) activity *in vivo* model (Male Sprague-Dawley rats) treated with 30-mg/kg/day doxycycline after arterial injury (125), suggesting that if this drug were to be used for cancer therapy, its toxic side effects might be negligible (119, 126, 127). Mechanistically, doxycycline inhibits matrix-metalloproteinases (MMPs) and the formation of the tumor-sphere in cellular models of OC like SKOV3, ES2 and Tov21G (119). Doxycycline from 50 μM to 500 μM did not affect the viability of normal fibroblasts (hTERT-BJ1) and MCF7 cells (119). Doxycycline treatment reduced tumor growth by 80% in pancreatic tumor xenografts of PANC-1 cells (128). The antibiotic also reduced bone and bone-associated soft-tissue tumor mass by >60% and ~80%, respectively, in a xenograft model of breast cancer bone metastasis that involved MDA-MB-231 cells (129). The anti-cancer activity of doxycycline was attributed to the inhibition of MMPs rather than the targeting of mitochondrial biogenesis (119). Doxycycline exhibited a marked suppression of both invasive and migratory behaviors in human oral squamous cell carcinoma (SCC-15 cells) *in vitro*, with inhibition levels exceeding 75% at a concentration of 10 μg/ml. Additionally, daily administration of doxycycline at a dosage of 3 mg/mice effectively impeded tumor progression in SCC-15 xenografted nude mice, resulting in an 85.6% inhibition rate. Following doxycycline treatment, *MMP-9* mRNA levels in fresh tumor tissue notably decreased compared to the control group treated with normal saline ($P < 0.01$), while *MMP-2* mRNA levels remained unchanged (130).

Glycylcyclines and tetracyclines impair protein synthesis in bacteria (131, 132). These molecules bind to the bacterial 30S ribosomal unit, inhibiting the binding of aminoacyl-tRNA to the ribosomal A-site. Thus, glycylcyclines could be used to inhibit mitochondrial biogenesis in a similar manner to the one discussed above (119). Pyrvinium pamoate is an anti-helminthic drug which inhibits OXPHOS under normoxic and hypoxic environments and also prevents the formation of the tumor-sphere (119). Finally, tigecycline was shown to also inhibit the formation of a mammo-sphere in SKOV3, ES2 and Tov21G OC cell lines (119).

Monensin is primarily used as a veterinary antibiotic and feed additive for livestock, especially in the prevention and control of coccidiosis. The use of Monensin in human medicine is not authorized, and it is not prescribed for human consumption. However, experiments in SKOV-3, A2780, OVCAR-3 and CAOV-3 cells yielded promising results as a potential repurposed drug against OC. Monensin was shown to regulate the expression molecules linked to the epithelial-mesenchymal transition (EMT) and the mitogen-activated protein kinase (MEK)-extracellular signal-regulated kinase (ERK) pathway (61). This drug inhibited the proliferation of A2780, OVCAR3 and CAOV-3 cell lines from 0.2 μM (low inhibitory effect) until 5 μM (complete inhibitory effect) and impaired the invasive properties of SKOV-3 cells. Furthermore, *in vivo* experiments where SKOV-3 cells were injected into nude mice, followed by monensin administration (0, 8, and 16 mg/kg), resulted in reduced tumor masses in monensein-

treated animals, compared to control groups (61). Mechanistically, monensin stimulated the SUMOylation of MEK1, impaired the growth, migration, and invasive capabilities of the A2780, OVCAR3, CAOV-3 and SKOV-3 OC cell lines and in the *in vivo* murine ovarian cancer xenograft model. Thus, monensin holds promise for OC treatment by augmenting MEK1 SUMOylation by suppressing the MEK-ERK signaling pathway (61). To investigate the potential SUMOylation of MEK in OC cell lines, MEK1 and SUMO1 were co-expressed in the non-tumorous cell line HEK293. Immunoprecipitation and western blot analyses of MEK1 revealed that monensin augmented the SUMOylation of MEK1, in a dose- and time-dependent manner (61). However, this drug still needs to be evaluated for approval and usage in human patients.

Bithionol is an anthelmintic drug, historically used for the treatment of intestinal worm infections (133). Bithionol is believed to interfere with the energy metabolism of the parasites, leading to their death. Bithionol has also been used as an antibacterial and antifungal agent in some topical formulations (134, 135). However, due to potential side effects and the availability of other effective treatments, its use in medical practice has been limited. Bithonol causes cell death via caspases-3/7-mediated apoptosis, arrest cell cycle progression, promote the production of Reactive Oxygen Species (ROS) and inhibits Autotaxin (ATX) (136). Autotaxin is an enzyme involved in the production of the signaling molecule lysophosphatidic acid (LPA). ATX and LPA have been implicated in cancer progression, including tumor growth, invasion, and metastasis (137–146). ATX is often overexpressed in several types of cancer, and elevated levels of LPA have been associated with promoting cancer cell survival, migration, and angiogenesis (147–149). In human OC biopsies LPA_2 and LPA_3 are highly expressed in comparison with normal ovaries or low malignancy tumors. Furthermore, there is a significant correlation between the expression ratios of $LPA_{2\text{-}3}$ and VEGF in patients with cancer (150). Thus, research has been focused to understand ways to inhibit ATX or block the LPA pathways to impede cancer progression. Since ATX is associated with an increase in invasiveness and aggressiveness of tumor cells, and with the grade of tumor development, the inhibition of ATX by bithionol might have an important repercussion in OC treatment (151). In addition, bithionol has been shown to also induce DNA fragmentation, loss of mitochondrial potential and overexpression and activation of apoptotic biomarkers, such as cleaved PARP and caspase-7 (136, 151).

Itraconazole, an anti-fungal drug, has an anti-angiogenic activity and inhibits the Hedgehog pathway inducing autophagic growth arrest (152–155). This drug has been proposed for the treatment of several cancers such as leukemia, ovarian, breast and pancreatic (156). Out of 55 patients with refractory OC, 19 individuals received a combination of itraconazole and chemotherapy. The median progression-free survival (PFS) was 103 days for those receiving chemotherapy (platinum and taxane administration) with itraconazole, compared to 53 days for those without itraconazole (p=0.014). Similarly, the median overall survival was 642 days and 139 days for patients with and without itraconazole, respectively (p=0.006). A proportional hazards regression model (Cox) was employed for multivariate analysis of progression-free survival (PFS) and overall survival (defined as the duration from the commencement of chemotherapy after becoming refractory to death by any cause) following itraconazole exposure alongside chemotherapy. The analysis was adjusted for factors including age, race, Eastern Cooperative Oncology Group (ECOG) performance status (PS), carcinoma histology, number of prior regimens, and platinum sensitivity status. The study demonstrated that the hazard ratio for PFS was 0.24 (p=0.002), and for overall survival, it was 0.27 (p=0.006) in the group receiving itraconazole therapy (157). This data strongly suggested that combining classic chemotherapy with itraconazole may improve the median overall survival rate due to a potential synergistic effect of itraconazole in the treatment of refractory OC (157).

The antiparasitic drug ivermectin, which binds to the glutamic acid operative chloride ion channel (GluCls) (158, 159) has been repurposed for OC treatment (160–162). Ivermectin arrests cell cycle at G0-G1 phase by increasing the synthesis of p21, reducing proliferating cell nuclear antigen (PCNA), cyclin E, and cyclin D protein levels in breast cancer cell lines (MCF-7, MDA-MB-231 and MDA-MB-468) (163). Ivermectin also reduces viability and colony-forming ability in cancer stem-like malignant populations in the SKOV-3 cellular model (163). Furthermore, ivermectin inactivates the P21 (RAC1) Activated Kinase 1 (PAK1), resulting in the inhibition of the phosphorylation of kinase Raf1 (RAF-1) in TYK-nu and RMUG-S OC cells (160). The proliferation rate of TYK-nu, KOC7c, SKOV3, and RMUG-S cell lines was also diminished (160). Ivermectin targets the yes-associated protein 1 (YAP1) (164), which promotes tumorigenesis in breast and liver cancers (165, 166), suggesting a potential application in the treatment of OC, where YAP1 is considered a prognostic marker of the disease (167, 168). Mechanistically, ivermectin blocks the activity of Karyopherin Subunit β1 (KPNB1) in the OC model SKOV3 and OVCAR3 cells, impairing proliferation by targeting several signal pathways, related to cell cycle progression and inducing apoptosis (169, 170). When combined with paclitaxel, these compounds present a synergistic anti-tumor action (171).

Mebendazole is another antiparasitic drug with anti-cancer activity. In several cultured cellular models of OC (MESOV, ES2, A2780, SKOV3 null p53, SKOV3 R248W p53, and SKOV3 R273H p53), mebendazole hindered cell proliferation and activated apoptosis via p53-independent induction of p21 and tubule depolymerization (172). The premise behind exploring these drugs as potential cancer treatments lies in their ability to destabilize microtubules (173–175). Importantly, mebendazole also inhibited cell proliferation and migration in the cisplatin-resistant human OC cell lines OVCAR8CR and OVCAR8 and further induced apoptosis in OVCAR8CR and SKOV3CR cells (176). Mechanistically, this drug modulates essential signaling pathways, such as MYC (Basic Helix-Loop-Helix protein transcription factor)/MAX (MYC Associated Factor X), ELK (ETS (E-twenty six) transcription factor)/SRF (Serum Response Factor), E2F (transcription factor)/DP1 (differentiation regulated

transcription factor protein), and nuclear factor kappa B (NF-κB) (176). In addition, in a xenograft murine model of athymic nude mice injected with SKOV3CR cells, mebendazole acted cooperatively with cisplatin to inhibit proliferation, promote apoptosis, and decrease ovarian tumor growth (176). These findings support the possible application of mebendazole in the treatment and maintenance of OC (172), which in combination with cisplatin holds promise for treating chemoresistant OC cases (176).

Peroxisome proliferator-activated receptors (PPARs) have a crucial role in ovarian physiology by regulating the expression and activation of proteases (177–179). PPARγ is regulated by the luteinizing hormone and is highly expressed during ovulation (180). Furthermore, PPARγ(+/−) mice exhibited an approximately 3-fold rise in mammary adenocarcinomas ($P<0.05$), a more than 3-fold increase in ovarian granulosa cell carcinomas ($P<0.05$), a greater than 3-fold increase in malignant tumors ($P<0.02$), and a 4.6-fold elevation in metastatic incidence (181). In mice, PPARγ(+/−) has an increased susceptibility to ovarian carcinogenesis generated by dimethyl benzanthracene (DMBA, 7,12-dimethylbenz[α] anthracene) (181). In a murine model of PPARγ heterozygous female knockout ($Ppar\gamma^{+/-}$) and congenic wild-type littermate controls ($Ppar\gamma^{+/+}$), treated with the carcinogen DMBA, at the 25th week from the initiation of the study, KO mice exhibited significantly higher skin papilloma multiplicity (0.87 papillomas/mouse) compared to controls (0.52 papillomas/mouse; $P<0.05$) (182). By the end of the observation period, ∼41% (18 out of 44) of controls ($Ppar\gamma^{+/+}$) and ∼61% (24 out of 39) of knockout ($Ppar\gamma^{+/-}$) mice died or had to be killed due to morbidity resulting from tumor progression (181). Tumors in $Ppar\gamma^{+/-}$ mice were found to be in a more advanced state compared to wild-type controls. Although the total ovarian tumor multiplicity did not differ between the two genotypes, $Ppar\gamma^{+/-}$ mice displayed a significantly higher multiplicity of malignant tumors per mouse compared to wild-type controls when tumors were categorized as benign or malignant. In particular, among the total ovarian tumors, there were 3 carcinomas out of 12 in wild-type mice and 10 carcinomas out of 13 in $Ppar\gamma^{+/-}$ mice, reaching a significance level of $P < 0.02$ (181). The increased susceptibility of $Ppar\gamma^{+/-}$ mice to DMBA-induced carcinogenesis implies that PPARγ may function as a tumor modifier. Consequently, PPARγ-specific ligands could potentially play a beneficial role in chemo preventing ovarian carcinogenesis (181.

Activating ligands of PPARγ, such as ciglitazone, pioglitazone, and *t*-butyl [1,1-bis(3′-indolyl)-1-(*p*-*t*-butyl)methane (DIM-C-pPhtBu) have been proposed to inhibit OC by impairing proliferation and tumor development and also by triggering apoptosis (183–186). Specifically, ciglitazone inhibits cell proliferation by blocking cell cycle progression and promoting apoptosis (183, 184). In addition, ciglitazone enhanced PAR1-triggered prostaglandin E2 (PGE2) production and cyclooxygenase 2 (COX-2) expression in the normal rat gastric epithelial cell line (RGM1) (187).

Treatment with ciglitazone reduces *Cox-2* mRNA expression and PGE2 production, while also decreasing COX-2 promoter activity. Additionally, it upregulates PPRE (putative PPAR response element) promoter activity in human non-small-cell lung cancer cells (A427 and A549) (188). Ciglitazone decreases expression levels of glucose transporter-1 (GLUT-1), inhibits glucose uptake, and increases tumor cell apoptosis in A2780 and OVCAR3 OC cells (189). Additionally, it reduces expressions of specific protein 1 (Sp-1) and β-catenin while increasing phosphorylation levels of adenosine monophosphate (AMP)-activated protein kinase and enhancing chromatin condensation and fragmentations (189). In an *in vivo* model utilizing eight-week-old female NOD-scid IL2R γ null (NSG) mice injected with A2780 OC cells, ciglitazone significantly decreases OC mass transplanted onto the back of the mice. GLUT-1 expression is increased in high-grade serous ovarian carcinoma, with expression levels proportional to cancer stage severity (189). Mechanistically, DIM-C-pPhtBu induces PPARγ-dependent p21 and reduces PPARγ-independent cyclin D1, resulting in cell cycle arrest, inhibition of cell proliferation, and apoptosis induction (185).

Clofibric acid, commonly used for the treatment of hyperlipidemia, was shown to reduce the growth of OVCAR-3 tumors transplanted subcutaneously and notably prolonged the survival of cancerous peritonitis mouse model with malignant ascites originating from DISS cells compared to the control group (190). Moreover, clofibric acid exhibited dose-dependent suppression of cell proliferation in OVCAR-3 cells. In both implanted OVCAR-3 tumors and cultured OVCAR-3 cells, clofibric acid treatment induced the expression of carbonyl reductase (CR), which promotes the conversion of PGE2 to PGF2α (prostaglandin F2α) (190). Clofibric acid treatment also reduced the levels of PGE2 and VEGF in OVCAR-3 tumors and DISS-derived ascites. Solid OVCAR-3 tumors treated with clofibric acid exhibited reduced microvessel density and increased apoptosis (190).

Disulfiram, a medication used to treat alcohol dependence, has been studied for its potential anticancer effects in OC. Research suggests that disulfiram may inhibit cancer cell growth and metastasis in copper (Cu)-dependent manner due to its ability to bind this ion (191, 192). Approximately 60% of breast cancer patients have elevated levels of Cu in serum (average 3.25 μg/mL) compared with healthy individuals (average 2 μg/mL) (193). The disulfiram-Cu complex was shown to be is a potent inhibitor of proteasomal activity and to trigger apoptosis in the cultured breast cancer cell lines MDA-MB-231 and MCF10DCIS.com, with no effect in non-tumorigenic immortalized MCF-10A cells (192). In mice with MDA-MB-231 tumor xenografts, disulfiram notably suppressed tumor growth by 74%. This effect was attributed to apoptosis induction and proteasome inhibition, which rendered accumulation of ubiquitinated proteins and the natural proteasome substrates p27 and Bax (BCL2 associated X, apoptosis regulator) (192). Disulfiram-Cu complex increases intracellular Cu concentration both *in vitro* and *in vivo*, bypassing the requirement for Cu-membrane transporters, such as Ctr1, suggesting that the classical transporter Ctr1 may not play a significant role in disulfiram-mediated Cu accumulation (194, 195). This complex antagonized NFκB signaling, suppressed aldehyde dehydrogenase activity and antioxidant levels, thereby inducing

apoptosis mediated by oxidative stress in the inflammatory breast cancer model SUM149, rSUM149 cells (194, 195).

In a murine model, the disulfiram-Cu complex markedly suppressed tumor growth without notable toxicity, inducing apoptosis exclusively in tumor cells. This underscores that inflammatory breast cancer tumors are highly redox-adapted, potentially conferring resistance to ROS-inducing therapies (194, 195). Hence, the redox modulation capabilities of disulfiram represents a promising avenue for treating tumors enhancing the efficacy of traditional therapies (192). As such, in cultured OC models, disulfiram promoted oxidative stress through an Cu-dependent mechanism, resulting in death of OVCAR-3, SKOV-3, OVMZ-30, OVMZ-31, OVMZ-37, and OVMZ-38 cells (196). It has been reported that the ditiocarb-Cu complex, a metabolite of disulfiram, is responsible for the anti-cancer effects. Additionally, functional, and biophysical analyses identified NPL4 (nuclear protein localization protein 4 homolog) as the molecular target underlying the tumor-suppressing effects of disulfiram (191). NPL4 acts as an adaptor of p97, also known as ATPase valosin-containing protein (VCP) segregase, which is crucial for protein turnover in various regulatory and stress-response pathways within cells (191).

Disulfiram, combined with Cu, enhances cisplatin-induced apoptosis in IGROV1, SKOV3, and SKOV3IP1 cells, sensitizing cancer cells to cisplatin treatment and decreasing cell viability by 50-80%% (197). This combination targets acetaldehyde dehydrogenase (ALDH)+ cells, favoring cisplatin sensitivity in H460/CisR, H1299/CisR, and SKMES-1/CisR cells (198). Additionally, disulfiram and Cu supplementation reduces NF-κB activity and sensitizes H630WT and HCT116WT cell lines to gemcitabine (199). Disulfiram reverses doxorubicin (DOX) resistance by increasing c-Jun NH2-terminal kinase (JNK) expression and phosphorylation in HL60 cells (200). Effective cell death in OVCAR3 and SKOV3 cells is mediated by disulfiram, promoting an oxidative intracellular environment and causing irreversible cell damage associated with the expression of heat shock proteins HSP32, HSP40, and HSP70 (196). Furthermore, the combination of disulfiram and Cu, induces disulfide bond-mediated dimerization of HSP27, resulting in its inactivation and rapid detachment of OVCAR-3 cells, an effect not detected with disulfiram alone (196). Combinatory treatment of disulfiram with auranofin, an anti-rheumatic drug, enhances cytotoxic effects in OVCAR3 cells (188).

Fluphenazine is an antipsychotic drug that exerts its effects on the postsynaptic dopaminergic D1 and D2 receptors by inhibiting the release of dopamine. In OC OVCAR-3 cells, fluphenazine plays an essential role in the phosphorylation of AKT dependent on epidermal growth factor (EGF) (201, 202). Moreover, fluphenazine targets pyruvate dehydrogenase kinase 1 (PDK1), which is part of the PDK1/Akt pathway mediating cell survival, proliferation and tumorigenesis (201). Thus, the inhibition of PDK1/Akt kinase pathway suppressed the EFG-dependent proliferation phenotype and survival of cancer OVCAR-3 cells by inducing apoptosis (201). The proposed mechanism of action for fluphenazine is related to an enhancement of genomic DNA-oligonucleosomal cleavage, and to the activity of the caspase substrate polyadenosine diphosphatase ribose. These pathways trigger caspase-dependent apoptotic cell death (201).

Metformin, a frequently prescribed medication for type 2 diabetes mellitus, reduces proliferation of SKOV3ip1, OVCAR-5, HeyA8 and K-ras/PTEN cells. The K-ras/PTEN mouse OvCa cell line was established from ovarian tumors generated using a genetic mouse model (203, 204)). Mechanistically, metformin causes cell cycle arrest in G0/G1 phase by decreasing the expression of cyclin-dependent kinase 4 (CDK4) and Cyclin D1, with no evidence of triggering apoptosis (204). Metformin treatment results in reduced number and mass of ovarian tumors. For instance, female athymic nude mice pretreated with metformin (250 mg/kg/d) exhibited significantly fewer ovarian tumor implants compared to controls (mean number of tumors: placebo, 116; metformin, 47; P<.005) (204). In SKOV3ip1 xenograft mice, treatment with metformin in combination with paclitaxel resulted in a 60% reduction in tumor weight compared to controls (P=.02) (204). This combination demonstrated a stronger effect than each compound tested separately (204). Metabolically, metformin modifies adenosine monophosphate-activated protein kinase (AMPK) activity, lipid synthesis, and glycolysis. Notably, metformin induces apoptosis in OC cell lines in an AMPK-dependent manner (205–207).

Furthermore, a study of OC patients where a cohort of individuals was treated with metformin resulted in an increased survival rate (67%) of individuals treated with metformin compared to the non-treated group (47%) (208). Patients who consumed this drug exhibited a markedly enhanced 5-year survival rate (51%) compared to those who did not use metformin (8%) or those without diabetes (23%) (209). In combined metformin/cisplatin treatment, increasing metformin concentrations led to a notable reduction in the half-maximal inhibitory concentration of cisplatin (209). Consequently, research in ovarian cancer patients, alongside *in vivo* and *in vitro* models, highlights the inhibitory effect of metformin on tumor growth, its ability to enhance chemotherapy sensitivity, and its potential to prolong the life expectancy of affected individuals.

Naftopidil is an α1-adrenergic receptor antagonist that is primarily used for the treatment of benign prostatic hyperplasia (BPH), a condition characterized by an enlarged prostate gland in men (210–212). By blocking the α-1 adrenergic receptors in the prostate, naftopidil helps to relax the smooth muscles in the prostate and bladder neck, relieving symptoms of BPH and improving urine flow (213). In studies using cellular models of OC, naftopidil inhibited proliferation without eliciting apoptosis, leading to a cytostatic effect observed in SKOV-3 and IGROV1-R10 cell lines (214). Furthermore, this medication enhances the production of proapoptotic BH3-only proteins, namely Bim (BCL2-like 11, member of the Bcl-2 family that promotes apoptosis), Noxa (phorbol-12-myristate-13-acetate-induced protein 1), and Puma (BCL2 binding component 3). Two different mechanisms have been identified for naftopidil in OC-cultured models. For instance, in SKOV3 cells, an ER stress-induced response by the activating transcription factor 4 (ATF4), which is responsible for the phenotype, while in the IGROV1-R10 cell line,

the JNK pathway is the leading pathway (214). Considering the mechanisms by which naftopidil induces the expression of Puma by the JNK/c-Jun pathway, resulting in a new alternative to OC management (214).

Nelfinavir is a protease inhibitor primarily used in the treatment of HIV (human immunodeficiency virus). Experiments in HGSOC cells showed that treatment with this drug reduces the cell number, clonogenic survival and viability (215). Additionally, nelfinavir favors a pro-apoptotic environment characterized by elevated levels of phospho-eIF2α (Eukaryotic Translation Initiation Factor 2A), DNA Damage Inducible Transcript 3 (DDIT3, also known as CHOP), and ATF4, as well as an increased ratio of Bax/Bcl-2 and cleaving of the executor caspase 7 (215). Nelfinavir triggered a dose-dependent reduction in the HGSOC cell number and viability and a parallel increase in hypo-diploid DNA content, independently of platinum sensitivity (215). DNA damage induced by nelfinavir was detected by the phosphorylation of the histone marker, H2AX (H2A.X variant histone) in PEO1 and PEO4 cell lines, in a process linked to reduced proliferation and survival mediated by the ERK and AKT pathways (215). In the PEO1 and PEO4 cellular models, a synergistic effect of nelfinavir with the protease inhibitor, bortezomib, enhanced the ability to induce short-term cell cycle arrest and long-term toxicity (215). So far, bortezomib has been used in the treatment of multiple myeloma and mantle cell lymphoma, but similarly to nelfinavir possess the potential as a treatment against OC.

Ritonavir is another protease inhibitor, largely used in the treatment of HIV, in combination with other antiretroviral medications to slow the progression of the disease. Ritonavir inhibits the activity of the HIV protease enzyme, which is necessary for the virus to replicate and produce new infectious viral particles (216). By inhibiting protease, Ritonavir helps reduce the viral load in the body. Additionally, ritonavir is often used as a "booster" medication, as it increases the levels of other protease inhibitors in the blood, enhancing their effectiveness. This boosting effect allows for lower doses of other protease inhibitors when used in combination with nucleoside analog reverse transcriptase inhibitors (NRTI), resulting in highly effective antiretroviral therapy. In the context of OC repurposing, ritonavir was shown to prevent cell cycle progression in MDH-2774 and SKOV-3 cultured models (217). Furthermore, in MDH-2774 and SKOV-3 cell lines, this drug promoted apoptosis and cell cycle arrest in G1 phase by depleting the phosphorylation of retinoblastoma (RB), and by reducing the expression of G1 cyclin and cyclin-dependent kinase (217). In MDAH 2774 and SKOV-3 cells, ritonavir also increased levels of phosphorylated AKT, thus inhibiting the PI3K-AKT pathway, which resulted in an antitumor effect that led to apoptosis (217–219). In xenograft models, nude mice injected with human ovarian adenocarcinoma A2780 cells and treated with ritonavir exhibited reduced tumor burden compared to untreated controls. Additionally, ritonavir-treated mice showed larger areas of necrosis and increased activated caspase-3 staining, indicating induction of apoptosis in the tumor cells (219).

Non-steroidal anti-inflammatory drugs (NSAIDs) are a class of medications commonly used to reduce inflammation, relieve pain, and lower fever. NSAIDs inhibit the production of prostaglandins by blocking cyclooxygenases (COX), which play a role in inflammation and pain (220). Thus, NSAIDs have anti-inflammatory and analgesic (pain-relieving) properties, often used to manage conditions characterized by inflammation, such as arthritis, osteoarthritis, rheumatoid arthritis, and to alleviate systemic pain in cases of menstrual cramps, headaches, muscle aches, and minor injuries (221–223).

Examples of NSAIDs include ibuprofen (e.g., Advil, Motrin), naproxen (e.g., Aleve), aspirin, diclofenac, and meloxicam. Among these, aspirin has been investigated for its potential to reduce the risk of ovarian cancer development and progression. Aspirin inhibits NF-κB, COX, and the PI3K/mTOR signaling pathway, concurrently activating AMPK (224). Some studies suggest that regular aspirin use may be associated with a reduced risk of OC incidence and mortality (225). Aspirin was shown to inhibit the proliferation of OCT2 and OVCAR-3 cells and to reduce PPARδ function by inhibiting ERK1/2 (226). Therefore, NSAIDs show promise as therapeutic treatments against OC; however, dosage seems to be a key feature requiring further investigation (158).

Cancer chemotherapeutic treatment often results in a significant upregulation of transmembrane efflux pumps, which contribute to the development of multiple drug resistance, a major impediment in effective cancer treatment. Highly resistant tumors might be eradicated using chemosensitizers that block the efflux of the drug and increase the entry of the drug into the cell (227). In this regard, sertraline is a selective serotonin reuptake inhibitor, commonly prescribed for the treatment of various mental health conditions, particularly depression, anxiety disorders, obsessive-compulsive disorder, and panic disorder (228). Sertraline increases the levels of serotonin, a neurotransmitter in the brain, which is believed to have a positive impact on mood and emotional well-being (229). For instance, P-glycoprotein (P-gp) is a transmembrane efflux pump that actively transports and eliminates drugs and other chemical compounds from cells. This protective function prevents the buildup of potentially harmful substances within cells, negatively impacting the therapeutic effectiveness of the drugs. Thus, P-gp is linked to multidrug resistance observed in cancer cells that develop resistance to multiple chemotherapeutic drugs (230). The significant implications for pharmacokinetics, where P-gp influences the absorption, distribution, and elimination of drugs, lead to altered bioavailability and distribution patterns for drugs that are substrates for P-gp (231). Certain drugs can either inhibit or induce P-gp activity, affecting the cellular concentrations of various substrate drugs. Ongoing research focuses on P-gp in drug development to enhance drug efficacy and address multidrug resistance, with efforts directed at designing drugs that can bypass or inhibit P-gp when necessary. This knowledge is essential for healthcare professionals and researchers navigating drug interactions and optimizing therapeutic outcomes. P-gp pumps are expressed and functional in the chemoresistant ovarian adenocarcinoma cell line OVCAR-8 and in the derived drug-resistant models (human ovarian adenocarcinoma cell line NCI/ADR-Res (NAR) cells) (227). Among these, sertraline has been shown to enhance the

cytotoxicity of DOX and reduce DOX efflux in NAR cells (227). Studies conducted in human ovarian adenocarcinoma xenograft models demonstrated that combining sertraline with DOXIL® (pegylated liposomal DOX) effectively reverses multiple drug resistance (MDR). Sertraline acts as a chemosensitizer by blocking extrusion pumps, thereby allowing the drug delivered via the nanomedicine to accumulate inside the cell (227). Hence, the combined therapy of nanomedicine with chemosensitizers like sertraline is poised to amplify therapeutic responses in highly resistant tumors. This approach increases drug influx through nanomedicine while reducing drug efflux by employing a chemosensitizer (227). Moreover, findings from a xenograft murine model revealed that combining sertraline with DOX significantly enhances cytotoxicity, delaying tumor growth and improving survival rates by 1.5-fold (227). This combined treatment holds promise in mitigating multiple drug resistance phenotypes attributed to P-gp pumps, such as Multidrug Resistance 1 (MDR1, also known as ABCB1), which are ATP-dependent efflux pumps of the ABC protein superfamily (227, 232).

Thalidomide was initially marketed as a sedative-hypnotic drug with anti-emetic activity against morning sickness of early pregnancy, but was withdrawn from the market in the early sixties as it was found to cause severe fetal malformations (233–235). It is a medication with immunomodulatory and antiangiogenic properties that has been investigated for its potential to inhibit tumor growth and angiogenesis in ovarian cancer. Studies suggest that thalidomide may exert anticancer effects by modulating immune responses and disrupting tumor microenvironment interactions (10). Thalidomide inhibits TNF-α production in lipopolysaccharide-stimulated monocytes (236). Thalidomide decreased the capacity of SKOV-3 cells and primary epithelial ovarian carcinoma cells to secrete TNF-α, but this drug did not significantly affect the proliferation and growth of SKOV-3 cells (237). Thalidomide notably decreased the capacity of SKOV-3 cells to secrete MMP-9 and MMP-2, yet it did not have the same effect on primary epithelial ovarian carcinoma cells. However, thalidomide did not affect the secretion of IL-6 in either SKOV-3 cells or primary epithelial ovarian carcinoma cells (237). Thalidomide inhibits the processing of the *TNF-α* and the angiogenic factor *VEGF* transcripts (238). Sixty-six patients, comprising 37 women and 29 men, with advanced cancer (19 ovarian, 18 renal, 17 melanoma, 12 breast cancer) received daily treatments ofthalidomide at a dose of 100 mg. Out of the 18 patients with renal cancer, three showed partial responses, and an additional three patients experienced disease stabilization for up to 6 months. Although no conclusive responses were observed in patients, there was an improvement in the sleep quality ($P<0.05$) and preserved appetite ($P<0.05$) in these individuals (239). Women (138) diagnosed with biochemical-recurrent epithelial OC, primary peritoneal cancer, or fallopian tube carcinoma were eligible for a randomized phase III trial of tamoxifen versus thalidomide (240). Results suggested that thalidomide treatment was associated with a similar risk of progression (HR=1.31, 95% confidence interval [CI] =0.93–1.85), an increased risk of death (HR=1.76, 95% CI=1.16–2.68) and more grades 3 and 4 toxicities (55% versus 3%) in comparison with tamoxifen treatment (240). Therefore, thalidomide was not more effective than tamoxifen in delaying recurrence or death but was more toxic (240).

Repurposed kinase inhibitors

Several kinase inhibitors, originally developed for different pathologies, have been investigated for their potential to target specific signaling pathways implicated in OC. Examples include dasatinib, a Src kinase inhibitor, and imatinib, a BCR-ABL tyrosine kinase inhibitor, which have shown promise in preclinical studies of ovarian cancer (241).

Dasatinib is an inhibitor of Src/Abl family kinases used for the treatment of Philadelphia chromosome-positive acute lymphoblastic leukemia or chronic myeloid leukemia (242). Dasatinib inhibited cell growth by partially inducing apoptosis with a significant effect in autophagy activation in the SKOV3 and Hey cell lines (243). Dasatinib reduced the phosphorylation of AKT, mTOR, p70S6K, and S6 kinase expression and reduced Bcl-2 expression and activity. Dasatinib induces autophagy in Hey and SKOV3 cells that partially depends on beclin 1, AKT and Bcl-2. Overexpression of Bcl-2 partially prevented dasatinib-induced autophagy. In a Hey xenograft model, dasatinib inhibited tumor growth and induced both autophagy and apoptosis (243). Elevated levels of p-Src (phosphorylated Src family tyrosine kinases) protein expression were detected in A2780, HO8910, OVCAR3, CAOV3, and COC1 cell lines compared to healthy cells. This observation suggests activation of the Src signaling pathway (244). Combining dasatinib and paclitaxel significantly inhibited proliferation and boosted apoptosis in A2780 and HO8910 cells compared to controls. This combination showed tumor growth inhibitory rates of 76.7% and 58.5% in A2780 and HO8910 cell lines, respectively, outperforming paclitaxel treatment alone (244). In A2780 and HO8910 xenografts models, dasatinib treatment inhibited tumor growth by 43.2% and 34.0%, respectively (244). Paclitaxel treatment increased Src activation in Hey OC cells, inducing the expression of EpCAM (epithelial cell adhesion molecule) marker expression in Hey cells, while upregulated the expression of SSEA-4 (stage-specific embryonic antigen-4) and CD133 (prominin 1) markers (245). In this sense, dasatinib combined with paclitaxel significantly suppressed p-Src in Hey cells and xenografts but had no effect on the expression of these markers (245). However, this combination did not enhance the proliferative, tumorigenic, and vasculogenic of paclitaxel alone in HEY cell-induced ovarian tumors (245). Importantly, administration of dasatinib and paclitaxel in murine models reduced the invasion of cancer cells into the pancreas and liver, major organs affected by ovarian tumor metastasis. Thus, the evidence points to a significant potential of dasatinib in targeting intra-peritoneal dissemination of OC (245).

Imatinib inhibits the proliferation of several OC cell lines (C272-hTert/E7, C889/hTert, CSOC848, CSOC908, and CSOC918) that expressed elevated levels of PDGFRα (platelet-derived growth factor receptor α) (246). SKOV3 and CAOV3

cells do not express PDGFRα are insensitive to the effects of imatinib, suggesting that the inhibition of cell proliferation by imatinib is in a PDGFRα-specific manner. Imatinib induces antiproliferative effects by arresting cell progression at G0-G1 and impeding advancement through the S phase. Additionally, at a concentration of 1 μm, Imatinib inhibits both PDGFRα and Akt phosphorylation (246). However administration of imatinib to patients with epithelial OC, had minimal effect as a single treatment (247). A phase II trial of imatinib administered to patients with platinum-resistant OC, showed that imatinib mesylate, when used alone, lacks significant clinical efficacy in c-Kit and/or PDGFR positive, recurrent OC, particularly in heavily pretreated patients (248). Thus, imatinib may be considered as a supplementary drug to be used in combination with other treatments.

Hormonal therapy is an emerging treatment that utilizes hormones or hormone-blocking agents to interfere with the growth and progression of OC cells. While hormonal therapy is not a standard treatment for most OC, it may be considered in specific cases where the cancer cells express hormone receptors, such as ER and PR. This strategy can be particularly useful for endometrioid OC and some ovarian stromal tumors that may express these hormone receptors. Among the drugs utilized in hormonal therapy is tamoxifen, a Selective ER Modulator (SERM) commonly used in breast cancer treatment and has been investigated in some cases of OC with hormone receptor expression (249, 250). Aromatase inhibitors, such as letrozole and anastrozole, which prevent the synthesis of estrogen, are mainly used in the treatment of breast cancer and oftentimes as fertility treatments, are sometimes used in ER+ OC cases (251–255). In a phase II trial involving 50 patients with relapsed ovarian cancer, the antitumor activity of letrozole was assessed using Union International Contre Cancer (UICC) and CA125 (cancer antigen 125) marker criteria. Tumors categorized as stable disease by UICC criteria showed significantly higher ER (P=0.027) and PR (P=0.0066) values compared to those categorized as progressive disease (251). The combined presence of these receptors strongly correlated with stable disease (P<0.0001). Similarly, according to CA125 criteria, tumors with higher ER (P=0.013), lower erbB2 (P=0.026), and higher epidermal growth factor receptor (P=0.009) levels were associated with CA125 stable/responsive disease compared to progressive disease (251). In another phase II trial, letrozole was administered at a daily dosage of 2.5 mg until either clinical or marker evidence indicated disease progression. This trial focused on ER-positive OC patients with rising CA125 levels, indicative of progression according to Rustin's criteria (252). Among the 42 patients assessed for CA125 response, 7 (17%) showed a response, defined as a decrease of more than 50%, while 11 (26%) patients did not experience progression, indicated by a doubling of CA125 levels, after 6 months of treatment (252). Of the 33 patients evaluable for radiological response, 3 (9%) had a partial remission, and 14 (42%) had stable disease at 12 weeks (252). Subgroup analysis based on ER status showed CA125 response rates of 0% (immunoscore of 150-199), 12% (immunoscore of 200-249), and 33% (immunoscore of 250-300), with a significant trend observed (P = 0.028, $\chi 2$ for trend). Additionally, expression levels of HER2, insulin-like growth factor binding protein 5 (IGFBP5), trefoil factor 1 (TFF1), and vimentin correlated with changes in CA125 levels during treatment (252). Finally, a 2.5 mg daily oral dose of letrozole was administrated to thirty-three women with recurrent ER+ epithelial ovary or peritoneum carcinoma enrolled in a phase II trial (253). Among these patients, 26% of the individuals diagnosed with ER^{-+}, platinum- and taxane-resistant high-grade ovarian and primary peritoneal cancer who received letrozole treatment experienced a clinical benefit, defined as either stabilization of disease or partial response (3% of patients) (253).

Ormeloxifene is a SERM primarily used as an oral contraceptive and for the treatment of conditions related to the female reproductive system. It inhibits the action of estrogen on the uterus, leading to changes in the cervical mucus chemistry and endometrium. These physiological changes create a challenging environment for the sperm to reach the egg and for a fertilized egg to successfully implant in the uterus. In the context of OC repurposing, *in vitro* experiments showed that ormeloxifene hindered cell proliferation and triggered apoptosis in cisplatin-resistant in the A2780, A2780-CP and SKOV-3 cell lines (256). At the molecular level, ormeloxifene reduced AKT phosphorylation, enhanced p53 phosphorylation, and altered the synthesis and localization patterns of cyclin D1, cyclin E, p27, and CDK2 (256). In xenograft murine models, injecting 50 or 100 μg ormeloxifene once a week for 5 weeks reduced tumorigenesis and metastasis within the peritoneal cavity (256). Within 2 weeks of A2780-CP cell injection, all mice treated with vehicle displayed a swollen abdomen, indicative of ascites formation, along with significant peritoneal carcinomatosis and numerous solid tumors (256). Conversely, mice treated with 100 μg of ormeloxifene showed no detectable tumors (256). This suggests that ormeloxifene holds promise as a compound for OC treatment. Despite the potential benefits, hormonal therapy is not widely used in OC yet and is only considered when other standard treatments are not effective and in specific cases of OC patients expressing the hormone receptors. It is noteworthy that while hormonal therapy has potential in OC treatment, standard treatments such as surgery and chemotherapy remain the mainstay of ovarian cancer management. As clinical research and trials progress, this treatment option may become an efficient alternative to OC care.

Model-informed drug repurposing

Model-informed drug repurposing (MIDR) might be used to accelerate the repositioning of drugs (257). MIDR is a rapidly expanding *in silico* approach to drug discovery and development that involves mathematical models, computational tools, and data-driven techniques to identify new therapeutic uses for existing drugs (257). The development of powerful computational methods, such as bioinformatics, systems biology, and quantitative pharmacology modeling, and the combination of these techniques, allow the

analysis of large datasets to identify potential connections between drugs and diseases. This is further achieved by consolidating diverse data sources, such as genomic, transcriptomic, proteomic, and clinical records. In addition, network pharmacology, as well as pharmacokinetic and pharmacodynamic modeling, further refine the understanding of complex interactions among drugs, targets, and diseases. Ultimately, these approaches are now being integrated into machine learning algorithms and artificial intelligence pipelines to combine complex datasets and efficiently predict drug-disease relationships. These *in silico* models can also help identify synergistic effects of drug combinations for improved therapeutic outcomes. This powerful experimental approach is now being utilized in the treatment of cancer.

As an example, a recent report that involved a literature search coupled to *in silico* analyses and screening process involving preclinical research, explored the testing of approved compounds for human use in treating OC (258). The combination of these approaches rendered four compounds used regularly in the clinic, metformin, celecoxib, lurbinectedin, and 5-azacytidine, as drugs with significant potential for repurposing in the context of myeloid-derived suppressor cells (MDSC) within the OC tumor microenvironment (258). MDSC suppresses the immune response in OC through several mechanisms; therefore, finding potential drug candidates for repositioning has been a challenging process (258). As example is the emerging evidence for lurbinectedin, a synthetic compound derived from the marine organism *Ecteinascidia turbinate*. lurbinectedin is an alkylating anticancer drug. It targets specific DNA repair mechanisms in cancer cells, leading to DNA damage and cell death (259). Lurbinectedin decreases myeloid-derived suppressor cell (MDSC) percentages *in vitro* in chronic lymphocytic leukemia (CLL) patient-derived studies (260). It induces cell death in a dose and time-dependent manner and reduces the expression of chemokine receptor CCR7 implicated in B-CLL cell migration (260). Notably, malignant B cells from patients with clinical lymph node involvement exhibit higher trans-endothelial cell migration (TEM) in response to CCL21 and CCL19 compared to those without such organomegaly (260). There is a correlation between CCR7 expression, receptor for both CCL21 and CCL19, and clinical lymphadenopathy, and blocking CCR7 suppresses TEM of CLL cells (260). Lurbinectedin has shown promise in treating various solid tumors, including small-cell lung cancer and relapsed OC (261). This drug received accelerated approval from the U.S. FDA for metastatic small-cell lung cancer that has progressed after platinum-based chemotherapy (262). *In vitro* studies revealed significant antitumor effects of lurbinectedin on both chemosensitive and chemoresistant clear cell carcinoma (CCC) of the ovary cells (RMG1, RMG2, KOC7C, and HAC2) (263). Evaluation of mouse CCC cell xenografts confirmed that lurbinectedin effectively suppressed tumor growth. Notably, combining lurbinectedin with SN-38 (7-ethyl-10-hydroxycamptothecin) demonstrated a significant synergistic effect, particularly evident in both cisplatin-resistant and paclitaxel-resistant CCC cell lines. These findings indicate potent antitumor activity of lurbinectedin in both cisplatin-sensitive and cisplatin-resistant OC (263). Furthermore, lurbinectedin is under investigation in clinical trials for potential efficacy in other cancer types, including advanced ovarian, endometrial, and breast cancers, relapsed hematological malignancies like acute myeloid leukemia (AML) and lymphomas, and soft tissue sarcomas including liposarcoma and leiomyosarcoma (261, 264, 265). Combination therapies involving lurbinectedin are being assessed, including with immune checkpoint inhibitors, PARP inhibitors, and other targeted therapies, to explore potential synergistic effects.

Celecoxib, a selective COX-2 inhibitor used to treat pain and inflammation, has been investigated for its potential to inhibit OC growth and metastasis. Evidence suggested that celecoxib may exert anticancer effects in OC cells by inhibiting COX-2-mediated signaling pathways involved in tumor progression (266). In areas of active tumor growth in a murine model for mesothelioma, large numbers of MDSCs co-localize with COX-2 expression (267). Celecoxib effectively reduced PGE2 levels both *in vitro* (mesothelioma AB1 cell line) and *in vivo* (BALB/c mice) (267). Furthermore, celecoxib treatment decreased levels of ROS in immature myeloid subtypes (MO-MDSC, PMN-MDSC, and Gr-1lowSubset 2) from the spleen of tumor-bearing mice and improved cytotoxic T cell function (267). Ten days after injection with a lethal dose of 0.5×10^6 AB1 tumor cells, the absolute number of MDSCs was significantly lower in mice receiving the celecoxib diet compared with mice receiving the control diet. This difference was more pronounced at day 22 after tumor injection, and mice receiving the celecoxib diet did not exhibit any discernible side effects (267). These findings highlight the potential of celecoxib as an adjunctive therapy in cancer treatment strategies.

Finally, 5-azacytidine is a nucleoside analog that is incorporated into DNA and RNA and inhibits DNA methyltransferase enzymes leading to subsequent DNA hypomethylation. It is primarily used as a demethylating agent in the treatment of certain hematological malignancies, particularly myelodysplastic syndromes, where it can help to restore normal hematopoiesis by reversing aberrant DNA methylation patterns (268–270). The inhibition of methylation via 5-azacytidine increases the formation of invadopodia and enhances the extracellular matrix degradation in SKOV3 and A2780 cells and further promotes cell migration and invasion of SKOV3 cells (271). Moreover, in SKOV3 cells, 5-azacytidine induce the expression of genes and proteins involved in actin-regulating signaling pathways [*PIK3CA* (phosphatidylinositol-4,5-bisphosphate 3-kinase catalytic subunit alpha), *SRC* (SRC proto-oncogene, non-receptor tyrosine kinase), *RhoC* (ras homolog family member C), *RhoA* (ras homolog family member A), *RAC1* (Rac family small GTPase 1), and *AFAP* (actin filament associated protein 1) (271). Furthermore, the 5-azacytidine increased the phosphorylation of AKT and p110 alpha (PI3-kinase isoform), suggesting that the PI3K-AKT pathway is activated in SKOV3 and A2780 cells (271). In mouse xenograft models, 5-azacytidine treatment suppressed tumor growth and increased the occurrence of metastatic nodules, indicating an enhanced metastatic potential due to DNA demethylation (271). Methylation inhibition led to increased transcription of PIK3CA and upregulation of genes associated with the PI3K-AKT signaling pathway (271). This induction likely occurs through epigenetic regulation of *PIK3CA*, as analysis of DNA methylation levels in the *PIK3CA* promoter region indicated decreased methylation of CpG islands in SKOV3 and A2780 cells following 5- azacytidine treatment (271). The impact of trichostatin A (TSA) and 5-azacytidine (5-aza-

2′-deoxycytidine), either alone or in conjunction with low-dose cisplatin, was assessed on Hey, SKOV3 and A2780 lines *in vitro* (272). Combined treatment exhibited superior efficacy compared to individual drugs and notably suppressed cell viability, migration, and spheroid formation and growth in Hey, SKOV3 and A2780 cells (272). Sequential administration of cisplatin (1 mg kg^{-1}) followed by TSA (0.3 mg kg^{-1}) significantly suppressed the tumorigenicity of Hey xenografts by inhibiting the expression of epithelial to mesenchymal transition (EMT) markers (Twist, Snail, Slug, E-cadherin, and N-cadherin), and reducing the pluripotency of ovarian cancer cells (272). Finally, a clinical trial in patients with platinum-resistant OC showed the effect of oral 5-azacytidine in combination with pembrolizumab (NCT02900560). Pembrolizumab is a monoclonal antibody medication used as immune checkpoint inhibitor for immunotherapy of various types of cancer (273). This study helped to establish an optimal dosing schedule for oral azacitidine in combination with pembrolizumab for platinum-resistant/refractory OC patients (274). Additional preclinical studies using 5-azacytidine alone and in combination with a small molecule histone deacetylase (HDAC) inhibitor, entinostat, showed high potential in OC treatment as well (258).

Despite the enticing results from the *in silico* analyses, it is important to note that it is of the essence to perform subsequent *in vitro* and *in vivo* validations prior to clinical applications. However, computational approaches can provide information and further hypotheses for model-informed drug repurposing. As summarized in this review, Figure 5 provides a schematic representation of central metabolic pathways associated with the anti-tumor activities of repurposed drugs. This overview encompasses antiparasitic drugs, antiretrovirals, antibiotics, hypocholesterolemia treatments, and other drugs and metabolites.

Conclusion

This review provides valuable insights into the utility of drug repositioning for OC treatment, highlighting the importance of cell line and animal models in initial screening and drug testing.

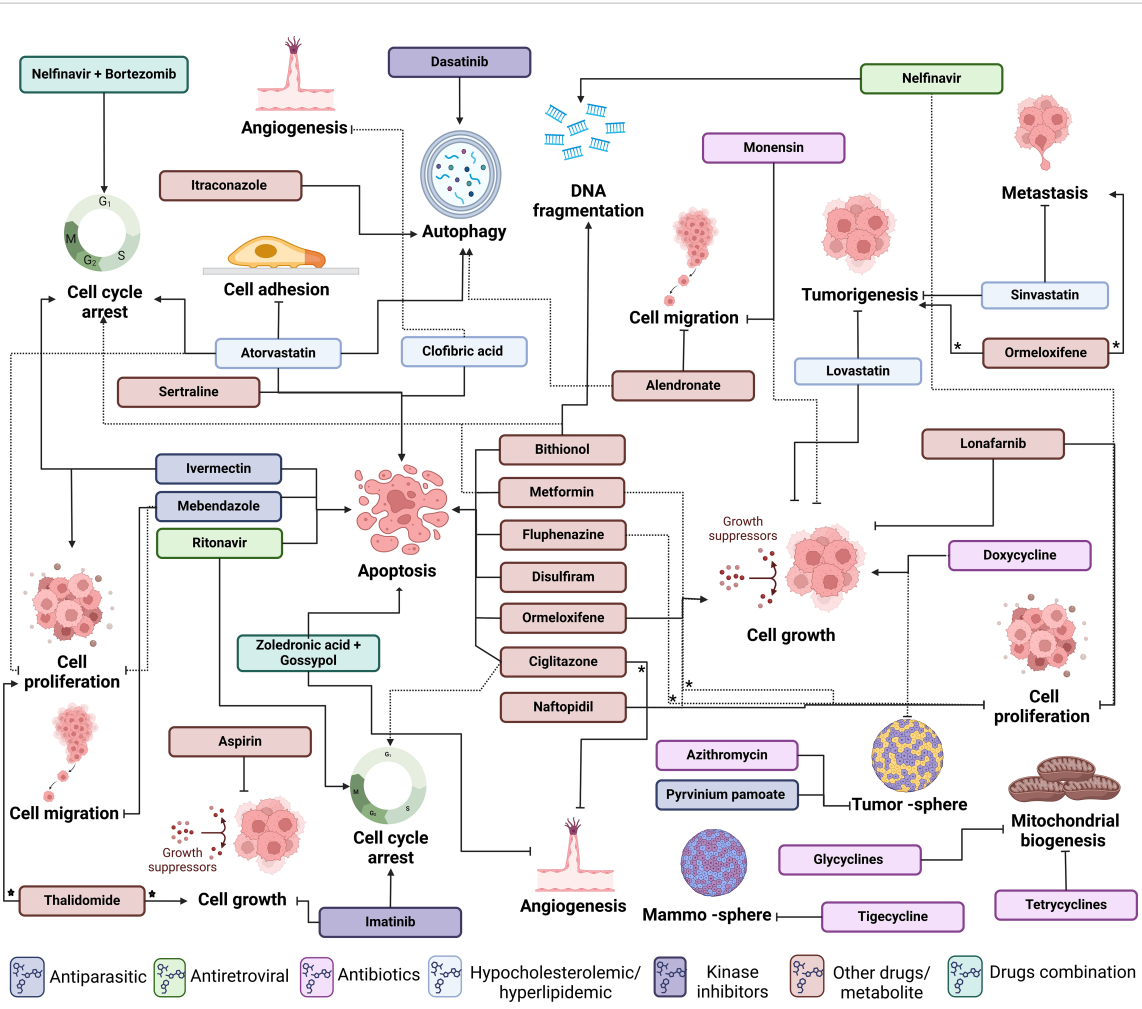

FIGURE 5
Cancer hallmarks involved in the drug reposition for ovarian cancer treatment. Schematic representation of the main metabolic pathways related to anti-tumor activities of repositioned drugs. The summary includes antiparasitic drugs (dark blue boxes), antiretroviral (light green boxes), antibiotics (grape boxes), compounds to treat hypocholesterolemia (light blue boxes), and other drugs and metabolites (red boxes). Compounds used in combinatorial treatments are also represented (dark green boxes). Induction (→), reduction (*), or inhibition (⊣) of the cancer hallmarks is indicated within the figure (Figure created with Biorender).

Although clinical translation remains in its early stages, these models form a crucial foundation for future studies. Overcoming the challenges of translating preclinical findings into successful human therapies will require careful consideration of drug interactions, personalized medicine approaches, and extensive clinical validation. We provided a critical discussion of the potential of drug repositioning for OC treatment, highlighting current advances in the area, which does not represent a clinical investigation. Our analysis focused on *in vitro* experiments across multiple cancer cell lines and short-term *in vivo* models, and the limited information available from clinical trials. The discussion revealed encouraging evidence of the efficacy of existing drugs in targeting OC. Despite these promising findings, we recognize the limitations inherent in *in vitro* and preclinical models. These systems, while informative, fail to capture the full complexity, heterogeneity, and microenvironment of OC in human patients, which limits the direct translation of findings to clinical practice. Key challenges include differences in pharmacokinetics and pharmacodynamics between preclinical models and human systems, which may influence therapeutic efficacy and safety profiles. Furthermore, *in vivo* and *in vitro* studies do not account for the complex pharmacological interactions that occur in real-world scenarios, such as those between drugs, dietary supplements, and food, which could either amplify or attenuate therapeutic effects. Careful optimization of dosing regimens is crucial to balance efficacy and minimize adverse outcomes. Looking forward, systematic approaches that integrate high-throughput screening, computational modeling, and patient-derived models offer a path to refining drug combinations and tailoring therapies to individual patients. These methodologies, combined with biomarker-driven approaches, enable the identification of molecular pathways most relevant to OC progression and therapeutic response. Leveraging genomics and proteomics can further clarify the pharmacokinetics and pharmacodynamics of repositioned drugs, supporting their clinical application.

Drug repositioning is particularly advantageous in oncology due to its ability to shorten the timeline for bringing effective therapies to patients, compared to the 10 - 15 years typically required for *de novo* drug development, as evidenced above. Despite the potential usage of a wide range of available drugs, the clinical validation of these therapies requires robust longitudinal studies and clinical trials to assess safety, efficacy, and optimal combination strategies in the context of OC. Ultimately, drug repositioning holds significant promise for overcoming challenges in OC treatment, particularly drug resistance. By addressing pharmacokinetic challenges, optimizing dosing strategies, and incorporating personalized medicine principles, repositioned drugs can offer cost-effective and innovative solutions. Nonetheless, clinical trials remain indispensable to substantiating preclinical findings and ensuring that repositioned therapies fulfill their potential in improving outcomes for OC patients. This review point to the critical role of multidisciplinary approaches in advancing the utility of drug repositioning for OC, with the ultimate goal of enhancing patient survival and quality of life.

Author contributions

EV-V: Data curation, Investigation, Writing – original draft. FM-C: Data curation, Investigation, Writing – original draft. OR-H: Conceptualization, Funding acquisition, Project administration, Resources, Supervision, Writing – review & editing. AB-G: Data curation, Writing – original draft. LB-M: Data curation, Investigation, Software, Writing – original draft. TP-B: Data curation, Funding acquisition, Investigation, Writing – review & editing. LQ-G: Investigation, Writing – original draft, Writing – review & editing. GF-G: Conceptualization, Funding acquisition, Project administration, Resources, Supervision, Writing – review & editing.

Funding

The author(s) declare financial support was received for the research, authorship, and/or publication of this article. This work was supported by PAPIIT (projects IA208422 and IA206724 awarded to GF-G and projects IN222321 and IN221824 awarded to OR-H). EV-V is a recipient of a postdoctoral fellowship from Dirección General de Asuntos del Personal Académico (DGAPA) from Universidad Autónoma de Mexico (UNAM). TP-B and AB-G were supported by Wesleyan University institutional funds.

Conflict of interest

The authors declare that the research was conducted in the absence of any commercial or financial relationships that could be construed as a potential conflict of interest.

The author(s) declared that they were an editorial board member of Frontiers, at the time of submission. This had no impact on the peer review process and the final decision.

Generative AI statement

The author(s) declare that no Generative AI was used in the creation of this manuscript.

Publisher's note

References

1. Banno K, Iida M, Yanokura M, Irie H, Masuda K, Kobayashi Y, et al. Drug repositioning for gynecologic tumors: a new therapeutic strategy for cancer. *Sci World J*. (2015) 2015:1–10. doi: 10.1155/tswj.v2015.1

2. Power A, Berger AC, Ginsburg GS. Genomics-enabled drug repositioning and repurposing: insights from an IOM Roundtable activity. *Jama*. (2014) 311:2063–4. doi: 10.1001/jama.2014.3002

3. Hernandez L, Kim MK, Lyle LT, Bunch KP, House CD, Ning F, et al. Characterization of ovarian cancer cell lines as *in vivo* models for preclinical studies. *Gynecol Oncol*. (2016) 142:332–40. doi: 10.1016/j.ygyno.2016.05.028

4. Qin T, Fan J, Lu F, Zhang L, Liu C, Xiong Q, et al. Harnessing preclinical models for the interrogation of ovarian cancer. *J Exp Clin Cancer Res*. (2022) 41:277. doi: 10.1186/s13046-022-02486-z

5. Mirabelli P, Coppola L, Salvatore M. Cancer cell lines are useful model systems for medical research. *Cancers (Basel)*. (2019) 11:1–18. doi: 10.3390/cancers11081098

6. Li Z, Zheng W, Wang H, Cheng Y, Fang Y, Wu F, et al. Application of animal models in cancer research: recent progress and future prospects. *Cancer Manag Res*. (2021) 13:2455–75. doi: 10.2147/CMAR.S302565

7. Zhou Y, Xia J, Xu S, She T, Zhang Y, Sun Y, et al. Experimental mouse models for translational human cancer research. *Front Immunol*. (2023) 14:1095388. doi: 10.3389/fimmu.2023.1095388

8. Overgaard NH, Fan TM, Schachtschneider KM, Principe DR, Schook LB, Jungersen G. Of mice, dogs, pigs, and men: choosing the appropriate model for immuno-oncology research. *ILAR J*. (2018) 59:247–62. doi: 10.1093/ilar/ily014

9. Berek JS, Hacker NF. *Berek and Hacker's gynecologic oncology*. United States: Lippincott Williams & Wilkins (2010).

10. Jayson GC, Kohn EC, Kitchener HC, Ledermann JA. Ovarian cancer. *Lancet*. (2014) 384:1376–88. doi: 10.1016/S0140-6736(13)62146-7

11. Sung H, Ferlay J, Siegel RL, Laversanne M, Soerjomataram I, Jemal A, et al. Global cancer statistics 2020: GLOBOCAN estimates of incidence and mortality worldwide for 36 cancers in 185 countries. *CA: Cancer J Clin*. (2021) 71:209–49. doi: 10.3322/caac.21660

12. Huang J, Chan WC, Ngai CH, Lok V, Zhang L, Lucero-Prisno DE III, et al. Worldwide burden, risk factors, and temporal trends of ovarian cancer: A global study. *Cancers*. (2022) 14:2230. doi: 10.3390/cancers14092230

13. Young R. *WHO classification of tumours of female reproductive organs. Monodermal teratomas and somatic-type tumours arising from a dermoid cyst*. France: International Agency for Research on Cancer, Vol. 63-6. (2014).

14. Lheureux S, Gourley C, Vergote I, Oza AM. Epithelial ovarian cancer. *Lancet*. (2019) 393:1240–53. doi: 10.1016/S0140-6736(18)32552-2

15. Barnes BM, Nelson L, Tighe A, Burghel GJ, Lin I-H, Desai S, et al. Distinct transcriptional programs stratify ovarian cancer cell lines into the five major histological subtypes. *Genome Med*. (2021) 13:1–19. doi: 10.1186/s13073-021-00952-5

16. Kurman RJ, Carcangiu ML, Herrington CS. *World Health Organisation classification of tumours of the female reproductive organs*. Geneva, Switzerland: International agency for research on cancer (2014).

17. Malpica A, Deavers MT, Lu K, Bodurka DC, Atkinson EN, Gershenson DM, et al. Grading ovarian serous carcinoma using a two-tier system. *Am J Surg Pathol*. (2004) 28:496–504. doi: 10.1097/00000478-200404000-00009

18. Slomovitz B, Gourley C, Carey MS, Malpica A, Shih I-M, Huntsman D, et al. Low-grade serous ovarian cancer: state of the science. *Gynecologic Oncol*. (2020) 156:715–25. doi: 10.1016/j.ygyno.2019.12.033

19. Ahn G, Folkins AK, McKenney JK, Longacre TA. Low-grade serous carcinoma of the ovary. *Am J Surg Pathol*. (2016) 40:1165–76. doi: 10.1097/PAS.0000000000000693

20. Soovares P, Pasanen A, Similä-Maarala J, Bützow R, Lassus H. Clinical factors and biomarker profiles associated with patient outcome in endometrioid ovarian carcinoma-Emphasis on tumor grade. *Gynecologic Oncol*. (2022) 164:187–94. doi: 10.1016/j.ygyno.2021.10.078

21. Hollis RL, Thomson JP, Stanley B, Churchman M, Meynert AM, Rye T, et al. Molecular stratification of endometrioid ovarian carcinoma predicts clinical outcome. *Nat Commun*. (2020) 11:4995. doi: 10.1038/s41467-020-18819-5

22. Köbel M, Rahimi K, Rambau PF, Naugler C, Le Page C, Meunier L, et al. An immunohistochemical algorithm for ovarian carcinoma typing. *Int J Gynecological Pathol*. (2016) 35:430. doi: 10.1097/PGP.0000000000000274

23. McCluggage WG. Morphological subtypes of ovarian carcinoma: a review with emphasis on new developments and pathogenesis. *Pathology*. (2011) 43:420–32. doi: 10.1097/PAT.0b013e328348a6e7

24. Iida Y, Okamoto A, Hollis RL, Gourley C, Herrington CS. Clear cell carcinoma of the ovary: a clinical and molecular perspective. *Int J Gynecologic Cancer*. (2020) 34:ijgc–2020-001656. doi: 10.1136/ijgc-2020-001656

25. Kang EY, Cheasley D, LePage C, Wakefield MJ, da Cunha Torres M, Rowley S, et al. Refined cut-off for TP53 immunohistochemistry improves prediction of TP53 mutation status in ovarian mucinous tumors: implications for outcome analyses. *Modern Pathol*. (2021) 34:194–206. doi: 10.1038/s41379-020-0618-9

26. Network CGAR. Integrated genomic analyses of ovarian carcinoma. *Nature*. (2011) 474:609. doi: 10.1038/nature10166

27. Baldwin RL, Nemeth E, Tran H, Shvartsman H, Cass I, Narod S, et al. BRCA1 promoter region hypermethylation in ovarian carcinoma: a population-based study. *Cancer Res*. (2000) 60:5329–33.

28. Hilton JL, Geisler JP, Rathe JA, Hattermann-Zogg MA, DeYoung B, Buller RE. Inactivation of BRCA1 and BRCA2 in ovarian cancer. *J Natl Cancer Institute*. (2002) 94:1396–406. doi: 10.1093/jnci/94.18.1396

29. Strathdee G, Appleton K, Illand M, Millan DW, Sargent J, Paul J, et al. Primary ovarian carcinomas display multiple methylator phenotypes involving known tumor suppressor genes. *Am J Pathol*. (2001) 158:1121–7. doi: 10.1016/S0002-9440(10)64059-X

30. Wang C, Horiuchi A, Imai T, Ohira S, Itoh K, Nikaido T, et al. Expression of BRCA1 protein in benign, borderline, and Malignant epithelial ovarian neoplasms and its relationship to methylation and allelic loss of the BRCA1 gene. *J Pathology: A J Pathological Soc Great Britain Ireland*. (2004) 202:215–23. doi: 10.1002/path.v202:2

31. Prat J, Oncology FCoG. Staging classification for cancer of the ovary, fallopian tube, and peritoneum. *Int J Gynecology Obstetrics*. (2014) 124:1–5. doi: 10.1016/j.ijgo.2013.10.001

32. Height T. *Ovarian Epithelial, Fallopian Tube, and Primary Peritoneal Cancer Treatment (PDQ®) Health Professional Version*. United States: National Cancer Institute (2024).

33. Society AC. *Ovarian Cancer Stages*. United States: American Cancer Society (2020).

34. Momenimovahed Z, Tiznobaik A, Taheri S, Salehiniya H. Ovarian cancer in the world: epidemiology and risk factors. *Int J women's Health*. (2019) 11:287–99. doi: 10.2147/IJWH.S197604

35. Antoniou A, Pharoah PD, Narod S, Risch HA, Eyfjord JE, Hopper JL, et al. Average risks of breast and ovarian cancer associated with BRCA1 or BRCA2 mutations detected in case series unselected for family history: a combined analysis of 22 studies. *Am J Hum Genet*. (2003) 72:1117–30. doi: 10.1086/375033

36. Lu HK, Broaddus RR. Gynecologic cancers in Lynch syndrome/HNPCC. *Familial Cancer*. (2005) 4:249–54. doi: 10.1007/s10689-005-1838-3

37. Salehi F, Dunfield L, Phillips KP, Krewski D, Vanderhyden BC. Risk factors for ovarian cancer: an overview with emphasis on hormonal factors. *J Toxicol Environ Health Part B*. (2008) 11:301–21. doi: 10.1080/10937400701876095

38. Beral V, Bull D, Green J, Reeves G. Ovarian cancer and hormone replacement therapy–Authors' reply. *Lancet*. (2007) 370:932–3. doi: 10.1016/S0140-6736(07)61437-8

39. Cancer CGoESoO. Ovarian cancer and smoking: individual participant meta-analysis including 28 114 women with ovarian cancer from 51 epidemiological studies. *Lancet Oncol*. (2012) 13:946–56. doi: 10.1016/S1470-2045(12)70322-4

40. Terry KL, Karageorgi S, Shvetsov YB, Merritt MA, Lurie G, Thompson PJ, et al. Genital powder use and risk of ovarian cancer: a pooled analysis of 8,525 cases and 9,859 controls. *Cancer Prev Res*. (2013) 6:811–21. doi: 10.1158/1940-6207.CAPR-13-0037

41. Braicu EI, Darb-Esfahani S, Schmitt WD, Koistinen KM, Heiskanen L, Pöhö P, et al. High-grade ovarian serous carcinoma patients exhibit profound alterations in lipid metabolism. *Oncotarget*. (2017) 8:102912. doi: 10.18632/oncotarget.22076

42. Minlikeeva AN, Freudenheim JL, Cannioto RA, Szender JB, Eng KH, Modugno F, et al. History of hypertension, heart disease, and diabetes and ovarian cancer patient survival: evidence from the ovarian cancer association consortium. *Cancer causes control*. (2017) 28:469–86. doi: 10.1007/s10552-017-0867-1

43. Shah MM, Erickson BK, Matin T, McGwin G Jr, Martin JY, Daily LB, et al. Diabetes mellitus and ovarian cancer: more complex than just increasing risk. *Gynecologic Oncol*. (2014) 135:273–7. doi: 10.1016/j.ygyno.2014.09.004

44. Zhang D, Li N, Xi Y, Zhao Y, Wang T. Diabetes mellitus and risk of ovarian cancer. A systematic review and meta-analysis of 15 cohort studies. *Diabetes Res Clin Pract*. (2017) 130:43–52. doi: 10.1016/j.diabres.2017.04.005

45. O'Donnell AJ, Macleod KG, Burns DJ, Smyth JF, Langdon SP. Estrogen receptor-α mediates gene expression changes and growth response in ovarian cancer cells exposed to estrogen. *Endocrine-related Cancer*. (2005) 12:851–66. doi: 10.1677/erc.1.01039

46. Chen Y, Zhang L, Liu W, Wang K. Case-control study of metabolic syndrome and ovarian cancer in Chinese population. *Nutr Metab*. (2017) 14:1–9. doi: 10.1186/s12986-017-0176-4

47. Ostrand-Rosenberg S. Myeloid-derived suppressor cells: more mechanisms for inhibiting antitumor immunity. *Cancer immunology immunotherapy*. (2010) 59:1593–600. doi: 10.1007/s00262-010-0855-8

48. Ness RB, Grisso JA, Cottreau C, Klapper J, Vergona R, Wheeler JE, et al. Factors related to inflammation of the ovarian epithelium and risk of ovarian cancer. *Epidemiology*. (2000) 11:111–7. doi: 10.1097/00001648-200003000-00006

49. Group UCSW. *US cancer statistics data visualizations tool, based on November 2018 submission data (1999–2016): US Department of Health and Human Services, Centers for Disease Control and Prevention and National Cancer Institute*. United States: Centers for Disease Control and Prevention and National Cancer Institute (2019).

50. Grossman DC, Curry SJ, Owens DK, Barry MJ, Davidson KW, Doubeni CA, et al. Screening for ovarian cancer: US preventive services task force recommendation statement. *Jama*. (2018) 319:588–94. doi: 10.1001/jama.2017.21926

51. Moorman PG, Palmieri RT, Akushevich L, Berchuck A, Schildkraut JM. Ovarian cancer risk factors in African-American and white women. *Am J Epidemiol*. (2009) 170:598–606. doi: 10.1093/aje/kwp176

52. Zheng L, Cui C, Shi O, Lu X, Li Y-K, Wang W, et al. Incidence and mortality of ovarian cancer at the global, regional, and national levels, 1990–2017. *Gynecologic Oncol*. (2020) 159:239–47. doi: 10.1016/j.ygyno.2020.07.008

53. Cabasag CJ, Fagan PJ, Ferlay J, Vignat J, Laversanne M, Liu L, et al. Ovarian cancer today and tomorrow: A global assessment by world region and Human Development Index using GLOBOCAN 2020. *Int J Cancer*. (2022) 151:1535–41. doi: 10.1002/ijc.v151.9

54. Gaona-Luviano P, Medina-Gaona LA, Magaña-Pérez K. Epidemiology of ovarian cancer. *Chin Clin Oncol*. (2020) 9:47. doi: 10.21037/cco-20-34

55. Chien J, Poole EM. Ovarian cancer prevention, screening, and early detection: report from the 11th biennial ovarian cancer research symposium. *Int J Gynecologic Cancer*. (2017) 27:S20–2. doi: 10.1097/IGC.0000000000001118

56. Baldwin LA, Huang B, Miller RW, Tucker T, Goodrich ST, Podzielinski I, et al. Ten-year relative survival for epithelial ovarian cancer. *Obstetrics Gynecology*. (2012) 120:612–8. doi: 10.1097/AOG.0b013e318264f794

57. Vargas AN. Natural history of ovarian cancer. *ecancermedicalscience*. (2014) 8:780–96. doi: 10.3332/ecancer.2014.465

58. Oncology NCPGi. *Ovarian Cancer. Including Fallopian Tube Cancer and Primary Peritoneal Cancer. Version 2.2020*. Plymouth Meeting, United States: National Comprehensive Cancer Network (2021).

59. Colombo N, Sessa C, du Bois A, Ledermann J, McCluggage WG, McNeish I, et al. ESMO–ESGO consensus conference recommendations on ovarian cancer: pathology and molecular biology, early and advanced stages, borderline tumours and recurrent disease. *Ann Oncol*. (2019) 30:672–705. doi: 10.1093/annonc/mdz062

60. Arora N, Talhouk A, McAlpine JN, Law MR, Hanley GE. Long-term mortality among women with epithelial ovarian cancer: a population-based study in British Columbia, Canada. *BMC cancer*. (2018) 18:1–9. doi: 10.1186/s12885-018-4970-9

61. Yao S, Wang W, Zhou B, Cui X, Yang H, Zhang S. Monensin suppresses cell proliferation and invasion in ovarian cancer by enhancing MEK1 SUMOylation. *Exp Ther Med*. (2021) 22:1–10. doi: 10.3892/etm.2021.10826

62. King M-C, Marks JH, Mandell JB. Breast and ovarian cancer risks due to inherited mutations in BRCA1 and BRCA2. *Science*. (2003) 302:643–6. doi: 10.1126/science.1088759

63. ICON, Research EOf, Neoplasm ToCCACIO. International Collaborative Ovarian Neoplasm trial 1 and Adjuvant ChemoTherapy In Ovarian Neoplasm trial: two parallel randomized phase III trials of adjuvant chemotherapy in patients with early-stage ovarian carcinoma. *J Natl Cancer Institute*. (2003) 95:105–12. doi: 10.1093/jnci/95.2.105

64. Trimbos JB, Vergote I, Bolis G, Vermorken JB, Mangioni C, Madronal C, et al. Impact of adjuvant chemotherapy and surgical staging in early-stage ovarian carcinoma: European Organisation for Research and Treatment of Cancer–Adjuvant ChemoTherapy In Ovarian Neoplasm trial. *J Natl Cancer Institute*. (2003) 95:113–25. doi: 10.1093/jnci/95.2.113

65. Ledermann J, Raja F, Fotopoulou C, Gonzalez-Martin A, Colombo N, Sessa C. Newly diagnosed and relapsed epithelial ovarian carcinoma: ESMO Clinical Practice Guidelines for diagnosis, treatment and follow-up. *Ann Oncol*. (2013) 24:vi24–32. doi: 10.1093/annonc/mdt333

66. Ashing-Giwa K, Ganz PA, Petersen L. Quality of life of African-American and white long term breast carcinoma survivors. *Cancer: Interdiscip Int J Am Cancer Soc*. (1999) 85:418–26. doi: 10.1002/(SICI)1097-0142(19990115)85:2<418::AID-CNCR20>3.0.CO;2-9

67. McGuire WP, Hoskins WJ, Brady MF, Kucera PR, Partridge EE, Look KY, et al. Cyclophosphamide and cisplatin compared with paclitaxel and cisplatin in patients with stage III and stage IV ovarian cancer. *New Engl J Med*. (1996) 334:1–6. doi: 10.1056/NEJM199601043340101

68. Ozols RF, Bundy BN, Greer BE, Fowler JM, Clarke-Pearson D, Burger RA, et al. Phase III trial of carboplatin and paclitaxel compared with cisplatin and paclitaxel in patients with optimally resected stage III ovarian cancer: a Gynecologic Oncology Group study. *J Clin Oncol*. (2003) 21:3194–200. doi: 10.1200/JCO.2003.02.153

69. Vasey PA, Jayson GC, Gordon A, Gabra H, Coleman R, Atkinson R, et al. Phase III randomized trial of docetaxel–carboplatin versus paclitaxel–carboplatin as first-line chemotherapy for ovarian carcinoma. *J Natl Cancer Institute*. (2004) 96:1682–91. doi: 10.1093/jnci/djh323

70. Ortiz M, Wabel E, Mitchell K, Horibata S. Mechanisms of chemotherapy resistance in ovarian cancer. *Cancer Drug Resistance*. (2022) 5:304. doi: 10.20517/cdr.2021.147

71. Lee JM, Minasian L, Kohn EC. New strategies in ovarian cancer treatment. *Cancer*. (2019) 125:4623–9. doi: 10.1002/cncr.v125.s24

72. Conic I, Stanojevic Z, Jankovic Velickovic L, Stojnev S, Ristic Petrovic A, Krstic M, et al. Epithelial ovarian cancer with CD117 phenotype is highly aggressive and resistant to chemotherapy. *J Obstetrics Gynaecology Res*. (2015) 41:1630–7. doi: 10.1111/jog.2015.41.issue-10

73. Farley J, Brady WE, Vathipadiekal V, Lankes HA, Coleman R, Morgan MA, et al. Selumetinib in women with recurrent low-grade serous carcinoma of the ovary or peritoneum: an open-label, single-arm, phase 2 study. *Lancet Oncol*. (2013) 14:134–40. doi: 10.1016/S1470-2045(12)70572-7

74. Parmar MK, Sydes MR, Cafferty FH, Choodari-Oskooei B, Langley RE, Brown L, et al. Testing many treatments within a single protocol over 10 years at MRC Clinical Trials Unit at UCL: Multi-arm, multi-stage platform, umbrella and basket protocols. *Clin trials*. (2017) 14:451–61. doi: 10.1177/1740774517725697

75. Lheureux S, McCourt C, Rimel B, Duska L, Fleming G, Mackay H, et al. Moving forward with actionable therapeutic targets and opportunities in endometrial cancer: a NCI clinical trials planning meeting report. *Gynecologic Oncol*. (2018) 149:442–6. doi: 10.1016/j.ygyno.2018.02.005

76. Rundle S, Bradbury A, Drew Y, Curtin NJ. Targeting the ATR-CHK1 axis in cancer therapy. *Cancers*. (2017) 9:41. doi: 10.3390/cancers9050041

77. Haynes B, Murai J, Lee J-M. Restored replication fork stabilization, a mechanism of PARP inhibitor resistance, can be overcome by cell cycle checkpoint inhibition. *Cancer Treat Rev*. (2018) 71:1–7. doi: 10.1016/j.ctrv.2018.09.003

78. Lin AB, McNeely SC, Beckmann RP. Achieving precision death with cell-cycle inhibitors that target DNA replication and repair. *Clin Cancer Res*. (2017) 23:3232–40. doi: 10.1158/1078-0432.CCR-16-0083

79. Lee J-M, Nair J, Zimmer A, Lipkowitz S, Annunziata CM, Merino MJ, et al. Prexasertib, a cell cycle checkpoint kinase 1 and 2 inhibitor, in BRCA wild-type recurrent high-grade serous ovarian cancer: a first-in-class proof-of-concept phase 2 study. *Lancet Oncol*. (2018) 19:207–15. doi: 10.1016/S1470-2045(18)30009-3

80. Carrassa L, Damia G. DNA damage response inhibitors: Mechanisms and potential applications in cancer therapy. *Cancer Treat Rev*. (2017) 60:139–51. doi: 10.1016/j.ctrv.2017.08.013

81. Do K, Wilsker D, Ji J, Zlott J, Freshwater T, Kinders RJ, et al. Phase I study of single-agent AZD1775 (MK-1775), a Wee1 kinase inhibitor, in patients with refractory solid tumors. *J Clin Oncol*. (2015) 33:3409. doi: 10.1200/JCO.2014.60.4009

82. Parsels LA, Karnak D, Parsels JD, Zhang Q, Vélez-Padilla J, Reichert ZR, et al. PARP1 trapping and DNA replication stress enhance radiosensitization with combined WEE1 and PARP inhibitors. *Mol Cancer Res*. (2018) 16:222–32. doi: 10.1158/1541-7786.MCR-17-0455

83. Burger RA, Brady MF, Bookman MA, Fleming GF, Monk BJ, Huang H, et al. Incorporation of bevacizumab in the primary treatment of ovarian cancer. *New Engl J Med*. (2011) 365:2473–83. doi: 10.1056/NEJMoa1104390

84. Oza AM, Cook AD, Pfisterer J, Embleton A, Ledermann JA, Pujade-Lauraine E, et al. Standard chemotherapy with or without bevacizumab for women with newly diagnosed ovarian cancer (ICON7): overall survival results of a phase 3 randomised trial. *Lancet Oncol*. (2015) 16:928–36. doi: 10.1016/S1470-2045(15)00086-8

85. Aghajanian C, Blank SV, Goff BA, Judson PL, Teneriello MG, Husain A, et al. OCEANS: a randomized, double-blind, placebo-controlled phase III trial of chemotherapy with or without bevacizumab in patients with platinum-sensitive recurrent epithelial ovarian, primary peritoneal, or fallopian tube cancer. *J Clin Oncol*. (2012) 30:2039. doi: 10.1200/JCO.2012.42.0505

86. Coleman RL, Brady MF, Herzog TJ, Sabbatini P, Armstrong DK, Walker JL, et al. Bevacizumab and paclitaxel–carboplatin chemotherapy and secondary cytoreduction in recurrent, platinum-sensitive ovarian cancer (NRG Oncology/Gynecologic Oncology Group study GOG-0213): a multicentre, open-label, randomised, phase 3 trial. *Lancet Oncol*. (2017) 18:779–91. doi: 10.1016/S1470-2045(17)30279-6

87. Pujade-Lauraine E, Hilpert F, Weber B, Reuss A, Poveda A, Kristensen G, et al. Bevacizumab combined with chemotherapy for platinum-resistant recurrent ovarian cancer: the AURELIA open-label randomized phase III trial. *Obstetrical Gynecological Survey*. (2014) 69:402–4. doi: 10.1097/01.ogx.0000452705.82050.e4

88. Liu JF, Barry WT, Birrer M, Lee J-M, Buckanovich RJ, Fleming GF, et al. Combination cediranib and olaparib versus olaparib alone for women with recurrent platinum-sensitive ovarian cancer: a randomised phase 2 study. *Lancet Oncol*. (2014) 15:1207–14. doi: 10.1016/S1470-2045(14)70391-2

89. Liu J, Barry W, Birrer M, Lee J-M, Buckanovich R, Fleming G, et al. Overall survival and updated progression-free survival outcomes in a randomized phase II study of combination cediranib and olaparib versus olaparib in relapsed platinum-sensitive ovarian cancer. *Ann Oncol*. (2019) 30:551–7. doi: 10.1093/annonc/mdz018

90. Verma S, Miles D, Gianni L, Krop IE, Welslau M, Baselga J, et al. Trastuzumab emtansine for HER2-positive advanced breast cancer. *New Engl J Med*. (2012) 367:1783–91. doi: 10.1056/NEJMoa1209124

91. Vergote I, Armstrong D, Scambia G, Teneriello M, Sehouli J, Schweizer C, et al. A randomized, double-blind, placebo-controlled, phase III study to assess efficacy and safety of weekly farletuzumab in combination with carboplatin and taxane in patients with ovarian cancer in first platinum-sensitive relapse. *J Clin Oncol*. (2016) 34:2271–8. doi: 10.1200/JCO.2015.63.2596

92. Ab O, Whiteman KR, Bartle LM, Sun X, Singh R, Tavares D, et al. IMGN853, a folate receptor-α (FRα)–targeting antibody–drug conjugate, exhibits potent targeted

antitumor activity against FRα-expressing tumors. *Mol Cancer Ther*. (2015) 14:1605–13. doi: 10.1158/1535-7163.MCT-14-1095

93. Martin LP, Konner JA, Moore KN, Seward SM, Matulonis UA, Perez RP, et al. Characterization of folate receptor alpha (FRα) expression in archival tumor and biopsy samples from relapsed epithelial ovarian cancer patients: A phase I expansion study of the FRα-targeting antibody-drug conjugate mirvetuximab soravtansine. *Gynecologic Oncol*. (2017) 147:402–7. doi: 10.1016/j.ygyno.2017.08.015

94. Moore KN, Vergote I, Oaknin A, Colombo N, Banerjee S, Oza A, et al. FORWARD I: a Phase III study of mirvetuximab soravtansine versus chemotherapy in platinum-resistant ovarian cancer. *Future Oncol*. (2018) 14:1669–78. doi: 10.2217/fon-2017-0646

95. Bradbury A, Zenke FT, Curtin NJ, Drew Y. The role of ATR inhibitors in ovarian cancer: investigating predictive biomarkers of response. *Cells*. (2022) 11:2361. doi: 10.3390/cells11152361

96. Montemorano L, Lightfoot MD, Bixel K. Role of olaparib as maintenance treatment for ovarian cancer: the evidence to date. *OncoTargets Ther*. (2019) 12:11497. doi: 10.2147/OTT.S195552

97. Kazazi-Hyseni F, Beijnen JH, Schellens JH. Bevacizumab. *oncologist*. (2010) 15:819. doi: 10.1634/theoncologist.2009-0317

98. Brahmer JR, Tykodi SS, Chow LQ, Hwu W-J, Topalian SL, Hwu P, et al. Safety and activity of anti–PD-L1 antibody in patients with advanced cancer. *New Engl J Med*. (2012) 366:2455–65. doi: 10.1056/NEJMoa1200694

99. Feingold KR, Anawalt B, Boyce A, Chrousos G, de Herder WW, Dhatariya K, et al. *Endotext*. South Dartmouth (MA: MDText.com, Inc (2000). Available at: https://www.ncbi.nlm.nih.gov/sites/books/NBK278943/.

100. Goldstein JL, Brown MS. Regulation of the mevalonate pathway. *Nature*. (1990) 343:425–30. doi: 10.1038/343425a0

101. Wong WW, Dimitroulakos J, Minden M, Penn L. HMG-CoA reductase inhibitors and the Malignant cell: the statin family of drugs as triggers of tumor-specific apoptosis. *Leukemia*. (2002) 16:508–19. doi: 10.1038/sj.leu.2402476

102. Jones HM, Fang Z, Sun W, Clark LH, Stine JE, Tran A-Q, et al. Atorvastatin exhibits anti-tumorigenic and anti-metastatic effects in ovarian cancer *in vitro*. *Am J Cancer Res*. (2017) 7:2478.

103. Toepfer N, Childress C, Parikh A, Rukstalis D, Yang W. Atorvastatin induces autophagy in prostate cancer PC3 cells through activation of LC3 transcription. *Cancer Biol Ther*. (2011) 12:691–9. doi: 10.4161/cbt.12.8.15978

104. Kobayashi Y, Kashima H, Wu R-C, Jung J-G, Kuan J-C, Gu J, et al. Mevalonate pathway antagonist suppresses formation of serous tubal intraepithelial carcinoma and ovarian carcinoma in mouse models. *Clin Cancer Res*. (2015) 21:4652–62. doi: 10.1158/1078-0432.CCR-14-3368

105. Martirosyan A, Clendening JW, Goard CA, Penn LZ. Lovastatin induces apoptosis of ovarian cancer cells and synergizes with doxorubicin: potential therapeutic relevance. *BMC Cancer*. (2010) 10:1–13. doi: 10.1186/1471-2407-10-103

106. Greenaway JB, Virtanen C, Revay T, Hardy D, Shepherd T, DiMattia G, et al. Ovarian tumour growth is characterized by mevalonate pathway gene signature in an orthotopic, syngeneic model of epithelial ovarian cancer. *Oncotarget*. (2016) 7:47343. doi: 10.18632/oncotarget.10121

107. Stine JE, Guo H, Sheng X, Han X, Schointuch MN, Gilliam TP, et al. The HMG-CoA reductase inhibitor, simvastatin, exhibits anti-metastatic and anti-tumorigenic effects in ovarian cancer. *Oncotarget*. (2016) 7:946. doi: 10.18632/oncotarget.5834

108. Kobayashi Y, Kashima H, Rahmanto YS, Banno K, Yu Y, Matoba Y, et al. Drug repositioning of mevalonate pathway inhibitors as antitumor agents for ovarian cancer. *Oncotarget*. (2017) 8:72147. doi: 10.18632/oncotarget.20046

109. Sawada K, Morishige K-i, Tahara M, Kawagishi R, Ikebuchi Y, Tasaka K, et al. Alendronate inhibits lysophosphatidic acid-induced migration of human ovarian cancer cells by attenuating the activation of rho. *Cancer Res*. (2002) 62:6015–20.

110. Hashimoto K, Morishige K-I, Sawada K, Tahara M, Kawagishi R, Ikebuchi Y, et al. Alendronate inhibits intraperitoneal dissemination in *in vivo* ovarian cancer model. *Cancer Res*. (2005) 65:540–5. doi: 10.1158/0008-5472.540.65.2

111. Boonen S, Reginster J-Y, Kaufman J-M, Lippuner K, Zanchetta J, Langdahl B, et al. Fracture risk and zoledronic acid therapy in men with osteoporosis. *New Engl J Med*. (2012) 367:1714–23. doi: 10.1056/NEJMoa1204061

112. Crawford BA, Kam C, Pavlovic J, Byth K, Handelsman DJ, Angus PW, et al. Zoledronic acid prevents bone loss after liver transplantation: a randomized, double-blind, placebo-controlled trial. *Ann Internal Med*. (2006) 144:239–48. doi: 10.7326/0003-4819-144-4-200602210-00005

113. Major PP, Coleman RE. Zoledronic acid in the treatment of hypercalcemia of Malignancy: results of the international clinical development program. *Semin Oncol*. (2001) 28:17–24. doi: 10.1016/S0093-7754(01)90261-1

114. Rosen LS, Gordon D, Kaminski M, Howell A, Belch A, Mackey J, et al. Zoledronic acid versus pamidronate in the treatment of skeletal metastases in patients with breast cancer or osteolytic lesions of multiple myeloma: a phase III, double-blind, comparative trial. *Cancer J (Sudbury Mass)*. (2001) 7:377–87.

115. Atmaca H, Gorumlu G, Karaca B, Degirmenci M, Tunali D, Cirak Y, et al. Combined gossypol and zoledronic acid treatment results in synergistic induction of cell death and regulates angiogenic molecules in ovarian cancer cells. *Eur Cytokine Network*. (2009) 20:121–30. doi: 10.1684/ecn.2009.0159

116. Schmidmaier R, Simsek M, Baumann P, Emmerich B, Meinhardt G. Synergistic antimyeloma effects of zoledronate and simvastatin. *Anti-cancer Drugs*. (2006) 17:621–9. doi: 10.1097/01.cad.0000215058.85813.02

117. Knight LA, Kurbacher CM, Glaysher S, Fernando A, Reichelt R, Dexel S, et al. Activity of mevalonate pathway inhibitors against breast and ovarian cancers in the ATP-based tumour chemosensitivity assay. *BMC Cancer*. (2009) 9:1–10. doi: 10.1186/1471-2407-9-38

118. Lamb R, Harrison H, Hulit J, Smith DL, Lisanti MP, Sotgia F. Mitochondria as new therapeutic targets for eradicating cancer stem cells: Quantitative proteomics and functional validation *via* MCT1/2 inhibition. *Oncotarget*. (2014) 5:11029. doi: 10.18632/oncotarget.v5i22

119. Lamb R, Ozsvari B, Lisanti CL, Tanowitz HB, Howell A, Martinez-Outschoorn UE, et al. Antibiotics that target mitochondria effectively eradicate cancer stem cells, across multiple tumor types: treating cancer like an infectious disease. *Oncotarget*. (2015) 6:4569. doi: 10.18632/oncotarget.3174

120. Hirsch HA, Iliopoulos D, Tsichlis PN, Struhl K. Metformin selectively targets cancer stem cells, and acts together with chemotherapy to block tumor growth and prolong remission. *Cancer Res*. (2009) 69:7507–11. doi: 10.1158/0008-5472.CAN-09-2994

121. Rattan R, Ali Fehmi R, Munkarah A. Metformin: an emerging new therapeutic option for targeting cancer stem cells and metastasis. *J Oncol*. (2012) 2012:1–12. doi: 10.1155/2012/928127

122. Sun X, Lin T, Fang J, Liu J, Yao W, Geng L, et al. Clinical efficacy analysis of biofeedback electrical stimulation combined with doxycycline in the treatment of type IIIA chronic prostatitis. *Evidence-Based Complementary Altern Med*. (2022) 2022:1–7. doi: 10.1155/2022/7150204

123. White CR, Jodlowski TZ, Atkins DT, Holland NG. Successful doxycycline therapy in a patient with Escherichia coli and multidrug-resistant Klebsiella pneumoniae urinary tract infection. *J Pharm Pract*. (2017) 30:464–7. doi: 10.1177/0897190016642362

124. Joseph BB. Subantimicrobial dose doxycycline for acne and rosacea. *SKINmed: Dermatol Clinician*. (2003) 2:234–46. doi: 10.1111/j.1540-9740.2003.03014.x

125. Bendeck MP, Conte M, Zhang M, Nili N, Strauss BH, Farwell SM. Doxycycline modulates smooth muscle cell growth, migration, and matrix remodeling after arterial injury. *Am J Pathol*. (2002) 160:1089–95. doi: 10.1016/S0002-9440(10)64929-2

126. Chang M-Y, Rhee Y-H, Yi S-H, Lee S-J, Kim R-K, Kim H, et al. Doxycycline enhances survival and self-renewal of human pluripotent stem cells. *Stem Cell Rep*. (2014) 3:353–64. doi: 10.1016/j.stemcr.2014.06.013

127. Krakauer T, Buckley M. Doxycycline is anti-inflammatory and inhibits staphylococcal exotoxin-induced cytokines and chemokines. *Antimicrob Agents Chemother*. (2003) 11:3630–3. doi: 10.1128/aac.47.11.3630-3633.2003

128. Son K, Fujioka S, Iida T, Furukawa K, Fujita T, Yamada H, et al. Doxycycline induces apoptosis in PANC-1 pancreatic cancer cells. *Anticancer Res*. (2009) 29:3995–4003.

129. Duivenvoorden WC, Popovic SV, Lhoták S, Seidlitz E, Hirte HW, Tozer RG, et al. Doxycycline decreases tumor burden in a bone metastasis model of human breast cancer. *Cancer Res*. (2002) 62:1588–91.

130. Shen L-C, Chen Y-K, Lin L-M, Shaw S-Y. Anti-invasion and anti-tumor growth effect of doxycycline treatment for human oral squamous-cell carcinoma–*in vitro* and *in vivo* studies. *Oral Oncol*. (2010) 46:178–84. doi: 10.1016/j.oraloncology.2009.11.013

131. Chopra I, Roberts M. Tetracycline antibiotics: mode of action, applications, molecular biology, and epidemiology of bacterial resistance. *Microbiol Mol Biol Rev*. (2001) 65:232–60. doi: 10.1128/MMBR.65.2.232-260.2001

132. MacDougall C, Chambers H. Protein synthesis inhibitors and miscellaneous antibacterial agents. In: *Goodman and Gilman's the pharmacological basis of therapeutics*. McGraw-Hill, New York (2011). p. 1521–47.

133. Yang S-p, Lin C-c. Treatment of paragonimiasis with bithionol and bithionol sulfoxide. *Dis Chest*. (1967) 52:220–32. doi: 10.1378/chest.52.2.220

134. Guo W, Liu Y, Yao Z, Zhou H, Wang X, Huang Z, et al. Bithionol restores sensitivity of multidrug-resistant gram-negative bacteria to colistin with antimicrobial and anti-biofilm effects. *ACS Infect Dis*. (2023) 9:1634–46. doi: 10.1021/acsinfecdis.3c00257

135. Kim JH, Chan KL, Cheng LW, Tell LA, Byrne BA, Clothier K, et al. High efficiency drug repurposing design for new antifungal agents. *Methods Protoc*. (2019) 2:31. doi: 10.3390/mps2020031

136. Ayyagari VN, Brard L. Bithionol inhibits ovarian cancer cell growth *in vitro*-studies on mechanism (s) of action. *BMC Cancer*. (2014) 14:1–17. doi: 10.1186/1471-2407-14-61

137. Kawagoe H, Stracke ML, Nakamura H, Sano K. Expression and transcriptional regulation of the PD-Iα/autotaxin gene in neuroblastoma. *Cancer Res*. (1997) 57:2516–21.

138. Hoelzinger DB, Mariani L, Weis J, Woyke T, Berens TJ, McDonough W, et al. Gene expression profile of glioblastoma multiforme invasive phenotype points to new therapeutic targets. *Neoplasia*. (2005) 7:7–16. doi: 10.1593/neo.04535

139. Stassar M, Devitt G, Brosius M, Rinnab L, Prang J, Schradin T, et al. Identification of human renal cell carcinoma associated genes by suppression subtractive hybridization. *Br J Cancer*. (2001) 85:1372–82. doi: 10.1054/bjoc.2001.2074

140. Kehlen A, Englert N, Seifert A, Klonisch T, Dralle H, Langner J, et al. Expression, regulation and function of autotaxin in thyroid carcinomas. *Int J Cancer*. (2004) 109:833–8. doi: 10.1002/ijc.v109:6

141. Yang SY, Lee J, Park CG, Kim S, Hong S, Chung HC, et al. Expression of autotaxin (NPP-2) is closely linked to invasiveness of breast cancer cells. *Clin Exp metastasis*. (2002) 19:603–8. doi: 10.1023/A:1020950420196

142. Wu J-M, Xu Y, Skill NJ, Sheng H, Zhao Z, Yu M, et al. Autotaxin expression and its connection with the TNF-alpha-NF-κB axis in human hepatocellular carcinoma. *Mol Cancer*. (2010) 9:1–14. doi: 10.1186/1476-4598-9-71

143. Liu S, Umezu-Goto M, Murph M, Lu Y, Liu W, Zhang F, et al. Expression of autotaxin and lysophosphatidic acid receptors increases mammary tumorigenesis, invasion, and metastases. *Cancer Cell*. (2009) 15:539–50. doi: 10.1016/j.ccr.2009.03.027

144. Kato K, Yoshikawa K, Tanabe E, Kitayoshi M, Fukui R, Fukushima N, et al. Opposite roles of LPA 1 and LPA 3 on cell motile and invasive activities of pancreatic cancer cells. *Tumor Biol*. (2012) 33:1739–44. doi: 10.1007/s13277-012-0433-0

145. Nam SW, Clair T, Campo CK, Lee HY, Liotta LA, Stracke ML. Autotaxin (ATX), a potent tumor motogen, augments invasive and metastatic potential of ras-transformed cells. *Oncogene*. (2000) 19:241–7. doi: 10.1038/sj.onc.1203263

146. Auciello FR, Bulusu V, Oon C, Tait-Mulder J, Berry M, Bhattacharyya S, et al. A stromal lysolipid–autotaxin signaling axis promotes pancreatic tumor progression. *Cancer Discovery*. (2019) 9:617–27. doi: 10.1158/2159-8290.CD-18-1212

147. Yu S, Murph MM, Lu Y, Liu S, Hall HS, Liu J, et al. Lysophosphatidic acid receptors determine tumorigenicity and aggressiveness of ovarian cancer cells. *JNCI: J Natl Cancer Institute*. (2008) 100:1630–42. doi: 10.1093/jnci/djn378

148. Nam SW, Clair T, Kim Y-S, McMarlin A, Schiffmann E, Liotta LA, et al. Autotaxin (NPP-2), a metastasis-enhancing motogen, is an angiogenic factor. *Cancer Res*. (2001) 61:6938–44.

149. Hu Y-L, Tee M-K, Goetzl EJ, Auersperg N, Mills GB, Ferrara N, et al. Lysophosphatidic acid induction of vascular endothelial growth factor expression in human ovarian cancer cells. *J Natl Cancer Institute*. (2001) 93:762–7. doi: 10.1093/jnci/93.10.762

150. Fujita T, Miyamoto S, Onoyama I, Sonoda K, Mekada E, Nakano H. Expression of lysophosphatidic acid receptors and vascular endothelial growth factor mediating lysophosphatidic acid in the development of human ovarian cancer. *Cancer Lett*. (2003) 192:161–9. doi: 10.1016/S0304-3835(02)00713-9

151. Ayyagari VN, Johnston NA, Brard L. Assessment of the anti-tumor potential of Bithionol *in vivo* using a xenograft model of ovarian cancer. *Anti-cancer Drugs*. (2016) 27:547. doi: 10.1097/CAD.0000000000000364

152. Odds F, Bossche HV. Antifungal activity of itraconazole compared with hydroxy-itraconazole *in vitro*. *J Antimicrobial Chemotherapy*. (2000) 45:371–3. doi: 10.1093/jac/45.3.371

153. Aftab BT, Dobromilskaya I, Liu JO, Rudin CM. Itraconazole inhibits angiogenesis and tumor growth in non–small cell lung cancer. *Cancer Res*. (2011) 71:6764–72. doi: 10.1158/0008-5472.CAN-11-0691

154. Wei X, Liu W, Wang JQ, Tang Z. Hedgehog pathway": a potential target of itraconazole in the treatment of cancer. *J Cancer Res Clin Oncol*. (2020) 146:297–304. doi: 10.1007/s00432-019-03117-5

155. Deng H, Huang L, Liao Z, Liu M, Li Q, Xu R. Itraconazole inhibits the Hedgehog signaling pathway thereby inducing autophagy-mediated apoptosis of colon cancer cells. *Cell Death Dis*. (2020) 11:539. doi: 10.1038/s41419-020-02742-0

156. Pantziarka P, Sukhatme V, Bouche G, Meheus L, Sukhatme VP. Repurposing Drugs in Oncology (ReDO)—itraconazole as an anti-cancer agent. *Ecancermedicalscience*. (2015) 9:1–16. doi: 10.3332/ecancer.2015.521

157. Tsubamoto H, Sonoda T, Yamasaki M, Inoue K. Impact of combination chemotherapy with itraconazole on survival of patients with refractory ovarian cancer. *Anticancer Res*. (2014) 34:2481–7.

158. McCavera S, Rogers AT, Yates DM, Woods DJ, Wolstenholme AJ. An ivermectin-sensitive glutamate-gated chloride channel from the parasitic nematode Haemonchus contortus. *Mol Pharmacol*. (2009) 75:1347–55. doi: 10.1124/mol.108.053363

159. Moreno Y, Nabhan JF, Solomon J, Mackenzie CD, Geary TG. Ivermectin disrupts the function of the excretory-secretory apparatus in microfilariae of Brugia malayi. *Proc Natl Acad Sci*. (2010) 107:20120–5. doi: 10.1073/pnas.1011983107

160. Hashimoto H, Messerli SM, Sudo T, Maruta H. Ivermectin inactivates the kinase PAK1 and blocks the PAK1-dependent growth of human ovarian cancer and NF2 tumor cell lines. *Drug Discovery Ther*. (2009) 3:243–6.

161. Li N, Zhan X. Anti-parasite drug ivermectin can suppress ovarian cancer by regulating lncRNA-EIF4A3-mRNA axes. *EPMA J*. (2020) 11:289–309. doi: 10.1007/s13167-020-00209-y

162. Zhang X, Qin T, Zhu Z, Hong F, Xu Y, Zhang X, et al. Ivermectin augments the *in vitro* and *in vivo* efficacy of cisplatin in epithelial ovarian cancer by suppressing Akt/mTOR signaling. *Am J Med Sci*. (2020) 359:123–9. doi: 10.1016/j.amjms.2019.11.001

163. Juarez M, Schcolnik-Cabrera A, Dominguez-Gomez G, Chavez-Blanco A, Diaz-Chavez J, Duenas-Gonzalez A. Antitumor effects of ivermectin at clinically feasible concentrations support its clinical development as a repositioned cancer drug. *Cancer Chemotherapy Pharmacol*. (2020) 85:1153–63. doi: 10.1007/s00280-020-04041-z

164. Nishio M, Sugimachi K, Goto H, Wang J, Morikawa T, Miyachi Y, et al. Dysregulated YAP1/TAZ and TGF-β signaling mediate hepatocarcinogenesis in Mob1a/1b-deficient mice. *Proc Natl Acad Sci*. (2016) 113:E71–80. doi: 10.1073/pnas.1517188113

165. Overholtzer M, Zhang J, Smolen GA, Muir B, Li W, Sgroi DC, et al. Transforming properties of YAP, a candidate oncogene on the chromosome 11q22 amplicon. *Proc Natl Acad Sci*. (2006) 103:12405–10. doi: 10.1073/pnas.0605579103

166. Zender L, Spector MS, Xue W, Flemming P, Cordon-Cardo C, Silke J, et al. Identification and validation of oncogenes in liver cancer using an integrative oncogenomic approach. *Cell*. (2006) 125:1253–67. doi: 10.1016/j.cell.2006.05.030

167. Kang W, Tong JH, Chan AW, Lee T-L, Lung RW, Leung PP, et al. Yes-associated protein 1 exhibits oncogenic property in gastric cancer and its nuclear accumulation associates with poor prognosis. *Clin Cancer Res*. (2011) 17:2130–9. doi: 10.1158/1078-0432.CCR-10-2467

168. Xia Y, Chang T, Wang Y, Liu Y, Li W, Li M, et al. Correction: YAP promotes ovarian cancer cell tumorigenesis and is indicative of a poor prognosis for ovarian cancer patients. *PloS One*. (2016) 11:e0152712. doi: 10.1371/journal.pone.0152712

169. Kodama M, Kodama T, Newberg JY, Katayama H, Kobayashi M, Hanash SM, et al. *In vivo* loss-of-function screens identify KPNB1 as a new druggable oncogene in epithelial ovarian cancer. *Proc Natl Acad Sci*. (2017) 114:E7301–E10. doi: 10.1073/pnas.1705441114

170. Tang M, Hu X, Wang Y, Yao X, Zhang W, Yu C, et al. Ivermectin, a potential anticancer drug derived from an antiparasitic drug. *Pharmacol Res*. (2021) 163:105207. doi: 10.1016/j.phrs.2020.105207

171. Kobayashi Y, Banno K, Kunitomi H, Tominaga E, Aoki D. Current state and outlook for drug repositioning anticipated in the field of ovarian cancer. *J gynecologic Oncol*. (2019) 30:1–13. doi: 10.3802/jgo.2019.30.e10

172. Elayapillai S, Ramraj S, Benbrook DM, Bieniasz M, Wang L, Pathuri G, et al. Potential and mechanism of mebendazole for treatment and maintenance of ovarian cancer. *Gynecologic Oncol*. (2021) 160:302–11. doi: 10.1016/j.ygyno.2020.10.010

173. Spagnuolo PA, Hu J, Hurren R, Wang X, Gronda M, Sukhai MA, et al. The antihelmintic flubendazole inhibits microtubule function through a mechanism distinct from Vinca alkaloids and displays preclinical activity in leukemia and myeloma. *Blood J Am Soc Hematol*. (2010) 115:4824–33. doi: 10.1182/blood-2009-09-243055

174. Dogra N, Kumar A, Mukhopadhyay T. Fenbendazole acts as a moderate microtubule destabilizing agent and causes cancer cell death by modulating multiple cellular pathways. *Sci Rep*. (2018) 8:1–15. doi: 10.1038/s41598-018-30158-6

175. Doudican N, Rodriguez A, Osman I, Orlow SJ. Mebendazole induces apoptosis *via* Bcl-2 inactivation in chemoresistant melanoma cells. *Mol Cancer Res*. (2008) 6:1308–15. doi: 10.1158/1541-7786.MCR-07-2159

176. Huang L, Zhao L, Zhang J, He F, Wang H, Liu Q, et al. Antiparasitic mebendazole (MBZ) effectively overcomes cisplatin resistance in human ovarian cancer cells by inhibiting multiple cancer-associated signaling pathways. *Aging (Albany NY)*. (2021) 13:17407. doi: 10.18632/aging.203232

177. Marx N, Schoünbeck U, Lazar MA, Libby P, Plutzky J. Peroxisome proliferator-activated receptor gamma activators inhibit gene expression and migration in human vascular smooth muscle cells. *Circ Res*. (1998) 83:1097–103. doi: 10.1161/01.RES.83.11.1097

178. Ricote M, Li AC, Willson TM, Kelly CJ, Glass CK. The peroxisome proliferator-activated receptor-γ is a negative regulator of macrophage activation. *Nature*. (1998) 391:79–82. doi: 10.1038/34178

179. Xin X, Yang S, Kowalski J, Gerritsen ME. Peroxisome proliferator-activated receptor γ ligands are potent inhibitors of angiogenesis *in vitro* and *in vivo*. *J Biol Chem*. (1999) 274:9116–21. doi: 10.1074/jbc.274.13.9116

180. Banerjee J, Komar CM. Effects of luteinizing hormone on peroxisome proliferator-activated receptor γ in the rat ovary before and after the gonadotropin surge. *Reproduction*. (2006) 131:93–101. doi: 10.1530/rep.1.00730

181. Nicol CJ, Yoon M, Ward JM, Yamashita M, Fukamachi K, Peters JM, et al. PPARγ influences susceptibility to DMBA-induced mammary, ovarian and skin carcinogenesis. *Carcinogenesis*. (2004) 25:1747–55. doi: 10.1093/carcin/bgh160

182. Fischer SM, Conti CJ, Locniskar M, Belury MA, Maldve RE, Lee ML, et al. The effect of dietary fat on the rapid development of mammary tumors induced by 7, 12-dimethylbenz (a) anthracene in SENCAR mice. *Cancer Res*. (1992) 52:662–6.

183. Vignati S, Albertini V, Rinaldi A, Kwee I, Riva C, Oldrini R, et al. Cellular, molecular consequences of peroxisome proliferator-activated receptor-δ activation in ovarian cancer cells. *Neoplasia*. (2006) 8:851–IN12. doi: 10.1593/neo.06433

184. Zhang X, Young HA. PPAR and immune system—what do we know? *Int Immunopharmacol*. (2002) 2:1029–44. doi: 10.1016/S1567-5769(02)00057-7

185. Lei P, Abdelrahim M, Safe S. 1, 1-Bis (3′-indolyl)-1-(p-substituted phenyl) methanes inhibit ovarian cancer cell growth through peroxisome proliferator–activated receptor–dependent and independent pathways. *Mol Cancer Ther*. (2006) 5:2324–36. doi: 10.1158/1535-7163.MCT-06-0184

186. Shigeto T, Yokoyama Y, Xin B, Mizunuma H. Peroxisome proliferator-activated receptor α and γ ligands inhibit the growth of human ovarian cancer. *Oncol Rep*. (2007) 18:833–40. doi: 10.3892/or.18.4.833

187. Takaoka K, Sekiguchi F, Shigi H, Maeda Y, Nishikawa H, Kawabata A. Opposite effects of two thiazolidinediones, ciglitazone and troglitazone, on

proteinase-activated receptor-1-triggered prostaglandin E2 release. *Toxicology*. (2010) 268:40–5. doi: 10.1016/j.tox.2009.11.020

188. Hazra S, Dubinett SM. Ciglitazone mediates COX-2 dependent suppression of PGE2 in human non-small cell lung cancer cells. *Prostaglandins leukotrienes essential Fatty Acids*. (2007) 77:51–8. doi: 10.1016/j.plefa.2007.05.006

189. Shin SJ, Kim JY, Kwon SY, Mun K-C, Cho CH, Ha E. Ciglitazone enhances ovarian cancer cell death *via* inhibition of glucose transporter-1. *Eur J Pharmacol*. (2014) 743:17–23. doi: 10.1016/j.ejphar.2014.09.013

190. Yokoyama Y, Xin B, Shigeto T, Umemoto M, Kasai-Sakamoto A, Futagami M, et al. Clofibric acid, a peroxisome proliferator–activated receptor α ligand, inhibits growth of human ovarian cancer. *Mol Cancer Ther*. (2007) 6:1379–86. doi: 10.1158/1535-7163.MCT-06-0722

191. Skrott Z, Mistrik M, Andersen KK, Friis S, Majera D, Gursky J, et al. Alcohol-abuse drug disulfiram targets cancer *via* p97 segregase adaptor NPL4. *Nature*. (2017) 552:194–9. doi: 10.1038/nature25016

192. Chen D, Cui QC, Yang H, Dou QP. Disulfiram, a clinically used anti-alcoholism drug and copper-binding agent, induces apoptotic cell death in breast cancer cultures and xenografts *via* inhibition of the proteasome activity. *Cancer Res*. (2006) 66:10425–33. doi: 10.1158/0008-5472.CAN-06-2126

193. Majumder S, Chatterjee S, Pal S, Biswas J, Efferth T, Choudhuri SK. The role of copper in drug-resistant murine and human tumors. *Biometals*. (2009) 22:377–84. doi: 10.1007/s10534-008-9174-3

194. Guo W, Zhang X, Lin L, Wang H, He E, Wang G, et al. The disulfiram/copper complex induces apoptosis and inhibits tumour growth in human osteosarcoma by activating the ROS/JNK signalling pathway. *J Biochem*. (2021) 170:275–87. doi: 10.1093/jb/mvab045

195. Xu Y, Zhou Q, Feng X, Dai Y, Jiang Y, Jiang W, et al. Disulfiram/copper markedly induced myeloma cell apoptosis through activation of JNK and intrinsic and extrinsic apoptosis pathways. *Biomedicine Pharmacotherapy*. (2020) 126:110048. doi: 10.1016/j.biopha.2020.110048

196. Papaioannou M, Mylonas I, Kast RE, Brüning A. Disulfiram/copper causes redox-related proteotoxicity and concomitant heat shock response in ovarian cancer cells that is augmented by auranofin-mediated thioredoxin inhibition. *Oncoscience*. (2014) 1:21. doi: 10.18632/oncoscience.v1i1

197. Guo F, Yang Z, Kulbe H, Albers AE, Sehouli J, Kaufmann AM. Inhibitory effect on ovarian cancer ALDH+ stem-like cells by Disulfiram and Copper treatment through ALDH and ROS modulation. *Biomedicine Pharmacotherapy*. (2019) 118:109371. doi: 10.1016/j.biopha.2019.109371

198. MacDonagh L, Gallagher M, Ffrench B, Gasch C, Breen E, Gray S, et al. Targeting the cancer stem cell marker, aldehyde dehydrogenase 1, to circumvent cisplatin resistance in NSCLC. *Oncotarget*. (2017) 8:72544–63. doi: 10.18632/oncotarget.19881

199. Guo X, Xu B, Pandey S, Goessl E, Brown J, Armesilla AL, et al. Disulfiram/copper complex inhibiting NFκB activity and potentiating cytotoxic effect of gemcitabine on colon and breast cancer cell lines. *Cancer Lett*. (2010) 290:104–13. doi: 10.1016/j.canlet.2009.09.002

200. Xu B, Shi P, Fombon IS, Zhang Y, Huang F, Wang W, et al. Disulfiram/copper complex activated JNK/c-jun pathway and sensitized cytotoxicity of doxorubicin in doxorubicin resistant leukemia HL60 cells. *Blood Cells Molecules Dis*. (2011) 47:264–9. doi: 10.1016/j.bcmd.2011.08.004

201. Choi JH, Yang YR, Lee SK, Kim SH, Kim YH, Cha JY, et al. Potential inhibition of PDK1/Akt signaling by phenothiazines suppresses cancer cell proliferation and survival. *Ann New York Acad Sci*. (2008) 1138:393–403. doi: 10.1196/nyas.2008.1138.issue-1

202. Duarte D, Vale N. Antipsychotic drug fluphenazine against human cancer cells. *Biomolecules*. (2022) 12:1360. doi: 10.3390/biom12101360

203. Romero IL, Gordon IO, Jagadeeswaran S, Mui KL, Lee WS, Dinulescu DM, et al. Effects of oral contraceptives or a gonadotropin-releasing hormone agonist on ovarian carcinogenesis in genetically engineered mice. *Cancer Prev Res*. (2009) 2:792–9. doi: 10.1158/1940-6207.CAPR-08-0236

204. Lengyel E, Litchfield LM, Mitra AK, Nieman KM, Mukherjee A, Zhang Y, et al. Metformin inhibits ovarian cancer growth and increases sensitivity to paclitaxel in mouse models. *Am J obstetrics gynecology*. (2015) 212:479. e1–. e10. doi: 10.1016/j.ajog.2014.10.026

205. Bowker SL, Majumdar SR, Veugelers P, Johnson JA. Increased cancer-related mortality for patients with type 2 diabetes who use sulfonylureas or insulin. *Diabetes Care*. (2006) 29:254–8. doi: 10.2337/diacare.29.02.06.dc05-1558

206. Landman GW, Kleefstra N, van Hateren KJ, Groenier KH, Gans RO, Bilo HJ. Metformin associated with lower cancer mortality in type 2 diabetes: ZODIAC-16. *Diabetes Care*. (2010) 33:322–6. doi: 10.2337/dc09-1380

207. Libby G, Donnelly LA, Donnan PT, Alessi DR, Morris AD, Evans JM. New users of metformin are at low risk of incident cancer: a cohort study among people with type 2 diabetes. *Diabetes Care*. (2009) 32:1620–5. doi: 10.2337/dc08-2175

208. Kumar S, Meuter A, Thapa P, Langstraat C, Giri S, Chien J, et al. Metformin intake is associated with better survival in ovarian cancer: A case-control study. *Cancer*. (2013) 119:555–62. doi: 10.1002/cncr.v119.3

209. Romero IL, McCormick A, McEwen KA, Park S, Karrison T, Yamada SD, et al. Relationship of type II diabetes and metformin use to ovarian cancer progression, survival, and chemosensitivity. *Obstetrics gynecology*. (2012) 119:61. doi: 10.1097/AOG.0b013e3182393ab3

210. Yokoyama T, Kumon H, Nasu Y, Takamoto H, Watanabe T. Comparison of 25 and 75 mg/day naftopidil for lower urinary tract symptoms associated with benign prostatic hyperplasia: a prospective, randomized controlled study. *Int J Urol*. (2006) 13:932–8. doi: 10.1111/j.1442-2042.2006.01443.x

211. Oh-oka H. Usefulness of naftopidil for dysuria in benign prostatic hyperplasia and its optimal dose–comparison between 75 and 50 mg. *Urologia Internationalis*. (2009) 82:136–42. doi: 10.1159/000200787

212. Funahashi Y, Hattori R, Matsukawa Y, Komatsu T, Sassa N, Gotoh M. Clinical efficacy of a loading dose of naftopidil for patients with benign prostate hyperplasia. *World J Urol*. (2011) 29:225–31. doi: 10.1007/s00345-010-0528-4

213. Thomas TS. *Implementation of Lifestyle Modifications as First Line Therapies for the Management of Benign Prostatic Hyperplasia*. Kent State University, United States: Kent State University (2023).

214. Florent R, Weiswald L-B, Lambert B, Brotin E, Abeilard E, Louis M-H, et al. Bim, Puma and Noxa upregulation by Naftopidil sensitizes ovarian cancer to the BH3-mimetic ABT-737 and the MEK inhibitor Trametinib. *Cell Death Dis*. (2020) 11:380. doi: 10.1038/s41419-020-2588-8

215. Subeha MR, Goyeneche AA, Bustamante P, Lisio MA, Burnier JV, Telleria CM. Nelfinavir induces cytotoxicity towards high-grade serous ovarian cancer cells, involving induction of the unfolded protein response, modulation of protein synthesis, DNA damage, lysosomal impairment, and potentiation of toxicity caused by proteasome inhibition. *Cancers*. (2021) 14:99. doi: 10.3390/cancers14010099

216. Markowitz M, Saag M, Powderly WG, Hurley AM, Hsu A, Valdes JM, et al. A preliminary study of ritonavir, an inhibitor of HIV-1 protease, to treat HIV-1 infection. *New Engl J Med*. (1995) 333:1534–40. doi: 10.1056/NEJM199512073332204

217. Kumar S, Bryant CS, Chamala S, Qazi A, Seward S, Pal J, et al. Ritonavir blocks AKT signaling, activates apoptosis and inhibits migration and invasion in ovarian cancer cells. *Mol Cancer*. (2009) 8:1–12. doi: 10.1186/1476-4598-8-26

218. Kumar S, Bryant C, Qazi A, Morris R, Imudia A, Steffes C, et al. Ritonavir blocks Akt signaling and exhibits antineoplastic activity in ovarian cancer cell lines. *Cancer Res*. (2008) 68:3381–.

219. Winterhoff B, Teoman A, Freyer L, Von Bismarck A, Dowdy S, Schmalfeldt B, et al. The HIV protease inhibitor ritonavir induces cell cycle arrest and apoptosis in the A2780 ovarian cancer cell line *in vitro* and *in vivo*. *Gynecologic Oncol*. (2013) 130:e138. doi: 10.1016/j.ygyno.2013.04.393

220. Wallace JL. Distribution and expression of cyclooxygenase (COX) isoenzymes, their physiological roles, and the categorization of nonsteroidal anti-inflammatory drugs (NSAIDs). *Am J Med*. (1999) 107:11–6. doi: 10.1016/S0002-9343(99)00363-0

221. Marjoribanks J, Ayeleke RO, Farquhar C, Proctor M, Gynaecology C, Group F. Nonsteroidal anti-inflammatory drugs for dysmenorrhoea. *Cochrane Database systematic Rev*. (1996) 2015:1–139. doi: 10.1002/14651858.CD001751

222. Affaitati G, Martelletti P, Lopopolo M, Tana C, Massimini F, Cipollone F, et al. Use of nonsteroidal anti-inflammatory drugs for symptomatic treatment of episodic headache. *Pain Pract*. (2017) 17:392–401. doi: 10.1111/papr.2017.17.issue-3

223. Malanga G, Wolff E. Evidence-informed management of chronic low back pain with nonsteroidal anti-inflammatory drugs, muscle relaxants, and simple analgesics. *Spine J*. (2008) 8:173–84. doi: 10.1016/j.spinee.2007.10.013

224. Thun MJ, Jacobs EJ, Patrono C. The role of aspirin in cancer prevention. *Nat Rev Clin Oncol*. (2012) 9:259–67. doi: 10.1038/nrclinonc.2011.199

225. Trabert B, Ness RB, Lo-Ciganic W-H, Murphy MA, Goode EL, Poole EM, et al. Aspirin, nonaspirin nonsteroidal anti-inflammatory drug, and acetaminophen use and risk of invasive epithelial ovarian cancer: a pooled analysis in the Ovarian Cancer Association Consortium. *J Natl Cancer Institute*. (2014) 106:djt431. doi: 10.1093/jnci/djt431

226. Daikoku T, Tranguch S, Chakrabarty A, Wang D, Khabele D, Orsulic S, et al. Extracellular signal-regulated kinase is a target of cyclooxygenase-1-peroxisome proliferator-activated receptor-δ signaling in epithelial ovarian cancer. *Cancer Res*. (2007) 67:5285–92. doi: 10.1158/0008-5472.CAN-07-0828

227. Drinberg V, Bitcover R, Rajchenbach W, Peer D. Modulating cancer multidrug resistance by sertraline in combination with a nanomedicine. *Cancer Lett*. (2014) 354:290–8. doi: 10.1016/j.canlet.2014.08.026

228. MacQueen G, Born L, Steiner M. The selective serotonin reuptake inhibitor sertraline: its profile and use in psychiatric disorders. *CNS Drug Rev*. (2001) 7:1–24. doi: 10.1111/j.1527-3458.2001.tb00188.x

229. Kitaichi Y, Inoue T, Nakagawa S, Boku S, Kakuta A, Izumi T, et al. Sertraline increases extracellular levels not only of serotonin, but also of dopamine in the nucleus accumbens and striatum of rats. *Eur J Pharmacol*. (2010) 647:90–6. doi: 10.1016/j.ejphar.2010.08.026

230. Gottesman MM, Pastan I, Ambudkar SV. P-glycoprotein and multidrug resistance. *Curr Opin Genet Dev*. (1996) 6:610–7. doi: 10.1016/S0959-437X(96)80091-8

231. Lin JH, Yamazaki M. Role of P-glycoprotein in pharmacokinetics: clinical implications. *Clin Pharmacokinet*. (2003) 42:59–98. doi: 10.2165/00003088-200342010-00003

232. Fletcher JI, Haber M, Henderson MJ, Norris MD. ABC transporters in cancer: more than just drug efflux pumps. *Nat Rev Cancer*. (2010) 10:147–56. doi: 10.1038/nrc2789

233. Franks ME, Macpherson GR, Figg WD. Thalidomide. *Lancet*. (2004) 363:1802–11. doi: 10.1016/S0140-6736(04)16308-3

234. Kumar S, Rajkumar SV. Thalidomide and lenalidomide in the treatment of multiple myeloma. *Eur J Cancer*. (2006) 42:1612–22. doi: 10.1016/j.ejca.2006.04.004

235. Braña MF, Acero N, Anorbe L, Mingarro DM, Llinares F, Domínguez G. Discovering a new analogue of thalidomide which may be used as a potent modulator of TNF-α production. *Eur J medicinal Chem*. (2009) 44:3533–42. doi: 10.1016/j.ejmech.2009.03.018

236. Sampaio EP, Sarno EN, Galilly R, Cohn ZA, Kaplan G. Thalidomide selectively inhibits tumor necrosis factor alpha production by stimulated human monocytes. *J Exp Med*. (1991) 173:699–703. doi: 10.1084/jem.173.3.699

237. Piura B, Medina L, Rabinovich A, Dyomin V, Huleihel M. Thalidomide distinctly affected TNF-α, IL-6 and MMP secretion by an ovarian cancer cell line (SKOV-3) and primary ovarian cancer cells. *Eur Cytokine Netw*. (2013) 24:122–9. doi: 10.1684/ecn.2013.0342

238. Ching L, Xu Z, Gummer B, Palmer B, Joseph W, Baguley B. Effect of thalidomide on tumour necrosis factor production and anti-tumour activity induced by 5, 6-dimethylxanthenone-4-acetic acid. *Br J Cancer*. (1995) 72:339–43. doi: 10.1038/bjc.1995.335

239. Eisen T, Boshoff C, Mak I, Sapunar F, Vaughan M, Pyle L, et al. Continuous low dose thalidomide: a phase II study in advanced melanoma, renal cell, ovarian and breast cancer. *Br J Cancer*. (2000) 82:812–7. doi: 10.1054/bjoc.1999.1004

240. Hurteau JA, Brady MF, Darcy KM, McGuire WP, Edmonds P, Pearl ML, et al. Randomized phase III trial of tamoxifen versus thalidomide in women with biochemical-recurrent-only epithelial ovarian, fallopian tube or primary peritoneal carcinoma after a complete response to first-line platinum/taxane chemotherapy with an evaluation of serum vascular endothelial growth factor (VEGF): A Gynecologic Oncology Group Study. *Gynecologic Oncol.* (2010) 119:444–50. doi: 10.1016/j.ygyno.2010.08.002

241. Matei D, Emerson R, Lai Y, Baldridge L, Rao J, Yiannoutsos C, et al. Autocrine activation of PDGFRα promotes the progression of ovarian cancer. *Oncogene*. (2006) 25:2060–9. doi: 10.1038/sj.onc.1209232

242. Chen R, Chen B. The role of dasatinib in the management of chronic myeloid leukemia. *Drug design Dev Ther*. (2015) 9:773–9. doi: 10.2147/DDDT.S80207

243. Le XF, Mao W, Lu Z, Carter BZ, Bast RC Jr. Dasatinib induces autophagic cell death in human ovarian cancer. *Cancer*. (2010) 116:4980–90. doi: 10.1002/cncr.v116:21

244. Xiao J, Xu M, Hou T, Huang Y, Yang C, Li J. Dasatinib enhances antitumor activity of paclitaxel in ovarian cancer through Src signaling. *Mol Med Rep*. (2015) 12:3249–56. doi: 10.3892/mmr.2015.3784

245. Kadife E, Chan E, Luwor R, Kannourakis G, Findlay J, Ahmed N. Paclitaxel-induced Src activation is inhibited by dasatinib treatment, independently of cancer stem cell properties, in a mouse model of ovarian cancer. *Cancers*. (2019) 11:243. doi: 10.3390/cancers11020243

246. Matei D, Chang DD, Jeng M-H. Imatinib mesylate (Gleevec) inhibits ovarian cancer cell growth through a mechanism dependent on platelet-derived growth factor receptor α and Akt inactivation. *Clin Cancer Res*. (2004) 10:681–90. doi: 10.1158/1078-0432.CCR-0754-03

247. Posadas EM, Kwitkowski V, Kotz HL, Espina V, Minasian L, Tchabo N, et al. A prospective analysis of imatinib-induced c-KIT modulation in ovarian cancer: a phase II clinical study with proteomic profiling. *Cancer*. (2007) 110:309–17. doi: 10.1002/cncr.v110:2

248. Alberts DS, Liu PY, Wilczynski SP, Jang A, Moon J, Ward JH, et al. Phase II trial of imatinib mesylate in recurrent, biomarker positive, ovarian cancer (Southwest Oncology Group Protocol S0211). *Int J Gynecologic Cancer*. (2007) 17:784. doi: 10.1136/ijgc-00009577-200707000-00005

249. Trope C, Marth C, Kaern J. Tamoxifen in the treatment of recurrent ovarian carcinoma. *Eur J Cancer*. (2000) 36:59–61. doi: 10.1016/S0959-8049(00)00228-8

250. Trédan O, Provansal M, Abdeddaim C, Lardy-Cleaud A, Hardy-Bessard A-C, Kalbacher E, et al. Regorafenib or tamoxifen for platinum-sensitive recurrent ovarian cancer with rising CA125 and no evidence of clinical or RECIST progression: a GINECO randomized phase II trial (REGOVAR). *Gynecologic Oncol*. (2022) 164:18–26. doi: 10.1016/j.ygyno.2021.09.024

251. Bowman A, Gabra H, Langdon SP, Lessells A, Stewart M, Young A, et al. CA125 response is associated with estrogen receptor expression in a phase II trial of letrozole in ovarian cancer: identification of an endocrine-sensitive subgroup. *Clin Cancer Res*. (2002) 8:2233–9.

252. Smyth JF, Gourley C, Walker G, MacKean MJ, Stevenson A, Williams AR, et al. Antiestrogen therapy is active in selected ovarian cancer cases: the use of letrozole in estrogen receptor–positive patients. *Clin Cancer Res*. (2007) 13:3617–22. doi: 10.1158/1078-0432.CCR-06-2878

253. Ramirez PT, Schmeler KM, Milam MR, Slomovitz BM, Smith JA, Kavanagh JJ, et al. Efficacy of letrozole in the treatment of recurrent platinum-and taxane-resistant high-grade cancer of the ovary or peritoneum. *Gynecologic Oncol*. (2008) 110:56–9. doi: 10.1016/j.ygyno.2008.03.014

254. Papadimitriou CA, Markaki S, Siapkaras J, Vlachos G, Efstathiou E, Grimani I, et al. Hormonal therapy with letrozole for relapsed epithelial ovarian cancerLong-term results of a phase II study. *Oncology*. (2004) 66:112–7. doi: 10.1159/000077436

255. del Carmen MG, Fuller AF, Matulonis U, Horick NK, Goodman A, Duska LR, et al. Phase II trial of anastrozole in women with asymptomatic müllerian cancer. *Gynecologic Oncol*. (2003) 91:596–602. doi: 10.1016/j.ygyno.2003.08.021

256. Maher DM, Khan S, Nordquist JL, Ebeling MC, Bauer NA, Kopel L, et al. Ormeloxifene efficiently inhibits ovarian cancer growth. *Cancer Lett*. (2015) 356:606–12. doi: 10.1016/j.canlet.2014.10.009

257. Dodds M, Xiong Y, Mouksassi S, Kirkpatrick CM, Hui K, Doyle E, et al. Model-informed drug repurposing: a pharmacometric approach to novel pathogen preparedness, response and retrospection. *Br J Clin Pharmacol*. (2021) 87:3388–97. doi: 10.1111/bcp.14760

258. Berckmans Y, Hoffert Y, Vankerckhoven A, Dreesen E, Coosemans A. Drug repurposing for targeting myeloid-derived suppressor-cell-generated immunosuppression in ovarian cancer: A literature review of potential candidates. *Pharmaceutics*. (2023) 15:1792. doi: 10.3390/pharmaceutics15071792

259. Markham A. Lurbinectedin: first approval. *Drugs*. (2020) 80:1345–53. doi: 10.1007/s40265-020-01374-0

260. Till KJ, Lin K, Zuzel M, Cawley JC. The chemokine receptor CCR7 and α4 integrin are important for migration of chronic lymphocytic leukemia cells into lymph nodes. *Blood J Am Soc Hematol*. (2002) 99:2977–84. doi: 10.1182/blood.V99.8.2977

261. Trigo J, Subbiah V, Besse B, Moreno V, López R, Sala MA, et al. Lurbinectedin as second-line treatment for patients with small-cell lung cancer: a single-arm, open-label, phase 2 basket trial. *Lancet Oncol*. (2020) 21:645–54. doi: 10.1016/S1470-2045(20)30068-1

262. Singh S, Jaigirdar AA, Mulkey F, Cheng J, Hamed SS, Li Y, et al. FDA approval summary: lurbinectedin for the treatment of metastatic small cell lung cancer. *Clin Cancer Res*. (2021) 27:2378–82. doi: 10.1158/1078-0432.CCR-20-3901

263. Takahashi R, Mabuchi S, Kawano M, Sasano T, Matsumoto Y, Kuroda H, et al. Preclinical investigations of PM01183 (lurbinectedin) as a single agent or in combination with other anticancer agents for clear cell carcinoma of the ovary. *PloS One*. (2016) 11:e0151050. doi: 10.1371/journal.pone.0151050

264. Cruz C, Llop-Guevara A, Garber JE, Arun BK, Fidalgo JAP, Lluch A, et al. Multicenter phase II study of lurbinectedin in BRCA-mutated and unselected metastatic advanced breast cancer and biomarker assessment substudy. *J Clin Oncol*. (2018) 36:3134. doi: 10.1200/JCO.2018.78.6558

265. Elez ME, Tabernero J, Geary D, Macarulla T, Kang SP, Kahatt C, et al. First-in-human phase I study of Lurbinectedin (PM01183) in patients with advanced solid tumors. *Clin Cancer Res*. (2014) 20:2205–14. doi: 10.1158/1078-0432.CCR-13-1880

266. Dannenberg AJ, Altorki NK, Boyle JO, Dang C, Howe LR, Weksler BB, et al. Cyclo-oxygenase 2: a pharmacological target for the prevention of cancer. *Lancet Oncol*. (2001) 2:544–51. doi: 10.1016/S1470-2045(01)00488-0

267. Veltman JD, Lambers ME, van Nimwegen M, Hendriks RW, Hoogsteden HC, Aerts JG, et al. COX-2 inhibition improves immunotherapy and is associated with decreased numbers of myeloid-derived suppressor cells in mesothelioma. *Celecoxib influences MDSC Funct BMC Cancer*. (2010) 10:1–13. doi: 10.1186/1471-2407-10-464

268. Kantarjian H, Issa JPJ, Rosenfeld CS, Bennett JM, Albitar M, DiPersio J, et al. Decitabine improves patient outcomes in myelodysplastic syndromes: results of a phase III randomized study. *Cancer: Interdiscip Int J Am Cancer Soc*. (2006) 106:1794–803. doi: 10.1002/cncr.v106:8

269. Silverman LR, Demakos EP, Peterson BL, Kornblith AB, Holland JC, Odchimar-Reissig R, et al. Randomized controlled trial of azacitidine in patients with the myelodysplastic syndrome: a study of the cancer and leukemia group B. *J Clin Oncol*. (2002) 20:2429–40. doi: 10.1200/JCO.2002.04.117

270. Fenaux P, Mufti GJ, Hellstrom-Lindberg E, Santini V, Finelli C, Giagounidis A, et al. Efficacy of azacitidine compared with that of conventional care regimens in the treatment of higher-risk myelodysplastic syndromes: a randomised, open-label, phase III study. *Lancet Oncol*. (2009) 10:223–32. doi: 10.1016/S1470-2045(09)70003-8

271. Cao D, Li D, Huang Y, Ma Y, Zhang B, Zhao C, et al. 5-Azacytidine promotes invadopodia formation and tumor metastasis through the upregulation of PI3K in ovarian cancer cells. *Oncotarget*. (2017) 8:60173. doi: 10.18632/oncotarget.18580

272. Meng F, Sun G, Zhong M, Yu Y, Brewer M. Anticancer efficacy of cisplatin and trichostatin A or 5-aza-2′-deoxycytidine on ovarian cancer. *Br J Cancer*. (2013) 108:579–86. doi: 10.1038/bjc.2013.10

273. Robert C, Ribas A, Wolchok JD, Hodi FS, Hamid O, Kefford R, et al. Anti-programmed-death-receptor-1 treatment with pembrolizumab in ipilimumab-refractory advanced melanoma: a randomised dose-comparison cohort of a phase 1 trial. *Lancet*. (2014) 384:1109–17. doi: 10.1016/S0140-6736(14)60958-2

274. Zhao L, Chen X, Wu H, He Q, Ding L, Yang B. Strategies to synergize PD-1/PD-L1 targeted cancer immunotherapies to enhance antitumor responses in ovarian cancer. *Biochem Pharmacol*. (2023) 215:115724. doi: 10.1016/j.bcp.2023.115724

275. Xin B, Yokoyama Y, Shigeto T, Futagami M, Mizunuma H. Inhibitory effect of meloxicam, a selective cyclooxygenase-2 inhibitor, and ciglitazone, a peroxisome proliferator-activated receptor gamma ligand, on the growth of human ovarian cancers. *Cancer: Interdiscip Int J Am Cancer Soc*. (2007) 110:791–800. doi: 10.1002/cncr.v110:4

276. Yokoyama Y, Xin B, Shigeto T, Mizunuma H. Combination of ciglitazone, a peroxisome proliferator-activated receptor gamma ligand, and cisplatin enhances the inhibition of growth of human ovarian cancers. *J Cancer Res Clin Oncol*. (2011) 137:1219–28. doi: 10.1007/s00432-011-0993-1

frontiers | Frontiers in Oncology

TYPE Review
PUBLISHED 21 March 2025
DOI 10.3389/fonc.2025.1520985

OPEN ACCESS

EDITED BY
Teresita Padilla-Benavides,
Wesleyan University, United States

REVIEWED BY
Kulbhushan Thakur,
University of Delhi, India
Praveen Koganti,
Sanford Burnham Prebys Medical Discovery Institute, United States

*CORRESPONDENCE
Nancy Martínez-Montiel
fcb.colaborador03@correo.buap.mx

RECEIVED 01 November 2024
ACCEPTED 04 February 2025
PUBLISHED 21 March 2025

CITATION
Martínez-Montiel N, Vite-Arciniega JdJ, Rosas-Murrieta NH and Martínez-Contreras RD (2025) Repurposing alternative splicing events as potential targets for the design of diagnostic and therapeutic tools in PCa. *Front. Oncol.* 15:1520985. doi: 10.3389/fonc.2025.1520985

Repurposing alternative splicing events as potential targets for the design of diagnostic and therapeutic tools in PCa

Nancy Martínez-Montiel[1*], José de Jesús Vite-Arciniega[1], Nora Hilda Rosas-Murrieta[2] and Rebeca D. Martínez-Contreras[1]

[1]Laboratorio de Ecología Molecular Microbiana, Centro de Investigaciones en Ciencias Microbiológicas, Instituto de Ciencias, Benemérita Universidad Autónoma de Puebla, Puebla, Mexico, [2]Laboratorio de Bioquímica y Biología Molecular, Centro de Química, Instituto de Ciencias, Benemérita Universidad Autónoma de Puebla, Puebla, Mexico

Alternative splicing is a key mechanism responsible for protein diversity in eukaryotes. Even when the relevance of this process was initially overlooked, it is now clear that splicing decisions have a strong impact on the physiology of organisms. Moreover, aberrant splicing products have been clearly related to different diseases, including cancer. Deregulation of splicing factors or mutations at the immature mRNA level could be responsible of generating these aberrant products that are involved in cell biology processes, including migration, angiogenesis, differentiation, cell cycle, DNA repair and so on. For this reason, alternative splicing is now considered a hallmark of cancer. Prostate cancer is one of the most frequently diagnosed types of cancer and some of the leading global cause of cancer death men. Prostate cancer shows an important incidence in the developing world, while the mortality rate is growing because of limited medical infrastructure and awareness. Here, we present some of the key alternative splicing events related to prostate cancer and even when the exact role of these isoforms in the development of the disease has not been fully understood, we believe that the correction of these aberrant splicing events represents an attractive target for the design of innovative diagnostic and therapeutic tools.

KEYWORDS

splicing, prostate cancer, diagnosis, treatment, RNA

1 Introduction

Prostate cancer (PCa) is the second most common cancer diagnosed in men (after skin cancer) and the second most common cause of cancer death in men (after lung cancer). Advances in screening, diagnosis, and treatment of PCa have been improving outcomes for thousands of men. In the US, approximately 1 in 44 men will die from PCa in 2024, with an estimated total of 35,250 men, with a 5-year relative survival rate of 97% (1).

Most PCas are found early and are asymptomatic. If symptoms are present, patients may experience difficulty urinating, blood in urine or semen, back pain, or erectile dysfunction.

Screening for PCa is conducted with a PSA test. Although PSA screening can result in early detection of PCa, it is not completely reliable due to the possibility to generate false-positive results and overdiagnosis (2). Due to this possibility, routine PCa screening is not recommended for men at average risk but most organizations endorse shared decision-making to educate men about the pros and cons of PSA screening. In most countries including the US, the course of treatment is not always clear, and there is much debate over which strategies are most effective for PCa in the long term. This landscape urge the necessity to establish a clear correlation between the molecular characteristics and the cellular behavior of the tumor, in order to develop accurate diagnostic tools and effective therapeutic management.

2 Current tools for PCa diagnosis

PCa diagnosis requires a combined approach including magnetic resonance imaging (MRI), computed tomography (CT), and positron emission tomography (PET). Additional noninvasive procedures for PCa include serum prostate-specific antigen (PSA) levels and digital rectal examination. Finally, to determine the size and histological grade of the tumor, transrectal and transperineal biopsy, as well as transurethral resection of the prostate, may be performed (3).

In order to properly determine the stage of PCa, the following critical characteristics should be addressed: tumor size and spread to neighboring organs; spread of tumor to lymph nodes; metastasis; histologic grade of the tumor, based on the Gleason score; and PSA levels at the time of diagnosis (4).

Most therapies for early stages of PCa involve either surgically removing the tumor or active surveillance. Because many PCas require testosterone to grow, hormonal therapies aimed at reducing the amount of testosterone are frequently used in addition to medical procedures. Castration-resistant PCa (CRPC) refers to tumors that continue to grow in the absence of testosterone (5). Chemotherapy, immunotherapy, and radio-ligand targeted therapy can be used for CRPC or aggressive and recurrent disease.

Chemotherapeutic agents for PCa include: Cabazitaxel, Carboplatin, Docetaxel and Mitoxantrone hydrochloride. Pembrolizumab and sipuleucel-T are immunotherapy agents used for treating PCa (6).

Targeted therapy can be useful for PCa when the patient has specific mutations or the tumor expresses unique molecular characteristics. The following targeted therapies are applied for PCa: Lutetium lu 177 vipivotide tetraxetan; Olaparib; Radium 223 dichloride and Rucaparib camsylate (6).

Finally, hormonal therapy could be applied for PCa patients in order to reduce testosterone, which is required for tumor growth. The following therapies that work on a patient's hormonal system are approved for use in PCa: Abiraterone acetate; Apalutamide; Bicalutamide; Darolutamide; Degarelix; Enzalutamide; Flutamide; Goserelin acetate; Leuprolide acetate; Nilutamide; and Relugolix (6).

Even when all these therapeutic tools could be applied in combination to reduce or revert the advance of PCa, most of them are recommended for treatment in advanced stages. In order to produce novel therapies, researchers continue to investigate additional molecular targets for the treatment of PCa.

3 Alternative splicing relevance in cancer

Alternative splicing (AS) is a co-transcriptional mechanism that regulates eukaryotic gene expression that affects over 90% of human genes (7, 8). In this mechanism, different combinations of exons and introns can be identified and removed from the pre-mRNA, allowing multiple mRNA configurations of joined sequences to arise from a single gene, increasing the coding potential of the genome (9).

Malfunctions of alternative splicing events can affect the natural expression of a large number of transcripts, including several factors involved in apoptosis or cell survival, molecular processes intimately associated with cancer evolution (10, 11). In many cases, specific splicing factors or mutated components of the splicing machinery are linked to an anomalous event. Moreover, a switch in specific splicing events occurs in particular types of cancer where the concomitant outcome is the production of non-functional proteins with added, deleted, or altered domains affecting tumorigenesis (12). With all this evidence, several strategies have been developed to regulate alternative splicing, some oriented to improve cancer prognosis, therapeutic and treatment.

Alternatively spliced messenger RNA often produce proteins with distinct or even opposing functions (i.e. Bcl-x produces a pro-apoptotic and an anti-apoptotic versions). It is estimated that as much as 50% of all genetic disorders may be caused by mutations that alter pre-mRNA splicing (13). There is increasing evidence regarding genes involved in different stages of cancer, whose alternative splicing is affected, with consequences in different processes such as cellular invasion and proliferation, resistance to apoptosis and susceptibility to different chemotherapeutic agents. In accordance with the information provided by the Cancer Genome Project of the Wellcome Trust Sanger Institute, 488 human genes possess mutations associated with some type of cancer. More relevant, 63 of them present mutations that somehow affect their alternative splicing. Despite the relevance of splicing to diseases, few approaches exist to control this mechanism with therapeutic purposes (14).

4 Alternative splicing events related to PCa

Even when more evidence concerning the relevance of alternative splicing in cancer is unraveled every day, further studies are needed in order to analyze the molecular mechanisms regulating aberrant splicing events and the cellular pathways altered by these splicing decisions. Here, we present some of the key splicing events associated to PCa development. Each case is presented separately and the key information is summarized in Table 1.

4.1 The androgen receptor

Alternative splicing of the androgen receptor is one of the most studied events for PCa. This nuclear receptor for male sex hormones is a multidomain protein that possess the ability to dimerize when binding to an androgen molecule and the activation of this route starts different mechanisms of cell development and proliferation (42).

TABLE 1 Splicing events relevant to prostate cancer.

Gene official symbol/ Official full name	Splicing events, mutations	Functional impacts	Potential as therapeutic targets	Reference
AR androgen receptor	Aberrant alternative splicing	Synthesis of two truncated isoforms of the constitutively active receptor, called AR-V7 and AR-V9, which lack the LBD domain (exons 5 to 8). The isoforms correlate with cell proliferation, resistance and protection against hormonal treatments.		(15) (16) (17)
	Dysregulation and overexpression of the SRSF1 splicing factor	Synthesis of aberrant AR-V7 and AR-V9 isoforms correlates with SRSF1 overexpression.		(18)
BCL2L1 BCL2 like 1 or *BCL-X* gene	Isoforms BCL-XL and BCL-XS from two alternative 5' splice sites in the exon 2. Regulation of isoforms expression by the cell cycle and activation of phosphatases.	Prostate cell lines expressing BCL XL (phosphorylation-activated protein) exhibit a high resistance to apoptosis, as well as resistance to various treatments, from chemotherapy to radiotherapy.	Phosphorylase inhibitor drugs.	(21) (22)
CCND1 cyclin D1	SNP G/A870 at the end of exon 4 and beginning of intron 4.	The isoform called cyclin D1b retains a portion of intron 4 that includes a premature stop codon. Cyclin D1b is in the nucleus and correlates with decreased activation of the androgen receptor.		(23)
CD44 CD44 molecule (IN blood group)	Dysregulation of alternative splicing with diverse isoforms at different stages of the disease.	There is a downregulation of CD44 expression in metastatic stages of prostate cancer, while migration is decreased.	CD44 and CD44v6 could be markers for finding prostate metastatic cells in liquid biopsies.	(24)
		CD44v6 is expressed in the epithelial to mesenchymal transition.		(25)
KLK3 kallikrein related peptidase 3 (Prostate Specific Antigen)	Highly complex alternative splicing events, SNPs.	Overexpression of KLK3 degrades the extracellular matrix and thus expands cancer tissue, and correlates with increased angiogenesis.	New and improved diagnostic and therapeutic tools based on	(26)
	Highly complex alternative splicing events, SNPs.		KLK3 variants to assess disease progression.	(27)
FOXA1 forkhead box A1	High rate of mutagenesis in any endoderm-derived tissue, such as the prostate gland.	The effect on splicing regulation is not yet fully understood.		(28) (29)
IGF1 insulin like growth factor 1	Alternative splicing, three isoforms called IGF-IEa, IGF-IEb and IGF-IEc.	In PCa epithelial cells, the IGF-IEc isoform is highly expressed with an increase in proliferation mediated by activation of the IGF-1R receptor. Association between increased circulating levels of IGF-1 and the risk of developing solid malignancies.	IGF-1 and IGF-IEc could act as circulating biomarkers.	(30) (31)
KLF6 KLF transcription factor 6	IVSΔA allele generate the alternative isoforms not functional: KLF6-V1, KLF6-V2 and KLF6-V3. The IVSΔA allele has a G/A polymorphism that generates a new splice site near the boundary between the first intron and the second exon called the IVS1-27 point.	The isoforms act as antagonists of the functional KLF6 isoform, cancers tend to be aggressive and metastasis.	IVSΔA allele related to PCa in men, in the American population.	(32) (33)

(Continued)

TABLE 1 Continued

Gene official symbol/ Official full name	Splicing events, mutations	Functional impacts	Potential as therapeutic targets	Reference
ERG/TMPRSS2 ERG ETS transcription factor ERG TMPRSS2 transmembrane serine protease 2	Gene fusion with the androgen-driven promoter of the TMPRSS2 gene through chromosomal translocation or by interstitial deletion of the intergenic region between TMPRSS2 and ERG.	ERG/TMPRSS2 deletion is present in approximately 50% of PCas.	Modify the splicing events of ERG gene.	(34)
	Up to 30 alternative transcripts of the ERG gene.	ERG is phosphorylated by ERK kinase, triggering the posttranslational activity that drives cell proliferation.		(35) (36)
NF-YA nuclear transcription factor Y subunit alpha	Alternative splicing produces the NF-YAL and NF-YAS isoforms.	Increased NF-YAS induces cancer cell proliferation, while overexpression of NF-YAL increases cell mobility.	New molecular strategy for risk assessment of PCa patients.	(37, 38)
VEGFA vascular endothelial growth factor A	Alternative slicing produces angiogenic and anti-angiogenic isoforms.	In PCa cell lines, the ratio between these pro-angiogenic and anti-angiogenic isoforms is affected, with a tendency to increase for proangiogenic isoforms.		(39) (40)
	Dysregulation of the SRSF1 factor.	Dysregulation of the SRSF1 factor increases the expression of VEGFA121 (angiogenic) and decreases the isoform with better anti-angiogenic potential.		(41)

The gene coding for the AR consists of 8 exons, where exons 5 to 8 encode the ligand-binding domain (LBD). Interestingly, in prostatic cancer cells the expression of this gene is modified and an aberrant alternative splicing occurs (Figure 1A), generating two truncated isoforms of the receptor, named AR-V7 and AR-V9 (43). These isoforms completely lack the LBD domain and therefore they are not able to bind to androgens, but they are constitutively active, so that they cannot be negatively regulated and will be constantly generating proliferation, conferring resistance and protection against hormonal treatments (15–17).

The expression of these aberrant isoforms derived from a deregulated alternative splicing event is not directly associated with a mutation in the gene for the androgen receptor, however it has been pointed out that the level of expression of these isoforms is related to an increase in the number of copies within the locus containing the gene in the cell. Moreover, it has been depicted that a deregulation and overexpression of the SRSF1 splicing factor correlates with the appearance of aberrant isoforms (18).

4.2 BCL2L1

The *BCL-X* gene (or *BCL2L1*) regulates apoptosis and therefore has an extremely important role in cancer (19, 20). This gene is constituted by 3 exons with the ability to generate 2 isoforms due to the selection of two alternative 5' splice sites in exon 2, resulting in isoforms BCL-X_L (B-Cell Lymphoma xtra large) and BCL-X_S (B-Cell Lymphoma xtra small). Both isoforms have opposite functions where BCL-X_S is proapoptotic being part of the core apoptosome, while on the contrary BCL-X_L is antiapoptotic by antagonizing proapoptotic functions of other molecules belonging to the BCL-2 family (Figure 1B).

The regulation of the expression of these isoforms is determined by the regulation of the cell cycle and with this, the activation of different phosphatases. At the level of splicing regulation, it is known that the expression of BCL-X_S is determined by hnRNP H and F, SAM68 and RBM25 (44–46). On the other hand, the expression of BCL-X_L is regulated by SR proteins such as SRSF1, SRSF9 and SAP155 (45–48) that must be phosphorylated and this modification usually occurs during the initiation of cell replication (22). The disruption of the delicate balance between BCL-X_L and BCL-X_S isoforms has not been related to a specific mutation; however, it is believed that it has to do with the appearance of epigenetic changes that affect the cell cycle, but further evidence is needed to fully demonstrate this observation.

In the context of PCa, it has been determined that prostatic cell lines expressing BCL-X_L show a fairly high resistance to apoptosis generating resistance to various treatments from chemotherapy to radiotherapy (21). As an alternative, phosphorylase inhibitor drugs have been implemented for cancer treatment, although this could generate negative effects in other healthy tissues.

4.3 CCND1

The *CCND1* gene consists of 5 exons and encodes the cyclin D1 protein which is a proto-oncogene given its ability to activate cyclin-dependent kinases (CDK) 4 and 6 forming a complex that phosphorylates and thus activates molecules that allow cell cycle progression from G1 to S phase promoting cell proliferation. Moreover, cyclin D1 sequesters inhibitors of CDK kinases such as p27.

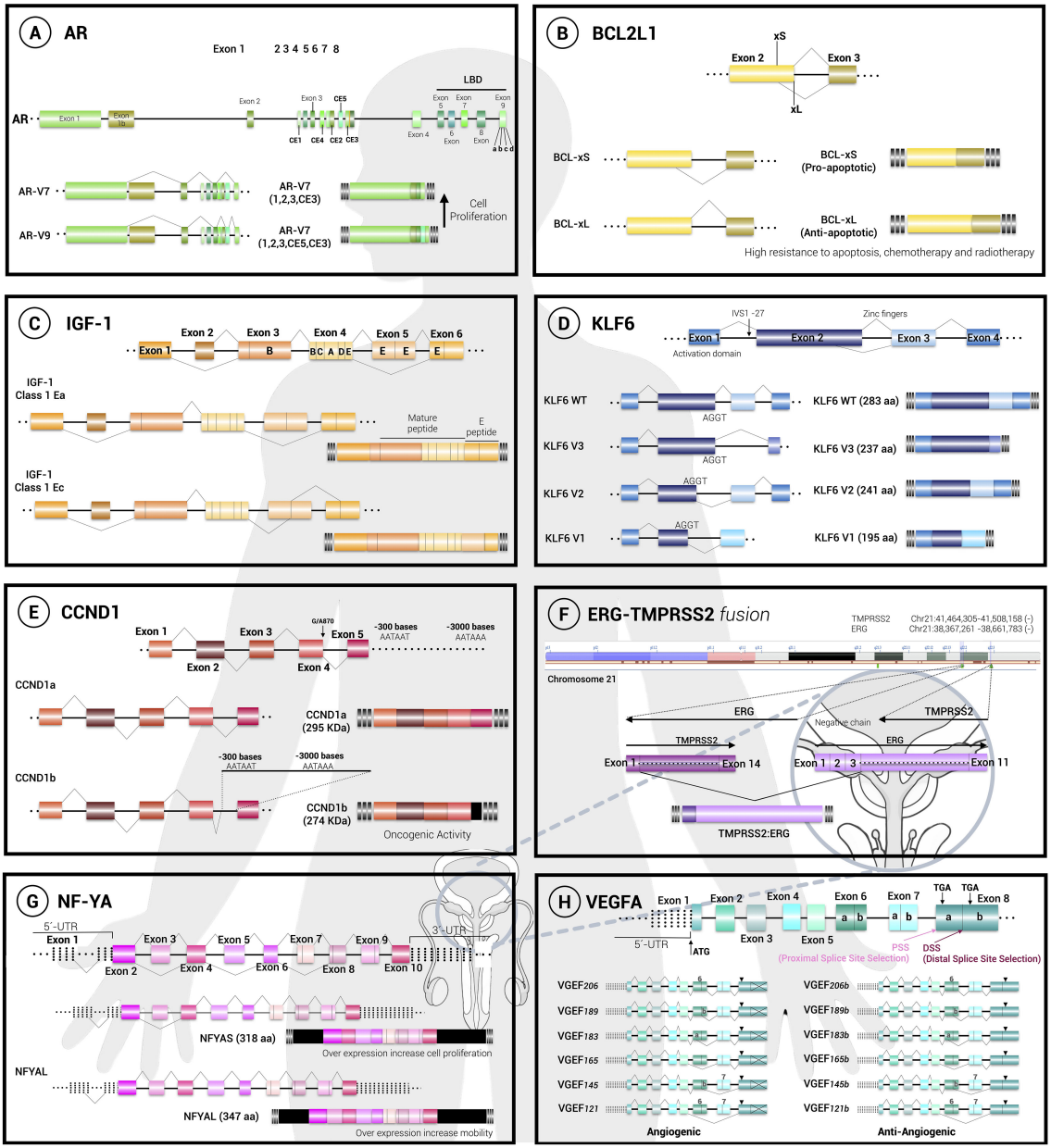

FIGURE 1
Alternative splicing decisions regulate cell fate. The general structure and splicing choices are depicted for 8 pre-mRNAs, as follows: **(A)** the androgen receptor (AR), **(B)** the BCL-X gene (BCL2L1), **(C)** the insuline-like growth factor (IGF), **(D)** the krüppel-like transcription factor 6 (KLF6), **(E)** D1 (CCND1), **(F)** the fusion between the ETS-related gene and the transmembrane serine protease 2 gene (ERG/ TMPRSS2), **(G)** the nuclear factor Y (NF-YA) and **(H)** the vascular endothelial growth factor A (VEGFA). The cellular effect of the isoforms generated is mentioned. Exons are represented with boxes while lines correspond to introns.

Usually, the mRNA resulting from the *CCND1* gene does not undergo alternative splicing; however, it has been seen that in multiple cancers and tumors there are translocations and deletions that promote the activation of this gene (49). In PCa, it has been determined that a single nucleotide polymorphism for this gene is common, this allele called *G/A870* consists of the change of a guanine by an adenine in the vicinity of the end of exon 4 and beginning of intron 4. This mutation causes a decrease in the recognition of the usual splice sites and favors the formation of a transcript that retains a fraction of intron 4 that includes a premature stop codon, generating the isoform called cyclin D1b (Figure 1E). This isoform always resides in the nucleus, unlike the normal isoform that shuttles between the nucleus and the cytoplasm according to the signals in the cell. The expression of this isoform also correlates with a decrease in the activation of the androgen receptor in PCa (23).

4.4 CD44 and *KLK3*

CD44 is an adhesion glycoprotein expressed in the epithelial cells of prostate tissue. The *CD44* gene consists of 20 exons, where

intermediate exons v2 to v10 are mutually exclusive and could be included due to alternative splicing decisions. It has been reported that during PCa a deregulation of this alternative splicing selection occurs, generating various isoforms at different stages of the disease. However, it has been observed that in metastatic stages of PCa there is a negative regulation in the expression of this glycoprotein while migration is decreased (24). One report proposes that CD44v6 is expressed in epithelial to mesenchymal transition (25). Considering this evidence, CD44 and CD44v6 could be an interesting marker to find prostatic metastatic cells in liquid biopsies.

The *KLK3* gene encodes the protein peptidase related to kallikrein 3 (KLK3), better known as the prostate specific antigen (PSA). KLK3 functions as a protease and it plays an extremely important role during the development of PCa, where it is overexpressed in order to degrade the extracellular matrix and thus expand the cancerous tissue (26). Moreover, an increase in angiogenesis also correlates with the overexpression of KLK3 in the context of PCa (27).

KLK3 consists of 5 exons and 8 isoforms of the KLK3 protein are known. Even when different attempts have been made in order to relate the different isoforms of KLK3 with malignancy and progression of PCa, no irrefutable evidence has been found yet and it becomes interesting to explore alternative splicing regulation for this PCa biomarker (26).

Both the *CD44* and *KLK3* genes are important in the development of PCa disease and although they are well studied, alternative splicing events are highly complex, and not only have polymorphisms been reported that modify the dynamics of splicing, It has also been seen that this modification can be orchestrated by epigenetic mutations and therefore are not very useful as a therapeutic target. Interestingly, there was a sharp decline in the overall incidence of PCa from 2007 to 2014 in the US, which correlated with a reduction in prostate specific antigen (PSA) screening as a result of changes to US Preventive Services Task Force recommendations. Variations in PCa incidence rates mainly reflect the use of PSA screening, which typically detects localized disease. In 2023, it was estimated that 55% of American men with metastatic PCa were initially diagnosed with localized or regional disease, reflecting the importance of PSA detection. Even when the full impact of splicing decisions for CD44 and KLK3 in the onset an evolution of PCa remains elusive, it results interesting to analyze the expression of splicing variants during the progression of the disease in order to develop new and improved diagnostic and therapeutic tools.

4.5 FOXA1

FOXA1 is a transcriptional factor responsible for the modulation of key splicing factors such as hnRNPK and SRSF1 (50). Although several mutations have been detected in the FOXA1 gene, the effect of these mutations on the expression of genes regulated by splicing factors including SRSF1 (like AR or VEGFA) has not been fully understood yet. The *FOXA1* gene has been found to have a very high mutagenesis rate, which is reflected in the ability to generate tumors in basically any endoderm-derived tissue, including the prostate gland (28).

The relationship between FOXA1 and splicing regulation in the context of PCa is still not fully understood (29), but we believe that the analysis of this cellular cascade in the following years could mean a significant advance for the development of diagnostic targets.

4.6 IGF-I

Insulin-like growth factor I (IGF-I), also called somatomedin C, is essential in developmental and proliferative functions in many tissues, besides maintaining homeostasis of several hormones including insulin. This factor is secreted mainly by the liver and some other tissues such as the prostate in a paracrine manner.

The gene encoding this factor (*IGF-I)* consists of 6 exons that generate 3 different isoforms: IGF-IEa, IGF-IEb and IGF-IEc (30) and the IGF-IEc isoform is highly expressed during PCa and this has been directly related to an increase in proliferation mediated by the activation of the IGF-1R receptor in PCa epithelial cells (Figure 1C). Interestingly, several studies have shown an association between increased levels of circulating IGF-1 and the risk of developing solid malignancies, including PCa (31). The IGF-IEc isoform is overexpressed in human PCa tissues and in human PC-3 and LNCaP cells. This preferential IGF-IEc mRNA expression generates the MGF E peptide that possesses mitogenic activity through mechanisms independent of IGF-1R, IR, and hybrid IGF-1R/IR (51). Altogether, these observations suggest that IGF-1 and IGF-IEc could act as circulating biomarkers for PCa diagnosis.

There are also reports of mutations that favor the formation of other IGF-I isoforms, although they have not yet been related to PCa.

4.7 KLF6

The *KLF6* gene (krüppel-like transcription factor 6), consisting of 3 DNA-binding zinc domains, regulates the cell cycle by inducing the expression of the cell cycle inhibitor p21 and preventing replication as its main function; however, KLF6 is a factor that can also be one of several modulators of cell differentiation, apoptosis and development and is therefore considered a tumor suppressor.

Usually, KLF6 is expressed without undergoing alternative splicing (wtKLF6 isoform). However, individuals possessing the IVSΔA allele generate 3 alternative isoforms: KLF6-V1, KLF6-V2 and KLF6-V3. These isoforms lack one (KLF6-V2) or 2 zinc domains (KLF6-V1 and KLF6-V3) and therefore are not functional (Figure 1D). In addition, alternative variants can also act as antagonists of the functional isoform wtKLF6 in such a way that it behaves as a dominant allele and therefore cancers related to this isoform tend to be aggressive and generate metastasis. The IVSΔA allele possesses a unique G/A polymorphism that generates a new splice site near the boundary between the first intron and the second exon (called IVS1 -27 point) that is recognized by the SRp40 protein and promotes the expression of isoforms lacking zinc domains (32).

The presence of the IVSΔA allele has been studied only in the American population and it has been determined that it is related to lung and PCa in men (33).

4.8 ERG/TMPRSS2

The *ERG* gene (ETS-related gene) is a member of the E-26 transformation-specific (ETS) family of transcription factors. The ETS transcription factors have a pivotal role in development and cell differentiation with roles in different cell types, where it regulates embryogenesis, vasculogenesis, angiogenesis, haematopoiesis and neuronal development. This transcription factor regulates the expression of genes involved in the regulation of cellular architecture, cell migration, invasion and cell permeability.

There are several descriptions of *ERG*'s gene and exon/intron structure. The *ERG* locus is approximately 300 kb long and includes at least 12 exons producing up to 30 alternative *ERG* transcripts that are expressed and encoding at least 15 protein variants (Figure 1F).

Prostate epithelia do not normally express *ERG*, but it has been reported that *ERG* is overexpressed in a high proportion of prostate carcinomas as a result of a gene fusion with the androgen-driven promoter of the *TMPRSS2* gene. This fusion is caused by chromosomal translocation or by interstitial deletion of the intergenic region between *TMPRSS2* and *ERG* (34). Deletions may occur because of fragile sites and breakpoints found in intron 2 of *ERG* and in introns 1 and 2 of *TMPRSS2* that resemble Alu repeat elements. These elements are involved in gene expression at different levels, including alternative splicing. This aberrant ERG represses a number of prostate epithelium-specific genes, including *KLK3*, suggesting that ERG promotes the de-differentiaton of prostate epithelium (52).

Another alternative splicing decision relevant for ERG expression in prostate cancer involves cassette exons 7 and 7b. It has been reported that when exon 7b is included, ERG is phosphorylated by ERK kinase, triggering the posttranslational activity that drives cell proliferation (35).

It has been seen that this *ERG/TMPRSS2* deletion is present in approximately 50% of PCas and it has been demonstrated that inhibiting the insertion of exon 7b decreases cell proliferation and migration. Due to the complexity of this gene, no trans acting splicing regulatory factors have been described yet but the development of tools designed to modify these splicing events are attractive (36).

4.9 Nuclear factor Y

The transcription factor NF-Y supports cell proliferation by activating the transcription of various molecules that allow transformation and proliferation. This factor comprises 3 subunits: NF-YA, NF-YB and NF-YC. The gene coding for the NF-YA subunit consists of 9 exons where the first exon corresponds to a non-coding sequence and the third exon undergoes alternative splicing that encodes 28 amino acids (Figure 1G), producing the NF-YA_L and NF-YA_S isoforms, respectively (37). Although the dynamics that deregulates the expression of these isoforms is not fully known, it has been seen that other epithelial cancers such as lung adenocarcinoma overexpress the long isoform NF-YA_L which has been related to cell migration, while the short isoform NF-YA_S is related to endometrial cancer tumors. In PCa, it has been observed that the increase of NF-YA_S induces cancer cell proliferation, while NF-YA_I overexpression increases cell motility. We believe that evaluation of NF-YA splicing may represent a new molecular strategy for risk assessment of PCa patients (38).

4.10 VEGFA

The vascular endothelial growth factor or VEGFA promotes angiogenesis and the gene that encodes this factor can generate different angiogenic isoforms that are generally referred to as "VEGFAxxx" where xxx refers to the number of amino acids present in the protein. According to this, each isoform has a different half-life and activates various signaling pathways (Figure 1H).

The angiogenic isoforms VEGFA121, VEGFA145, VEGFA148, VEGFA165 and VEGFA206 are normally expressed in cells but they show a certain ratio with the anti-angiogenic isoforms (VEGFA121b, VEGFA145b, VEGFA148b, VEGFA165b, VEGFA206b), so the regulation of their expression is essential for the correct functioning of the tissue (39). However, in PCa cell lines it has been found that the ratio between these pro-angiogenic and anti-angiogenic isoforms is affected and expression tends to be enhanced for the pro-angiogenic isoforms (40). As in the case of the androgen receptor (AR), this change in isoform regulation is not related to a mutation in the VEGFA gene so far, but it is the dysregulation of the SRSF1 factor that mainly increases the expression of VEGFA121 and decreases the isoform with the best anti-angiogenic potential (41).

5 Concluding remarks

Alternative splicing has a key role in the physiology of prostate cancer. In the near future, it will be interesting to direct our efforts to connect the molecular evidence with the cellular behavior that prevails in the context of prostate cancer. This landscape could help us to properly develop new tools to innovate diagnostic and therapeutic tools in order to improve the outcome for cancer patients. The possibility to monitor splicing events in liquid biopsies would be a non-invasive tool for cancer diagnosis, while RNA molecules designed with therapeutic applications is now a reality. With all this in mind, we hope that alternative splicing modulation will become an alternative for prostate cancer patients.

Author contributions

RM-C: Conceptualization, Investigation, Writing – original draft, Writing – review & editing. JV-A: Investigation, Writing – original draft. NR-M: Investigation, Writing – original draft. NM-

M: Investigation, Supervision, Writing – original draft, Writing – review & editing.

Funding

The author(s) declare that no financial support was received for the research and/or publication of this article.

Conflict of interest

The authors declare that the research was conducted in the absence of any commercial or financial relationships that could be construed as a potential conflict of interest.

Generative AI statement

The author(s) declare that no Generative AI was used in the creation of this manuscript.

Publisher's note

References

1. Siegel RL, Giaquinto AN, Jemal A. Cancer statistics 2024. *CA Cancer J Clin*. (2024) 74:12–49. doi: 10.3322/caac.21820

2. Devasia TP, Mariotto AB, Nyame YA, Etzioni R. Estimating the number of men living with metastatic prostate cancer in the united states. *Cancer Epidemiol Biomarkers Prev*. (2023) 32:659–65. doi: 10.1158/1055-9965.EPI-22-1038

3. NCI. *Prostate cancer treatment (PDQ®)–health professional version. national cancer institute. Updated February 13, 2023*. (2023). Available online at: https://www.cancer.gov/types/prostate/hp/prostate-treatment-pdq (Accessed May 17, 2023).

4. ACS. *Prostate cancer stages. american cancer society. Updated November 22, 2023*. (2023) (Accessed February 8, 2024).

5. NCI. *NCCN clinical practice guidelines in oncology (NCCN Guidelines®), prostate cancer*. National Comprehensive Cancer Network (2023).

6. NCI. *Drugs approved for prostate cancer. national cancer institute. Updated August 25, 2023*. (2023) (Accessed February 8, 2024).

7. Pan Q, Shai O, Lee LJ, Frey BJ, Blencowe BJ. Deep surveying of alternative splicing complexity in the human transcriptome by high throughput sequencing. *Nat Genet*. (2008) 40:1413–5. doi: 10.1038/ng.259

8. Wang ET, Sandberg R, Luo S, Khrebtukova I, Zhang L, Mayr C, et al. Alternative isoform regulation in human tissue transcriptomes. *Nature*. (2008) 456:470–6. doi: 10.1038/nature07509

9. Lander ES, Linton LM, Birren B, Nusbaum C, Zody MC, Baldwin J, et al. Initial sequencing and analysis of the human genome. *Nature*. (2021) 409:860–921. doi: 10.1038/35057062

10. Ladomery M. Aberrant alternative splicing is another hallmark of cancer. *Int J Cell Biol*. (2013) 2013:463786. doi: 10.1155/2013/463786

11. Martínez-Contreras R, Martínez-Montiel N. Chapter 3. the role of splicing factors in cancer prognosis and treatment. In: Massey E, editor. *Alternative splicing and disease*. New York: Nova Science Publishers (2016). p. 51–82.

12. Martínez-Montiel N, Rosas-Murrieta NH, Martínez-Contreras R. Alternative´ splicing regulation: Implications in cancer diagnosis and treatment. *Med Clin*. (2015) 144:317–23. doi: 10.1016/j.medcli.2014.02.021

13. Tazi J, Bakkour N, Stamm S. Alternative splicing and disease. *Biochim Biophys Acta*. (2009) 1792:14–26. doi: 10.1016/j.bbadis.2008.09.017

14. Martínez-Montiel N, Rosas-Murrieta NH, Martínez-Montiel M, Gaspariano-Cholula MP, Martínez-Contreras RD. Microbial and natural metabolites that inhibit splicing: A powerful alternative for cancer treatment. *BioMed Res Int*. (2016) 2016:3681094. doi: 10.1155/2016/3681094

15. Yu Z, Chen S, Sowalsky AG, Voznesensky OS, Mostaghel EA, Nelson PS, et al. Rapid induction of androgen receptor splice variants by androgen deprivation in prostate cancer. *Clin Cancer Res*. (2014) 20:1590–600.

16. Liang J, Wang L, Poluben L, Nouri M, Arai S, Xie L, et al. Androgen receptor splice variant 7 functions independently of the full length receptor in prostate cancer cells. *Cancer Lett*. (2021) 519:172–84. doi: 10.1016/j.canlet.2021.07.013

17. Han D, Labaf M, Zhao Y, Owiredu J, Zhang S, Patel K, et al. Androgen receptor splice variants drive castration-resistant prostate cancer metastasis by activating distinct transcriptional programs. *J Clin Invest*. (2024) 30:e168649. doi: 10.1172/JCI168649

18. Saini T, Gupta P, Raut R, Nayak V, Bharathnaveen P, Mishra P, et al. AR-V7 expression facilitates accelerated G2/M phase transition in castration-resistant prostate cancer. *Exp Cell Res*. (2024) 438:114026. doi: 10.1016/j.yexcr.2024.114026

19. Boise LH, González-García M, Postema CE, Ding L, Lindsten T, Turka LA, et al. Bcl-x, a bcl-2-related gene that functions as a dominant regulator of apoptotic cell death. *Cell*. (1993) 74:597–608. doi: 10.1016/0092-8674(93)90508-n

20. Pistritto G, Trisciuoglio D, Ceci C, Garuf A, D'orazi G. Apoptosis as anticancer mechanism: function and dysfunction of its modulators and targeted therapeutic strategies. *Aging (Albany NY)*. (2016) 8:603–19. doi: 10.18632/aging.100934

21. Baltogiannis D, Charalabopoulos K, Giannakopoulos X, Karakosta A, Sofkitis N. Combined use of antisense oligonucleotides and chemotherapeutics in the treatment of refractory prostate cancer. *Exp Oncol*. (2005) 27:91–3.

22. Naro C, Barbagallo F, Chieff P, Bourgeois CF, Paronetto MP, Sette C. The centrosomal kinase NEK2 is a novel splicing factor kinase involved in cell survival. *Nucleic Acids Res*. (2014) 42:3218–27. doi: 10.1093/nar/gkt1307

23. Knudsen KE. The cyclin D1b splice variant: an old oncogene learns new tricks. *Cell Div*. (2006) 24:1 –5. doi: 10.1186/1747-1028-1-15

24. Iczkowski KA. Cell adhesion molecule CD44: its functional roles in prostate cancer. *Am J Transl Res*. (2010) 3:1–7.

25. Hernández JR, Kim JJ, Verdone JE, Liu X, Torga G, Pienta KJ, et al. Alternative CD44 splicing identifies epithelial prostate cancer cells from the mesenchymal counterparts. *Med Oncol*. (2015) 32:159. doi: 10.1007/s12032-015-0593-z

26. Pampalakis G, Scorilas A, Sotiropoulou G. Novel splice variants of prostate specifc antigen and applications in diagnosis of prostate cancer. *Clin Biochem*. (2008) 41:591–7. doi: 10.1016/j.clinbiochem.2007.12.022

27. Koistinen H, Künnapuu J, Jeltsch M. KLK3 in the regulation of angiogenesis–tumorigenic or not? *Int J Mol Sci*. (2021) 22:13545. doi: 10.3390/ijms222413545

28. Parolia A, Cieslik M, Chu SC, Xiao L, Ouchi T, Zhang Y, et al. Distinct structural classes of activating FOXA1 alterations in advanced prostate cancer. *Nature*. (2019) 571:413–8. doi: 10.1038/s41586-019-1347-4

29. Baca SC, Takeda DY, Seo JH, Hwang J, Ku SY, Arafeh R, et al. Reprogramming of the FOXA1 cistrome in treatment-emergent neuroendocrine prostate cancer. *Nat Commun*. (2021) 12:1979. doi: 10.1038/s41467-021-22139-7

30. Philippou A, Maridaki M, Pneumaticos S, Koutsilieris M. The complexity of the IGF1 gene splicing, posttranslational modifcation and bioactivity. *Mol Med*. (2014) 20:202–14. doi: 10.2119/molmed.2014.00011

31. Matsushita M, Fujita K, Hatano K, De Velasco MA, Uemura H, Nonomura N. Connecting the dots between the gut-IGF-1-prostate axis: A role of IGF-1 in prostate carcinogenesis. *Front Endocrinol*. (2022) 13:852382. doi: 10.3389/fendo.2022.852382

32. Narla G, Difeo A, Reeves HL, Schaid DJ, Hirshfeld J, Hod E, et al. A germline DNA polymorphism enhances alternative splicing of the KLF6 tumor suppressor gene and is associated with increased prostate cancer risk. *Cancer Res*. (2005) 65:1213–22. doi: 10.1158/0008-5472.CAN-04-4249

33. DiFeo A, Martignetti JA, Narla G. The role of KLF6 and its splice variants in cancer therapy. *Drug Resistance Updates*. (2009) 12:1–7. doi: 10.1016/j.drup.2008.11.001

34. Wang J, Cai Y, Yu W, Ren C, Spencer DM, Ittmann M. Pleiotropic biological activities of alternatively spliced TMPRSS2/ERG fusion gene transcripts. *Cancer Res*. (2008) 68:8516–24. doi: 10.1158/0008-5472.CAN-08-1147

35. Jumbe SL, Porazinski SR, Oltean S, Mansell JP, Vahabi B, Wilson ID, et al. The evolutionarily conserved cassette exon 7b drives ERG's oncogenic properties. *Transl Oncol*. (2019) 12:134–42. doi: 10.1016/j.tranon.2018.09.001

36. Li L, Hobson L, Perry L, Clark B, Heavy S, Haider A, et al. S- targeting the ERG oncogene with splice-switching oligonucleotides as a novel therapeutic strategy in prostate cancer. *Br J Cancer*. (2020) 123:1024–32. doi: 10.1038/s41416-020-0951-2

37. Li XY, Hooft van Huijsduijnen R, Mantovani R, Benoist C, Mathis D. Intron exon organization of the NF-Y genes. tissue-specifc splicing modifes an activation domain. *JBC*. (1992) 267:8984–90. doi: 10.1016/S0021-9258(19)50377-5

38. Belluti S, Semeghini V, Rigillo G, Ronzio M, Benati D, Torricelli F, et al. Alternative splicing of NF-YA promotes prostate cancer aggressiveness and represents a new molecular marker for clinical stratifcation of patients. *J Exp Clin Cancer Res*. (2021) 40:362. doi: 10.1186/s13046-021-02166-4

39. Stevens M, Oltean S. Modulation of VEGF-a alternative splicing as a novel treatment in chronic kidney disease. *Genes*. (2018) 9:98. doi: 10.3390/genes9020098

40. Wang X, Bove AM, Simone G, Ma B. Molecular bases of VEGFR-2-mediated physiological function and pathological role. *Front Cell Dev Biol*. (2020) 8:599281. doi: 10.3389/fcell.2020.599281

41. Harper SJ, Bates DO. VEGF-a splicing: the key to anti-angiogenic therapeutics? *Nat Rev Cancer*. (2008) 8:880–7. doi: 10.1038/nrc2505

42. Green SM, Mostaghel EA, Nelson PS. Androgen action and metabolism in prostate cancer. *Mol Cell Endocrinol*. (2012) 360:3–13. doi: 10.1016/j.mce.2011.09.046

43. Dehm SM, Tindall DJ. Alternatively spliced androgen receptor variants. *Endocr Relat Cancer*. (2011) 18:R183–96. doi: 10.1530/ERC-11-0141

44. Garneau D, Revil T, Fisette JF, Chabot B. Heterogeneous nuclear ribonucleoprotein F/H proteins modulate the alternative splicing of the apoptotic mediator Bcl-x. *J Biol Chem*. (2005) 280:22641–50. doi: 10.1074/jbc.M501070200

45. Paronetto MP, Achsel T, Massiello A, Chalfant CE, Sette C. The RNA-binding protein Sam68 modulates the alternative splicing of Bcl-x. *J Cell Biol*. (2007) 176:929–39. doi: 10.1083/jcb.200701005

46. Zhou A, Ou AC, Cho A, Benz-Jr EJ, Huang SC. Novel splicing factor RBM25 modulates Bcl-x pre-mRNA 5' splice site selection. *Mol Cell Biol*. (2008) 28:5924–36. doi: 10.1128/MCB.00560-08

47. Cloutier P, Toutant J, Shkreta L, Goekjian S, Revil T, Chabot B. Antagonistic effects of the SRp30c protein and cryptic 5' splice sites on the alternative splicing of the apoptotic regulator Bcl-x. *J Biol Chem*. (2008) 283:21315–24.

48. Massiello A, Roesser JR, Chalfant CE. SAP155 binds to ceramide-responsive RNA cis-element 1 and regulates the alternative 5' splice site selection of Bcl-x pre mRNA. *FASEB J*. (2006) 20:1680–2. doi: 10.1096/fj.05-5021fje

49. Knudsen KE, Diehl JA, Haiman CA, Knudsen ES. Cyclin D1: polymorphism, aberrant splicing and cancer risk. *Oncogene*. (2006) 25:1620–8. doi: 10.1038/sj.onc.1209371

50. Del Giudice M, Foster JG, Peirone S, Rissone A, Caizzi L, Gaudino F, et al. FOXA1 regulates alternative splicing in prostate cancer. *Cell Rep*. (2022) 40:111404. doi: 10.1016/j.celrep.2022.111404

51. Armakolas A, Philippou A, Panteleakou Z, Nezos A, Sourla A, Petraki C, et al. Preferential expression of IGF-1Ec (MGF) transcript in cancerous tissues of human prostate: Evidence for a novel and autonomous growth factor activity of MGF E peptide in human prostate cancer cells. *Prostate*. (2010) 70:1233–42. doi: 10.1002/pros.v70:11

52. Adamo P, Ladomery M. The oncogene ERG: a key factor in prostate cancer. *Oncogene*. (2016) 35:403–14. doi: 10.1038/onc.2015.109

frontiers | Frontiers in Oncology

TYPE Systematic Review
PUBLISHED 24 March 2025
DOI 10.3389/fonc.2025.1505889

OPEN ACCESS

EDITED BY
Alma D. Campos-Parra,
Universidad Veracruzana, Mexico

REVIEWED BY
Oscar Medina-Contreras,
Mexico Children's Hospital, Mexico
Weimin Gao,
Barrow Neurological Institute (BNI),
United States

*CORRESPONDENCE
Gisou Erabi
gisou.erabi@gmail.com
Niloofar Deravi
niloofarderavi@sbmu.ac.ir

†These authors share first authorship

RECEIVED 03 October 2024
ACCEPTED 27 February 2025
PUBLISHED 24 March 2025

CITATION
Hajihosseini S, Emami E, Zakavi SA, Jochin P, Shahrokhi M, Khoshravesh S, Goli M, Belbasi M, Erabi G and Deravi N (2025) Olaparib monotherapy or combination therapy in lung cancer: an updated systematic review and meta- analysis. *Front. Oncol.* 15:1505889. doi: 10.3389/fonc.2025.1505889

Olaparib monotherapy or combination therapy in lung cancer: an updated systematic review and meta- analysis

Sajjad Hajihosseini[1†], Ehsan Emami[1†], Seyed Amirali Zakavi[2†], Parnia Jochin[3], Mehregan Shahrokhi[3], Sahar Khoshravesh[4], Mitra Goli[5], Mohaddeseh Belbasi[6], Gisou Erabi[7*] and Niloofar Deravi[8*]

[1]Student Research Committee, Tehran University of Medical Sciences, Tehran, Iran, [2]Students Research Committee, School Of Medicine, Ardabil University of Medical Sciences, Ardabil, Iran, [3]School of Medicine, Shiraz University of Medical Sciences, Shiraz, Iran, [4]School of Medicine, Shahid Beheshti University of Medical Sciences, Tehran, Iran, [5]Department of Medical-Surgical Nursing, School of Nursing and Midwifery, Shahid Beheshti University of Medical Sciences, Tehran, Iran, [6]Students Research Committee, School of Pharmacy, Zanjan University of Medical Sciences, Zanjan, Iran, [7]Student Research Committee, Urmia University of Medical Sciences, Urmia, Iran, [8]Student Research Committee, Shahid Beheshti University of Medical Science, Tehran, Iran

Background and aims: Impaired double strand DNA repair by homologous repair deficiency (HRD) leads to sensitivity to poly ADP ribose polymerase (PARP) inhibition. A subset of non-small cell lung cancers (NSCLCs) harbour impaired DNA double strand break repair. This study aims to investigate meta-analysis on the olaparib monotherapy or combination therapy in lung cancer.

Methods: A comprehensive search was conducted in Pubmed, Scopus and Google Scholar data bases up to August 13, 2023 related articles were extracted title, abstract and full text of articles were screened. The quality included articles were assessing the data was extracted and hence analysis.

Results: After screening 5208 articles, 9 were selected for final review based on relevance to the topic. Olaparib monotherapy increased progression free survival (PFS) level [ES= 7.76; 95% CI= 0.16 to 1.36; P=0.208]. Olaparib maintenance therapy increased PFS compared to placebo in platinum-sensitive NSCLC patients [ES= 0.9; 95% CI= 0.9 to 0.9]. Combination therapy with durvalumab and olaparib decreased PFS level compared to the olaparib group [ES=6.07; 95% confidence interval (95% CI) = 0.67 to 11.46; P=0.000]. Adding gefitinib to olaparib decreased PFS compared to olaparib only group, significantly (ES=3.39; 95% CI=-0.78 to 7.56; P=0.609).

Conclusions: Our study demonstrated olaparib as monotherapy can increase the PFS of patients with lung cancer, but the combination of olaparib and gefitinib or the combination of olaparib plus durvalumab couldn't have a significant effect. According to the high heterogeneous rate of studies further large-scale randomized control trials are still required to progress association.

Systematic Review Registration: Open Science Framework (OSF).

KEYWORDS

olaparib, lung cancer, NSCLCs, gefitinib, durvalumab

1 Introduction

Lung cancer remains the most common cancer site in men, accounting for 17% of all new cancer diagnoses and a staggering 23% of cancer-related deaths (1). The vast majority of lung cancers, approximately 80-85%, are classified as non-small cell lung cancer (NSCLC), which encompasses several histological subtypes including squamous cell carcinoma, adenocarcinoma, and large-cell carcinoma (2). Also, small cell lung cancer (SCLC) ranks as the sixth most common cause of cancer-related deaths, contributing to approximately 13–15% of all lung cancer cases (3, 4).

Poly (ADP-ribose) polymerase (PARP) enzymes constitute a family of nuclear enzymes that are responsible for identifying and repairing single-strand breaks in DNA (5–7). The primary function of PARP involves the poly-ADP ribosylation of essential chromatin components and various proteins that are integral to the DNA repair process (8). PARP1, in particular, has the ability to relax chromatin structure, thereby allowing DNA repair factors to access the damaged sites more effectively (9). Given the crucial role of PARP enzymes in DNA repair, PARP inhibitors have emerged as a promising avenue of research for the treatment of lung cancer, particularly NSCLC (10). In a study conducted by Byers et al. in 2012, it was found that SCLC cell lines exhibited significantly higher levels of PARP1 protein expression compared to NSCLC lines (11).

Numerous preclinical investigations have suggested that PARP inhibitors possess the ability to heighten the sensitivity of SCLC cells to a range of chemotherapeutic agents (12). Byers et al. were the first to report that incorporating olaparib into the standard chemotherapy regimen of cisplatin and etoposide enhanced the anti-tumor effects in SCLC (11). As another illustrative example, research conducted by Murai et al. revealed that the PARP inhibitor talazoparib enhances the cytotoxic effects of the DNA-alkylating agent temozolomide in cancer cells (12). Lallo et al. demonstrated that combining the PARP inhibitor (Olaparib) with the Wee1 kinase inhibitor (adavosertib) significantly enhances the effectiveness of olaparib as a single agent in patient-derived xenografts of SCLC (13). Additionally, an abstract study by Gay et al. highlighted a synergistic effect between an ataxia telangiectasia and Rad3 related (ATR) kinase inhibitor and olaparib, which resulted in increased cytotoxicity in SCLC cell lines. Collectively, these findings underscore the potential of a combinatorial approach as a promising therapeutic strategy for integrating PARP inhibitors into the treatment of SCLC (14).

But in clinical studies, a case report by Lin in 2024 presents a novel treatment approach involving the combination of osimertinib and olaparib for the management of concurrent lung and ovarian cancers. The authors describe two potential treatment approaches with this combination: an alternating schedule or a short-term concurrent administration (15). Maintenance therapy with the combination of durvalumab and olaparib in patients with metastatic NSCLC couldn't demonstrate a statistically significant improvement in progression free survival (PFS) compared to durvalumab monotherapy; The length of time during and after the treatment of a disease, such as cancer, that a patient lives with the disease but it doesn't get worse. However, a numerical improvement in PFS was observed with the combination regimen (16, 17). The results from a study by Fennell in 2022 indicate that while the primary endpoint of PFS was numerically longer in the olaparib treatment arm compared to the control group, this difference couldn't meet the threshold for statistical significance. This suggests that PARP inhibitor monotherapy olaparib, may have the potential to achieve meaningful tumor control in chemosensitive NSCLC patients (18). Reduced levels of BRCA1 mRNA have been associated with longer PFS in patients with EGFR-mutant NSCLC treated with erlotinib. Given that PARP inhibitors may diminish or inhibit BRCA1 expression, combining olaparib with gefitinib could potentially enhance outcomes for patients with advanced EGFR-mutant NSCLC. However, the study conducted by Garcia-Campelo et al. didn't show a significant advantage from the combination treatment of gefitinib and olaparib (19).

To the best of our knowledge for the first time, this meta-analysis aims to association between olaparib monotherapy and combination therapy with other agents like durvalumab for lung cancer.

2 Methods

In this systematic review and meta-analysis, we intended to specify the treatment of lung cancer by olaparib as monotherapy to combination of olaparib plus gefitinib, and combination of olaparib plus durvalumab. Our methodology cohere to the PROSPERO guidelines (International Prospective Register of Systematic Reviews). The research protocol of this review was registered to Open Science Framework (OSF) (https://api.osf.io/v2/nodes/3748c/?version=2.20).

2.1 Search strategy

An advanced literature search was performed up to August 13, 2023 to replevy applicable articles from following databases: Pubmed, Scopus and Google Scholar. The search strategy contained four main subgroups of keywords. The subgroups involved terms related to lung cancer, olaparib for monotherapy, gefitinib and durvalumab for combination therapy, as well. The subgroups were collaborated using the 'AND' operator, and no restrictions were applied concerning the date, publication type, or language. The search strategy was adjusted according to the format of query for each database. To make sure all the related articles were included, we screened the reference lists of applicable systematic reviews and included studies that were obtainable in our study. All steps were independently performed by two reviewers, and any controversy were resolved through discussion between the reviewers.

2.2 Inclusion and exclusion criteria

The following criteria were considered in order to select the papers for our meta-analysis study:

1. Observational methodology (in order to exclude the invalidate effect of any intervention).
2. The main goal was to compare olaparib as monotherapy to combination of olaparib plus gefitinib, and combination of olaparib plus durvalumab.

3. Study population consisted of patients suffering from lung cancer.

Studies that used other types of methodology, were executed on animal models, or were performed in cellular and molecular level, and commentary or editorial ones were excluded, and studies including interventional and observational methods plus systematic reviews were included.

2.3 Data extraction and quality assessment

Two independent reviewers appraised each study's title and abstract to dispose its suitability for inclusion in this meta-analysis. Studies that didn't fulfill our criteria were excluded. The full texts of the existing studies were screened and suitable studies entered the data extraction process. Afterwards, the following items were derived for extraction in four sets: 1. Study characteristics (i.e. authors, year,location, and type of study); 2. patient-specific factors (i.e. the eligibility criteria for patients suffering lung cancer); 3. Study Design (i.e. number of participants, method and period of drug administration, proper follow-up of the patients, technique used to evaluate the patients' response to relative therapies); 4. Outcomes (i.e. progression free survival of the patients). Then, our reviewer used the critical appraisal checklists for Randomized Control Trial studies developed by the Joanna Briggs Institute (JBI) (https://jbi.global/critical-appraisal-tools). Another author assisted in the process in case of disparity.

2.5 Statistical analysis

We used STATA 13.1 software, developed by StataCorp LP in College Station, TX, USA, for our data analysis. Results were reported as pooled odds ratios (ORs) with a 95% confidence interval, visualized in a forest plot. We evaluated heterogeneity among the eligible studies using the I2 statistic (20) and used the random effects model when significant heterogeneity was detected (I2 > 50%) (21). Furthermore, we organized a sensitivity analysis and no paper was excluded. Finally, to explore the potential for publication bias, we applied visual inspection of funnel plot symmetry and Egger's regression analysis (22).

3 Results

3.1 Study selection

After searching in (PubMed, Google Scholar, and Scopus) databases total of 5208 number articles were obtained, and 512 duplicates were Removed. After reviewing the title & abstract screening 174 studies remained. The final review includes 9 articles of the final full-text results, the rest of which had unrelated data were deleted. The study selection process is outlined in Figure 1.

3.2 Study characteristics

A summary of the included studies is given in Table 1. The trial characteristics of the eight included studies are summarized in the table below. Briefly, the trials were published between 2020 and 2023 and included 595 participants in RCTs (226 in the olaparib monotherapy group and 369 participants in the combination therapy group). The mean age of participants ranged from 36 to 89 years. The intervention duration in all RCTs was 0.3-67.1 weeks for olaparib and 4.0-63.0 weeks for durvalumab, and the dose administered ranged from 200 mg BID to 300mg BID (200mg TDS) for olaparib and 1500 mg IV for durvalumab or 250mg gefitinib. The included studies were from the UK, USA Spain, Korea, China, And France countries.

3.3 Meta-analysis

WMD levels were reported in 7 included studies (Figure 1). Compared to baseline, olaparib monotherapy increased PFS level [ES= 7.76; 95% CI= 0.16 to 1.36; P=0.208]; however, between-study heterogeneity was reported low (I2 = 30.2%). Olaparib maintenance therapy increased PFS compared to placebo in platinum-sensitive NSCLC patients [ES= 0.9; 95% CI= 0.9 to 0.9]. Also, the obtained results indicate that olaparib as maintenance treatment, both in the form of BD [ES= 1.20; 95% CI= -0.01 to 2.41] and in the form of TDS [ES= 1.10; 95% CI= -0.24 to 2.44], in patients with chemosensitive SCLC didn't create a statistically significant difference in improving PFS or OS, and more studies are needed in this regard (Figure 2A).

Using olaparib, either alone or in combination with ceralasertib, couldn't achieve the predefined efficacy endpoint. Nevertheless, there was a noticeable increase in disease stabilization within the combination treatment group. To enhance efficacy, further exploration of olaparib in SCLC is warranted [ES= -1.50; 95% CI= -3.30 to 0.30].

Although between-study heterogeneity was high (I2 = 89.2%), combination therapy with durvalumab and olaparib decreased PFS level compared to the olaparib group according to 3 studies [ES=6.07; 95% confidence interval (95% CI) = 0.67 to 11.46; P=0.000] (Figure 2B).

The effect of combination therapy with gefitinib and olaparib on PFS was reported in 2 studies. Adding gefitinib to olaparib decreased PFS compared to olaparib only group, significantly (ES=3.39; 95% CI=-0.78 to 7.56; P=0.609); however, between-study heterogeneity was low (I2 = 0.0%; Figure 2C).

3.4 Risk of bias of included studies

The methodological quality of included studies was assessed using the JBI tool. All of the studies demonstrated excellent quality. Funnel plot was symmetric with pseudo 95% confidence limits and the study was not biased.

4 Discussion

This meta-analysis investigated the efficacy of olaparib in NSCLC. A total of 518 patients from seven studies were included.

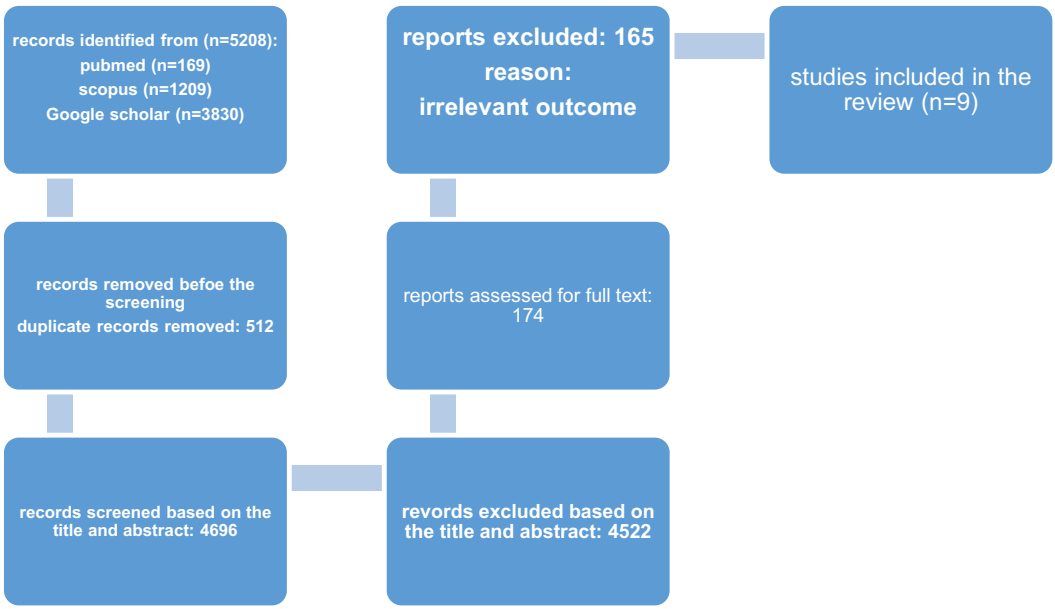

FIGURE 1
PRISMA flow diagram for current systematic.

Olaparib demonstrated a significant improvement in PFS when administered as a monotherapy. However, due to limited data, the efficacy of olaparib in combination with gefitinib or durvalumab for NSCLC remains inconclusive. Further research is warranted to elucidate the potential benefits of these therapeutic regimens.

While clinically approved PARP inhibitors — including olaparib, niraparib, rucaparib, talazoparib, and veliparib — demonstrably block PARP1 and PARP2 with similar efficacy, their capacity to induce PARP trapping varies significantly. These disparities in trapping potency are considered a key factor underlying the differing dosage guidelines for these agents, as heightened PARP trapping correlates strongly with severe myelosuppressive effects (30, 31).

In 2018, olaparib gained approval for treating BRCA-mutated HER2-negative metastatic breast cancer. This progress continued with its approval for pancreatic cancer in 2019 and metastatic castrate-resistant prostate cancer in 2021 (32).

A randomized trial of 91 patients with EGFR-mutant NSCLC evaluated the impact of BRCA1 mRNA expression on PFS when treated with olaparib plus gefitinib or gefitinib alone. Patients with high BRCA1 mRNA expression exhibited significantly longer PFS in the combination group (12.9 months) compared to the gefitinib-only group (9.2 months). This effect was more pronounced in patients with high BRCA1 levels. Conversely, patients with low BRCA1 levels had longer PFS when treated with gefitinib alone. Additionally, low CTLp mRNA levels, a subtype of BRCA1 C complexes, were associated with prolonged PFS in EGFR-mutant patients receiving olaparib plus gefitinib (29).

The GOAL study, a randomized, phase IB/II trial, evaluated the efficacy of olaparib combined with gefitinib compared to gefitinib alone in 182 patients with EGFR-mutant NSCLC. While the combination group demonstrated higher response rates and longer durations of response, there was no significant difference in median PFS between the two groups (10.9 months vs. 12.8 months). Previous research has linked low BRCA1 mRNA levels to improved PFS in patients with EGFR-mutant NSCLC treated with erlotinib (19). It is hypothesized that adding olaparib to gefitinib might enhance treatment outcomes in EGFR-mutant advanced NSCLC by inhibiting BRCA1 expression (19, 29).

The PIPSeN trial, a phase 2 randomized study, investigated the use of maintenance olaparib in 60 patients with platinum-sensitive NSCLC. While patients in the olaparib group experienced a slightly longer median PFS (2.9 months) compared to the placebo group (2 months), there was no significant difference in overall survival (OS) between the two groups (9.4 months vs. 9.5 months). Due to early termination, this study was underpowered to detect significant differences. Platinum sensitivity is a biomarker associated with PARP inhibitor sensitivity. Therefore, evaluating olaparib in platinum-sensitive advanced NSCLC patients as a PARP inhibitor is warranted (18).

The MEDIOLA study, an open-label, phase 1/2 basket trial, evaluated the efficacy of olaparib plus durvalumab in relapsed SCLC. Although 40 patients were enrolled, only 38 were assessed for efficacy. The prespecified target of a 12-week disease control rate (DCR) was not met. However, in the pretreated SCLC population, median overall survival (OS) was promising. Given the potential for PARP inhibitors to enhance antitumor activity and the potential synergy with immune checkpoint inhibitors, further exploration of this combination in relapsed platinum-sensitive SCLC is warranted (24).

The TRIDENT trial, a single-arm, phase 2 study, evaluated the efficacy of olaparib plus Durvalumab as maintenance therapy in patients with extensive-stage (ES)-SCLC who had received first-line treatment with Durvalumab plus chemotherapy. The combination demonstrated promising antitumor activity without any new safety concerns. PARP inhibitors are known to modify tumor immunogenicity, exhibit antitumor activity, and can increase sensitivity to anti-PD-1/PD-L1 therapies. These characteristics suggest that PARP inhibitors may be

TABLE 1 Characteristics of included studies.

Author/ reference	Country	Year	Study design	Participants	Sex (Fe)	Mean age	Intervention	Duration	Quality Assessment
Fennell et al. (18)	UK	2020	Randomised, double-blind, placebo-controlled, parallel arm, phase 2 trial	Patients had advanced (stage IIIB/IV) SCLC NSCLC, and had to be chemo-naive	1. Olaparib group (N=32): (Male=50%) (Female=50%) 2. Placebo group (N=38): (Male=63%) (Female=37%)	Age - median (IQR): 1. Olaparib group: 65 (61–72) 2. Placebo groupe: 63 (59–70)	The initial study dose of oral olaparib or placebo tablets was 300mg administered twice daily in 21-day cycles until disease progression, unacceptable toxicity, or patient withdrawal of consent. Dose interruption was allowed for any grade of toxicity for a maximum of 14 days until complete recovery or reversion to Common Terminology Criteria for Adverse Events (CTCAE) version 4.03 grade 1. Dose reductions were allowed to 250mg twice daily (dose level -1) or 200 mg twice daily (dose level -2). Dose escalations were not permitted	Between 27th August 2014 and 14th November 2017	12/13
Garcia-Campelo et al. (19)	Spain & Mexico	2020	Randomized phase IB/ II study	Patients with treatment-naïve, pathologically confirmed stage IV NSCLC, with centrally confirmed EGFR mutations and measurable disease	Arm A: gefitinib (N=91): Female 62.64% Arm B: gefitinib plus olaparib (N=91): Female 72.53%	Arm A: gefitinib (N=91): 68 (36-85) Arm B: gefitinib plus olaparib (N=91): 65 (39-85)	182 patients underwent randomization, 91 received gefitinib and 91 received gefitinib plus olaparib. Patients were randomly allocated (1:1) to receive gefitinib 250 mg daily or gefitinib 250 mg daily plus olaparib 200 mg three times daily in 28-day cycles. The primary endpoint was PFS. Secondary endpoints included overall survival (OS), response rate, safety and tolerability	3 years (Between September 2013, and July 2016)	13/13
Desmond et al. (23)	USA	2022	An expansion cohort of a proof-of-concept phase I/II study (NCT02484404)	Fifteen individuals with advanced NSCLC who had received at least one prior platinum-based regimen.	—	Median age: 66 years	Eligible participants were enrolled in an expansion cohort of a proof-of-concept phase I/II study and received O 300 mg PO BID with D 1500 mg IV every 4 weeks until disease progression or unacceptable toxicity. The primary end-point was PFS	Between July 2016 and July 2021	9/13
Krebs et al. (24)	UK	2023	A phase 1/2, open-label, single-arm, multicenter, international basket study	Patients with histologically or cytologically confirmed relapsed limited or extensive-stage SCLC.	Patients (n = 38): Male= 55.3%	Patients (n = 38): Median (range)= 62.5 (44–76)	Patients with previously treated limited or extensive-stage SCLC received oral olaparib 300 mg twice daily, as run-in for 4 weeks, then with durvalumab (1500 mg intravenously every 4 weeks) until disease progression. As previously described for breast cancer, all patients in the SCLC cohort received olaparib monotherapy (300 mg, oral tablet, twice daily) for 4 weeks, followed by a combination of olaparib (300 mg orally twice daily) and durvalumab (1500 mg, intravenously), administered every 4 weeks (28-day cycle) until disease progression or intolerable toxicity.	Median total treatment duration (range) was 12.1 weeks (0.3–67.1 weeks) for olaparib and 8.0 weeks (4.0–63.0 weeks) for durvalumab. Median investigator-assessed duration of response was 3.6 months (IQR, 2.6–4.6 months)	12/13

(Continued)

10.3389/fonc.2025.1505889

TABLE 1 Continued

Author/ reference	Country	Year	Study design	Participants	Sex (Fe)	Mean age	Intervention	Duration	Quality Assessment
Huang et al. (25)	China	2023	TRIDENT is a single arm, multicenter, phase 2 study	Patients with treatment-naïve ES-SCLC aged >18 with ECOG PS 0-2	—	—	Durvalumab (1500 mg) was concurrently administered with platinum-etoposide every 3 weeks for 4 cycles, followed by durvalumab 1500 mg every 4 weeks plus olaparib 300 mg twice daily until disease progression or unacceptable toxicity	Between August 2021 and August 2022. At the data cutoff on August 9, 2023, the median duration of follow-up was 13.0 months	11/13
Woll et al. (26)	UK	2022	Randomised, double-blind, placebo-controlled, phase II trial,	Patients with pathologically confirmed SCLC (including limited and extensive stage disease) and had achieved a complete or partial response after at least three cycles of first line chemotherapy with etoposide and either cisplatin or carboplatin	Placebo: Male=46% Olaparib BD: Male=49% Olaparib TDS: Male=42%	Placebo (N = 74): Median (Range) = 64 (43-86) Olaparib BD (N = 73): Median (Range) = 66 (43-89) Olaparib TDS (N = 73): Median (Range) = 63(42-82)	Patients received oral olaparib 300 mg BD or 200 mg TDS or matching placebo in continuous 28 day cycles for two years or until disease progression, death, unacceptable toxicity, or withdrawal of patient consent	Between 21 November 2013 and 11 December 2015	
Postel-Vinay et al. (27)	France & Spain	2023	Randomized double-blind phase II trial		Arm Placebo (N = 27): Male= 85% Arm olaparib (N = 33): Male= 82%	Arm Placebo: Median (range) = 65 (47-82) Arm olaparib: Median (range) = 62 (53-86)	Patients initially received the standard-of-care: four to six 21-day cycles of any platinum-doublet therapy, excluding taxane-based doublets. Patients with partial or complete response (based on RECIST v1.1) after 4–6 cycles of platinum-based chemotherapy were randomly assigned, in a one-to-one ratio, to receive maintenance olaparib or placebo. Olaparib or placebo was administered orally, at a dose of 300 mg twice a day in 28-day cycles, and started no later than 6 weeks after the last administration of chemotherapy. Treatment was administered until disease progression or unacceptable toxicity. Crossover to olaparib was not allowed	The median duration of follow-up was 39.3 months [CI 95%: 27.3–46.0]	13/13

(Continued)

10.3389/fonc.2025.1505889

TABLE 1 Continued

Author/ reference	Country	Year	Study design	Participants	Sex (Fe)	Mean age	Intervention	Duration	Quality Assessment
Park et al. (28)	Republic of Korea	2023	This study was designed as a biomarker-driven umbrella trial called SUKSES (Small Cell Lung Cancer Umbrella Korea Studies) as previously reported.	Patients with SCLC and SUKSES-S experienced disease progression during or within 6 months after first-line platinum-based chemotherapy. Patients who relapsed >6 months after the last dose of first-line therapy were allowed to participate in the trial after second-line platinum chemotherapy (with participation in SUKSES as third-line therapy). All patients had an Eastern Clinical Oncology Group Performance Score of 0 or 1, normal organ and bone marrow function, and a life expectancy of ≥16 weeks	SUKSES-B (olaparib, n = 15): Male = 93.3% SUKSES-N2 (olaparib and ceralasertib, n = 26): Male = 92.3%	SUKSES-B: Median (range) = 68 (48–76) SUKSES-N2: Median (range) = 66 (47–78)	In the olaparib monotherapy arm, olaparib 300 mg by mouth was administered every 12 hours with approximately 240 mL of water. Each cycle of treatment was 21 days in duration. A computed tomography scan was conducted every 6 weeks for response evaluation. In the olaparib and ceralasertib combination arm, the same dosing schedule of olaparib was performed but with the addition of ceralasertib at 160 mg by mouth, every day from day 1 to day 7 of each cycle. One cycle of treatment was 28 days, and a computed tomography scan was conducted every 8 weeks	From August 2016 to December 2020. The median follow-up duration of the olaparib monotherapy arm was 8.1 months (95% CI, 5.1–16.5). The median follow-up duration of the olaparib and ceralasertib combination arm was 7.2 months (95% CI, 6.0–10.2).	
Karachaliou et al. (29)	Spain	2020	A phase 1B and 2B study treatment	Patients with metastatic EGFR-mutant NSCLC	Gefitinib (N = 51): Male = 35% Gefitinib + Olaparib (N = 40): Male = 25%	Gefitinib: median age (range) = 70 (36-85) Gefitinib + Olaparib: median age (range) = 65 (39-85)	In the phase 1B dose escalation part of the study, tolerance in the absence of pharmacokinetic interactions and the activity of gefitinib plus olaparib were confirmed in 22 patients with EGFR-mutant NSCLC. The recommended phase 2 dose was 250 mg of gefitinib once daily plus 200 mg of olaparib three times daily	Between July 2013 and July 2016. PFS and OS were evaluated at the final data cutoff point on July 2017	12/13

10.3389/fonc.2025.1505889

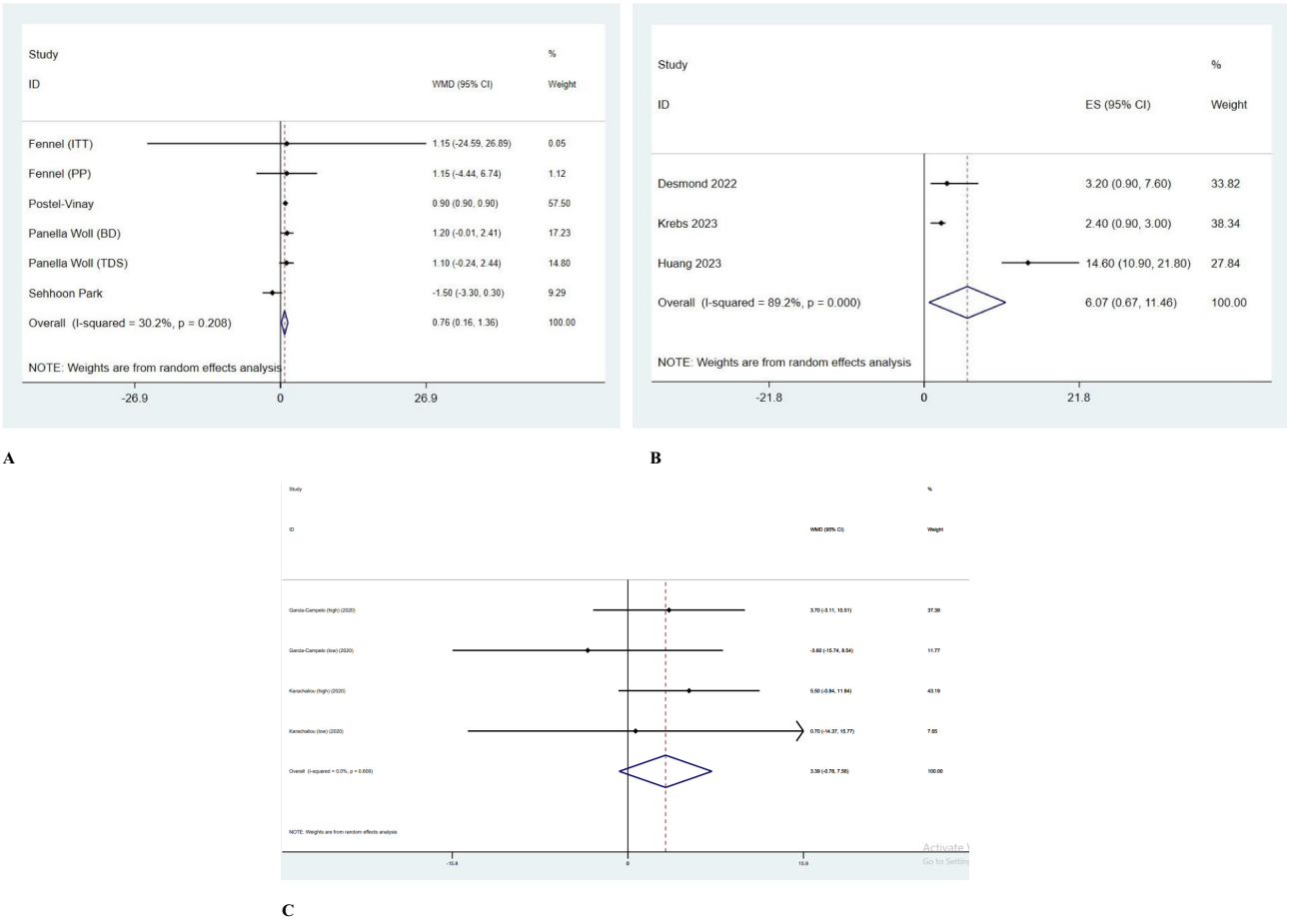

FIGURE 2
(A) Forrest plot of olaparib monotherapy. **(B)** Forrest plot of olaparib and durvalumab combination therapy. **(C)** Forrest plot of olaparib and gefitinib combination therapy.

valuable in combination with immune checkpoint inhibitors like durvalumab for ES-SCLC patients (33).

In an expansion cohort of a phase II study, the combination of olaparib plus durvalumab was evaluated in 15 patients with advanced, previously treated NSCLC. While a modest efficacy was observed overall, patients with high PD-L1 expression (>50%) and prior immune checkpoint inhibitor (ICI) therapy demonstrated a trend towards longer PFS, although this difference was not statistically significant. Preclinical research suggests that PARP inhibitors can potentially enhance the response to ICIs due to their immunostimulatory effects (23).

A study conducted by Thomas et al. found that combining PARP inhibitors with durvalumab immunotherapy could lead to a notable increase in PFS (over 5 months); however, the result wasn't statistically significant (34). A comparable study was carried out four years later by Krebs et al., which found that combining PARP inhibitors with durvalumab immunotherapy showed no significant difference in OS and PFS, with median values of 2.4 and 7.6, respectively, when compared to other therapy combinations (24).

Unlike breast or ovarian cancer, which have a relatively high BRCA mutation rate, BRCA mutations in SCLC were found in less than 3% of the population (35). A promising method for selecting suitable SCLC patients for PARP inhibitors therapy involves the measurement of biomarkers. Among the most extensively studied is SLFN11, a biomarker whose expression levels are linked to sensitivity to DNA-damaging therapies. SLFN11 is a DNA or RNA helicase that is recruited to stalled replication forks when single-strand breaks or double-strand breaks occur during the intra-S phase checkpoint. It plays a key role by disrupting homologous recombination repair, which leads to cell cycle arrest and eventually cell death (36). Higher levels of SLFN11 have been linked to increased sensitivity to DNA-damaging chemotherapies, including PARP inhibitors, leading to improved PFS and OS in triple-negative breast cancer (37). Conversely, the absence or low expression of SLFN11 has been associated with resistance to various DNA-damaging agents, including platinum-based drugs and PARP inhibitors (38). SLFN11 was found to be significantly overexpressed, even more so than in non-small cell lung cancer, making it a potential biomarker for predicting response to PARP inhibitors in SCLC (39). Another potential marker for predicting sensitivity to PARP inhibitors is E-Cadherin. When combined with LDH measurement, it may assist in patient stratification and provide insights into the overall prognosis of SCLC patients (40, 41). However, further research is required to validate these markers and identify new ones with greater predictive value.

The reduced efficacy of combination therapy relative to monotherapy may stem from several mechanisms. First, excessive DNA damage induction that in it, combining PARP inhibitors (e.g., olaparib) with chemotherapy or radiation can exceed cellular repair

capacities, causing indiscriminate cell death in both cancerous and healthy tissues. The clinical development of PARP inhibitor and platinum-based drug combinations faces complexities due to shared toxicity profiles, notably myelosuppression. A critical limitation of this approach lies in its narrow therapeutic window, stemming from the non-selective impact of both agents on healthy tissues, which exacerbates chemotherapy-induced toxicities; As happened in the BROCADE3 trial, adverse events led to study drug discontinuation (30, 42, 43). Second issue is unintended pathway activation that in it, Pairing PARP inhibitors with other DNA-damaging therapies may trigger alternative repair mechanisms (e.g., non-homologous end joining), circumventing the targeted cell death mechanism (synthetic lethality). Combining PARP inhibitors with tumor-infiltrating lymphocytes — harvested from tumors and cultured outside the body — may offer a viable therapeutic strategy for triple-negative breast cancer. Nevertheless, studies indicate that PARP inhibitors use may inadvertently increase PD-L1 levels, amplifying immunosuppressive mechanisms within the tumor microenvironment (44).

Pharmacokinetic interactions may further complicate combination approaches. For instance, olaparib is primarily processed through the CYP3A4/5 enzymatic pathway, meaning drugs that boost CYP3A activity lower plasma concentrations of olaparib, whereas CYP3A inhibitors elevate drug exposure. Additionally, overlapping toxicities may pose some challenges; PARP inhibitors (associated with blood cell deficiencies and fatigue) interact adversely with chemotherapies (e.g., drugs causing bone marrow suppression) or immunotherapies (e.g., liver toxicity from checkpoint inhibitors), often requiring dose reductions that undermine therapeutic efficacy. In patients with previously untreated metastatic nonsquamous NSCLC lacking actionable genetic mutations, the combination of pembrolizumab and maintenance olaparib showed no significant improvement in PFS or OS when compared to pembrolizumab paired with pemetrexed-based chemotherapy (45, 46).

Designing clinical trials for PARP inhibitor-chemotherapy combinations involves navigating variables such as drug characteristics (e.g., pharmacokinetics), combination partners, dosing protocols, target patient groups, and evolving regulatory standards. For instance, the FDA's approval of cisplatin/paclitaxel/bevacizumab hindered veliparib-based regimen development. Regulatory approval requires demonstrating the combination's superiority over individual agents, supported by robust preclinical evidence. Success demands sustained collaboration among researchers, sponsors, and patients, along with flexibility to adapt to shifting clinical environments (42).

This study presents a comprehensive analysis of three different treatment regimens for lung cancer: olaparib monotherapy, olaparib plus gefitinib, and olaparib plus durvalumab. As the first systematic review and meta-analysis on this topic, our findings provide a valuable initial assessment. Future research is warranted to further investigate the efficacy and safety of these regimens, both individually and in combination. Because of the few results have been obtained, it isn't possible to give a definitive opinion; Therefore, it is necessary to do more studies. While our study is the first of its kind, it is limited by the relatively small number of studies available and the lack of significant improvements in PFS with the current combination therapies. Despite these limitations, the findings can be extrapolated to other populations.

5 Conclusion and implications

Combining PARP inhibitors with chemotherapy represents an emerging yet complex strategy aimed at amplifying the anticancer efficacy of both therapies, potentially broadening their use to more patients. Our analysis demonstrated that olaparib monotherapy can improve PFS in patients with lung cancer. However, we couldn't find significant benefits with the combination of olaparib and gefitinib or olaparib and durvalumab. Given the heterogeneity and limited number of studies, larger and more robust trials are needed to evaluate the efficacy of these regimens in improving PFS and treating lung cancer. Despite the success of PARP inhibitors in cancers with DNA repair defects, personalized patient selection remains crucial. Advances in multi-omics and ongoing clinical trials are poised to address these challenges, enabling tailored therapies and improved resistance management in the near future.

Data availability statement

The original contributions presented in the study are included in the article/supplementary material. Further inquiries can be directed to the corresponding author.

Author contributions

SH: Writing – original draft. EE: Writing – original draft. SZ: Writing – original draft. PJ: Writing – review & editing. MS: Writing – review & editing. SK: Writing – review & editing. MG: Writing – review & editing. MB: Writing – review & editing. GE: Writing – original draft. ND: Writing – review & editing.

Funding

The author(s) declare that no financial support was received for the research and/or publication of this article.

Acknowledgments

We appreciate all authors of included studies.

Conflict of interest

The authors declare that the research was conducted in the absence of any commercial or financial relationships that could be construed as a potential conflict of interest.

Generative AI statement

The author(s) declare that no Generative AI was used in the creation of this manuscript.

Publisher's note

References

1. Jemal A, Bray F, Center MM, Ferlay J, Ward E, Forman D, et al. Global cancer statistics. *CA Cancer J Clin*. (2011) 61:69–90. doi: 10.3322/caac.20107

2. Sun S, Schiller JH, Spinola M, Minna JD. New molecularly targeted therapies for lung cancer. *J Clin Invest*. (2007) 117:2740–50. doi: 10.1172/JCI31809

3. Govindan R, Page N, Morgensztern D, Read W, Tierney R, Vlahiotis A, et al. Changing epidemiology of small-cell lung cancer in the United States over the last 30 years: analysis of the surveillance, epidemiologic, and end results database. *J Clin Oncol*. (2006) 24:4539–44. doi: 10.1200/JCO.2005.04.4859

4. GBD 2017 Causes of Death Collaborators, Roth GA, Abate D, Abate KH, Abay SM, Abbafati C, et al. Global, regional, and national age-sex-specific mortality for 282 causes of death in 195 countries and territories, 1980-2017: a systematic analysis for the Global Burden of Disease Study 2017. *Lancet*. (2018) 392:1736–88. doi: 10.1016/S0140-6736(18)32203-7

5. Slade D. PARP and PARG inhibitors in cancer treatment. *Genes Dev*. (2020) 34:360–94. doi: 10.1101/gad.334516.119

6. D'Andrea AD. Mechanisms of PARP inhibitor sensitivity and resistance. *DNA Repair (Amst)*. (2018) 71:172–6. doi: 10.1016/j.dnarep.2018.08.021

7. Wang Y, Luo W, Wang Y. PARP-1 and its associated nucleases in DNA damage response. *DNA Repair (Amst)*. (2019) 81:102651. doi: 10.1016/j.dnarep.2019.102651

8. Dantzer F, Ame JC, Schreiber VR, Nakamura J, Nissier-DE Murcia JME, Murcia GDE. Poly(ADP-ribose) polymerase-1 activation during DNA damage and repair. *Methods Enzymol*. (2006) 409:493–510. doi: 10.1016/S0076-6879(05)09029-4

9. Huber A, Bai P, de Murcia JM, de Murcia G. PARP-1, PARP-2 and ATM in the DNA damage response: functional synergy in mouse development. *DNA Repair (Amst)*. (2004) 3:1103–8. doi: 10.1016/j.dnarep.2004.06.002

10. Levra MG, Olaussen KA, Novello S, Soria J-C. PARP inhibitors: an interesting pathway also for non-small cell lung cancer? *Curr Pharm Des*. (2014) 20:3875–82. doi: 10.2174/13816128113196660765

11. Byers LA, Wang J, Nilsson MB, Fujimoto J, Saintigny P, Yordy J, et al. Proteomic profiling identifies dysregulated pathways in small cell lung cancer and novel therapeutic targets including PARP1. *Cancer Discovery*. (2012) 2:798–811. doi: 10.1158/2159-8290.CD-12-0112

12. Lok BH, Gardner EE, Schneeberger VE, Ni A, Desmeules P, Rekhtman N, et al. PARP inhibitor activity correlates with SLFN11 expression and demonstrates synergy with temozolomide in small cell lung cancer. *Clin Cancer Res*. (2017) 23:523–35. doi: 10.1158/1078-0432.CCR-16-1040

13. Lallo A, Frese KK, Morrow CJ, Sloane R, Gulati S, Schenk MW, et al. The combination of the PARP inhibitor olaparib and the WEE1 inhibitor AZD1775 as a new therapeutic option for small cell lung cancer. *Clin Cancer Res*. (2018) 24:5153–64. doi: 10.1158/1078-0432.CCR-17-2805

14. Gay CM, Tong P, Li L, Stewart CA, Sen T, Glisson BS. Abstract 2822: ATR inhibitors are active as single agents and in combination with PARP1 and ATM inhibitors in molecularly distinct subsets of small cell lung cancer models. *Cancer Res*. (2018) 78:2822–2. doi: 10.1158/1538-7445.AM2018-2822

15. Lin J, Welch S, Sanatani M, Ramadan S. Combination of osimertinib and olaparib therapy to treat non-small cell lung cancer and high-grade serous ovarian carcinoma: A case report. *Curr Oncol*. (2024) 31:558–65. doi: 10.3390/curroncol31010039

16. Ahn M-J, Bondarenko I, Kalinka E, Cho BC, Sugawara S, Gálffy G, et al. Durvalumab in combination with olaparib versus durvalumab alone as maintenance therapy in metastatic NSCLC: the phase 2 ORION study. *J Thorac Oncol*. (2023) 18:1594–606. doi: 10.1016/j.jtho.2023.06.013

17. progression-free survival. In: *NCI Dictionary of Cancer Terms*. United states: National Cancer Institute (2024). Available online at: https://www.cancer.gov/publications/dictionaries/cancer-terms/def/progression-free-survival (Accessed March 2024).

18. Fennell DA, Porter C, Lester J, Danson S, Blackhall F, Nicolson M, et al. Olaparib maintenance versus placebo monotherapy in patients with advanced non-small cell lung cancer (PIN): A multicentre, randomised, controlled, phase 2 trial. *EClinicalMedicine*. (2022) 52:101595. doi: 10.1016/j.eclinm.2022.101595

19. Garcia-Campelo R, Arrieta O, Massuti B, Rodriguez-Abreu D, Granados ALO, Majem M, et al. Combination of gefitinib and olaparib versus gefitinib alone in EGFR mutant non-small-cell lung cancer (NSCLC): A multicenter, randomized phase II study (GOAL). *Lung Cancer*. (2020) 150:62–9. doi: 10.1016/j.lungcan.2020.09.018

20. Higgins JP, Thompson SG. Quantifying heterogeneity in a meta-analysis. *Stat Med*. (2002) 21:1539–58. doi: 10.1002/sim.v21:11

21. DerSimonian R, Kacker R. Random-effects model for meta-analysis of clinical trials: an update. *Contemp Clin trials*. (2007) 28:105–14. doi: 10.1016/j.cct.2006.04.004

22. Sterne JA, Harbord RM. Funnel plots in meta-analysis. *stata J*. (2004) 4:127–41. doi: 10.1177/1536867X0400400204

23. Desmond D, Vilimas R, Mullenix C, Zhao C, Szabo E, Shelat M, et al. Durvalumab (D) in combination with olaparib (O) for advanced, previously treated non-small cell lung cancer (NSCLC). *J Clin Oncol*. (2022) 40:e21153–3. doi: 10.1200/JCO.2022.40.16_suppl.e21153

24. Krebs MG, Delord J-P, Evans TRJ, De Jonge M, Kim S-W, Meurer M, et al. Olaparib and durvalumab in patients with relapsed small cell lung cancer (MEDIOLA): An open-label, multicenter, phase 1/2, basket study. *Lung Cancer*. (2023) 180:107216. doi: 10.1016/j.lungcan.2023.107216

25. Huang Y, Jia J, Wang Q, Liu X, Li Z. Phase II study of durvalumab plus olaparib as maintenance therapy in extensive-stage small-cell lung cancer (TRIDENT): Preliminary efficacy and safety results. *J Clin Oncol*. (2023) 41:8518–8. doi: 10.1200/JCO.2023.41.16_suppl.8518

26. Woll P, Gaunt P, Danson S, Steele N, Ahmed S, Mulatero C, et al. Olaparib as maintenance treatment in patients with chemosensitive small cell lung cancer (STOMP): A randomised, double-blind, placebo-controlled phase II trial. *Lung Cancer*. (2022) 171:26–33. doi: 10.1016/j.lungcan.2022.07.007

27. Postel-Vinay S, Planchard D, Antigny M, Coves Sarto J, Domine Gomez M, de las Penas Bataller R, et al. Olaparib maintenance versus placebo in platinum-sensitive non-small cell lung cancer: the Phase 2 randomized PIPSeN trial. *Br J Cancer*. (2024) 130:417–24. doi: 10.1038/s41416-023-02514-5

28. Park S, Kim YJ, Min YJ, Mortimer PGS, Kim H-J, Smith SA, et al. Biomarker-driven phase 2 umbrella trial: Clinical efficacy of olaparib monotherapy and combination with ceralasertib (AZD6738) in small cell lung cancer. *Cancer*. (2024) 130:541–52. doi: 10.1002/cncr.v130.4

29. Karachaliou N, Arrieta O, Giménez-Capitán A, Aldeguer E, Drozdowskyj A, Chaib I, et al. BRCA1 expression and outcome in patients with EGFR-mutant NSCLC treated with gefitinib alone or in combination with olaparib. *JTO Clin Res Rep*. (2021) 2:100113. doi: 10.1016/j.jtocrr.2020.100113

30. Luo L, Keyomarsi K. PARP inhibitors as single agents and in combination therapy: the most promising treatment strategies in clinical trials for BRCA-mutant ovarian and triple-negative breast cancers. *Expert Opin Investig Drugs*. (2022) 31:607–31. doi: 10.1080/13543784.2022.2067527

31. Hopkins TA, Ainsworth WB, Ellis PA, Donawho CK, DiGiammarino EL, Panchal SC, et al. PARP1 trapping by PARP inhibitors drives cytotoxicity in both cancer cells and healthy bone marrow. *Mol Cancer Res*. (2019) 17:409–19. doi: 10.1158/1541-7786.MCR-18-0138

32. Kim D, Nam HJ. PARP inhibitors: clinical limitations and recent attempts to overcome them. *Int J Mol Sci*. (2022) 23:1–18. doi: 10.3390/ijms23158412

33. Huang Y, Jia J, Wang Q, Liu X, Zhang L. 86P Durvalumab plus olaparib as maintenance therapy in extensive-stage small-cell lung cancer (TRIDENT): Updated efficacy and safety analysis. *Immuno-Oncology Technol*. (2023) 20:12. doi: 10.1016/j.iotech.2023.100558

34. Thomas A, Vilimas R, Trindade C, Erwin-Cohen R, Roper N, Xi L, et al. Durvalumab in combination with olaparib in patients with relapsed SCLC: results from a phase II study. *J Thorac Oncol*. (2019) 14:1447–57. doi: 10.1016/j.jtho.2019.04.026

35. George J, Lim JS, Jang SJ, Cun Y, Ozretić L, Kong G, et al. Comprehensive genomic profiles of small cell lung cancer. *Nature*. (2015) 524:47–53. doi: 10.1038/nature14664

36. Coleman N, Zhang B, Byers LA, Yap TA. The role of Schlafen 11 (SLFN11) as a predictive biomarker for targeting the DNA damage response. *Br J Cancer*. (2021) 124:857–9. doi: 10.1038/s41416-020-01202-y

37. Coussy F, El-Botty R, Château-Joubert S, Dahmani A, Montaudon E, Leboucher S, et al. BRCAness, SLFN11, and RB1 loss predict response to topoisomerase I inhibitors in triple-negative breast cancers. *Sci Transl Med*. (2020) 12:1–12. doi: 10.1126/scitranslmed.aax2625

38. Willis SE, Winkler C, Roudier MP, Baird T, Marco-Casanova P, Jones EV, et al. Retrospective analysis of Schlafen11 (SLFN11) to predict the outcomes to therapies affecting the DNA damage response. *Br J Cancer*. (2021) 125:1666–76. doi: 10.1038/s41416-021-01560-1

39. Venugopala KN. Targeting the DNA damage response machinery for lung cancer treatment. *Pharm (Basel)*. (2022) 15:1–22. doi: 10.3390/ph15121475

40. Zhang X, Guoa M, Fana J, Lva Z, Huang Q, Han J, et al. Prognostic significance of serum LDH in small cell lung cancer: A systematic review with meta-analysis. *Cancer biomark*. (2016) 16:415–23. doi: 10.3233/CBM-160580

41. Allison Stewart C, Tong P, Cardnell RJ, Sen T, Li L, Gay CM, et al. Dynamic variations in epithelial-to-mesenchymal transition (EMT), ATM, and SLFN11 govern response to PARP inhibitors and cisplatin in small cell lung cancer. *Oncotarget*. (2017) 8:28575–87. doi: 10.18632/oncotarget.15338

42. Matulonis UA, Monk BJ. PARP inhibitor and chemotherapy combination trials for the treatment of advanced Malignancies: does a development pathway forward exist? *Ann Oncol*. (2017) 28:443–7. doi: 10.1093/annonc/mdw697

43. Ayoub J, Friedlander ML, Dieras VC, Wildiers H, Arun B, Han HS, et al. 140O veliparib plus carboplatin-paclitaxel in patients with HER2-negative advanced/metastatic gBRCA-associated breast cancer: results in hormone receptor-positive and triple-negative breast cancer subgroups from the phase III BROCADE3 trial. *Ann Oncol*. (2020) 31:S65. doi: 10.1016/j.annonc.2020.03.241

44. Jiao S, Xia W, Yamaguchi H, Wei Y, Chen M-K, Hsu JM, et al. PARP inhibitor upregulates PD-L1 expression and enhances cancer-associated immunosuppression. *Clin Cancer Res*. (2017) 23:3711–20. doi: 10.1158/1078-0432.CCR-16-3215

45. Gray JE, Schenker M, Şendur MAN, Leonova V, Kowalski D, Kato T, et al. The phase 3 KEYLYNK-006 study of pembrolizumab plus olaparib versus pembrolizumab plus pemetrexed as maintenance therapy for metastatic nonsquamous NSCLC. *J Thorac Oncol*. (2025) 20:219–32. doi: 10.1016/j.jtho.2024.10.026

46. Paller CJ, Bradbury PA, Ivy SP, Seymour L, LoRusso PM, Baker L, et al. Design of phase I combination trials: recommendations of the Clinical Trial Design Task Force of the NCI Investigational Drug Steering Committee. *Clin Cancer Res*. (2014) 20:4210–7. doi: 10.1158/1078-0432.CCR-14-0521

Frontiers in Oncology

Advances knowledge of carcinogenesis and tumor progression for better treatment and management

The third most-cited oncology journal, which highlights research in carcinogenesis and tumor progression, bridging the gap between basic research and applications to imrpove diagnosis, therapeutics and management strategies.

Discover the latest Research Topics

See more →

Frontiers

Avenue du Tribunal-Fédéral 34
1005 Lausanne, Switzerland
frontiersin.org

Contact us

+41 (0)21 510 17 00
frontiersin.org/about/contact